



UNIVERSIDAD DE GRANADA

FACULTAD DE CIENCIAS

Departamento de Química Analítica

Centro de Investigación y Desarrollo del Alimento Funcional (CIDAF)



TESIS DOCTORAL

**CARACTERIZACIÓN ANALÍTICA DE EXTRACTOS VEGETALES Y EVALUACIÓN DE
SU ACTIVIDAD EN MODELOS CELULARES Y ANIMALES**

presentada por

Salvador Fernández Arroyo

para optar al grado de

Doctor Internacional por la Universidad de Granada

Tesis doctoral dirigida por:

D. Alberto Fernández Gutiérrez

D. Antonio Segura Carretero

D. Vicente Micol Molina

Granada, 2012

Editor: Editorial de la Universidad de Granada
Autor: Úaçaá[;A^!; } } á^: ÁE! [^[
D.L.: ÖÜAG €€€FG
ISBN: Jí ì È | È € È í Ì È





Esta tesis doctoral ha sido realizada gracias a una beca predoctoral concedida por la Junta de Andalucía (P07-AGR-02619) y a la financiación con cargo a fondos del Centro de Investigación y Desarrollo del Alimento Funcional (CIDAF), procedentes de diferentes proyectos, contratos y subvenciones de las Administraciones central y autonómica, plan propio de investigación de la UGR, así como de empresas interesadas en los resultados de la investigación.

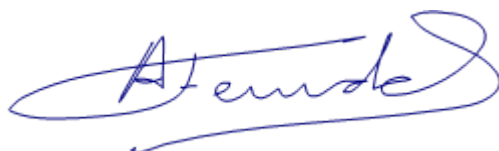


**CARACTERIZACIÓN ANALÍTICA DE EXTRACTOS VEGETALES Y EVALUACIÓN DE
SU ACTIVIDAD BIOLÓGICA EN MODELOS CELULARES Y ANIMALES**

por

Salvador Fernández Arroyo

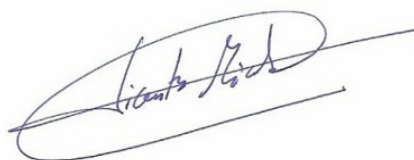
Visado en Granada a 21 de Marzo de 2010



Fdo: Prof. Dr. D. Alberto Fernández Gutiérrez
Catedrático del Departamento de Química Analítica
Facultad de Ciencias. Universidad de Granada

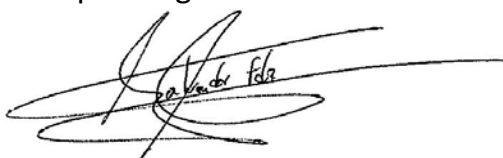


Fdo: Dr. D. Antonio Segura Carretero
Catedrático del Departamento de Química Analítica
Facultad de Ciencias. Universidad de Granada



Fdo: Dr. D. Vicente Micol Molina
Profesor de la Universidad Miguel Hernández
Instituto de Biología Molecular y Celular. Universidad Miguel Hernández

Trabajo presentado para optar al grado de Doctor Internacional por la UGR:



Fdo: Salvador Fernández Arroyo

El Prof. Dr. D. ALBERTO FERNÁNDEZ GUTIÉRREZ, Catedrático de Universidad en el Departamento de Química Analítica “Profesor Fermín Capitán” y Director del CIDAF,

CERTIFICA:

Que el trabajo que se presenta en esta tesis doctoral con el título: **“CARACTERIZACIÓN ANALÍTICA DE EXTRACTOS VEGETALES Y EVALUACIÓN DE SU ACTIVIDAD BIOLÓGICA EN MODELOS CELULARES Y ANIMALES”**, que ha sido realizado bajo mi dirección y la de los Drs. D. Antonio Segura Carretero y D. Vicente Micol Molina en los laboratorios que el Centro de Investigación y Desarrollo del Alimento Funcional (CIDAF) tiene en las instalaciones del Parque Tecnológico de la Salud (PTS) de Armillay también, parcialmente, en el Instituto de Biología Molecular y Celular (IBMC) de la Universidad Miguel Hernández de Elche, en el Departamento de Bioquímica de la Escuela Universitaria de Óptica de la Universidad Complutense de Madrid y en el grupo de investigación U781 “Génétique et épigénétique des maladies métaboliques, neurosensorielles et du développement” del Institut National de la Santé et de la Recherche Médicale (INSERM) de París, reúne todos los requisitos legales, académicos y científicos para hacer que el doctorando D. Salvador Fernández Arroyo pueda optar al grado de Doctor Internacional por la Universidad de Granada.

Y para que así conste, expido y firmo el presente certificado en Granada a 21 de Marzo de 2012:

Prof. D. Alberto Fernández Gutiérrez





ÍNDICE





ÍNDICE GENERAL

ÍNDICE DE FIGURAS	14
RESUMEN	18
RÉSUMÉ	24
OBJETIVOS.....	30
INTRODUCCIÓN.....	36
1. LA MEDICINA NATURAL EN LA HISTORIA.	37
2. EXTRACTOS VEGETALES COMO FUENTE NATURAL DE COMPUESTOS BIOACTIVOS. 39	
2.1. <i>Cistus spp.</i>	39
2.1.1. Generalidades del género <i>Cistus</i>	40
2.1.2. <i>Cistus ladanifer</i>	40
2.1.3. <i>Cistus populifolius</i>	42
2.1.4. Otras especies del género <i>Cistus</i>	43
2.2. <i>Olea europaea</i> y aceite de oliva virgen extra.	46
2.3. <i>Hibiscus sabdariffa</i>	49
3. POLIFENOLES: BIOSÍNTESIS Y CARACTERÍSTICAS.	50
4. POLIFENOLES Y BIOACTIVIDAD.	55
4.1. Infección bacteriana y polifenoles.	55
4.2. Cáncer y polifenoles.....	56
4.2.1. Cáncer de mama.	59
4.2.2. Cáncer de colon.....	62
4.3. Envejecimiento y polifenoles.	64
4.4. Obesidad y Polifenoles.....	66
4.5. Patologías huérfanas y polifenoles.	69
4.5.1. Condrodisplasias.	70
5. TÉCNICAS ANALÍTICAS PARA EL ANÁLISIS DE POLIFENOLES.....	73
5.1. Técnicas separativas.	73
5.1.1. Cromatografía líquida de alta resolución (HPLC).....	74

5.1.2. Nanocromatografía líquida (nLC).	75
5.2. Sistemas de detección en cromatografía líquida.	77
5.2.1. Espectroscopía de absorción molecular Ultravioleta-Visible (UV-Vis).....	77
5.2.2. Espectrometría de masas.	79
6. ENSAYOS <i>IN VITRO</i> E <i>IN VIVO</i> Y METODOLOGÍAS PARA LA DETERMINACIÓN DE LA BIOACTIVIDAD.	81
6.1. Ensayos <i>in vitro</i>	83
6.1.1. Cultivos microbianos.	83
6.1.2. Cultivos celulares animales.	85
6.2. Ensayos <i>in vivo</i> . Animales de experimentación.....	87
6.2.1. Marco legal.....	87
6.2.2. Modelos animales.	88
6.3. Metodología para la determinación de la bioactividad	90
6.3.1. Capacidad antioxidante.....	90
6.3.2. Capacidad antimicrobiana.....	92
6.3.3. Western Blot	93
6.3.4. Viabilidad celular en cultivos animales.....	94
7. METABOLISMO Y BIODISPONIBILIDAD DE LOS POLIFENOLES	94
7.1. Metabolismo de los polifenoles	94
7.2. Farmacocinética y biodisponibilidad.....	97
BLOQUE I. <i>Cistus spp.</i>	101
BLOQUE II. ACEITE DE OLIVA VIRGEN EXTRA.....	143
BLOQUE III. <i>Hibiscus sabdariffa</i>	201
CONCLUSIONES.....	279
CONCLUSIONS.....	289
ABREVIATURAS.....	299
BIBLIOGRAFÍA.....	305



ÍNDICE DE FIGURAS

Figura 1. Papiro de Ebers (1700 a.C.) egipcio (superior) y De materia medica (siglo I d.C.) de Discórides (inferior).....	37
Figura 2. <i>C. ladanifer</i> . Superior: arbusto; inferior izquierda: detalle de la flor; inferior derecha: detalle de hojas y fruto.	40
Figura 3. <i>C. populifolius</i> . Superior: detalle de las flores; inferior: detalle del fruto.	42
Figura 4. Diferentes especies del género <i>Cistus</i> . Superior izquierda: <i>C. salviifolius</i> ; superior centro: <i>C. clusii</i> ; superior derecha: <i>C. laurifolius</i> ; centro izquierda: <i>C. monspeliensis</i> ; centro derecha: <i>C. libanotis</i> ; inferior izquierda: <i>C. albidus</i> ; inferior centro: <i>C. incanus</i> ; inferior derecha: <i>C. crispus</i>	44
Figura 5. Aceitunas (fruto de <i>Olea europaea</i>) y aceite de oliva obtenido de éstas.	46
Figura 6. <i>H. sabdariffa</i> , detalle de las flores.	48
Figura 7. Principales familias de compuestos fenólicos y clases de flavonoides con los esqueletos básicos de cada una de ellas.	51
Figura 8. Biosíntesis simplificada de los compuestos fenólicos siguiendo las rutas del ácido shikímico y del acetato. Abreviaturas: E4P, eritrosa-4-fosfato; PEP, ácido fosfoenolpirúvico; CoA, coenzima A; 3-DHS, ácido 3-dehidroshikímico; FA, fenilalanina; Tyr, tirosina.	53
Figura 9. Esquema simplificado del control por parte de las ciclinas y las kinasas dependientes de ciclina (cdk) en el ciclo celular.	56
Figura 10. Carcinoma lobular de mama.....	58
Figura 11. Evolución del adenocarcinoma colorectal.....	62
Figura 12. Esquema simplificado de la transición epitelial-mesenquimal.	64
Figura 13. Relación entre obesidad e inflamación y moléculas señalizadoras implicadas. IGF: factor de crecimiento insulínico; TNF- α : factor de necrosis tumoral α ; IL: interleuquina; MCP-1: proteína quimioatrayente de monocitos 1.	67
Figura 14. Tyrion Lanister encarnado por Peter Dinklage en la serie Juego de Tronos.	70



Figura 15. Vías de señalización en la activación del receptor FGFR3. FGF: factor de crecimiento fibroblástico; FGFR3: receptor 3 del factor de crecimiento fibroblástico; RAS: proteína del sarcoma de rata (GTPasa); RAF: acelerador rápido del fibrosarcoma (serin-treonin kinasa); MEK1/2: kinasas 1 y 2 de la MAPK; ERK1/2 (MAPK1/2): proteínas kinasas 1 y 2 activadas por mitógenos; Stat1: transductor de señal y activador de la transcripción 1.....	71
Figura 16. Sistema de HPLC de los años 1970.	73
Figura 17. Equipo de nanocromatografía líquida (nLC).....	75
Figura 18. Equipo de espectroscopía de absorción basado en un detector de batería de diodos (DAD).	77
Figura 19. Analizadores de masas. Superior, trampa de iones; inferior, tiempo de vuelo.	79
Figura 20. Tinción de Gram (izquierda) y esquema simplificado de la composición de la envuelta (derecha) de una bacteria Gram negativa como <i>E. coli</i> (superior) y una bacteria Gram positiva como <i>S. aureus</i> (inferior).	83
Figura 21. Fases del crecimiento bacteriano.	84
Figura 22. Cultivo celular de condrocitos de la línea RCJ de ratón.	85
Figura 23. Rata Wistar.....	87
Figura 24. Ratón de la cepa C57BL/6J silvestre (izquierda) y knock-out LDLr ^{-/-} (derecha).88	
Figura 25. Esquema simplificado de los mecanismos de acción de los métodos SET (superior) y HAT (inferior).	89
Figura 26. Imágenes de microscopía de <i>Staphylococcus aureus</i> (izquierda) y <i>Escherichia coli</i> (derecha).....	92
Figura 27. Absorción de polifenoles y metabolismo que sufren.....	96
Figura 28. Curva de concentración plasmática frente al tiempo.	97











Los compuestos fenólicos constituyen un grupo de metabolitos secundarios en las plantas con una amplia actividad biológica, por lo que muchas de las investigaciones realizadas en varias áreas de la ciencia (bioquímica, farmacia, medicina, etc.) se centran en ellos.

La presente tesis doctoral, dividida en tres bloques, se ha enfocado en el estudio de este tipo de compuestos en diferentes fuentes vegetales y en la bioactividad que presentan *in vitro* e *in vivo*.

En el primer bloque, llevado a cabo en colaboración con el Instituto de Biología Molecular y Celular (IBMC) de la Universidad Miguel Hernández y con la empresa Químicas del Vinalopó se ha dedicado al estudio de especies del género *Cistus*. Este género comprende especies ampliamente distribuidas en la región mediterránea y especialmente abundantes en la península Ibérica y noroeste de África. Aunque sus aceites esenciales han sido muy estudiados, existe muy poca información sobre el contenido polifenólico de estas plantas, pudiendo suponer una fuente abundante y de bajo coste para la obtención de polifenoles con potencial uso en diversas aplicaciones. Por esta razón, en el capítulo 1 se ha procedido a caracterizar por primera vez un extracto acuoso obtenido de *Cistus ladanifer* mediante cromatografía líquida de alta resolución acoplada a espectroscopía UV/Visible y espectrometría de masas con analizador de tiempo de vuelo y trampa de iones (HPLC-DAD-ESI-TOF-MS/IT-MS/MS). La caracterización de *C. ladanifer* ha servido como base para, en el capítulo segundo, caracterizar los compuestos más importantes de las especies de este género y poder llevar a cabo un análisis comparativo sobre el perfil polifenólico de las especies de *Cistus* más comunes en España, y relacionar evolutivamente los diferentes subgéneros. El estudio de la bioactividad de *C. ladanifer* y *C. populifolius* (seleccionadas por su elevado contenido en elagitaninos) se ha llevado a cabo en el tercer capítulo de este primer bloque, analizando su actividad antioxidante mediante diversos métodos basados en transferencia de electrones y en transferencia de átomos de hidrógeno, su actividad



antimicrobiana contra bacterias Gram negativas y Gram positivas y su actividad anticancerígena en varias líneas celulares.

En el segundo bloque de esta tesis doctoral se ha evaluado la bioactividad en cáncer de mama y colon de 14 aceites pertenecientes a 5 variedades distintas que difieren en su perfil polifenólico. El aceite de oliva virgen extra, un importante ingrediente de la dieta mediterránea, es conocido por sus múltiples propiedades beneficiosas para el organismo. Gran parte de estos efectos saludables se deben a los compuestos fenólicos que se encuentran presentes en el aceite. En el capítulo 4 se ha estudiado la relación entre la capacidad antiproliferativa de estos aceites en una línea celular de cáncer de mama resistente a los tratamientos anti-HER2 y el perfil polifenólico que presentan, en colaboración con el Instituto Catalán de Oncología (ICO) de Girona. En el capítulo 5, también en colaboración con el ICO, se estudia la capacidad de estos mismos aceites para prevenir la transición que sufren las células epiteliales hacia un fenotipo mesenquimal en algunas enfermedades, dando como resultado una fibrosis excesiva o, en el caso del cáncer, metástasis. Para finalizar este segundo bloque, en el capítulo 6, y en colaboración con el IBMC de la Universidad Miguel Hernández, se ha llevado a cabo un estudio de absorción, metabolización y capacidad anticancerígena de los compuestos fenólicos presentes en extractos de aceites de oliva virgen extra en las líneas celulares HT29 y SW480 de adenocarcinoma de colon, utilizando para ello nLC-ESI-TOF-MS.

El tercer bloque se ha dedicado al estudio de *Hibiscus sabdariffa* mediante una colaboración multidisciplinar entre el IBMC de la UMH, el Centre de Recerca Biomèdica del Hospital Universitari Sant Joan de Reus, el Departamento de Bioquímica de la Escuela de Óptica de la Universidad Complutense de Madrid y el Institut National de la Santé et de la Recherche Médicale (INSERM) del Hôpital Necker-Enfants Malades de París y las empresas Monteloeder y NDN. En el capítulo 7 se han cuantificado los compuestos de un extracto acuoso de *H. sabdariffa* mediante HPLC-DAD-ESI-TOF-MS y se ha validado el método calculando la reproducibilidad, repetitividad y los límites de detección y



cuantificación. Además, se ha evaluado la capacidad antihiperlipémica de este extracto en ratones *knock-out* LDLr^{-/-}. En el capítulo 8 se ha caracterizado y cuantificado un extracto polifenólico enriquecido de *H. sabdariffa* así como diferentes fracciones obtenidas a partir de éste. Se ha evaluado la capacidad que poseen mejorando el estrés oxidativo e inflamatorio e inhibiendo la adipogénesis en preadipocitos 3T3-L1, en adipocitos maduros y en adipocitos hipertrofiados resistentes a insulina. En el capítulo 9 se ha llevado a cabo un estudio de biodisponibilidad en ratas de los compuestos fenólicos y la metabolización que sufren tras una ingesta forzada del extracto polifenólico enriquecido de *H. sabdariffa* mediante HPLC-ESI-TOF-MS, relacionándolo con el estatus oxidativo del plasma. Por último, en el capítulo 10, se pone de manifiesto que en enfermedades para las que actualmente no existe tratamiento como es el caso de las condrodisplasias, la búsqueda de nuevos compuestos bioactivos en extractos vegetales es una buena aproximación para mejorar, desde un punto de vista molecular y celular, los trastornos ocasionados por estas enfermedades.





RÉSUMÉ





Les composés phénoliques constituent un groupe de métabolites secondaires chez les plantes avec une grande activité biologique, et pourtant, de nombreuses recherches réalisées dans plusieurs domaines d'intérêt scientifique (biochimie, pharmacie, médecine, etc.) sont centrées sur eux.

La présente thèse doctorale, divisée en trois blocs, a mis l'accent sur l'étude de ce type de composés de différentes sources végétales et leur bioactivité présentée *in vitro* et *in vivo*.

Le premier bloc, réalisé en collaboration avec l'Institut de Biologie Moléculaire et Cellulaire (IBMC) de l'Université Miguel Hernández (UMH) et l'entreprise Químicas del Vinalopó, est consacré à l'étude des espèces du genre *Cistus*. Ce genre comprend des espèces largement distribuées dans la région méditerranéenne et particulièrement abondantes dans la région de la péninsule Ibérique et le nord-ouest de l'Afrique. Bien que ces huiles essentielles ont été très étudiées, il n'y a presque aucune information sur la teneur polyphénolique dans ces plantes, alors qu'elles pourraient être une source abondante et peu coûteuse de polyphénols, avec la possibilité de les utiliser dans diverses applications. Pour cette raison, dans le chapitre 1, on a caractérisé pour la première fois un extrait aqueux obtenu à partir de *Cistus ladanifer* en utilisant la chromatographie liquide d'haute résolution couplée à spectroscopie UV/Vis et la spectrométrie de masses avec analyseur de temps de vol et piège à ions (HPLC-DAD-ESI-TOF-MS/IT-MS/MS). La caractérisation de *C. ladanifer* a servi de base pour, dans le deuxième chapitre, caractériser les plus importants composés des espèces de ce genre et effectuer une analyse comparative sur le profil polyphénolique dans les espèces plus communes de *Cistus* en Espagne et mettre en relation l'évolution des différents sous-genres. L'étude de la bioactivité de *C. ladanifer* et *C. populifolius* (sélectionnés selon leur haute teneur en elagitannins) est effectuée dans le troisième chapitre de ce premier bloc, où l'on a analysé son activité antioxydante à l'aide de diverses méthodes fondées sur le transfert d'électron et le transfert des atomes d'hydrogène, leur activité



antimicrobienne contre les bactéries Gram-négatives et Gram-positives et leur activité anticancéreuse dans plusieurs lignées cellulaires .

Dans le deuxième bloc de cette thèse doctorale, on a évalué la bioactivité, dans le cancer du sein et du côlon, de 14 huiles appartenants à 5 variétés différentes qui diffèrent dans leur profil polyphénolique. L'huile d'olive extra vierge, un ingrédient important de la gastronomie méditerranéenne, est connue pour ses multiples propriétés bénéfiques pour la santé. Une grande partie de ces effets sont dus aux composés phénoliques qui sont présents dans l'huile. Dans le chapitre 4, on a étudié la relation entre la capacité antiproliférative de ces huiles dans une lignée cellulaire de cancer du sein résistante aux traitements anti-HER2 et le profil polyphénolique de ces huiles, en collaboration avec l'Institut Catalan d'Oncologie (ICO) de Gérone. Dans le chapitre 5, aussi en collaboration avec l'ICO, on a examiné la capacité de ces mêmes huiles d'empêcher la transformation des cellules épithéliales vers un phénotype mésenchymateuse qui se déroule dans certaines maladies, résultant dans une fibrose excessive ou, dans le cas du cancer, en métastase. Pour terminer ce deuxième bloc, au chapitre 6 et en collaboration avec l'IBMC de l'Université Miguel Hernández, on a mené une étude d'absorption, de métabolisation et de capacité anticancéreuse des composés phénoliques présents dans les extraits d'huile d'olive extra vierge dans les lignées cellulaires HT29 et SW480 d'adénocarcinome du côlon, à l'aide de la nanochromatographie liquide couplée à la spectrométrie de masses avec analyseur de temps de vol (nLC-ESI-TOF-MS).

Le troisième bloc est dédié à l'étude d'*Hibiscus sabdariffa* grâce à une collaboration multidisciplinaire entre l'IBMC de l'UMH, le Centre de Recherche Biomédicale de l'Hôpital Universitaire Sant Joan de Reus, le Département de Biochimie de l'École d'Optique de l'Université Complutense de Madrid, l'Institut National de la Santé et de la Recherche Médicale (INSERM) de l'Hôpital Necker-Enfants Malades de Paris et les entreprises Monteloeder et NDN. Dans le chapitre 7 on a quantifié les composés d'un extrait aqueux d'*H. sabdariffa* par HPLC-DAD-ESI-TOF-MS et la méthode a été validée en



calculant la répétabilité, la reproductibilité et les limites de détection et de quantification. En outre, on a évalué la capacité antihyperlipémique de cet extrait dans des souris *knock-out* pour les récepteurs des LDL (souris LDL^{-/-}). Dans le chapitre 8 a été caractérisé et quantifié un extrait d'*H. sabdariffa* enrichi en polyphénols ainsi que différentes fractions obtenues de lui. On a évalué leur capacité en améliorant le stress oxydatif et inflammatoire et en inhibant l'adipogénèse en preadipocytes 3T3-L1 et des adipocytes matures et dans adipocytes hypertrophiés résistant à l'insuline. Au chapitre 9 on a mené une étude de biodisponibilité chez les rats des composés phénoliques et la métabolisation dont souffrent après une consommation forcée d'extrait polyphénolique enrichi d'*H. sabdariffa* par HPLC-ESI-TOF-MS, et leur relation concernant le statut oxydatif du plasma. Pour finir, au chapitre 10, il apparaît évident que, pour certaines maladies actuellement incurables, comme les chondrodysplasies, la recherche de nouveaux composés bioactifs dans les extraits de plantes est une bonne approche pour améliorer les problèmes causés par ces maladies, du point de vue moléculaire et cellulaire.





OBJETIVOS







La búsqueda de extractos naturales de origen vegetal y de principios bioactivos a partir de éstos como preventivos, mejoramiento o tratamiento de diversas enfermedades es un campo de la ciencia muy activo en estos últimos años. Para ello no sólo es importante conocer la bioactividad que presenta sobre ciertas enfermedades un extracto vegetal, sino también caracterizar perfectamente los compuestos presentes en él. Por ello, los objetivos planteados en la presente tesis doctoral son los siguientes:

- En el primer bloque de la tesis se pretende caracterizar un extracto acuoso de *Cistus ladanifer* mediante una potente plataforma analítica como es el acoplamiento entre cromatografía líquida de alta resolución (HPLC) a espectroscopía UV-Vis con detector de batería de diodos (DAD), espectrometría de masas con analizador de tiempo de vuelo (TOF-MS) y trampa de iones (IT-MS/MS). Además, se comprobará si el perfil polifenólico de diferentes especies del género *Cistus* pertenecientes a sus tres subgéneros puede utilizarse para construir y/o corroborar los árboles filogenéticos establecidos. Por último, se pretende evaluar la bioactividad de *Cistus ladanifer* y *Cistus populifolius* analizando su capacidad antioxidante, antibacteriana y su citotoxicidad frente diferentes líneas celulares cancerígenas.
- En el segundo bloque de la presente tesis doctoral se comprobará la actividad anticancerígena y el mecanismo de acción de los polifenoles obtenidos de 14 aceites de oliva virgen extra pertenecientes a 5 variedades distintas en la línea celular JIMT-1 de cáncer de mama resistente a los tratamientos anti-HER2 y la capacidad de inhibición de la transición epitelial-mesenquimal que sufren las células en varios tipos de enfermedades, desencadenando una fibrosis excesiva, o metástasis en el caso del cáncer. Por último se valorará la capacidad antiproliferativa de los polifenoles del aceite de oliva virgen extra en dos líneas celulares de adenocarcinoma de colon (HT29 y SW480) y se realizará un análisis



metabolómico de los compuestos fenólicos originales del aceite de oliva y la metabolización que sufren tanto en el medio de cultivo como en el citoplasma celular utilizando para ello la nanocromatografía líquida (nLC) acompañada a espectrometría de masas con analizador de tiempo de vuelo (TOF-MS)

- En el tercer y último bloque, los objetivos consisten en validar un método analítico para caracterizar y cuantificar los compuestos fenólicos presentes en un extracto acuoso de *Hibiscus sabdariffa*, en un extracto polifenólico enriquecido obtenido a partir de éste y en subfracciones purificadas mediante HPLC-DAD-ESI-TOF-MS. A continuación se ensayará la bioactividad que presentan estos extractos mediante ensayos de capacidad antioxidante, de capacidad antihiperlipémica en ratones knock-out LDLr^{-/-} y su capacidad antiadipogénica en la línea celular adipocítica 3T3-L1. A continuación se realizará un estudio de biodisponibilidad y metabolización de los compuestos de *Hibiscus sabdariffa* en ratas wistar tras una ingesta forzada del extracto polifenólico enriquecido y la relación con el estatus oxidativo del plasma sanguíneo. Para finalizar, se realizará una búsqueda de nuevos compuestos bioactivos en extractos vegetales y el mecanismo de acción a nivel molecular y celular que presentan, como tratamiento de enfermedades huérfanas como es el caso de las condrodisplasias.







INTRODUCCIÓN





1. LA MEDICINA NATURAL EN LA HISTORIA.

La utilización de plantas como herramientas para la curación de diferentes trastornos de la salud está ampliamente documentada desde la antigüedad en todas las culturas. El tratamiento de las enfermedades en la prehistoria del ser humano comenzó, probablemente, en el íntimo contacto con la naturaleza, con la observación de las costumbres de otros animales y con la experiencia acumulada tras la ingestión accidental o provocada de algunas especies vegetales.



Figura 1. Papiro de Ebers (1700 a.C.) egipcio (superior) y De materia medica (siglo I d.C.) de Discórides (inferior).

Las raíces de la filosofía de la medicina natural son milenarias. Los conocimientos sobre las plantas medicinales, antes del nacimiento de la escritura, se realizaban oralmente. Entre los textos más antiguos encontrados donde se describen plantas medicinales figuran una tablilla de arcilla sumeria (3000 a.C.) y el “*Pen Tsao*” (2.800 a.C.) de origen asiático. Posteriormente, los egipcios en el “*papiro de Ebers*” datado del 1700 a.C. citan aproximadamente 700 plantas utilizadas con fines medicinales (Figura 1, superior). Ya en la época clásica, Hipócrates (400 a.C.) hizo referencia a la “*vix medicatrix naturae*” -la naturaleza sana por sí misma- y posteriormente Discórides en el siglo I d.C. en su trabajo “*De materia medica*” (Figura 1, inferior) describió unas 600 plantas usadas en tratamientos médicos.

No fue hasta los siglos XVIII y XIX cuando se dio lugar a un gran avance de estas ciencias, de la patología y de la clínica. Por una parte gracias al estudio químico de la composición



de los productos naturales así como sus sustancias activas, y por otra el análisis fisiológico de los mecanismos de acción, gracias a la fructífera relación entre la química y la medicina.

2. EXTRACTOS VEGETALES COMO FUENTE NATURAL DE COMPUESTOS BIOACTIVOS.

La creciente preocupación social por el impacto sobre la salud humana y el medio ambiente de las sustancias y preparados químicos peligrosos ha estimulado la búsqueda de soluciones para producir productos más ecológicos, a trabajar con más firmeza a favor del medio ambiente y a controlar mejor el rendimiento ecológico de los productos en todo su ciclo de vida.

En la actualidad, la búsqueda de principios bioactivos centrada en especies vegetales como fuente de compuestos con acciones beneficiosas sobre el hombre y otras especies animales es un campo de la ciencia muy activo. Además de obtenerse compuestos con aplicaciones concretas, esta actividad contribuye a disminuir la liberación de sustancias potencialmente tóxicas y xenobióticas al medio ambiente (como alternativa al sector petroquímico) y, además, disminuir el riesgo de aparición de cepas microbianas resistentes a antibióticos sintéticos ofreciendo una alternativa terapéutica, aplicando el *“Principio de Precaución y Sustitución”* definido en el *“Libro Blanco de la Comisión Europea sobre la Estrategia para la futura política en materia de sustancias y preparados peligrosos”* publicado en febrero de 2001.

Es debido a todas estas razones por las que en la presente tesis doctoral se ha querido estudiar en profundidad las siguientes plantas (o productos derivados), tanto de una forma analítica como la bioactividad que presentan.



2.1. *Cistus spp.*

2.1.1. Generalidades del género *Cistus*.

Las especies del género *Cistus* (Orden *Malvales*, Familia *Cistaceae*) son conocidas vulgarmente como Jaras o Estepas, aunque esta denominación también se aplica a algunas especies del género *Halimium*, íntimamente relacionado con ellas.

Las plantas del género *Cistus* son perennifolias, arbustivas y leñosas que se extienden por suelos ácidos, áridos y secos, graníticos y pizarrosos de la cuenca mediterránea, y raramente en suelos calizos. Crecen en los suelos más degradados, por lo que su presencia suele indicar suelos muy pobres. Estas plantas producen alelopáticos que inhiben el crecimiento de otras especies vegetales a su alrededor, con lo que son capaces de crear grandes masas arbustivas compactas en el hábitat donde habitan. Además, son especies pioneras en la recuperación de suelos degradados especialmente tras un incendio forestal, ya que las semillas tienen un carácter pirófilo y ven favorecida su germinación por la acción del fuego. Las flores son hermafroditas y pentámeras y con numerosos estambres. La polinización suele ser por zoofilia y la dispersión de sus semillas es por anemocoria/zoocoria/autocoria.

Dentro del género *Cistus* podemos encontrar tres subgéneros:

Leucocistus, al que pertenecen *C. ladanifer*, *C. salviifolius*, *C. populifolius*, *C. laurifolius* y *C. monspeliensis*.

Cistus, representado por *C. crispus*, *C. incanus* y *C. albidus*.

Halimioides, que engloba a *C. libanotis* y *C. clusii*.

2.1.2. *Cistus ladanifer*.

C. ladanifer (jara común, jara pringosa, jara de las cinco llagas, estepa de ládano) (Figura 2) es llamada así por la esencia de ládano que exuda la planta, una oleorresina compuesta básicamente por ladaniol ($C_{17}H_{30}O$), sesquiterpenos, ésteres y taninos. Ha sido declarada como especie de interés especial según el Anexo I al Decreto 50/2003 de 30 de Mayo. Boletín Oficial de la Región de Murcia de 10 de junio de 2003.



Figura 2. *C. ladanifer*. Superior: arbusto; inferior izquierda: detalle de la flor; inferior derecha: detalle de hojas y fruto.

Es un arbusto de hasta 3 m de altura, erecto, con leño duro y corteza pegajosa pardo-rojiza. Muy oloroso. Sus hojas son opuestas, simples, sésiles o cortamente pecioladas, lanceoladas, estrechas y de color verde oscuro, muy viscosas y pegajosas al tacto, con el envés cubierto de pelos estrellados y el haz glabrescente. Presenta flores solitarias y terminales de color blanco, de hasta 11 cm de diámetro, y a menudo con un anillo de cinco manchas purpúreas. La floración suele ser entre marzo y mayo.

El fruto es una cápsula globosa de hasta 10 lóculos con un indumento denso que se abren en la madurez en otras tantas valvas. Es muy abundante en la península Ibérica por toda la región Mediterránea occidental, desde Portugal y Marruecos hasta la Costa Azul y Argelia. Suelen ser un elemento constituyente de encinares y alcornoques de los pisos termomediterráneo y mesomediterráneo.



La resina de ládano que exuda es muy inflamable, por lo que ante un incendio, la jara hará que éste se propague más rápidamente. El ládano es, además, un alelopático¹⁻³ y también le sirve de protección frente al calor y la sequía, ya que refleja los rayos del sol y protege a la planta de sobrecalentamientos. El agua que pierde por transpiración también es menor gracias a esta capa aceitosa que la recubre.

La resina de ládano tiene un sabor amargo que tradicionalmente se ha utilizado como bálsamo contra la tos, tranquilizante y analgésico en tratamientos de artritis, etc⁴. Sin embargo, el ládano es neurotóxico, hepatotóxico, nefrotóxico, e inhibe la relajación muscular⁵ por lo que su administración oral no es recomendada.

En la actualidad, el uso que se le da al ládano es principalmente industrial, especialmente en perfumería, donde una vez refinada la resina, se utiliza para fijar y dar olor a las pinturas, siendo España la principal exportadora de esta esencia. La madera de *Cistus ladanifer*, por ser durísima se usa en la fabricación de pequeñas herramientas o piezas que vayan a sufrir gran rozamiento, y también como excelente leña.

Sin embargo, aunque su resina ha sido muy estudiada⁶, muy poco se conoce de su perfil polifenólico.

2.1.3. *Cistus populifolius*.

Cistus populifolius (jara macho, jarón, jara cervuna) (Figura 3) se caracteriza por ser un arbusto recto de hasta 1.5 metros de altura de tallos rojizos. Sus hojas son aovadas, de forma acorazonada y estrechadas en la punta, simples, opuestas y de largo peciolo, rugosas, glabrescentes y muy grandes. Sus flores blancas son solitarias o en cimbras paucifloras y presentan 5 sépalos rojizos, de forma acorazonada, envolviendo los 2 de los extremos a los demás. El fruto es una cápsula ovoide, subpentagonal, que se abre en 5 valvas repletas de pequeñas semillas.



Figura 3. *C. populifolius*. Superior: detalle de las flores; inferior: detalle del fruto.

Su hábitat suele ser muy similar al de *C. ladanifer*, aunque al ser una planta menos heliófila, suele encontrarse preferentemente en zonas frescas y de umbría.

Cistus populifolius ha sido ampliamente utilizado en la medicina popular debido a sus propiedades antiinflamatorias, antiespasmódicas, cicatrizantes antimicrobianas, antiulcerogénicas, y vasodilatadoras⁷⁻⁹. Aunque se haya estudiado la bioactividad del extracto acuoso de *C. populifolius*, poco se conoce de su perfil polifenólico.

2.1.4. Otras especies del género *Cistus*.

Cistus salviifolius (jara negra, estepa negra, jaguarzo morisco) (Figura 4, superior izquierda) es un arbusto de hasta 1 metro de altura con corteza grisácea o negruzca. Sus hojas presentan pelos tanto por el haz como por el envés, y sus flores son de color blanco con la base de los pétalos amarillenta. Su hábitat se extiende por suelos arenosos, rocosos, silíceos y arcillosos, formando parte en pinares, alcornoques y encinares. Se adapta bien a condiciones xéricas. A esta especie vegetal se le atribuyen propiedades astringentes, cicatrizantes, antioxidantes^{10,11} e hipoglicémicas¹². Aunque el extracto hidroalcohólico de esta especie se ha caracterizado^{13,14}, nada se conoce de la fracción polifenólica de un extracto acuoso.

Cistus clusii (romero macho, jaguarzo) (Figura 4, superior centro) es un arbusto de hasta 1 metro de altura que en su estado vegetativo puede confundirse con el romero. Sus hojas son opuestas, brillantes por el haz y blanco tomentosas por el envés. Sus



inflorescencias son umbeliformes con hasta 8 pequeñas flores de color blanco. Su hábitat se da por suelos calizos (aunque puede encontrarse incluso en suelos arenosos y yesosos) aguantando bien el calor y la sequía. Forma parte de zonas con pino carrasco y encinas. Tradicionalmente se ha utilizado como antiinflamatorio¹⁵ y contra la caída del cabello¹⁶. Sin embargo, apenas existen datos sobre los compuestos fenólicos de *C. clusii*.

Cistus laurifolius (jara o estepa de montaña) (Figura 4, superior derecha) es un arbusto de hasta 2 metros de altura, con corteza de color grisáceo. Sus hojas tienen forma oval-lanceoladas de haz verde oscuro y envés blanco tomentoso. Sus flores se reúnen en inflorescencias cimosas umbeliformes de hasta 9 flores de color blanco y base amarilla. Su fruto globoso se abre en 5 valvas. Suele crecer en pinares, encinares, robledales y estepas. Tradicionalmente se le han atribuido propiedades antiinflamatorias y antinociceptivas¹⁷. El perfil polifenólico de *C. laurifolius* se conoce desde hace algunos años¹⁸.

Cistus monspeliensis (estepa negra, jara de Montpellier) (Figura 4, centro izquierda) se caracteriza por ser una especie subarborescente, de hasta 1.5 metros de altura. Sus hojas son estrechas, opuestas y sésiles, de un color verde intenso por el haz y más pálido por el envés hirsuto. Las hojas son muy pegajosas y con un fuerte olor debido al ládano que exuda. Sus flores de color blanco suelen ser solitarias o en grupos de 8-10. Su hábitat se da preferentemente por suelos silíceos, aunque es poco exigente en cuanto al tipo de suelo. Crece en climas cálidos y aguanta bien las solanas, pero no resiste las heladas. Actualmente se utiliza en jardinería ornamental y en repoblaciones forestales. Recientemente se ha descubierto su actividad antiproliferativa en la hipertrofia prostática benigna¹⁹. Sobre su perfil polifenólico se conoce únicamente su composición en catequinas²⁰.

Cistus libanotis (jara del Líbano, romerina) (Figura 4, centro derecha) es un arbusto de hasta 1 metro de altura. Sus hojas son estrechas, lampiñas y verde oscuras por el haz y

con pelos en el envés. Sus flores son blancas con una mancha amarilla en la base y largamente pedunculadas. Su fruto es una cápsula globosa de seis valvas. Su hábitat se extiende por suelos arenosos costeros bajo pinares. Ni sobre sus aplicaciones medicinales ni sobre su composición polifenólica existen referencias actualmente.

Cistus albidus (jara blanca, estepilla) (Figura 4, inferior izquierda) es un arbusto de hasta 0.15 metros de altura y de corteza grisácea. Sus hojas son opuestas y sésiles, ovaladas y planas, con muchos pelos estrellados tanto por el haz como por el envés. Sus flores son terminales agrupadas, de color rosado purpúreo. El fruto es una cápsula enteramente pelosa dehiscente en cinco valvas. Su hábitat se extiende por suelos preferentemente calizos, aunque también por otros tipos como los arenosos y muy pobres. Soporta muy bien las sequías y suele encontrarse en encinares y otros bosques mediterráneos. Tradicionalmente se ha utilizado *C. albidus* para combatir el dolor de estómago, en

contracturas y neuralgias.

Recientemente se ha realizado un estudio sobre su capacidad antioxidante y su actividad inhibidora de la proliferación celular *in vitro*²¹. Sobre su perfil polifenólico, sólo se conoce de forma parcial las proantocianidinas oligoméricas que presenta²².



Figura 4. Diferentes especies del género *Cistus*. Superior izquierda: *C. salviifolius*; superior centro: *C. clusii*; superior derecha: *C. laurifolius*; centro izquierda: *C. monspeliensis*; centro derecha: *C. libanotis*; inferior izquierda: *C. albidus*; inferior centro: *C. incanus*; inferior derecha: *C. crispus*.

Cistus incanus (jara gris) (Figura 4, inferior centro) es un arbusto de hasta 1 metro de altura y recubierto de pelos. Sus hojas son pequeñas, ovaladas, de bordes ondulados y cubiertas por pelos grisáceos. Sus



flores son de un color rosa púrpura con pétalos arrugados y crecen agrupadas de forma terminal. Esta planta crece sobre suelos secos y calcáreos. A *C. incanus* se le han atribuido efectos antibacterianos y antifúngicos²³, citotóxicos²⁴, anticancerígenos¹⁹, antiinflamatorios²⁵, gastroprotectores²⁶ y antivirales²⁷. Existen varios estudios en los que se han caracterizado la fracción fenólica de esta planta^{13,28,29}.

Cistus crispus (jara rizada) (Figura 4, inferior derecha) es un arbusto postrado de hasta 0.6 metros de altura. Sus hojas son pelosas, sésiles, con los márgenes rizados, haz verde rugoso y el envés más claro. Las flores son de color púrpura, cortamente pecioladas, que aparecen solitarias o en grupos. Su hábitat se encuentra en alcornocales, encinares, pinares, jarales y brezales. Puede aparecer sobre suelos pedregosos o incluso arcillosos. No tiene usos tradicionales atribuidos y todavía no se conoce nada respecto a su perfil polifenólico.

2.2. *Olea europaea* y aceite de oliva virgen extra.

El olivo (*Olea europaea* L.) es un árbol perennifolio que puede alcanzar hasta los 15 metros de altura, con un tronco estriado en canal y cuyas hojas coriáceas y lanceoladas son de color verde oscuro por el haz y verde grisáceo por el envés, glabras, de márgenes lisos y pedúnculo corto. Sus flores son bisexuales o polígamas y el fruto, la aceituna, es una drupa succulenta globosa muy aceitosa, del que se obtiene el aceite de oliva. Actualmente se cultiva en todos los países de la cuenca Mediterránea, especialmente en el centro y el sur de España e Italia, y en Grecia, Turquía, Túnez y Marruecos entre otros. España es el principal productor de aceite de oliva con un 40 % de la producción mundial.

La dieta mediterránea engloba los hábitos alimenticios típicos de algunas regiones mediterráneas, tales como España, Creta, Grecia e Italia. En los años 60 se descubrió que la esperanza de vida de estas poblaciones era más alta en comparación con la del resto

del mundo, mientras que las tasas de enfermedad coronaria, algunos tipos de cáncer y otras enfermedades crónicas directamente relacionadas con la dieta eran más bajas. Al estudiar los hábitos alimenticios de las distintas poblaciones se comprobó que la alimentación de los países del Mediterráneo, compuesta por verduras, hortalizas, legumbres, frutas, pescado, aceite de oliva y vino, podía ser la condicionante de las reducidas cifras de colesterol que presentaban los mediterráneos cuando eran comparados con los habitantes de América del Norte, anglosajones y centroeuropeos, quienes consumían una dieta con mayor contenido calórico, basada en grasas y proteínas de origen animal, productos lácteos y dulces que cocinaban con mantequilla o derivados. Como consecuencia de este hecho y de las conclusiones del estudio se acuñó el término de Dieta Mediterránea como dieta saludable, especialmente por su efecto beneficioso sobre las enfermedades cardiovasculares, ya que disminuye los niveles de colesterol en sangre y reduce la presión arterial, previniendo así de la presencia de coágulos de sangre, y protegiendo contra los radicales libres.



Figura 5. Aceitunas (fruto de *Olea europaea*) y aceite de oliva obtenido de éstas.

El aceite de oliva (Figura 5) es un elemento clave en la dieta mediterránea. Su composición varía en función de múltiples factores, tales como la variedad de aceituna, la exposición solar, la localización geográfica, las características del olivar, la forma de extracción y la conservación del aceite³⁰⁻³².

En general pueden distinguirse dos fracciones en la composición del aceite de oliva virgen: una saponificable y otra insaponificable.



La fracción saponificable representa entre el 98.5% y el 99.5% del peso del aceite de oliva. Los ácidos grasos del aceite de oliva son básicamente monoinsaturados, como el ácido oleico que representa entre el 60-80 % del total de ácidos grasos. También podemos encontrar ácidos grasos saturados (13-20%), fundamentalmente palmítico (11-17%) y esteárico, y ácidos grasos poliinsaturados entre los que se encuentran los ácidos grasos esenciales linoleico (4-20%) y linolénico (0.9%).

La fracción insaponificable, también denominados componentes minoritarios, constituye entre el 0.5 y el 1.5% de los aceites y. Esta fracción es, en parte, la responsable de la estabilidad oxidativa y las características organolépticas excepcionales de estos aceites. Los componentes minoritarios de los aceites vegetales se eliminan mayoritariamente durante los procesos de refinación. Es por ello que el aceite de oliva virgen, al ser obtenido únicamente mediante los procesos de lavado, prensado, centrifugación y filtración, conserva todos estos componentes. Este grupo de compuestos incluye a los hidrocarburos, esteroides, tocoferoles, pigmentos, alcoholes grasos, compuestos volátiles y aromáticos y compuestos fenólicos.

Son las propiedades antioxidantes y bioactivas de los polifenoles del aceite de oliva las que han estimulado numerosas investigaciones para establecer el perfil de estos compuestos. En el aceite de oliva se han descrito compuestos pertenecientes al grupo de los alcoholes fenólicos, incluyendo hidroxitirosol y tirosol, ácidos cinámicos como el cumárico, cafeico, ferúlico y sinápico, lignanos (pinoresinol y derivados), flavonas (luteolina y apigenina), flavonoles y ácidos benzoicos entre los que encontramos los ácidos gálico, sirínico, vanílico, etcétera. Pero los compuestos mayoritarios son los secoiridoides como las agliconas de la oleuropeína y del ligustrósido, definidos como ésteres heterosídico del ácido elenólico con el hidroxitirosol o el tirosol respectivamente, así como sus formas dialdehídicas^{33,34}.



La dieta mediterránea y especialmente el aceite de oliva han demostrado diversos efectos beneficiosos en el organismo, como la disminución del riesgo de padecer enfermedades cardiovasculares³⁵, la reducción del LDL-colesterol en sangre³⁶⁻³⁸, la prevención de la aterosclerosis^{35,39}, disminución de la hipertensión^{40,41}, mejora de la obesidad^{40,41}, diabetes tipo 2^{40,42}, síndrome metabólico y alzheimer⁴³, potente antioxidante y antiinflamatorio^{37,42,44}, y anticancerígeno (especialmente en cáncer de mama, colorectal y de próstata)⁴⁵⁻⁴⁸.

2.3. *Hibiscus sabdariffa*.

Hibiscus sabdariffa (Orden *Malvales*, Familia *Malvaceae*) (Figura 6) comúnmente conocida como flor de Jamaica, rosella y en árabe como karkade, crece mayoritariamente en África Central y occidental, y en el sur y este de Asia. Forma un género amplio de alrededor de 220 especies. El género *Hibiscus* incluye plantas anuales o



Figura 6. *H. sabdariffa*, detalle de las flores.

perennes desde pequeños arbustos a pequeños árboles. Las hojas son alternas y simples y las flores son largas, conspicuas, con forma de trompeta, con cinco pétalos, de tonos rojos o morados. La planta se usa mundialmente como bebida refrescante o como infusión. Estos extractos se han usado tradicionalmente en medicina popular⁴⁹ en aplicaciones que incluyen el tratamiento de

la hipertensión⁵⁰⁻⁵², enfermedades hepáticas⁵³⁻⁵⁵, y como antioxidante⁵⁶⁻⁶⁰, antimicrobiano^{61,62}, antiinflamatorio⁶³⁻⁶⁶, neuroprotector^{58,67}, antimutagénico^{68,69} y anticancerígeno⁷⁰⁻⁷². Sin embargo, el principal uso que se le da a *Hibiscus sabdariffa* es su actividad hipolipemiante e hipocolesterolemica^{54,73-77}, combatiendo la obesidad y protegiendo de esta manera, junto con sus otras actividades, el padecer enfermedades



coronarias o relacionadas con éstas^{78,79}. Es una variedad de té que apenas contiene sustancias excitantes, por lo que su ingesta es muy recomendable en todo tipo de personas. El alto contenido del té de hibisco en flavonoides es lo que le dota de estas todas estas actividades.

Una de las ventajas industriales de esta planta es su rápida reproducción y la simplicidad y bajo coste para la obtención del extracto. El color rojo característico se debe a los antocianos, delfinidina-3-O-sambubiósido y cianidina-3-O-sambubiósido entre otras. Las antocianinas que contiene son usadas como colorantes naturales en comidas⁸⁰. La composición química de *Hibiscus sabdariffa* se conoce relativamente. Ensayos con TLC y HPLC han revelado la presencia de quercetina, luteolina y sus glicósidos, ácido clorogénico, gopipetin, hibiscetin y sus glicósidos, fenoles y ácidos fenólicos (ácido protocatecuico y pelargonidínico), eugenol y los esteroides β -sitosterol y ergosterol entre otros⁸¹⁻⁸³. Además, el ácido hidroxícitrico y su lactona son dos importantes componentes de esta planta⁸⁴.

3. POLIFENOLES: BIOSÍNTESIS Y CARACTERÍSTICAS.

Los productos naturales constituyen hoy día una fuente prolífica de compuestos bioactivos para el desarrollo de nuevos medicamentos o como preventivos de diversas enfermedades. Debido a su gran diversidad estructural, estos compuestos representan una fuente complementaria imprescindible frente a los compuestos sintetizados en los laboratorios. Sin embargo, los grandes cambios que han tenido lugar en el proceso de descubrimiento de nuevos medicamentos en la última década han introducido nuevos requerimientos en el campo de la investigación de los productos naturales. Las aproximaciones clásicas han dado lugar a conceptos y aproximaciones más modernas. Las nuevas tendencias van encaminadas a la necesidad de identificar el candidato más



prometedor de una mezcla compleja y acelerar el proceso de purificación y evaluación de ese candidato⁸⁵.

Estas tendencias van dirigidas a la aplicación de bioensayos de los extractos crudos para identificar aquellos que podrían contener compuestos bioactivos que puedan ser luego fraccionados y aislados de una forma biodirigida. Convencionalmente este proceso incluye la extracción de cantidades significativas de la fuente vegetal, seguido por el uso de técnicas separativas como la cromatografía para identificar y caracterizar los compuestos, utilizando para ello diferentes sistemas de detección como pueden ser UV-Vis, IR, MS o RMN.

Los compuestos fenólicos o polifenoles constituyen uno de los principales grupos de metabolitos secundarios con una gran diversidad de estructuras y funciones, pero generalmente constan de un anillo aromático con uno o más sustituyentes hidroxilo. Se consideran metabolitos secundarios de las plantas aquellos compuestos que no son esenciales para su supervivencia en su conjunto o de alguna de sus partes⁸⁶. Los compuestos fenólicos o polifenoles constituyen uno de los grupos de sustancias más numerosos y ampliamente distribuidos en el reino vegetal, con más de 8000 estructuras fenólicas conocidas actualmente. Entre las principales familias de compuestos fenólicos podemos encontrar los fenoles simples, benzoquinonas, ácidos fenólicos, ácidos fenilacéticos, acetofenonas, ácidos hidroxicinámicos, fenilpropenos, cumarinas, cromonas, naftoquinonas, xantonas, estilbenos, antraquinonas, flavonoides, lignanos, ligninos y taninos hidrosolubles (Figura 7).

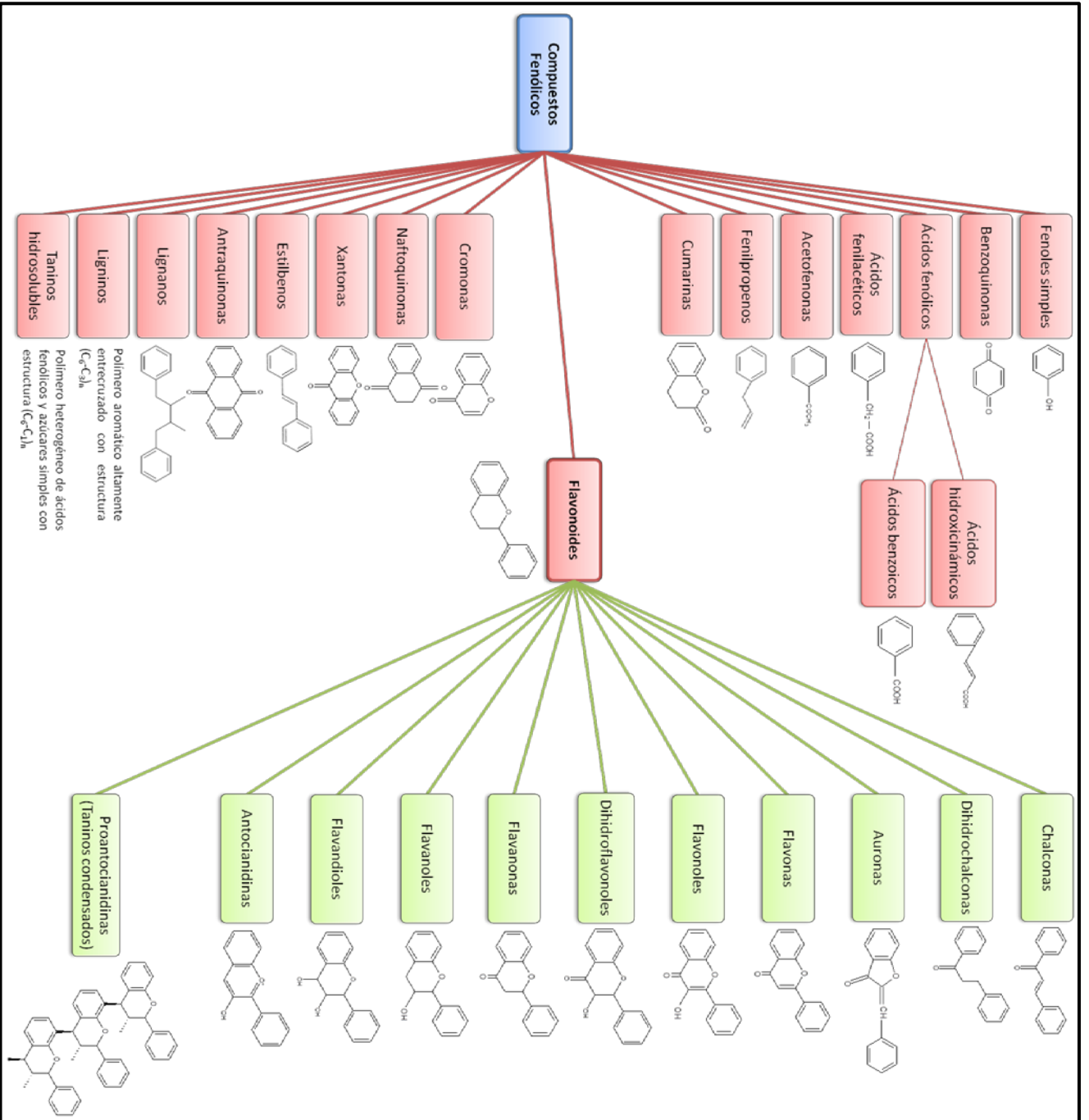


Figura 7. Principales familias de compuestos fenólicos y clases de flavonoides con los esqueletos básicos de cada una de ellas.



Los flavonoides, cuyo esqueleto básico es del tipo C6-C3-C6, constituyen la familia más importante y ampliamente distribuida en la naturaleza, y a su vez se puede subdividir en distintas clases: chalconas, dihidrochalconas, auronas, flavonas, flavonoles, dihidroflavonoles, flavanonas, flavanoles, flavandioles (leucoantocianidinas), antocianidinas y proantocianidinas (taninos condensados) (Figura 7).

Los compuestos fenólicos surgen de dos principales rutas metabólicas: la ruta del ácido shikímico y la ruta del acetato (Figura 8) y se generan durante el desarrollo normal de la planta aunque el contenido en algunos de ellos puede incrementarse bajo condiciones de estrés como radiación UV, infección por patógenos y parásitos, polución del aire y exposición a temperaturas extremas, o disminuir por acción de las enzimas polifenoloxidasas (PPOs) ante daño celular tanto por causas físicas como infecciosas. El nivel de compuestos fenólicos en vegetales también se ve afectado por otros factores como tipo y técnicas de cultivo, condiciones de crecimiento, proceso de maduración, así como condiciones de procesado y almacenamiento.

En los alimentos derivados de fuentes vegetales, los compuestos fenólicos están íntimamente relacionados con sus cualidades sensoriales y nutricionales, de forma que pueden contribuir al amargor, astringencia, color, flavor, olor y estabilidad oxidativa del alimento⁸⁷. Otra característica esencial de los polifenoles es su habilidad para interactuar con proteínas, lo cual es responsable de la percepción de astringencia que resulta de la interacción de los taninos con las proteínas salivares, por formación de precipitados e inhibición de ciertas enzimas, reduciendo la digestión de las proteínas de la dieta.

Además, diversos estudios han demostrado que los compuestos fenólicos exhiben un amplio rango de propiedades fisiológicas, como antialérgicas⁸⁸, antiaterogénicas^{39,89,90}, antiinflamatorias^{89,91}, antimicrobianas⁹², antioxidantes^{90,93} y cardioprotectoras⁹⁴ y anticancerígenas entre otras.



Esta demostrada bioactividad de los polifenoles los convierte en importantes compuestos funcionales y por tanto, es de gran interés su determinación en matrices tanto vegetales como biológicas.

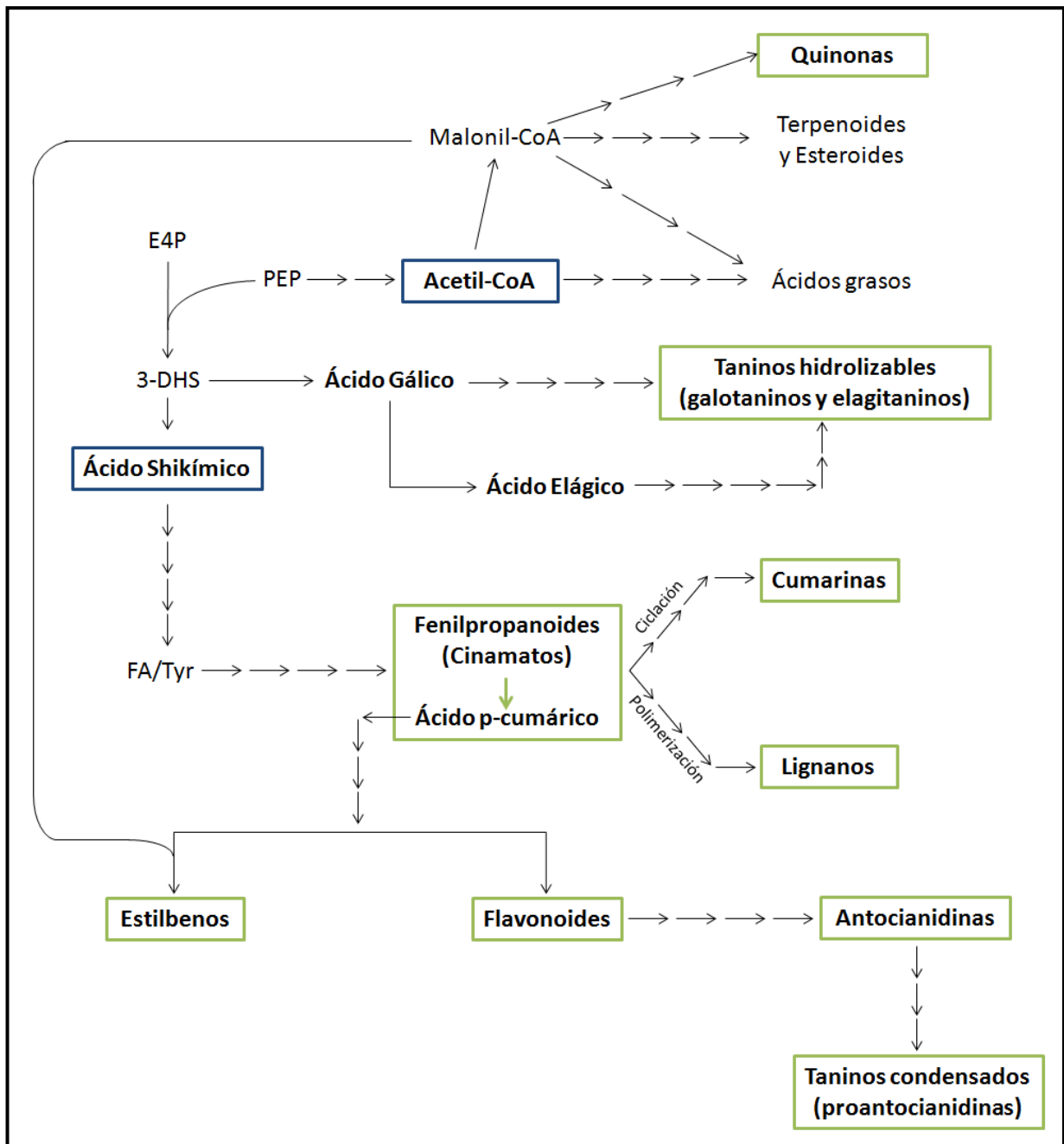


Figura 8. Biosíntesis simplificada de los compuestos fenólicos siguiendo las rutas del ácido shikímico y del acetato. Abreviaturas: E4P, eritrosa-4-fosfato; PEP, ácido fosfoenolpirúvico; CoA, coenzima A; 3-DHS, ácido 3-dehidroshikímico; FA, fenilalanina; Tyr, tirosina.



4. POLIFENOLES Y BIOACTIVIDAD.

En los últimos años se ha dado un aumento en el interés de identificar fitoquímicos o compuestos vegetales que tienen efectos positivos en la salud, los cuales han cubierto una amplia área de investigación, que incluye, entre otros, estudios sobre la actividad antioxidante, anticancerígena, la disminución de obesidad, del colesterol y de enfermedades cardiovasculares relacionadas. Con frecuencia, el éxito de la caracterización de un fitoquímico puede conducir al desarrollo de nuevos alimentos o suplementos con actividades que favorecen a la salud. Durante las últimas décadas, estos alimentos han sido denominados alimentos funcionales, que son generalmente aceptados como aquellos que contienen, de forma natural y más allá de sus nutrientes básicos, cualidades beneficiosas para la salud.

4.1. Infección bacteriana y polifenoles.

La infección se define como la colonización de un organismo huésped por especies patógenas comprometiendo el correcto funcionamiento y supervivencia del huésped. La infección puede ser localizada cuando afecta a una parte del organismo o generalizada cuando se extiende por todo el cuerpo.

Los factores que afectan a la aparición y desarrollo de un proceso infeccioso son, entre otros, la ruta de entrada del organismo patógeno, la carga bacteriana, el periodo de incubación, la virulencia intrínseca y toxicidad del patógeno, el poder invasivo y el estado inmune del huésped.

Estas bacterias infecciosas se van a reproducir rápidamente en el organismo huésped excretando toxinas que dañen los tejidos y produciendo una afluencia de glóbulos



blancos (neutrófilos) que fagocitarán a estos microorganismos agresores y comenzando así un proceso inflamatorio asociado a la infección.

Es interesante estudiar las propiedades antibacterianas de las plantas para ayudar a combatir o frenar estas infecciones combinadas o no con los tratamientos típicos basados en antibióticos y por ello numerosos estudios se han llevado a cabo en este campo con multitud de matrices vegetales^{92,95}.

4.2. Cáncer y polifenoles.

El cáncer comprende un grupo de enfermedades caracterizadas por la proliferación autónoma de células neoplásicas que tienen varias alteraciones, incluyendo mutaciones e inestabilidad genética.

Según la OMS, el cáncer es una de las principales causas de muerte a nivel mundial, atribuyéndole alrededor de un 15 % del total de defunciones, situándose a la cabeza los cánceres de pulmón, estómago, hígado, colorrectal y de mama⁹⁶.

El cáncer se desarrolla a partir de alteraciones genéticas y epigenéticas que permiten a las células sobrevivir, replicarse y evadir mecanismos reguladores de apoptosis, de la proliferación y del ciclo celular⁹⁷.

El ciclo celular se define como el intervalo entre cada división celular y comprende cuatro fases estrictamente reguladas: fase G1, S, G2 y M. En la fase S (de síntesis) el material genético se duplica, en la fase M (mitosis/meiosis) la célula se divide, y entre ambas fases se encuentran las fases G1 y G2 en las que la célula se detiene para crecer lo necesario antes de continuar la división. Existe una fase denominada G0 en la cual las células están



en un estado quiescente sin dividirse. Los factores que regulan la salida de G0 y entrada en G1 son cruciales para determinar la frecuencia del crecimiento⁹⁸.

Entre cada una de las fases del ciclo celular encontramos puntos de control con los que asegurar la correcta duplicación del ADN y la corrección de errores que se hayan podido producir durante su replicación. Se necesita de la acción de proteínas específicas para que la célula pueda superar esos puntos de control y asegurar una correcta división celular (Figura 9).

Entre estas proteínas encontramos la familia de las ciclinas dependientes de kinasas (cdk)⁹⁹, que comprende 11 proteínas diferentes. Las ciclinas, proteínas diana de la fosforilación de las cdk, son sintetizadas durante la interfase y son destruidas abruptamente al final de la mitosis. Actualmente se conocen seis familias de ciclinas en mamíferos, y se clasifican según el punto de control del ciclo celular donde ejercen su función. Las ciclinas más importantes en el ciclo celular son las ciclinas A, B, D y E¹⁰⁰ (Figura 9).

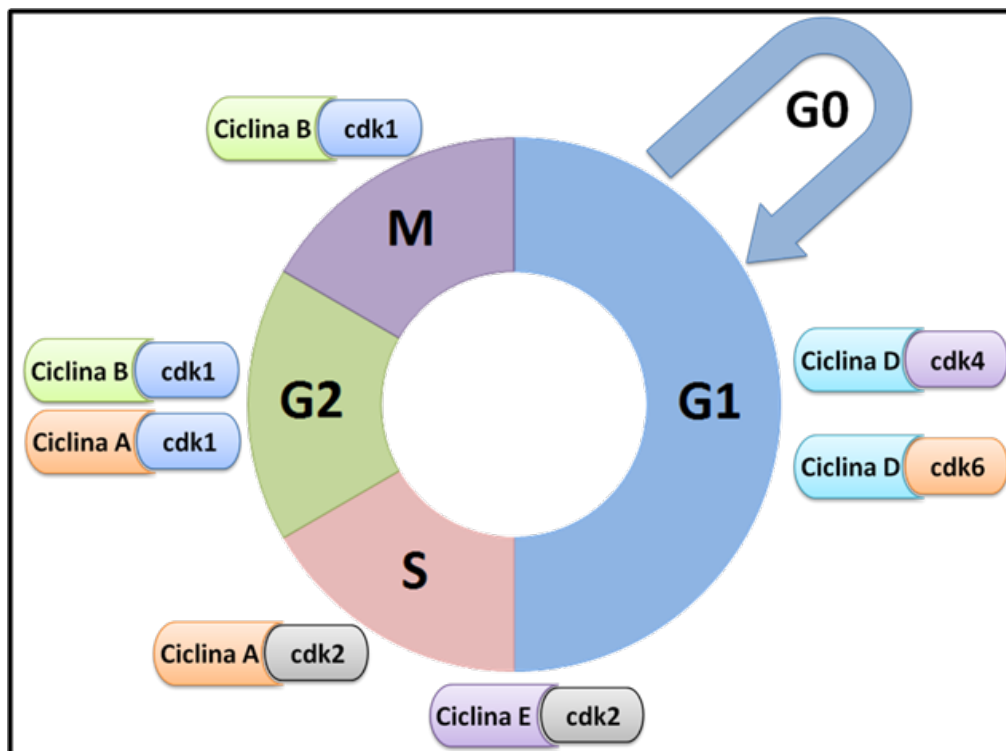


Figura 9. Esquema simplificado del control por parte de las ciclinas y las kinasas dependientes de ciclina (cdk) en el ciclo celular.



Existen ciertas proteínas que actúan como “centinelas” del ciclo celular, como es el caso de la proteína p53, que detiene el ciclo celular en G1/S ó G2/M ante un daño en el ADN y activa enzimas reparadoras de este daño como son las proteínas de la familia GADD45 (growth arrest and DNA damage). Si el daño en el ADN es reparado, p53 se degrada y permite a la célula continuar con un ciclo celular normal. En el caso contrario, la célula entra en apoptosis y muere^{101,102}.

Las histonas H2AX también tienen un papel importante en el ciclo celular. La fosforilación de esta histona (γ -H2AX) indica un daño en el ADN localizado, deteniendo el ciclo celular hasta que se repare el ADN^{103,104}. Por otro lado, las acetiltransferasas (HAT) y desacetilasas (HDAC) de histonas son las encargadas de introducir o eliminar grupos acetilo en residuos de lisina de las histonas. La presencia de grupos acetilo en estas proteínas hará más fuerte su unión con el ADN y, por tanto, aumentarán la condensación de éste, impidiendo que se desempaquete. Esta acetilación/desacetilación de las histonas es crucial en la regulación de la transcripción génica, permitiendo o impidiendo que la cromatina esté accesible a las proteínas encargadas de transcribir el ARN mensajero. La hiperacetilación de las histonas (ya sea por activación de las HAT o inhibición de las HDAC) provoca la parada del ciclo celular por impedir la expresión de genes implicados en la proliferación y el reclutamiento de varios factores que promueven la expresión de genes supresores de tumores^{105,106}.

Otras proteínas implicadas merecen atención por estar en puntos clave de varias vías de señalización. Entre ellas encontramos la AKT1 (PKB, protein kinase B), implicada en el ciclo celular y parada en G1 o G2 si esta proteína está fosforilada¹⁰⁷; MEK1 (MAP2K1, mitogen-activated protein kinase kinase 1) y Stat3 (signal transducer and activator of transcription 3) que pueden promover un aumento de la proliferación o la apoptosis según su grado de activación^{108,109}; NF- κ B (nuclear factor kappa-light-chain-enhancer of activated B cells) es un factor transcripcional de respuesta rápida formado por dos subunidades, p65/p50, implicado, al igual que las demás, en la proliferación celular y entrada en apoptosis si la

subunidad p65 se encuentra fosforilada¹¹⁰; por último, MAPK/p38 (mitogen-activated protein kinase de 38 KDa) interviene en la regulación de la apoptosis y en la parada del ciclo celular, induce la diferenciación celular y la producción de citoquinas en la inflamación¹¹¹.

4.2.1. Cáncer de mama.

El cáncer de mama (Figura 10) es el tipo de cáncer más frecuente en las mujeres occidentales. Representa alrededor del 30% de todos los tumores, y aproximadamente el 20% de todas las muertes relacionadas con esta enfermedad. En España, el cáncer de mama ha pasado a constituir en las últimas décadas un problema sanitario de primera magnitud.

Cada año se diagnostican más de 15.000 nuevos casos en nuestro país, lo cual supone un aumento de la incidencia de un 3% anual desde los años ochenta. Aún así, los datos de prevalencia de cáncer de mama para los países de la Unión Europea ponen de manifiesto

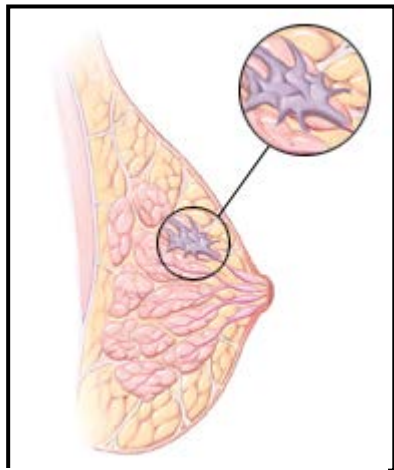


Figura 10. Carcinoma lobular de mama.

cierta distribución heterogénea, en países como Italia, Grecia, Portugal y España, y en general los países localizados en la franja mediterránea, presentan un número de casos de cáncer de mama significativamente menor que el resto de países integrantes de la Unión Europea (con reducciones de hasta el 25% en el riesgo de padecer cáncer de mama cuando se comparan mujeres que consumen grandes cantidades de aceite de oliva virgen con aquéllas que consumen otro tipo de aceite o grasa).

Muchos de los tumores de mama presentan una particularidad que los distingue de la mayoría de los otros tumores: la hormonodependencia de estrógenos para su desarrollo y crecimiento¹¹²⁻¹¹⁴. El tejido mamario requiere del aporte de estrógenos para su



crecimiento, y en consecuencia, los tumores originados a partir de este tejido van a conservar la dependencia de los estrógenos para su proliferación. Los tumores que se encuentran en este estadio son tratados en la mayoría de las ocasiones mediante terapias antiestrogénicas las cuales son, en un principio, capaces de controlar el crecimiento del tumor en un gran número de casos.

Sin embargo, en muchos de los casos, la hormonodependencia del tumor se pierde, las células cancerosas sufren una serie de transformaciones adicionales que las vuelven hormonoindependientes¹¹² y las hace capaces de crecer en ausencia de estrógenos. En este nuevo estadio, los tumores presentan un peor pronóstico, ya que la adquisición de la independencia a estrógenos se acompaña de un aumento en la agresividad del tumor, lo que provoca la utilización de tratamientos más agresivos (quimioterapia y radioterapia)^{112,113,115}.

El receptor de estrógenos (RE) es el principal encargado de recibir los estímulos estrogénicos y convertirlos en una respuesta que implique la proliferación de las células; por tanto, en cualquier alteración de la respuesta a los estímulos estrogénicos, forzosamente debe estar implicado el receptor de estrógenos. El RE es un receptor nuclear que a su vez actúa como un factor de transcripción que controla la expresión de un determinado número de genes, en su mayoría relacionados con la proliferación¹¹⁶. Las células RE positivas pueden tratarse con antiestrogénicos (como el Tamoxifeno), siendo estos tumores los que presentan un mejor pronóstico.

Otro receptor que aparece mutado en aproximadamente un 30 % de los casos es el receptor ErbB2 (HER2), asociado a la activación de la proliferación celular. El cáncer de mama HER2 positivo se trata actualmente con anticuerpos anti-HER2 (Trastuzumab), aunque el pronóstico de este tipo de cánceres tiene un peor pronóstico.



Sin embargo, y como se ha dicho anteriormente, los tumores RE positivos pueden perder su hormonodependencia, al igual que los HER2 positivos pueden insensibilizarse al tratamiento con anticuerpos, siendo, en este último caso, tumores con un tratamiento especialmente complicado y desfavorable.

Es por esto último que cada vez más se buscan tratamientos alternativos para el cáncer de mama, en especial en los casos más complicados de la enfermedad. En las últimas dos décadas son numerosos los estudios que se han realizado al respecto. Desde el año 1995 ha cobrado principal relevancia el estudio del té verde en diferentes líneas celulares de cáncer de mama¹¹⁷⁻¹²⁰, animales de experimentación^{117,121} y estudios epidemiológicos en la población femenina^{122,123}. Todos estos estudios ponen de manifiesto el importante papel que juega la epigalocatequina galato (EGCG) extraída de ésta matriz vegetal. Sin embargo, no pueden descartarse sinergismos con otras moléculas o incluso con los medicamentos utilizados actualmente que potencien los efectos de este flavonoide^{120,124-126}.

También han sido objeto de estudio en el cáncer de mama los polifenoles del vino tinto^{127,128}, y de la granada^{129,130}. Del primero, parece ser el resveratrol el principal responsable de la bioactividad en este tipo de tumores¹³¹⁻¹³⁵. Sin embargo, como se ha comentado anteriormente, no se pueden descartar efectos sinérgicos que aumenten esta bioactividad antiproliferativa^{125,136,137}. En el caso de la granada, no está muy claro cuál podría ser el compuesto bioactivo responsable, aunque se sospecha del ácido elágico¹³⁸.

Otros muchos compuestos y extractos vegetales han sido utilizados en el tratamiento a nivel celular del cáncer de mama, como la curcumina^{123,139,140}, antocianos del arándano¹⁴¹, la genisteína de la soja¹⁴², y otros tipos de matrices que contienen polifenoles^{119,137,143-147}.



Sin embargo, en la última década, los polifenoles del aceite de oliva están cobrando una relevancia especial. Estos estudios empezaron comparando la clínica e histología de pacientes que consumían regularmente aceite de oliva con aquellas que tomaban otros aceites diferentes¹⁴⁸. El ácido oleico, ácido graso monoinsaturado característico del aceite de oliva, tuvo un buen resultado como coadyuvante del Trastuzumab en la terapia del cáncer de mama HER2 positivo¹⁴⁹ y formando complejos inhibitorios de la transcripción del gen PEA3, implicado en la proliferación de los tumores¹⁵⁰. Por otro lado, los polifenoles del aceite de oliva y en especial la oleuropeína aglicona han tenido excelentes resultados en el tratamiento de tumores HER2 positivos que han adquirido resistencia al Trastuzumab¹⁵¹. Además, estos polifenoles también son capaces de inhibir la autofosforilación del receptor HER2 (impidiendo su activación)⁴⁵ y promover su autodegradación en los proteosomas¹⁵², inhibir la sintasa de ácidos grasos (FAS) que está sobreexpresada en los tumores de mama HER2 positivos¹⁵³ e inhibir la proliferación celular de células RE positivas / HER2 negativas en la fase G1/S induciendo apoptosis¹⁵⁴ e interfiriendo en la activación de las MAP kinasas ERK1/2⁴⁶.

4.2.2. Cáncer de colon.

El cáncer de colon o cáncer colorectal (CCR) (Figura 11) es la segunda causa de muerte por cáncer, después del cáncer de pulmón en el hombre y de el de mama, en la mujer. Entre un 22% y un 36% de los casos, se presenta la enfermedad avanzada y, en estos casos, el índice de supervivencia es prácticamente de cero. En nuestro país se producen 11.000 nuevos casos por año y la mortalidad inducida por este cáncer es de 10 muertes por cada 100.000 habitantes¹⁵⁵.

Como factores de riesgo en el CCR se pueden señalar la existencia previa (en el individuo o en su familia) de poliposis adenomatosa, síndrome de Lynch, enfermedades inflamatorias del colon (enfermedad de Chron y colitis ulcerosa) y por último, factores de la dieta^{156,157}.



Figura 11. Evolución del adenocarcinoma colorectal.

El CCR puede dividirse en tres grupos: esporádicos (representando un 70% de los casos aproximadamente), hereditarios (con una incidencia menor del 10%) y familiar (con hasta un 25% de los casos).

Mutaciones en varios genes intervienen en la aparición de un CCR^{158,159}. En los casos en los que el CCR se hereda, se encuentra como responsable una mutación en el gen APC^{159,160}, que da lugar a una poliposis adenomatosa familiar y posteriormente a un CCR. Otros casos de CCR heredado se dan sin poliposis, y en ellos se encuentran mutados genes reparadores como el MSH2 y el MLH1¹⁶¹. Otro gen frecuentemente mutado es el oncogén *K-ras*^{162,163}, estimulándose el crecimiento de las células tumorales. En muchos casos también se ha visto mutado el gen supresor de tumores que codifica para la proteína p53^{164,165}.

Las investigaciones de los compuestos fenólicos en el tratamiento del CCR están llevándose a cabo desde hace veinte años, aunque sólo en los últimos siete años a cobrado especial interés. Los primeros estudios se realizaron con la quercetina¹⁶⁶ y los ácidos elálgico y clorogénico¹⁶⁷. Los estudios posteriores con el té verde también dieron buenos resultados¹⁶⁸, especialmente con la epigallocatequina galato^{169,170}. Además, otras matrices vegetales han sido utilizadas como antiproliferativas del CCR^{171,172}. Sin embargo, la quercetina ha sido el compuesto fenólico más estudiado en el cáncer de colon^{166,169,173-175}.

Cabe destacar la importancia del aceite de oliva en el tratamiento del CCR, pues numerosos estudios se han realizado siguen realizándose. El primer compuesto ensayado fue el hidroxitirosol extraído del aceite de oliva¹⁷⁶, el cual detenía el ciclo celular en fase



G1 e inducía apoptosis en las células cancerígenas. Los ensayos con el perfil fenólico completo del aceite de oliva dio como resultado efectos antimetastásicos^{177,178}, anticancerígenos^{179,180}, quimiopreventivos¹⁸¹, antiproliferativos y proapoptóticos¹⁸⁰, en algunos casos por inhibición de la sintasa de ácidos grasos (FAS)⁴⁷ e incluso mejorando la colitis ulcerosa asociada al CCR¹⁸². Varios estudios con compuestos fenólicos individuales presentes en el aceite de oliva han demostrado la gran actividad del hidroxitirosol como molécula antiproliferativa¹⁷⁶ ya que induce parada del ciclo celular mediante inhibición de las quinasas ERK1/2 y la ciclina D¹⁸³ y el pinosinol como molécula activadora de la proteína supresora de tumores p53^{184,185}. Todos estos datos, unidos a los buenos resultados con la quercetina (también presente en el aceite de oliva) hacen de esta matriz un buen candidato para profundizar en el tratamiento del CCR.

4.3. Envejecimiento y polifenoles.

Nuestro organismo, a consecuencia del transcurso de su metabolismo, produce radicales libres, agentes oxidantes que causan deterioro celular y tisular. Los efectos perjudiciales de los radicales libres son varios, desde daños en el ADN, peroxidación lipídica, alteración de proteínas y de reacciones enzimáticas, hasta daños en el tejido conjuntivo y daños tisulares asociados. Las células tienen mecanismos para eliminar estos radicales libres mediante enzimas antioxidantes, como la superóxido dismutasa (SOD) y la catalasa. Mientras que la primera se encarga de eliminar radicales superóxido (O_2^-), la segunda neutraliza el peróxido de hidrógeno (H_2O_2).

Sin embargo, el envejecimiento de las células es causado por muchos otros motivos. Entre ellos destacan los factores genéticos (acortamiento de los telómeros), hormonales, hábitos de vida, dieta, etc.

El mecanismo de diferenciación epitelial a mesenquimal (EMT, Epithelial-to-Mesenchymal Transition) (Figura 12) es un modelo idóneo para estudiar el efecto antienviejamiento de los polifenoles. Esta transición permite que las células epiteliales puedan convertirse en células migratorias, acción que está inhibida en un organismo adulto. Sin embargo, su reactivación está presente en enfermedades acompañadas de fibrosis o algunos tumores¹⁸⁶.

Esta transición ocurre cuando las células epiteliales pierden sus uniones célula-célula debido a la desaparición de las uniones adherentes formadas especialmente por E-cadherina (debido a la represión del gen que la codifica). Además, las células epiteliales pierden de esta forma su polaridad apico-basal, sufre cambios en su citoesqueleto, se desorganiza la membrana y finalmente se delaminan y migran. Esto es especialmente importante en las fases metastásicas del cáncer^{187,188}.

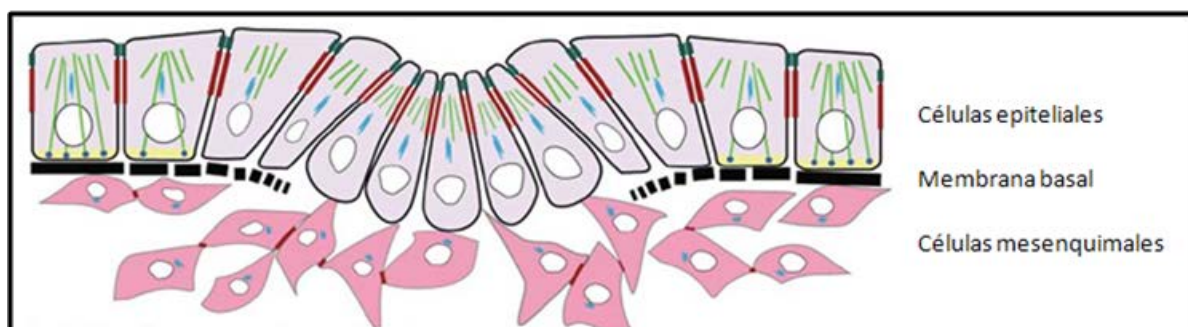


Figura 12. Esquema simplificado de la transición epitelial-mesenquimal.

La principal responsable de esta transición es la citoquina denominada factor de transformación del crecimiento β (TGF- β , transforming growth factor- β). La unión de esta citoquina a su receptor TGFBR crea una cascada de señalización donde se activan proteínas de la familia SMAD (transductoras de la señal del TGF- β) que se translocan al núcleo celular y se unen a cofactores transcripcionales de la familia SNAIL como SNAI2 (Slug), impidiendo la expresión del gen que codifica para la cadherina E y activando la transición celular hacia un fenotipo mesenquimal, produciéndose proteínas como la vimentina o la fibronectina. Estos eventos desembocan en una fibrosis excesiva



acompañada de producción de colágeno y de matriz extracelular en el órgano afectado^{189,190} y dotando a estas células propiedades invasivas.

Aunque existen numerosos estudios sobre el efecto de los polifenoles como compuestos antienviejimiento, son escasos los estudios comprobando este efecto en el modelo EMT, y principalmente están basados en el té verde y específicamente, en la EGCG¹⁹¹⁻¹⁹³.

4.4. Obesidad y Polifenoles.

La hiperlipidemia (o exceso de lípidos en sangre) se debe, en la mayoría de los casos, a una mutación en las lipoproteínas de baja densidad (LDL), bien por alteraciones en ellas mismas o por alteraciones en el receptor de las LDL. Malos hábitos en la dieta son la principal causa de hiperlipidemia, si bien existen factores genéticos heredados u otras enfermedades hormonales que pueden condicionarla. Aunque la hiperlipidemia en sí no puede considerarse una patología, sí es un desajuste metabólico que puede causar multitud de enfermedades, especialmente enfermedades cardiovasculares y obesidad.

La obesidad es una patología ampliamente extendida, de elevada prevalencia en los países industrializados (más de 1500 millones de adultos tienen sobrepeso, de los cuales más de un tercio son obesos), y se considera uno de los principales problemas de salud de la sociedad moderna¹⁹⁴.

La obesidad se define como un exceso de almacenamiento de energía en forma de grasa dentro de los adipocitos que forman el tejido adiposo, y por lo tanto se acompaña de un aumento en el tamaño de estas células (hipertrofia) y del número de éstas (hiperplasia). Esta enfermedad tiene un origen multifactorial, abarcando, entre otros, factores genéticos, neuroendocrinos, dieta, sedentarismo, y el uso de algunos fármacos (antidepresivos, anticonceptivos o glucocorticoides).



La leptina, un neuropéptido, es secretada por los adipocitos y actúa a nivel hipotalámico, controlando el apetito de tal forma que la leptinemia es reflejo de las reservas grasas del cuerpo. Una expresión elevada de leptina conyeva una hiperfagia que dará lugar a la obesidad.

Estudios *in vitro* sugieren que factores liberados localmente por los adipocitos hipertrofiados, como el factor de necrosis tumoral α (TNF- α) y el factor de crecimiento insulínico 1 (IGF-1) estimulan la hiperplasia¹⁹⁵ y por lo tanto favorecen la diferenciación de los preadipocitos a adipocitos maduros (Figura 13). Por otro lado, el receptor γ activador de la proliferación del peroxisoma (PPAR- γ) es uno de los receptores nucleares más importantes que estimula la hiperplasia del adipocito.

Como es lógico, para suministrar oxígeno y nutrientes al tejido adiposo en expansión, se incrementa el número y el tamaño de los vasos sanguíneos. En consecuencia, la fase inicial de la adipogénesis se vincula de manera pronunciada con la angiogénesis. El factor de crecimiento vascular endotelial (VEGF) liberado por los adipocitos en crecimiento es el principal mediador de esta angiogénesis¹⁹⁶.

Existen varias enfermedades y trastornos asociados con la obesidad, especialmente diabetes, cáncer, enfermedades cardiovasculares, hígado graso no alcohólico (NASH) e inflamación¹⁹⁷.

La relación de la obesidad y la inflamación (Figura 13) se pone de manifiesto al estudiar los niveles de expresión de adipoquinas como las interleuquinas (IL) 1 y 6, el TNF- α y la proteína quimioatrayente de monocitos 1 (MCP-1), todas ellas aumentadas en la obesidad. La elevada producción de estas proteínas va a potenciar el estado inflamatorio en el tejido adiposo favoreciendo la activación e infiltración de macrófagos maduros. De hecho, se ha observado que el incremento en la secreción de citoquinas como el TNF- α puede estimular a los preadipocitos y a las células endoteliales a producir MCP-1,



atrayendo a los macrófagos al tejido adiposo. Una vez infiltrados en el tejido adiposo, los macrófagos comienzan a secretar citoquinas y quimioquinas tales como TNF- α , IL-1, IL-6, y MCP-1. Este patrón de secreción, junto con el producido por adipocitos y otros tipos celulares, puede perpetuar un círculo vicioso de reclutamiento de macrófagos y producción de citoquinas inflamatorias, llevando a una inflamación primaria local en el tejido adiposo^{195,198}.

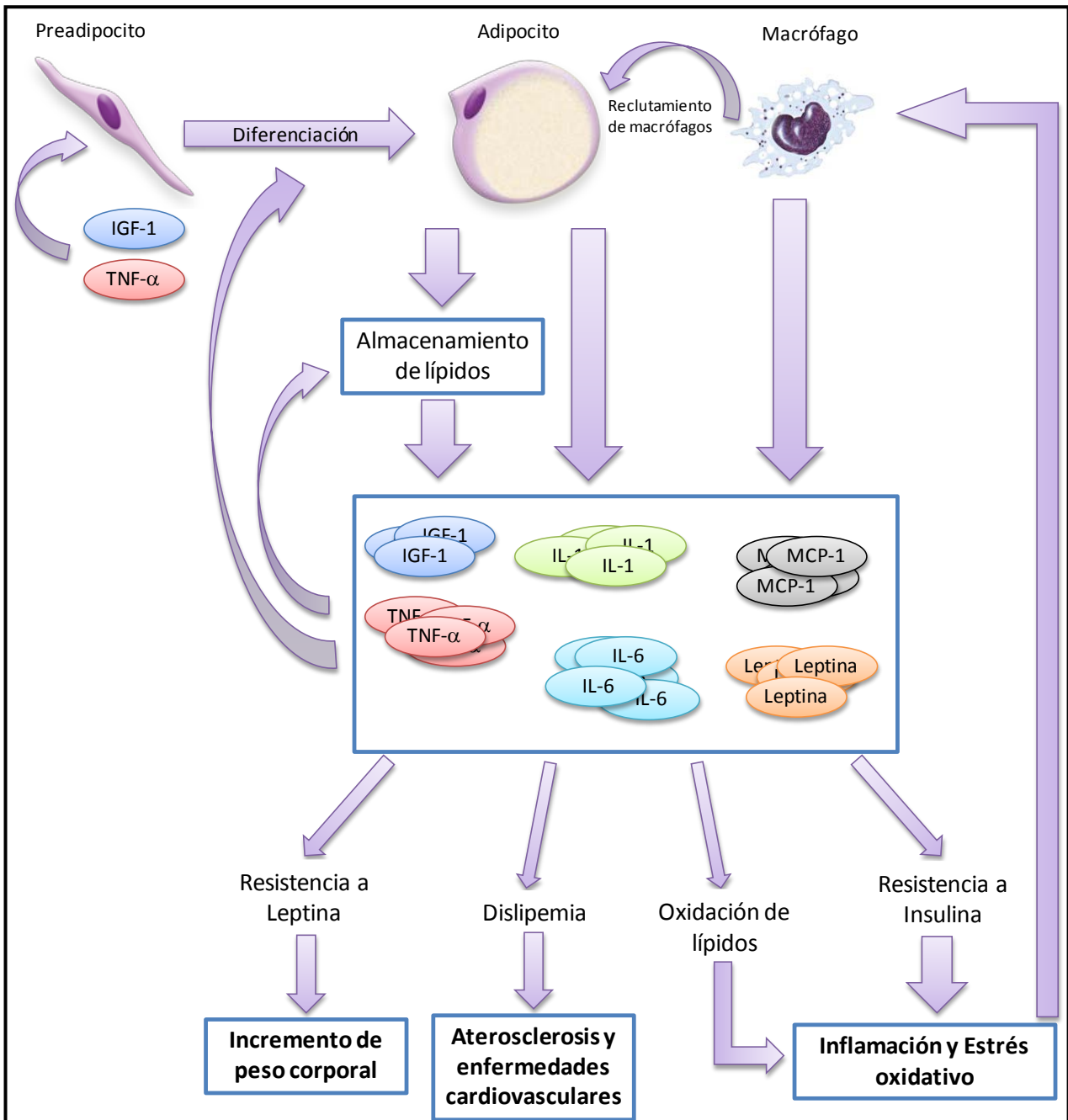


Figura 13. Relación entre obesidad e inflamación y moléculas señalizadoras implicadas. IGF: factor de crecimiento insulínico; TNF- α : factor de necrosis tumoral α ; IL: interleuquina; MCP-1: proteína quimioatrayente de monocitos 1.



La secreción de todos estos mediadores inflamatorios va a generar especies reactivas del oxígeno (ERO) como el anión superóxido (O_2^-), el radical hidroxilo ($OH\cdot$), el peróxido de hidrógeno (H_2O_2) y el oxígeno singlete (1O_2). Estas ERO aumentarán el daño celular y tisular activando la producción de todas las citoquinas implicadas en la inflamación y por consiguiente prolongarán esta respuesta inflamatoria.

Numerosos estudios con extractos vegetales y compuestos polifenólicos purificados han sido llevados a cabo para prevenir o disminuir la obesidad. Cabe destacar la investigación del té verde y las catequinas que lo componen (especialmente la EGCG)¹⁹⁹⁻²⁰³ y de los polifenoles de uva²⁰⁴⁻²⁰⁶. Otros polifenoles con demostrada bioactividad mejorando la obesidad son la curcumina^{207,208} y la quercetina²⁰⁹.

4.5. Patologías huérfanas y polifenoles.

Según la definición de la Unión Europea, en su Reglamento CE nº 141/2000 1, “las enfermedades huérfanas son enfermedades potencialmente mortales, o debilitantes a largo plazo, de baja prevalencia y alto nivel de complejidad. La mayoría de ellas son enfermedades genéticas; otras son cánceres poco frecuentes, enfermedades autoinmunitarias, malformaciones congénitas, o enfermedades tóxicas e infecciosas, entre otras categorías. Para abordarlas es preciso un planteamiento global, con esfuerzos especiales y combinados, para prevenir la morbilidad significativa o evitar la mortalidad prematura, y para mejorar la calidad de vida o el potencial socioeconómico de las personas afectadas”. Este tipo de enfermedades tienen una prevalencia menor de 5 casos por cada 10.000 habitantes.

Entre los principales problemas que deben afrontar aquellos pacientes con enfermedades huérfanas es la inexistencia de tratamiento farmacológico o, en aquellas que sí lo tienen, la reticencia de las industrias farmacéuticas a comercializarlos en el



mercado al no amortizarlos con las ventas previstas sin ningún tipo de incentivo. Además, hay que sumar a estos problemas el retraso en los diagnósticos o la inexistencia de estos hasta estadíos avanzados de la enfermedad (bien por escasez de conocimientos especializados, por diagnóstico equivocado o por dificultades de acceso a la asistencia).

Es debido a que muchas de estas patologías no tienen hoy en día tratamiento específico por lo que se plantea una serie de nuevas estrategias encaminadas al tratamiento de enfermedades huérfanas mediante la utilización de extractos vegetales como fuente natural de moléculas bioactivas dirigidas contra dianas específicas de estas enfermedades.

4.5.1. Condrodisplasias.

El crecimiento de los huesos largos depende de la proliferación y maduración de las células que constituyen el cartílago, los condrocitos. Estas células van a ser reemplazadas de modo gradual por el tejido óseo durante el crecimiento del individuo. Los condrocitos, en su proceso de maduración, pasan por una primera etapa en la que se hipertrofian para posteriormente morir en un proceso de tipo apoptótico²¹⁰. El crecimiento y desarrollo de los condrocitos en los cartílagos que flanquean los huesos está controlado por los factores de crecimiento de fibroblastos (FGF). Estos factores activan cuatro tipos diferentes de receptores denominados FGFR1, FGFR2, FGFR3 y FGFR4, estando los tres primeros implicados en enfermedades congénitas esqueléticas y craneales.

Las enfermedades óseas o condrodisplasias, también llamadas displasias esqueléticas, son trastornos esqueléticos hereditarios. Es un desorden genético que se manifiesta con deformidades de las extremidades y otras partes del cuerpo. Estas enfermedades se pueden delimitar en diferentes grupos: la displasia distrófica, debida a distintas mutaciones del gen que codifica para una proteína transportadora de sulfato (DTDST) originando proteoglicanos poco sulfatados en la matriz cartilaginosa; colagenopatías de



Figura 14. Tyrion Lanister encarnado por Peter Dinklage en la serie Juego de Tronos.

tipo II, las cuales se producen por mutaciones del gen COL2A1, impidiéndose la formación del colágeno tipo II; y la acondroplasia, la forma más común de enanismo congénito (Figura 14), originada por mutaciones en el receptor 3 del factor de crecimiento fibroblástico (FGFR3)²¹¹.

Como se ha indicado, la acondroplasia se caracteriza por una mutación en el receptor FGFR3 cuyo gen se localiza en el extremo distal del brazo corto del cromosoma 4. Estudios previos realizados en distintas poblaciones han establecido la existencia de una mutación frecuente consistente en el cambio de la glicina 380 por arginina (G380R) en el dominio transmembrana del receptor²¹². Mediante ratones knock-out para el receptor FGFR3 se ha demostrado que este receptor es un regulador negativo en el crecimiento del hueso. La activación del receptor y su posterior dimerización provocan la autofosforilación de residuos de tirosina, lo que sirve de sitio de unión de proteínas y efectores que propagan las señales de FGFR3, como son las proteínas ERK1/2 y STAT1²¹³. La mutación G380R origina una estabilización del dímero y por lo tanto una activación continua del receptor incluso en ausencia de agonistas²¹¹. Una vez producida esta activación sostenida del receptor, se ocasionando una fosforilación continuada de las proteínas ERK1/2 (p-ERK1/2), una acumulación de Cl⁻ a nivel intracelular, una disminución de la generación de matriz extracelular y una bajada de la proliferación celular^{213-215,216} (Figura 15). Todos estos eventos hacen que se altere el equilibrio normal entre los procesos de proliferación y maduración inhibiéndose el correcto crecimiento de la placa ósea.

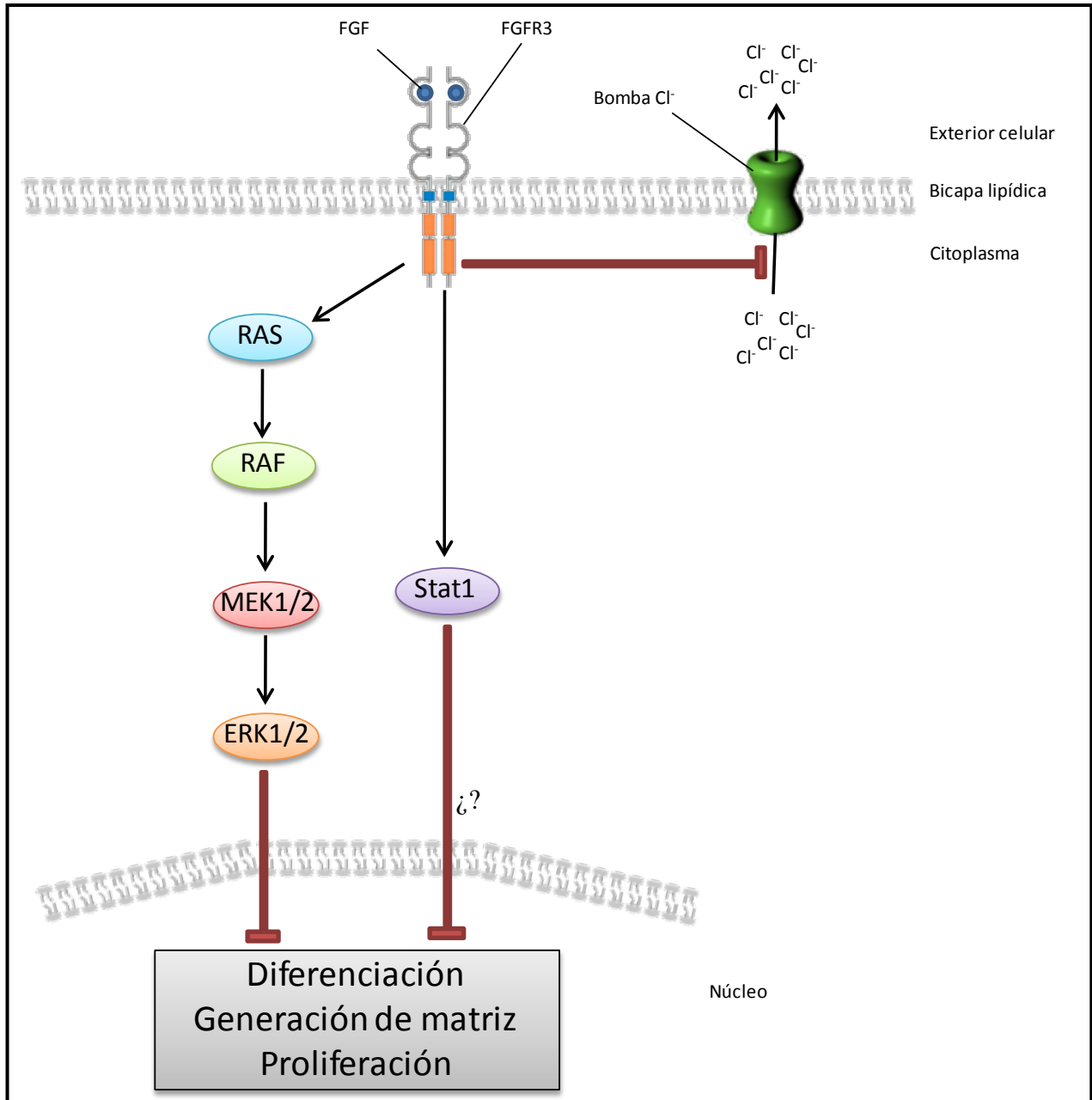


Figura 15. Vías de señalización en la activación del receptor FGFR3. FGF: factor de crecimiento fibroblástico; FGFR3: receptor 3 del factor de crecimiento fibroblástico; RAS: proteína del sarcoma de rata (GTPasa); RAF: acelerador rápido del fibrosarcoma (serin-treonin quinasa); MEK1/2: kinasas 1 y 2 de la MAPK; ERK1/2 (MAPK1/2): proteínas kinasas 1 y 2 activadas por mitógenos; Stat1: transductor de señal y activador de la transcripción 1.



5. TÉCNICAS ANALÍTICAS PARA EL ANÁLISIS DE POLIFENOLES.

El desarrollo del estudio de los polifenoles se aceleró sustancialmente por la aparición de la fitoquímica como rama de la química y la evolución de los estudios sistemáticos de clasificación quimiotaxonómicos, los métodos de extracción, purificación y análisis de fenoles así como la implementación de las técnicas de análisis químico orgánico como herramienta fundamental en la elucidación de estructuras complejas.

Las técnicas analíticas más empleadas en la actualidad pueden englobarse en dos grandes grupos: técnicas separativas y técnicas espectrométricas. Las técnicas separativas se utilizan para resolver los componentes de una mezcla; por otro lado, las técnicas espectrométricas proporcionan, para cada compuesto analizado, una información compleja, relacionada con sus características estructurales específicas.

5.1. Técnicas separativas.

Hasta mediados del siglo XX la separación de los compuestos de una mezcla compleja se llevaban a cabo mediante destilación, precipitación y extracción. Hoy en día, sin embargo, se utilizan especialmente la cromatografía y electroforesis en la separación analítica.

Aunque la separación de los compuestos fenólicos se ha llevado a cabo en varios vegetales usando técnicas electroforéticas^{217,218} y cromatografía de gases^{219,220}, la técnica más potente para la separación de estos compuestos es la cromatografía líquida de alta resolución (HPLC).



5.1.1. Cromatografía líquida de alta resolución (HPLC).

La cromatografía comprende un conjunto de técnicas que permite separar componentes estrechamente relacionados en mezclas complejas, lo que en muchas ocasiones resulta imposible por otros medios. La cromatografía se basa en la distinta distribución de las sustancias a separar entre dos fases, una móvil y otra estacionaria, en función de sus propiedades físico-químicas (carga, polaridad, potencial redox o masa molecular). Según el estado físico de la fase móvil se pueden distinguir tres tipos de técnicas cromatográficas: cromatografía líquida, de gases y de fluidos supercríticos.



Figura 16. Sistema de HPLC de los años 1970.

La cromatografía líquida en columna fue inventada a principios del siglo XX por el botánico ruso Mikhail Tswett, quien empleó la técnica para separar varios pigmentos vegetales como clorofilas y xantofilas, haciendo pasar disoluciones de estos compuestos a través de una columna de vidrio rellena con carbonato de calcio. Las especies separadas aparecían como bandas coloreadas en la columna, lo que

justifica el nombre que eligió para la técnica (del griego “*chroma*” que significa color, y “*graphein*” que significa escribir).

En los años 1950, Howard y Marlin introdujeron una nueva modalidad de cromatografía a la que llamaron de fase reversa. Hasta ese momento la cromatografía se había utilizado para separar sustancias polares usando una fase estacionaria polar y fases móviles apolares. Estos científicos revirtieron la polaridad de las fases móvil y estacionaria con el objetivo de separar ácidos grasos, de tal forma que usaron una fase estacionaria apolar y una fase móvil polar.



A finales de los años 1960 se vio que la eficiencia de la técnica podía aumentar disminuyendo el tamaño de partícula de la fase estacionaria. Así, empezaron a emplearse rellenos de columna con tamaño de partícula entre 3 y 10 μm . A la tecnología que se puso a punto para poder utilizar este tipo de columnas se le llamó Cromatografía Líquida de Alta Resolución (HPLC) (Figura 16). Los equipos de HPLC disponen de varios módulos: bombas capaces de impulsar la fase móvil a través de estas columnas con alto grado de empaquetamiento proporcionando la presión necesaria para ello; un sistema de inyección de muestra que permite su introducción en el flujo de la fase móvil de forma reproducible y sin despresurización del sistema; y en la mayoría de los casos, un detector acoplado con el que obtener, además de la información adicional que nos proporcione, parámetros cromatográficos como el tiempo de retención y el área de pico de los compuestos que eluyen de la columna. El tiempo de retención del analito dependerá de lo fuerte que interaccione con la fase estacionaria, las dimensiones y el tamaño de partícula de la columna y de la composición, flujo y temperatura de la fase móvil utilizada.

La primera vez que se utilizó un equipo de HPLC para la separación de polifenoles fue en el año 1973 por Bruckner y colaboradores para la separación de los compuestos de una muestra de cerveza²²¹. Esta técnica ha evolucionado notablemente y a día de hoy, sólo entre los años 2010 y 2011, se pueden encontrar más de 5000 publicaciones acerca del uso del HPLC en el análisis de compuestos fenólicos (según ScienceDirect), lo cual nos da idea de la importancia y el potencial de esta técnica en la caracterización de los compuestos fenólicos en matrices vegetales.

5.1.2. Nanocromatografía líquida (nLC).

La nanocromatografía líquida (nLC) (Figura 17) es una técnica relativamente reciente que vio la luz hace aproximadamente 20 años. Esta técnica cromatográfica usa diámetros

internos de columna muy pequeños (10-100 μm) y flujos de fase móvil de 10-1000 nL/min.

Los primeros intentos de usar este tipo de columnas se llevaron a cabo por Karlsson y Novotny en el año 1988²²² quienes evaluaron columnas de 20 a 70 μm . Más adelante, en el 1996, Hsieh y Jorgenson²²³ desarrollaron columnas mucho más pequeñas de 12 a 33 μm .

Las características de la nLC son varias: una gran disminución del consumo de disolventes con la subsecuente disminución de residuos y de coste económico; una disminución del diámetro interno de la columna que se traduce en un incremento de la sensibilidad y en volúmenes de muestra más pequeños; y un mayor empaquetamiento de la columna (y menor tamaño de poro) lo que aumenta la eficiencia de separación y disminuye el ensanchamiento de los picos.



Figura 17. Equipo de nanocromatografía líquida (nLC).

Esta técnica es especialmente potente en el ámbito de la proteómica, campo en el que se han hecho la mayoría de avances analíticos, aunque también se han desarrollado aplicaciones para análisis farmacológicos, ambientales y enantioméricos²²⁴⁻²²⁶. Sin embargo, la nLC tiene todavía poca aplicación en el campo del análisis de compuestos fenólicos, habiéndose descrito algunas aplicaciones, entre las que destaca un método de cuantificación de polifenoles en aceite de oliva²²⁷.



5.2. Sistemas de detección en cromatografía líquida.

Un detector debe cumplir, idealmente, con las siguientes características: presentar una elevada sensibilidad y reproducibilidad, límites bajos de detección, pequeña fluctuación de la señal de fondo, una respuesta rápida, ser robusto, no interferir con la eficacia de la separación, no ser destructivo y ser económico.

Existen numerosos sistemas de detección que pueden acoplarse a un sistema de HPLC, pero los más comúnmente usados son los detectores espectrofotométricos y los espectrómetros de masas.

5.2.1. Espectroscopía de absorción molecular Ultravioleta-Visible (UV-Vis).

Los inicios de la espectroscopía se remontan al año 1704 cuando Newton descubrió el fenómeno de dispersión de la luz. Pero no fue hasta mucho más adelante cuando Bunsen y Kirchhoff en 1859 dieron a conocer que cada elemento químico posee un espectro de emisión de líneas características y construyeron un equipo capaz de medir esa emisión llamado espectroscopio. Mientras que la espectroscopía de emisión atómica ya tenía varias aplicaciones prácticas a finales del siglo XIX, no fue hasta los años 30 del siglo XX que la espectroscopía de absorción molecular empezó a desarrollarse al descubrir que las vitaminas (especialmente la vitamina A) absorbían radiación ultravioleta. En el año 1940 la casa comercial National Technologies Laboratories (la que más adelante pasó a ser Beckman Instruments) desarrolló el DU UV-Vis Model A, el primer espectrofotómetro comercial. En 1954 se desarrolló el primer equipo de doble haz, lo que permitía medidas más rápidas y precisas al permitir la medida de la muestra y la de una disolución de referencia al mismo tiempo. Hasta este momento se usaban lámparas de tungsteno para el espectro visible y lámparas de deuterio para el ultravioleta con la única opción de seleccionar una longitud de onda para la medida. En 1969 se fabricó el primer detector acoplable a HPLC, con longitud de onda variable sin necesidad de cambiar los filtros o las



lámparas. Diez años después, en 1979, se inventó el detector de batería de diodos (DAD) (Figura 18), cuya aparición permitió la detección simultánea de un rango de longitudes de onda en segundos con el fin de obtener espectros de absorción, especialmente en muestras que pasan rápidamente por una celda.

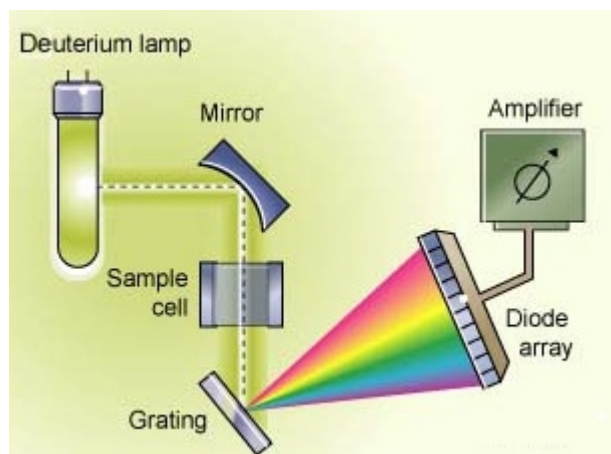


Figura 18. Equipo de espectroscopía de absorción basado en un detector de batería de diodos (DAD).

La espectroscopía de absorción molecular UV-Vis se basa en la capacidad de las moléculas de absorber radiación en el rango de los 190-800 nm aproximadamente del espectro electromagnético, causando la promoción de un electrón de su estado fundamental a uno excitado. La espectroscopía UV-Vis mide, generalmente, la absorbancia del analito, definida como la cantidad de intensidad de luz que es capaz

de absorber una molécula. Esta absorción está relacionada de forma lineal (dentro de un rango) con la concentración de la sustancia, siguiendo la ley de Lambert-Beer.

Los múltiples enlaces conjugados presentes en los compuestos fenólicos los convierten en cromóforos que presentan bandas de absorción en la región UV (generalmente en torno a los 220 y 280 nm) e incluso en el visible como es el caso de las antocianidinas y algunos flavonoles.

La espectroscopía de absorción UV-Vis tiene una gran aplicación en la identificación y cuantificación de multitud de moléculas y probablemente sea la técnica de análisis cuantitativo más utilizada en todo el mundo debido a su posibilidad para determinar un gran número de compuestos y grupos funcionales y su facilidad de manejo, a pesar de que su sensibilidad es mucho menor que la de otros sistemas de detección.



5.2.2. Espectrometría de masas.

La espectrometría de masas es uno de los pocos sistemas de detección que proporcionan información estructural, por lo que la combinación de una técnica de separación de alta eficacia como el HPLC con la espectrometría de masas como sistema de detección da lugar a una herramienta muy útil en el análisis de muestras complejas, tanto en su caracterización analítica como estructural (incluso medir la relación isotópica de átomos y/o moléculas), además de presentar una aceptable sensibilidad, selectividad y universalidad. Sin embargo, el coste de adquisición de estos aparatos es muy elevado, presentan una deriva mayor y las interferencias son más problemáticas.

Podría considerarse a Thomson como el padre de la espectrometría de masas. Se basó en los trabajos previos de Goldstein a finales del siglo XIX en los que descubrió que los rayos luminosos en un tubo de descarga que contenía gases a baja presión viajaban en línea recta desde los agujeros de un disco metálico usado como cátodo hasta la parte opuesta usada como ánodo. La continuación de estos estudios, junto con los descubrimientos de que esos rayos luminosos podían deflectarse en un campo magnético, llevaron a Thomson a crear el primer equipo que era capaz de medir las diferencias en la relación masa/carga (m/z) de los átomos. Varios años después, Aston refinó los equipos fabricados por Thomson y construyó el llamado espectrógrafo de masas.

Debido a que este tipo de detectores necesitan que la muestra se encuentre en estado gaseoso, los primeros acoplamientos con equipos de cromatografía se llevaron a cabo con la cromatografía de gases en los años 1960. No fue hasta la década de los 70 cuando se empezaron a desarrollar interfases capaces de desolvatar las muestras líquidas dejando las moléculas ionizadas en fase gaseosa cuando se pudo realizar el acoplamiento con HPLC, aunque hasta los años 80 este acoplamiento no fue del todo práctico.

Todos los espectrómetros de masas cuentan esencialmente con las siguientes partes:

- Un sistema de ionización o interfase que permita la desolvatación e ionización de la muestra. Las interfases más utilizadas en los acoplamientos con HPLC son la ESI (ionización por electrospray), en el que la muestra en solución se hace pasar a través de un fino capilar al cuyo extremo se aplica un alto potencial eléctrico, se forma un spray a la salida del capilar y el disolvente se evapora liberando moléculas cargadas, la APCI (ionización química a presión atmosférica) donde la muestra gaseosa se ioniza al colisionar con los iones producidos al bombardear con electrones un exceso de gas reactivo y EI (impacto electrónico) en la que la muestra se calienta a alta temperatura para producir un vapor molecular, que se ioniza al ser bombardeado con un haz de electrones de alta energía.

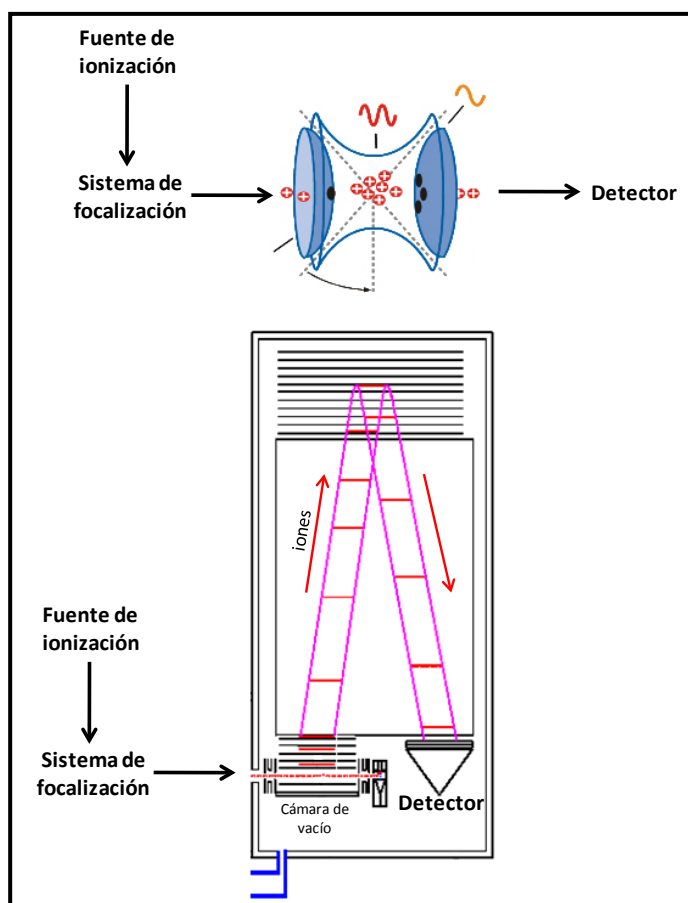


Figura 19. Analizadores de masas. Superior, trampa de iones; inferior, tiempo de vuelo.

- Un analizador de masas, que idealmente sea capaz de separar eficientemente los iones en función de su relación m/z . Estos analizadores también puede ser de varios tipos. **La trampa de iones (IT)** (Figura 19, superior) que aplica diferentes voltajes generando un campo electromagnético tridimensional en la cavidad de la trampa que atrapa y concentra los iones. La aplicación de una rampa lineal de radiofrecuencia provoca inestabilidad en las trayectorias de los iones y son expulsados en función de su relación m/z dando lugar a un espectro de masas. Una vez que los iones se

encuentran atrapados dentro de este analizador se puede llevar a cabo bien el análisis de



sus masas o bien el aislamiento de uno o varios iones precursores y su posterior fragmentación con lo que se obtendrá un patrón de fragmentación que proporciona información estructural de las moléculas. Otro analizador de masas es el **tiempo de vuelo (TOF)** (Figura 19, inferior), cuyo fundamento consiste en la separación de los iones según la distinta velocidad que adquieren en el interior del tubo de vuelo en función de su relación m/z . Los iones de mayor m/z “volarán” a menor velocidad que los de menor m/z . Los analizadores de tiempo de vuelo ortogonales son capaces de proporcionar la masa exacta de los iones, que junto con la distribución isotópica de éstas permite la obtención de una fórmula molecular prácticamente inequívoca.

- Un detector donde la corriente de los iones proveniente del analizador se transforme en una señal medible. El detector más convencional es el multiplicador de electrones, constituido por un cátodo que al recibir los iones procedentes del analizador emitirá electrones, que a su vez impactarán sobre sucesivos dínodos que amplificarán la señal electrónica.

La primera aplicación de la espectrometría de masas en la determinación de polifenoles en matrices vegetales se llevó a cabo por Pellizza y colaboradores en el año 1969 acoplando este detector a cromatografía de gases²²⁸. Sin embargo, la caracterización analítica de estos compuestos fenólicos utilizando un acoplamiento HPLC-MS tuvo que esperar hasta bien entrada la década de los años 90.

6. ENSAYOS *IN VITRO* E *IN VIVO* Y METODOLOGÍAS PARA LA DETERMINACIÓN DE LA BIOACTIVIDAD.

Para la determinación de la bioactividad de un extracto vegetal o de los compuestos que lo componen es necesario evaluar su eficacia y mecanismo de acción en las diferentes



patologías que se pretenden abordar. Para ello, es necesario el uso de diferentes ensayos *in vitro* e *in vivo* que proporcionen los resultados necesarios para comprender cómo actuarán en el organismo.

Los ensayos *in vitro* (del latín “dentro del vidrio”) son aquellos que se realizan fuera de un sistema vivo en un ambiente controlado. Los ensayos *in vivo* (del latín “dentro de lo vivo”) son los que se realizan en tejidos de organismos vivos.

Ambos tipos de ensayos tienen sus ventajas e inconvenientes:

- Las cuestiones éticas y morales que la experimentación animal suscita en la sociedad e incluso en los propios investigadores tal vez sea la mayor desventaja de la experimentación *in vivo* comparada con la *in vitro*.
- Económicas: el mantenimiento y utilización de los animales de experimentación tiene costes mucho más elevados que los ensayos *in vitro*.
- Científicas: los ensayos *in vitro* permiten una gran versatilidad en el diseño experimental y un número elevado de réplicas, permitiendo la monitorización y automatización y obteniendo resultados de forma rápida y fiable. Esto es más difícil cuando se utilizan animales de experimentación ya que la variación biológica existente entre ellos hace que los resultados no siempre sean totalmente reproducibles, además de que se necesita de personal muy cualificado para planificar y llevar a cabo los experimentos. Sin embargo, para los ensayos *in vitro* existe una necesidad de validación de los métodos y la imposibilidad en muchas ocasiones de extrapolar los resultados ya que no se tiene en cuenta el organismo vivo al completo. Además, los pacientes desarrollan patologías paralelas y otras complicaciones que sólo pueden estudiarse en un organismo vivo. Por último, el estudio y desarrollo de nuevos compuestos bioactivos sólo es posible utilizando animales de experimentación, con el fin de establecer la dosis y



posología, la cinética y metabolismo y las incompatibilidades y efectos secundarios de los compuestos bioactivos; son necesarios animales para la producción de anticuerpos mono y policlonales, para el estudio de respuestas conductuales a psicofármacos, establecer la eficacia de vacunas, estudiar la respuesta a implantes, etc.

- Legales: que impiden el uso de animales de experimentación según se recoge en la Directiva del Consejo 86/609/CEE y en el Real Decreto 1201/2005, que establece que *“no deberá realizarse un experimento si se dispone de otro método científicamente satisfactorio y contrastado que permita obtener las mismas conclusiones sin implicar la utilización de animales”*.

6.1. Ensayos *in vitro*.

Los ensayos *in vitro* tienen como objetivo describir los efectos de una variable experimental en un subconjunto de las partes constitutivas de un organismo (órganos, tejidos, células, componentes celulares, proteínas y/o biomoléculas). Este tipo de experimentos es el más apropiado para conocer el mecanismo de acción de una sustancia ya que al tener en el sistema muy pocas variables y reacciones paralelas, los resultados son mucho más fáciles de interpretar.

6.1.1. Cultivos microbianos.

Las bacterias pueden englobarse en dos grandes grupos: las Gram negativas, como *Escherichia coli*, que no se tiñen de azul en la tinción de Gram debido a la organización de su envuelta celular, basada en dos membranas lipídicas que envuelven a una fina pared de peptidoglicanos. Por el contrario, las bacterias Gram positivas como *Staphylococcus aureus* poseen una única membrana lipídica y una gruesa pared de peptidoglicanos, tiñéndose de azul en la tinción de Gram (Figura 20).

Un microorganismo se puede sembrar en un medio líquido o en la superficie de un medio sólido de agar. Los medios de cultivo contienen distintos nutrientes como son azúcares simples o sustancias complejas como la sangre o el extracto de caldo de carne.

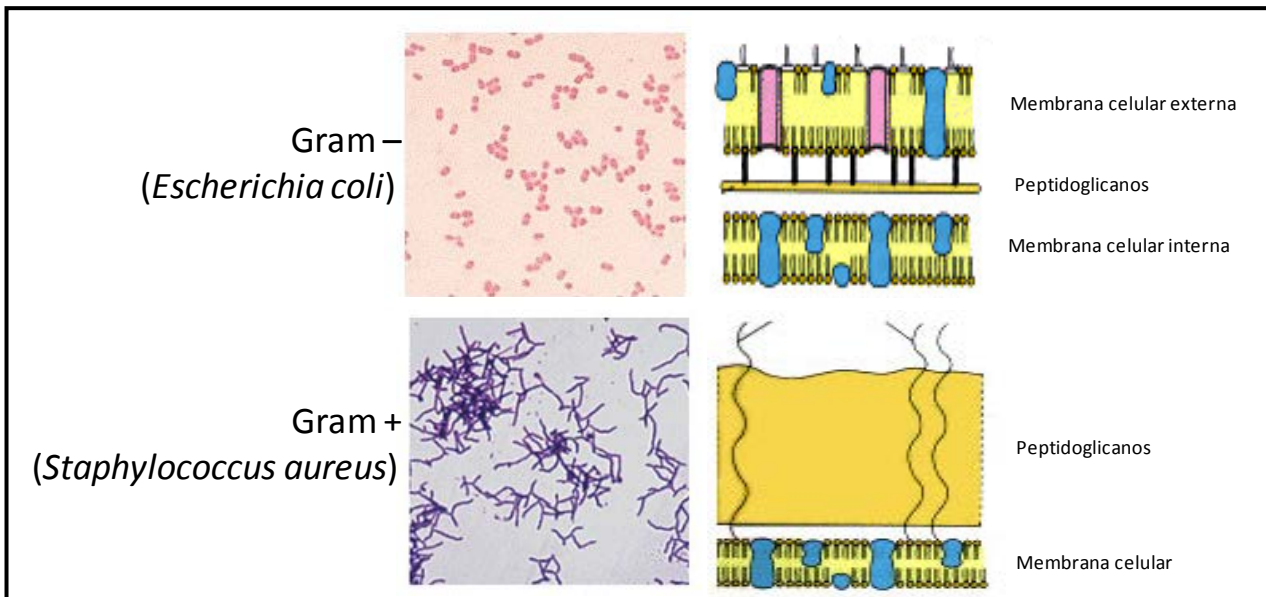


Figura 20. Tinción de Gram (izquierda) y esquema simplificado de la composición de la envuelta (derecha) de una bacteria Gram negativa como *E. coli* (superior) y una bacteria Gram positiva como *S. aureus* (inferior).

Para su crecimiento, los microorganismos necesitan de unas condiciones ambientales (luz/oscuridad, O_2/CO_2 , temperatura, pH del medio, etc.) y de esterilidad adecuadas. El crecimiento de los microorganismos consta de varias fases (Figura 21):

- 1) Fase de latencia: en el que las bacterias que han sido transferidas a un nuevo medio de cultivo se adaptan a él y empiezan a prepararse para volver a dividirse activamente.
- 2) Fase exponencial: en la que las bacterias duplican su población a su velocidad máxima de división.
- 3) Fase estacionaria: en la que, bien porque el medio de cultivo se agota, o porque se acumula alguna sustancia de deshecho inhibitoria del crecimiento, las bacterias dejan de dividirse.



4) Fase de muerte: en la que las bacterias se quedan sin nutrientes y empiezan a morir.

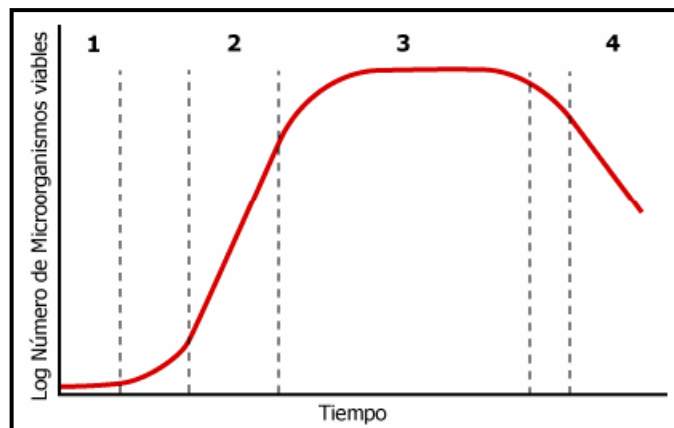


Figura 21. Fases del crecimiento bacteriano.

6.1.2. Cultivos celulares animales.

El cultivo celular es el proceso mediante el cual las células crecen bajo condiciones controladas, generalmente a una temperatura de 37 °C y una mezcla de gases consistente en un 95 % de O₂ y un 5 % de CO₂. Sin embargo, las condiciones de cultivo y, especialmente los medios nutritivos, varían enormemente de una línea celular a otra, siendo los más utilizados el DMEM y el RPMI. Estos medios de cultivo contienen sales, ácidos grasos y aminoácidos esenciales, oligoelementos, etc. Normalmente se suelen suplementar con un porcentaje variable de suero fetal bovino (FBS) que aportan otros nutrientes y diferentes factores de crecimiento. Además, se deben utilizar antibióticos que eviten la contaminación por hongos, bacterias u otros patógenos (Figura 22).

Los cultivos celulares tienen una serie de ventajas que los hacen un modelo muy útil de estudio. Entre ellas destacan las siguientes:

- Se pueden controlar de forma precisa todos los factores ambientales (composición del medio de cultivo, pH, temperatura, % O₂/CO₂, etc.) y fisiológicos (hormonas, factores de crecimiento, densidad celular,...).

- Se puede obtener fácilmente y de una forma rápida un número elevado de células, las cuales son idénticas y homogéneas, evitando así la heterogeneidad biológica que presenta el uso de animales de experimentación.
- Se minimiza el uso de las sustancias a ensayar debido a que el acceso a las células es directo y por tanto las concentraciones necesarias son mucho más bajas que en modelos animales. Esto se traduce en una disminución en el coste de los experimentos.
- Motivaciones éticas. El cultivo celular es una alternativa válida en muchas situaciones a la experimentación *in vivo* con la que se sacrifican al año muchos miles de animales. Sin embargo, no hay que olvidar que el cultivo celular no puede reemplazar siempre al estudio con animales de experimentación.

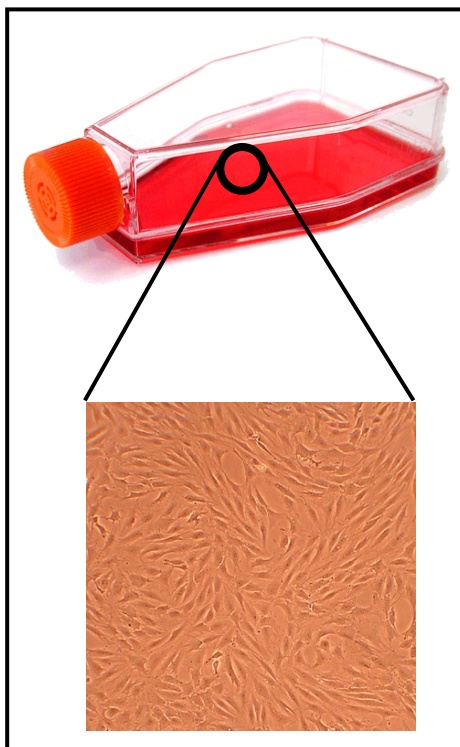


Figura 22. Cultivo celular de condrocitos de la línea RCJ de ratón.

Sin embargo, existen ciertos inconvenientes a tener en cuenta:

- Las células animales en cultivo crecen mucho más lentas que los organismos patógenos (bacterias, hongos, micoplasmas, etc.), por lo que se debe ser muy estricto con las condiciones de asepsia y disponer de instrumental específico y personal cualificado para este tipo de experimentos.
- Muchas de las líneas celulares que se utilizan hoy en día son inestables debido a la dotación cromosómica aneuploide que poseen. Esto supone un problema si alguna de estas subpoblaciones logra crecer más rápido que la original, obteniendo diferencias de una generación a la siguiente. La solución, no siempre posible, es emplear líneas estables preestablecidas.



- Se necesita validar el modelo *in vitro* ya que se diferencia bastante de un tejido intacto (se pierde la organización espacial y carecen de sistemas de regulación de la homeostasis *in vivo*).

Los cultivos celulares son utilizados en multitud de estudios. Entre ellos se pueden destacar la investigación del cáncer, los ensayos de actividad celular, el flujo intracelular de sustancias o señales, las interacciones celulares, la virología, la inmunología, la ingeniería de proteínas, el diagnóstico de enfermedades, la producción de tejidos para trasplantes, las aplicaciones industriales agronómicas de reproducción *in vitro* de clones de plantas de interés comercial, y un largo etcétera.

6.2. Ensayos *in vivo*. Animales de experimentación.

La búsqueda de las bases moleculares y procesos implicados en cualquier patología dependen de la disponibilidad de modelos experimentales con los que compartan similitudes fisiológicas, anatómicas y metabólicas con los humanos. Los modelos animales más comúnmente utilizados son la rata (*Rattus norvegicus*) y el ratón (*Mus musculus*), ya que presentan la ventaja de poder ser manipulados genéticamente y con precisión, tienen un coste relativamente bajo con respecto a otros modelos animales y ofrecen la posibilidad de poder controlar los factores ambientales que pueden influir en la progresión de las enfermedades que se quieren estudiar.

6.2.1. Marco legal.

No hay que olvidar que el trabajo con animales de experimentación requiere unas consideraciones éticas importantes que deben comenzar ya en el diseño del experimento. La experimentación animal está regulada por varias leyes en vigor a nivel autonómico, nacional (Real Decreto 1201/2005, de 10 de octubre, “sobre protección de

los animales utilizados para experimentación y otros fines científicos” y Ley 32/2007, de 7 de noviembre, “para el cuidado de los animales, en su explotación, transporte, experimentación y sacrificio”) y Europeo (Directiva 2010/63/UE del Parlamento Europeo y del Consejo, de 22 de septiembre, “relativa a la protección de los animales utilizados para fines científicos”).

Además, también se regulan siguiendo el principio de las 3 R's: Reemplazo, Reducción y Refinamiento. Este principio fue creado como medida alternativa al uso de animales de experimentación, y se basa en el concepto de: 1) Reemplazar el uso de animales de experimentación cuando se puedan usar otras vías de investigación; 2) Reducir al máximo el número de animales a utilizar; y 3) Refinar el método de trabajo existente para disminuir el dolor y malestar de los animales. El seguimiento de este principio se consigue con la creación de comités de ética de experimentación animal en el que participan diferentes estamentos sociales que valoran la hipótesis y los protocolos de trabajo propuestos por los investigadores.

6.2.2. Modelos animales.

Muchas cepas silvestres son utilizadas en experimentación animal. Las ratas de la cepa Wistar (ratas albinas creadas en 1906 por el Instituto Wistar) (Figura 23) son las más usadas en estudios de fisiología, etología, farmacología y toxicología. Estas ratas son el primer organismo modelo utilizado en investigaciones biomédicas por ser fáciles de criar, de rápida reproducción, de fácil manejo y docilidad y por presentar una fisiología parecida al humano.



Figura 23. Rata Wistar.

Sin embargo, cuando se quiere estudiar una patología específica, se necesitan modelos animales especialmente diseñados para tal fin. La generación



de nuevos animales de experimentación facilita el estudio de condiciones específicas que se encuentran en patologías humanas, y se basan en la creación de modelos mediante técnicas de manipulación genética. Entre estos modelos se encuentran los Knock-out y Knock-in con una mutación dirigida basada en la eliminación (knock-out) o inserción (Knock-in) de un gen de interés, y los modelos transgénicos que contienen un segmento de ADN recombinante portador de información genética específica.

Los modelos experimentales de obesidad se han convertido en una herramienta esencial para el estudio de esta patología y de los trastornos metabólicos asociados como la esteatosis hepática o la resistencia a la insulina. La utilización de estos modelos ha permitido profundizar en el conocimiento de la enfermedad y realizando además aproximaciones difícilmente viables en humanos.

Existen múltiples modelos de obesidad, cada uno de ellos con determinadas características útiles para abordar diferentes objetivos concretos. Entre ellas, la cepa C57BL/6J que posee un mismo fondo genético presentan predisposición a la obesidad bajo dietas hipercalóricas. Un ejemplo de ellos son los ratones C57BL/6J LDLr knock-out ($LDLr^{-/-}$) (Figura 24),

deficientes en los receptores de las lipoproteínas de baja densidad, causando hipercolesterolemia familiar, una enfermedad humana caracterizada por aterosclerosis prematura y una elevación importante en la concentración plasmática de colesterol LDL²²⁹. Los ratones LDLr knock-out ($LDLr^{-/-}$) alimentados con una dieta rica en grasa, desarrollan esteatohepatitis no alcohólica (NASH) asociada con cuatro o cinco componentes del síndrome metabólico.



Figura 24. Ratón de la cepa C57BL/6J silvestre (izquierda) y knock-out $LDLr^{-/-}$ (derecha).

6.3. Metodología para la determinación de la bioactividad

6.3.1. Capacidad antioxidante.

Los métodos de determinación de la actividad antioxidante se basan en distintos sistemas generadores de radicales libres. Dichos radicales reaccionan con la muestra y en virtud de la capacidad antioxidante de ésta se inhibiría la generación de los primeros.

En la actualidad, debido a la complejidad de los procesos de oxidación, no existe un método que refleje de forma completa el perfil antioxidante de una muestra, por tanto, es bueno trabajar con varios métodos para facilitar la comparación e interpretación de los resultados.

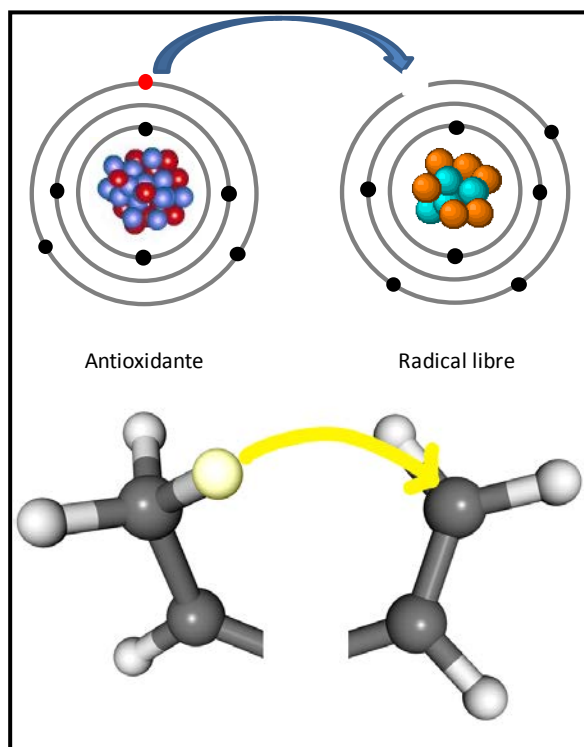


Figura 25. Esquema simplificado de los mecanismos de acción de los métodos SET (superior) y HAT (inferior).

Los antioxidantes pueden dividirse en aquellos biosintetizados por el propio organismo (como los antioxidantes enzimáticos superóxido dismutasa (SOD), catalasa, glutatión peroxidasa, etc. o los no enzimáticos como el glutatión, coenzima Q o el ácido úrico) y aquellos que deben ingerirse con la dieta (como por ejemplo los polifenoles).

Los mecanismos de acción de los compuestos antioxidantes no enzimáticos pueden clasificarse en dos grandes grupos: SET (single electron transfer) en los que la molécula antioxidante estabiliza a los radicales libres



cediéndoles un electrón y HAT (hydrogen atom transfer) en los que el antioxidante cede un átomo de hidrógeno completo²³⁰ (Figura 25).

Dentro de los métodos basados en un mecanismo SET están los métodos TEAC y FRAP. El primero mide la capacidad antioxidante en equivalentes de Trolox, mientras que el segundo mide el poder antioxidante para reducir iones férricos.

En el caso del mecanismo HAT, los métodos más utilizados son el ORAC (capacidad para absorber radicales de oxígeno) y el TBARS (sustancias reactivas al ácido tiobarbitúrico).

El método TEAC se basa en generar un radical $ABTS^{\bullet+}$ a partir de su precursor, el ácido 2,2'-azinobis (3-etilbenzotiazolín)-6-sulfónico (ABTS) utilizando persulfato potásico. El radical catiónico obtenido es un compuesto de color verde-azulado, estable y medible espectrofotométricamente a 734 nm. La estabilización de este radical hace que pierda su color.

El método FRAP se basa en el poder que tiene una sustancia antioxidante para reducir el Fe^{3+} a Fe^{2+} . El complejo férrico-2,4,6-tripiridil-s-triazina ($TPTZ-Fe^{+3}$) incoloro es reducido al complejo ferroso ($TPTZ-Fe^{+2}$) de color azul intenso medible espectrofotométricamente a 595 nm.

El fundamento del método ORAC se basa en medir la pérdida de fluorescencia de la sonda Fluoresceína. Esta sonda presenta una λ de excitación y de emisión de 485 y 520 nm respectivamente. En este método, el radical AAPH (2,2'-Azobis-(2-aminopropano)-dihidrocloruro) oxida a la fluoresceína de forma que ésta pierde su fluorescencia. Así, las sustancias antioxidantes presentes en el extracto vegetal retrasarán dicha pérdida de fluorescencia.

Por último, el método TBARS se basa en la medida de generación de malondialdehído (MDA), un producto producido por la peroxidación lipídica. Este compuesto es capaz de reaccionar con el ácido tiobarbitúrico (TBA) en una reacción estequiométrica 1:2, dando



un complejo que se excita a 500 nm y emite fluorescencia a 530 nm. Un extracto que sea capaz de inhibir la peroxidación lipídica da como resultado una disminución en la producción de MDA y por lo tanto una bajada en la emisión de fluorescencia.

También es posible realizar ensayos antioxidantes *in vivo*, midiendo la actividad de la enzima superóxido dismutasa (SOD) plasmática (isoforma SOD3). Esta enzima es una fuerte defensa natural que poseen las células para detoxificar radicales del oxígeno, y se encarga de dismutar el ión superóxido (O_2^-) en oxígeno molecular (O_2) y peróxido de hidrógeno (H_2O_2) en dos etapas de reacción. Este ensayo se basa en la generación de aniones superóxido por oxidación de la xantina a ácido úrico mediante la enzima xantina oxidasa. Estos aniones O_2^- reducirán al citocromo C y esta reacción puede medirse espectrofotométricamente a 550 nm. Una elevada actividad de la SOD eliminará los aniones superóxido e impedirá la reducción del citocromo C con la consecuente disminución en la absorbancia.

6.3.2. Capacidad antimicrobiana.

Los extractos de plantas se han convertido en potenciales alternativas para la industria de medicamentos debido a la elevada actividad antimicrobiana de los compuestos naturales y al desarrollo de multirresistencia por parte de los microorganismos a los antibióticos de uso común. Por esta razón se realizan ensayos antimicrobianos con los que calcular la concentración mínima inhibitoria (MIC_{50}) del extracto vegetal a la cual el 50 % de las bacterias mueren. Estos ensayos se realizan utilizando *Escherichia coli* (como modelo de bacteria gram negativa) y *Staphylococcus aureus* (como bacteria gram positiva) (Figura 26).

El fundamento del método consiste en incubar las bacterias en un medio de cultivo basado en agar a 37 °C en presencia de diferentes concentraciones del extracto. Como colorante se usa el cloruro de 2-(p-iodofenil)-3-(p-nitrofenil)5-feniltetrazolio (INT), una

sal de tetrazolio que se reduce rápidamente por las deshidrogenasas de la cadena de transporte de electrones asociada a la respiración de las bacterias. Esta sales, al reducirse, precipitan formando un complejo insoluble en agua de color rojo intenso medible espectrofotométricamente a 570 nm.

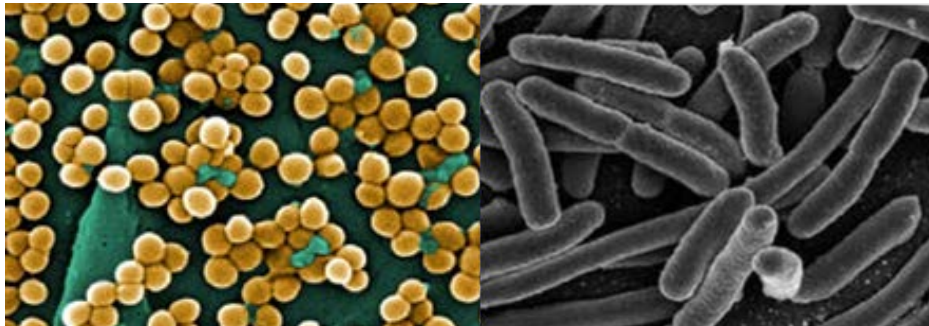


Figura 26. Imágenes de microscopía de *Staphylococcus aureus* (izquierda) y *Escherichia coli* (derecha).

6.3.3. Western Blot

El Western Blot es una técnica utilizada para la detección de proteínas en una muestra celular o tisular. Se basa en la separación (ya sea por tamaño, hidrofobicidad, etc) de las proteínas desnaturalizadas mediante una electroforesis (generalmente usando un gel de poliacrilamida). Las proteínas son trasferidas a continuación desde el gel hacia una membrana (normalmente de nitrocelulosa), donde son detectadas utilizando anticuerpos específicos para la proteína. De esta forma se podrá comparar la cantidad de proteína presentes en distintas muestras. Las aplicaciones del Western blot son innumerables. A *grosso modo*, dentro del campo de la biomedicina, tiene aplicaciones diagnósticas en enfermedades infecciosas, enfermedades hereditarias y congénitas, enfermedades autoinmunitarias, y cada vez es más utilizada en el cáncer, tanto para el diagnóstico precoz y el tratamiento como en investigación básica y aplicada. Otros campos en los que se utiliza esta técnica son la inmunología y áreas relacionadas con ésta, como la inflamación y el envejecimiento celular, y también en el ámbito de la microbiología, la genética y la genómica.



6.3.4. Viabilidad celular en cultivos animales

La viabilidad celular puede determinarse de varias formas: mediante citometría de flujo, en la que a las células se les obliga a pasar alineadas una a una frente a un haz láser mediante un flujo continuo. Cada célula, a la vez que dispersa la luz, emite luz fluorescente como consecuencia de la excitación láser a la que es sometida. O bien mediante ensayos colorimétricos como el MTT (una sal de tetrazolio) que al reducirse mediante la succinato deshidrogenasa de las mitocondrias funcionales dará lugar al formazán, de color azul intenso. La viabilidad celular es un fiel indicador de la citotoxicidad del tratamiento o condiciones a los que se somete a las células.

7. METABOLISMO Y BIODISPONIBILIDAD DE LOS POLIFENOLES

El metabolismo que van a sufrir los compuestos fenólicos y su biodisponibilidad en el organismo son dos conceptos muy interrelacionados entre sí.

De forma general, la biodisponibilidad de los polifenoles va a estar determinada por la facilidad que tengan para atravesar la barrera epitelial del intestino, las modificaciones metabólicas que sufran a su través y la tasa de eliminación de estos compuestos antes de alcanzar los tejidos diana.

7.1. Metabolismo de los polifenoles

El metabolismo se define como el conjunto de reacciones químicas que dan lugar a una conversión química o transformación de fármacos o sustancias endógenas en otros



compuestos. Estas modificaciones pueden producir metabolitos activos, metabolitos inactivos, o productos metabólicos con menor, mayor o distinta actividad farmacológica.

Los compuestos activos que entran en el organismo van a sufrir biotransformaciones por acción del metabolismo de fase I y de fase II^{231,232}.

Las reacciones que se producen en la fase I del metabolismo suelen ser oxidaciones y reducciones llevadas a cabo por el sistema enzimático del citocromo P450 o hidrólisis (incluyendo la eliminación de los azúcares unidos y la formación de su respectiva aglicona). La hidroxilación llevada a cabo por el citocromo P450 requiere que en el anillo B de los compuestos fenólicos no existan grupos hidroxilo o que exista únicamente uno. Dos o más grupos hidroxilo en este anillo impiden la hidroxilación por parte del citocromo P450. Por lo tanto, una estructura catecol en este anillo impide la hidroxilación del compuesto fenólico²³³. Por otro lado se ha observado la imposibilidad de los compuestos fenólicos glicosilados para atravesar la barrera intestinal. Para ello, en una primera etapa deben eliminarse estos residuos de azúcar. Debido a que la hidrólisis de estos azúcares no ocurre en las condiciones ácidas del estómago, es necesaria una acción enzimática mediante glicosidasas presentes en el propio alimento ingerido, en las células intestinales o, mayoritariamente, por glicosidasas de la flora intestinal²³⁴ (Figura 27). En mamíferos existen 2 enzimas capaces de hidrolizar los glicósidos de los compuestos fenólicos. Esta desconjugación es producida por dos enzimas, la LPH (lactasa floridzin hidrolasa) presente únicamente en la cara externa de la membrana de los enterocitos del cepillo intestinal, y la CBG (β -glucosidasa citosólica) que se encuentra en el citoplasma de muchos tejidos, especialmente en hígado. Sin embargo, se han observado ciertos flavonoides glicosilados que han sido absorbidos intactos y han llegado al plasma (especialmente glucósidos de quercetina y varias antocianinas)²³⁴, aunque no queda claro el mecanismo por el cual estos glucósidos pueden ser absorbidos.



En la fase II del metabolismo suelen darse reacciones de conjugación en las que se unen al compuesto grupos metilo, sulfato, acetato, glucurónido o glutatión. El metabolismo de fase II pretende aumentar la polaridad de los compuestos para facilitar su excreción por orina o bilis. Estas rutas de conjugación son comunes tanto para el metabolismo de fármacos (u otros xenobióticos) como para el metabolismo de los polifenoles. Gran parte de esta fase II del metabolismo puede darse en las células intestinales. En el hígado, y en menor medida en el riñón, ocurren reacciones de metilación y sulfatación de forma secundaria, quedando estos órganos en segundo plano especialmente cuando las dosis de compuestos son bajas²³⁴ (Figura 27). Las enzimas encargadas de unir grupos metilo a los polifenoles son las COMT (catecol-*O*-metiltransferasas) presentes en multitud de tejidos. Estas enzimas son capaces de transferir un grupo metilo desde la *S*-adenosilmetionina tanto al grupo hidroxilo del carbono 3' como al 4' del anillo catecol de los flavonoles. Sin embargo, el citocromo P450 presenta una acción desmetilasa específica de la posición 4' y no de la 3'. Por lo tanto, en cuanto a los flavonoles se refiere, será más común encontrar la conjugación del grupo metilo en la posición 3' del anillo catecol²³⁵.

Las enzimas UGT (UDP glucuronil transferasa) son las responsables de la conjugación de los polifenoles con glucurónidos. Esta enzima está presente en el retículo endoplásmico de una gran variedad de tejidos, aunque las principales responsables de esta acción en los polifenoles son las UGT de la familia UGT1A, predominantes en intestino, hígado y riñón²³⁴. Es en el hígado donde se darán predominantemente las conjugaciones con glucurónido. Las fenol sulfotransferasas (P-PST o SULT) son enzimas citosólicas que también están presentes en todos los tejidos. Existen también varias familias de esta enzima. Cabe resaltar la SULT1A1 predominante en hígado y la SULT1A3 presente en el colon y con mayor afinidad por los grupos catecol²³⁴. Las enzimas que catalizan las reacciones de acetilación (N-acetiltransferasas) y de conjugación con el glutatión (glutatión transferasas) no tienen demasiada importancia en el metabolismo de los polifenoles y su papel es minoritario²³⁶.

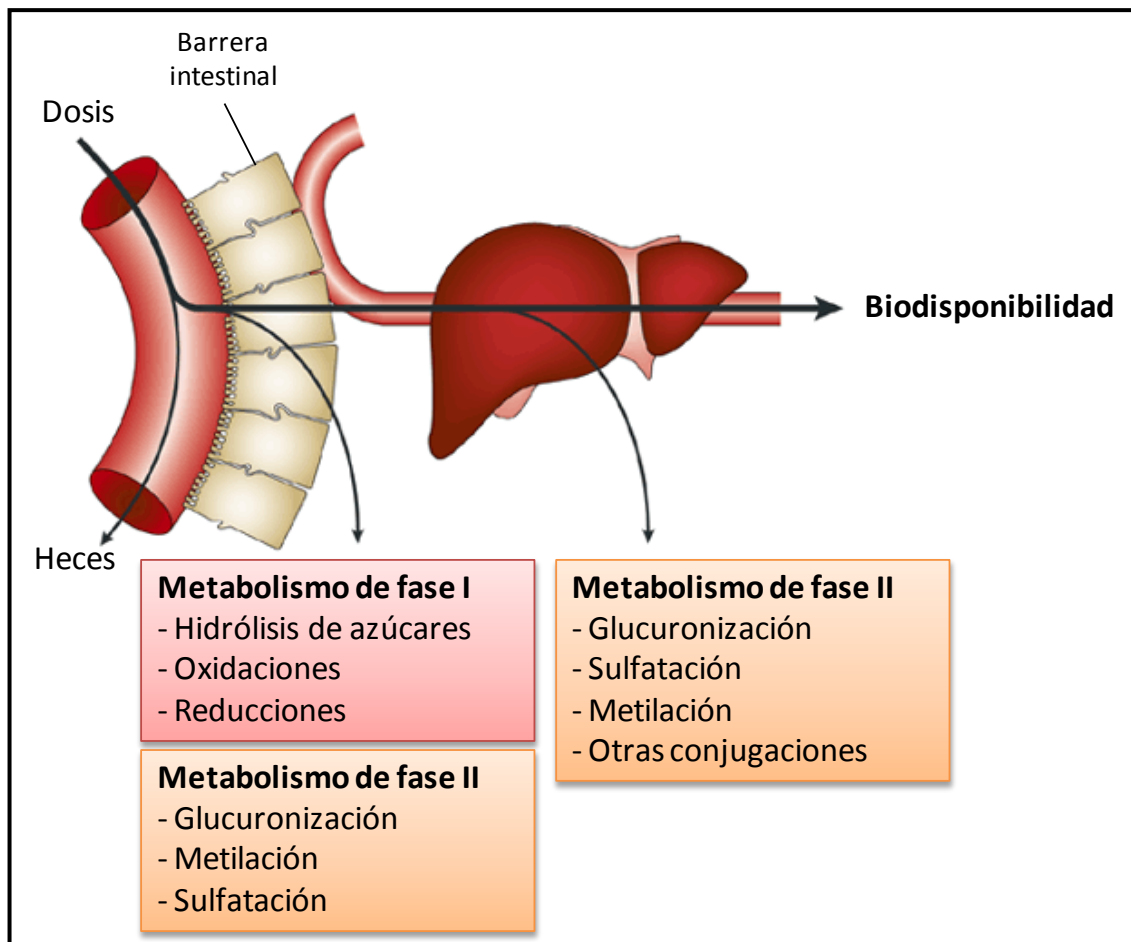


Figura 27. Absorción de polifenoles y metabolismo que sufren.

7.2. Farmacocinética y biodisponibilidad.

La farmacocinética se define, en términos generales, como el estudio de la evolución temporal de las concentraciones de un compuesto activo y sus metabolitos en el organismo tras la administración de una dosis determinada, lo que incluye su absorción, paso al torrente circulatorio, distribución a los diferentes tejidos y órganos y eliminación del organismo, además de la construcción de modelos adecuados para interpretar los datos obtenidos²³⁷.

La farmacocinética cuantifica los procesos de absorción, distribución y eliminación de un compuesto activo en el organismo. La medida de la concentración de dicho compuesto,



generalmente en plasma, a diferentes tiempos tras su administración, origina una curva de concentraciones plasmáticas vs tiempo²³⁸.

Las curvas de farmacocinética muestran directamente los valores de dos parámetros: la concentración máxima (C_{max}), y el tiempo máximo (t_{max}) que es el tiempo necesario para que se alcance C_{max} . La C_{max} va a depender de la dosis administrada y de la relación entre las constantes de velocidad de absorción (K_{abs}) y eliminación (K_{el}), mientras que el tiempo máximo es proporcional a la velocidad media de absorción y al tiempo de vida medio del compuesto ($t_{1/2}$) calculado como el $\ln 2/t_{max}$ (Figura 28). A partir de estas curvas también se obtiene información sobre el área bajo la curva (AUC), relacionada con la cantidad de compuesto activo que accede inalterado a la circulación sistémica.

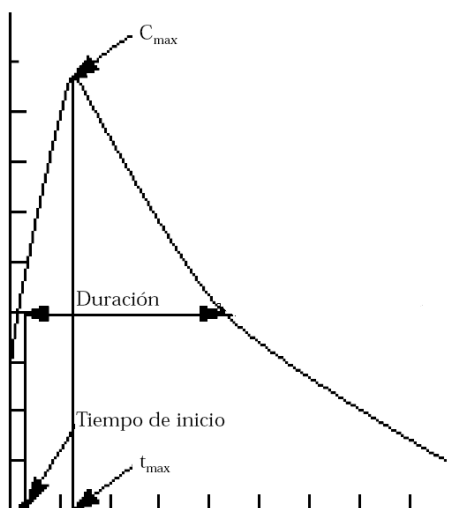


Figura 28. Curva de concentración plasmática frente al tiempo.

El concepto de biodisponibilidad, ampliamente utilizado en la actualidad, expresa la fracción de la dosis administrada que accede en forma inalterada a la circulación sistémica y la velocidad a la que se produce. La biodisponibilidad de un compuesto activo no depende sólo de la absorción sino también de aquellos procesos que disminuyen su entrada en el organismo denominados “efecto del primer paso” en los que el compuesto administrado se elimina durante el primer paso a través de la pared intestinal y el hígado.

En cuanto a los compuestos fenólicos, su absorción viene determinada por su estructura básica, el grado de glicosilación/acetilación, conjugación con otros compuestos fenólicos, masa molecular, grado de polimerización y solubilidad²³⁹. Por norma general, los polifenoles de bajo peso molecular, los taninos hidrolizables y algunas proantocianidinas



se absorben más fácilmente que aquellos polifenoles de elevado peso molecular, con alto grado de polimerización o aquellos que están unidos a proteínas o fibra²³⁹.

La distribución es el proceso mediante el cual el compuesto activo se incorpora desde la circulación sanguínea a los diferentes órganos y tejidos corporales. Los procesos de distribución son, en consecuencia, procesos cinéticos en los que se realiza una transferencia, en general reversible, del compuesto activo entre distintos compartimientos corporales. La distribución tisular depende de características del compuesto activo, del régimen de dosificación y de la situación fisiopatológica de quien lo consume. A su vez, las propiedades fisicoquímicas (peso molecular, coeficiente de distribución, pK_a) y las propiedades farmacocinéticas (volumen de distribución, velocidad de eliminación, grado de fijación a proteínas plasmáticas) también condicionan el acceso del compuesto activo a diferentes órganos y tejidos corporales.

Los compuestos activos se unen en diferentes grados a las proteínas plasmáticas en un proceso inmediato y de naturaleza reversible. Sólo la fracción no unida a proteínas presenta actividad farmacológica, es decir, sólo la fracción de principio activo que permanece libre en el plasma tiene capacidad para difundir a los espacios extravasculares.

La eliminación engloba los procesos que contribuyen a la desaparición del compuesto activo del organismo, es decir, la biotransformación (fase I y II del metabolismo) y la excreción.







BLOQUE I.

Cistus spp.







CAPÍTULO 1. High-performance liquid chromatography with diode array detection coupled to electrospray time-of-flight and ion-trap tandem mass spectrometry to identify phenolic compounds from a *Cistus ladanifer* aqueous extract.





High-performance Liquid Chromatography with Diode Array Detection Coupled to Electrospray Time-of-flight and Ion-trap Tandem Mass Spectrometry to Identify Phenolic Compounds from a *Cistus ladanifer* Aqueous Extract

S. Fernández-Arroyo,^b E. Barraón-Catalán,^{b,c} V. Micol,^b
A. Segura-Carretero^{a*} and A. Fernández-Gutiérrez^a

ABSTRACT:

Introduction – *Cistus ladanifer* is an aromatic shrub that is widespread in the Mediterranean region. The labdanum exudate is used in the fragrance industry and has been characterised. However, there is not enough information about the phenolic content of the raw plant, the aerial part of it being a very rich source of bioactive compounds.

Objective – Characterisation of the bioactive compounds of the raw plant and its aerial parts.

Methodology – High-performance liquid chromatography with diode array and electrospray ionisation mass spectrometric detection was used to carry out the comprehensive characterisation of a *Cistus ladanifer* shrub aqueous extract. Two different MS techniques were coupled to HPLC: time-of-flight mass spectrometry and tandem mass spectrometry.

Results – Many well-known compounds present in *Cistus ladanifer* were characterised, such as flavonoids, phenolic acids, ellagitannins, hexahydroxydiphenol and derivatives, and other compounds.

Conclusion – The method described simultaneously separated a wide range of phenolic compounds and the proposed characterisation of the major compounds of this extract was carried out. It is important to highlight that, to our knowledge, this is the first time that a *Cistus ladanifer* aqueous extract from the raw plant has been characterised. Copyright © 2009 John Wiley & Sons, Ltd.

Keywords: *Cistus ladanifer*; high-performance liquid chromatography; mass spectrometry; UV-vis; flavonoids; ellagitannins; hexahydroxydiphenol; phenolic acids

Introduction

The *Cistus ladanifer* shrub, also commonly known as rock rose or 'sticky jara', is a native and widespread species in the Mediterranean region (Teixera *et al.*, 2007; Andrade *et al.*, 2009) that belongs to the *Cistaceae* family. It is especially abundant in the Iberian Peninsula and northwestern Africa. This aromatic shrub is an important part of the semiarid-Mediterranean ecosystem and forms dense stands on siliceous soils (Robles *et al.*, 2003), colonising degraded areas and inhibiting the growth of other plants (Dias and Moreira, 2002), by restricting aerial growth of plants or inhibiting germination and growth of other species, due to its phytotoxicity to other plants and even to the soil (Chaves *et al.*, 2001a, b). The abundance of this plant is also due to its capacity to repopulates easily after wildfires (Ferrandis *et al.*, 1999).

Cistus ladanifer produces different types of secondary metabolites. Among them phenols, terpenes, alkaloids, polyacetylenes, fatty acids and steroids have been reported in the literature. Some of these compounds have been partly identified before (Chaves *et al.*, 2001a, b; Dias and Moreira, 2002; Andrade *et al.*,

2009). The phenolic and flavonoid fraction has been related to the reported antioxidant activity of *C. ladanifer* extracts (Andrade *et al.*, 2009).

C. ladanifer is also the main source of very valuable bee pollen in Spain and other Mediterranean countries (Ortiz, 1994). In addition, this pollen and its extract are rich in flavonoids which have exhibited significant antioxidant activity in several *in vitro* assays

* Correspondence to: A. Segura-Carretero, Department of Analytical Chemistry, University of Granada, Avda. Fuentenueva s/n, 18003 Granada, Spain. E-mail: ansegura@ugr.es

^a Department of Analytical Chemistry, University of Granada, Avda. Fuentenueva s/n, 18003 Granada, Spain

^b Molecular and Cellular Biology Institut (IBMC), Miguel Hernández University, Avenida de la Universidad s/n, 03202 Elche, Alicante, Spain

^c R&D Department of Endemic Biotech, S.L. C/ Collado de Novelda no. 3, 03640 Monóvar, Alicante, Spain



(Tomas *et al.*, 1992; Nagai *et al.*, 2002). The honey derived from this pollen has a unique and pleasant taste and a high economic value (Fuentes-Sánchez, 1996)

The plant also exudates a resin with a strong aromatic odour known as *labdanum*, which is highly appreciated in the fragrance industry. This exudate has shown strong inhibition of calcium transport in skeletal muscle (Sosa *et al.*, 2004) and contributes to inhibition of the germination of neighbouring plants (Chaves *et al.*, 2001a, b). Traditionally, it has been used from ancient times to treat diarrhea, dysentery, catarrh and menstruation difficulties. This resin is very rich in polyphenols and has been characterised in previous studies (Robles *et al.*, 2003; Gomes *et al.*, 2005). However, there is little information available about the polyphenolic content of the raw plant and its aerial part as a source of potential bioactive compounds.

Ecological cultivation practices and sustainable processes are increasing in importance and social acceptance and have focused on obtaining products with minimum environmental impact. Hence, the aim of this study was to characterise an aqueous extract from *Cistus ladanifer* obtained in the absence of organic solvents or chemicals and compatible with organic certification. In addition, the use of *C. ladanifer* as a raw material for the manufacture of polyphenolic extracts would eliminate part of the undesirable vegetable biomass in the forest regions, which poses a serious fire risk, especially in summer.

Here we present a complete and exhaustive analysis of an aqueous extract of *Cistus ladanifer* aerial parts using HPLC-DAD-ESI-TOF-MS/IT-MS/MS to characterise the polyphenolic fraction and other related compounds. This complete analysis of the composition of *Cistus ladanifer* may help in the future design and formulation of nutraceutical and cosmetic preparations and will be the base of new investigations into the activities of the various compounds found in *C. ladanifer*.

Experimental

Chemicals

All chemicals were of analytical reagent grade and used as received. Acetic acid and acetonitrile for HPLC were purchased from Fluka, Sigma-Aldrich (Steinheim, Germany) and Lab-Scan (Gliwice, Sowińskiego, Poland), respectively. Solvents were filtered using a Solvent Filtration Apparatus 58061 (Supelco, Bellefonte, PA, USA). Water was purified by a Milli-Q system from Millipore (Bedford, MA, USA).

Sample preparation

The aerial part of the raw plant of *Cistus ladanifer* was selected and crushed with a mechanical mill and then extracted with distilled water at 40°C with gentle agitation for 4 h. Then the samples were centrifuged at 2000 rpm, decanted and finally filtered through 0.45 µm filter before use. Then, samples were directly injected into the HPLC system.

Instrumentation

Analyses were carried out using an Agilent 1200 Series Rapid Resolution LC system (Agilent Technologies, Palo Alto, CA, USA), including a standard autosampler and a diode array detector. The HPLC column used was a Zorbax Eclipse Plus C₁₈ (1.8 µm, 150 × 4.6 mm). The HPLC system was coupled to a microTOF mass spectrometer (Bruker Daltonics, Bremen, Germany; see Bruker Daltonics technical note no. 008, 'Molecular formula determination under automation') equipped with an ESI interface. MS/MS analysis was performed using a Bruker Daltonics Esquire 2000 IT mass spectrometer (Bruker Daltonics, Bremen, Germany), also equipped with an ESI interface.

Chromatographic procedure and UV-vis conditions

The separation of the compounds from *C. ladanifer* aqueous extract was carried out at room temperature with a gradient elution program at a flow rate of 0.8 mL/min. The mobile phases consisted of acetic acid 0.5% (A) and acetonitrile (B). The following multi-step linear gradient was applied: 0 min, 0% B; 20 min, 20% B; 30 min, 30% B; 40 min, 50% B; 50 min, 75% B; 60 min, 100% B. The initial conditions were held for 10 min. The injection volume in the HPLC system was 15 µL. The UV-vis detection was performed in the 190–600 nm range.

ESI-TOF-MS detection

As the flow rate at chromatographic conditions was set at 0.8 mL/min, the use of a splitter of the flow was required for the coupling with the MS detector as the flow arriving at the ESI-TOF detector had to be 0.25 mL/min, in order to obtain reproducible results and stable spray. The HPLC system was coupled to a TOF mass spectrometer equipped with an ESI interface operating in negative ion mode using a capillary voltage of +4.5 kV. The other optimum values of the ESI-TOF parameters were drying gas temperature, 190°C; drying gas flow, 9 L/min and nebulising gas pressure, 2 bar. The detection was carried out considering a mass range of 50–1100 *m/z*.

The accurate mass data of the molecular ions were processed through the software DataAnalysis 3.4 (Bruker Daltonics), which provided a list of possible elemental formulas using Generate Molecular Formula Editor. This uses a CHNO algorithm, which provides standard functionalities such as minimum/maximum elemental range, electron configuration and ring-plus double bond equivalents, as well as a sophisticated comparison of the theoretical with the measured isotope pattern (σ value) for increased confidence in the suggested molecular formula. The widely accepted accuracy threshold for confirmation of elemental compositions has been established at 5 ppm (Bringmann *et al.*, 2005). Even with very high mass accuracy (<3 ppm in most of the cases), many chemically possible formulae are obtained depending on the mass regions considered. Therefore, high mass accuracy alone is not enough to exclude enough candidates with complex elemental compositions. The use of isotopic abundance patterns as a single further constraint removes >95% of false candidates. This orthogonal filter can condense several thousand candidates down to only a small number of molecular formulas.

During the development of the HPLC method, external instrument calibration was performed using a 74900-00-05 Cole Palmer syringe pump (Vernon Hills, IL, USA) directly connected to the interface, with a sodium formate cluster solution passing through containing 5 mM sodium hydroxide and 0.2% formic acid in water:isopropanol 1:1 v/v. The calibration solution was injected at the beginning of each run and all the spectra were calibrated prior to the compound identification. By using this method, an exact calibration curve based on numerous cluster masses each differing by 68 Da (NaCHO₂) was obtained. Because of the compensation of temperature drift in the TOF, this external calibration provided accurate mass values (better than 5 ppm) for a complete run without the need for a dual sprayer setup for internal mass calibration.

ESI-IT-MS/MS detection

The IT-MS spectrometer was run in the negative ion mode and the capillary voltage was set at 4000 V. IT instrument scanned at 50–1100 *m/z* range. The other parameters were dry temperature, 300°C; drying gas flow, 9 L/min; nebulising gas pressure, 30 psi. The instrument was controlled by a personal computer running Esquire NT software from Bruker Daltonics.

Results and Discussion

The base peak chromatogram from *C. ladanifer* by HPLC-ESI-TOF is shown in Fig. 1. The characterised compounds are presented in Table 1 identified with the numbers 1–36 considering the

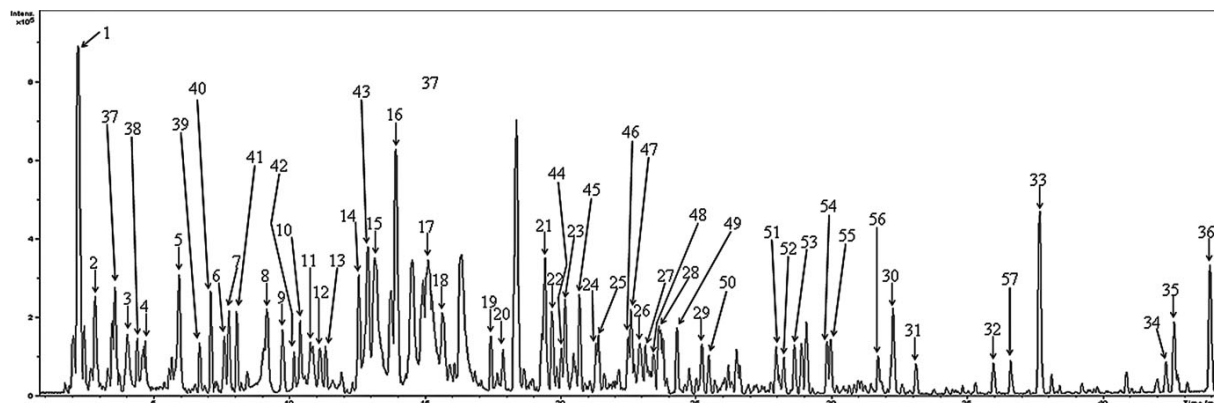


Figure 1. Base peak chromatogram of *Cistus ladanifer* aqueous extract.

elution order. In the present work, the phenolic compounds are classified into five groups: hexahydroxydiphenyl (HHDP) and derivatives, phenolic acids and derivatives, ellagic acid and derivatives, flavonoids and derivatives, and other compounds. All the compounds were characterised by the interpretation of their UV-vis absorbance band, the mass spectra obtained with the TOF-MS and the MS/MS spectra acquired with the IT-MS, and also taking into account the data provided by the literature.

Hexahydroxydiphenyl and derivatives

It has been reported that HHDP yields ellagic acid by spontaneous lactonisation (Arapitsas *et al.*, 2007). As there are many compounds derived from HHDP, we have summarised its derivatives in this section. Three isomers of hexahydroxydiphenyl- β -D-glucoside (peaks 3–5) have been identified. The fragmentation pattern in all cases resulted in two fragments at m/z 301 and 275. The fragment at m/z 301 represents the HHDP moiety (loss of glucose via cleavage of ester link and spontaneous lactonisation in ellagic acid). The loss of a CO group from the HHDP moiety produces the corresponding fragment at m/z 275. The fragment at m/z 421 found in peak 4 is caused by the loss of a group $C_2H_4O_2$ in glucose residue. Peak 12, corresponding to pedunculagin, showed fragments at m/z 481 (loss of one HHDP group), 301 and 275 (according to the fragmentation pathway described for peaks 3–5). Strictinin, assigned to peak 16, presented a fragment at m/z 301 obtained for spontaneous lactonisation of HHDP moiety.

Phenolic acids and derivatives

Peak 6 was characterised as gallic acid. The MS² spectrum provided a fragment at m/z 125, corresponding to the loss of a CO₂ molecule. Peaks 7 and 10 were determined as glucogallin isomers, with a fragmentation pattern at m/z 169 (corresponding to the loss of glucose moiety) and m/z 125 (decarboxylation of galloyl group). Peak 9 corresponded to gentsioid glucoside, with a MS/MS pattern at m/z 153 and 109 due to the loss of glucose moiety and CO₂ successively. Peak 11 was characterised as digalloyl- β -D-glucopyranoside. The fragmentation pattern is shown in Fig. 2(a). Peak 14 corresponded to uralenneoside, and its MS² spectrum showed two fragments at m/z 153 and 109 due to the loss of xilose residue and CO₂ successively. Finally, peak 19 was characterised as miriciaphenone B with a fragmentation pattern as shown in Fig. 2(b).

Ellagic acid and derivatives

Peaks 15 and 17 were identified as punicalagins isomers at m/z 1083.059. Three fragments at m/z 781, 601 and 301 were found, corresponding to cleavage of punicalagin to obtain punicalin, gallagic acid and ellagic acid successively, according to the proposed fragmentation pattern by Seeram *et al.* (2005). Peak 8 was identified as punicalin. Only one fragment at m/z 601 was obtained, which corresponded to gallagic acid (Seeram *et al.*, 2005). Peak 18 was identified as cornusiin B and its fragmentation pattern is shown in Fig. 3. Peaks 24 and 29 were identified as ellagic acid-7-xyloside and methylated ellagic acid-7-xyloside (ducheside A), respectively. The fragment obtained at m/z 301 in peak 24 and 315 in peak 29 corresponded to the loss of xylose moiety. This corresponded to the ellagic acid and methylated ellagic acid, respectively. Peak 26 was identified as ellagic acid. Its fragmentation pattern showed two fragments at m/z 257 (loss of CO₂) and 229 (successively loss of one CO group from the fragment at m/z 257).

Flavonoids

Thirteen peaks were identified as flavonoids. The ion found at m/z 350.066 (peak 13) corresponded to epigallocatechin, a flavan-3-ol. The MS² fragmentation at m/z 261 and 179 corresponded to the loss of CO₂ and C₆H₆O₃, respectively, from the precursor ion. The loss of C₆H₆O₃ was due to heterocyclic ring fission (Gu *et al.*, 2003).

Peaks 21, 23, 25, 27, 30, 31, 33 and 36 were identified as flavonols. Peaks 21 and 25 were both characterised as quercetin diglycosides. The fragments at m/z 463 and 301 found in the compound 21 were consistent with the loss of two hexose moieties successively. The MS/MS spectrum of peak 25 showed a fragment at m/z 301 corresponding to the loss of one hexose and one pentose groups simultaneously. The peak 27 was characterised as quercetin glucoside, with a fragmentation pattern at m/z 301 (loss of glucose) and 151 (via heterolytic cleavage). Peaks 23, 30 and 31 were characterised as kaempferol diglycosides. These three peaks presented the same fragmentation pattern at m/z 447 and 285, due to the loss of two hexose groups for peak 23, and the loss of rhamnosyl and hexosyl group for peaks 30 and 31. Peaks 33 and 36 were identified as kaempferol methylether and kaempferol dimethylether, respectively. The fragment at m/z 165 in peak 33 corresponded to the loss of C₈H₆O₂ (cleavage ^{1,3}A')

**Table 1.** Mass spectral and UV data negative mode in the *Cistus ladanifer* aqueous extract

Peak number	RT (min)	UV λ (nm)	[M - H] ⁻	MS/MS	Molecular formula	Error (ppm)	Sigma	Proposed compound
1	2.40	218	191.0556	161, 127, 85	C ₇ H ₁₁ O ₆	2.9	0.0134	Quinic acid
2	2.90	212	173.0455	93	C ₇ H ₉ O ₅	0.5	0.0095	Shikimic acid
3	4.10	257, 365	481.0624	301, 275	C ₂₀ H ₁₇ O ₁₄	0.0	0.0130	Hexahydroxydiphenyl-D-glucose (isomer)
4	4.70	257, 365	481.0625	421, 301, 275	C ₂₀ H ₁₇ O ₁₄	-0.2	0.0170	Hexahydroxydiphenyl-D-glucose (isomer)
5	6.00	257, 365	481.0625	301, 275	C ₂₀ H ₁₇ O ₁₄	-0.2	0.0044	Hexahydroxydiphenyl-D-glucose (isomer)
6	7.60	270	169.0144	125	C ₇ H ₉ O ₅	-1.1	0.0021	Galic acid
7	7.80	266	331.0677	169, 125	C ₁₃ H ₁₅ O ₁₀	-1.8	0.0084	Glucogallin (isomer)
8	9.20	218, 259, 380	781.0531	721, 601, 271	C ₃₄ H ₂₁ O ₂₂	-0.1	0.0029	Punicalin
9	9.80	261, 312	315.0722	225, 153, 109	C ₁₃ H ₁₅ O ₉	0.0	0.0076	Gentisoin glucoside
10	10.40	257, 378	331.0665	169, 125	C ₁₃ H ₁₅ O ₁₀	1.8	0.0075	Glucogallin (isomer)
11	10.80	257, 296, 378	483.0779	331, 169	C ₂₀ H ₁₉ O ₁₄	0.2	0.0088	Digaloi- β -D-glucopiranoside
12	11.10	258, 376	783.0680	481, 301, 275	C ₃₄ H ₂₃ O ₂₂	0.8	0.0080	Pedunculagin
13	11.40	260	305.0659	261, 179	C ₁₅ H ₁₃ O ₇	2.4	0.0056	Epigallocatechin
14	12.60	256, 310	285.0617	153, 109	C ₉ H ₁₃ O ₈	-0.3	0.0025	Uralennoiside
15	13.20	216, 261, 378	1083.0593	781, 601, 301	C ₄₈ H ₂₉ O ₃₀	0.0	0.0053	Punicalagin (isomer)
16	13.90	257, 376	633.0758	301	C ₂₇ H ₂₁ O ₁₈	-3.9	0.0089	Strictinin
17	15.10	216, 264, 378	1083.0595	781, 601, 301	C ₄₈ H ₂₉ O ₃₀	-0.2	0.0174	Punicalagin (isomer)
18	15.60	256, 376	1085.0745	783, 451, 425, 301	C ₄₈ H ₂₉ O ₃₀	0.4	0.0088	Cornusilin B
19	17.40	253	481.0947	437, 313, 169	C ₂₁ H ₂₁ O ₁₃	2.9	0.0177	Mirciaphenone B
20	17.80	260, 376	327.1071	165, 101	C ₁₅ H ₁₉ O ₈	3.9	0.0030	3,4'-Dihydroxypropiofenone-3- β -D-glucoside
21	19.40	269, 350	625.1414	463, 301	C ₂₇ H ₂₉ O ₁₇	-0.5	0.0142	Quercetin diglycoside
22	19.70	233, 258	415.1609	369, 311, 191, 149	C ₁₉ H ₂₇ O ₁₀	0.1	0.0031	Phenethyl- β -primeveroside
23	20.00	272, 351	609.1458	447, 285	C ₂₇ H ₂₉ O ₁₆	0.5	0.0054	Kaempferol diglycoside
24	21.30	253, 360	433.0407	301	C ₁₉ H ₁₃ O ₁₂	1.2	0.0054	Ellagic acid-7-xyloside
25	21.40	255, 355	595.1294	301	C ₂₆ H ₂₇ O ₁₆	1.7	0.0076	Quercetin diglycoside
26	23.00	254, 368	300.9986	257, 229	C ₁₄ H ₅ O ₈	1.3	0.0016	Ellagic acid
27	23.10	260, 360	463.0883	301, 151	C ₂₁ H ₁₉ O ₁₂	-0.1	0.0052	Quercetin glucoside
28	23.80	233, 280	505.2081	359	C ₂₆ H ₁₃ O ₁₀	-0.3	0.0023	Dihydrodehydrodiconiferil alcohol 9'-O- α -L-rhamnocide
29	25.20	245, 362	447.0558	315	C ₂₀ H ₁₅ O ₁₂	2.5	0.0068	Ducheside A
30	32.20	265, 346	593.1302	447, 285	C ₃₀ H ₂₅ O ₁₃	-0.2	0.0102	Kaempferol diglycoside
31	33.10	266, 346	593.1284	447, 285	C ₃₀ H ₂₅ O ₁₃	2.8	0.0163	Kaempferol diglycoside
32	35.90	262, 342	269.0448	231, 225, 191, 151, 107	C ₁₅ H ₉ O ₅	2.9	0.0084	Apigenin
33	37.60	266, 350	299.0562	255, 235, 201, 165, 109	C ₁₆ H ₁₁ O ₆	-0.4	0.0109	Kaempferol methylether
34	42.25	272, 336	283.0609	Not fragmented	C ₁₆ H ₁₁ O ₅	1.0	0.0198	Apigenin methylether (isomer)
35	42.60	266, 340	283.0613	Not fragmented	C ₁₆ H ₁₁ O ₅	-0.5	0.0178	Apigenin methylether (isomer)
36	43.90	266, 350	313.0718	Not fragmented	C ₁₇ H ₁₃ O ₆	-0.2	0.0036	Kaempferol dimethylether

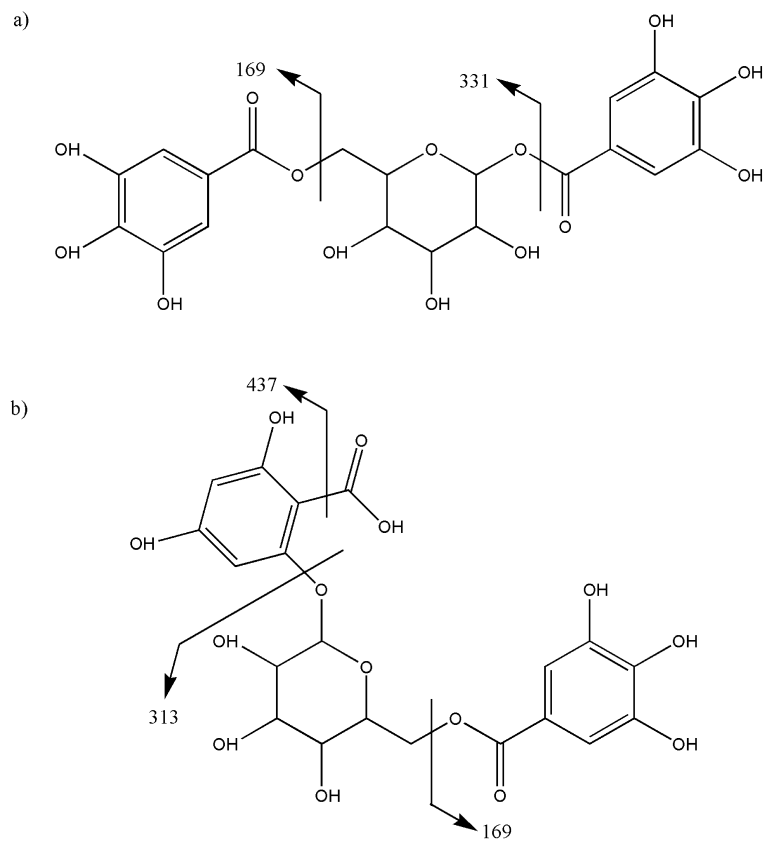


Figure 2. Fragmentation pattern for (a) digalloyl- β -D-glucopyranoside and (b) mirciaphenone B.

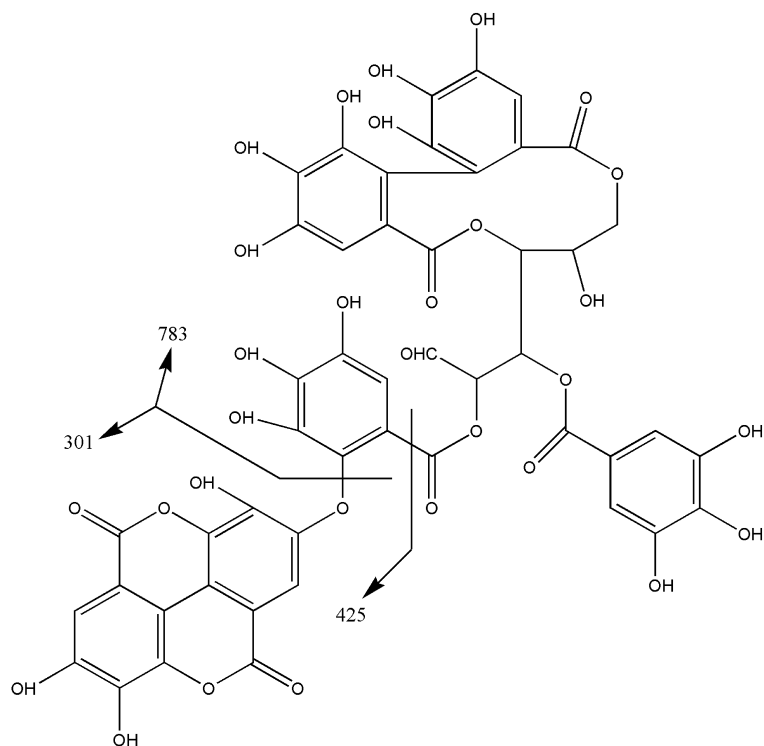


Figure 3. MS/MS spectra for cornusiin B.

**Table 2.** Unknown compounds from *C. ladanifer* aqueous extract

Peak number	RT (min)	UV bands λ (nm)	[M - H] ⁻	MS/MS fragments	Molecular formula	Error (ppm)	Sigma
37	3.60	230	337.0777	277	C ₁₂ H ₁₇ O ₁₁	-0.3	0.0024
38	4.40	220, 260	297.1190	Not fragmented	C ₁₁ H ₂₁ O ₉	0.5	0.0066
39	6.70	219	737.2373	705, 661, 529, 485, 449, 397, 337, 305, 265	C ₂₇ H ₄₅ O ₂₃	2.2	0.0090
40	7.10	219, 270	647.2056	605, 457, 397, 265	C ₂₄ H ₃₉ O ₂₀	-2.4	0.0077
41	8.10	219, 262	779.2476	719, 661, 601, 379, 283	C ₄₇ H ₃₉ O ₁₁	2.8	0.1714
42	10.20	221, 260, 378	279.1079	179, 117	C ₁₁ H ₁₆ O ₈	2.4	0.0055
43	12.90	222, 254, 374	469.0054	Not fragmented	C ₂₁ H ₉ O ₁₃	-1.2	0.0018
44	20.14	226, 270	479.1194	461, 313, 169	C ₂₂ H ₂₃ O ₁₂	0.2	0.0033
45	20.70	228, 276, 325	507.1137	463, 313, 169	C ₂₃ H ₂₅ O ₁₃	1.4	0.0088
46	22.50	233, 270	565.2287	550, 519, 419, 233, 202	C ₂₈ H ₃₇ O ₁₂	0.6	0.0040
47	22.60	231, 266, 335	431.0984	341, 311	C ₂₁ H ₁₉ O ₁₀	-0.1	0.0349
48	23.60	233, 274	509.2028	491, 461, 367, 311, 163	C ₂₅ H ₃₃ O ₁₁	-1.0	0.0061
49	24.30	233, 266	523.2181	475, 327	C ₂₆ H ₃₅ O ₁₁	0.8	0.0205
50	25.40	237, 265	447.0905	315, 225, 151	C ₂₁ H ₁₉ O ₁₁	6.1	0.0081
51	27.90	238, 261, 354	475.1230	460, 313	C ₂₃ H ₂₃ O ₁₁	3.3	0.0157
52	28.20	210, 238, 268	461.1089	341, 299	C ₂₂ H ₂₁ O ₁₁	0.1	0.0143
53	28.60	210, 236, 300	473.1443	307, 145	C ₂₄ H ₂₅ O ₁₀	2.3	0.0121
54	29.80	210, 238, 275	477.1402	313, 169	C ₂₃ H ₂₅ O ₁₁	0.2	0.0034
55	30.00	210, 238	445.2082	313, 293, 191, 161	C ₂₁ H ₃₃ O ₁₀	-0.6	0.0271
56	31.70	210, 238	447.2226	429, 373, 311, 251, 221, 191, 149, 131	C ₂₁ H ₂₅ O ₁₀	2.2	0.0080
57	36.55	—	339.2542	321, 279, 223, 179, 139	C ₂₀ H ₃₃ O ₄	-0.4	0.0054

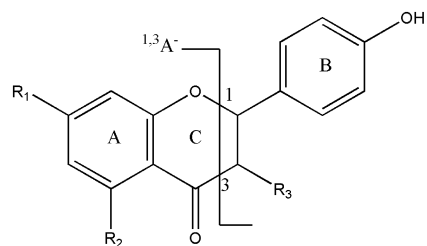


Figure 4. Cleavage via $1,3A^-$ for kaempferol methylether ($R_1 = OH$ or Me, $R_2 = OH$ or Me, $R_3 = OH$) and apigenin ($R_1 = OH$, $R_2 = OH$, $R_3 = H$).

(Fig. 4). This fragmentation pattern indicated that the methyl ether group is in position 5 or 7 on the A ring.

Peaks 32, 34 and 35 were characterised as flavones. Peak 32 was identified as apigenin. The MS/MS spectrum showed a fragment at m/z 151 (cleavage $1,3A^-$), m/z 107 (cleavage $1,3A^- - CO_2$) and m/z 225 ($[M - H - CO_2]^-$) (Fig. 4).

Other compounds

Peak 1 corresponded to quinic acid. The most important fragment of quinic acid appeared at m/z 127 ($[M - H - CO - 2H_2O]^-$). Peak 2 was identified as shikimic acid, with a fragmentation pattern at m/z 93 ($[M - H - CO_2 - 2H_2O]^-$). Peak 20 was identified as 3,4'-dihydroxypropiophenone-3- β -D-glucoside. The fragment obtained at m/z 165 corresponded to the loss of glucose moiety. Peak 22 was assigned to phenethyl- β -primeveroside. The fragment at m/z 369 corresponded to the loss of one CO and H₂O from the xylose group of primeveroside moiety. The fragment at m/z 311 corresponded to primeverose moiety. The cleavage of glucose showed a fragment obtained at m/z 191 and corresponded to the primeverose residue. Finally, at m/z 149, a fragment was obtained corresponding to the xylose group of primeveroside moiety. The oxygen from the glucosidic bond remained with the latter. Finally, peak 28 was identified as dihydrodehydrodiconiferyl alcohol 9'-O- α -L-ramnoside. Its fragmentation pattern showed a fragment at m/z 359 corresponding to the loss of the ramnose moiety.

Unknown compounds

Table 2 shows a list of compounds for which it was not possible to elucidate a structure even when the MS/MS experiment was carried out. There was not enough evidence to come up with a proposed structure. The table includes retention time, UV band, experimental m/z , MS/MS fragments, molecular formulae, errors and σ values.

Acknowledgements

This investigation has been supported by grants AGL2007-60778, P07-AGR-02619 and AGL2008-05108-C03-03 and a Torres-Quevedo (PTQ-08-03-08076) fellowship to E. Barrajon from MEC,

and grants IMIDTD/2006/523 and IMIDTA/2008/653 from IMPIVA (Valencian Regional Government). We also thank Químicas del Vinalopó SL and Endemic Biotech SL for their financial support and for providing us with the plant material. The authors also thank Inmaculada Rodríguez, Rosa Quirantes and Jesús Lozano from the Analytical Chemistry Department, University of Granada, and Lorena Funes from IBMC, for their invaluable help.

References

- Andrade D, Gil C, Breitenfeld L, Domingues F, Duarte AP. 2009. Bioactive extracts from *Cistus ladanifer* and *Arbutus unedo* L. *Ind Crop Prod* **30**: 165–167.
- Arapitsas P, Menichetti S, Vincieri SS, Romani A. 2007. Hydrolyzable tannins with the hexahydroxydiphenoyl unit and the m-depsidic link: HPLC-DAD-MS. Identification and model synthesis. *J Agric Food Chem* **55**: 48–55.
- Bringmann G, Kajahn I, Nuesüß C, Pelzing M, Laug S, Unger M, Holzgrabe U. 2005. Analysis of the glucosinolate pattern of *Arabidopsis thaliana* seeds by capillary zone electrophoresis coupled to electrospray ionization–mass spectrometry. *Electrophoresis* **26**: 1513–1522.
- Chaves N, Sosa T, Alias JC, Escudero JC. 2001a. Identification and effects of interaction phytotoxic compounds from exudate of *Cistus ladanifer* leaves. *J Chem Ecol* **27**: 611–621.
- Chaves N, Sosa T, Escudero JC. 2001b. Plant growth inhibiting flavonoids in exudate of *Cistus ladanifer* and in associated soils. *J Chem Ecol* **27**: 623–631.
- Dias LS, Moreira I. 2002. Interaction between water soluble and volatile compounds of *Cistus ladanifer* L. *Chemoecology* **12**: 77–82.
- Ferrandis P, Herrantz JM, Martínez-Sánchez JJ. 1999. Effect of fire on hard-coated Cistaceae seed banks and its influence on techniques for quantifying seed banks. *Plant Ecol* **144**: 103–114.
- Fuentes-Sánchez C. 1996. La miel de encina, jara y tomillo. *Agricultura: Revista agropecuaria* **769**: 690–691.
- Gomes PB, Mata VG, Rodrigues AE. 2005. Characterization of the Portuguese-grown *Cistus ladanifer* essential oil. *Journal of Essential Oil Research* **17**: 160–165.
- Gu L, Kelem MA, Hammerstone JF, Beecher G, Holden J, Haytowitz D, Prior RL. 2003. Screening of foods containing proanthocyanidins and their structural characterization using LC-MS/MS and thiolytic degradation. *J Agric Food Chem* **51**: 7513–7521.
- Nagai T, Inoue R, Inoue H, Suzuki N. 2002. Scavenging capacities of pollen extracts from *cistus ladaniferus* on autoxidation, superoxide radicals, hydroxyl radicals, and DPPH radicals. *Nutr Res* **22**: 519–526.
- Ortis PL. 1994. The Cistaceae as food resources for honeybees in South West Spain. *J Apic Res* **33**: 136–144.
- Robles C, Bousquet-Mélou A, Garzino S, Bonin G. 2003. Comparison of essential oil composition of two varieties of *Cistus ladanifer*. *Biochem Systemat Ecol* **31**: 339–343.
- Seeram N, Lee R, Hardy M, Heber D. 2005. Rapid large scale purification of ellagitannins from pomegranate husk, a by-product of the commercial juice industry. *Sep Purif Technol* **41**: 49–55.
- Sosa T, Chaves N, Alias JC, Escudero JC, Henao F, Gutiérrez-Merino C. 2004. Inhibition of mouth skeletal muscle relaxation by flavonoids of *Cistus ladanifer* L.: a plant defense mechanism against herbivores. *J Chem Ecol* **30**: 1087–1101.
- Teixeira S, Mendes A, Alves A, Santos L. 2007. Simultaneous distillation–extraction of high-value volatile compounds from *Cistus ladanifer* L. *Anal Chim Acta* **548**: 439–446.
- Tomas LF, Garcia GMM, Nieto JL, Tomas BF. 1992. Flavonoids from *Cistus ladanifer* bee pollen. *Phytochemistry* **31**: 2027–2029.









CAPÍTULO 2. A systematic study of the polyphenolic composition of aqueous extracts deriving from several *Cistus* genus species: evolutionary relationship.





A Systematic Study of the Polyphenolic Composition of Aqueous Extracts Deriving from Several *Cistus* Genus Species: Evolutionary Relationship

Enrique Barrajón-Catalán,^{a,b} Salvador Fernández-Arroyo,^c Cristina Roldán,^c Emilio Guillén,^b Domingo Saura,^a Antonio Segura-Carretero^c and Vicente Micol^{a*}

ABSTRACT:

Introduction – *Cistaceae* is a large family of shrubs widely spread over the Mediterranean area. It includes *Helianthemum*, *Halimium* and *Cistus* genus. *Cistus* genus contains approximately 20 species distributed in three subgenus. The essential oil of *Cistus* species has been thoroughly studied, but the polyphenolic composition of the aerial parts of the different *Cistus* species needs further characterisation.

Objective – To perform a comparative analysis of the qualitative and quantitative polyphenolic composition of the aerial parts of the most commonly distributed Spanish *Cistus* species in order to find a relationship between chemotype and subgenus.

Methodology – Thirteen aqueous extracts derived from 10 different *Cistus* species were analysed by using HPLC with diode array-detection coupled to electrospray ion trap mass spectrometry technique (HPLC-DAD-ESI-MS/MS). Their major compounds were identified and ellagitannins were quantified. Principal component analysis (PCA) was performed on the most relevant compounds to find out the statistical association between chemotype and variety.

Results – Three main groups of compounds were found, i.e. ellagitannins, flavonoids and phenolic acids derivatives. The polyphenolic profile was specific for each species, although the abundance of some compounds also varied depending on the soil type. Whereas *C. ladanifer*, *C. salviifolius*, *C. populifolius* and *C. libanotis* were specially rich in ellagitannins, *C. clusii*, *C. laurifolius* and *C. monspeliensis* contained significant amounts of flavonoids and much less ellagitannins. In contrast, *C. crispus*, *C. incanus* and *C. albidus* showed a polyphenolic profile mostly based on flavonoids. PCA analysis showed a strong relationship between *Cistus* subgenus and its chemotype based on the most relevant water-soluble polyphenolic compounds.

Conclusions – Chemical composition of the leaves' aqueous extracts from plants belonging to the *Cistus* genus is strongly related to their subgenus, in agreement to previous taxonomical and phylogenetic divisions. In contrast, soil and climate are less influencing factors. *Leucocistus* and *Halimioides* subgenus showed a higher content in ellagitannins. However, *Cistus* subgenus had higher flavonoid content. Copyright © 2011 John Wiley & Sons, Ltd.

Supporting information may be found in the online version of this article.

Keywords: *Cistaceae*; *Cistus*; HPLC-DAD-ESI-MS/MS; chemotype; ellagitannins; flavonoids

Introduction

The *Cistaceae* is a Mediterranean native family of almost 200 species of shrubs. Most members of this family are very fragrant and sweet-smelling, being much appreciated in the perfume industry and for ornamental purposes. Also, *Cistaceae* plants adapt easily to wildfires that destroy large forest areas, their seeds resisting and repopulating rapidly in the following season (Ferrandis *et al.*, 1999).

This family is formed by different genus, including *Helianthemum*, *Halimium* and *Cistus*. *Cistus* genus contains between 16 and 28 different species, depending on the source (Guzmán and Vargas, 2005). *Cistus* genus is divided into three subgenus: *Cistus*, *Halimioides* and *Leucocistus*. The first one includes purple flowered plants and the last two comprise species showing white flowers. Previously reported phylogenetic and taxonomic studies (Guzmán *et al.*, 2009) have pointed out the relationship between these subgenus, which is summarised in Fig. 1.

Some of the *Cistus* species are endemic and others are widespread in the Iberian Peninsula (Portugal and Spain), Canary Islands, northwestern Africa, Italy, Greece and Turkey (Andrade *et al.*, 2009). The species are disseminated over different areas of the Mediterranean area, but not all the species are distributed

* Correspondence to: V. Micol, Molecular and Cellular Biology Institute (IBMC), Miguel Hernández University, Avenida de la Universidad s/n, E-03202 Elche, Alicante, Spain. E-mail: vmicol@umh.es

^a Molecular and Cellular Biology Institute (IBMC), Miguel Hernández University, Avenida de la Universidad s/n, E-03202 Elche, Alicante, Spain

^b R&D Department of ENDEMIC BIOTECH, S.L. Monóvar, C/ Collado de Novelda no. 3, 03640 Monóvar, Alicante, Spain

^c Department of Analytical Chemistry, Faculty of Sciences, University of Granada, Granada 18071, Spain

following the same pattern. Thereby, each area is colonised by different *Cistus* species depending on climatological and soil conditions.

Traditional folk medicine has used *Cistus* species for anti-inflammatory, antiulcerogenic, wound healing, antimicrobial, cytotoxic and vasodilator remedies. Recent studies reveal some information on the possible candidate compounds for these effects, and new activities are being discovered and attributed to *Cistus* extracts. These include antimicrobial, antioxidant, antitumor, antinociceptive and analgesic effects (De Andres *et al.*, 1999; Küpeli and Yesilada, 2007; Barrajón-Catalán *et al.*, 2010).

Leucocistus subgenus is the most numerous of the *Cistus* genus. *Cistus ladanifer* (sticky or common rockrose) belongs to the *Leucocistus* subgenus. *C. ladanifer* contains several types of identified secondary metabolites (Chaves *et al.*, 1997, 2001). The resin or excretion of *C. ladanifer*, which holds much interest for the fragrance industry, has been characterised in detail (Dias *et al.*, 2005). Recently, we have reported a comprehensive study on the qualitative composition of the aqueous extract of *C. ladanifer* leaves (Fernandez-Arroyo *et al.*, 2010). The composition of hydroalcoholic extracts from *Cistus salviifolius* has also been reported (Kreimeyer *et al.*, 1998; Saracini *et al.*, 2005), but no information is available on its aqueous extracts. *Cistus populifolius* (male rockrose) has been used in folk medicine due to its anti-inflammatory, antiulcerogenic, wound healing, antimicrobial, cytotoxic, vasodilator and antispasmodic properties (De Andres *et al.*, 1999). Aqueous extracts of *C. populifolius* have been studied before for different biological activities, but its polyphenolic fraction has not been characterised in detail (De Andres *et al.*, 1999).

Previous studies on *Cistus laurifolius* (mountain rockrose), have reported anti-inflammatory and antinociceptive activities in ethanolic extracts containing different flavonols (Küpeli and Yesilada, 2007). The polyphenolic profile of methanolic extracts of *C. laurifolius* has also been studied (Sadhu *et al.*, 2006) but no study on the polyphenolic fraction of its aqueous extract has been reported. Moreover, catechin-related compounds were also identified in the aqueous extracts of *C. monspeliensis* (black rockrose; Pomponio *et al.*, 2003).

Three *Cistaceae* species belonging to the *Cistus* subgenus also grow in the Iberian Peninsula: *Cistus crispus* (curly rockrose), *Cistus incanus* (*Cistus creticus*, pink rockrose or hairy rockrose) and *Cistus albidus* (white rockrose). Some studies have reported the existence of monomeric and polymeric flavanols, gallic acid, rutin and diterpenes in several parts of *C. incanus* (Chinou *et al.*, 1994; Kreimeyer *et al.*, 1998; Santagati *et al.*, 2008). Previous studies have shown the presence of oligomeric proanthocyanidins in *C. albidus* (Qa'dan *et al.*, 2003), but no systematic analysis has been performed before on the leaves of this plant. No previous reports on the composition of *C. crispus* are available.

Finally, there are two *Cistaceae* belonging to the *Halimioides* subgenus and growing in the Iberian Peninsula: *Cistus libanotis* (Lebanon rockrose) and *Cistus clusii*. This latter has been traditionally used as an anti-inflammatory (Guinea *et al.*, 1990) and hair growth remedy (Stübing and Peris, 1998). No previous reports have been found on the composition of the aerial parts of these plants.

Most previous studies on *Cistus* have been focused on the essential oil composition, due to the interest of these plants for perfumery. However, few studies have reported the polyphenolic composition of *Cistus* species. Here we present a comparative qualitative and quantitative study of the composition of aqueous extracts from the aerial parts of 10 out of 12 *Cistus* species grown in Spain. The studied species belong to three different *Cistus* subgenus (Table 1), including *C. ladanifer*, *C. salviifolius*, *C. populifolius*, *C. laurifolius*, *C. monspeliensis*, *C. crispus*, *C. incanus*, *C. albidus*, *C. libanotis* and *C. clusii*. The composition of these extracts was analysed through HPLC with diode array detection coupled to electrospray and ion-trap mass spectrometry. A comparative quantitation of the identified ellagitannins was performed on the

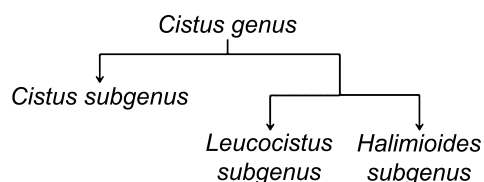


Figure 1. Taxonomic relationship between different subgenus contained in *Cistus* genus from the *Cistaceae* family.

Table 1. Information of the subgenus, soil, climate and location shown in Fig. 2 of the different *Cistus* samples analysed in the study

Species	Subgenus	Soil	Climate	Location
<i>Cistus ladanifer</i> (1)	<i>Leucocistus</i>	Volcanic sandstone	Continental	A
<i>Cistus ladanifer</i> (2)	<i>Leucocistus</i>	Volcanic sandstone*	Continental	A*
<i>Cistus salviifolius</i> (1)	<i>Leucocistus</i>	Volcanic sandstone	Continental	A
<i>Cistus salviifolius</i> (2)	<i>Leucocistus</i>	Siliceous	Wet Mediterranean	B
<i>Cistus populifolius</i>	<i>Leucocistus</i>	Siliceous	Wet Mediterranean	D
<i>Cistus laurifolius</i>	<i>Leucocistus</i>	Calcareous	Mediterranean	E
<i>Cistus monspeliensis</i>	<i>Leucocistus</i>	Siliceous	Wet Mediterranean	B
<i>Cistus crispus</i>	<i>Cistus</i>	Volcanic sandstone	Continental	A
<i>Cistus incanus</i>	<i>Cistus</i>	Calcareous	Wet Mediterranean	C
<i>Cistus albidus</i> (1)	<i>Cistus</i>	Limy	Dry Mediterranean	D
<i>Cistus albidus</i> (2)	<i>Cistus</i>	Siliceous	Wet Mediterranean	B
<i>Cistus libanotis</i>	<i>Halimioides</i>	Volcanic sandstone	Continental	A
<i>Cistus clusii</i>	<i>Halimioides</i>	Limy	Dry Mediterranean	B

* A more mineralised soil.

Polyphenolic Characterization of *Cistus* Aqueous Extracts

studied species. The relationship between the chemotype, based on the polyphenolic composition of the species, and their taxonomical classification is proposed. In addition, the composition of some of the species studied here is being reported for the first time.

Experimental

Extracts processing

Cistus plant materials were obtained from natural parks or reserves of Ciudad Real, Valencia and Alicante provinces (Spain) in early spring, according to flowering time and reserves' rules (Fig. 2). In all cases, fresh aerial parts were selected and washed for subsequent processing. This vegetable material was first crushed using a mechanical mill to a maximum size of 3–5 mm and then extracted with distilled water at a temperature below 65°C, with gentle agitation for approximately 2 h and a plant–solvent ratio of 1:5. After that, the material was filtered using a Büchner device, and then centrifuged to eliminate solid insoluble components. The extracts were concentrated by rotatory evaporation, and kept at 4°C until use. Although other alternative solvents (ethanol, methanol) were tested, water was selected as the extracting solvent choice, for ecological and environmental reasons.

HPLC-DAD-ESI-MS/MS

The different *Cistaceae* extracts were analysed and quantitated using an Agilent LC 1100 series (Agilent Technologies, Inc., Palo Alto, CA, USA) controlled by Chemstation software and equipped with a pump, autosampler, column oven and UV–vis diode array detector. The HPLC instrument was coupled to an Esquire 3000+ (Bruker Daltonics, GmbH, Germany) mass spectrometer equipped with an ESI source and ion trap mass analyser, and controlled by Esquire control and data analysis software. A Merck LiChrospher 100 RP₁₈, 5 µm, 250 × 4 mm (i.d.) column was used for analytical purposes.

Separation was carried out using a linear gradient protocol as previously reported (Fernandez-Arroyo *et al.*, 2010). For the accurate performance of the LC-MS pump, 10% organic solvent was premixed in the water phase. The flow rate was 0.5 mL/min. Diode-array detection was set at 280, 320 and 340 nm. Mass spectrometry operating conditions were optimised in order to achieve maximum sensitivity values. The ESI source was operated in negative mode to generate [M – H][–] ions using the following conditions: desolvation temperature at 360°C and vaporiser temperature at 400°C; dry gas (nitrogen) and nebuliser were set at 12 L/min

and 70 psi, respectively. The MS data were acquired as full-scan mass spectra at 50–1100 *m/z* using 200 ms for collection of the ions in the trap.

Identification of the main compounds was performed by HPLC-DAD analysis using a home-made library of phenolic compounds and comparing the retention times, UV spectra and MS/MS data of the peaks in the samples with those of authentic standards or data reported in the literature (Fernandez-Arroyo *et al.*, 2010). These compounds were divided into three structure-related categories for convenience. The first category was gallic acid, ellagic acid and gallo/ellagitannins (Table 2). The second one was composed of flavonoids (Table 3), and the last was formed by phenolic acids derivatives (Table 4). The chromatograms at 280 nm, as the most representative wavelength, of the different species are shown in Figs 3–5.

Quantitation of punicalagins content was performed using punicalagin commercial standard (Phytolab, Vestenbergsgreuth, Germany). The software ChemStation for LC 3D (Agilent Technologies Life Sciences and Chemical Analysis, Waldbronn, Germany) was used for quantitation purposes. The linearity range of the responses was determined on eight concentration levels (ranging from 0.25 µg/mL to 0.25 mg/mL) with three injections for each level. Calibration graphs for the quantitative evaluation of the compounds were performed by means of a six-point regression curve ($r^2 > 0.996$).

Statistical analysis

To analyse the relationship between the abundance of the analysed phenolic compounds and *Cistus* subgenus, first we selected those compounds with a stronger statistical association between the abundance of the compound and the *Cistus* specie. Then, principal component analysis (PCA) was applied to the abundance of the selected compounds. The selection of the compounds was based on a chi-square test performed over each compound. Two categorical variables were defined: *Cistus* subgenus (*Leucocistus*, *Cistus* or *Halimoides*) and abundance of the compound (area obtained by HPLC-MS, above or below a given threshold). Threshold was selected as that maximising χ^2 , since higher χ^2 values imply a strong association between the categorical variables. Then, the selected compounds were those exhibiting the highest χ^2 . Based on this selection criterion, each *Cistus* sample was represented as a vector, where each component was HPLC-MS area for each one of the selected compounds. Finally, PCA analysis was applied to the areas of the selected compounds.

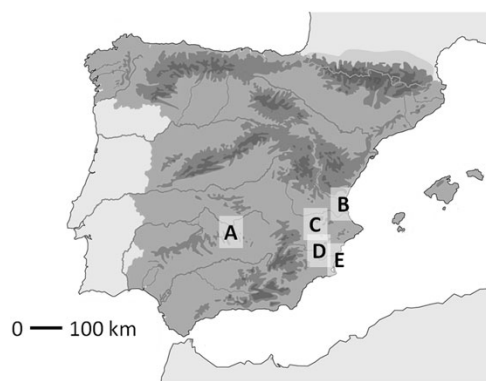


Figure 2. Locations of the different areas of Spain from where *Cistus* specimens were collected. (A) Continental localisation in Ciudad Real province; (B) mountain area in Valencia province; (C) southern mountain area in Valencia province; (D) semidesertic area in Alicante province; (E) Mediterranean area in Alicante province.

Table 2. Gallic and ellagic acids, and gallo/ellagitannins in *Cistus* extracts (E)

Species	Peak number								
	E1	E2	E3	E4	E5	E6	E7	E8	E9
<i>Cistus ladanifer</i> (1)	+	+	+	+	+	–	–	+	–
<i>Cistus ladanifer</i> (2)	+	+	+	+	–	–	–	+	–
<i>Cistus salviifolius</i> (1)	+	+	+	+	–	+	–	+	–
<i>Cistus salviifolius</i> (2)	+	+	+	+	+	+	–	+	–
<i>Cistus populifolius</i>	+	+	+	+	+	+	–	+	+
<i>Cistus laurifolius</i>	+	+	+	+	–	–	+	+	–
<i>Cistus monspeliensis</i>	+	+	+	–	–	–	–	+	–
<i>Cistus crispus</i>	+	–	–	–	–	–	–	+	–
<i>Cistus incanus</i>	+	–	–	–	–	–	–	+	–
<i>Cistus albidus</i> (1)	+	–	–	–	–	–	+	+	+
<i>Cistus albidus</i> (2)	+	–	–	–	–	–	–	+	–
<i>Cistus libanotis</i>	+	+	+	+	–	+	–	+	–
<i>Cistus clusii</i>	+	+	+	+	–	–	–	+	–

E1, gallic acid; E2, punicalin; E3, punicalagin; E4, punicalagin-gallate; E5, cornusii B; E6, 7-xyloside ellagic acid; E7, pedunculagin; E8, Hexahydroxydiphenol-glucose; E9, glucogallin. Peak labels in the table correspond to those shown in the chromatograms.

**Table 3.** Flavonoids-related compounds in *Cistus* extracts (F)

Species	Peak number																
	F2	F3	F4	F5	F6	F7	F8	F9	F10	F11	F12	F13	F14	F15	F16	F17	
<i>Cistus ladanifer</i> (1)	+	-	-	-	-	-	-	-	-	-	-	-	-	-	-	-	
<i>Cistus ladanifer</i> (2)	-	-	-	-	-	-	-	-	-	-	-	-	-	-	-	-	
<i>Cistus salviifolius</i> (1)	-	+	-	-	-	-	-	-	-	+	-	+	-	-	-	-	
<i>Cistus salviifolius</i> (2)	-	+	-	-	-	-	-	-	-	+	-	+	-	-	-	-	
<i>Cistus populifolius</i>	-	+	-	-	-	-	-	-	-	-	-	-	-	-	-	-	
<i>Cistus laurifolius</i>	-	+	-	-	-	-	-	+	-	-	+	+	-	-	-	+	
<i>Cistus monspeliensis</i>	+	-	-	-	-	-	-	-	-	-	-	-	-	-	-	+	
<i>Cistus crispus</i>	-	+	-	-	-	-	+	+	-	-	-	+	+	-	-	+	
<i>Cistus incanus</i>	-	-	-	+	-	+	+	+	-	-	+	-	+	+	+	+	
<i>Cistus albidus</i> (1)	+	-	-	-	-	+	+	+	+	-	+	-	+	+	-	+	
<i>Cistus albidus</i> (2)	+	-	-	-	-	+	+	+	+	-	+	-	+	+	-	+	
<i>Cistus libanotis</i>	-	-	-	-	-	-	-	-	-	-	-	-	-	-	-	-	
<i>Cistus clusii</i>	-	-	+	-	+	+	-	-	-	-	-	-	-	+	-	-	

F2, apigenin diglucoside; F3, quercetin glucoside; F4, kaempferol diglucoside; F5, kaempferol 3-O-rutinoside; F6, isorhamnetin-O-rutinoside; F7, rutin; F8, (-)-(epi)catechin; F9, (-)-(epi)gallocatechin; F10, quercetin 3-O-(2'-cumaroyl) rutinoside; F11, (-)-(epi)gallocatechin gallate; F12, quercitrin; F13, myricetin hexoside; F14, (-)-(epi)catechin-(epi)gallocatechin dimer; F15, (-)-(epi)gallocatechin-(epi)gallocatechin dimer; F16, quercetin-3-O-rutinoside-7-O-hexoside or quercetin-3-O-(2'-caffeoyl)-rutinoside; F17, myricitrin. Peak labels in the table correspond to those shown in the chromatograms.

Table 4. Phenolic acids derivatives (O)

Species	Peak number								
	O2	O3	O4	O5	O6	O7	O8	O9	
<i>Cistus ladanifer</i> (1)	-	-	-	-	-	-	-	-	
<i>Cistus ladanifer</i> (2)	-	-	-	-	-	-	-	+	
<i>Cistus salviifolius</i> (1)	-	-	-	-	-	-	-	+	
<i>Cistus salviifolius</i> (2)	-	-	-	-	-	-	-	+	
<i>Cistus populifolius</i>	-	-	-	-	-	-	+	-	
<i>Cistus laurifolius</i>	-	-	+	+	-	+	+	-	
<i>Cistus monspeliensis</i>	-	+	-	-	-	+	+	+	
<i>Cistus crispus</i>	+	-	-	-	-	+	-	-	
<i>Cistus incanus</i>	-	-	-	-	-	+	-	-	
<i>Cistus albidus</i> (1)	-	-	-	-	+	+	-	-	
<i>Cistus albidus</i> (2)	-	-	-	-	+	+	-	-	
<i>Cistus libanotis</i>	-	-	-	-	-	-	-	-	
<i>Cistus clusii</i>	-	-	-	-	-	+	+	+	

O2, caffeoyl-quinic acid; O3, hydroxy-ferulic acid hexoside; O4, 3-p-coumaroyl-quinic acid; O5, myrciaphenone B; O6, hydroxy-ferulic acid rhamnoside; O7, uralennoiside; O8, gentisoyl glucoside; O9, 3,4'-dihydroxypropiofenone-3-β-D-glucoside. Peak labels in the table correspond to those shown in the chromatograms.

Results and Discussion

Leucocistus subgenus

***Cistus ladanifer*.** Two different samples of *C. ladanifer* were analysed, both deriving from a volcanic sandstone soil located in a continental and warm area of Ciudad Real, Spain (place A, Fig. 2). Sample 1 derived from a less mineralised soil than sample 2 according to natural park staff. Their chromatograms were quite similar (Fig. 3A) and showed abundance of hydrolysable tannins

derived from gallic and ellagic acids (Table 2). Peak E1 was identified as gallic acid, which showed a base peak at m/z 169 corresponding to $[M - H]^-$ and a fragment ion at m/z 125 ($[M - H - 44]^-$). Peak E2, which performs as a doublet peak, was identified as punicalin, which exhibited $[M - H]^-$ ion at m/z 781, with main fragment ions at m/z 601 and m/z 301 (Gil *et al.*, 2000). Several peaks, all labelled as E3, exhibited the same base peak with a parental ion at m/z 1083, and fragment ions at m/z 781, 601 and 301. Therefore, these peaks were assigned to punicalagin isomers. Another group of peaks, labelled as E4, exhibited a parental ion at m/z 1251 and were assigned to punicalagin gallate, which showed a fragmentation profile with main fragments at m/z 1207, 1083 and 603 (Saracini *et al.*, 2005). The peak numbered as E8 was identified as hexahydroxydiphenoyl-D-glucose (HHDP-Glc) and showed a parental ion at m/z 481, with fragments at m/z 301 and 275. Compounds E2, E3, E4 and E8, which belonged to the ellagitannins family, were present in both samples of *C. ladanifer* (Fernandez-Arroyo *et al.*, 2010). Sample 1 (grey trace in Fig. 3A), obtained from the poorest soil (less mineralised), showed a peak labelled as E5, identified as cornusini B, showing a parental ion at m/z 1085, and fragments at m/z 783, 451 and 301 (Fernandez-Arroyo *et al.*, 2010). Sample 1 also showed a flavone structure (peak F2) tentatively assigned to a diglycosylated apigenin with a parental ion at m/z 593, and fragments at m/z 473 and 353 (Parejo *et al.*, 2004). Flavonoids have been also found in excretions of *C. ladanifer* leaves, but most of them were aglycones or methylated forms (Chaves *et al.*, 1997, 2001). Sample 2, obtained from a richer soil, presented a compound belonging to the phenolic acids derivatives category (peak O9) identified as 3,4'-dihydroxypropiofenone-3-β-D-glucoside, with a parental ion at m/z 327 and main fragment at m/z 165. These results confirm those previously reported showing that ellagitannins are the most significant family of compounds present in *C. ladanifer* aqueous extracts (Fernandez-Arroyo *et al.*, 2010). Considering that samples 1 and 2 derived from different soil types and showed similar polyphenolic profile, it may be concluded that soil is a less influential factor in the composition of *C. ladanifer*.

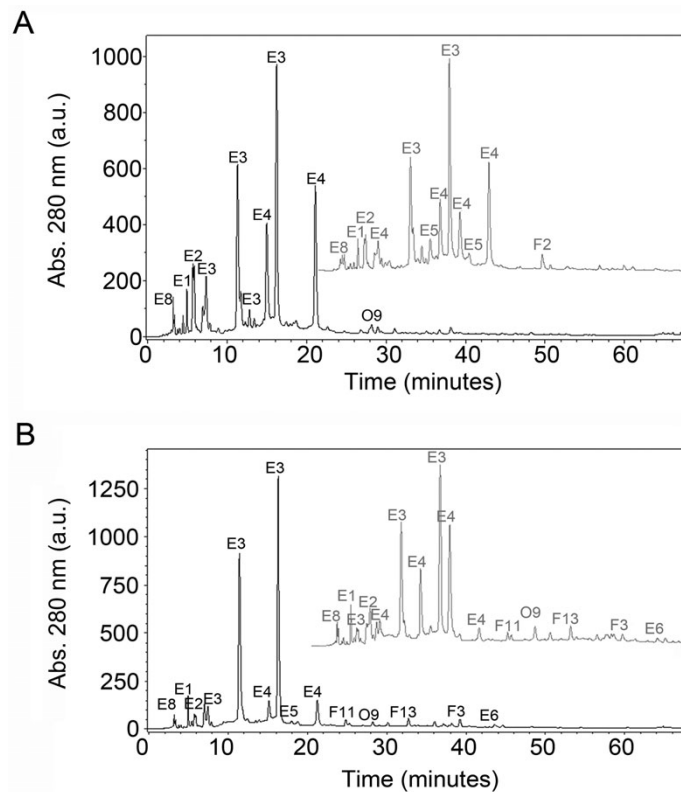


Figure 3. HPLC-DAD profiles at 280 nm of *Cistus* species belonging to the *Leucocistus* subgenus. (A) *C. ladanifer* sample 1, from volcanic sandstone soil (grey trace) and *C. ladanifer* sample 2, from a more mineralised volcanic sandstone soil (black trace) (A in Fig. 2). (B) *C. salviifolius* sample 1 from volcanic sandstone soil, (A in Fig. 2) (grey trace) and *C. salviifolius* sample 2, from a siliceous soil, (B in Fig. 2) (black trace). Profiles in each box show the same time/absorbance scales.

***Cistus salviifolius*.** Two different samples were analysed, one of them derived from the continental and warm area of Ciudad Real (place A in Fig. 2), grown on a volcanic sandstone soil (sample 1). The other one (sample 2) was obtained from a siliceous soil of a mountain area in Valencia (place B, Fig. 2), referred to as 'wet Mediterranean' in Table 2, more humid and moderate. As occurred with *C. ladanifer*, HPLC profiles of both *C. salviifolius* samples (Fig. 3B) were qualitatively similar, but some quantitative differences were clearly found, especially regarding the ellagitannins group. Gallic acid (E1) and HHDP-Glc (E8) were present as occurred in all *Cistus* species studied. In addition, punicalin, punicalagin and punicalagin gallate (peaks E2, E3 and E4 respectively) were present in both samples, while cornusiin B (E5) was only detectable in the sample from clay soil. Another additional ellagitannin was identified in both samples (E6), which was assigned to 7-xyloside ellagic acid, with a parental ion at m/z 433 and a fragment at m/z 301 (Fernandez-Arroyo *et al.*, 2010).

Flavonoids were more abundant in *C. salviifolius* than in *C. ladanifer*. Two compounds with flavanol backbone were identified in both *C. salviifolius* samples. The compound labelled as F3, identified as quercetin-glucoside, showed a parental ion at m/z 463 and two main fragments at m/z 301 and 151 (Fernandez-Arroyo *et al.*, 2010). Compound F13 was assigned to myricetin-hexoside, which showed a parental ion at m/z 479 and fragments at m/z 316, 271 and 179 (Määttä *et al.*, 2003).

A flavanol was also identified (F11) and assigned to (–)-epigallocatechin gallate (parental ion at m/z 457, with fragments at m/z 305 and 169; Del Rio *et al.*, 2004). Finally, both *C. salviifolius* samples contained, as seen for *C. ladanifer*, 3,4'-dihydroxypropiofenone-3- β -D-glucoside (O9). Most of these compounds were previously reported in *C. salviifolius* hydroalcoholic extracts, what confirms our results (Saracini *et al.*, 2005). The quantitative differences observed between the two samples reveal that soil and/or climate may have some influence on the polyphenolic composition of this plant.

***Cistus populifolius*.** The plant analysed in this study derived from a mountain area located in Valencia province (place B, Fig. 2). *C. populifolius* contained gallic acid, HHDP-Glc and a great variety of ellagitannins (Fig. 4A), including punicalin, punicalagin, punicalagin gallate, cornusiin-B and 7-xyloside ellagic (peaks E2–6). A new gallotannin was identified as glucogallin (labelled as E9), with a parental ion at m/z 331 and fragmentation at m/z 169 and 125 (Fernandez-Arroyo *et al.*, 2010). The compounds quercetin glucoside (F3) and gentsioglucoside (O8) were also detected in this aqueous extract. As occurred to *C. ladanifer*, *C. populifolius* aqueous extracts exhibited low flavonoids content, but were very rich in ellagitannins. Both species had the lowest content in flavonoids (flavanols and flavonols) of this study.

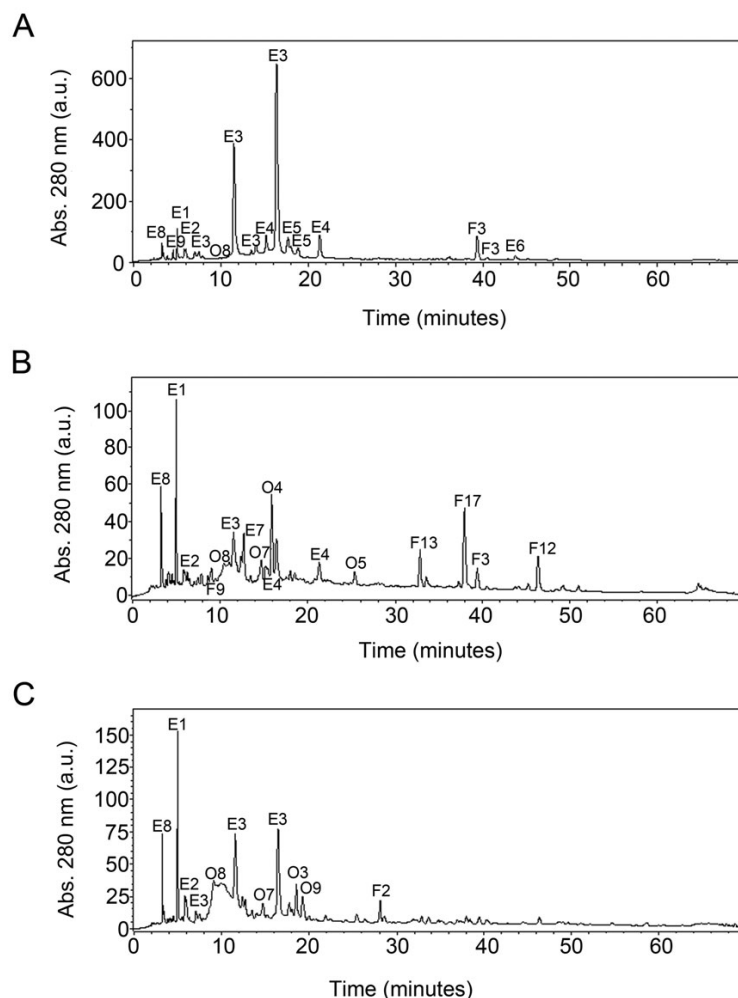


Figure 4. HPLC-DAD profiles at 280 nm of *C. populifolius* (A), *C. laurifolius* (B) and *C. monspeliensis* (C) aqueous extracts (all belonging to *Leucocistus* subgenus).

Cistus laurifolius

Here, a plant growing on calcareous soil located in the interior of Alicante province (place D, Fig. 2) was analysed. Gallic acid and HHDP-Glc were present and accompanied by the ellagitannins punicalin, punicalagin and punicalagin gallate (peaks E2, E3 and E4; Fig. 4B). Another ellagitannin was identified as pedunculagin (E7), with a parental ion at m/z 783, and fragments at m/z 481, 301 and 275 (Fernandez-Arroyo *et al.*, 2010). Several flavonoids were also identified in this extract. The flavanol (-)-(epi)gallocatechin was identified (F9), with a parental ion at m/z 305 and main fragments at m/z 261 and 179 (Fernandez-Arroyo *et al.*, 2010). Several flavonols were identified: quercitrin (F12), with a parental ion at m/z 447 and main fragments at m/z 301 and 179 (Gao *et al.*, 2009); myricetin rhamnoside or myricitrin (F17) (MassBank Record PR100670), with a parental ion at m/z 463 and main fragments at m/z 316, 271, 179 and 151; quercetin glucoside (F3); and myricetin hexoside (F13). Although the profile of flavonoids was not identical to those previously reported for extracts obtained with

organic solvents (Sadhu *et al.*, 2006; K3peli and Yesilada, 2007), they shared some similarities.

In the third category of compounds, peak O7 was assigned to uralennoiside, with parental ion at m/z 285 and main fragments at m/z 153 and 109; gentisoyl glucoside (O8) with a parental ion at m/z 315 and fragments at m/z 153 and 109; *p*-coumaroylquinic acid (O4) showing a parental ion at m/z 337 and main fragment at m/z 163 (Gao *et al.*, 2009); and myrciaphenone-B (O5) with a parental ion at m/z 481 (Fernandez-Arroyo *et al.*, 2010).

***Cistus monspeliensis*.** Qualitatively, *C. monspeliensis* extract (mountain area B in Valencia, Fig. 2) looked very similar to that of other *Leucocistus* species (Fig. 4C), especially *C. laurifolius*, presenting gallic acid, HHDP-Glc and ellagitannins such as punicalin and punicalagin (peaks E1, E2, E3 and E8). The diglycosylated apigenin (F2) was the only flavonoid identified. Catechins previously reported in other studies (Pomponio *et al.*, 2003) were not found in our study, probably due to differences in the extractive procedure. Among phenolic acid derivatives, uralennoiside,

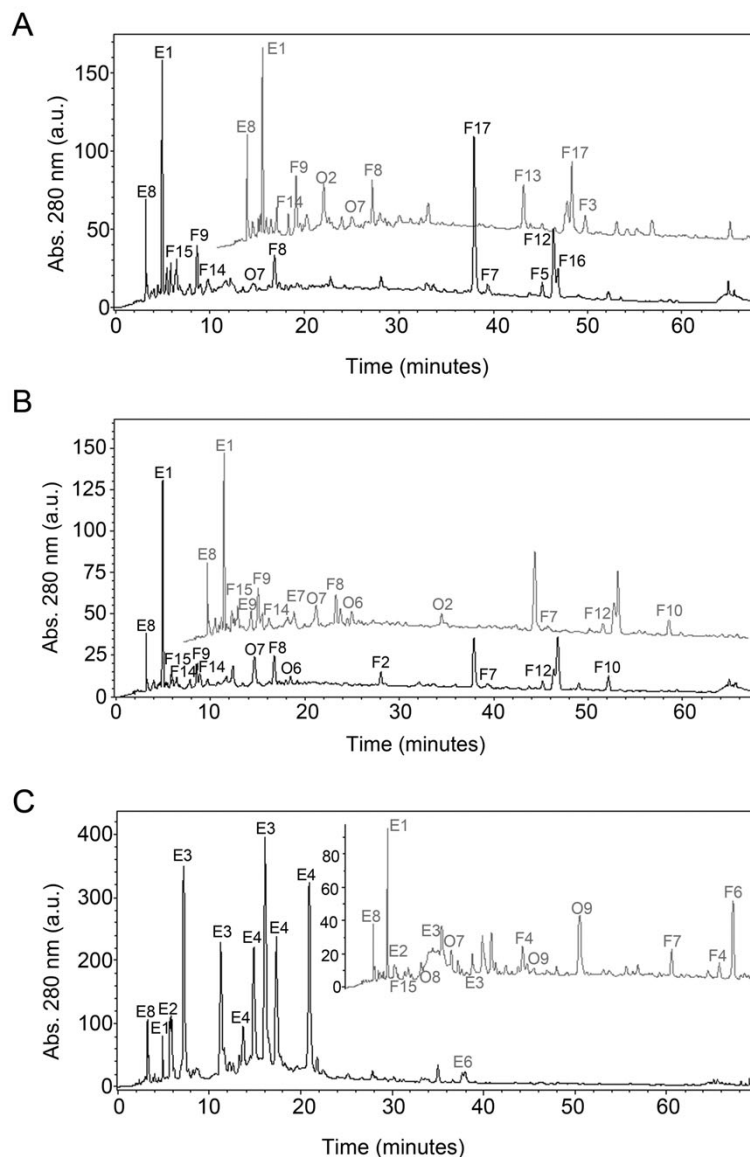


Figure 5. HPLC-DAD profiles at 280 nm of several *Cistus* species. (A) *C. crispus* (grey trace) and *C. incanus* (black trace), both from *Cistus* subgenus. (B) *C. albidus* sample 1, from a limy soil (E in Fig. 2) (grey trace) and *C. albidus* sample 2 from a siliceous soil (B in Fig. 2) (black trace), both from *Cistus* subgenus. (C) *C. libanotis* (black trace) and *C. clusii* (grey trace), both from *Halimioides* subgenus. Profiles in each box show the same time/absorbance scales.

gentisoyl glucoside and 3,4'-dihydroxypropiofenone-3- β -D-glucoside (peaks O7–9) were identified. Moreover, a new one was identified, i.e. hydroxyferulic acid rhamnoside (O3), with a parental ion at m/z 355 and fragment ions at m/z 209 and 191 (Simirgiotis *et al.*, 2009).

Cistus subgenus

***Cistus crispus*.** The chromatogram at 280 nm (Fig. 5A) of the specimen of *C. crispus* analysed in this study (area of Ciudad Real, place A, Fig. 2) looked quite different from those of the *Leucocistus* species, indicating that their evolutionary origin drastically influenced extract composition. In contrast, *C. crispus* extract did

not contain ellagitannins; only gallic acid and HHDP-Glc (E1 and E8) were detected. As these compounds may be the precursors of the biosynthesis of polymeric tannins, we might conclude that aqueous extracts of *C. crispus* lack complex ellagitannins. On the contrary, flavonoids were much more abundant. The flavonols quercetin-glucoside (F3), myricetin hexoside (F13) and myricetin rhamnoside (F17), previously described in other *Cistus* species, were found in this extract. A group of additional flavanols was also identified. F8 was assigned to (+)-catechin/(–)-epicatechin (any of the isomers), with a parental ion at m/z 289 and main fragments at m/z 245, 205 and 179 (Stöggel *et al.*, 2004). Compound F9 was assigned to (–)-(epi)gallocatechin and F14 to (–)-(epi)gallocatechin-(epi)catechin dimer, showing a parental ion at



m/z 593 and a main fragment at *m/z* 425 (Määttä *et al.*, 2003). Finally, two compounds belonging to the 'phenolic acids derivatives' category were identified: uralenneoside (O7) and caffeoyl-quinic acid (O2), with a parental ion at *m/z* 354 and a fragmentation at *m/z* 191 and 136 (Clifford *et al.*, 2003).

Cistus incanus. The black trace in Fig. 5(A) shows the chromatogram at 280 nm for *C. incanus* extract (deriving from a southern mountain area of Valencia with moderate climate and calcareous soil; place C, Fig. 2). As occurred in other members of the *Cistus* subgenus, tannins were absent, with the exception of the precursors HHDP-Glc (E8) and gallic acid (E1). On the contrary, flavonoids were abundant. Nine different flavonoids were identified in *C. incanus* leaves. Four flavanols were identified, i.e. (+)-catechin/(-)-epicatechin (F8); (-)-(epi)gallocatechin (F9); (-)-(epi)gallocatechin-(epi)catechin dimer (F14); and (-)-(epi)gallocatechin-(epi)gallocatechin dimer (F15) with a parental ion at *m/z* 610 and a main fragment at *m/z* 441 (Määttä *et al.*, 2003). Moreover, five flavonols derivatives were identified: rutin (F7); myricitrin (F17); kaempferol-3-*O*-rutinoside (F5), with a parental ion at *m/z* 593 and main fragment at *m/z* 285; quercetin-3-*O*-rutinoside-7-*O*-hexoside or quercetin-3-*O*-(2'-caffeoyl)-rutinoside (peak F16), with a parental ion at *m/z* 771 and fragments at *m/z* 609 and 301 (Simirgiotis *et al.*, 2009); and quercitrin (F12) with a parental ion at *m/z* 447 (Gao *et al.*, 2009). In the third category of compounds, only uralenneoside (O7) was found in this extract.

Cistus albidus. Two specimens were analysed: sample 1 (Fig. 5B, grey trace) from a dry Mediterranean area (semiarid) in the heart of Alicante province (place E, Fig. 2) growing on limy soil, and sample 2 (Fig. 5B, black trace), from the mountain area in Valencia with wet Mediterranean climate (place B, Fig. 2). Besides gallic acid and HHDP-Glc, some ellagitannins, such as pedunculagin (E7) and glucogallin (E9), were detected, but only in sample 1. However, flavonoids were the most relevant compounds in *C. albidus*. Several flavanols were found, i.e. (+)-catechin/(-)-epicatechin (F8); (-)-(epi)gallocatechin (F9); (-)-(epi)gallocatechin-(epi)catechin dimer (F14); and (-)-(epi)gallocatechin-(epi)gallocatechin dimer (F15) (Santagati *et al.*, 2008). Among flavonols, a diglycosylated apigenin (F2), rutin (F7), myricitrin (F17) and quercitrin (F12) were present in both samples. Other new flavonols were found in both *C. albidus* samples, such as peak F10, which was assigned to quercetin-3-*O*-(2'-cumaryl) rutinoside, with a parental ion at *m/z* 755 and fragmentation ions at *m/z* 609, 591 and 301 (Simirgiotis *et al.*, 2009). Within the category of phenolic acids derivatives, uralenneoside (O7) and hydroxyferulic acid rhamnoside (O6), with a parental ion at *m/z* 355 and main fragments at 209 and 191, were found in both samples (Simirgiotis *et al.*, 2009). No significant qualitative or quantitative differences were found between the two *C. albidus* samples despite their different soil. This confirms once again that soil and/or climate influences the composition of the *Cistus* extracts in a lesser degree than the type of species. The polyphenolic composition was also very similar to other members of *Cistus* subgenus, such as *C. crispus* and *C. incanus*, and differed considerably to that one of the species belonging to *Halimioides* or *Leucocistus* subgenus.

***Halimioides* Subgenus**

Cistus libanotis. The sample collected for this study derived from Ciudad Real (place A, Fig. 2). *C. libanotis* aqueous extract

HPLC profile (Fig. 5C, black profile) contained gallic acid (E1) and ellagitannins such as punicalin, punicalagin, punicalagin gallate, 7-xyloside ellagic acid and HHDP-Glc (peaks E2, E3, E4, E6 and E8 respectively). Neither flavonoids nor phenolic acids derivatives were identified in *C. libanotis* aqueous extract. The polyphenolic profile of *C. libanotis* aqueous extract was similar to that shown by some species belonging to *Leucocistus* subgenus, such as *C. ladanifer* and *C. salviifolius*. This fact may indicate that *Leucocistus* and *Halimioides* subgenus are more related one to another than to *Cistus* subgenus.

Cistus clusii. The specimen analysed in this study derived from a limy soil in the dry area of the Alicante province (area E, Fig. 2). The HPLC-DAD profile at 280 nm (Fig. 5C, dark grey trace) showed the presence of gallic acid and HHDP-Glc, and some ellagitannins, i.e. punicalin, punicalagin and punicalagin gallate (peaks E2–4). Unlike *C. libanotis*, *C. clusii* contained several flavonoids, such as the flavanol (-)-(epi)gallocatechin-(epi)gallocatechin dimer (F15) and the flavonol rutin (F7), with parental ion at *m/z* 609 and fragments at *m/z* 301 and 179 (Santagati *et al.*, 2008). Two more flavonols were identified in this source for the first time, i.e. isorhamnetin-*O*-rutinoside (F6), with a parental ion at *m/z* 623 and main fragment at *m/z* 315; and kaempferol diglucoside (F4), with a parental ion at *m/z* 593 and main fragment at *m/z* 285 (Fernandez-Arroyo *et al.*, 2010). As regards to the group of phenolic acids derivatives, uralenneoside, gentisoyl glucoside and 3,4'-dihydroxypropiofenone-3- β -D-glucoside (peaks O7–9) were also identified in this extract. The results reveal that *C. clusii* displays a polyphenolic profile that combines ellagitannins and flavonoids, which looks more similar to that shown by some members of the *Leucocistus* subgenus such as *C. laurifolius*.

Ellagitannins quantitative analysis

Ellagitannins are the largest group of tannins and possess antioxidant, antitumor, antiatherosclerotic, anti-inflammatory, antibacterial, anti-hepatotoxic and antiviral activities (Bakkalbasi *et al.*, 2009). Ellagitannins have been used since ancient times in the tannery industry and have important cosmetic applications. Hence, ellagitannins were quantified in all aqueous extracts deriving from the different *Cistus* species studied (Table 5). *Leuco-*

Table 5. Concentration of ellagitannins in the different *Cistaceae* aqueous extracts determined as punicalagin equivalents in mg/mL. Subgenus is also indicated

Species	Concentration (mg/mL)	Subgenus
<i>Cistus ladanifer</i> (1)	11.7	<i>Leucocistus</i>
<i>Cistus ladanifer</i> (2)	15.12	<i>Leucocistus</i>
<i>Cistus salviifolius</i> (1)	15.79	<i>Leucocistus</i>
<i>Cistus salviifolius</i> (2)	14.27	<i>Leucocistus</i>
<i>Cistus populifolius</i>	7.86	<i>Leucocistus</i>
<i>Cistus laurifolius</i>	0.74	<i>Leucocistus</i>
<i>Cistus monspeliensis</i>	0.95	<i>Leucocistus</i>
<i>Cistus crispus</i>	0	<i>Cistus</i>
<i>Cistus incanus</i>	0	<i>Cistus</i>
<i>Cistus albidus</i> (1)	0.2	<i>Cistus</i>
<i>Cistus albidus</i> (2)	0	<i>Cistus</i>
<i>Cistus libanotis</i>	8.42	<i>Halimioides</i>
<i>Cistus clusii</i>	0.63	<i>Halimioides</i>



cistus subgenus, with some exceptions, contained the highest concentration of ellagitannins, especially *C. salvifolius* and *C. ladanifer*, and, to a lower degree *C. populifolius*. Two species of this subgenus contained significantly less ellagitannins, i.e. *C. laurifolius* and *C. monspeliensis*. We hypothesise that this result might be more related to the evolutionary origin of these species than to soil or climatological conditions. In fact, a recently reported evolutionary study (Guzmán *et al.*, 2009) indicates that *C. laurifolius*, *C. monspeliensis* and *C. populifolius* separated from the other *Leucocistus* species (*C. salvifolius* and *C. ladanifer*) at an early stage.

The two species belonging to *Halimioides* subgenus also contained ellagitannins, but *C. libanotis* exhibited a much higher content (13-fold) than *C. clusii*, almost comparable to that of some members of the *Leucocistus* subgenus. However, additional differences were observed, since *C. clusii* contained four flavonoids and *C. libanotis* was devoid of such compounds. *C. clusii* was collected from a more mineralised soil with a sunnier and drier climate, which could explain the presence of flavonols, compounds traditionally considered as photoprotective agents (Svobodová *et al.*, 2003). Finally, no ellagitannins were detected in the *Cistus* subgenus, with the exception of a residual presence of glucogallin in one of the *C. albidus* samples.

Comparison between samples of the same species also brings interesting conclusions. HPLC profiles of *C. ladanifer* samples did not show qualitative differences between them. Nevertheless, the more mineralised the soil was, higher abundance of ellagitannins was found, suggesting a relationship between soil quality and the abundance of these compounds. On the contrary, *C.*

albidus samples did not show significant differences, indicating that soil and climate factors were not influential. In *C. salvifolius* samples, neither qualitative nor quantitative significant differences in ellagitannins were found. Sample 1 showed a slightly higher concentration of ellagitannins, and punicalagins were the most abundant compounds. In contrast, sample 2 contained as much punicalagins as punicalagins gallates. This might also relate to the influence of soil and/or climate factors in *C. salvifolius* extracts. In any case, all these statements may need further analysis on more plant specimens to be confirmed.

Principal component analysis and evolutionary relationship

Phenolic compounds exhibiting a stronger statistical association between their abundance and the *Cistus* variety were selected through a χ^2 test, as described in the Experimental section. Five compounds showing highest χ^2 and lowest p -values were selected for PCA analysis (see Supporting Information, the first five compounds in Table S1). Those compounds not included presented lower χ^2 and higher p -values. A PCA (principal component analysis) based on correlation matrix was applied to the areas of the above-mentioned selected compounds. The first principal component (PC1) contained 63.4% of the variance, and the first and second (PC2) principal components contained 89.2%. Figure 6 shows PC1 and PC2 for the 13 samples belonging to the three *Cistus* genus studied. PC1 provides a clear separation between *Cistus* and the other two subgenus, while PC 2 seems to be useful to separate between *Leucocistus* and *Halimioides*. Therefore, a strong relationship between *Cistus* subgenus and its

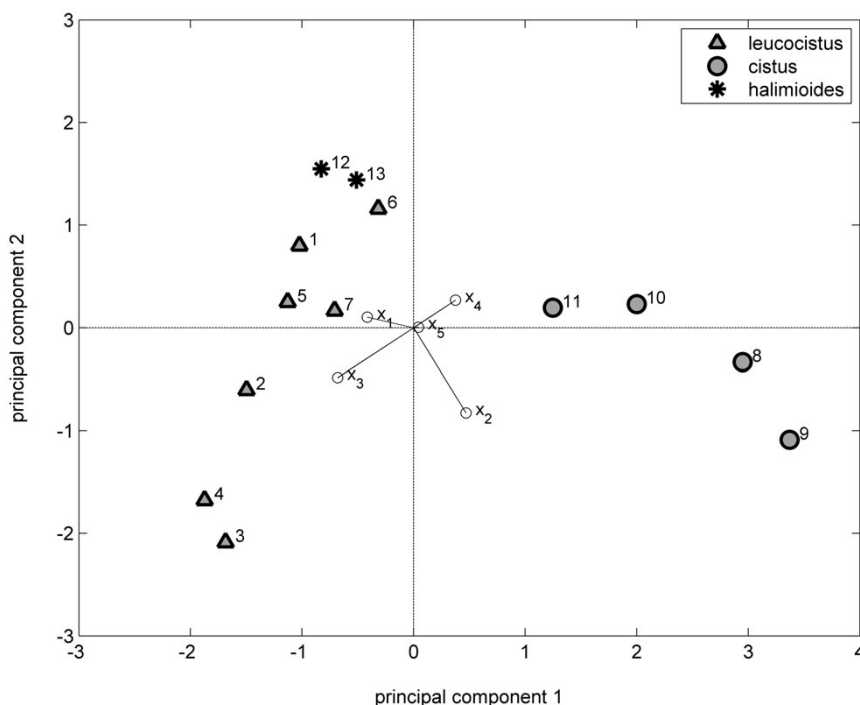


Figure 6. Diagram of the first and second principal components provided by the PCA analysis performed over the areas of the selected compounds. The plot illustrates the PC space for the thirteen samples (indicated by numbers 1–13) and the five normalised areas of the selected compounds: x1, E2-punicalagin; x2, E8-hexahydroxydiphenoyl-glucose; x3, F8-(–)-(epi)catechin; x4, F9-(–)-(epi)gallocatechin; x5, F14-(–)-(epi)catechin-(epi)gallocatechin dimer. Samples are numbered as follows: 1, *C. ladanifer* (1); 2, *C. ladanifer* (2); 3, *C. salvifolius* (1); 4, *C. salvifolius* (2); 5, *C. populifolius*; 6, *C. laurifolius*; 7, *C. monspeliensis*; 8, *C. crispus*; 9, *C. incanus*; 10, *C. albidus* (1); 11, *C. albidus* (2); 12, *C. libanotis*; 13, *C. clusii*.



chemotype based on the most relevant water-soluble polyphenolic compounds was found, confirming previous taxonomic and evolutionary studies.

The analysis presented here points out that the most important factors determining the polyphenolic composition of aqueous extracts deriving from several Mediterranean *Cistus* species are related to their evolutionary origin and subgenus. Soil and climate exert minor influences. HPLC polyphenolic profiles of *Cistus* subgenus were quite different from the *Leucocistus* and *Halimioides* subgenus. *Cistus* subgenus, which is, as indicated by previous taxonomic studies, evolutionarily separated from the two other subgenus (*Leucocistus* and *Halimioides*), is devoid of ellagitannins, but contains a higher amount of flavonoids. On the contrary, *Leucocistus* and *Halimioides*, sharing a common evolutionary origin (Fig. 1), are enriched in ellagitannins, especially *Leucocistus* subgenus, and contain a smaller amount of flavonoids. The results presented here confirm previous evolutionary and phylogenetic studies (Guzmán and Vargas, 2005; Guzmán *et al.*, 2009), reinforcing the idea that plant development and evolution are closely related to their polyphenolic profile (Taylor and Grotewold, 2005). Nevertheless, further detailed studies on the polyphenolic composition of these species would be required to corroborate this hypothesis.

Supporting information

Supporting information can be found in the online version of this article.

Acknowledgements

This investigation has been supported by grant AGL2007-60778 and Torres-Quevedo (PTQ-08-03-08076) fellowship to E. Barrajón-Catalán from MEC, and grants IMIDTD/2006/523, IMIDTA/2008/653 and ACOMP/2010/107 from Generalitat Valenciana. We also thank Químicas del Vinalopó, S.L. and Endemic Biotech, S.L. for their financial support and for providing us with the raw materials.

References

- Andrade D, Gil C, Breitenfeld L, Domingues F, Duarte AP. 2009. Bioactive extracts from *Cistus ladanifer* and *Arbutus unedo* L. *Ind Crop Prod* **30**: 165–167.
- Bakkalbasi E, Mentis O, Artik N. 2009. Food ellagitannins—occurrence, effects of processing and storage. *Crit Rev Food Sci Nutr* **49**: 283–298.
- Barrajón-Catalán E, Fernández-Arroyo S, Guillén E, Segura-Carretero A, Fernández-Gutiérrez A, Micol V. 2010. *Cistaceae* aqueous extracts containing ellagitannins show antioxidant and antimicrobial capacity, and cytotoxic activity against human cancer cells. *Food Chem Toxicol* **48**: 2273–2282.
- Clifford MN, Johnston KL, Knight S, Kuhnert N. 2003. Hierarchical scheme for LC-MS_n identification of chlorogenic acids. *J Agric Food Chem* **51**: 2900–2911.
- Chaves N, Escudero JC, Gutierrez-Merino C. 1997. Quantitative variation of flavonoids among individuals of a *Cistus ladanifer* population. *Biochem Syst Ecol* **25**: 429–435.
- Chaves N, Sosa T, Escudero JC. 2001. Plant growth inhibiting flavonoids in exudate of *Cistus ladanifer* and in associated soils. *J Chem Ecol* **27**: 623–631.
- Chinou I, Demetzos C, Harvala C, Roussakis C, Verbist JF. 1994. Cytotoxic and antibacterial labdane-type diterpenes from the aerial parts of *Cistus incanus* subsp. *creticus*. *Planta Medica* **60**: 34–36.
- De Andres AI, Gomez-Serranillos MP, Iglesias I, Villar AM. 1999. Effects of extract of *Cistus populifolius* L. on the central nervous system. *Phytother Res* **13**: 575–579.
- Del Rio D, Stewart AJ, Mullen W, Burns J, Lean MEJ, Brighenti F, Crozier A. 2004. HPLC-MS_n analysis of phenolic compounds and purine alkaloids in green and black tea. *J Agric Food Chem* **52**: 2807–2815.
- Dias AS, Costa CT, Dias LS. 2005. Allelopathic plants. XVII. *Cistus ladanifer* L. *Allelopathy J* **16**: 1–30.
- Fernandez-Arroyo S, Barrajón-Catalán E, Micol V, Segura-Carretero A, Fernández-Gutiérrez A. 2010. High-performance liquid chromatography with diode array detection coupled to electrospray time-of-flight and ion-trap tandem mass spectrometry to identify phenolic compounds from a *Cistus ladanifer* aqueous extract. *Phytochem Anal* **21**: 307–313.
- Ferrandis P, Herranz JM, Martínez-Sánchez JJ. 1999. Effect of fire on hard-coated *Cistaceae* seed banks and its influence on techniques for quantifying seed banks. *Plant Ecol* **144**(1):103–114.
- Gao WN, Luo JG, Kong LY. 2009. Quality evaluation of *Hypericum japonicum* by using high-performance liquid chromatography coupled with photodiode array detector and electrospray ionization tandem mass spectrometry. *Biomed Chromatogr* **23**: 1022–1030.
- Gil MI, Tomas-Barberan FA, Hess-Pierce B, Holcroft DM, Kader AA. 2000. Antioxidant activity of pomegranate juice and its relationship with phenolic composition and processing. *J Agric Food Chem* **48**: 4581–4589.
- Guinea M, Elbl G, Wagner H. 1990. Screening of *Cistus clusii* extract for cyclooxygenase and angiotensin-converting enzyme inhibitory activity. *Planta Medica* **56**: 664.
- Guzmán B, Vargas P. 2005. Systematics, character evolution, and biogeography of *Cistus* L. (*Cistaceae*) based on ITS, trnL-trnF, and matK sequences. *Mol Phylogenet Evol* **37**: 644–660.
- Guzmán B, Lledó MD, Vargas P. 2009. Adaptive radiation in Mediterranean *Cistus* (*Cistaceae*). *PLoS ONE* **4**: e6362.
- Kreimeyer J, Petereit F, Nahrstedt A. 1998. Separations of flavan-3-ols and dimeric proanthocyanidins by capillary electrophoresis. *Planta Med* **64**: 63–67.
- Küpeli E, Yesilada E. 2007. Flavonoids with anti-inflammatory and antinociceptive activity from *Cistus laurifolius* L. leaves through bioassay-guided procedures. *J Ethnopharmacol* **112**: 524–530.
- Määttä KR, Kamal-Eldin A, Riitta Törrönen A. 2003. High-performance liquid chromatography (HPLC) analysis of phenolic compounds in berries with diode array and electrospray ionization mass spectrometric (MS) detection: *Ribes* species. *J Agric Food Chem* **51**: 6736–6744.
- Parejo I, Jauregui O, Sanchez-Rabaneda F, Viladomat F, Bastida J, Codina C. 2004. Separation and characterization of phenolic compounds in fennel (*Foeniculum vulgare*) using liquid chromatography–negative electrospray ionization tandem mass spectrometry. *J Agric Food Chem* **52**: 3679–3687.
- Pomponio R, Gotti R, Santagati NA, Cavrini V. 2003. Analysis of catechins in extracts of *Cistus* species by microemulsion electrokinetic chromatography. *J Chromatogr A* **990**: 215–223.
- Qa'dan F, Petereit F, Nahrstedt A. 2003. Prodelphinidin trimers and characterization of a proanthocyanidin oligomer from *Cistus albidus*. *Pharmazie* **58**: 416–419.
- Sadhu SK, Okuyama E, Fujimoto H, Ishibashi M, Yesilada E. 2006. Prostaglandin inhibitory and antioxidant components of *Cistus laurifolius*, a Turkish medicinal plant. *J Ethnopharmacol* **108**: 371–378.
- Santagati NA, Salerno L, Attaguiile G, Savoca F, Ronisvalle G. 2008. Simultaneous determination of catechins, rutin, and gallic acid in *Cistus* species extracts by HPLC with diode array detection. *J Chromatogr Sci* **46**: 150–156.
- Saracini E, Tattini M, Traversi ML, Vincieri FF, Pinelli P. 2005. Simultaneous LC-DAD and LC-MS determination of ellagitannins, flavonoid glycosides, and acyl-glycosyl flavonoids in *Cistus salvifolius* L. leaves. *Chromatographia* **62**: 245–249.
- Simirgiotis MJ, Caligari PDS, Schmeda-Hirschmann G. 2009. Identification of phenolic compounds from the fruits of the mountain papaya *Vasconcellea pubescens* A. DC. grown in Chile by liquid chromatography–UV detection–mass spectrometry. *Food Chem* **115**: 775–784.
- Stöggel WM, Huck CW, Bonn GK. 2004. Structural elucidation of catechin and epicatechin in sorrel leaf extracts using liquid-chromatography coupled to diode array-, fluorescence-, and mass spectrometric detection. *J Sep Sci* **27**: 524–528.
- Stübing G, Peris JB. 1998. *Plantas Medicinales de la Comunidad Valenciana*. Generalitat Valenciana. Conselleria de Medio Ambiente: Valencia; 133.
- Svobodová A, Psoťová J, Walterová D. 2003. Natural phenolics in the prevention of UV-induced skin damage. A review. *Biomed Pap Med Fac Univ Palacky Olomouc Czech Republic* **147**: 137–145.
- Taylor LP, Grotewold E. 2005. Flavonoids as developmental regulators. *Curr Opin Plant Biol* **8**: 317–23.







CAPÍTULO 3. *Cistaceae* aqueous extracts containing ellagitannins show antioxidant and antimicrobial capacity, and cytotoxic activity against human cancer cells.





Contents lists available at ScienceDirect

Food and Chemical Toxicology

journal homepage: www.elsevier.com/locate/foodchemtox

Cistaceae aqueous extracts containing ellagitannins show antioxidant and antimicrobial capacity, and cytotoxic activity against human cancer cells

Enrique Barrajon-Catalan^{a,c}, Salvador Fernandez-Arroyo^b, Domingo Saura^a, Emilio Guillen^c, Alberto Fernandez-Gutierrez^b, Antonio Segura-Carretero^b, Vicente Micol^{a,*}

^a Molecular and Cellular Biology Institute (IBMC), Miguel Hernandez University, Avenida de la Universidad s/n, E-03202 Elche, Alicante, Spain

^b Department of Analytical Chemistry, Faculty of Sciences, University of Granada, Granada 18071, Spain

^c R&D Department of ENDEMIC BIOTECH – QUÍMICAS DEL VINALOPÓ, S.L. Monóvar, C/ Collado de Novelda no. 3, 03640 Monóvar, Alicante, Spain

ARTICLE INFO

Article history:

Received 17 February 2010

Accepted 20 May 2010

Keywords:

Cistus

HPLC-DAD-ESI-MS/MS

Antioxidant

Antimicrobial

Antitumor

Ellagitannins

ABSTRACT

Roots and aerial parts of *Cistaceae* have been used since ancient times in the Mediterranean cultures for its medicinal properties. In this study, phenolic and tannin content of *C. ladanifer* and *C. populifolius* leaves aqueous extracts were determined and their antioxidant and antimicrobial activity were fully studied by several *in vitro* assays. Their major compounds were identified and quantitated by high-performance liquid chromatography with diode array detection coupled to electrospray ion-trap mass spectrometry. Cytotoxicity on a panel of human cancer cells was also determined. *C. populifolius* extract was stronger antioxidant than *C. ladanifer* extract in electron transfer reaction based assays but *C. ladanifer* extract was more effective to inhibit peroxy radicals. The major compounds in both extracts were ellagitannins, especially punicalagins derivatives, showing *C. populifolius* a higher content. *C. ladanifer* showed noteworthy antibacterial activity against *Staphylococcus aureus*, whereas *C. populifolius* was effective against *Escherichia coli*, with MICs values of 154 and 123 µg/mL, respectively. Last, both extracts showed a notorious capacity to inhibit the proliferation of M220 pancreatic cancer cells and MCF7/HER2 and JIMT-1 breast cancer cells. The leaves of these plants suppose a source for water-soluble ellagitannins-enriched polyphenolic extracts with antioxidant and antimicrobial activities. Their cytotoxic activity against several cancer cells may deserve further attention.

© 2010 Elsevier Ltd. All rights reserved.

1. Introduction

The *Cistaceae* is a Mediterranean native family of almost 200 species of shrubs. Some of these plants are autochthonous and widespread in the south-east of Iberian “Peninsula”, northwestern Africa, Greece and Portugal (Andrade et al., 2009; Teixeira et al., 2007). Most members of this family are very fragrant and sweet-smelling, being much appreciated in the perfume industry and for ornamental purposes.

Among the *Cistaceae* family, *Cistus ladanifer* (“sticky shrub”) and *Cistus populifolius* show one of the largest biomass productivity in the wilderness and natural parks of the south area of Spain (Paton et al., 1998). *C. ladanifer* is an important member of the flora within

the semiarid Mediterranean ecosystems and forms dense stands on siliceous soils (Robles et al., 2003). These two species, especially *C. ladanifer*, are very abundant along the Spanish forest and landscape, and their overgrowth may lead to environmental problems. This shrub colonizes degraded areas and inhibits the growth of other plants (Dias and Moreira, 2002), by restricting aerial growth of plants or by inhibiting germination of other species, due to its phytotoxicity over other plants and soil (Chaves et al., 2001a,b). *Cistaceae* also adapts easily to wildfires that destroy large forest areas, as their seeds resist fires and repopulate fast in the following season (Ferrandis et al., 1999).

C. ladanifer has been used since ancient times due to its aromatic exudate or resin, commonly known as *labdanum*, which has been used to treat diarrhea, dysentery, catarrh and menstruation discomfort. Nowadays, *labdanum* is extraordinarily interesting for the fragrance industry. *C. ladanifer* essential oil is also antiseptic, astringent, tonic, expectorant, balsamic and an emmenagogue. Others species from the same family such as *Cistus populifolius* have been also used in folk medicine due to properties like: anti-inflammatory, antiulcerogenic, wound healing, antimicrobial, cytotoxic, vasodilator and antispasmodic (De Andres et al., 1999).

Abbreviations: GAE, gallic acid equivalent; TAE, tannic acid equivalent; dw, dry weight; ORAC, oxygen radical absorbance capacity; TEAC, Trolox equivalent antioxidant capacity; FRAP, ferric-reducing ability power; TBARS, thiobarbituric acid-reactive substances; CC50, 50% cytotoxic concentration; HPLC-DAD-ESI-MS/MS, HPLC with diode array detection coupled to electrospray and ion-trap mass spectrometry.

* Corresponding author. Tel.: +34 96 6658430; fax: +34 96 6658758.

E-mail address: vmicol@umh.es (V. Micol).



Both species produce several types of secondary metabolites. Among them, phenolics, terpenes, alkaloids, polyacetylenes, fatty acids, and steroids have been partially identified before (Andrade et al., 2009; Chaves et al., 2001a; Dias and Moreira, 2002; Pascual et al., 1977). Although the resin of *C. ladanifer* has been deeply characterized in previous studies (Gomes et al., 2005; Robles et al., 2003), little information about the polyphenolic content of the aerial part of the plant as a source of potential bioactive compounds is available (Kupeli and Yesilada, 2007; Santagati et al., 2008; Ustun et al., 2006). Recently, we have reported the characterization of *C. ladanifer* leaves using HPLC coupled to electrospray time-of-flight and ion-trap tandem mass spectrometry (Fernandez-Arroyo et al., 2009).

Previous studies have reported the biological activity of *Cistaceae* species. For instance, the antiviral activity of *C. incanus* and *C. populifolius* has been studied in cell culture and animal models (Abad et al., 1997; Droebner et al., 2007; Ehrhardt et al., 2007). Moreover, the antioxidant activity of *C. ladanifer* (Andrade et al., 2009), and the vasodilator properties of *C. populifolius* (Somoza et al., 1996) have also been reported. *C. ladanifer* exudates have shown strong inhibition of the calcium transport in skeletal muscle (Sosa et al., 2004). Nevertheless, most of these studies were performed in extracts of unknown composition. Here, a comprehensive and comparative study of the biological activity and composition of *C. ladanifer* and *C. populifolius* aqueous extracts is shown for the first time.

The aim of this study was to obtain extracts from the above mentioned *Cistaceae* species following sustainable methods and cultivation practices. For this purpose, the first action taken was using non-organic solvents or chemicals and also following the rules indicated by organic certification organizations (ECOCERT). In addition, the management of this raw material would eliminate part of the undesirable vegetable biomass of the forest regions which suppose a serious risk of fire, especially in summer.

In this study, extracts deriving from *C. ladanifer* and *C. populifolius* aerial parts were prepared using aqueous extraction. The composition of these extracts was analyzed through HPLC with diode array detection coupled to electrospray and ion-trap mass spectrometry. Their flavonoid and tannin contents were determined. The antioxidant and the antimicrobial activities of these extracts were fully characterized through several methods. Moreover, the cytotoxic activity against a panel of human cancer cell lines was assayed.

2. Material and methods

2.1. Plant material and processing

In order to use autochthonous Spanish specimens of *Cistus*, plants were obtained from natural parks of Ciudad Real and Cuenca provinces (Spain) after summer, according to flowering time care and parks' rules. Specimens were identified by the authors and processed independently. Fresh aerial parts were selected avoiding woody parts and then washed and milled obtaining a particle size of 0.3–0.5 cm diameter. The material was then extracted with distilled water (always below 65 °C), with agitation for approximately 1 h and plant/solvent ratio of 1:5. Afterwards, the samples were filtered through 1–2.5 µm cellulose filters, freeze-dried and stored at 4 °C in the dark. Immediately before the *in vitro* or cellular assays, the extracts were resuspended in distilled water and centrifuged at 2000 rpm to discard any insoluble material. For the cellular assays, samples were sterile-filtered through 0.22 µm filters.

2.2. HPLC-DAD-MS/MS

The different *Cistaceae* extracts were analyzed and quantitated using an Agilent LC 1100 series (Agilent Technologies, Inc., Palo Alto, CA, USA) controlled by the Chemstation software and equipped with a pump, autosampler, column oven and UV–vis diode array detector. The HPLC instrument was coupled to an Esquire 3000+ (Bruker Daltonics, GmbH, Germany) mass spectrometer equipped with an ESI source and ion-trap mass analyzer, and controlled by Esquire control and data analysis software. A Merck LiChrospher 100 RP-18, 5 µm, 250 × 4 mm (i.d.) column was used for analytical purposes.

Separation was carried out through a linear gradient method using 1% formic acid (A) and acetonitrile (B). The gradient started with 4% B, 25%B at 25 min, 100% B at 80 min, 4% B at 82 min and 5 more minutes for reequilibration. For the accurate performance of the LC-MS pump, 10% of organic solvent was premixed in the water phase. The flow rate was 0.5 mL/min. Diode-array detection was set at 280, 320 and 340 nm. Mass spectrometry operating conditions were optimized in order to achieve maximum sensitivity values. The ESI source was operated in negative mode to generate $[M-H]^-$ ions using the following conditions: desolvation temperature at 360 °C and vaporizer temperature at 400 °C; dry gas (nitrogen) and nebulizer were set at 12 L min⁻¹ and 70 psi, respectively. The MS data were acquired as full scan mass spectra at 50–1100 *m/z* by using 200 ms for collection of the ions in the trap.

Identification of the main compounds was performed by HPLC-DAD analysis, comparing the retention time, UV spectra and MS/MS data of the peaks in the samples with those of authentic standards or data reported in the literature.

Quantitation of punicalagins and gallic acid content was performed using commercial standards of gallic acid (Sigma–Aldrich, Europe) and punicalagin (Phytolab, Vestenbergsgreuth, Germany). The software ChemStation for LC 3D (Agilent Technologies Life Sciences and Chemical Analysis, Waldbronn, Germany) was used for quantitation purposes. The linearity range of the responses was determined on eight concentration levels with three injections for each level. Calibration graphs for HPLC were recorded with sample amount ranging from 0.25 µg/mL to 0.25 mg/mL ($r^2 > 0.9999$). Quantitative evaluation of the compounds was performed by means of a six-point regression curve ($r^2 > 0.996$) in a concentration range between 0.25 µg/mL and 0.1 mg/mL, using external standards and evaluated at 280 nm.

2.3. Phenolic, flavonoid and tannins quantitation

Total flavonoid content was quantified following a method previously described (Pourmorad et al., 2006) using quercetin (Sigma–Aldrich, Europe) as standard. Briefly, samples were incubated in the presence of potassium acetate and AlCl₃, then the colored product of the reaction was quantified by measuring absorbance at 415 nm. Total polyphenolic content was determined using the Folin–Ciocalteu method (Huang et al., 2005) and gallic acid (Sigma–Aldrich, Europe) as standard. Tannin content was determined with the use of two alternative techniques. The first one consisted on the precipitation of tannins with 0.6 mg/mL BSA (Sigma–Aldrich, Europe) at acidic pH and then resuspension in 1% SDS, 5% triethanolamine buffer (Makkar, 1989). Afterwards, FeCl₃ was added to the reaction and the formed chromogen was quantified by measuring absorbance at 510 nm. The second method was performed through precipitation of polyphenols with 1.6 mg/mL BSA at pH 7.4, and later tannins' precipitate was discarded. Then, polyphenolic content was determined again in the supernatant by Folin–Ciocalteu method and tannins' content calculated by weight difference.

2.4. Measurement of the Trolox equivalent antioxidant capacity (TEAC)

The Trolox equivalent antioxidant capacity (TEAC) assay, which measures the reduction of the radical cation of ABTS by antioxidants, was performed as previously described (Laporta et al., 2007b). Briefly, ABTS radical cation (ABTS^{•+}) was produced by reacting ABTS (Sigma–Aldrich, Europe) stock solution with 2.45 mM potassium persulfate (final concentration) and allowing the mixture to stay in the dark at room temperature for 12–24 h before use. To perform the antioxidant assay with *Cistaceae* extracts, the ABTS^{•+} solution was diluted with water up to reaching an absorbance value of 0.70 (±0.02) at 734 nm. For the photometric assay, 1 ml of the ABTS^{•+} solution and 100 µL of the antioxidant extract were mixed for 45 s and measured immediately after 5 min at 734 nm (absorbance did not change significantly up to 10 min).

2.5. Radical-scavenging capacity by thiobarbituric acid-reactive substances assay (TBARS)

The quantitative evaluation of the antioxidant capacity of the compounds against lipid peroxidation was determined through TBARS assay. Small unilamellar vesicles (SUVs) were prepared as previously described (Caturla et al., 2003) by sonication of multilamellar vesicles (MLVs) of egg yolk phosphatidylcholine (EYPC) (Lipoid GmbH, Ludwigshafen, Germany). One milliliter of SUVs dispersion was incubated for 10 min at 37 °C with the extracts and after that, the free radical generator AAPH (Sigma–Aldrich, Europe) was added (10 mM final concentration) to the mixture in order to induce peroxidation of unsaturated fatty acids. The reaction was incubated at 37 °C with occasional vortexing, stopped after 60 min by adding 200 µL of BHT (4% p/v in ethanol) and frozen at –80 °C until use. The colorimetric reaction with thiobarbituric acid was then carried out by adding 250 µL of sodium dodecyl sulfate (3% p/v), 500 µL of TBA (1% p/v) (Sigma–Aldrich, Europe) and 500 µL of HCl 7 mM to the samples, and incubating at 95 °C for 15 min. Then, TBA–MDA chromogen was determined using HPLC system as previously described (Laporta et al., 2007b).

2.6. Assay of the oxygen radical absorbance capacity (ORAC)

To assay the capacity of the extracts to scavenge peroxy radicals, a validated ORAC method was used (Ou et al., 2001). Briefly, the automated ORAC assay was carried out on a Fluostar Galaxy spectrofluorometric analyzer (BMG Labtechnolo-



gies GmbH; Offenburg, Germany). In the final assay mixture (200 µL total volume), fluorescein (FL) and AAPH were used at 90 nM and 12.8 mM, respectively. Several dilutions of Trolox (1–40 µM) were used to construct the calibration curve. A freshly prepared AAPH solution was used for each experiment. The temperature of the incubator was set at 37 °C and the FL fluorescence was recorded every minute after the addition of AAPH. The final ORAC values were calculated by using a regression equation between the Trolox concentration and the net area of the FL decay curve (area under curve, AUC) as previously described in Laporta et al. (2007b).

2.7. Ferric-reducing ability power (FRAP)

The FRAP assay was made as previously described (Benzie and Strain, 1996). Briefly, 40 µL of the extracts were mixed on a 96-well plate with 250 µL of freshly prepared FRAP reagent. Samples were incubated for 10 min at 37 °C, and then, absorbance at 593 nm was recorded during 4 min on a microplate reader (SPECTROstar Omega, BMG LabTech GmbH, Offenburg, Germany). FRAP values were calculated using FeSO₄·7H₂O as standard.

2.8. Antibacterial assay

Escherichia coli and *Staphylococcus aureus* were used as models for Gram-negative and Gram-positive bacteria, respectively. The microplate method was used to determine the minimal inhibitory concentration (MIC) values for the extracts (Eloff, 1998). The *Cistaceae* extracts were dissolved in sterile water. Briefly, cells were grown overnight at 37 °C in LB and diluted in the same medium. The 96-well round-bottomed sterile plates were prepared by dispensing 160 µL of LB no-salt medium and 20 µL of bacteria to give final inoculum of 10⁴/10³/10² CFU/ml into each one of the wells. 20 µL aliquots of the extracts were added (in octuplicates). The antibiotic neomycin (Sigma–Aldrich, Europe) was included in each assay as positive control, while broth without extracts was used as a negative control. The microplates were covered and incubated overnight at 37 °C. As an indicator of bacterial growth, 50 µL of 0.2 mg/ml *p*-iodonitrotetrazolium violet (INT) (Sigma–Aldrich, Europe) was added to each well and the plates incubated at 37 °C for 30 min. MIC₅₀ values were recorded as the concentration of the antibacterial agent that inhibited 50% of the bacterial growth.

2.9. Cell lines and cultures

The human breast carcinoma cell line SKBr3 was obtained from the American Type Culture Collection (ATCC, Manassas, VA, USA) and derives from a pleural metastasis effusion from a primary breast adenocarcinoma. MCF-7 breast cancer cells stably overexpressing HER2 oncogene (MCF-7/HER2) (Menendez et al., 2007), and the cell line JIMT-1, derived from a breast cancer clinically resistant to trastuzumab (Tanner et al., 2004), were kindly provided by Institut Català d’Oncoologia (Girona, Spain). M186 and M220, also known as IMIM-PC1 and IMIM-PC2 respectively, were derived from human pancreatic adenocarcinoma primary tumoral cells (García-Morales et al., 2005). HS-766T cells derived from a pancreatic carcinoma metastasis to a lymph node and HT29 cells came from a human colon cancer carcinoma. M186, M220, HS-766T and HT29 cancer cells were kindly provided by Dra. Pilar García Morales from *Elche University Hospital, Biomedic Research Foundation* (Elche, Spain). All cells were routinely grown in DMEM + GlutaMAX medium supplemented with 10% of heat-inactivated fetal bovine serum (GIBCO) containing 50 U/ml penicillin and 50 mg/mL of streptomycin (GIBCO). Cells were incubated at 37 °C in a humidified 5% CO₂ air atmosphere.

2.10. Determination of cytotoxic activity in human cancer cells by MTT assay

Cell viability of all cell lines was determined through the MTT assay (Mosmann, 1983). Briefly, cells were plated in 96-well plates at a density yielding 80–90% confluence when the cytotoxicity assay was performed. Complete medium was refreshed and eight replicates cultures were treated with different doses of the extracts for 24 h. Control samples were treated only with buffer. Viability was then measured by the bioreduction of 3-(4,5-dimethylthiazol-2-yl)-2,5-diphenyltetrazolium-bromide (MTT) (Sigma–Aldrich, Europe) to a colored formazan product that was dissolved in 100 µL of DMSO and measured at 570 nm with a microplate reader. The optical density obtained was directly correlated with cell quantity. All the results corresponding to MTT experiments were expressed as the mean of a minimum of 6–8 replicates. The 50% cytotoxic concentration values (CC50) were determined from the survival plots.

3. Results

3.1. Yield and preparation of the extracts

The extracts were obtained as described in the methods section. The dried extracts obtained were brown, nicely aromatized and

water-soluble with an approximate yield of 7–10% (w/w) respect to fresh raw material. Although other alternative solvents (ethanol, methanol) were tested for extraction with discreetly better results in total phenolic composition (data not shown), water was selected as the extracting solvent choice, due to ecological and environmental reasons.

3.2. Total phenolic, flavonoid and tannin content

As previous step to the measurement of the antioxidant activity, the total polyphenol content of the extract was quantified using the Folin–Ciocalteu method (Huang et al., 2005), as this value correlates in most cases with the antioxidant capacity of the extract. The obtained values for each plant are shown in Table 1. *C. ladanifer* phenolic content was higher than that of other aqueous extracts previously reported (Dudonni et al., 2009), and almost similar to that one of ethanolic *C. ladanifer* extracts (Andrade et al., 2009). In agreement to the phenolic content, flavonoids’ content, determined as quercetin equivalent, was also higher in *C. populifolius* compared to that one found in *C. ladanifer* extract (Table 1).

There is a great variability of methods in literature to quantify tannins (Makkar, 1989). As a first approach, the so-called FeCl₃ method carried out using an acidic pH (pH 4.0), was performed. The results of this test showed that both *Cistus* extracts had a similar ability to precipitate proteins, although *C. populifolius* extract exhibited a little higher one (Table 2). Tannins supposed a significant proportion of the total dry matter, i.e. 6.8% for *C. ladanifer*, and 8.2% in the case of *C. populifolius*.

In order to explore the capacity of *Cistus* tannins to precipitate proteins at more physiological pH values, the tannin assay was performed at pH 7.4. For that, a modification of the Folin–Ciocalteu assay, in which polyphenols were allowed to interact with BSA at neutral pH, was performed. Then, the pellets were removed by centrifugation and regular Folin–Ciocalteu assay was followed on the supernatants. The results showed that the amount of this type of tannins was considerably higher in *C. populifolius* than those ones in *C. ladanifer* (Table 3), 5.88% of total polyphenols in *C. ladanifer* extract vs. 32.67% in *C. populifolius* extract.

Table 1
Values for different antioxidant measurements performed with *C. ladanifer* and *C. populifolius* aqueous extracts. Values are expressed as mean ± SD, n = 8.

Antioxidant assay (units)	<i>C. ladanifer</i>	<i>C. populifolius</i>
Folin–Ciocalteu (g GAE ^a /100 g dw ^d)	22.93 ± 1.08	31.89 ± 1.08
Flavonoid content (mg quercetin eq/100 mg dw)	3.04 ± 0.49	5.95 ± 1.08
TEAC (mmol TE ^b /100 g dw)	35.85 ± 1.25	45.74 ± 1.52
FRAP (mmol Fe ²⁺ /100 g dw)	117.72 ± 4.38	179.10 ± 3.34
TBARS (% inhibition) ^c	72.13 ± 8.12	84.61 ± 23.04
ORAC (µmol TE ^b /g dw)	3329.0 ± 182.1	2348.4 ± 325.3

^a Gallic acid equivalents.
^b Trolox equivalents.
^c % inhibition of lipid peroxidation at a concentration of 0.375 mg/mL.
^d Dry weight.

Table 2
Tannin quantitation in *C. ladanifer* and *C. populifolius* aqueous extracts using different methods as described in Section 2. Values are expressed as mean ± SD, n = 8.

Tannin assay (units)	<i>C. ladanifer</i>	<i>C. populifolius</i>
FeCl ₃ -based (g TAE ^a /100 g dw ^b)	6.81 ± 0.61	8.18 ± 0.98
Folin-based (% of total polyphenols)	5.88 ± 4.77	32.67 ± 4.38

^a Tannic acid equivalent.
^b Dry weight.

3.3. HPLC-DAD-MS/MS characterization

The aqueous extracts from *C. ladanifer* and *C. populifolius* were further studied by using HPLC-DAD-ESI-MS/MS technique, in order to identify their major compounds. Several peaks were identified using a library of phenolic compounds and comparing their retention time, UV spectra and MS/MS data with those of commercial standards or those reported in literature (Fernandez-Arroyo et al., 2009). Fig. 1 shows the chromatograms obtained at 280 nm for *C. ladanifer* (Fig. 1A) and *Cistus populifolius* (Fig. 2A) and their respective base peak chromatograms (BPC) (Figs. 1B and 2B).

Four major phenolic compounds were identified, which appeared in both *Cistus* species. Peak number 1 was identified as gallic acid (Fig. 2), which showed a base peak at m/z 169 corresponding to $[M-H]^-$ and a fragment ion at m/z 125 ($[M-H-44]^-$), corresponding to the loss of CO_2 . Peak number 2 exhibited $[M-H]^-$ ion at m/z 781, with main fragment ion at m/z 601, consistent with gallagic acid (Gil et al., 2000), and other fragment at m/z 301, which is characteristic of ellagic acid. The results obtained for peak number 2 were compatible with the punicalin structure (Fig. 2). Peaks number 3 and 4 exhibited the same base peak with a parental ion at m/z 1083, and their fragmentation yielded fragment ions at m/z 781 (consistent with the loss of hexahydroxydiphenoyl moiety), 601 (gallagic acid) and 301 (ellagic acid). Therefore, both peaks were assigned to punicalagin isomers (Fig. 2).

The quantitation of these compounds showed that gallic acid represented 0.242 ± 0.004 % (w/w) of *C. ladanifer* aqueous extract and all ellagitannins, (Fig. 1; peaks 2–4) accounted for 3.50 ± 0.02 % (w/w). *C. populifolius* showed 0.315 ± 0.005 % (w/w) of gallic acid, but much higher content in ellagitannins, i.e. 15.43 ± 0.02 % (w/w). This was in agreement to the results obtained in the tannin assay (Table 2) that indicated a higher content in tannins able to precipitate

proteins at neutral pH for *C. populifolius*. We postulate that most of these tannins may correspond to ellagitannins.

Other compounds, which could not be identified by MS/MS, showed absorption spectra maximum at 320 nm and 350 nm, which is typical for the flavonol structure. These compounds were assigned to kaempferol and quercetin glycosylated derivatives and probably contributed to the flavonoids' content previously determined for both *Cistaceae*. Nevertheless, their identity could not be confirmed with the use of their respective aglycones as standards.

3.4. Antioxidant activity

A complete set of antioxidant assays was performed in order to deeply characterize the antioxidant potential of these plants (Table 1). TEAC assay is a single-electron transfer-based method which has been used in a large variety of food samples (Huang et al., 2005) and it uses Trolox as standard.

FRAP assay (ferric ion reducing antioxidant power) is also based in a single-electron transfer mechanism, but it's specially indicated for determining the antioxidant capacity of biological samples (Benzie and Strain, 1996). The results obtained for *C. ladanifer* were comparable to those previously reported (Dudonni et al., 2009), but no FRAP data are available for *C. populifolius* in the bibliography. However, FRAP values were also higher for *C. populifolius* than those for *C. ladanifer*, which correlates with the results obtained in TEAC and phenolic content assays (Table 1).

TBARS assay is specially indicated for measuring the level of oxidation in lipid samples such as oils and emulsions (Huang et al., 2005). Nonetheless, it is also used to study the capacity of an antioxidant compound to inhibit the generation of thiobarbituric acid-reactive substances, malondialdehyde among them,

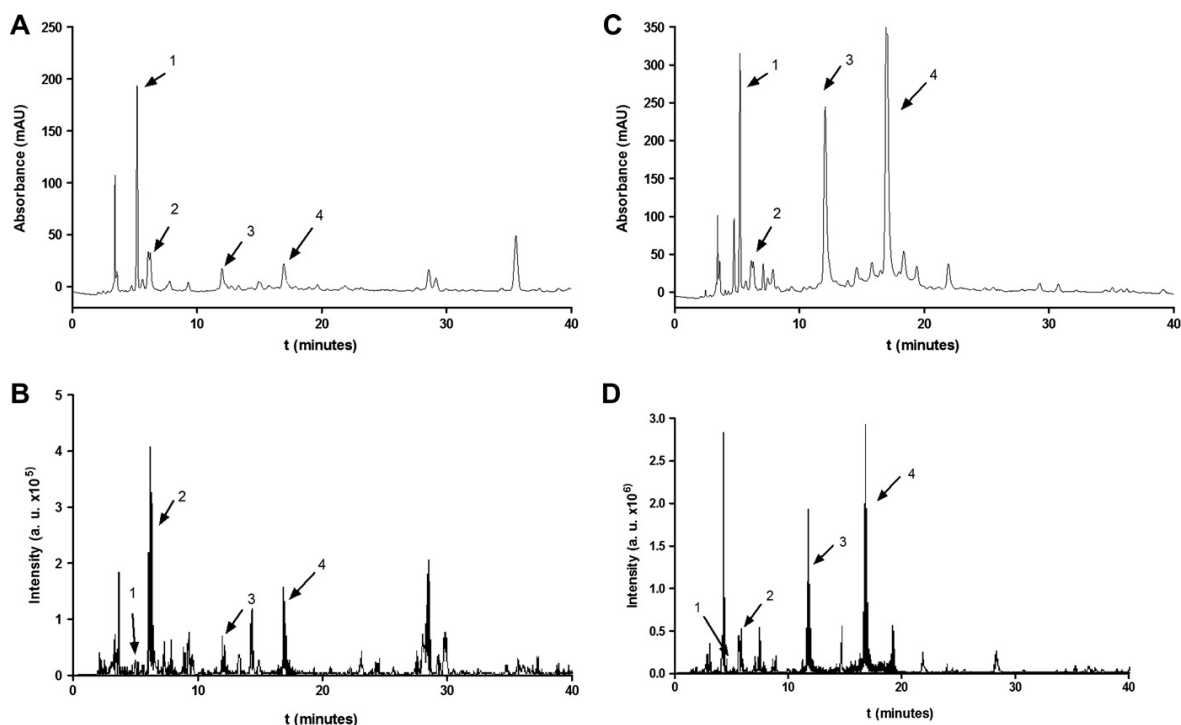


Fig. 1. HPLC-DAD chromatograms for *C. ladanifer* (A) and *C. populifolius* (C) at 280 nm. Base peak chromatograms obtained by HPLC-DAD-ESI-MS/MS of *C. ladanifer* (B) and *C. populifolius* (D). 1, Gallic acid; 2, punicalin; 3, punicalagin isomer; 4, punicalagin isomer.

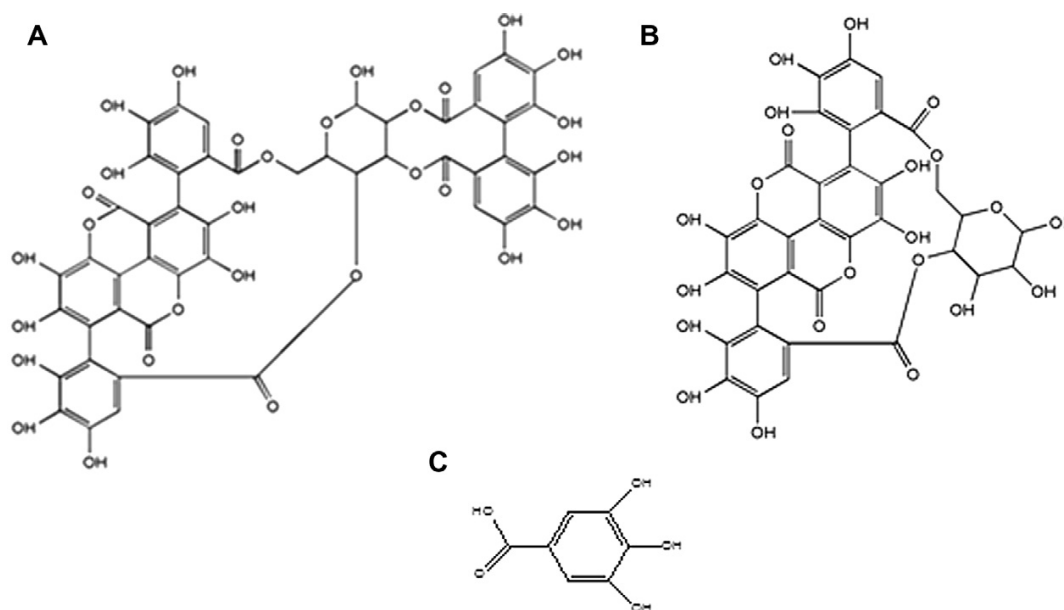


Fig. 2. Chemical structures of punicalagin (A), punicalin (B) and gallic acid (C).

which are generated in the complex process involved in lipid peroxidation. For this test, a phospholipid vesicles system was used and the capacity of the extracts to inhibit the formation of lipid peroxy radicals was determined. In agreement to what observed in the previous antioxidant measurements, *C. populifolius* extract also showed a little stronger capacity than *C. ladanifer* extract in the TBARS assay (Table 1), since the level of lipid peroxidation measured as % oxidation inhibition was higher than that one observed for *C. ladanifer*, both determined at 0.375 mg/mL of extract.

ORAC (Oxygen Radical Absorbance Capacity) assay was performed in order to test the capacity of the extracts to quench peroxy radicals. ORAC method is a hydrogen atom transfer-based assay and has become one of the most widely accepted methods to measure the antioxidant capacity of food, botanical and biological samples (Huang et al., 2005). In contrast to the results obtained in previous antioxidant measurements, *C. ladanifer* extract was more potent than *C. populifolius* (Table 1), and both showed higher values than those recently reported for *C. ladanifer* aqueous extract (Dudonni et al., 2009).

3.5. Antimicrobial activity

The antibacterial activity was measured as described in methods using two different bacterial strains which are widely used as models for Gram-positive and Gram-negative bacteria, such as *Staphylococcus aureus* and *Escherichia coli*, respectively. The concentrations of extracts corresponding to 50% bacterial growth inhibition (MIC_{50}) were determined for *C. ladanifer* and *C. populifolius* aqueous extracts (Table 3). *C. ladanifer* extract was more potent against Gram-positive bacteria compared to Gram-negative ones. In contrast, *C. populifolius* extract exhibited a higher efficacy against *E. coli*, i.e. a Gram-negative one.

3.6. In vitro cytotoxicity against human cancer cells

The cytotoxic activity of two *Cistus* extracts over an extensive collection of cancer cell lines, including pancreatic, colon and

Table 3

MIC_{50} values for *C. ladanifer* and *C. populifolius* aqueous extracts against *E. coli* and *S. aureus*. Values are expressed in mg of dry extract per mL. Values are expressed as mean \pm SD, $n = 8$.

	<i>E. coli</i>	<i>S. aureus</i>
<i>C. ladanifer</i>	0.900 \pm 0.047	0.154 \pm 0.028
<i>C. populifolius</i>	0.123 \pm 0.042	0.344 \pm 0.028
Neomycin	0.10 \pm 0.01	0.10 \pm 0.01

breast cancer cells was determined. The antitumor activity was measured on subconfluent (80–90% confluent) cells as the capacity of the extracts to inhibit cell proliferation measured through the MTT assay.

Figs. 3 and 4 show the dose–response survival curves for the treatments of the different cancer cells in the presence of *C. ladanifer* or *C. populifolius* aqueous extracts for 24 h. Table 4 shows the 50% cytotoxic concentration (CC50) values corresponding to the plots shown in Figs. 3 and 4. Both *Cistus* extracts had a similar behavior against pancreatic cancer cells (Fig. 3). HS-766T and M186 cells were somehow resistant to these extracts, whereas M220 cells were highly sensitive, showing CC50 values of 0.49 and 0.66 mg/ml for *C. ladanifer* and *C. populifolius* extracts, respectively.

Regarding breast cancer cells, MCF7/HER2 and JIMT-1 cells were the most sensitive to *Cistus* extracts showing CC50 values within the range of 0.5–1 mg/ml for MCF7/HER2 and 1.6–2 mg/ml for JIMT-1 cells. SKBr3 breast cancer cells and HT29 colon cancer cells were more resistant to the *Cistus* extracts in this order.

4. Discussion

Phenolic compounds have been traditionally associated to biological activities such as antioxidant, antimicrobial or cytotoxic. The *Cistus* aqueous extracts studied here showed a significant phenolic content as shown in the previous section. *C. populifolius* aqueous extract exhibited higher polyphenolic content than that one of *C. ladanifer*. As far as we are concerned, although previous

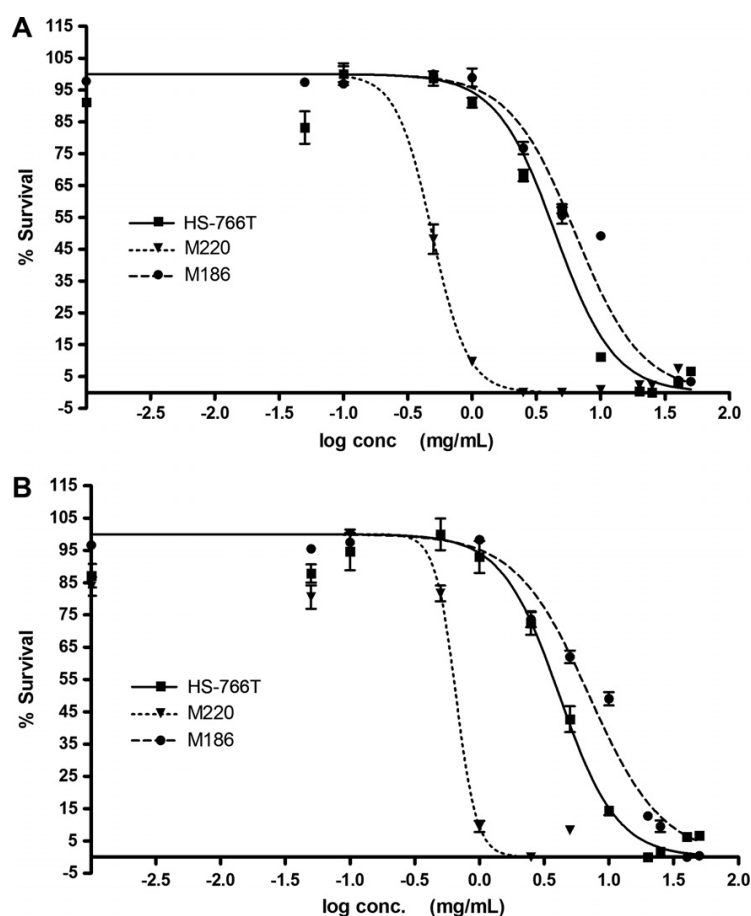


Fig. 3. Survival plots obtained using the MTT assay for HS-766T, M220 and M186 pancreatic cancer cells treated with *C. ladanifer* (A) or *C. populifolius* (B) extracts for 24 h.

data of *C. ladanifer* are available, data of *C. populifolius* extracts has not been found, so this is the first time reported. The higher phenolic content of *C. populifolius* aqueous extract determined through Folin–Ciocalteu reagent correlated to its higher antioxidant capacity observed in TEAC and FRAP assays. This is consistent with the fact that the three assays are based on electron–transfer mechanism (Huang et al., 2005).

Tannins are a subfamily of polyphenols which show the ability to precipitate proteins. Tannins have been used since ancient times in tannery industry and have important cosmetic applications. Traditionally *Cistus* species have been also used as antiarrheic, which is one of the pharmacological activities of tannins, acting through the shrinkage of intestine mucous membranes and decrease of mucous secretions. It has been reported that BSA is significantly precipitated by condensed tannins only at pH 3.0–5.0 (Hagerman and Butler, 1978). Hence, it must be assumed that those tannins, able to precipitate BSA at neutral pH values, may be of different type, probably gallo- or ellagitannins (hydrolyzable tannins). According to this hypothesis, *C. ladanifer* tannins would belong to the condensed type, whereas *C. populifolius* aqueous extract would contain a higher amount of hydrolysable or gallo/ellagitannins. The concentration of tannins in plants is not only species-specific but it also depends on soil fertility and pH, light intensity, plant age or temperature stress (Adamczyk et al., 2008). All these factors make tannins concentrations to differ significantly among

plant species and make their comparison complicated. Anyhow, the values obtained here for *Cistus* species are comparable to those reported for species such as *Vaccinium myrtillus*, *Vaccinium vitis-idaea*, *Betula pendula*, *Pinus sylvestris* or *Picea abies*, all of them with values between 9 and 20 g TAE/100 g dw (Adamczyk et al., 2008).

After the identification of the major phenolic compounds present in the *Cistaceae* extracts, the amount of gallic acid and punicalagins were quantified. The presence of gallic acid has been earlier reported in the *Cistaceae* family (Santagati et al., 2008). This compound has exhibited several interesting biological activities such as antioxidant (Kim, 2007; Vaher et al., 2005), antitumor (Inoue et al., 1995; Perchellet et al., 1992) and antimicrobial (Kang et al., 2008). Punicalagins belong to the family of ellagitannins, which are structurally derived from ellagic acid and are known to be effective antioxidants (Gil et al., 2000; Seeram et al., 2004) and anticarcinogenic (Kulkarni et al., 2007; Perchellet et al., 1992) compounds.

The presence of flavonoids in *Cistus* has been documented before. Previous reports have found apigenin, quercetin and kaempferol derivatives in exudates of *C. ladanifer* leaves and soil where these plants grew (Chaves et al., 1997; 2001b). The latter fact has been related to its allelopathic potential. The presence of flavonols' derivatives and ellagitannins has been previously reported in other *Cistaceae* species, such as *C. laurifolius* (Enomoto et al., 2004; Santagati et al., 2008; Saracini et al., 2005).

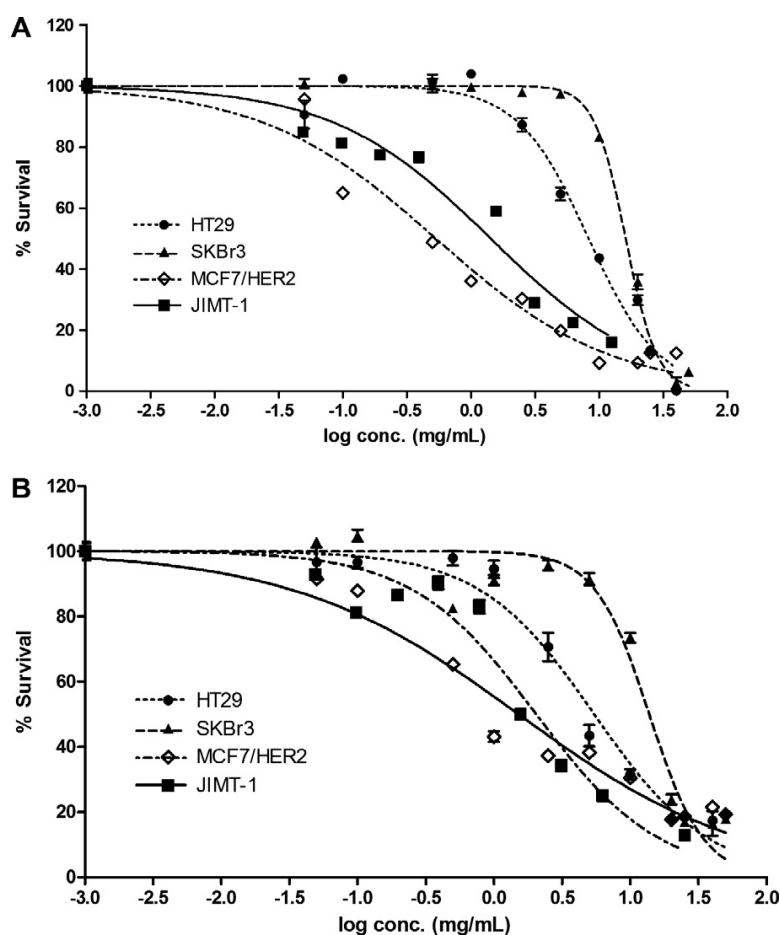


Fig. 4. Survival plots obtained using the MTT assay for HT29 colon cancer cells and SKBr3, MCF7/HER2 and JIMT-1 breast cancer cell lines treated with *C. ladanifer* (A) or *C. populifolius* (B) extracts for 24 h.

Table 4
CC50 values for different human cancer cell lines when treated with *C. ladanifer* or *C. populifolius* aqueous extracts for 24 h. Values are expressed in mg of dry extract per mL, and were determined from Figs. 3 and 4. Values are expressed as mean \pm SD, n = 8.

Cell line	<i>C. ladanifer</i>	<i>C. populifolius</i>
HS-766T	4.37 \pm 0.49	4.14 \pm 0.50
M220	0.49 \pm 0.03	0.66 \pm 0.07
M186	6.34 \pm 0.04	7.04 \pm 0.03
HT29	8.27 \pm 0.08	5.43 \pm 0.67
SKBr3	16.10 \pm 0.52	13.78 \pm 1.22
MCF7/HER2	0.53 \pm 0.07	1.15 \pm 0.22
JIMT-1	1.69 \pm 0.24	2.04 \pm 0.28

The ability of antioxidant nutrients to scavenge free radicals and to chelate metals has been associated to the inhibition of the overproduction of reactive oxygen species (ROS). The inhibition of ROS has been also linked to positive impact on human health through the modulation of the pathogenesis of many diseases such as atherosclerosis, hypertension, cardiovascular disease, ischemia/reperfusion injury, diabetes mellitus, cancer and neurodegenerative diseases (Seifried et al., 2007; Valko et al., 2007). Hence, the antioxidant activity of *C. ladanifer* and *C. populifolius* aqueous extracts was fully evaluated in this study through several *in vitro* methods. *C.*

populifolius extract exhibited higher antioxidant activity in most of the assays performed (TEAC, FRAP and TBARS) except for the ORAC assay, in which *C. ladanifer* showed higher potency. TEAC values observed for the *Cistus* species were a bit lower than those of other potent antioxidant extracts obtained with hydroalcoholic solvents and having higher polyphenolic content, such as olive leaf, orange peel bioflavonoid, or lemon verbena extracts (Funes et al., 2009). Nevertheless, the values obtained here were comparable to other reported for traditional medicinal plants (Kirca and Arslan, 2008; Li et al., 2008; Surveswaran et al., 2007). The capacity of *Cistaceae* extracts to inhibit lipid peroxidation, measured in TBARS assay, was lower than that one reported for other potent antioxidants (Funes et al., 2009; Laporta et al., 2007b), but it was still relevant.

ORAC method is based on hydrogen atom transfer mechanism and measures the capacity to eliminate peroxy radicals, which play a critical role in lipid oxidation (Huang et al., 2005). Therefore, *C. ladanifer* extract must be more efficient than *C. populifolius* extract in inhibiting peroxy radicals formation, which goes beyond than just reducing capacity, and is related to other aspects of the “total antioxidant capacity” such as radical-scavenging capacity, metal chelating capacity or ability to inhibit oxidative enzymes. This result might reveal interesting applications for the aqueous *C. ladanifer* extract as peroxy radicals preventing agent, which causes lipid oxidation in food and biological systems. Considering that



strong antioxidant ethanolic extracts such as olive leaf (25% oleuropein) and tea catechins (70% catechins) have reported ORAC values within the range of 4500–5000 TE/g dw (Laporta et al., 2007b), the values found here for *Cistus* extracts can be considered as notorious, and close to the level reported for lemon verbena extract (25% verbascoside) (Funes et al., 2009).

The MIC values for the *Cistaceae* extracts were compared to those previously published for other antimicrobial extracts such as *Hypoxis rooperi* extract and its bioactive compounds, hypoxoside and rooperol, performed in identical conditions (Laporta et al., 2007a). It can be concluded that although antimicrobial capacity of *Cistus* extracts was lower than some pure compounds such as rooperol, aqueous *Cistaceae* extracts were more effective than that reported for the antimicrobial *Hypoxis rooperi* extract (Laporta et al., 2007a). Considering that pure catechins have shown MIC values in the range of 0.064–0.128 mg/ml (Stapleton et al., 2004), the studied *Cistus* extracts can be rated as good antimicrobial agents. It has to be also remarked that *Cistus* extracts were, in some cases, as effective as the antibiotic neomycin (Table 3), which suggests potential applications for these extracts as antimicrobial agents. As regard to this, gallic acid and gallotannins, which are the main compounds of the extract may contribute significantly to this antibacterial capacity as reported (Kang et al., 2008; Taguri et al., 2004). The MIC values found here were comparable to those reported for other ellagitannins-enriched extracts (Al-Zoreky, 2009; Machado et al., 2002), or even to that of pure punicalagin (Taguri et al., 2004). This fact may indicate a synergistic interaction between the different compounds of the extract. The stronger inhibitory capacity of *C. populifolius* aqueous extract on *E. coli* might be related to its higher content in ellagitannins, which have been reported as efficient antimicrobial compounds (Al-Zoreky, 2009; Machado et al., 2002; Reddy et al., 2007). Nevertheless, the complexity of the extracts makes conclusions difficult to draw.

Natural extracts have been previously documented as a potential source of anticarcinogenic compounds (Kaefer and Milner, 2008; Perchellet et al., 1992; Shoemaker et al., 2005). In this sense, it is accepted that the chemopreventive and tumor-inhibitory effect associated to some dietary antioxidant polyphenols could be due to their capacity to inhibit oxygen reactive species (ROS) or free radicals (Halliwell, 1996). More recently, a large body of studies is evidencing the ability of these compounds to modulate uncontrolled proliferation pathways or protooncogen expression (Menendez et al., 2007). Therefore, it is certainly plausible that the cytotoxicity against cancer cells of these compounds is unrelated to their radical scavenging activity.

A recent study on the anticancer activity of several tea extracts with high polyphenolic content has reported CC50 values within the range 0.1–0.5 mg/ml for several cancer cell lines (Friedman et al., 2007). Precisely, punicalagins have shown their anticancer potential in previous studies (Seeram et al., 2005; Syed et al., 2007). Previous studies on ellagitannins-enriched extracts (Kulkarni et al., 2007) reported CC50 values around 0.55 mg/ml. Nevertheless, combination of ellagitannins were more effective than pure ellagitannins against cancer cells (Heber, 2008). Therefore, the concentration range of *Cistus* extracts displaying cytotoxicity against M220 (pancreas), MCF7/HER2 and JIMT-1 (breast) cancer cells might be significant to support further studies, especially in MCF7/HER2 and JIMT-1, where a dose–response was clearly obtained. In this sense, the overexpression of HER2 in these cells suggests that *Cistus* extracts may be exerting its cytotoxic activity by a HER2-related mechanism as reported before for other polyphenols (Menendez et al., 2007). Moreover, the results obtained regarding JIMT-1 cells might have some interesting clinical applications since JIMT-1 breast cancer cells have shown to be insensitive to trastuzumab therapy, a clinically used antibody-drug against breast cancer cells, both *in vitro* and in xenograft tumors (Tanner et al.,

2004). We have previously reported that treatment of MCF7/HER2 or JIMT-1 breast cancer cells using up to 100 µg/ml trastuzumab did not affect cell viability after four days treatment (Barrajón-Catalán et al., 2010). However, since JIMT-1 cells growth seems to be HER2-independent, the cytotoxic mechanism of the *Cistus* extracts observed in this study could take place through the modulation of cell proliferation signaling cascades (Köninki et al., 2010), rather than through an HER2-related mechanism.

5. Conclusion

In summary, *C. ladanifer* and *Cistus populifolius* suppose an abundant vegetable biomass in the forest regions and natural parks in the South of Spain and other Mediterranean regions. Since these plants are allelopathic for other species, their use to produce aqueous vegetable extracts may support a sustainably developed model and benefit the environment of the semiarid regions. Besides the well-known applications in the perfume industry, *C. ladanifer* and *C. populifolius* may provide with a source of polyphenolic extracts with significant antioxidant activity against peroxy radicals for food or biological systems. The antimicrobial activity observed for the *Cistus* extracts, which might be due to the combination of ellagitannins present in the extracts, demands for further antimicrobial studies in other bacterial strains. Moreover, the preliminary cytotoxic activity of the *Cistaceae* aqueous extracts, observed for the first time in this study against breast cancer cells, deserve further investigations in order to determine the compounds, or their combinations, which are the main responsible for such activity, and its potential mechanism.

Conflict of interest statement

The authors declare no conflicts of interest.

Acknowledgements

This investigation has been supported by Grant AGL2007–60778 and Torres-Quevedo (PTQ-08-03-08076) fellowship to E. Barrajón from MEC, and Grants IMIDTD/2006/523 and IMIDTA/2008/653 from IMPIVA (Generalitat Valenciana). We also thank Químicas del Vinalopó, S.L. and Emdemic Biotech, SL for their financial support and for providing us with the raw materials.

References

- Abad, M.J., Bermejo, P., Villar, A., Sanchez Palomino, S., Carrasco, L., 1997. Antiviral activity of medicinal plant extracts. *Phytother. Res.* 11, 198–202.
- Adamczyk, B., Kitunen, V., Smolander, A., 2008. Protein precipitation by tannins in soil organic horizon and vegetation in relation to tree species. *Biol. Fert. Soils* 45, 55–64.
- Al-Zoreky, N.S., 2009. Antimicrobial activity of pomegranate (*Punica granatum* L.) fruit peels. *Int. J. Food Microbiol.* 134, 244–248.
- Andrade, D., Gil, C., Breitenfeld, L., Domingues, F., Duarte, A.P., 2009. Bioactive extracts from *Cistus ladanifer* and *Arbutus unedo* L. *Ind. Crops Prod.*, doi:10.1016/j.indcrop.2009.1001.1009.
- Barrajón-Catalán, E., Menéndez-Gutiérrez, M.P., Falco, A., Carrato, A., Saceda, M., Micol, V., 2010. Selective death of human breast cancer cells by lytic immunoliposomes: correlation with their HER2 expression level. *Cancer Lett.* 290, 192–203.
- Benzie, I.F., Strain, J.J., 1996. The ferric reducing ability of plasma (FRAP) as a measure of "antioxidant power": the FRAP assay. *Anal. Biochem.* 239, 70–76.
- Caturla, N., Vera-Samper, E., Villalain, J., Mateo, C.R., Micol, V., 2003. The relationship between the antioxidant and the antibacterial properties of galloylated catechins and the structure of phospholipid model membranes. *Free Radic. Biol. Med.* 34, 648–662.
- Chaves, N., Escudero, J.C., Gutierrez-Merino, C., 1997. Quantitative variation of flavonoids among individuals of a *Cistus ladanifer* population. *Biochem. Syst. Ecol.* 25, 429–435.
- Chaves, N., Sosa, T., Alías, J.C., Escudero, J.C., 2001a. Identification and effects of interaction phytotoxic compounds from exudate of *Cistus ladanifer* leaves. *J. Chem. Ecol.* 27, 611–621.



- Chaves, N., Sosa, T., Escudero, J.C., 2001b. Plant growth inhibiting flavonoids in exudate of *Cistus ladanifer* and in associated soils. *J. Chem. Ecol.* 27, 623–631.
- De Andres, A.I., Gomez-Serranillos, M.P., Iglesias, I., Villar, A.M., 1999. Effects of extract of *Cistus populifolius* L. On the central nervous system. *Phytother. Res.* 13, 575–579.
- Dias, L.S., Moreira, I., 2002. Interaction between water soluble and volatile compounds of *Cistus ladanifer* L. *Chemoecology* 12, 77–82.
- Droebner, K., Ehrhardt, C., Poetter, A., Ludwig, S., Planz, O., 2007. CYSTUS052, a polyphenol-rich plant extract, exerts anti-influenza virus activity in mice. *Antiviral Res.* 76, 1–10.
- Dudonni, S., Vitrac, X., Coutière, P., Woillez, M., Mérillon, J.M., 2009. Comparative study of antioxidant properties and total phenolic content of 30 plant extracts of industrial interest using DPPH, ABTS, FRAP, SOD, and ORAC assays. *J. Agric. Food Chem.* 57, 1768–1774.
- Ehrhardt, C., Hrinčius, E.R., Korte, V., Mazur, I., Droebner, K., Poetter, A., Dreschers, S., Schmolke, M., Planz, O., Ludwig, S., 2007. A polyphenol rich plant extract, CYSTUS052, exerts anti influenza virus activity in cell culture without toxic side effects or the tendency to induce viral resistance. *Antiviral Res.* 76, 38–47.
- Eloff, J.N., 1998. A sensitive and quick microplate method to determine the minimal inhibitory concentration of plant extracts for bacteria. *Planta Med.* 64, 711–713.
- Enomoto, S., Okada, Y., Guvenc, A., Erdurak, C.S., Coskun, M., Okuyama, T., 2004. Inhibitory effect of traditional Turkish folk medicines on aldose reductase (AR) and hematological activity, and on AR inhibitory activity of curcetin-3-O-methyl ether isolated from *Cistus laurifolius* L. *Biol. Pharm. Bull.* 27, 1140–1143.
- Fernandez-Arroyo, S., Barrajoán-Catalán, E., Micol, V., Segura-Carretero, A., Fernandez-Gutierrez, A., 2009. High-performance liquid chromatography with diode array detection coupled to electrospray time-of-flight and ion-trap tandem mass spectrometry to identify phenolic compounds from a *Cistus ladanifer* aqueous extract. *Phytochem. Anal. doi:10.1002/pca.1200*.
- Ferrandis, P., Herranz, J.M., Martínez-Sánchez, J.J., 1999. Effect of fire on hard-coated Cistaceae seed banks and its influence on techniques for quantifying seed banks. *Plant Ecol.* 144, 103–114.
- Friedman, M., Mackey, B.E., Kim, H.J., Lee, I.S., Lee, K.R., Lee, S.U., Kozukue, E., Kozukue, N., 2007. Structure-activity relationships of tea compounds against human cancer cells. *J. Agric. Food Chem.* 55, 243–253.
- Funes, L., Fernández-Arroyo, S., Laporta, O., Pons, A., Roche, E., Segura-Carretero, A., Fernández-Gutiérrez, A., Micol, V., 2009. Correlation between plasma antioxidant capacity and verbascoside levels in rats after oral administration of lemon verbena extract. *Food Chem.* 117, 589–598.
- García-Morales, P., Gómez-Martínez, A., Carrato, A., Martínez-Lacaci, I., Barberá, V.M., Soto, J.L., Carrasco-García, E., Menéndez-Gutiérrez, M.P., Castro-Galache, M.D., Ferragut, J.A., Saceda, M., 2005. Histone deacetylase inhibitors induced caspase-independent apoptosis in human pancreatic adenocarcinoma cell lines. *Mol. Cancer Ther.* 4, 1222–1230.
- Gil, M.I., Tomas-Barberán, F.A., Hess-Pierce, B., Holcroft, D.M., Kader, A.A., 2000. Antioxidant activity of pomegranate juice and its relationship with phenolic composition and processing. *J. Agric. Food Chem.* 48, 4581–4589.
- Gomes, P.B., Mata, V.G., Rodrigues, A.E., 2005. Characterization of the Portuguese-grown *cistus ladanifer* essential oil. *J. Essent. Oil Res.* 17, 160–165.
- Hagerman, A.E., Butler, L.G., 1978. Protein precipitation method for the quantitative determination of tannins. *J. Agric. Food Chem.* 26, 809–811.
- Halliwel, B., 1996. Antioxidants in human health and disease. *Ann. Rev. Nut.* 16, 33–50.
- Heber, D., 2008. Multitargeted therapy of cancer by ellagitannins. *Cancer Lett.* 269, 262–268.
- Huang, D., Boxin, O.U., Prior, R.L., 2005. The chemistry behind antioxidant capacity assays. *J. Agric. Food Chem.* 53, 1841–1856.
- Inoue, M., Suzuki, R., Sakaguchi, N., Li, Z., Takeda, T., Ogiwara, Y., Jiang, B.Y., Chen, Y., 1995. Selective induction of cell death in cancer cells by gallic acid. *Biol. Pharm. Bull.* 18, 1526–1530.
- Kaefer, C.M., Milner, J.A., 2008. The role of herbs and spices in cancer prevention. *J. Nutr. Biochem.* 19, 347–361.
- Kang, M.S., Oh, J.S., Kang, I.C., Hong, S.J., Choi, C.H., 2008. Inhibitory effect of methyl gallate and gallic acid on oral bacteria. *J. Microbiol.* 46, 744–750.
- Kim, Y., 2007. Antimelanogenic and antioxidant properties of gallic acid. *Biol. Pharm. Bull.* 30, 1052–1055.
- Kirca, A., Arslan, E., 2008. Antioxidant capacity and total phenolic content of selected plants from Turkey. *Int. J. Food Sci. Tech.* 43, 2038–2046.
- Köninki, K., Barok, M., Tanner, M., Staff, S., Pitkänen, J., Hemmilä, P., Ilvesaro, J., Isola, J., 2010. Multiple molecular mechanisms underlying trastuzumab and lapatinib resistance in JM1-1 breast cancer cells. *Cancer Letters doi:10.1016/j.canlet.2010.02.002*.
- Kulkarni, A.P., Mahal, H.S., Kapoor, S., Aradhya, S.M., 2007. In vitro studies on the binding, antioxidant, and cytotoxic action of punicalagin. *J. Agric. Food Chem.* 55, 1491–1500.
- Kupeli, E., Yesilada, E., 2007. Flavonoids with anti-inflammatory and antinociceptive activity from *Cistus laurifolius* L. leaves through bioassay-guided procedures. *J. Ethnopharmacol.* 112, 524–530.
- Laporta, O., Funes, L., Garzón, M.T., Villalain, J., Micol, V., 2007a. Role of membranes on the antibacterial and anti-inflammatory activities of the bioactive compounds from *Hypoxis rooperi* corm extract. *Arch. Biochem. Biophys.* 467, 119–131.
- Laporta, O., Pérez-Fons, L., Mallavia, R., Caturla, N., Micol, V., 2007b. Isolation, characterization and antioxidant capacity assessment of the bioactive compounds derived from *Hypoxis rooperi* corm extract (African potato). *Food Chem.* 101, 1425–1437.
- Li, H.B., Wong, C.C., Cheng, K.W., Chen, F., 2008. Antioxidant properties in vitro and total phenolic contents in methanol extracts from medicinal plants. *LWT – Food Sci. Technol.* 41, 385–390.
- Machado, T.D.B., Leal, I.C.R., Amaral, A.C.F., Dos Santos, K.R.N., Da Silva, M.G., Kuster, R.M., 2002. Antimicrobial ellagitannin of *Punica granatum* fruits. *J. Braz. Chem. Soc.* 13, 606–610.
- Makkar, H.P.S., 1989. Protein precipitation methods for quantitation of tannins: a review. *J. Agric. Food Chem.* 37, 1197–1202.
- Menendez, J.A., Vazquez-Martin, A., Colomer, R., Brunet, J., Carrasco-Pancorbo, A., García-Villalba, R., Fernandez-Gutierrez, A., Segura-Carretero, A., 2007. Olive oil's bitter principle reverses acquired autoresistance to trastuzumab (Herceptin) in HER2-overexpressing breast cancer cells. *BMC Cancer* 7, 80.
- Mosmann, T., 1983. Rapid colorimetric assay for cellular growth and survival: application to proliferation and cytotoxicity assays. *J. Immunol. Methods* 65, 55–63.
- Ou, B., Hampsch-Woodill, M., Prior, R.L., 2001. Development and validation of an improved oxygen radical absorbance capacity assay using fluorescein as the fluorescent probe. *J. Agric. Food Chem.* 49, 4619–4626.
- Pascual, T.J., Urones, J.G., Basaba, P., Nieto Pachó, M.J., 1977. Flavonoides de Cistaceae II *Cistus populifolius* L. y *Cistus hirsutus*. *Lam Anales de Química* 73, 1047–1048.
- Paton, D., Nuñez-Trujillo, J., Muñoz, A., Tovar, J., 1998. Prediction of browsing biomass of five shrub species of genus *Cistus* from Monfragüe natural park using multiple regressions. *Arch. Zootec.* 47, 95–105.
- Perchellet, J.P., Gali, H.U., Perchellet, E.M., Klish, D.S., Armbrust, A.D., 1992. Antitumor-promoting activities of tannic acid, ellagic acid, and several gallic acid derivatives in mouse skin. *Basic Life Sci.* 59, 783–801.
- Pourmorad, F., Hosseini-mehr, S.J., Shahabimajid, N., 2006. Antioxidant activity, phenol and flavonoid contents of some selected Iranian medicinal plants. *Afr. J. Biotechnol.* 5, 1142–1145.
- Reddy, M.K., Gupta, S.K., Jacob, M.R., Khan, S.I., Ferreira, D., 2007. Antioxidant, antimutagenic and antimicrobial activities of tannin-rich fractions, ellagitannins and phenolic acids from *Punica granatum* L. *Plan. Med.* 73, 461–467.
- Robles, C., Bousquet-Mélou, A., Garzino, S., Bonin, G., 2003. Comparison of essential oil composition of two varieties of *Cistus ladanifer*. *Biochem. Syst. Ecol.* 31, 339–343.
- Santagati, N.A., Salerno, L., Attagui, G., Savoca, F., Ronsisvalle, G., 2008. Simultaneous determination of catechins, rutin, and gallic acid in *Cistus* species extracts by HPLC with diode array detection. *J. Chromatogr. Sci.* 46, 150–156.
- Saracini, E., Tattini, M., Traversi, M.L., Vincieri, F.F., Pinelli, P., 2005. Simultaneous LC-DAD and LC-MS determination of ellagitannins, flavonoid glycosides, and acyl-glycosyl flavonoids in *Cistus salvifolius* L. Leaves. *Chromatographia* 62, 245–249.
- Seeram, N., Lee, R., Hardy, M., Heber, D., 2004. Rapid large scale purification of ellagitannins from pomegranate husk, a by-product of the commercial juice industry. *Sep. Purif. Technol.* 41, 49–55.
- Seeram, N.P., Adams, L.S., Henning, S.M., Niu, Y., Zhang, Y., Nair, M.G., Heber, D., 2005. In vitro antiproliferative, apoptotic and antioxidant activities of punicalagin, ellagic acid and a total pomegranate tannin extract are enhanced in combination with other polyphenols as found in pomegranate juice. *J. Nutr. Biochem.* 16, 360–367.
- Seifried, H.E., Anderson, D.E., Fisher, E.I., Milner, J.A., 2007. A review of the interaction among dietary antioxidants and reactive oxygen species. *J. Nutr. Biochem.* 18, 567–579.
- Shoemaker, M., Hamilton, B., Dairkee, S.H., Cohen, I., Campbell, M.J., 2005. In vitro anticancer activity of twelve Chinese medicinal herbs. *Phytother. Res.* 19, 649–651.
- Somoza, B., Sanchez De Rojas, V.R., Ortega, T., Villar, A.M., 1996. Vasodilator effects of the extract of the leaves of *Cistus populifolius* on rat thoracic aorta. *Phytother. Res.* 10, 304–308.
- Sosa, T., Chaves, N., Alias, J.C., Escudero, J.C., Henao, F., Gutiérrez-Merino, C., 2004. Inhibition of mouth skeletal muscle relaxation by flavonoids of *Cistus ladanifer* L.: a plant defense mechanism against herbivores. *J. Chem. Ecol.* 30, 1087–1101.
- Stapleton, P.D., Shah, S., Anderson, J.C., Hara, Y., Hamilton-Miller, J.M., Taylor, P.W., 2004. Modulation of beta-lactam resistance in *Staphylococcus aureus* by catechins and gallates. *Int. J. Antimicrob. Agents* 23, 462–467.
- Surveswaran, S., Cai, Y.Z., Corke, H., Sun, M., 2007. Systematic evaluation of natural phenolic antioxidants from 133 Indian medicinal plants. *Food Chem.* 102, 938–953.
- Syed, D.N., Afaq, F., Mukhtar, H., 2007. Pomegranate derived products for cancer chemoprevention. *Sem. Can. Biol.* 17, 377–385.
- Taguri, T., Tanaka, T., Kouno, I., 2004. Antimicrobial activity of 10 different plant polyphenols against bacteria causing food-borne disease. *Biol. Pharm. Bull.* 27, 1965–1969.
- Tanner, M., Kapanen, A.I., Junttila, T., Raheem, O., Grenman, S., Elo, J., Elenius, K., Isola, J., 2004. Characterization of a novel cell line established from a patient with Herceptin-resistant breast cancer. *Mol. Cancer Ther.* 3, 1585–1592.
- Teixeira, S., Mendes, A., Alves, A., Santos, L., 2007. Simultaneous distillation-extraction of high-value volatile compounds from *Cistus ladanifer* L. *Anal. Chim. Acta* 584, 439–446.
- Ustun, O., Ozcelik, B., Akyon, Y., Abbasoglu, U., Yesilada, E., 2006. Flavonoids with anti-Helicobacter pylori activity from *Cistus laurifolius* leaves. *J. Ethnopharmacol.* 108, 457–461.



2282

E. Barrajón-Catalán et al./Food and Chemical Toxicology 48 (2010) 2273–2282

Vaher, M., Ehala, S., Kaljurand, M., 2005. On-column capillary electrophoretic monitoring of rapid reaction kinetics for determination of the antioxidative potential of various bioactive phenols. *Electrophoresis* 26, 990–1000.

Valko, M., Leibfritz, D., Moncol, J., Cronin, M.T., Mazur, M., Telser, J., 2007. Free radicals and antioxidants in normal physiological functions and human disease. *Int. J. Biochem. Cell Biol.* 39, 44–84.







BLOQUE II.

Aceite de Oliva Virgen Extra







CAPÍTULO 4. Crude phenolic extracts from extra-virgin olive oil circumvent *de novo* breast cancer resistance to HER1/HER2-targeting drugs by inducing GADD45-sensed cellular stress, G2/M arrest and hyperacetylation of Histone H3.





Crude phenolic extracts from extra virgin olive oil circumvent *de novo* breast cancer resistance to HER1/HER2-targeting drugs by inducing GADD45-sensed cellular stress, G2/M arrest and hyperacetylation of Histone H3

CRISTINA OLIVERAS-FERRAROS^{1,2*}, SALVADOR FERNÁNDEZ-ARROYO^{3*}, ALEJANDRO VAZQUEZ-MARTIN^{1,2*}, JESÚS LOZANO-SÁNCHEZ³, SÍLVIA CUFÍ^{1,2}, JORGE JOVEN⁴, VICENT MICOL⁵, ALBERTO FERNÁNDEZ-GUTIÉRREZ³, ANTONIO SEGURA-CARRETERO³ and JAVIER A. MENENDEZ^{1,2*}

¹Catalan Institute of Oncology (ICO); ²Girona Biomedical Research Institute (IdIBGi), Girona, Catalonia; ³Department of Analytical Chemistry, Faculty of Sciences, University of Granada, Granada, Andalusia; ⁴Centre de Recerca Biomèdica, Hospital Universitari Sant Joan de Reus, Institut d'Investigació Sanitària Pere Virgili, Universitat Rovira i Virgili, Reus, Catalonia; ⁵Molecular and Cellular Biology Institute (IBMC), Miguel Hernández University, Elche Alicante, Spain

DOI: 10.3892/ijo_XXXXXXXX

1 **Abstract.** Characterization of the molecular function of complex
2 phenols naturally present in extra virgin olive oil (EVOO)
3 against the HER2-gene amplified JIMT-1 cell line, a unique
4 breast cancer model that inherently exhibits cross-resistance
5 to multiple HER1/2-targeted drugs including trastuzumab,
6 gefitinib, erlotinib and lapatinib, may underscore innovative
7 cancer molecules with novel therapeutic targets because they
8 should efficiently circumvent *de novo* resistance to HER1/2
9 inhibitors in order to elicit tumoricidal effects. We identified
10 pivotal signaling pathways associated with the efficacy of crude
11 phenolic extracts (PEs) obtained from 14 monovarietals of
12 Spanish EVOOs. i) MTT-based cell viability and HPLC coupled
13 to time-of-flight (TOF) mass spectrometry assays revealed
14 that anti-cancer activity of EVOO PEs positively correlated
15 with the phenolic index (i.e., total content of phenolics) and
16 with a higher presence of the complex polyphenols secoiridoids
17 instead of lignans. ii) Genome-wide analyses using 44 K
18 Agilent's whole human arrays followed by Gene Set Enrichment
19 Analysis (GSEA)-based screening of the Kyoto Encyclopedia
20 of Genes and Genomes (KEGG) pathway database revealed
21 a differential modulation of the JIMT-1 transcriptome at the
22 level of the cell cycle and p53 pathways. EVOO PEs differentially
23 impacted the expression status of stress-sensing, G2-M check-

point-related *GADD45* genes and of p53-related *CDKN1A*,
CDKN1C and *PMAIP-1* genes. iii) Cell cycle and fluorescence
microscopy analyses confirmed that secoiridoid-rich EVOO
PE inhibited mitosis to promote G2-M cell cycle arrest. This
was accompanied with the appearance of diffuse, even DNA
staining with γ H2AX and pan-nuclear hyperacetylation of
Histone H3 at Lysine 18. iv) Semi-quantitative Signaling Node
Multi-Target ELISAs determined that secoiridoid-rich EVOO
PE drastically activated the mitogen-activated protein kinases
MEK1 and p38 MAPK, a GADD45-related kinase involved in
Histone H3 acetylation. Secoiridoids, a family of complex
polyphenols characteristic of *Oleaceae* plants, appear to permit
histones to remain in hyperacetylated states and through the
resulting alterations in gene regulation to reduce mitotic viability
and metabolic competence of breast cancer cells inherently
refractory to HER-targeting therapies *ab initio*. *Oleaceae*
secoiridoids could provide a valuable phytochemical platform
for the design of more pharmacologically active second-
generation phytopharmaceutical anti-breast cancer molecules
with a unique mode of action.

Introduction

A significant amount of research has been dedicated in the last
few years to elucidate the molecular mechanisms that could
explain the appearance of acquired resistance to trastuzumab
(Hereceptin™) (1-3), a recombinant humanized antibody against
the HER2 receptor that was the first monoclonal antibody
approved for the treatment of a solid tumor by the FDA in
1998 (4-6). Moreover, not all *HER2* gene-amplified breast
carcinomas respond to treatment with trastuzumab *ab initio*.
Seventy percent of *HER2*-overexpressing metastatic breast
carcinomas show primary resistance to trastuzumab as a single
agent and approximately 15% of women diagnosed with early
HER2-positive disease are *de novo* resistant to trastuzumab and
relapse in spite of treatment with trastuzumab-based therapies

Correspondence to: Dr Javier A. Menendez, Catalan Institute of
Oncology, Girona (ICO-Girona) Dr Josep Trueta University Hospital
Ctra. França s/n, E-17007 Girona, Catalonia, Spain
E-mail: jmenendez@iconcologia.net; jmenendez@idibgi.org

*Contributed equally

Key words: olive oil, breast cancer, phenolics, GADD45, epigenome,
histones



(7,8). In this scenario, unraveling the ultimate responsible underlying *de novo* resistance to trastuzumab is a major challenge that is beginning to be addressed, and this dilemma is becoming increasingly important as pivotal trials showing clinical benefit of trastuzumab in combination with chemotherapy have led to a new standard of care for women in the adjuvant setting for HER2-overexpressing early-stage breast carcinomas (9,10). Unfortunately, there have been few studies addressing the ultimate molecular mechanisms that could explain *de novo* resistance to trastuzumab and other HER2-targeted therapies. Because of the lack of appropriate model systems, one can anticipate that this issue could be difficult to study and, accordingly, the precise molecular mechanisms underlying *de novo* non-sensitivity to trastuzumab remain largely obscure.

It is well established that the identification and the study with high-throughput techniques of phenotypes such as long-term survivors of untreatable malignancies, individuals protected against certain cancer diseases despite having a markedly risk for their development, or cancer patients displaying striking responses following a specific treatment, not only may unveil specific genetic/molecular alterations ultimately causing such characteristic phenotypes but may provide further innovative and clinically valuable therapeutic targets against these disease (11,12). We recently hypothesized that, in a counterintuitive manner, we could take advantage of extreme phenotype selection studies in the identification of clinically relevant molecular features explaining breast cancer resistance to HER2-targeted therapies *ab initio*. In this regard, intrinsic trastuzumab resistance in a cell line isolated from the pleural fluid of a HER2-positive breast cancer patient with progressive disease on trastuzumab (i.e., JIMT-1) constitutes an excellent scenario to discover alternative explanations for *de novo* resistance to trastuzumab (13,14). First, high-resolution genomic profiles have confirmed that, among intrinsic breast cancer molecular subtypes (15,16), trastuzumab-sensitive BT-474 and SKBR3 breast cancer cell lines (two *in vitro* models widely used as HER2-gene amplified trastuzumab-sensitive breast carcinomas) display a luminal B-like gene expression phenotype whereas trastuzumab-refractory JIMT-1 cells rather exhibit the closest resemblance to the actual HER2-positive gene expression breast cancer subtype (17). Second, JIMT-1 cells provide a valuable experimental model for the studies of resistance to HER-targeted therapies as they are largely insensitive to the growth inhibitory effects of the HER2/HER3 monoclonal antibodies trastuzumab and pertuzumab and to the HER1/HER2 tyrosine kinase inhibitors (TKIs) gefitinib, erlotinib, and lapatinib (13,14,17). Owing to redundant molecular mechanisms such as low levels of HER2 protein expression and activation despite HER2 gene amplification, loss of the phosphatase and tensin homolog (PTEN) tumor suppressor, activating mutation of the PIK3CA gene, and intrinsic enrichment in the CD44^{pos}CD24^{neg/low} phenotype with stem/progenitor cell properties (17,18), JIMT-1 cell line constitutes a naturally-occurring 'extreme phenotype' of *de novo* cross-refractoriness to multiple HER targeting therapies.

Extra virgin olive oil (EVOO)-derived complex polyphenols have been shown to exert significant anti-carcinogenic effects by directly modulating the activities of various types of receptor tyrosine kinases (RTKs), including HER2 (19-22). We here envisioned that, if HER2-positive JIMT-1 breast cancer cells

inherently refractory to multiple HER targeting therapies may retain sensitivity to EVOO phenolics, the genetic and functional study of the mode of actions involved may underscore therapeutic targets and innovative drug platforms aimed at circumventing intrinsic resistance to currently available HER targeting drugs. We evaluated the utility of genome-wide expression monitoring combined with functional validation approaches to delineate both the biological actions and the clinical value of complex multi-component phenolic extracts directly obtained from 14 monovarietals of Spanish EVOO. We now reveal for the first time that secoiridoids, a family of complex polyphenols characteristic of *Oleaceae* plants (23-25), may constitute a phytochemical platform for the development of novel anti-breast cancer drugs with a novel mode of action involving transcriptional activation of stress-responsive *GADD45* genes, G2/M cell cycle arrest, activation of the mitogen-activated protein kinases MEK1 and p38 MAPK, and histone acetylation-related chromatin remodeling (26-30). Our current elucidation of a molecular link between administration of complex polyphenols naturally occurring in EVOO and post-translational modification of histones, which can lead to epigenetic regulation of chromatin structure with attendant modulation of cell physiology in response to cellular stress, might suggest a novel antitumor therapeutic strategy able to efficiently circumvent intrinsic refractoriness of HER2-positive breast carcinomas to currently used HER1/2-targeted therapies.

Materials and methods

Collection of crude phenolic extracts from EVOO monovarietals. Solid phase extraction (SPE) with Diol-cartridges was employed to collect the phenolic fraction of EVOOs from all 14 monovarietals (31).

Quantification of total phenolic compounds. The Folin Ciocalteu method was employed for the quantification of total polyphenols in EVOO crude extracts (32). To calculate the percentage of each family of polyphenols, such as secoiridoids, phenolic alcohols, lignans, flavones and unknowns compounds, the 14 crude EVOO PE were injected into HPLC system (RRLC 1200 series, Agilent Technologies, Santa Clara, CA, USA) coupled to time-of-flight (TOF) mass spectrometer (Bruker Daltonics, Bremen, Germany). The conditions for HPLC and TOF have been described elsewhere (22). The area of each peak was calculated from the extracted ion chromatogram (EIC) by using Data Analysis software provided by Bruker Daltonics. The summation of all areas is the 100% of phenolic compounds.

Culture conditions. JIMT-1 human breast cancer cell line was established at Tampere University and is available from the German Collection of Microorganisms and Cell Cultures (<http://www.dsmz.de/>). JIMT-1 cells were grown in DMEM supplemented with 10% FBS and 2 mM L-glutamine. Cells were maintained at 37°C in a humidified atmosphere of 95% air and 5% CO₂.

Metabolic status assessment (MTT-based cell viability assays). JIMT-1 cells were seeded at a density of ~3,000 cells per well in a 96-well plate. The next day, cells were treated with



1 concentrations ranging from 0.0 to 0.1% (v/v) of the whole
 2 crude EVOO-PE dissolved in 1 ml of ethanol (stock solution).
 3 An appropriate amount of ethanol (v/v) was added to control
 4 cells. After 5 days of treatment (EVOO PE were not renewed
 5 during the entire period of culture treatment), cells were
 6 incubated with a solution of MTT [3-(4, 5-dimethylthiazol-
 7 2-yl)-2,5-diphenyltetrazolium bromide; Sigma, St. Louis,
 8 MO, USA] at a concentration of 5 mg/ml for 3 h at 37°C. The
 9 supernatants were then carefully aspirated, 100 µl of DMSO
 10 was added to each well, and the plates were agitated to dissolve
 11 the crystal product. Absorbances were read at 570 nm using a
 12 multi-well plate reader (Model Anthos Labtec 2010 1.7 reader).
 13 Cell viability effects upon exposure to EVOO-PE were analyzed
 14 as percentages of the absorbance obtained in untreated control
 15 cells. For each treatment, cell viability was evaluated as a
 16 percentage using the following equation: (A570 of treated
 17 sample/A570 of untreated sample) x 100. Cell sensitivity to
 18 crude EVOO-PE was expressed in terms of the concentration of
 19 PE (v/v) needed to decrease by 50% cell viability (IC₅₀ value).
 20 Since the percentage of control absorbance was considered to
 21 be the surviving fraction of cells, the IC₅₀ values were defined
 22 as the concentration of EVOO-PE that produced 50% reduction
 23 in control absorbance.
 24

25 *Agilent GeneChip analyses.* Total RNA isolated from JIMT-1
 26 cells grown in the absence or presence of 0.001% (v/v) EVOO
 27 PE for 6 h was isolated with TRIzol reagent (Invitrogen,
 28 Carlsbad, CA, USA), according to the manufacturer's
 29 instructions. RNA quantity and quality were determined using
 30 the RNA 6000 Nano Assay kit on an Agilent 2100 BioAnalyzer
 31 (Agilent Technologies, Palo Alto, CA, USA), as recommended.
 32 Agilent Human Whole Genome Microarrays (G4112F),
 33 containing 45,220 probes, were then hybridized. Briefly,
 34 500 ng of total RNA from each sample were amplified by
 35 Oligo-dT-T7 reverse transcription and labeled by *in vitro*
 36 transcription with T7 RNA polymerase in the presence of
 37 Cy5-CTP or Cy3-CTP using the QuickAmp Labeling Kit
 38 (Agilent) and purified using RNAeasy columns (Qiagen). After
 39 fragmentation, 825 ng of labeled cRNA from each of the
 40 two samples were co-hybridized in *in situ* hybridization buffer
 41 (Agilent) for 17 h at 65°C and washed at room temperature
 42 (RT) 1 min in Gene Expression Wash Buffer 1 (Agilent) and 1
 43 min at 37°C in Gene Expression Wash Buffer 2 (Agilent).
 44

45 *Statistical analysis of microarray data.* The images were
 46 generated on a confocal microarray scanner (G2565BA,
 47 Agilent) at 5 µm resolution and quantified using GenePix 6.0
 48 (Molecular Dynamics). Spots with signal intensities twice
 49 above the local background, not saturated and not flagged by
 50 GenePix were considered reliable. Extracted intensities were
 51 back-ground-corrected and the log₂ ratios were normalized in
 52 an intensity-dependent fashion by the global LOWESS
 53 method (intra-chip normalization). Normalized log₂ ratios
 54 were scaled between arrays to make all data comparable.
 55 Raw data were processed using MMARGE, a web
 56 implementation of LIMMA - a microarray analysis library
 57 developed within the Bioconductor project in the R statistical
 58 environment. To determine genes that were differentially
 59 expressed, the multiclass SAM (significance analysis of
 60 microarrays) procedure was applied. Probes with q-value

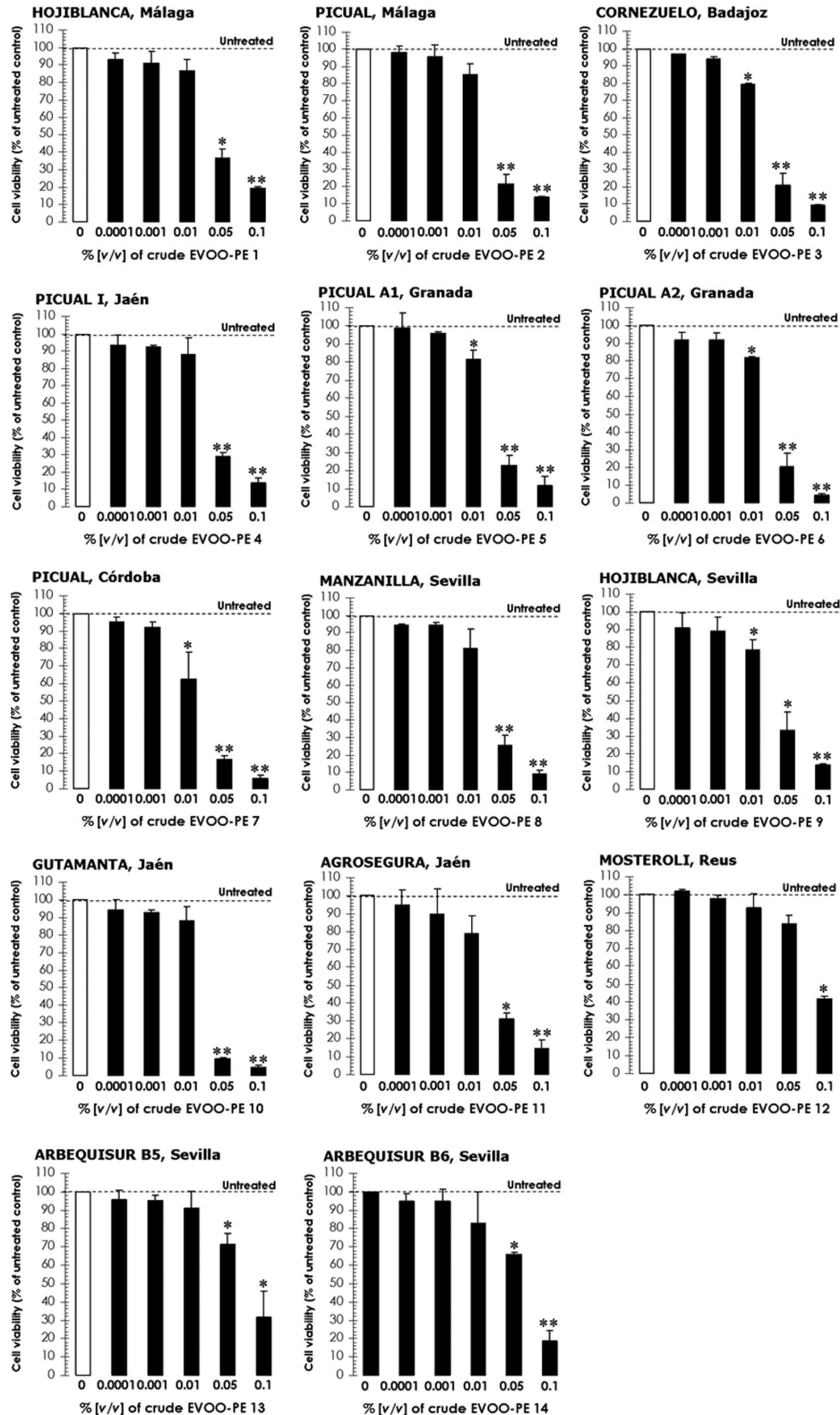
(FDR) <5% and additionally a fold change exceeding 1.2 in
 absolute value were selected as the relevant ones. Microarray
 probes were collapsed to genes by taking the median log₂
 ratio of the respective probes per gene.

Functional analysis of microarray data. To learn more about
 the biological context of the genes found to be regulated, we
 applied Gene Set Enrichment Analyses (GSEA). GSEA is a
 computational method that determines whether an *a priori*
 defined set of genes shows statistically significant, concordant
 differences between two biological states (e.g., phenotypes).
 Groups of related treatment comparison were built by using
 EVOO-PE 12 and EVOO-PE 7 as low-and high-responder
 phenotypes, respectively. Thus, the first group included the
 following comparisons: EVOO-PE 12 versus EVOO-PE 3,
 EVOO-PE 12 versus EVOO-PE 7 and EVOO-PE 12 versus
 EVOO-PE 10. The second group included the following
 comparisons: EVOO-PE 7 versus EVOO-PE 3, EVOO-PE 10
 versus EVOO-PE 7 and EVOO-PE 12 versus EVOO-PE 7. The
 combination of genes commonly regulated in those comparisons
 was then used as the list of interesting genes. Enrichment of
 the interesting genes within all available (i.e., 212) KEGG
 pathways that contained genes present on the used microarray
 platform was tested with Fisher's exact test. Pathways with
 q-value (FDR) <5% were considered as significantly enriched.

Cell cycle analysis. Adherent and detached cells were collected
 after trypsin detachment, washed in phosphate-buffered salt
 solution (PBS) and centrifuged at 1500 rpm. Cells were
 resuspended at 2x10⁶ cells/ml in PBS and fixed in ice-cold
 80% ethanol for, at least, 24 h. Fixed cells were centrifuged
 at 300 x g and each sample resuspended in propidium iodide
 (PI) stain buffer (0.1% Triton X-100[®], 200 µg of DNase-free
 RNase A, 20 µg of PI) in PBS for 30 min. After staining,
 samples were analyzed using a FACSCalibur (Becton-Dickinson,
 San Diego, CA, USA) and ModFit LT (Verity Software).

*Immunofluorescence staining and high-content confocal
 imaging.* Cells were seeded at ~5,000 cells/well in 96-well
 clear bottom imaging tissue culture plates (Becton-Dickinson
 Biosciences, San Jose, CA, USA) optimized for automated
 imaging applications. Triton X-100 permeabilization and
 blocking, primary antibody staining [phospho-Histone H2A.X
 (Ser139) 20E3 rabbit mAb #9718, Cell Signaling Technology,
 Inc. and Histone H3 modification antibody K18ac, Upstate
 Biotechnology, Millipore-both diluted according to the procedure
 suggested by the manufacturer], secondary antibody staining
 using Alexa Fluor[®] 488 goat anti-rabbit/mouse IgGs (Invitrogen,
 Molecular Probes, Eugene, OR, USA) and counterstaining
 (using Hoechst 33258; Invitrogen) were performed following
 BD Biosciences protocols. Images were captured in different
 channels for Alexa Fluor 488 (pseudo-colored green) and
 Hoechst 33258 (pseudo-colored blue) on a BD Pathway[™] 855
 Bioimager System (Becton-Dickinson) with x20 or x40
 objectives (NA 075 Olympus). Merged images were obtained
 according to the Recommended Assay Procedure using BD
 Attovision[™] software.

*Semi-quantitative determination of AKT, Stat3, p38 MAPK,
 MEK1 and NF-κB phosphorylation status.* CST's PathScan[®] 120



61
62
63
64
65
66
67
68
69
70
71
72
73
74
75
76
77
78
79
80
81
82
83
84
85
86
87
88
89
90
91
92
93
94
95
96
97
98
99
100
101
102
103
104
105
106
107
108
109
110
111
112
113
114
115
116
117
118
119
120

1
2
3
4
5
6
7
8
9
10
11
12
13
14
15
16
17
18
19
20
21
22
23
24
25
26
27
28
29
30
31
32
33
34
35
36
37
38
39
40
41
42
43
44
45
46
47
48
49
50
51
52
53
54
55
56
57
58
59
60

Figure 1. Effects of EVOO-PE on cell viability in JIMT-1 breast cancer cells. The metabolic status of trastuzumab-refractory JIMT-1 treated with graded concentrations of individual EVOO-PE was evaluated using a MTT-based cell viability assays and constructing dose-response graphs as % of untreated cells (dashed line, 100% cell viability). Results are means (columns) and 95% confidence intervals (bars) of three independent experiments made in triplicate. Statistically significant differences (one-factor ANOVA analysis) between experimental conditions and unsupplemented control cells are shown by asterisks (*P<0.01; **P<0.001). All statistical tests were two-sided.

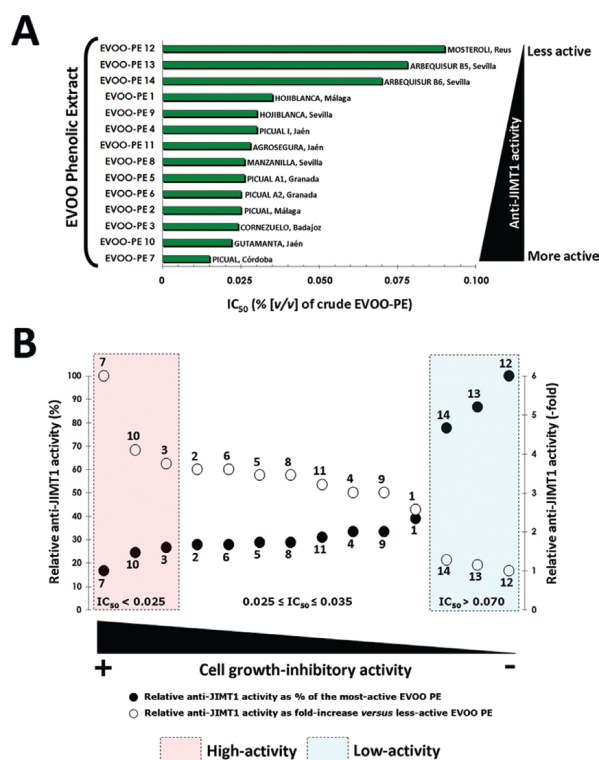


1 Signaling Nodes Multi-Target Sandwich ELISA Kit #7272
 2 was purchased from Cell Signaling Technology, Inc. This
 3 solid phase sandwich enzyme-linked ImmunoSorbent assay
 4 combines the reagents necessary to detect endogenous levels
 5 of AKT1, phospho-AKT1 (Ser473), phospho-MEK1
 6 (Ser217/221), phospho-p38 MAPK (Thr180/Tyr182), phospho-
 7 Stat3 (Tyr705) and phospho-NF- κ B p65 (Ser536). JIMT-1
 8 cells (75-80% confluent) were starved overnight and then
 9 cultured in the absence or presence of 0.001% v/v EVOO PE
 10 in 5% FBS-containing culture medium for 48 h. Cells were
 11 washed twice with cold-PBS and then lysed in buffer [20 mmol/l
 12 Tris pH 7.5, 150 mmol/l NaCl, 1 mmol/l EDTA, 1 mmol/l
 13 EGTA, 1% Triton X-100, 2.5 mmol/l sodium pyrophosphate,
 14 1 mmol/l β -glycerolphosphate, 1 mmol/l Na_3VO_4 , 1 $\mu\text{g/ml}$
 15 leupeptin, 1 mmol/l phenylmethylsulfonylfluoride, and complete
 16 protease inhibitor cocktail (Sigma-Chemicals)] for 30 min on
 17 ice. The lysates were cleared by centrifugation in an
 18 Eppendorf tube (15 min at 14,000 x g, 4°C). Protein content
 19 was determined against a standardized control using the
 20 Pierce Protein Assay Kit (Rockford, IL). Differential
 21 phosphorylation of AKT1, phospho-AKT, phospho-MEK1,
 22 phospho-p38 MAPK, phospho-Stat3 and phospho-NF- κ B p65
 23 was measured as per the manufacturer's instructions. Briefly,
 24 after incubation with cell lysates at a protein concentration of
 25 0.5 mg/ml, the target phospho-protein is captured by the
 26 antibody coated onto the microwells. Following extensive
 27 washing, a detection antibody is added to detect the captured
 28 target phospho-protein. An HRP-linked secondary antibody
 29 is then used to recognize the bound detection antibody. The
 30 HRP substrate TMB is added to develop color. The magnitude
 31 of absorbance (measured at 450 nm) for this developed color is
 32 proportional to the quantity of bound target protein.
 33

34 **Statistical analyses.** Two-group comparisons were performed by
 35 the Student's t-test for paired and unpaired values. Comparisons
 36 of means of ≥ 3 groups were performed by ANOVA and the
 37 existence of individual differences, in case of significant
 38 F-values at ANOVA, tested by Scheffé's multiple contrasts.
 39 For correlations between two parameters, the predicted lines
 40 were determined by simple linear regression analysis. The
 41 P-values and Pearson's linear correlation coefficient (r) were
 42 calculated with XLSTAT (Addinsoft™) and $P < 0.001$ was
 43 considered to be significant.
 44

45 **Results**

46
 47 **Cell growth inhibitory effects of crude EVOO-PE against**
 48 **JIMT-1 breast cancer cells.** To evaluate whether trastuzumab-
 49 refractory JIMT-1 cells, concentrations of the anti-HER2
 50 monoclonal antibody trastuzumab as high as 1000 $\mu\text{g/ml}$
 51 failed to significantly alter JIMT-1 cell viability as evaluated
 52 by the MTT assay (data not shown), retained sensitivity to
 53 crude PE directly obtained from 14 EVOO monovarietals,
 54 JIMT-1 cells were cultured in the absence or presence of a
 55 series of ethanolic dilutions (i.e., 0%, 0.0001, 0.001, 0.01, 0.05
 56 and 0.1 % v/v), which were prepared immediately before starting
 57 each experiment by diluting full strength EVOO-PE (100%)
 58 in fresh culture medium. The highest solvent concentration in
 59 the medium (0.1% v/v ethanol) has no significant effect on the
 60 metabolic status of JIMT-1 cells (data not shown). Although



61
62
63
64
65
66
67
68
69
70
71
72
73
74
75
76
77
78
79
80
81
82
83
84
85
86
87
88
89
90
91
92
93
94
95
96
97
98
99
100
101

Figure 2. Differential growth-inhibitory efficacy of EVOO-PE against JIMT-1 breast cancer cells. Top, sensitivity of JIMT-1 cells to individual EVOO-PE was expressed in terms of the concentration of PE [% (v/v)] required to decrease by 50% (IC₅₀) cell viability. Since the percentage of control absorbance in MTT-based cell viability assays (Fig. 1) was considered to be the surviving fraction of cells, the EVOO-PE IC₅₀ values were defined as the concentration of PE that produced 50% reduction in control absorbance (by interpolation upon construction of dose-response curves). Bottom, comparative efficacy of EVOO-PE against JIMT-1 cells was carried out by arbitrarily normalizing EVOO-PE IC₅₀ values as either % of the most-active EVOO-PE (EVOO-PE 7 = 100% activity) or fold-increases versus less-active EVOO PE (EVOO-PE 12 = 1.0-fold change). Statistically significant changes in curves slopes identified three groups of EVOO-PE with similar IC₅₀ values: 1, IC₅₀ < 0.025% v/v; 2, 0.025% v/v ≤ IC₅₀ ≤ 0.035% v/v; 3, IC₅₀ > 0.070% v/v.

102 all the crude EVOO-PE were capable of decreasing JIMT-1
 103 cell viability in a concentration-dependent manner (Fig. 1), we
 104 noted remarkable differences in the ability of individual
 105 EVOO-PE to elicit growth-inhibitory responses in JIMT-1
 106 cells. Thus, concentrations as low as 0.01% v/v notably
 107 decreased cell viability when employing PE obtained from
 108 EVOO mono-varietals 3 and 7. Conversely, concentrations as
 109 high as 0.1% v/v were needed to significantly decrease cell
 110 viability when employing PE obtained from EVOO mono-
 111 varietals 12, 13 and 14.

112 To accurately evaluate differences in the JIMT-1 breast
 113 cancer cell growth inhibitory activities among EVOO-PE,
 114 IC₅₀ values (i.e., the concentration of EVOO-PE needed to
 115 decrease cell viability by 50% relative to untreated control
 116 cells) were calculated by interpolation upon construction of
 117 dose-response curves. We obtained a wide series of IC₅₀ values
 118 ranging from 0.015% v/v (EVOO-PE 7) to 0.090% v/v
 119 (EVOOPE 12) (Fig. 2, top). Upon this approach, crude EVOO
 120 PE exhibited the following cytotoxic potencies: EVOO-PE 7 >



Table I. Total phenolic content in EVOO PE and percentage values for each family of polyphenols.

	Total phenolic index ^a	Secoiridoids ^b	Alcohols ^b	Lignans ^b	Flavones ^b	Unknown ^b
EVOO-PE1	206.66±0.31	88.14	3.94	1.24	5.27	1.41
EVOO-PE2	242.05±5.85	91.94	4.12	0.63	2.35	0.95
EVOO-PE3	229.14±0.46	93.72	1.02	0.50	2.89	1.87
EVOO-PE4	220.81±2.33	90.04	5.62	0.71	2.36	1.26
EVOO-PE5	208.64±2.31	92.41	3.46	0.60	2.63	0.90
EVOO-PE6	244.24±1.70	92.34	3.31	0.56	2.85	0.94
EVOO-PE7	302.13±1.77	94.06	2.15	0.51	2.61	0.67
EVOO-PE8	314.78±2.11	90.37	2.85	0.80	4.81	1.16
EVOO-PE9	292.27±1.67	87.23	2.19	1.05	8.41	1.12
EVOO-PE10	252.43±1.43	93.03	1.96	0.57	3.68	0.76
EVOO-PE11	285.47±4.62	89.19	4.79	0.73	4.36	0.93
EVOO-PE12	82.25±1.99	64.80	2.06	13.38	14.34	5.42
EVOO-PE13	142.27±1.39	80.77	1.81	6.62	7.33	3.47
EVOO-PE14	140.95±1.43	81.26	1.74	7.07	6.41	3.52

^aExpressed in ppm of caffeic acid equivalents. ^bRelative abundance expressed in %.

EVOO-PE 10 > EVOO-PE 3 > EVOO-PE 2 > EVOO-PE 6 > EVOO-PE 5 > EVOO-PE 8 > EVOO-PE 11 > EVOO-PE 4 > EVOO-PE 9 > EVOO-PE 1 > EVOO-PE 14 > EVOO-PE 13 > EVOO-PE 12 (Fig. 2, bottom). Anti-JIMT-1 activity was found to be up to 6-times higher when using EVOO-PE 7 than when using EVOO-PE 12. When JIMT-1 breast cancer cell growth-inhibitory potencies of EVOO-PE were arbitrarily normalized as % of the most-active EVOO-PE as well as fold-increase versus less-active EVOO-PE, curves slopes identified three groups of EVOO-PE with different anti-JIMT-1 behaviors (Fig. 2, bottom). Highly active PE from EVOOs 7 (Picual, Córdoba, Spain), 10 (Gutamanta, Jaén, Spain) and 3 (Cornezuelo, Badajoz, Spain) exhibited IC₅₀ values <0.025% v/v. Conversely, less-active PE from EVOOs 14 (Arbequisur B6, Sevilla, Spain), 13 (Arbequisur B5, Sevilla, Spain) and 12 (Mosteroli, Reus, Spain) exhibited IC₅₀ values >0.070% v/v. Most of the EVOO-PE exhibited intermediate IC₅₀ values ranging from 0.025 to 0.035% v/v.

Cytotoxic potencies of crude EVOO-PE relate to their relative content on secoiridoids. Table I shows the total phenolic content in individual EVOO monovarietals as assessed by the Folin Ciocalteu method. Table I shows also the percentage of each family of polyphenols in individual EVOO-PE. EVOO-PE appeared to differ little both in the total content and in the relative abundance of the main EVOO phenolic families (i.e., secoiridoids, lignans, flavones, phenolic alcohols), thus suggesting that small alterations in these parameters should significantly impact in the tumoricidal potency of individual EVOO-PE. This notion was supported further when IC₅₀ values for each EVOO-PE were plotted as a function (on a linear-linear scale) of the total phenolic content (Fig. 3A). Second-order polynomial regression analyses suggested a positive correlation between the growth inhibitory potencies of EVOO-PE and their total phenolic content ($R^2 = 0.7804$).

EVOO-PE displaying high phenolic indexes (>200 ppm of caffeic acid equivalents) were significantly more active than those bearing phenolic indexes <150 ppm of caffeic acid equivalents. An excellent correlation was found between the growth inhibitory potencies of EVOO-PE and their relative content of lignans/secoiridoids families of complex polyphenols (Fig. 3B, top). Whereas exacerbated growth-inhibitory responses positively related to the enrichment of individual EVOO-PE in their relative content of secoiridoid polyphenols, the substitution of secoiridoids by lignans rather related to loss of tumoricidal activity (Fig. 3B, bottom). The correlation between lignans content and growth-inhibitory activity fitted to a polynomial curve, showing an R² of 0.9155.

Effects of EVOO-PE on the JIMT-1 transcriptome: genome-wide analyses to identify key pathways associated with the degree of anti-tumoral potency among EVOO-PE. In an attempt to understand the existence of gene-based differences in the response of JIMT-1 cells to individual EVOO-PE differentially enriched in complex polyphenols such as secoiridoids and lignans, we employed microarray technology to clarify further the interaction between phenolic compounds with the transcriptome of trastuzumab-refractory HER2-positive JIMT-1 breast cancer cells. We evaluated the ability of individual crude EVOO-PE 7, 10, 3 and 12 to induce global changes in gene expression by using whole human genome microarrays (i.e., Agilent 44 K Whole Human genome Oligo Microarray containing 45,220 features, probes-representing 41,000 unique human genes and transcripts). RNA was extracted and prepared from JIMT-1 cells that had been cultured for 6 h at 70% confluence in the presence or absence of EVOO-PE 7, 10, 3 or 12 (0.001% v/v). After RNA hybridization to Agilent Technologies Whole Human Genome OligoMicroarrays, normalized and filtered data from all experimental groups were analyzed simultaneously using the significance analysis

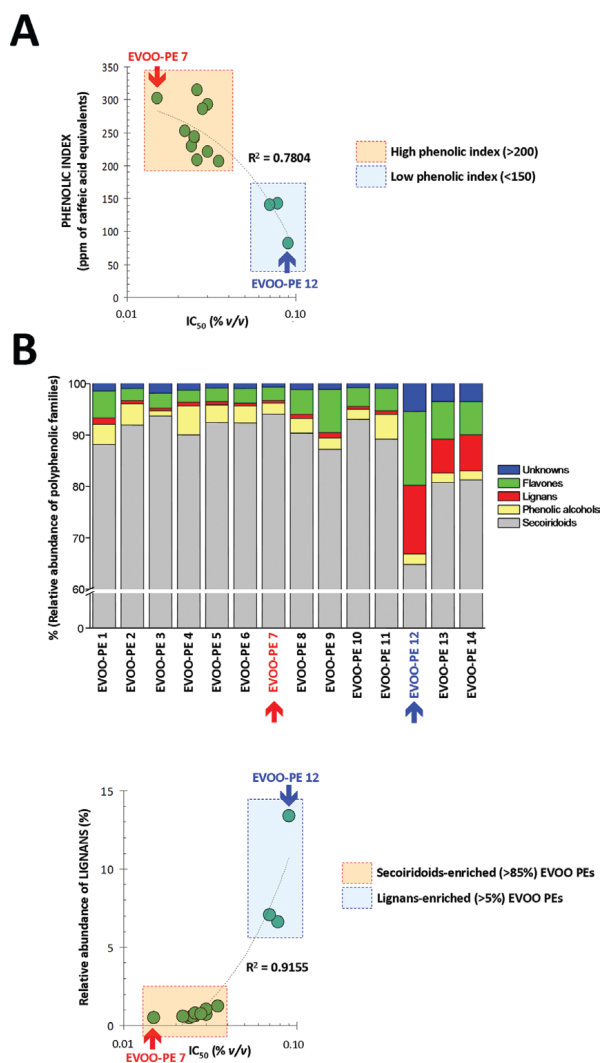


Figure 3. Correlations between chemical composition and growth inhibitory activity of EVOO-PE. Relationships between growth-inhibitory activities (expressed as IC₅₀ values) and either phenol concentrations of EVOO-PE (expressed as ppm of caffeic acid equivalents) (A) or relative abundance of lignans (expressed as % of total polyphenols) (B, bottom panel) in JIMT-1 cells. Considering the families of phenolic compounds that are naturally present in EVOO and performing the quantification in terms of flavones, lignans, phenolic alcohols and secoiridoids, results in terms of % of families of phenolic compounds are shown in (B, top panel). Data were expressed on linear rather than log scales. The obtained data were adjusted to a second-order polynomial curve (R² values are shown).

of microarray (SAM) algorithm. We set the significance cut-off at a median false discovery rate (FDR) of <5.0%. To determine the specific effects of crude EVOO-PE on gene expression, each treatment group was separately compared with the control group using a 2.0-fold change cut-off.

To identify key pathways/functions potentially associated with the degree of anti-tumoral activity among crude PE isolated from individual EVOO monovarietals, we focused on whole gene (functional) pathways instead of outlier-sum statistic gene groups. We performed this 'gene set' analysis using the Gene Set Enrichment Analysis (GSEA), an algorithm that is oriented to identify sets of functionally related genes

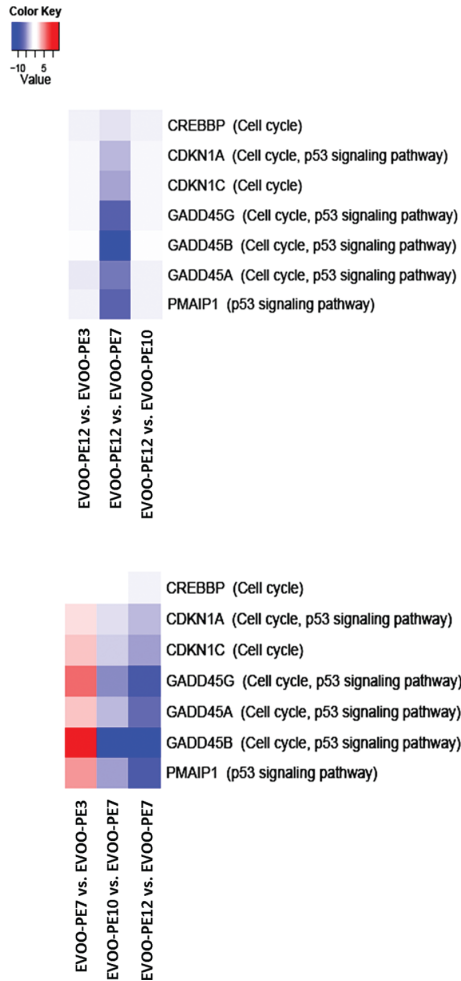
and is widely used in the analysis of microarray data. Screening the KEGG (Kyoto Encyclopedia of Genes and Genomes) pathway database by GSEA revealed that the sole enriched gene set responsible for the differential efficacy of secoiridoids-rich versus secoiridoids-low/null EVOO-PE was the cell cycle and p53 signaling pathway (Fig. 4, left panels). Analysis of individual genes within these classes revealed that differential regulation of just few cell cycle-related genes could largely explain the sensitivity of JIMT-1 cells to secoiridoid-rich EVOO-PE when compared to secoiridoids low/null-EVOO-PE. The enrichment of this pathway was driven by a group of genes including *CREBBP* (CREB binding protein, RSTS - Rubinstein-Taybi syndrome), *CDKN1A* (p21, Cip1), *CDKN1C* (p57, Kip2) and *PMAIP-1* (Noxa, APR). EVOO-PE 12, EVOO-PE 10 and EVOO-PE 3 failed to upregulate *CDKN1A*, *CDKN1C* and *PMAIP1* genes when compared to the up-regulatory effects elicited upon treatment with EVOO-PE 7. Remarkably, EVOO-PE had a dramatic differential impact on the expression of the stress-response family of *GADD45* genes. Whereas EVOO-PE 7 drastically up-regulated the expression of three members of the *GADD45* gene family including *GADD45A* (4.73-fold-increase), *GADD45G* (7.15-fold-increase) and *GADD45B* (11.40-fold-increase), the expression levels of *GADD45* genes were largely unchanged upon treatment with EVOO-PE 12, EVOO-PE 10 and EVOO-PE 3.

Differential effects of secoiridoid-rich EVOO PE in cell cycle progression: activation of the G2/M checkpoint in the absence of DNA damage. Because activation of *GADD45* stress-sensing genes has been demonstrated to play a crucial role in the G2/M checkpoint in response to DNA damage (26-29) (Fig. 4, right panels), we next examined whether treatment with EVOO-PE did modulate cell cycle progression in JIMT-1 cell cultures (Fig. 5, top panels). Cells were cultured in the absence or presence of trastuzumab, EVOO-PE 12 or EVOO-PE 7 for 24 h. Control (untreated) and treated cells were collected and stained with propidium iodide followed by FACS analysis. Likewise, a significant increase in the G2/M peak (36% at 24 h) was observed solely when JIMT-1 cells were cultured in the presence of EVOO-PE 7 compared with a 15% increase in the control group as well as in the presence of either trastuzumab (15%) or EVOO-PE 12 (14%). These findings strongly suggest that the differential impact of secoiridoid-rich EVOO-PE 7 in trastuzumab-refractory JIMT-1 cell viability is preceded by an acute arrest at the G2/M of the cell cycle, which may correlate with a differential activation of a *GADD45*-mediate G2/M checkpoint.

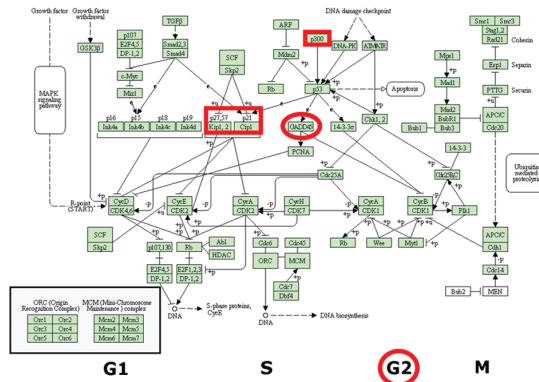
To evaluate whether the differential ability of secoiridoid-rich EVOO-PE 7 to activate the G2/M checkpoint related to a previous induction of DNA damage, we monitored Histone H2AX phosphorylation in the serine 139 residue, a sensitive marker for DNA double-strand breaks (DSBs). The phosphorylated H2AX, designated as γ H2AX, is visible within minutes of the induction of DSBs in the damaged cells as nuclear foci which are thought to serve as a platform for the assembly of protein involved in checkpoint responses and DNA repair - or during apoptotic chromatin fragmentation. We failed to observe phosphorylation or alterations in nuclear localization of H2AX in response to short-term (up to 6 h) treatments with EVOO-PE 12 and EVOO-PE 7 (data not shown). Accordingly, 120



1
2
3
4
5
6
7
8
9
10
11
12
13
14
15
16
17
18
19
20
21
22
23
24
25
26
27
28
29
30
31
32
33
34
35
36
37
38
39
40
41
42
43
44
45
46
47
48
49
50
51
52
53
54
55
56
57
58
59
60



Cell Cycle



p53 Signaling Pathway

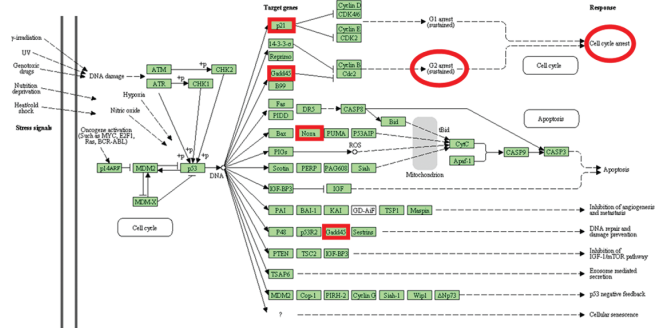


Figure 4. Gene Set Enrichment Analysis (GSEA) of EVOO-PE induced changes in the transcriptome of JIMT-1 cells. Left panels, a heat map showing the genes within the enriched gene set identified by GSEA in the comparative genome-wide analyses of the differential effects of EVOO-PE in the JIMT-1 transcriptome. The colors represent the expression values of the leading edge genes, in which the colors red, pink, light blue, dark blue show the range of expression values from high, moderate, low, to lowest in the comparison. Right diagrams, KEGG pathway maps of cell cycle (top) and p53 signaling pathway (bottom). Genes that were identified in the GSEA analyses (left panels) are shown by colored (red) rectangles.

staining with the vital nuclear stain Hoechst 33258 revealed that long-term exposure (24 and 48 h) to EVOO-PE 12 and EVOO-PE 7 fails to promote the appearance of apoptotic nuclei and nuclear fragments. Although long-term exposure to EVOO-PE failed also to induce the appearance of discrete γ H2AX foci in JIMT-1 cell nuclei, EVOO-PE notably differed in their ability to induce a diffuse, even, pan-nuclear γ H2AX DNA staining (Fig. 5, bottom panels). In agreement with earlier studies, activation of global γ H2AX DNA staining was observed during mitosis (i.e., maximal γ H2AX occurred at or near metaphase) in untreated (control) and EVOO-PE 12-treated JIMT-1 cell cultures. Intriguingly, a massive pan-nuclear γ H2AX DNA staining was readily apparent in the cell nuclei of JIMT-1 cells cultured in the presence of EVOO-PE 7. These findings suggested that GADD45-related activation of G2/M checkpoint control in response to secoiridoid-rich EVOO-PE may differ substantially from that induced by DNA damaging agents. This notion was supported further when analyzing

changes in the steady-state Histone H3 acetylation at Lys18 (H3K18). Indirect immunofluorescence using a specific antibody against Ach3/K18 revealed that, in untreated (control) cells, H3/K18 became acetylated in the condensed chromosomes of mitotic cells (Fig. 6, top panels). Notably, nuclei in JIMT-1 cells treated with EVOO-PE 7 but not with EVOO-PE 12, were strongly immunoreactive when stained with the specific antibody against anti-Ach3/K18 (Fig. 6, bottom panels), indicating that treatment with secoiridoid-rich EVOO PE successfully induced histone hyperacetylation in cell cycle arrested JIMT-1 cells.

Differential effects of secoiridoid-rich EVOO PE on the activation status of AKT1, MEK1, p38 MAPK, Stat3 and NF- κ B. To study further signaling cascades that may be involved in the regulation of G2/M cell cycle progression in response to the GADD45-sensed cellular stress induced by secoiridoids-rich EVOO PE, we finally assessed the activation

61
62
63
64
65
66
67
68
69
70
71
72
73
74
75
76
77
78
79
80
81
82
83
84
85
86
87
88
89
90
91
92
93
94
95
96
97
98
99
100
101
102
103
104
105
106
107
108
109
110
111
112
113
114
115
116
117
118
119
120

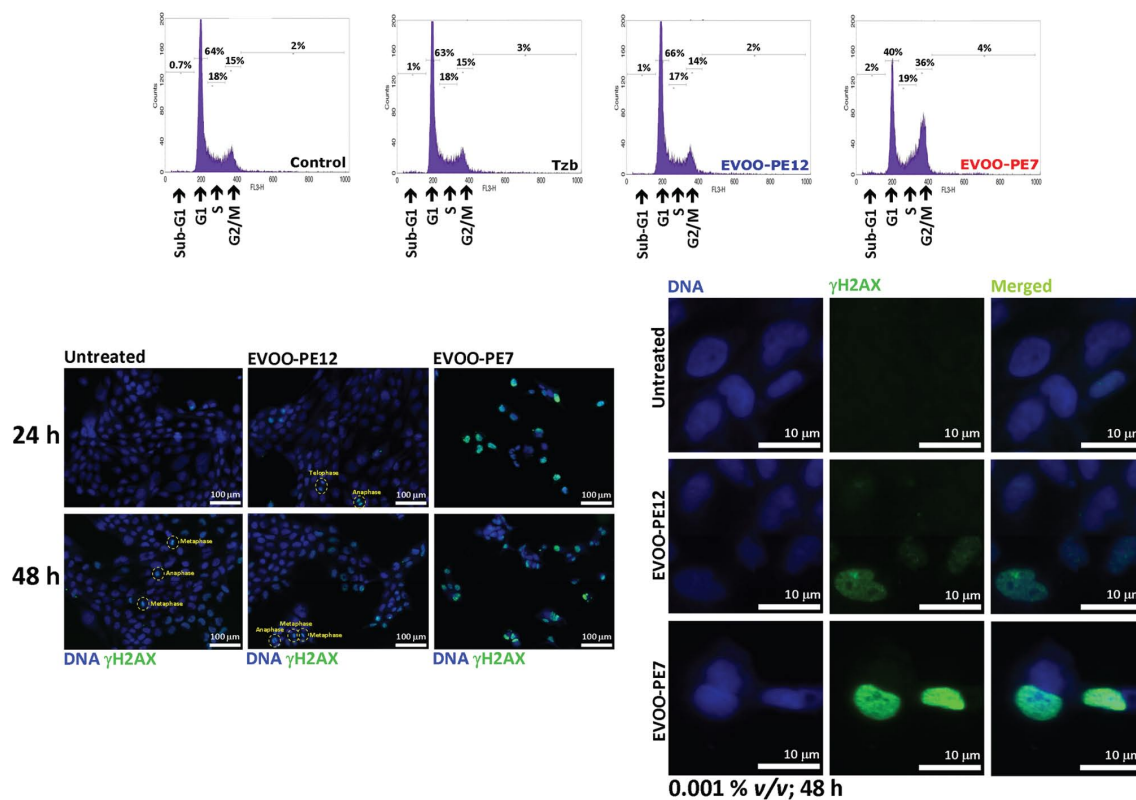


Figure 5. Differential effects of EVOO-PE on cell cycle progression in JIMT-1 breast cancer cells. Top, distribution of JIMT-1 cells in the different cell cycle compartments was analyzed by flow cytometry after 24 h in the absence or presence of trastuzumab (Tzb, 100 $\mu\text{g}/\text{ml}$), EVOO-PE 12 (0.001% v/v) and EVOO-PE 7 (0.001% v/v), as specified. The panels show representative flow cytometry profiles obtained from three independent experiments. Bottom, immunofluorescence of γH2AX after exposure to EVOO-PE 12 (0.001% v/v), EVOO-PE 7 (0.001% v/v) or mock treatment for 24 or 48 h, as specified. Nuclear DNA was counterstained with Hoechst 33258. Images show representative portion of JIMT-1 cell cultures captured in different channels for γH2AX (green) and Hoechst 33258 (blue) with either x20 (left, montages 2x2) or x40 (right) objectives, and merged on BD Pathway™ 855 Bioimager System using BD Attovision™ software.

status of convergence points and key regulatory proteins in several signaling pathways controlling cellular events such as growth and differentiation, energy homeostasis and the response to stress and inflammation. We took advantage of the CST's PathScan Signaling Nodes Multi-Target Sandwich ELISA kit, a semi-quantitative technology that combines the reagents necessary to detect endogenous levels of AKT1, phospho-AKT1 (Ser473), phospho-MEK1 (Ser217/221), phospho-p38 MAPK (Thr180/Tyr182), phospho-Stat3 (Tyr705) and phospho-NF- κB p65 (Ser536). Interestingly, the ability of EVOO-PE to inhibit JIMT-1 cell growth and to activate *GADD45* genes closely related to their ability to activate MEK1, p38 MAPK, Stat3, and NF- κB p65 (Fig. 7). EVOO-PE 12, 3, 10 and 7 failed to significantly modulate the activation status of AKT1. Crude PE obtained from secoiridoids-low/null EVOO-PE 12 failed to modulate the phospho-active status of MEK1, p38 MAPK, Stat3, and NF- κB p65. EVOO-PE 3 and EVOO-PE 10 slightly activated, but in a statistically significant manner-MEK1 (up to 5-fold enhancement), p38 MAPK, and NF- κB p65. Remarkably, secoiridoid-rich EVOOPE7 significantly activated Stat3 (~3-fold) and NF- κB p65 (~6-fold) and dramatically up-regulated up to 20- and 40-fold the activation status of MEK1 and p38 MAPK, respectively (Fig. 7).

Discussion

We are beginning to accumulate epidemiological, clinical and laboratory-based evidence suggesting that consumption of phenolic-enriched fruits, vegetables and herbs might reduce the risk of chronic diseases including human malignancies (33-35). In this regard, it has been repeatedly suggested that the ability of the so-called 'Mediterranean diet' (MD) (i.e., the dietary patterns found in olive-growing areas of the Mediterranean basin) to significantly reduce the risk of several types of human carcinomas including breast cancer (36-39), can be largely attributed to the unique healthy characteristics of EVOO, an integral ingredient of the traditional MD. Although these findings might suggest that, in the future, the use of supplements derived from EVOO will be a useful strategy for the prevention and/or treatment of cancer, both the specific components and the specific molecular mechanisms that exert EVOO-related anti-carcinogenic effects have not yet been thoroughly elucidated. Apart from the health benefits that can be expected from EVOO as the richest source of the mono-unsaturated fatty acid (MUFA) oleic acid (OA; 18:1n-9) (40), 1-2% of cold-pressed EVOO (i.e., the juice obtained from the olive fruit solely by mechanical means, without further treatment other than washing, filtration, decantation or centrifugation)

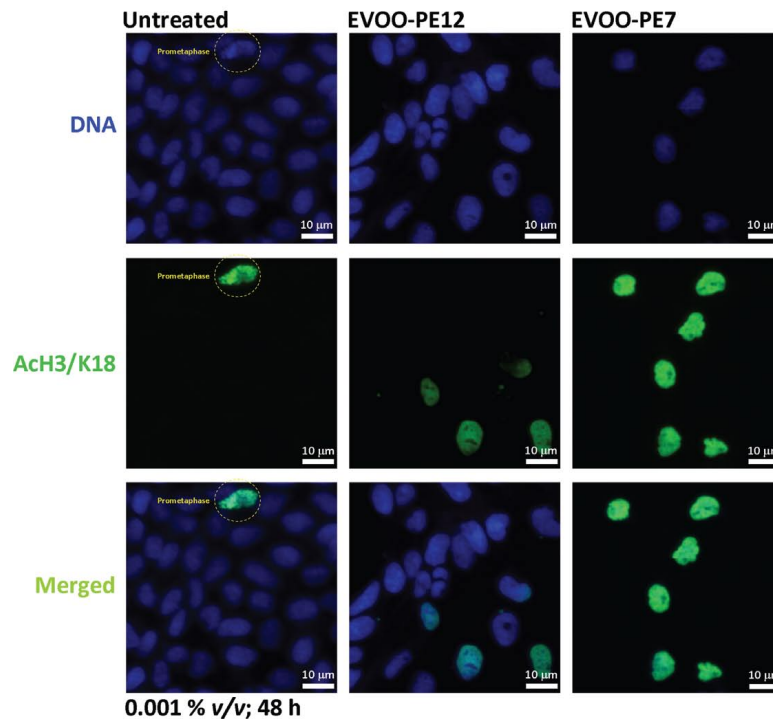
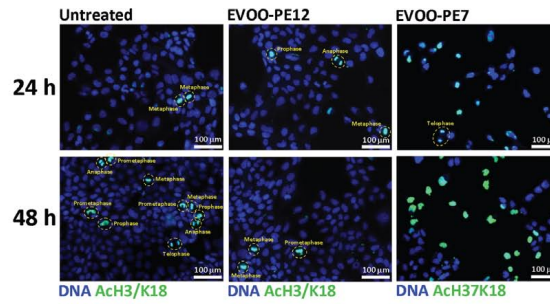


Figure 6. Differential effects of EVOO PE on the acetylation status of Histone H3 in JIMT-1 breast cancer cells. Immunofluorescence of AcH3/K18 after exposure to EVOO-PE 12 (0.001% v/v), EVOO-PE 7 (0.001% v/v) or mock treatment for 24 or 48 h, as specified. Nuclear DNA was counterstained with Hoechst 33258. Images show representative portion of JIMT-1 cell cultures captured in different channels for γ H2AX (green) and Hoechst 33258 (blue) with either x20 (top; montages 2x2) or x40 (bottom) objectives, and merged on BD Pathway 855 Bioimager System using BD Attovision software.

include minor components such as aliphatic and triterpenic alcohols, sterols, hydrocarbons, volatile compounds and several antioxidants (41-47). Although tocopherols and carotenes are also present, hydrophilic phenolics represent the most abundant family of bioactive EVOO compounds. As for many plant-derived phenolics, it has been largely assumed that EVOO-derived complex phenols such as secoiridoids (that include aglycone derivatives of oleuropein, dimethyloleuropein and ligstroside, which are also present in olive fruit) and lignans [such as (+)-pinoresinol and 1-(+)-acetoxypinoresinol] provide health benefits mainly because of their antioxidant activity (48-50). However, the antioxidant capacity of polyphenols does not directly correlate with their efficacy in terms of anti-cancer activity. Moreover, plasma concentrations of EVOO polyphenols when provided in the diet are often far lower than the levels required for protection against oxidation. It could be argued that metabolites of EVOO polyphenols can reach

several times higher concentrations in the bloodstream. These EVOO-derived compounds, however, tend to have a decreased antioxidant activity compared to parent compound (51,52).

Alternatively to general mechanisms largely related to the antioxidant and/or trapping activity of oxygen radicals commonly observed in many plant-derived phenolics, recent studies have demonstrated that complex polyphenols can exert an anti-carcinogenic effect by directly modulating the activities of various types of receptor tyrosine kinases (RTKs) including several members of the HER family (53-58). Results from our own laboratory support the notion that EVOO-derived complex polyphenols may constitute a previously unrecognized family of clinically valuable anti-cancer phytochemicals that significantly affect breast cancer cell proliferation and survival through a molecular mechanism involving the specific suppression of the activity, expression and signal transduction events of the Type I RTK HER2 (19-21). Similarly, trastuzumab-

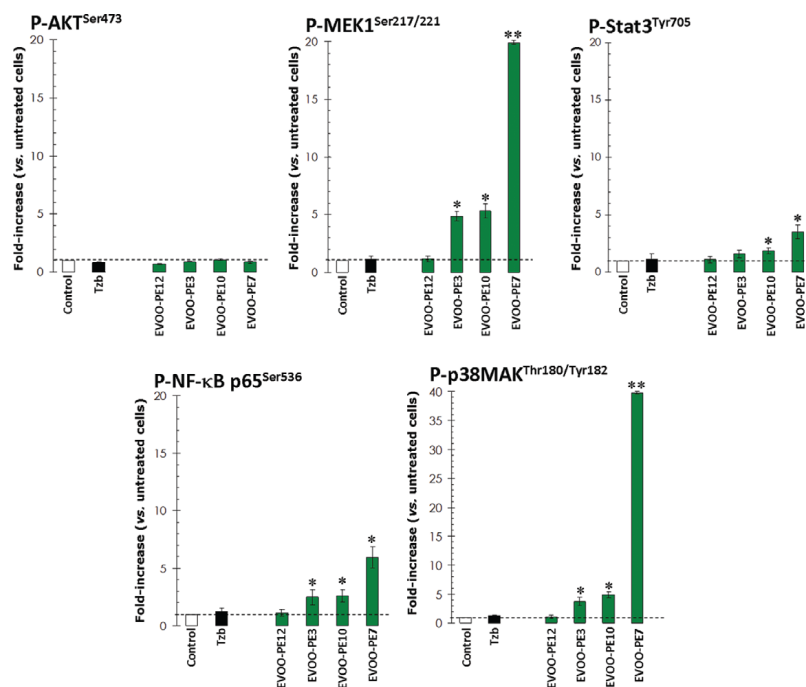


Figure 7. Effects of EVOO-PE on phospho-endogenous levels of AKT, MEK1, p38 MAPK, Stat3 and NF-κB p65 in JIMT-1 breast cancer cells. Cultures of JIMT-1 cells (75-80% confluent) were starved overnight and treated with either trastuzumab (TzB, 100 μg/ml) or 0.001% v/v of EVOO-PE 12, EVOO-PE 13, EVOO-PE 10 and EVOO-PE 7 for 48 h, as specified. Lysates were assayed at a protein of 0.5 mg/ml using the PathScan Signaling Nodes Multi-Target Sandwich ELISA Kit #7272 (Cell Signaling Technology, Inc.) as per the manufacturer's instructions. The absorbance readings at 450 nm were normalized to those obtained in untreated control cells cultured strictly in parallel. Results are means (columns) and 95% confidence intervals (bars) of two independent experiments made in duplicate. Statistically significant differences (one-factor ANOVA analysis) between experimental conditions and unsupplemented control cells are shown by asterisks (*P<0.01; **P<0.001). All statistical tests were two-sided.

induced HER2 internalization and down-regulation are thought to be causally related to the mechanism of action of the antibody (59,60). However, we are lacking formal proof for the hypothesis that knockdown of HER2 is sufficient to elicit anti-proliferative effects in HER2-positive tumor cells. In JIMT-1 breast cancer cells, a line recently established from a trastuzumab-resistant breast cancer patient that retains *HER2* gene amplification/*HER2* protein overexpression as well as trastuzumab resistance as a stable phenotype, *HER2* protein is internalized and down-regulated by trastuzumab treatment to an extent similar to that observed in trastuzumab-sensitive breast cancer cell lines (13,14,17,18). The very low level of *HER2* TK activity in cultured JIMT-1 implies that trastuzumab-induced *HER2* down-regulation does not result in a decreased activation state of key signaling transduction pathways and, therefore, *HER2* protein is a 'molecular fossil' that is not required for survival/proliferation of JIMT-1 cells (13,14,61). The ability of EVOO phenolics to suppress *HER2* protein expression while eliciting significant growth inhibitory activities against JIMT-1 cells would imply that, in addition to promoting *HER2* inhibition, they efficiently circumvent *de novo* trastuzumab resistance by affecting *HER2* downstream specific signaling pathways.

EVOO-derived phenolics with strong anti-JIMT-1 activity may underscore innovative cancer molecules with novel therapeutic targets because, in order to elicit tumoricidal effects, they should affect the expression and/or activity of

genes and transduction cascades closely involved in enhanced cancer cell survival. To test this hypothesis, we first obtained crude PE naturally bearing different amounts of phenolic families from 14 Spanish EVOO monovarietals. Although structural diversity and solubility generally impose a significant challenge in the extraction and analysis of phenolics (i.e., some reports estimate that approximately 30% of the errors in analytical measurements come from the sample preparation step), we were able to accurately estimate the relative levels of the phenolic compounds in individual EVOO-PE. Indeed, our current findings support the notion that high recoveries of EVOO-derived phenolic fractions and good analytical measurements can be obtained by using SPE with Diol-cartridges (31). We took advantage of a rapid resolution liquid chromatography method coupled to diode-array and time of flight mass spectrometry (TOF) recently developed in our laboratory to characterize and quantify phenolic compounds in EVOO monovarietals (22). The approach we adopted allows good peak resolutions to identify at least 19 different phenols in less than 20 min. Folin Ciocalteu-based quantification of total phenolics followed by identification of the relative abundance of the main EVOO phenolic families (i.e., secoiridoids, lignans, flavones, phenolic alcohols and other compounds yet unknown) and MTT-based cell viability assays revealed that trastuzumab-refractory JIMT-1 cells likewise retained an exquisite sensitivity to the cytotoxic effects elicited by increasing volumes of crude EVOO PE. More importantly, we described the occurrence of

61
62
63
64
65
66
67
68
69
70
71
72
73
74
75
76
77
78
79
80
81
82
83
84
85
86
87
88
89
90
91
92
93
94
95
96
97
98
99
100
101
102
103
104
105
106
107
108
109
110
111
112
113
114
115
116
117
118
119
120



1 correlations between the intrinsic phenolic composition of
2 EVOO-derived crude PE and their anti-proliferative abilities
3 toward JIMT-1 cells. When compared with lignan-rich
4 EVOO-PE, secoiridoid-rich EVOO-PE had a significantly
5 stronger ability (up to 6-times higher) to negatively affect
6 the metabolic status of JIMT-1 breast cancer cells. In this
7 scenario, we sought to identify possible molecular mediators
8 by interrogating the transcriptome of JIMT-1 cells cultured
9 in the absence or presence of poor- and highly active-crude
10 EVOO-PE. Both the duration of EVOO-PE treatment (6 h)
11 and the low concentration of EVOO PE (0.001% v/v) were
12 chosen to identify the earliest transcriptional events induced
13 by treatment with EVOO-PE, to minimize the detection of
14 gene expression changes due to apoptosis and, therefore, to
15 identify gene expression changes that preceded, and possibly
16 contributed to, the biological effects of EVOO-PE treatments
17 on JIMT-1 cells. When we examined whether differentially
18 expressed genes, which had disparate biological functions,
19 were part of one or more signal transduction pathways,
20 GSEA-based screening of the KEGG pathway database
21 concluded that EVOO-PE differentially modulated breast cancer
22 transcriptome at the level of the cell cycle pathway, with a
23 remarkable up-regulatory impact in G2/M checkpoint-related
24 stress sensor *GADD45* genes. Likewise, our results confirmed
25 that gene induction of all three *GADD45* isoforms inhibited
26 mitosis and promoted G2/M cell cycle arrest during (moderate)
27 cellular stress imposed by highly active, secoiridoid-rich
28 EVOO-PE (i.e., EVOO-PE 7). Further analyses, at higher
29 concentrations of secoiridoid-rich EVOO-PE and later time-
30 points, indicated that the mitotic population was preferentially
31 lost from the culture, an effect that correlated with the appearance
32 of a sub-G1 apoptotic peak on the FACScan (data not shown).
33 These results may be consistent with the suggestion that
34 mitotic cells are particularly sensitive to the cytotoxic effects
35 of the secoiridoid-rich EVOO-PE 7.

36 Secoiridoid-rich EVOO PE7-induced activation of the
37 *GADD45* sensing machinery ultimately led to a selective
38 induction of genes related to cell cycle arrest and apoptosis
39 including *CDKN1A* (p21^{Waf1/Cip1}) and *CDKN1C* (p57^{Kip2}), two
40 powerful inhibitors of cyclin-dependent kinases (62,63), and
41 *PMAIP-1* (phorbol-12-myristate-13-acetate-induced protein 1;
42 NOXA, APR) - a tumor suppressor gene that is crucial in
43 fine-tuning p53-related cell death decisions (64,65). The ability
44 of the secoiridoid-rich EVOO-PE 7 to functionally restore the
45 p53 pathway in p53-deficient JIMT-1 cells (13) while
46 efficiently activating the G2/M checkpoint might suggest that
47 natural phenolic molecules from EVOO might unexpectedly
48 function as regulators of histone deacetylase (HDAC) activity.
49 Although future studies appear necessary to definitely elucidate
50 these putative intriguing mechanisms, it should be noted that
51 secoiridoid-rich EVOO-PE 7 appeared to recapitulate well-
52 known effects of HDAC inhibitors (30,66-68). Supporting
53 this notion, treatment with the secoiridoid-rich EVOO-PE 7
54 markedly induced the expression of acetylated H3 histone
55 proteins. Because we confirmed also that the secoiridoid-rich
56 EVOO-PE 7 increased the cell cycle-regulated steady-state
57 phosphorylation status of histone H2AX but they did not work
58 as exogenous sources of significant DNA damage, breast cancer
59 cell growth inhibitory activities observed upon exogenous
60 supplementation with EVOO-derived complex polyphenols

may relate to their differentially ability to regulate gene
expression and chromatin structure at the epigenetic level.
HDAC inhibitors elicit histones to remain in an acetylated
state, and through the resulting alterations in gene expression
and chromatin structure, they cause a marked decrease in the
viability of cancer cells that associate with a cell-cycle arrest
at G2/M and transcriptional reactivation of dormant tumor-
suppressor genes, such as cyclin-dependent kinase inhibitors
(CKIs) belonging to the Cip/Kip family (e.g., p21^{Waf1/Cip1} and
p57^{Kip2}) (69-71). EVOO-PE-derived phenolics, by inhibiting
HDAC activity and promoting increased acetylation of histones,
can cause recruitment of transcription factors that might act
as critical regulators of cell cycle and phenotype by influencing
contemporaneously several CKI genes. Moreover, a previously
unrecognized ability of EVOO phenolics to work as powerful
inductors of acetylation of histones to restore the expression of
growth-inhibitory tumor-suppressor genes (which had generally
been silenced by hypo-acetylation during tumorigenesis) does
not preclude a previously described ability of EVOO phenolics
to inhibit HER2 activity and expression (19-21). By incorporating
HDAC inhibitory functionality into the pharmacophore of the
HER1 (EGFR) and HER2 inhibitors, Cai *et al* (72) recently
synthesized a novel series of compounds with potent,
multiacting HDAC, HER1, and HER2 inhibitory activities.
Based on their findings showing that a compound simultaneously
inhibiting HDAC, HER1, and HER2 displayed greater anti-
proliferative potencies than HDAC inhibitors (i.e., vorinostat),
EGFR inhibitors (i.e., erlotinib), HER2 inhibitors (i.e., lapatinib)
and combinations of vorinostat with erlotinib/lapatinib, the
author suggested that potent multi-acting HDAC, HER1, and
HER2 inhibitors may offer greater therapeutic benefits in
cancer over single-acting agents through the interference
with multiple pathways and potential synergy among HDAC
and HER1/HER2 inhibitors (73). In this scenario, our current
findings warrant forthcoming studies aimed to analyze
structure-activity (SAR) relationships evaluating individual
EVOO-derived phenolic candidates in HER kinase activity
assays as well as HDAC enzyme assays. Indeed, we cannot
exclude the possibility that previously described anti-HER2
effects of EVOO polyphenols due to proteasomal degradation
of HER2 protein (21) might include indirect effects by interacting
with chaperone (e.g., HSP90) function as is seen with HDAC
inhibition (74). Moreover, induction of G2/M arrest in JIMT-1
cells treated with the secoiridoid-rich EVOO-PE 7 occurred
in parallel with a dramatic overactivation of p38 activity. This
finding agrees with several reports demonstrating a functional
link between stress-activated mitogen-activated protein kinase
pathways and *GADD45* (26,27,75,76). In this regard, and
given that not only the p38 pathway promotes G2/M arrest via
GADD45 induction in response to cellular stressors such as
polyphenolic flavonoids (77) but also that P38 activity depends
on MEKK4 activation mediated by each of the three *GADD45*
proteins in response to a variety of stimuli (76,78,79), it is
reasonable to suggest that an autoregulatory loop consisting of
mitogen-activated protein pathways, *GADD45* protein and
cyclin-dependent kinase inhibitors appears to largely coordinate
induction of G2/M arrest versus apoptosis in dependence of
the nature of EVOO polyphenols and amplitude of cellular
stress effects. Moreover, p38 MAPK activity regulates chromatin
remodeling via Histone H3 acetylation (80,81), a regulatory 120



1 role where this MAP kinase controls acetylation by regulating
 2 acetyltransferase activity of p300/CBP (82-84), a transcriptional
 3 coactivator encoded by *CREBBP*, one of the genes differentially
 4 upregulated in response to secoiridoid-rich EVOO-PE. In the
 5 cellular response to secoiridoid-rich EVOO-PE, GADD45
 6 cross-regulated p38 signaling might therefore participate in
 7 the recruitment of co-activators with histone acetyltransferase
 8 activity thus directly contributing to the acetylation of histones
 9 leading to the activation and transcription of tumor suppressor
 10 genes (e.g., p21^{Waf1/Cip1} and p57^{Kip2}) with cell cycle suppressor
 11 activity.

12 As used in the present study, genomic data analyses of
 13 microarray technology in association with a functional validation
 14 approach could serve as a framework to identify EVOO-derived
 15 bioactive phenolics with novel anti-cancer therapeutic effects
 16 and clarify the molecular roles of structurally-related complex
 17 polyphenols (e.g., lignans, secoiridoids) in the physiological
 18 activity of crude PE directly obtained from EVOO (85). Our
 19 current findings therefore support the notion that high-throughput
 20 experimentation combining massive databases of genomic/
 21 proteomic data with efficient separation methods and powerful
 22 spectrometric methods for identification and structure
 23 elucidation can be used to obtain chemically standardized
 24 multi-component extracts simultaneously acting on multiple
 25 targets (86). Importantly, we here confirm that a broad repertoire
 26 of chemical entities (e.g., EVOO-derived polyphenols) can
 27 act together on multiple targets to differentially activate (e.g.,
 28 lignan-rich versus secoiridoids-rich EVOO-PE) defense,
 29 protective and repair epigenetic mechanisms rather than
 30 blocking a sole disease-causing molecular target (e.g., HER2
 31 oncogene). From a molecular perspective, the ability of some
 32 secoiridoid-rich EVOO PE to permit histones to remain in
 33 hyperacetylated states and through the resulting alterations in
 34 gene regulation to inhibit cell cycle progression and to cause a
 35 marked decrease in the viability of cancer cells may herald a
 36 previously unrecognized epigenetic antitumor therapeutic
 37 strategy based on complex polyphenols naturally occurring in
 38 EVOO. From a clinical perspective, the identification of a
 39 GADD45-sensed, p38 MAPK-related cell growth inhibitory
 40 pathway in *HER2* gene-amplified JIMT-1 cells molecularly
 41 bypasses an impediment to current HER1/2-targeted therapies
 42 and provides new targets for future therapeutic management
 43 of highly-aggressive basal-like/HER2-positive tumors with
 44 refractoriness to trastuzumab and/or lapatinib *ab initio* (18,87).

45 **Acknowledgments**

46 Javier A. Menendez is supported in part by the Instituto de
 47 Salud Carlos III (Ministerio de Sanidad y Consumo, Fondo de
 48 Investigación Sanitaria (FIS), Spain, Grants CP05-00090 and
 49 PI06-0778 and RD06-0020-0028), the Fundación Científica
 50 de la Asociación Española Contra el Cáncer (AECC, Spain), and
 51 by the Ministerio de Ciencia e Innovación (SAF2009-11579,
 52 Plan Nacional de I+D+I, MICINN, Spain). Alejandro Vazquez-
 53 Martín is the recipient of a ‘Sara Borrell’ post-doctoral contract
 54 (CD08/00283, Ministerio de Sanidad y Consumo, Fondo de
 55 Investigación Sanitaria (FIS), Spain. Silvia Cufí is the recipient
 56 of a Research Fellowship (Formación de Personal Investigador,
 57 FPI) by the Ministerio de Ciencia e Innovación (MICINN,
 58 Spain). Antonio Segura-Carretero is supported in part by the

Spanish Ministry of Education and Science (Grant AGL2008-
 05108-C03-03) and the Andalusian Regional Government
 Council of Innovation and Science (Grants P07AGR-02619
 and P09-CTS-4564).

66 **References**

67
 68 1. Nahta R and Esteva FJ: Herceptin: mechanisms of action and
 69 resistance. *Cancer Lett* 232: 123-138, 2006.
 70 2. Nahta R, Yu D, Hung MC, Hortobagyi GN and Esteva FJ:
 71 Mechanisms of disease: understanding resistance to HER2-
 72 targeted therapy in human breast cancer. *Nat Clin Pract Oncol* 3:
 73 269-280, 2006.
 74 3. Nahta R and Esteva FJ: HER2 therapy: molecular mechanisms
 75 of trastuzumab resistance. *Breast Cancer Res* 8: 215, 2006.
 76 4. Pegram MD, Lipton A, Hayes DF, Weber BL, Baselga JM,
 77 Tripathy D, Baly D, Baughman SA, Twaddell T, Glaspy JA and
 78 Slamon DJ: Phase II study of receptor-enhanced chemosensitivity
 79 using recombinant humanized anti-p185HER2/neu monoclonal
 80 antibody plus cisplatin in patients with HER2/neuoverexpressing
 81 metastatic breast cancer refractory to chemotherapy treatment. *J*
 82 *Clin Oncol* 16: 2659-2671, 1998.
 83 5. Baselga J, Norton L, Albanell J, Kim YM and Mendelsohn J:
 84 Recombinant humanized anti-HER2 antibody (Herceptin)
 85 enhances the antitumor activity of paclitaxel and doxorubicin
 86 against HER2/neu overexpressing human breast cancer xenografts.
 87 *Cancer Res* 58: 2825-2831, 1998.
 88 6. Nass SJ, Hahm HA and Davidson NE: Breast cancer biology
 89 blossoms in the clinic. *Nat Med* 4: 761-762, 1998.
 90 7. Spector NL and Blackwell KL: Understanding the mechanisms
 91 behind trastuzumab therapy for human epidermal growth factor
 92 receptor 2-positive breast cancer. *J Clin Oncol* 27: 5838-5847,
 93 2009.
 94 8. Esteva FJ, Yu D, Hung MC and Hortobagyi GN: Molecular
 95 predictors of response to trastuzumab and lapatinib in breast
 96 cancer. *Nat Rev Clin Oncol* 7: 98-107, 2010.
 97 9. Hortobagyi GN: Trastuzumab in the treatment of breast cancer.
 98 *N Engl J Med* 353: 1734-1736, 2005.
 99 10. Gonzalez-Angulo AM, Hortobagyi GN and Esteva FJ: Adjuvant
 100 therapy with trastuzumab for HER-2/neu-positive breast cancer.
 101 *Oncologist* 11: 857-867, 2006.
 102 11. Perez-Gracia JL, Gloria Ruiz-Ilundain M, Garcia-Ribas I and
 103 Maria Carrasco E: The role of extreme phenotype selection studies
 104 in the identification of clinically relevant genotypes in cancer
 105 research. *Cancer* 95: 1605-1610, 2002.
 106 12. Pérez-Gracia JL, Gúrpide A, Ruiz-Ilundain MG, Alfaro Alegría C,
 107 Colomer R, García-Foncillas J and Melero Bermejo I: Selection
 108 of extreme phenotypes: the role of clinical observation in
 109 translational research. *Clin Transl Oncol* 12: 174-180, 2010.
 110 13. Tanner M, Kapanen AI, Junttila T, Raheem O, Grenman S, Elo J,
 111 Elenius K and Isola J: Characterization of a novel cell line
 112 established from a patient with Herceptin-resistant breast cancer.
 113 *Mol Cancer Ther* 3: 1585-1592, 2004.
 114 14. Nagy P, Friedländer E, Tanner M, Kapanen AI, Carraway KL,
 115 Isola J and Jovin TM: Decreased accessibility and lack of activation
 116 of ErbB2 in JIMT-1, a herceptin-resistant, MUC4-expressing
 117 breast cancer cell line. *Cancer Res* 65: 473-482, 2005.
 118 15. Perou CM, Sørlie T, Eisen MB, van de Rijn M, Jeffrey SS,
 119 Rees CA, Pollack JR, Ross DT, Johnsen H, Akslen LA, Fluge O,
 120 Pergamenschikov A, Williams C, Zhu SX, Lønning PE,
 121 Børresen-Dale AL, Brown PO and Botstein D: Molecular portraits
 122 of human breast tumours. *Nature* 406: 747-752, 2000.
 123 16. Sorlie T, Tibshirani R, Parker J, Hastie T, Marron JS, Nobel A,
 124 Deng S, Johnsen H, Pesich R, Geisler S, Demeter J, Perou CM,
 125 Lønning PE, Brown PO, Børresen-Dale AL and Botstein D:
 126 Repeated observation of breast tumor subtypes in independent
 127 gene expression data sets. *Proc Natl Acad Sci USA* 100: 8418-8423,
 128 2003.
 129 17. Köninki K, Barok M, Tanner M, Staff S, Pitkänen J, Hemmilä P,
 130 Ilvesaro J and Isola J: Multiple molecular mechanisms underlying
 131 trastuzumab and lapatinib resistance in JIMT-1 breast cancer
 132 cells. *Cancer Lett* 294: 211-219, 2010.
 133 18. Oliveras-Ferreros C, Vazquez-Martin A, Martin-Castillo B,
 134 Cufí S, Del Barco S, Lopez-Bonet E, Brunet J and Menendez JA:
 135 Dynamic emergence of the mesenchymal CD44(pos)CD24(neg/
 136 low) phenotype in HER2-gene amplified breast cancer cells with
 137 *de novo* resistance to trastuzumab (Herceptin). *Biochem Biophys*
 138 *Res Commun* 397: 27-33, 2010.



- 1 19. Menendez JA, Vazquez-Martin A, Colomer R, Brunet J, Carrasco-Pancorbo A, Garcia-Villalba R, Fernandez-Gutierrez A and Segura-Carretero A: Olive oil's bitter principle reverses acquired autoresistance to trastuzumab (Herceptin) in HER2-overexpressing breast cancer cells. *BMC Cancer* 7: 80, 2007.
- 2
- 3
- 4 20. Menendez JA, Vazquez-Martin A, Oliveras-Ferreros C, Garcia-Villalba R, Carrasco-Pancorbo A, Fernandez-Gutierrez A and Segura-Carretero A: Extra-virgin olive oil polyphenols inhibit HER2 (erbB-2)-induced malignant transformation in human breast epithelial cells: relationship between the chemical structures of extra-virgin olive oil secoiridoids and lignans and their inhibitory activities on the tyrosine kinase activity of HER2. *Int J Oncol* 34: 43-51, 2009.
- 5
- 6
- 7
- 8
- 9
- 10 21. Menendez JA, Vazquez-Martin A, Garcia-Villalba R, Carrasco-Pancorbo A, Oliveras-Ferreros C, Fernandez-Gutierrez A and Segura-Carretero A: Anti-HER2 (erbB-2) oncogene effects of phenolic compounds directly isolated from commercial extra-virgin olive oil (EVOO). *BMC Cancer* 8: 377, 2008.
- 11
- 12
- 13
- 14 22. Garcia-Villalba R, Carrasco-Pancorbo A, Oliveras-Ferreros C, Vázquez-Martín A, Menéndez JA, Segura-Carretero A and Fernández-Gutiérrez A: Characterization and quantification of phenolic compounds of extra-virgin olive oils with anticancer properties by a rapid and resolutive LC-ESI-TOF MS method. *J Pharm Biomed Anal* 51: 416-429, 2010.
- 15
- 16
- 17
- 18 23. Jensen SR, Franzyk H and Wallander E: Chemotaxonomy of the Oleaceae: iridoids as taxonomic markers. *Phytochemistry* 60: 213-231, 2002.
- 19
- 20
- 21 24. Bendini A, Carretani L, Carrasco-Pancorbo A, Gómez-Caravaca AM, Segura-Carretero A, Fernández-Gutiérrez A and Lercker G: Phenolic molecules in virgin olive oils: a survey of their sensory properties, health effects, antioxidant activity and analytical methods. An overview of the last decade. *Molecules* 12: 1679-1719, 2007.
- 22
- 23
- 24
- 25
- 26 25. Obied HK, Prenzler PD, Ryan D, Servili M, Taticchi A, Esposto S and Robards K: Biosynthesis and biotransformations of phenol-conjugated oleosidic secoiridoids from *Olea europaea* L. *Nat Prod Rep* 25: 1167-1179, 2008.
- 27
- 28
- 29 26. Liebermann DA and Hoffman B: Gadd45 in stress signaling. *J Mol Signal* 3: 15, 2008.
- 30
- 31 27. Cretu A, Sha X, Tront J, Hoffman B and Liebermann DA: Stress sensor Gadd45 genes as therapeutic targets in cancer. *Cancer Ther* 7: 268-276, 2009.
- 32
- 33 28. Wang XW, Zhan Q, Coursen JD, Khan MA, Kontny HU, Yu L, Hollander MC, O'Connor PM, Fornace AJ Jr and Harris CC: GADD45 induction of a G2/M cell cycle checkpoint. *Proc Natl Acad Sci USA* 96: 3706-3711, 1999.
- 34
- 35 29. Jin S, Tong T, Fan W, Fan F, Antinore MJ, Zhu X, Mazzacurati L, Li X, Petrik KL, Rajasekaran B, Wu M and Zhan Q: GADD45-induced cell cycle G2-M arrest associates with altered subcellular distribution of cyclin B1 and is independent of p38 kinase activity. *Oncogene* 21: 8696-8704, 2002.
- 36
- 37
- 38
- 39 30. Zubia A, Ropero S, Otaegui D, Ballestar E, Fraga MF, Boix-Chornet M, Berdasco M, Martínez A, Coll-Mulet L, Gil J, Cossío FP and Esteller M: Identification of (1H)-pyrroles as histone deacetylase inhibitors with antitumoral activity. *Oncogene* 28: 1477-1484, 2009.
- 40
- 41
- 42
- 43 31. Carrasco-Pancorbo A, Neussus C, Pelzing M, Segura-Carretero A and Fernandez-Gutierrez A: CE- and HPLC-TOF-MS for the characterization of phenolic compounds in olive oil. *Electrophoresis* 28: 806-821, 2007.
- 44
- 45
- 46 32. Singleton VL and Rossi JA: Colorimetry of total phenolics with phophomolybdic-phosphotungstic acid reagent. *Am J Enol Vitic* 16: 144-158, 1956.
- 47
- 48 33. Hsu CL and Yen GC: Phenolic compounds: evidence for inhibitory effects against obesity and their underlying molecular signaling mechanisms. *Mol Nutr Food Res* 52: 53-61, 2008.
- 49
- 50 34. Crozier A, Jaganath IB and Clifford MN: Dietary phenolics: chemistry, bioavailability and effects on health. *Nat Prod Rep* 26: 1001-1043, 2009.
- 51
- 52
- 53 35. Cicerale S, Conlan XA, Sinclair AJ and Keast RS: Chemistry and health of olive oil phenolics. *Crit Rev Food Sci Nutr* 49: 218-236, 2009.
- 54
- 55 36. Colomer R and Menéndez JA: Mediterranean diet, olive oil and cancer. *Clin Transl Oncol* 8: 15-21, 2006.
- 56
- 57 37. Menendez JA and Lupu R: Mediterranean dietary traditions for the molecular treatment of human cancer: anti-oncogenic actions of the main olive oil's monounsaturated fatty acid oleic acid (18:1n-9). *Curr Pharm Biotechnol* 7: 495-502, 2006.
- 58
- 59 38. Escrich E, Moral R, Grau L, Costa I and Solanas M: Molecular mechanisms of the effects of olive oil and other dietary lipids on cancer. *Mol Nutr Food Res* 51: 1279-1292, 2007.
- 60
39. Colomer R, Lupu R, Papadimitropoulou A, Vellón L, Vázquez-Martín A, Brunet J, Fernández-Gutiérrez A, Segura-Carretero A and Menéndez JA: Giacomo Castelvetro's salads. Anti-HER2 oncogene nutraceuticals since the 17th century? *Clin Transl Oncol* 10: 30-34, 2008.
- 61
- 62
- 63
- 64 40. Escrich E, Solanas M, Moral R, Costa I and Grau L: Are the olive oil and other dietary lipids related to cancer? Experimental evidence. *Clin Transl Oncol* 8: 868-883, 2006.
- 65
- 66
- 67 41. Galli C and Visioli F: Antioxidant and other activities of phenolics in olives/olive oil, typical components of the Mediterranean diet. *Lipids* 34: 23-26, 1999.
- 68
- 69 42. Owen RW, Giacosa A, Hull WE, Haubner R, Spiegelhalter B and Bartsch H: The antioxidant/anticancer potential of phenolic compounds isolated from olive oil. *Eur J Cancer* 36: 1235-1147, 2000.
- 70
- 71
- 72 43. Owen RW, Mier W, Giacosa A, Hull WE, Spiegelhalter B and Bartsch H: Identification of lignans as major components in the phenolic fraction of olive oil. *Clin Chem* 46: 976-988, 2000.
- 73
- 74 44. Visioli F and Galli C: Phenolics from olive oil and its waste products. Biological activities in *in vitro* and *in vivo* studies. *World Rev Nutr Diet* 88: 233-237, 2001.
- 75
- 76 45. Visioli F, Poli A and Galli C: Antioxidant and other biological activities of phenols from olives and olive oil. *Med Res Rev* 22: 65-75, 2002.
- 77
- 78
- 79 46. Visioli F and Galli C: Biological properties of olive oil phytochemicals. *Crit Rev Food Sci Nutr* 42: 209-221, 2002.
- 80
- 81 47. Beauchamp GK, Keast RS, Morel D, Lin J, Pika J, Han Q, Lee CH, Smith AB and Breslin PA: Phytochemistry: ibuprofen-like activity in extra-virgin olive oil. *Nature* 437: 45-46, 2005.
- 82
- 83 48. Owen RW, Giacosa A, Hull WE, Haubner R, Würtele G, Spiegelhalter B and Bartsch H: Olive-oil consumption and health: the possible role of antioxidants. *Lancet Oncol* 1: 107-112, 2000.
- 84
- 85 49. Servili M, Esposto S, Fabiani R, Urbani S, Taticchi A, Mariucci F, Selvaggini R and Montedoro GF: Phenolic compounds in olive oil: antioxidant, health and organoleptic activities according to their chemical structure. *Inflammopharmacology* 17: 76-84, 2009.
- 86
- 87
- 88 50. Raederstorff D: Antioxidant activity of olive polyphenols in humans: a review. *Int J Vitam Nutr Res* 79: 152-165, 2009.
- 89
- 90 51. Sinclair DA: Toward a unified theory of caloric restriction and longevity regulation. *Mech Ageing Dev* 126: 987-1002, 2005.
- 91
- 92 52. Howitz KT and Sinclair DA: Xenohormesis: sensing the chemical cues of other species. *Cell* 133: 387-391, 2008.
- 93
- 94 53. Way TD, Kao MC and Lin JK: Apigenin induces apoptosis through proteasomal degradation of HER2/neu in HER2/neu-overexpressing breast cancer cells via the phosphatidylinositol 3-kinase/Akt-dependent pathway. *J Biol Chem* 279: 4479-4489, 2004.
- 95
- 96
- 97 54. Way TD, Kao MC and Lin JK: Degradation of HER2/neu by apigenin induces apoptosis through cytochrome c release and caspase-3 activation in HER2/neu-overexpressing breast cancer cells. *FEBS Lett* 579: 145-152, 2005.
- 98
- 99
- 100 55. Shimizu M, Deguchi A, Joe AK, Mckoy JF, Moriwaki H and Weinstein IB: EGCG inhibits activation of HER3 and expression of cyclooxygenase-2 in human colon cancer cells. *J Exp Ther Oncol* 5: 69-78, 2005.
- 101
- 102 56. Shimizu M, Deguchi A, Hara Y, Moriwaki H and Weinstein IB: EGCG inhibits activation of the insulin-like growth factor-1 receptor in human colon cancer cells. *Biochem Biophys Res Commun* 334: 947-953, 2005.
- 103
- 104 57. Shimizu M, Deguchi A, Lim JT, Moriwaki H, Kopelovich L and Weinstein IB: (-)-Epigallocatechin gallate and polyphenon E inhibit growth and activation of the epidermal growth factor receptor and human epidermal growth factor receptor-2 signaling pathways in human colon cancer cells. *Clin Cancer Res* 11: 2735-2746, 2005.
- 105
- 106
- 107 58. Chiang CT, Way TD and Lin JK: Sensitizing HER2-overexpressing cancer cells to luteolin-induced apoptosis through suppressing p21WAF1/CIP1 expression with rapamycin. *Mol Cancer Ther* 6: 2127-2138, 2007.
- 108
- 109
- 110 59. Baselga J, Albanell J, Molina MA and Arribas J: Mechanism of action of trastuzumab and scientific update. *Semin Oncol* 28: 4-11, 2001.
- 111
- 112 60. Molina MA, Codony-Servat J, Albanell J, Rojo F, Arribas J and Baselga J: Trastuzumab (herceptin), a humanized anti-Her2 receptor monoclonal antibody, inhibits basal and activated Her2 ectodomain cleavage in breast cancer cells. *Cancer Res* 61: 4744-4749, 2001.
- 113
- 114
- 115
- 116
- 117
- 118
- 119
- 120



1 61. O'Brien NA, Browne BC, Chow L, Wang Y, Ginther C, Arboleda
2 J, Duffy MJ, Crown J, O'Donovan N and Slamon DJ: Activated
3 Phosphoinositide 3-Kinase/AKT Signaling Confers Resistance
4 to Trastuzumab but not Lapatinib. *Mol Cancer Ther* 9: 1489-1502,
5 2010.

6 62. Weiss RH: p21^{Waf1/Cip1} as a therapeutic target in breast and other
7 cancers. *Cancer Cell* 4: 425-429, 2003.

8 63. Guo H, Tian T, Nan K and Wang W: p57: α multifunctional
9 protein in cancer (Review). *Int J Oncol* 36: 1321-1329, 2010.

10 64. Yu J and Zhang L: The transcriptional targets of p53 in apoptosis
11 control. *Biochem Biophys Res Commun* 331: 851-858, 2005.

12 65. Ploner C, Kofler R and Villunger A: Noxa: at the tip of the
13 balance between life and death. *Oncogene* 27 (Suppl. 1):
14 S84-S92, 2008.

15 66. Mork CN, Faller DV and Spanjaard R: A mechanistic approach
16 to anticancer therapy: targeting the cell cycle with histone
17 deacetylase inhibitors. *Curr Pharm Des* 11: 1091-1104, 2005.

18 67. Ocker M and Schneider-Stock R: Histone deacetylase inhibitors:
19 signalling towards p21^{suppl/waf1}. *Int J Biochem Cell Biol* 39:
20 1367-1374, 2007.

21 68. Martínez-Iglesias O, Ruiz-Llorente L, Sánchez-Martínez R,
22 García L, Zambrano A and Aranda A: Histone deacetylase
23 inhibitors: mechanism of action and therapeutic use in cancer.
24 *Clin Transl Oncol* 10: 395-398, 2008.

25 69. Sowa Y, Orita T, Hiranabe-Minamikawa S, Nakano K, Mizuno T,
26 Nomura H and Sakai T: Histone deacetylase inhibitor activates
27 the p21/WAF1/Cip1 gene promoter through the Sp1 sites. *Ann*
28 *NY Acad Sci* 886: 195-199, 1999.

29 70. Yokota T, Matsuzaki Y, Miyazawa K, Zindy F, Roussel MF
30 and Sakai T: Histone deacetylase inhibitors activate INK4d gene
31 through Sp1 site in its promoter. *Oncogene* 23: 5340-5349, 2004.

32 71. Cucciolla V, Borriello A, Criscuolo M, Sinisi AA, Bencivenga D,
33 Tramontano A, Scudieri AC, Oliva A, Zappia V and Della
34 Ragione F: Histone deacetylase inhibitors upregulate p57^{Kip2}
35 level by enhancing its expression through Sp1 transcription factor.
36 *Carcinogenesis* 29: 560-577, 2008.

37 72. Cai X, Zhai HX, Wang J, Forrester J, Qu H, Yin L, Lai CJ, Bao R
38 and Qian C: Discovery of 7-(4-(3-ethynylphenylamino)-7-
39 methoxyquinazolin-6-yloxy)-N-hydroxyheptanamide(CUDC101)
40 as a potent multi-acting HDAC, EGFR, and HER2 inhibitor for
41 the treatment of cancer. *J Med Chem* 3: 2000-2009, 2010.

42 73. Lai CJ, Bao R, Tao X, Wang J, Atoyan R, Qu H, Wang DG,
43 Yin L, Samson M, Forrester J, Zifcak B, Xu GX, DellaRocca S,
44 Zhai HX, Cai X, Munger WE, Keegan M, Pepicelli CV and
45 Qian C: CUDC-101, a multitargeted inhibitor of histone deacetylase,
46 epidermal growth factor receptor, and human epidermal growth
47 factor receptor 2, exerts potent anticancer activity. *Cancer Res* 70:
48 3647-3656, 2010.

49 74. Bali P, Pranpat M, Swaby R, Fiskus W, Yamaguchi H, Balasis
50 M, Rocha K, Wang HG, Richon V and Bhalla K: Activity of
51 sub-eroylanilide hydroxamic Acid against human breast cancer
52 cells with amplification of her-2. *Clin Cancer Res* 11: 6382-6389,
53 2005.

54 75. Kultz D, Madhany S and Burg MB: Hyperosmolality causes
55 growth arrest of murine kidney cells. Induction of GADD45 and
56 GADD153 by osmosensing via stress-activated protein kinase 2.
57 *J Biol Chem* 273: 13645-13651, 1998.

58 76. Takekawa M and Saito H: A family of stress-inducible GADD45-
59 like proteins mediate activation of the stress-responsive MTK1/
60 MEKK4 MAPKKK. *Cell* 95: 521-530, 1998.

61 77. O'Prey J, Brown J, Fleming J and Harrison PR: Effects of dietary
62 flavonoids on major signal transduction pathways in human
63 epithelial cells. *Biochem Pharmacol* 66: 2075-2088, 2003.

64 78. Chi H, Lu B, Takekawa M, Davis RJ and Flavell RA: GADD45beta/
65 GADD45gamma and MEKK4 comprise a genetic pathway
66 mediating STAT4-independent IFNgamma production in T cells.
67 *EMBO J* 23: 1576-1586, 2004.

68 79. Bulavin DV, Kovalsky O, Hollander MC and Fornace AJ Jr:
69 Loss of oncogenic H-rasinduced cell cycle arrest and p38 mitogen-
70 activated protein kinase activation by disruption of Gadd45a.
71 *Mol Cell Biol* 23: 3859-3871, 2003.

72 80. Wei GH, Zhao GW, Song W, Hao DL, Lv X, Liu DP and Liang CC:
73 Mechanisms of human gamma-globin transcriptional induction
74 by apicidin involves p38 signaling to chromatin. *Biochem Biophys*
75 *Res Commun* 363: 889-894, 2007.

76 81. Zhao Q, Barakat BM, Qin S, Ray A, El-Mahdy MA, Wani G,
77 Arafa el-S, Mir SN, Wang QE and Wani AA: The p38 mitogen-
78 activated protein kinase augments nucleotide excision repair by
79 mediating DDB2 degradation and chromatin relaxation. *J Biol*
80 *Chem* 283: 32553-32561, 2008.

81 82. Seo SB, McNamara P, Heo S, Turner A, Lane WS and
82 Chakravarti D: Regulation of histone acetylation and transcription
83 by INHAT, a human cellular complex containing the set onco-
84 protein. *Cell* 104: 119-130, 2001.

85 83. Saha RN, Jana M and Pahan K: MAPK p38 regulates transcriptional
86 activity of NF-kappaB in primary human astrocytes via acetylation
87 of p65. *J Immunol* 179: 7101-7109, 2007.

88 84. Liu X, Wang L, Zhao K, Thompson PR, Hwang Y, Marmorstein R
89 and Cole PA: The structural basis of protein acetylation by the
90 p300/CBP transcriptional coactivator. *Nature* 451: 846-850,
91 2008.

92 85. Chavan P, Joshi K and Patwardhan B: DNA microarrays in
93 herbal drug research. *Evid Based Complement Alternat Med* 3:
94 447-457, 2006.

95 86. Wermuth CG: Multitargeted drugs: the end of the 'one-target-
96 one-disease' philosophy? *Drug Discov Today* 9: 826-827, 2004.

97 87. Oliveras-Ferreros C, Vazquez-Martin A, Martin-Castillo B,
98 Pérez-Martínez MC, Cufí S, Del Barco S, Bernado L, Brunet J,
99 López-Bonet E and Menendez JA: Pathway-focused proteomic
100 signatures in HER2-overexpressing breast cancer with a basal-
101 like phenotype: new insights into *de novo* resistance to trastuzumab
102 (Herceptin). *Int J Oncol* 37: 669-678, 2010.

103
104
105
106
107
108
109
110
111
112
113
114
115
116
117
118
119
120









CAPÍTULO 5. Phenolic secoiridoids in extra-virgin olive oil impede fibrogenic and oncogenic epithelial-to-mesenchymal transition: extra-virgin olive oil as a source of novel antiaging phytochemicals.





Phenolic Secoiridoids in Extra Virgin Olive Oil Impede Fibrogenic and Oncogenic Epithelial-to-Mesenchymal Transition: Extra Virgin Olive Oil As a Source of Novel Antiaging Phytochemicals

Alejandro Vazquez-Martin,^{1,2,*} Salvador Fernández-Arroyo,^{3,*} Sílvia Cufí,^{1,2,*}
Cristina Oliveras-Ferraras,^{1,2,*} Jesús Lozano-Sánchez,^{3,*} Luciano Vellón,⁴ Vicente Micol,⁵
Jorge Joven,⁶ Antonio Segura-Carretero,^{3,†} and Javier A. Menendez^{1,2,†}

Abstract

The epithelial-to-mesenchymal transition (EMT) genetic program is a molecular convergence point in the life-threatening progression of organ fibrosis and cancer toward organ failure and metastasis, respectively. Here, we employed the EMT process as a functional screen for testing crude natural extracts for accelerated drug development in fibrosis and cancer. Because extra virgin olive oil (EVOO) (*i.e.*, the juice derived from the first cold pressing of the olives without any further refining process) naturally contains high levels of phenolic compounds associated with the health benefits derived from consuming an EVOO-rich Mediterranean diet, we have tested the ability of an EVOO-derived crude phenolic extract to regulate fibrogenic and oncogenic EMT *in vitro*. High-performance liquid chromatography (HPLC) coupled to time-of-flight (TOF) mass spectrometry assays revealed that the EVOO phenolic extract was mainly composed (~70%) of two members of the secoiridoid family of complex polyphenols, namely oleuropein aglycone—the bitter principle of olives—and its derivative decarboxymethyl oleuropein aglycone. EVOO secoiridoids efficiently prevented loss of proteins associated with polarized epithelial phenotype (*i.e.*, E-cadherin) as well as *de novo* synthesis of proteins associated with mesenchymal migratory morphology of transitioning cells (*i.e.*, vimentin). The ability of EVOO to impede transforming growth factor- β (TGF- β)-induced disintegration of E-cadherin-mediated cell-cell contacts apparently occurred as a consequence of the ability of EVOO phenolics to prevent the upregulation of SMAD4—a critical mediator of TGF- β signaling—and of the SMAD transcriptional cofactor SNAIL2 (Slug)—a well-recognized epithelial repressor. Indeed, EVOO phenolics efficiently prevented crucial TGF- β -induced EMT transcriptional events, including upregulation of *SNAI2*, *TCF4*, *VIM* (Vimentin), *FN* (fibronectin), and *SERPINE1* genes. While awaiting a better mechanistic understanding of how EVOO phenolics molecularly shut down the EMT differentiation process, it seems reasonable to suggest that nontoxic *Oleaceae* secoiridoids certainly merit to be considered for aging studies and, perhaps, for ulterior design of more pharmacologically active second-generation anti-EMT molecules.

¹Catalan Institute of Oncology, Girona, Catalonia, Spain.

²Girona Biomedical Research Institute, Girona, Catalonia, Spain.

³Department of Analytical Chemistry, Faculty of Sciences, University of Granada, Granada, Spain.

⁴Fundación INBIOMED, Cell Reprogramming Unit, San Sebastián. Basque Country, Spain.

⁵Molecular and Cellular Biology Institute (IBMC), Miguel Hernández University, Elche, Alicante, Spain.

⁶Centre de Recerca Biomèdica, Hospital Universitari Sant Joan de Reus, Institut d'Investigació Sanitària Pere Virgili, Universitat Rovira i Virgili, Reus, Catalonia, Spain.

*These authors have contributed equally to this research and are listed in random order.

†Co-senior authors.



Introduction

A DEREGULATED EPITHELIAL-TO-MESENCHYMAL (EMT) trans-differentiation process (*i.e.*, the generation of motile mesenchymal cells from epithelial sheets)^{1–3} is an ideal molecular scenario to test the notion that “an anti-aging drug must delay age-related diseases in order to extend lifespan (*i.e.*, unless a drug delays age-related diseases, it will not extend lifespan and vice versa, if a drug prevents age-related diseases, it must extend lifespan).”⁴ On the one hand, EMT overactivation is a critical phenomenon in age-related human diseases exhibiting end-state organ fibrosis (*e.g.*, kidney fibrosis in chronic renal disease, liver fibrosis in nonalcoholic steatohepatitis, or myocardial fibrosis in heart failure).^{5–8} The pleiotropic cytokine transforming growth factor- β (TGF- β) is a major regulator of these types of pathophysiological EMT.

Indeed, chronic diseases characterized by excessive fibrosis can be explained in terms of repeated and sustained infliction of TGF- β -induced EMT, which significantly increases synthesis and accumulation of collagen and extracellular matrix (ECM) in the affected organ.^{7,9–11} In this scenario, highly differentiated epithelial cells in the specific organs (*e.g.*, tubular epithelial cells in the kidney) will respond to noxious stimuli by undergoing TGF- β -driven EMT. Then, the transdifferentiated epithelial cells migrate into the interstitial space and some of them will become activated (*i.e.*, myofibroblasts *de novo* expressing mesenchymal markers such as α -smooth muscle cell actin [SMA]) to become the main source of excessive ECM. TGF- β -induced EMT not only constitutes a pivotal mechanism contributing to the supply of activated myofibroblasts in renal fibrosis but it also similarly turns adult hepatocytes into activated fibroblasts, contributing to liver fibrosis in nonalcoholic steatohepatitis.⁸ Spontaneous activation of TGF- β -driven EMT has also been shown to profibrotic responses during myocardial fibrosis in aged mice hearts.¹²

While end-stage renal disease will need lifelong renal replacement therapy with maintenance dialysis or kidney transplantation, it is also noteworthy that renal transplant recipients frequently start or restart dialysis because of the unusual propensity of these allografts to develop interstitial fibrosis and tubular atrophy as tubular epithelial cells react to certain fibrogenic stimuli to (re)engage in the process of EMT.^{13–16} Fibrosis, ranging from mild inflammation to severe sclerosing peritonitis and encapsulating sclerosing peritonitis, is also responsible for negative changes in the peritoneal membrane; this preservation is crucial for long-term survival in peritoneal dialysis. Glucose and glucose degradation products stimulate the profibrotic factor TGF- β by mesothelial cells and induce EMT, the pivotal triggering mechanism of peritoneal membrane fibrosis in peritoneal dialysis patients.^{17–19} Accordingly, the quality of life on renal replacement therapy is much impaired, and the life expectancy of these patients is substantially shorter when compared to the general population.²⁰

On the other hand, the EMT developmental process has gained much attention in oncology because some aspects of embryonic EMT are instrumentally employed by human cancer cells to facilitate metastasis. Tumor cells undergoing the EMT acquire the capacity to migrate and invade the surrounding stroma; they subsequently spread via blood and lymphatic vessels to repopulate distant sites as metas-

ases.^{21–25} More importantly, it has recently been discovered that tumor cells undergoing EMT acquire stem cell-like characteristics, thus showing a link between EMT and pathways involved in promoting cellular stemness.^{26–31} Induction of nontumorigenic, immortalized human mammary epithelial cells to the EMT phenotype likewise results in the loss of the epithelial phenotype (*e.g.*, downregulation and relocation of the epithelial marker E-cadherin) and the acquisition of the mesenchymal phenotype (*e.g.*, gain of the mesenchymal marker vimentin) concomitant with the acquisition of the CD44^{high}/CD24^{low} immunophenotype, a molecular signature associated with stem cells and increased tumor-initiating capacity in breast cancer disease.^{26,31} Because EMT-phenotypic tumor cells acquire stem-like cell signatures characterized by increased metastatic capacity and self-renewal ability, the stem-like cells or cancer stem cells (CSCs) generated from (*e.g.*, TGF- β driven) EMT induction provide a resource for cancer to recur because these cells are well known to be highly drug resistant.^{32–35}

A definitive understanding of the cellular and molecular events driving excessive fibrosis causally underlying end-state organ failures is crucial to designing effective and specifically targeted therapeutic interventions aimed to impede “fibrogenic EMT.” Similarly, a better molecular understanding and biological characterization of EMT phenotypic cells, cancer stem-like cells, and CSCs should allow us to screen for potential drugs that could cause selective killing of these cells that are the “root cause” of tumor development, maintenance, recurrence, and metastasis.^{36–38} Indeed, it is reasonable to suggest that molecular characterization of agents able to impede the generation of EMT-phenotypic tumor cells (*i.e.*, “oncogenic EMT”) will allow not only the development of newer therapies for complete eradication of tumors, which will certainly improve the overall survival of patients diagnosed with cancers, but also to ameliorate progressive tissue fibrosis in various age-related chronic diseases.^{2,39}

Supporting the hypothesis that EMT-focused studies can promise the generation of new anticancer and antifibrosis drugs, it should be noted that the gerosuppressant drug rapamycin (*i.e.*, a blocker of the nutrient-sensing mammalian target of rapamycin [mTOR] pathway that, by slowing down organismal aging, efficiently delays cancer)^{40–42} has been found to significantly enhance the expression of a protective gene for EMT (*i.e.*, E-cadherin) to impede TGF- β -induced EMT in cultured human peritoneal mesothelial cells.^{43,44} Similarly, the gerosuppressant agent metformin appears to molecularly behave as a *bona fide* antiaging modality owing its ability to prevent TGF- β -driven EMT in cultured Madin-Darby canine kidney (MDCK) cells (an *in vitro* mouse system model to study the critical involvement of the EMT phenomenon in renal fibrosis) and in cultured MCF-7 breast cancer epithelial cells (an *in vitro* human system model to study the loss of E-cadherin expression/function as the central molecular process required for EMT-driven acquisition of malignant and stem cell traits because post-EMT MCF-7/TGF- β mesenchymal phenotypic cells display increased tumorsphere-initiating stem cell-like features compared to their pre-EMT parental MCF-7 epithelial phenotypic cells).^{45,46} Accordingly, metformin treatment decreases both the self-renewal and the proliferation of breast CSC populations and efficiently prevents EMT-promoted ontogenesis



of the breast CSC molecular signature because it ablates the ability of TGF- β to increase the population of breast cancer cells that can form mammospheres in suspension—a feature endowed by CSCs.^{47–50}

Because crude phenolic extracts directly obtained from extra virgin olive oil (EVOO) and naturally enriched in secoiridoids (*i.e.*, a family of complex polyphenols characteristics of *Oleaceae* plants)^{51–54} can efficiently attack drug-resistant EMT-type breast cancer cells intrinsically enriched with CSC-like phenotypes,^{55,56} we recently envisioned that EVOO phenolics can negatively impact TGF- β -triggered fibrogenic and oncogenic EMT. Here we reveal for the first time that an EVOO-derived crude phenolic fraction is sufficient to efficiently impede fibrogenic and oncogenic EMT in cultured MDCK and MCF-7 cells, respectively. Our current study strongly suggests that *Oleaceae* secoiridoids might constitute a novel valuable phytochemical platform for the discovery of previously unrecognized antiaging biomolecules.

Materials and Methods

Olive oil

The EVOO employed in this study was from the mono-variety Picual obtained from Córdoba (Andalusia, Spain) in 2008. Picual olives were processed by continuous industrial plants equipped with a hammer crusher, a horizontal malaxator, and a two-phase decanter. Samples were stored in bottles without headspace at room temperature and in darkness before analysis.

Isolation of EVOO phenolic fraction

To isolate the phenolic fraction of Picual EVOO, we used solid-phase extraction (SPE) with Diol-cartridges. In all, 60 grams of Picual EVOO was dissolved in methanol and loaded onto the column. The cartridge was washed with 15 mL of hexane, which was then discarded to remove the nonpolar fraction of the EVOO. Finally, the sample was recovered by passing it through 40 mL of methanol; the solvent was evaporated under vacuum. The residue was dissolved with 2 mL of methanol and filtered through a 0.25-mm filter before characterization of the phenolic profile.

Qualitative and quantitative characterization of phenolic compounds

To characterize the phenolic profile in the Picual EVOO phenolic extract, rapid resolution liquid chromatography (RRLC) coupled to electrospray interface time-of-flight mass spectrometry (ESI-TOF-MS) was performed in an Agilent 1200-RRLC system (Agilent Technologies, Waldbronn, Germany) of the Series Rapid Resolution equipped with a vacuum degasser, an autosampler, a binary pump, and a UV-Vis detector. The chromatographic separation was carried out on a Zorbax Eclipse Plus C18 analytical column (4.6 mm \times 150 mm, 1.8- μ m particle size). The flow rate was 0.80 mL/min, and the temperature of the column was maintained at 25°C. The mobile phases used were water with 0.25% acetic acid as eluant A and methanol as eluant B. The total run time was 27 min.⁵³ Compounds were monitored in sequence first with diode array detection (DAD; 240 and 280 nm) and then with a mass analyzer (MA) detector. MS was performed using the microTOF (Bruker Daltonik, Bre-

men, Germany), which was coupled to the RRLC system. At this stage, the use of a splitter was required to the coupling with the MS detector because the flow that arrived to the TOF detector had to be 0.2 mL/min to obtain reproducible results and stable spray. The TOF mass spectrometer was equipped with an ESI (model G1607A from Agilent Technologies, Palo Alto, CA) operating in negative ion mode. External mass spectrometer calibration was performed with sodium formate clusters (5 mM sodium hydroxide in water/2-propanol 1/1 [vol/vol], with 0.2% of formic) in quadratic high-precision calibration (HPC) regression mode.

The calibration solution was injected at the beginning of the run, and all of the spectra were calibrated prior to identification of EVOO polyphenols. The optimum values of the source and transfer parameters were get for a good sensitivity and reasonable resolution of the mass range for compounds of interest (50–1000 *m/z*) to improve ionization performance.⁵³ The accurate mass data for the molecular ions were processed using the software Data Analysis 3.4 (Bruker Daltonik), which provided with a list of possible elemental formulas by using the Generate Molecular Formula Editor. The latter employs a CHNO algorithm that provides standard functionalities such as minimum/maximum elemental range, electron configuration, and ring-plus double bonds equivalent, as well as a sophisticated comparison of the theoretical with the measured isotopic pattern (sigma value) for increased confidence in the suggested molecular formula. The widely accepted accuracy threshold for confirmation of elemental compositions has been established at 5 ppm for most of the compounds.

The individual quantification of the identified phenolic compounds was carried out by RRLC-ESI-TOF using the validated method described above.⁵³ Ten standard calibration graphs for the quantification of the principal compounds found in the samples were prepared using the following commercial available standards. Hydroxytyrosol, tyrosol, vanillin, luteolin, apigenin, *p*-coumaric acid, ferulic acid, and vanillic acid were purchased from Sigma-Aldrich (St. Louis, MO), and (+)-pinoresinol was acquired from Arbo Nova (Turku, Finland). Oleuropein (Ole) was purchased from Extrasynthèse (Lyon, France).

As complementary information, the total phenolic content of the crude EVOO phenolic extract was determined by a spectrophotometric method based on the Folin-Ciocalteu technique.⁵⁷ The absorbance of the solution was measured at a wavelength of 725 nm in a Spectronic Genesys™ 5 spectrophotometer (Spectronic Instruments Inc. Rochester, NY). The extracts were diluted 1:10 with methanol. After this, a 50- μ L aliquot of the diluted methanolic extract of EVOO was used in this determination. Total polyphenols were expressed as caffeic acid equivalents. A calibration curve of freshly prepared caffeic acid solution was carried out. Three replicates of each analysis and for each calibration point were performed to obtain reproducible results.

Cell lines and culture conditions

MDCK cells were obtained from Dr. Manel Esteller (Cancer Epigenetics and Biology Program-PEBC, Bellvitge Biomedical Research Institute-IDIBELL, L'Hospitalet, Barcelona, Spain) and cultured in Dulbecco modified Eagle medium (DMEM; BioSource International; Invitrogen S.A., Barcelona, Spain) supplemented with 10% fetal bovine



TABLE 1. MAIN PHENOLIC COMPOUNDS IDENTIFIED IN EXTRA VIRGIN OLIVE OIL PHENOLIC EXTRACT BY HPLC-DAD-ESI-TOF

Number	Proposed compound	Retention time (min)	[M-H] ⁻	Molecular formula	Structure
1	Hydroxytyrosol	8	153.0557	C ₈ H ₁₀ O ₃	
2	Tyrosol	9,9	137.0608	C ₈ H ₁₀ O ₂	
3	Vanillin	11,7	151.0401	C ₈ H ₈ O ₃	
4	<i>p</i> -Coumaric acid	13,5	163.0401	C ₉ H ₈ O ₃	
5	Hydroxytyrosol acetate	14	195.0663	C ₁₀ H ₁₂ O ₄	
6	Elenolic acid	15	241.0718	C ₁₁ H ₁₄ O ₆	
7	Hydroxy elenolic acid	15,4	257.0667	C ₁₁ H ₁₄ O ₇	
8	Decarboxymethyl oleuropein aglycon	16,3	319.1187	C ₁₇ H ₂₀ O ₆	

(continued)



TABLE 1. (CONTINUED)

Number	Proposed compound	Retention time (min)	[M-H]-	Molecular formula	Structure
9	Hydroxy D-oleuropein aglycon	16,6	335.1136	C ₁₇ H ₂₀ O ₇	
10	Syringaresinol	18,2	417.1555	C ₂₂ H ₂₆ O ₈	
11	Pinoresinol	18,8	357.1344	C ₂₀ H ₂₂ O ₆	
12	Decarboxymethyl ligstroside aglycon	19,2	303.1229	C ₁₇ H ₂₀ O ₅	

(continued)



TABLE 1. (CONTINUED)

Number	Proposed compound	Retention time (min)	[M-H] ⁻	Molecular formula	Structure
13	Hydroxy D-ligstroside aglycon	19,9	319.1187	C ₁₇ H ₂₀ O ₆	
14	10-Hydroxy oleuropein aglycon	23	393.1191	C ₁₉ H ₂₂ O ₉	
15	Oleuropein aglycon	23,2	377.1242	C ₁₉ H ₂₂ O ₈	
16	Luteolin	23,7	285.0405	C ₁₅ H ₁₀ O ₆	
17	Methyl D-oleuropein aglycon	25,4	333.1344	C ₁₈ H ₂₂ O ₆	

(continued)



TABLE 1. (CONTINUED)

Number	Proposed compound	Retention time (min)	[M-H] ⁻	Molecular formula	Structure
18	Ligstroside aglycon	25,6	361.1293	C ₁₉ H ₂₂ O ₇	
19	Apigenin	25,8	269.0451	C ₁₅ H ₁₀ O ₅	
20	Methyl oleuropein aglycon	26,2	391.1398	C ₂₀ H ₂₄ O ₈	

serum (FBS), L-glutamine (2 mmol/L), and antibiotics (all from Biowhittaker, Madrid, Spain). MCF-7 human breast cancer cells were obtained from the American Type Culture Collection (ATCC) and they were routinely grown in improved MEM (IMEM) supplemented with 5% FBS and L-glutamine (2 mmol/L). Cells were maintained at 37°C in a humidified atmosphere of 95% air and 5% CO₂. Cells were screened periodically for *Mycoplasma* contamination.

TGF-β1

Recombinant human (carrier-free) TGF-β1 was purchased from R&D Systems Inc. (Minneapolis, MA).

Immunofluorescence staining and high-content confocal imaging

Cells were seeded at approximately 5,000 cells/well in 96-well, clear-bottomed imaging tissue culture plates (Becton Dickinson Biosciences; San Jose, CA) optimized for automated imaging applications. Triton X-100 permeabilization and blocking, primary antibody staining (1:50 dilution), secondary antibody staining using Alexa Fluor 488/594 goat anti-rabbit/mouse immunoglobulin Gs (IgGs) (Invitrogen, Molecular Probes, Eugene, OR), and counterstaining (using

Hoechst 33258; Invitrogen) were performed by following BD Biosciences protocols. Images were captured in different channels for Alexa Fluor 488 (pseudocolored green) and Hoechst 33258 (pseudocolored blue) on a BD Pathway™ 855 Bioimager System (Becton Dickinson Biosciences, San Jose, CA) with 20× or 40× objectives (NA 075 Olympus). Merged images were obtained according to the recommended assay procedure using BD Attovision™ software.

Quantitative, real-time polymerase chain reaction (qRT-PCR)

Total RNA was extracted from MCF-7 cell cultures supplemented with TGF-β (100 ng/mL), EVOO phenolics, or TGF-β plus EVOO phenolics as specified using a Qiagen RNeasy kit and QIAshredder columns according to the manufacturer's instructions (Qiagen, Valencia, CA). One microgram of total RNA was reverse-transcribed to cDNA using the Reaction Ready™ First Strand cDNA Synthesis Kit (SABiosciences, Frederick, MD) and applied to EMT PCR Arrays (cat. no. PAHS-090; 96-well format) following SABiosciences RT-PCR manual. Plates were processed in an Applied Biosystems 7500 Fast Real-Time PCR System (Applied Biosystems, Foster City, CA), using automated baseline



and threshold cycle detection. Data were interpreted by using SABiosciences' web-based PCR array analysis tool.

Results

Qualitative and quantitative characterization of phenolic compounds in EVOO phenolic extract was performed in a previously reported analytical approach.⁵³ Identification of phenolic compounds was performed by comparing both retention times and MS spectral data from EVOO methanolic extract and standards, as detailed in Materials and Methods. The remaining compounds, for which no commercial standards were available, were characterized by interpretation of their ultraviolet (UV) absorbance maxima, mass spectra provided by the TOF-MS, and other analytical information reported elsewhere because most of these compounds have been previously described in OO samples. Table 1 summarizes the main compounds identified in the Picual EVOO variety, including their structure and the information gen-

erated by TOF analyzer—retention time, calculated m/z , and molecular formula. Twenty compounds from different families (*i.e.*, simple phenols, flavonoids, lignans, and secoiridoids) were identified. Figure 1A shows the resulting chromatogram of EVOO phenolic extract. Several isomers of oleuropein aglycon were tentatively characterized in this sample. This compound and its isomers, for which there are no available commercial standards, have been previously described in OO,⁵⁸ and the accuracy of MS data provided enough confidence during their identification. The analysis of the true isotopic pattern by ESI-TOF-MS in combination with excellent mass resolution and mass accuracy is the perfect choice for molecular formula determination using the Generate Molecular Formula Editor as detailed in Materials and Methods.

Concentrations of individual phenolics were determined using the areas of each individual compound (three replicates) obtained by peak integration in their extracted ion chromatogram (EIC) and by interpolation in the corresponding

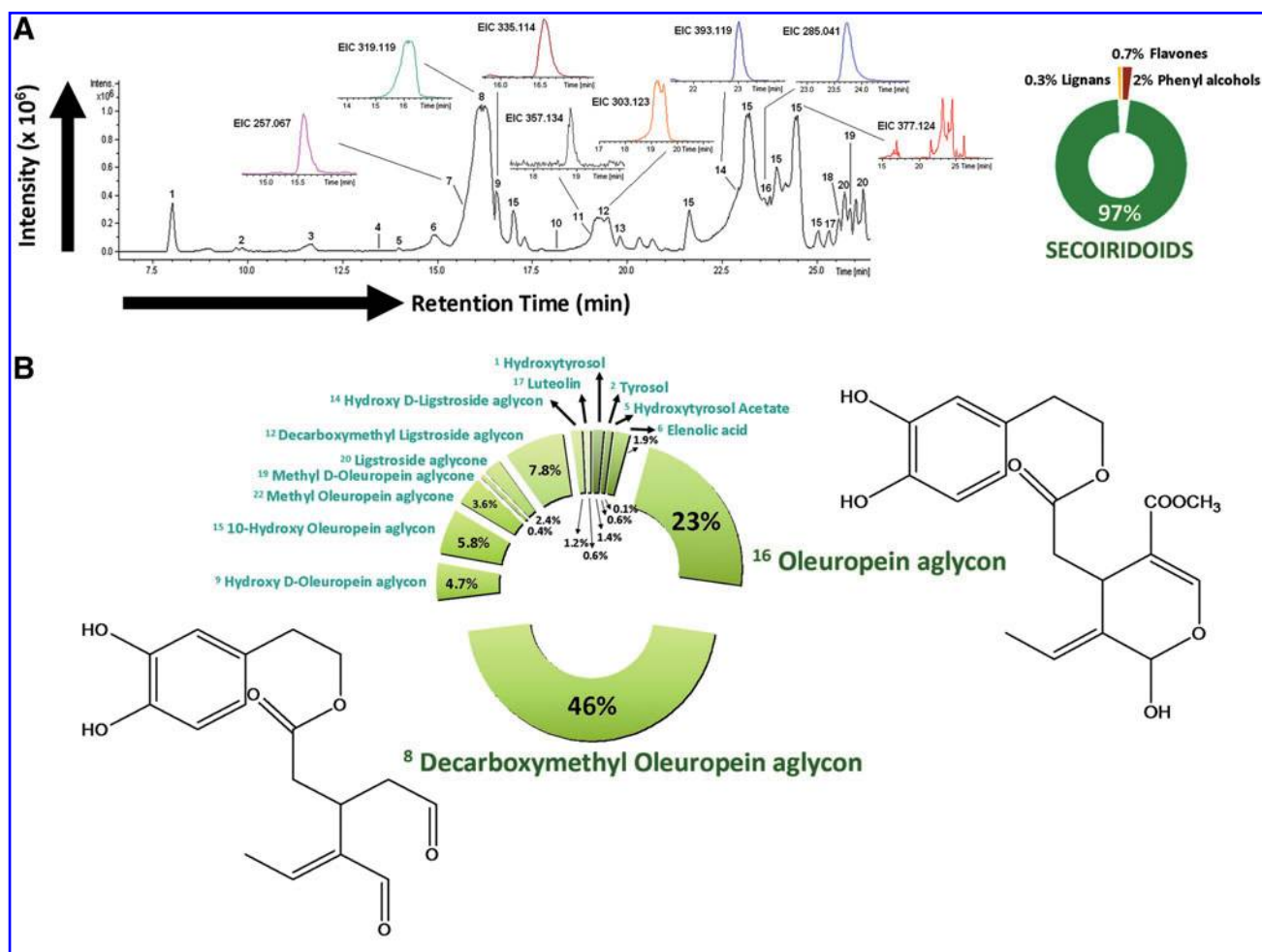


FIG. 1. (A) (Left) Base peak chromatogram (BPC) of extra virgin olive oil (EVOO) phenolic extract obtained by high-performance liquid chromatograph–electrospray ionization–time-of-flight mass spectrometry (HPLC-ESI-TOF) with the extracted ion chromatogram (EIC) of the main phenolic compounds. (Right) Percent distribution of main phenolic families identified in Picual EVOO phenolic extract. (B) Percent distribution of identified phenolic compounds in Picual EVOO phenolic extract. The figure shows chemical structures of oleuropein aglycone and its derivative decarboxymethyl oleuropein aglycone, the major components of the Picual EVOO phenolic extract.



calibration curve. EIC results of the main phenolic compounds are also shown in Fig. 1A. The phenolic compounds hydroxytyrosol, tyrosol, luteolin, and apigenin were quantified by their respective commercial standards prepared as previously described.⁵³ Other phenolic compounds, which had no commercial standards, were tentatively quantified on the basis of other compounds having similar structures. Secoiridoid and lignan groups were quantified with oleuropein and (+)-pinoresinol standards, respectively. Elenolic acid derivatives, which cannot be considered as true phenolic compounds, were expressed as oleuropein. It should be considered that response of the standards can be different from each one of the EVOO analytes included in the Picual variety, and consequently the quantification of these compounds was only an estimation of their actual concentrations.

Table 2 summarizes the amount of each phenolic from Picual EVOO, with the main components belonging to the secoiridoids group. Among these complex polyphenols, two derivatives of hydroxytyrosol (3,4-DHEPA) linked to the elenolic acid and its decarboxymethylated form, namely oleuropein aglycon (3,4-DHEPA-EA) and decarboxymethyl oleuropein aglycon (3,4-DHEPA-DEA), were the most abundant compounds as they constituted up to 23% and 46% of total phenolics, respectively (Fig. 1B). Regarding other phenolics belonging to the secoiridoid family, the relative contents of the decarboxymethylated form of ligstroside aglycon as well as the hydroxylated and methylated forms of oleuropein aglycon were significantly higher than other phenolic com-

pounds. Simple phenols (*e.g.*, tyrosol, hydroxytyrosol), lignans (*e.g.*, siringaresinol, [+]-pinoresinol), and flavones (*e.g.*, luteolin and apigenin) were notably underrepresented in the phenolic mixture. The average total polyphenols content was 683.579 ± 4.169 expressed as milligrams of analyte/kg of EVOO, as tentatively calculated as the sum of the individual phenolic compound concentrations.

Because an inherent problem with using crude natural extracts in cell-based screens is that many of them are toxic to cells at the dilutions that might generate optimal hit rates because of the high concentrations of salts and other materials they contain, the EVOO phenolic extract was not cytotoxic at tested concentration to avoid unacceptable false-positive results. On the basis of earlier studies using crude EVOO phenolic extracts in human breast cancer cell lines,^{53,54,56} we first confirmed that EVOO phenolics did not significantly alter viability at 200 ng/mL ($\sim 0.01\%$ vol/vol), the concentration employed during 72 hr to test modulation of the EMT process in MDCK and MCF-7 cells.

EVOO phenolics impede "fibrogenic EMT"

We first employed MDCK cells to evaluate the impact of the EVOO-derived crude phenolic extract on several TGF- β -altered EMT parameters including cell morphology. Thus, we established TGF- β -induced EMT and then we measured the response to EVOO phenolics (Fig. 2). Untreated MDCK control cells displayed a typical epithelial-like morphology with respect to their light-microscopic appearance. Upon treatment with TGF- β (50 ng/mL), the cells acquired a spindle-type morphology and a reduced number of cell-cell contacts. These alterations started after 24 hr and they were maximal after 72 hr of treatment, when TGF- β supplementation fully induced a complete conversion of parental MDCK epithelial cells to a fibroblast-like, spindle-shaped, elongated mesenchymal morphology. The changes of morphology were partially reversible when TGF- β treatment was carried out in the presence of the EVOO-derived crude phenolic extract. Whereas EVOO phenolics as sole treatment had no significant effects on EMT-related morphological changes, TGF- β -treated MDCK cells changed from scattered and fibroblast-like shapes in the absence of EVOO phenolics to a more packed cobblestone morphology in their presence. Although MDCK cells co-treated with TGF- β and the EVOO-derived crude phenolic extract failed to maintain entirely the compact cuboidal appearance of parental MDCK control cells, EVOO phenolics notably prevented TGF- β -induced cell scattering and reduced the number of TGF- β -induced spindle-shaped cells and pseudopodia.

Because the above-mentioned findings suggested that exposure to EVOO phenolics triggered molecular changes that were consistent with a partial reversion of the EMT phenomenon, we carried out immunostaining studies to assess the expression status of marker proteins of either the epithelial (*i.e.*, E-cadherin) or the mesenchymal (*i.e.*, vimentin) phenotype in MDCK cell populations (Fig. 2). Compared with untreated MDCK control cells, immunostaining studies showed the reduced expression of E-cadherin in TGF- β 1-treated MDCK cells, especially in the adherens junctions in which the expression of E-cadherin was not detected by immunofluorescence microscopy. The intermediate filament vimentin accumulated profusely in the cytoplasm of TGF- β 1-treated MDCK cells. The

TABLE 2. QUANTITATIVE RESULTS EXPRESSED IN MG ANALYTE/ KG OF PICUAL EXTRA VIRGIN OLIVE OIL PHENOLIC EXTRACT

Phenolic compounds	Concentration	Percent
Simple phenols	14.467 ± 0.285	2.116
Hydroxytyrosol	9.625 ± 0.208	1.408
Tyrosol	4.162 ± 0.109	0.609
Hydroxytyrosol acetate	0.680 ± 0.003	0.099
Secoiridoids	662.673 ± 4.782	96.942
Elenolic acid	13.123 ± 0.125	1.920
Hydroxy elenolic acid	0.097 ± 0.002	0.014
Oleuropein aglycon	157.917 ± 1.257	23.102
Decarboxymethyl oleuropein aglycon	314.429 ± 2.189	45.998
Hydroxy D-oleuropein aglycon	32.373 ± 1.584	4.736
10-Hydroxy oleuropein aglycon	39.479 ± 0.806	5.775
Methyl oleuropein aglycon	24.349 ± 0.516	3.562
Methyl D-oleuropein aglycon	2.903 ± 0.079	0.425
Ligstroside aglycon	16.261 ± 0.709	2.379
Decarboxymethyl ligstroside aglycon	53.652 ± 0.354	7.849
Hydroxy D-ligstroside aglycon	8.087 ± 0.353	1.183
Lignans	1.587 ± 0.061	0.232
Pinoresinol	0.815 ± 0.032	0.119
Syringaresinol	0.772 ± 0.029	0.113
Flavones	4.852 ± 0.084	0.710
Luteolin	4.041 ± 0.065	0.591
Apigenin	0.811 ± 0.040	0.119
Total phenolic contents	683.579 ± 4.169	100.000

Value = $X \pm$ standard deviation (SD). Percent distribution of identified phenolic compounds.

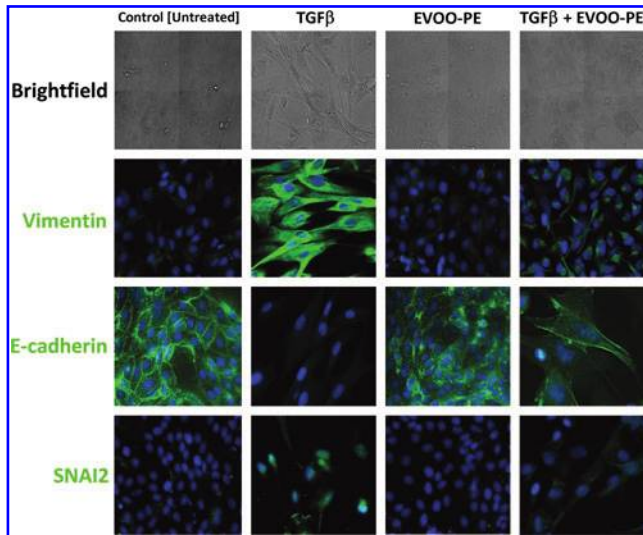


FIG. 2. Effects of extra virgin olive oil (EVOO) phenolics on transforming growth factor- β (TGF- β -induced changes in the morphology and expression of epithelial/mesenchymal markers of Madin–Darby canine kidney (MDCK) cells. MDCK cells were grown until 80% confluence, serum-starved for 24 hr, and then treated for 3 days with a minimal amount (0.1%) of fetal bovine serum (FBS) supplemented with vehicle (control [untreated]), TGF- β 1 alone (10 ng/mL), extra virgin olive oil phenolic extract (EVOO-PE) alone (200 ng/mL), or TGF- β 1 plus EVOO-PE. Phase-contrast and immunofluorescence images were obtained and merged on a BD Pathway™ 855 Bioimager System according to the recommended assay procedure using BD Attovision™ software. Images show representative portions of MDCK cultures showing subcellular distribution of vimentin, E-cadherin, and SNAI2 from two to three independent experiments.

EVOO-derived crude phenolic extract significantly prevented TGF- β 1-induced disintegration of E-cadherin at cell–cell contacts. Moreover, EVOO phenolics largely prevented the strong activation of the post-EMT marker vimentin that occurred upon treatment with TGF- β 1. We finally evaluated whether the EVOO-derived crude phenolic extract could impact the expression of EMT-promoting transcription factors such as SNAI2 (Slug), which not only functions as a bona fide epithelial repressor that inhibits *E-cadherin* gene expression through its direct binding to E-boxes within the *E-cadherin* promoter but also interacts with mesenchymal activators such as β -catenin to induce vimentin expression.³⁴ Likewise, SNAI2 protein was significantly upregulated during TGF- β 1-driven mesenchymal conversion of MDCK cells. Of note, the EVOO-derived crude phenolic extract negatively regulated nuclear accumulation of SNAI2 in response to TGF- β 1.

EVOO phenolics impede “oncogenic EMT”

We first confirmed that cellular changes (morphology and size) observed in MCF-7 breast cancer epithelial cells supplemented exogenously with TGF- β 1 resembled those of tumor cells undergoing EMT. Immunoreactivity of the epithelial cell marker E-cadherin was likewise found at sites of cell–cell contact in untreated MCF-7 control cells. This classical expression of E-cadherin in the basolateral membrane of epitheloid cells was significantly altered upon exposure to the

EMT promoter TGF- β 1, which promoted a drastic distribution of E-cadherin from a conspicuous, highly membranous staining to a more diffuse, barely detectable staining in the cytoplasm (Fig. 3). The EVOO-derived crude phenolic extract as sole treatment appeared to significantly accumulate E-cadherin protein expression at sites of cell–cell contact, thus promoting a more cuboidal appearance of MCF-7 cell cultures, which grew in more compact, homogeneously structured monolayers. Of note, TGF- β 1 failed to downregulate membranous E-cadherin when MCF-7 epithelial breast cancer cells were concurrently co-exposed to EVOO phenolics.

To make a preliminary evaluation of whether EVOO phenolics negatively impacted formation and activation of EMT-promoting SMAD complexes (*i.e.*, SMAD proteins [intracellular transcription factors and transducers of TGF- β signaling] have low affinity for DNA and need to interact and form a complex with EMT-promoting transcription factors, including SNAI1 and ZEB, to target the gene promoter of E-cadherin during TGF- β -driven EMT in breast epithelial cells), we employed immunofluorescence microscopy to monitor the expression status of SMAD4, SNAI2, and E-cadherin proteins of MCF-7 epithelial cells cultured with TGF- β 1 in the absence or presence of EVOO phenolics (Fig. 4). TGF- β 1 treatment of MCF-7 cells for 72 hr resulted in enhanced expression of SMAD4 and SNAI2, which paralleled loss of E-cadherin at intercellular junctions. The EVOO-derived crude phenolic extract significantly prevented the ability of TGF- β to upregulate SMAD4 and SNAI2.

EVOO phenolics prevent TGF- β 1-induced activation of the EMT transcriptional program

Finally, we decided to explore whether EVOO phenolics actively regulated a programmed series of genes events controlling TGF- β 1-induced EMT, as suggested by the immunofluorescence studies. Total RNA from untreated MCF-7 control cells and MCF-7 cells treated with TGF- β 1, EVOO phenolics, or TGF- β 1 plus EVOO phenolics were evaluated using qRT-PCR of genes specifically associated with EMT and the reciprocal mesenchymal-to-epithelial transition (MET) (Fig. 5). When a three-fold or greater difference in mRNA expression levels was used as the cutoff to determine significant regulatory effects on genes involved in the EMT genetic program, TGF- β 1 treatment was found to significantly upregulate a total of 11 of the 84 EMT gene regulators assessed in the experiment. MCF-7 cells treated with TGF- β 1 for 72 hr transcriptionally enhanced the expression of developmental EMT genes that have been repeatedly demonstrated to play pivotal roles in malignant progression, including *SNAI2* and *TCF4* (approximately four-fold increases).^{59,60} Accordingly, MCF-7/TGF- β 1 cells notably increased the expression of plasminogen activator inhibitor type-1 (*PAI-1*; *SERPINE1*), a prominent member of the subset of TGF- β -initiated EMT-related signaling events,^{61,62} and the mesenchymal markers vimentin (*VIM*; ~4-fold) and fibronectin (*FN*; ~4-fold). Supporting the notion that EVOO phenolics appear to negatively regulate oncogenic EMT, co-treatment of MCF-7 cells with the EVOO-derived crude phenolic extract efficiently prevented the occurrence of most of TGF- β 1-induced EMT transcriptional events, including up-regulation of *SNAI2*, *TCF4*, *VIM*, and *FN*. TGF- β 1-induced accumulation of *SERPINE1* decreased from ~15 times in the absence of EVOO phenolics to ~4 times in

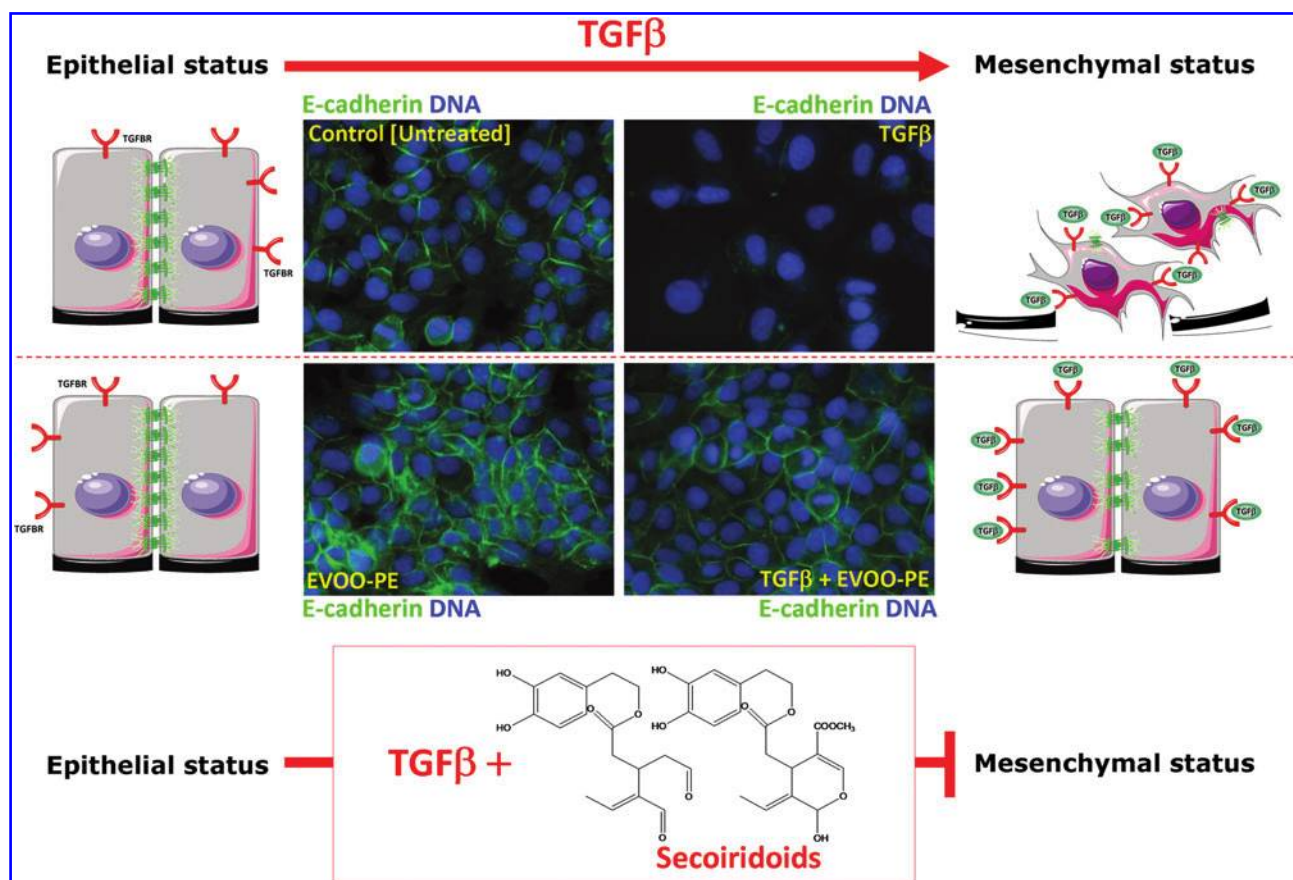


FIG. 3. Effect of extra virgin olive oil (EVOO) phenolics on distribution of the epithelial marker E-cadherin in MCF-7 cells. Subcellular distribution of E-cadherin was evaluated by indirect immunofluorescence in MCF-7 cells grown until 80% confluence, serum-starved for 24 hr, and then treated for 3 days with a minimal amount (0.1%) of fetal bovine serum (FBS) supplemented with vehicle (control [untreated]), transforming growth factor- β 1 (TGF- β 1) alone (10 ng/mL), EVOO phenolic extract (EVOO-PE) alone (200 ng/mL), or TGF- β 1 plus EVOO-PE. Images show representative portions ($n=3$) of MCF-7 cell cultures treated as specified for 3 days and captured in different channels for E-cadherin (green) and DNA (blue) on a BD Pathway™ 855 Bioimager System. The figure also shows a schematic summarizing EVOO phenolics' preventative activity against TGF- β -promoted downregulation or complete loss of the metastasis suppressor protein E-cadherin. Secoiridoids-targeted E-cadherin expression could efficiently prevent TGF- β -induced conversion of epithelial into migratory mesenchymal cells and may thus be a useful strategy to impede formation of migratory cancer stem cells (CSCs).

their presence. Regardless the presence of the EMT inducer TGF- β 1, the EVOO-derived crude phenolic extract significantly decreased by ~ 4 -fold the baseline expression of the mesenchymal marker osteopontin (*SPP1*, secreted phosphoprotein 1)^{63–65} independently of the presence of TGF- β 1.

Discussion

EVOO, the juice of the olive obtained solely by pressing and consumed without any further refining process, is unique among other vegetable oils because of its high level of naturally occurring phenolic compounds. Here, we have tested the hypothesis that prevention of TGF- β -induced EMT may represent a previously unrecognized mechanism through which phenolic molecules naturally occurring in EVOO might actively regulate the pathophysiology of many age-related human diseases, including end-state organ failures, due to excessive EMT-related fibrosis and cancer metastasis, given that the EMT genetic program is sufficient to

generate migrating CSCs by directly linking the acquisition of cellular motility with the maintenance and enhancement of tumor-initiating capacity.

Using canine MDCK kidney cells and human MCF-7 breast cancer cells, we directly evaluated the impact of a crude EVOO phenolic extract on several TGF- β -altered EMT parameters, including cell morphology and expression levels of epithelial and mesenchymal markers. EVOO phenolics significantly reduced TGF- β 1-induced cell scattering and TGF- β 1-increased intercellular spaces in MDCK cell cultures. The inhibitory effects of EVOO phenolics on TGF- β 1-induced conversion of MDCK epithelial cells to the spindle-like mesenchymal morphology was accompanied by a significant prevention of the cytoplasmic accumulation of the mesenchymal marker vimentin occurring in the TGF- β 1-induced mesenchymal state of MDCK cells. Perhaps more importantly, treatment with EVOO phenolics notably prevented the occurrence of hallmarks of TGF- β -induced acquisition of the mesenchymal phenotype, including the ability of TGF- β to

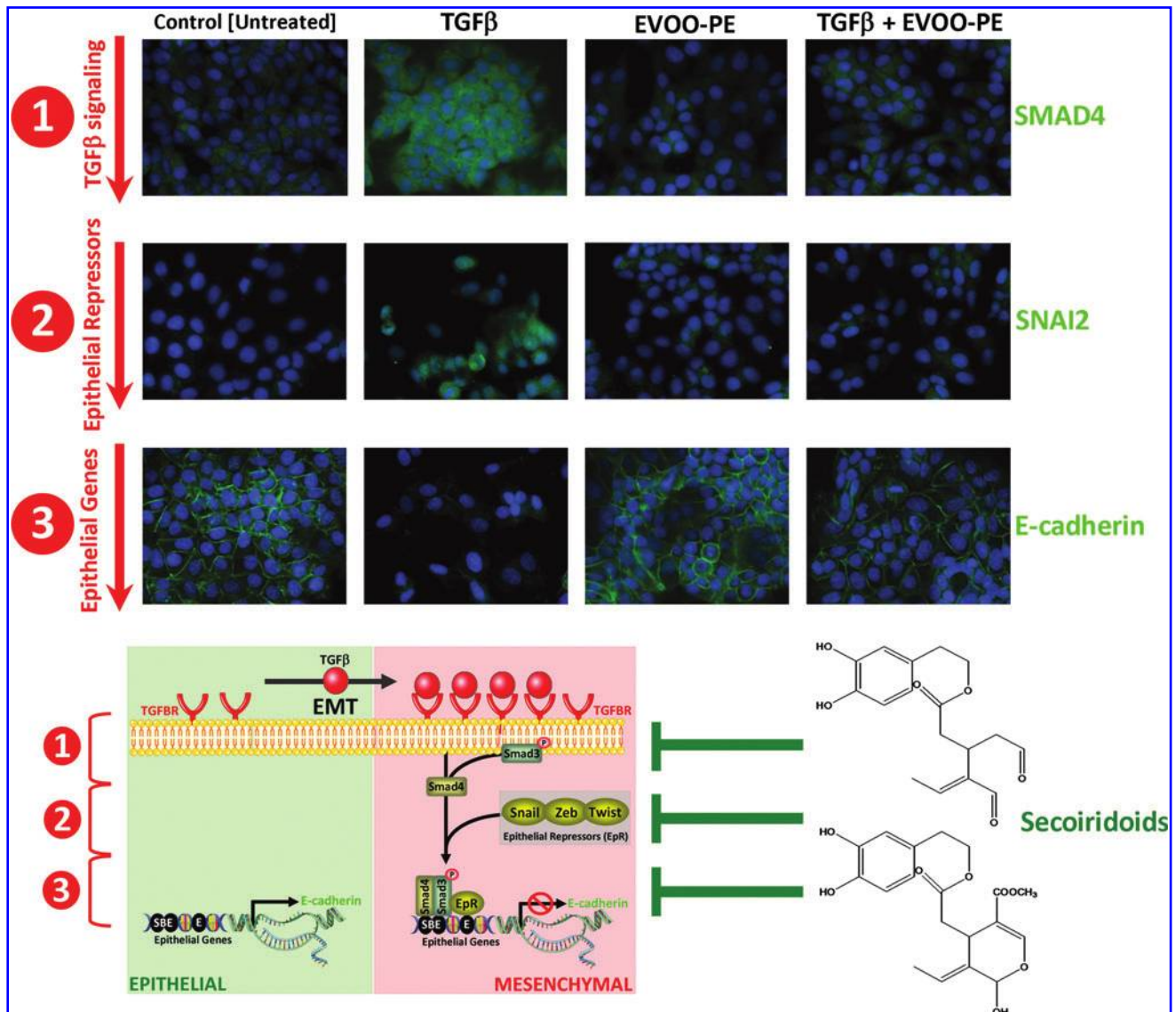


FIG. 4. Effects of extra virgin olive oil (EVOO) phenolics in transforming growth factor- β -regulated epithelial-to-mesenchymal transition (EMT) signaling cascade. Subcellular distribution of SMAD4, SNAI2, and E-cadherin was evaluated strictly in parallel by indirect immunofluorescence in MCF-7 cells grown until 80% confluence, serum-starved for 24 hr, and then treated for 3 days with a minimal amount (0.1%) of fetal bovine serum (FBS) supplemented with vehicle (control [untreated]), transforming growth factor- β 1 (TGF- β 1) alone (10 ng/mL), EVOO-phenolic extract (EVOO-PE) alone (200 ng/mL), or TGF- β 1 plus EVOO-PE. Images show representative portions ($n = 3$) of MCF-7 cell cultures treated as specified for 3 days and captured in different channels for E-cadherin (green) and DNA (blue) on a BD Pathway™ 855 Bioimager System. This figure also shows a schematic summarizing EVOO phenolics' preventative activity against TGF- β -driven EMT (1: Input layer [ligand/receptor/adaptors]; 2: Signal-processing layer [signaling cascade/transcription factors]; 3: Output layer [epithelial/mesenchymal markers]. TGF- β binding to its receptor (TGFBR) results in activation and nuclear translocation of SMAD transcription factors (e.g., SMAD4), which achieve target gene (e.g., E-cadherin) specificity through interaction with transcriptional cofactors (e.g., SNAI2). Epithelial-to-mesenchymal transition (EMT)-promoting transcription factors, including epithelial repressors such as SNAILs, ZEB, or TWIST, interact with SMADs, thus resulting in the formation of EMT-promoting SMAD complexes that can drive EMT by repressing epithelial genes such as E-cadherin. E, E-boxes; SBE, SMAD-binding elements.

cause loss of plasma membrane staining for E-cadherin and its ability to enhance cytoplasmic punctate and diffuse vesicle E-cadherin staining. Disintegration of cell-cell contacts (tight junctions, adherens junctions, and desmosomes) is a key feature of EMT.

More importantly, several lines of evidence have also substantiated that cell-cell contacts are not passive targets but

they are active regulators of EMT. Loss of the adherens junctions' component E-cadherin is well established to promote EMT in developmental biology and tumor models, whereas forced expression of E-cadherin can restore (noninvasive) epithelial phenotypes in (invasive) mesenchymal tumor cells. In terms of "fibrotic EMT," E-cadherin has been shown to play a central role in the EMT of renal tubular cells. In terms of

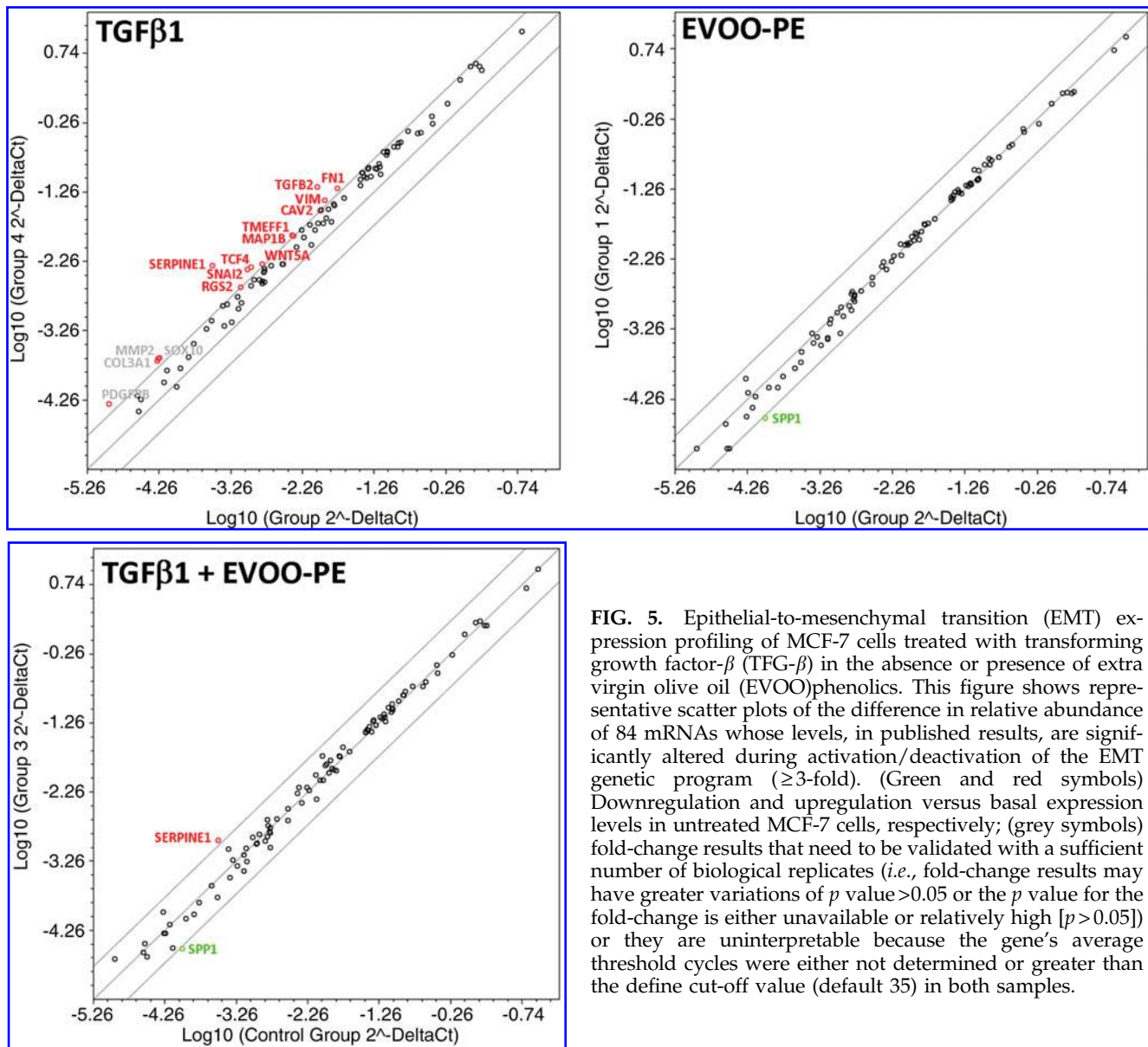


FIG. 5. Epithelial-to-mesenchymal transition (EMT) expression profiling of MCF-7 cells treated with transforming growth factor- β (TGF- β) in the absence or presence of extra virgin olive oil (EVOO) phenolics. This figure shows representative scatter plots of the difference in relative abundance of 84 mRNAs whose levels, in published results, are significantly altered during activation/deactivation of the EMT genetic program (≥ 3 -fold). (Green and red symbols) Downregulation and upregulation versus basal expression levels in untreated MCF-7 cells, respectively; (grey symbols) fold-change results that need to be validated with a sufficient number of biological replicates (*i.e.*, fold-change results may have greater variations of p value > 0.05 or the p value for the fold-change is either unavailable or relatively high [$p > 0.05$]) or they are uninterpretable because the gene's average threshold cycles were either not determined or greater than the define cut-off value (default 35) in both samples.

“oncogenic EMT,” activation of EMT in response to short hairpin (sh)RNA-mediated knockdown of E-cadherin expression has been shown to increase the tumorigenic CD44^{high}/CD24^{low} mesenchymal population in transformed breast cancer cells. Indeed, combined immunohistochemical staining of positive (*e.g.*, SNAIL) and negative (*e.g.*, E-cadherin) EMT markers together with SMAD3/4 has been proven to be an efficient approach to identify CSC-like EMT phenotypic cells in samples of invasive human ductal breast carcinomas.³⁴ In these studies, loss of E-cadherin at intercellular junctions significantly correlated with nuclear expression of SNAIL and SMAD3/4 at invasive regions, thus supporting a role for SNAIL-SMAD3/4 complexes in the repression of junction proteins during breast cancer cell invasion. In our hands, TGF- β treatment of MCF-7 breast epithelial cancer cells *in vitro* notably recapitulated the ability of EMT to promote ontogenesis of the breast cancer stem cell molecular signature *in vivo* because TGF- β -promoted loss of

E-cadherin took place upon activation of critical mediators of TGF β signaling, such as SMAD4, and epithelial repressors, such as the SMAD transcriptional cofactor SNAIL2. Remarkably, EVOO phenolics largely nullified upstream activation of TGF- β signaling to impede downstream formation of EMT-promoting SMAD repressor complexes. By weakening the ability of TGF- β to fully induce mesenchymal cell states, our current findings illustrate for the first time that the anti-EMT activity *in vitro* of EVOO phenolics might translate into antifibrotic and anti-CSCs *in vivo*.

From a mechanistic perspective, and considering that EVOO phenolics remarkably repressed the ability of TGF- β ability to transcriptionally reprogram MCF-7 breast cancer epithelial cells to express pivotal drivers and effectors of the EMT genetic program including *SNAIL2*, *TCF4*, *VIM*, and *FN*, whereas they failed to fully prevent TGF- β -induced EMT, as determined by cellular morphology in MDCK cells, it might be reasonable to suggest that EVOO phenolics efficiently



impede an important subset of TGF- β -regulated EMT changes but fail to complete the EMT reversal program (*i.e.*, MET). This scenario agrees with the hypothesis that reversal of EMT not only requires re-establishment of epithelial gene transcription but further a regain of structural components of the epithelial cytoskeleton.⁶⁶

Our current description of a significant anti-EMT activity of EVOO phenolics supports and expands further earlier studies showing that the green tea polyphenol epigallocatechin-3 gallate (EGCG) can significantly reduce the invasive breast cancer phenotype by upregulating the epithelial marker E-cadherin while downregulating the proinvasive *SNAIL* gene.^{67,68} Indeed, the common ability of a naturally occurring complex polyphenols to alter the expression of key regulators in the EMT pathway may suggest that they share an identical target that activation/deactivation prevents or reverses TGF- β -driven EMT. Activation of the energy sensor adenosine monophosphate-activated protein kinase (AMPK) is a plausible mechanism through which polyphenolic phytochemicals may reduce the ability of TGF- β to activate and maintain the mesenchymal molecular signature. On the one hand, AMPK activation has been shown to abrogate TGF- β -induced SMAD3-dependent transcription in cultured human primary mesangial cells and adult mouse cardiac fibroblasts.^{69,70} On the other hand, naturally occurring polyphenols such as EGCG significantly induce increases in the phosphorylation status of AMPK and in AMPK activity.^{71–73} If EVOO complex polyphenols behave molecularly in an EGCG-like manner, it might be tempting to suggest that, by acting as AMPK agonists, they can blunt TGF- β -activated EMT-related events (*e.g.*, phosphorylation of signal transducer and activator of transcription 3 [STAT3], which upregulates expression of several factors important for EMT induction).^{74–76} Another plausible mechanism through which EVOO phenolics might inhibit EMT and reactivate an epithelial phenotype might relate to their ability to molecularly mimic the anti-EMT effects of the polyphenol resveratrol, which has recently been found to inhibit the expression of *SNAIL*, *SLUG*, and *ZEB1* in pancreatic CSCs.⁷⁷

Although it remains to be elucidated whether a resveratrol-like up-regulation of silent information regulator T1 (SIRT1) deacetylase activity may counterintuitively regulate EVOO phenolics-induced enhancement and/or maintenance of epithelial versus mesenchymal phenotypes (*i.e.*, inhibition of SIRT1 increases acetylation of histone H3 at the E-cadherin gene promoter, thus increasing E-cadherin expression,⁷⁸ whereas activation of SIRT1 reverses acetylation of SMAD3, thus inhibiting TGF- β -induced renal fibrosis),^{79,80} it should be noted that the dietary bioflavonoid quercetin also inhibits the expression of EMT markers (*e.g.*, vimentin) as well as the transcription factors *SNAIL* and *SLUG* to inhibit CSC characteristics, including invasion, migration, and self-renewal.^{81,82} Polyphenolic phytochemicals, therefore, could all cause inhibition of fibrogenic and oncogenic EMT-driven phenomena. It is noteworthy that all of them had been reported to be either inhibitors of the mitochondrial respiratory chain or inhibitors of the mitochondrial adenosine triphosphate (ATP) synthesis, thus suggesting the hypothesis that these compounds can inhibit mitochondrial ATP production and therefore activate AMPK by increasing the intracellular AMP/ATP ratio.^{83–85} In addition, numerous lines of evidence suggest that most dietary polyphenols, including EGCG, resveratrol, and

EVOO phenolics, have the capacity to mitigate cellular damage induced via metabolic production of reactive oxygen species (ROS) by mitochondrial complex I.^{86–90} Given that complex I can control the nicotinamide adenine dinucleotide (NAD⁺)-to-NADH ratio, thus allowing the activation of SIRT1,⁹¹ it might tempting to suggest that EVOO phenolics-targeted functioning of mitochondrial complex I might connect the master energy regulatory proteins AMPK (which senses the AMP/ATP ratio) and sirtuins (which require NAD to deacetylate protein substrates) molecularly. In this regard, it has been recently demonstrated that AMPK and SIRT1 can be connected in a linear pathway because AMPK activation upregulates the gene encoding the NAD synthetic enzyme Nampt, thus providing the crucial link to the downstream activation of SIRT1.^{92–94}

We should express caution, however, when interpreting *in vitro* data to actual actions of EVOO polyphenols in the body, especially if no data have been collected regarding the action of physiological metabolites of tested EVOO polyphenols on the same cell systems. To produce their beneficial effects, other than on the gastrointestinal (GI) tract itself, EVOO polyphenols must be absorbed into the body after oral ingestion and be carried by the bloodstream from the absorption site to target tissues and organs. Obviously, our *in vitro* assays do not take into account the *in vivo* bioavailability issue and can lead to false-positive interpretations (*i.e.*, the *in vitro* active compound within the EVOO phenolic extract is quickly metabolized or has limited bioavailability to the target organ). Thus, if there is no evidence for the absorption of a particular EVOO polyphenol (*e.g.*, oleuropein aglycon, decarboxymethyl oleuropein aglycon), it could make no biological sense to gain mechanistical insights (*e.g.*, anti-EMT effects) by exposing it to cultured cells obtained from the kidney and/or the breast. We should acknowledge that, similar to most pharmaceuticals, the body will treat consumed EVOO polyphenols as xenobiotics, or foreign substances, and EVOO polyphenols will be therefore subjected to the same protective xenobiotic-metabolizing and efflux mechanisms, which result not only in major changes in biological activity but also in increased rates of excretion from the body.^{95–97} Because parental EVOO polyphenols contain suitable functional groups (*e.g.*, hydroxyl groups), they can undergo conjugation reactions with endogenous compounds to yield more polar and water-soluble derivatives. The principal conjugation reaction is the formation of β -glucuronides catalyzed by uridine diphosphoglucuronosyl transferases (UGTs), but conjugation with a sulfo moiety or glutathione catalyzed by sulfotransferases (SULTs) and glutathione-S-transferases, respectively, also occurs. Less-polar conjugates may also be formed by methylation, catalyzed by catechol-O-methyltransferase (COMT).

Although absorption and bioavailability studies have revealed that single phenols tyrosol and hydroxytyrosol can be retrieved in plasma and urine after OO consumption,⁹⁸ there is an urgent need for data regarding the plasma/urine concentration of the free forms of various secoiridoid aglycones. For instance, after ingestion of flavonoids, conjugates of the aglycon, such as glucuronides, sulfates, and methylated metabolites, have been found to predominate in the blood circulation rather than the original plant glycoside or aglycon.⁹⁹ Indeed, all of the conjugation mechanisms are highly efficient, and free aglycones are either absent or present in low concentrations in plasma after consumption of nutritional doses. Because in studies with green tea polyphenols, the metabolites mostly had reduced biological activity, it might be tempting to suggest that limited



bioavailability of EVOO complex polyphenols and their conversion into less-active metabolites (e.g., glucuronidated or sulfated forms) could negatively affect an anti-EMT effect, if any, *in vivo*. In some systems, however, polyphenols-derived metabolites were found to have the equivalent or even greater activity than the parental polyphenols.¹⁰⁰ Thus, whereas some studies have suggested that methylations can increase the bioavailability of polyphenols, other studies have indicated a decrease in the anticancer benefits of methylated polyphenols.¹⁰¹

Kinetics of penetration and elimination of EVOO polyphenols in tissues is largely unknown and data on actual bioavailability are scarce, thus it is plausible that cellular metabolites may differ from those obtained in plasma. Whether EVOO polyphenols could accumulate in specific organs remains to be ascertained, and the presence of cellular-specific mechanisms to incorporate polyphenols is still highly controversial.^{102–105} Recently, we employed a nano liquid chromatography–electrospray ionization–time-of-flight mass spectrometry (nanoLC-ESI-TOF MS) method to evaluate both the cellular uptake and the metabolism of EVOO phenolics in human breast carcinomas cells highly sensitive to the growth inhibitory effects of secoiridoid-rich EVOO phenolic extracts (Rocío García-Villalba, Alegría Carrasco-Pancorbo, Javier A. Menéndez, Antonio Segura-Carretero, Alberto Fernández-Gutiérrez, submitted manuscript). Most of free EVOO phenolics disappeared from the culture medium (*i.e.*, the extracellular milieu) in different extents and at different times according to the type of phenolic we tested. When the time course of cellular uptake of parental phenolics was expressed as percent of the quantity originally supplemented in culture medium, we concluded that, as early as 15 min, oleuropein aglycone and decarboxymethyl oleuropein aglycon were rapidly incorporated into the cell. Secoiridoids were also the phenolic group most extensively metabolized, and methylation was the preferential pathway for conjugation of oleuropein aglycone and decarboxymethyl oleuropein aglycon, which was followed or preceded, in some cases, by hydrogenation reactions. We observed extremely low intracellular accumulations of parental secoiridoids, with only traces of some compounds being detected in the cytoplasm and membranous structures. In addition, the amounts of methylated forms increased with time strictly in parallel with the disappearance of parental secoiridoids in the extracellular milieu, a process that reached a maximum after 2 hr of incubation, thus suggesting a crucial role for COMT at metabolizing EVOO polyphenols at target tissues such as breast carcinomas.

These findings might be crucial when designing synergy strategies aimed to improve the bioavailability and hence bioactivity of EVOO polyphenols.^{95,96,106} First, because metabolism of dietary polyphenols by gut bacteria constitutes a significant barrier to their bioavailability, modulation of intestinal microflora population can be modulated by antibiotics or other natural products (e.g., catechins).¹⁰⁷ Second, efflux transporter inhibitors and metabolism enzyme modulators can significantly affect phenolic absorption and metabolism, which consequently can improve their bioavailabilities. Third, pharmacological inhibition of glucuronidation using piperine^{108,109} can be expected to increase bioavailability of EVOO phenolics. *In vivo* studies have revealed that curcumin bioavailability can be drastically increased in human volunteers (up to 2000%) when curcumin is administered together with piperine.¹¹⁰ Piperine has been found to also increase the bio-

availability of green tea polyphenols in mice.¹¹¹ Recently, Johnson et al.¹¹² examined the hypothesis that piperine will enhance the pharmacokinetic parameters of resveratrol via inhibiting its glucuronidation, thereby slowing its rapid metabolism and elimination. By using animal models, the degree of exposure to resveratrol was enhanced to 229% and the maximum serum concentration was increased to 1544% with the addition of piperine.¹¹² Fourth, several nutraceuticals, including curcumin, green tea polyphenols, coenzyme Q, quercetin, and others, have been packaged as nanoparticles and proven to be useful in “nanochemoprevention” and “nanochemotherapy.”¹¹³ Efforts are currently underway in our laboratories to develop biocompatible, biodegradable, and nontoxic nano-size liposomal formulations that offer the possibility of carrying and delivering EVOO polyphenols in the prevention or treatment of several pathological conditions.

In summary, excessive fibrosis due to a sustained and unresolved EMT occurs in many age-related human diseases, including heart failure, sclerosis, nonalcoholic steatohepatitis, and progressive renal fibrosis. CSCs generated from EMT induction provide a resource for cancer to recur and metastasize because EMT-phenotypic tumor cells acquire stem-like increased metastatic capacity and self-renewal ability. Our current findings reveal for the first time that naturally occurring phenolics in EVOO efficiently impede EMT, the common link in the life-threatening progression of organ fibrosis and cancer toward organ failure and metastasis, respectively. Forthcoming studies should definitely establish whether, by targeting mitochondrial complex I, EVOO-derived complex polyphenols such as secoiridoids can mimic an energy limitation situation that enhances the net effect of ATP and NAD to activate AMPK and SIRT1 and lastly restrain the EMT differentiation process.

Because poor *in vivo* bioavailability of EVOO phenolics is being considered a major obstacle in translating in humans their multitude of health-promoting properties found in preclinical studies, future studies should focus on how to increase the bioavailabilities of EVOO so we can rapidly accelerate the development of this class of compounds into effective chemopreventing, anticancer, and/or antiaging agents.^{53,54,56,114–118} Nevertheless, *Oleaceae* secoiridoids, such as oleuropein aglycone and decarboxymethyl oleuropein aglycon, certainly merit consideration for longevity studies and, perhaps, for ulterior design of more pharmacologically active second-generation anti-EMT molecules.

Acknowledgments

Work at the laboratory of Javier A. Menendez is supported by the Instituto de Salud Carlos III (Ministerio de Sanidad y Consumo, Fondo de Investigación Sanitaria [FIS], Spain, grants CP05-00090 and PI06-0778 and RD06-0020-0028), the Fundación Científica de la Asociación Española Contra el Cáncer (AECC, Spain), and by the Ministerio de Ciencia e Innovación (SAF2009-11579, Plan Nacional de I+D+I, MICINN, Spain). Alejandro Vazquez-Martin is the recipient of a “Sara Borrell” postdoctoral contract (CD08/00283, Ministerio de Sanidad y Consumo, Fondo de Investigación Sanitaria [FIS], Spain). Sílvia Cufí is the recipient of a Research Fellowship (Formación de Personal Investigador [FPI]) by the Ministerio de Ciencia e Innovación (MICINN, Spain).



References

1. Moustakas A, Heldin CH. Signaling networks guiding epithelial-mesenchymal transitions during embryogenesis and cancer progression. *Cancer Sci* 2007;98:1512–1520.
2. Thiery JP, Acloque H, Huang RY, Nieto MA. Epithelial-mesenchymal transitions in development and disease. *Cell* 2009;139:871–890.
3. Kalluri R, Weinberg RA. The basics of epithelial-mesenchymal transition. *J Clin Invest* 2009;119:1420–1428.
4. Blagosklonny MV. Validation of anti-aging drugs by treating age-related diseases. *Aging (Albany NY)* 2009;1:281–288.
5. Stahl PJ, Felsen D. Transforming growth factor-beta, basement membrane and epithelial-mesenchymal transdifferentiation: implications for fibrosis in kidney disease. *Am J Pathol* 2001;159:1187–1192.
6. Iwano M, Plieth D, Danoff TM, Xue C, Okada H, Neilson EG. Evidence that fibroblasts derive from epithelium during tissue fibrosis. *J Clin Invest* 2002;110:341–350.
7. Zeisberg M, Yang C, Martino M, Duncan MB, Rieder F, Tanjore H, Kalluri R. Fibroblasts derive from hepatocytes in liver fibrosis via epithelial to mesenchymal transition. *J Biol Chem* 2007;282:23337–23347.
8. Syn WK, Jung Y, Omenetti A, Abdelmalek M, Guy CD, Yang L, Wang J, Witek RP, Fearing CM, Pereira TA, Teaberry V, Choi SS, Conde-Vancells J, Karaca GF, Diehl AM. Hedgehog-mediated epithelial-to-mesenchymal transition and fibrogenic repair in nonalcoholic fatty liver disease. *Gastroenterology* 2009;137:1478–1488.e8
9. Sato M, Muragaki Y, Saika S, Roberts AB, Ooshima A. Targeted disruption of TGF-beta1/Smad3 signaling protects against renal tubulointerstitial fibrosis induced by unilateral ureteral obstruction. *J Clin Invest* 2003;112:1486–1494.
10. Yeh YC, Wei WC, Wang YK, Lin SC, Sung JM, Tang MJ. Transforming growth factor-beta1 induces Smad3-dependent beta1 integrin gene expression in epithelial-to-mesenchymal transition during chronic tubulointerstitial fibrosis. *Am J Pathol* 2010;177:1743–1754.
11. Meindl-Beinker NM, Dooley S. Transforming growth factor-beta and hepatocyte transdifferentiation in liver fibrogenesis. *J Gastroenterol Hepatol* 2008;23(Suppl 1):S122–S127.
12. Ghosh AK, Bradham WS, Gleaves LA, De Taeye B, Murphy SB, Covington JW, Vaughan DE. Genetic deficiency of plasminogen activator inhibitor-1 promotes cardiac fibrosis in aged mice: involvement of constitutive transforming growth factor-beta signaling and endothelial-to-mesenchymal transition. *Circulation* 2010;122:1200–1209.
13. Wynn TA. Common and unique mechanisms regulate fibrosis in various fibroproliferative diseases. *J Clin Invest* 2007;117:524–549.
14. Bedi S, Vidyasagar A, Djamali A. Epithelial-to-mesenchymal transition and chronic allograft tubulointerstitial fibrosis. *Transplant Rev (Orlando)* 2008;22:1–5.
15. Djamali A, Samaniego M. Fibrogenesis in kidney transplantation: potential targets for prevention and therapy. *Transplantation* 2009;88:1149–1156.
16. Strutz F. Pathogenesis of tubulointerstitial fibrosis in chronic allograft dysfunction. *Clin Transplant* 2009;23(Suppl 21):26–32.
17. Aguilera A, Yáñez-Mo M, Selgas R, Sánchez-Madrid F, López-Cabrera M. Epithelial to mesenchymal transition as a triggering factor of peritoneal membrane fibrosis and angiogenesis in peritoneal dialysis patients. *Curr Opin Investig Drugs* 2005;6:262–268.
18. Selgas R, Bajo A, Jiménez-Heffernan JA, Sánchez-Tomero JA, Del Peso G, Aguilera A, López-Cabrera M. Epithelial-to-mesenchymal transition of the mesothelial cell—its role in the response of the peritoneum to dialysis. *Nephrol Dial Transplant* 2006;21(Suppl 2):ii2–ii7.
19. Aroeira LS, Aguilera A, Sánchez-Tomero JA, Bajo MA, del Peso G, Jiménez-Heffernan JA, Selgas R, López-Cabrera M. Epithelial to mesenchymal transition and peritoneal membrane failure in peritoneal dialysis patients: Pathologic significance and potential therapeutic interventions. *J Am Soc Nephrol* 2007;18:2004–2013.
20. Li C, Yang CW. The pathogenesis and treatment of chronic allograft nephropathy. *Nat Rev Nephrol* 2009;5:513–519.
21. Brabletz T, Jung A, Spaderna S, Hlubek F, Kirchner T. Opinion: migrating cancer stem cells - an integrated concept of malignant tumour progression. *Nat Rev Cancer* 2005;5:744–749.
22. Lee JM, Dedhar S, Kalluri R, Thompson EW. The epithelial-mesenchymal transition: New insights in signaling, development, and disease. *J Cell Biol* 2006;172:973–981.
23. Christiansen JJ, Rajasekaran AK. Reassessing epithelial to mesenchymal transition as a prerequisite for carcinoma invasion and metastasis. *Cancer Res* 2006;66:8319–8326.
24. Moustakas A, Heldin CH. Signaling networks guiding epithelial-mesenchymal transitions during embryogenesis and cancer progression. *Cancer Sci* 2007;98:1512–1520.
25. Guarino M, Rubino B, Ballabio G. The role of epithelial-mesenchymal transition in cancer pathology. *Pathology* 2007;39:305–318.
26. Mani SA, Guo W, Liao MJ, Eaton EN, Ayyanan A, Zhou AY, Brooks M, Reinhard F, Zhang CC, Shipitsin M, Campbell LL, Polyak K, Brisken C, Yang J, Weinberg RA. The epithelial-mesenchymal transition generates cells with properties of stem cells. *Cell* 2008;133:704–715.
27. Hollier BG, Evans K, Mani SA. The epithelial-to-mesenchymal transition and cancer stem cells: a coalition against cancer therapies. *J Mammary Gland Biol Neoplasia* 2009;14:29–43.
28. Singh A, Settleman J. EMT, cancer stem cells and drug resistance: an emerging axis of evil in the war on cancer. *Oncogene* 2010;29:4741–4751.
29. May CD, Sphyris N, Evans KW, Werden SJ, Guo W, Mani SA. Epithelial-mesenchymal transition and cancer stem cells: a dangerously dynamic duo in breast cancer progression. *Breast Cancer Res* 2011;13:202.
30. Kong D, Li Y, Wang Z, Sarkar FH. Cancer stem cells and epithelial-to-mesenchymal transition (EMT)-phenotypic cells: Are they cousin or twins? *Cancers* 2011;3:716–729.
31. Morel AP, Lièvre M, Thomas C, Hinkal G, Ansieau S, Puisieux A. Generation of breast cancer stem cells through epithelial-mesenchymal transition. *PLoS ONE* 2008;3:e2888.
32. Blick T, Hugo H, Widodo E, Waltham M, Pinto C, Mani SA, Weinberg RA, Neve RM, Lenburg ME, Thompson EW. Epithelial mesenchymal transition traits in human breast cancer cell lines parallel the CD44(hi)/CD24 (lo/-) stem cell phenotype in human breast cancer. *J Mammary Gland Biol Neoplasia* 2010;15:235–252.
33. Caja L, Bertran E, Campbell J, Fausto N, Fabregat I. The transforming growth factor-beta (TGF-beta) mediates acquisition of a mesenchymal stem cell-like phenotype in human liver cells. *J Cell Physiol* 2011;226:1214–1223.
34. Fuxe J, Vincent T, de Herreros AG. Transcriptional cross-talk between TGFbeta and stem cell pathways in tumor cell invasion: Role of EMT promoting Smad complexes. *Cell Cycle* 2010;9:2363–2374.



35. Phinney DG. Twist, epithelial-to-mesenchymal transition, and stem cells. *Stem Cells* 2011;29:3–4.
36. Gupta PB, Onder TT, Jiang G, Tao K, Kuperwasser C, Weinberg RA, Lander ES. Identification of selective inhibitors of cancer stem cells by high-throughput screening. *Cell* 2009;138:645–659.
37. Wang Z, Li Y, Ahmad A, Azmi AS, Kong D, Banerjee S, Sarkar FH. Targeting miRNAs involved in cancer stem cell and EMT regulation: An emerging concept in overcoming drug resistance. *Drug Resist Updat* 2010;13:109–118.
38. Li Y, VandenBoom TG 2nd, Kong D, Wang Z, Ali S, Philip PA, Sarkar FH. Up-regulation of miR-200 and let-7 by natural agents leads to the reversal of epithelial-to-mesenchymal transition in gemcitabine-resistant pancreatic cancer cells. *Cancer Res* 2009;69:6704–6712.
39. López-Novoa JM, Nieto MA. Inflammation and EMT: An alliance towards organ fibrosis and cancer progression. *EMBO Mol Med* 2009;1:303–314.
40. Anisimov VN, Zabezhinski MA, Popovich IG, Piskunova TS, Semchenko AV, Tyndyk ML, Yurova MN, Antoch MP, Blagosklonny MV. Rapamycin extends maximal lifespan in cancer-prone mice. *Am J Pathol* 2010;176:2092–2097.
41. Blagosklonny MV. Revisiting the antagonistic pleiotropy theory of aging: TOR-driven program and quasi-program. *Cell Cycle* 2010;9:3151–3156.
42. Blagosklonny MV. Rapamycin and quasi-programmed aging: Four years later. *Cell Cycle* 2010; 9:1859–1862.
43. Aguilera A, Aroeira LS, Ramirez-Huesca M, Perez-Lozano ML, Cirugeda A, Bajo MA, Del Peso G, Valenzuela-Fernandez A, Sanchez-Tomero JA, Lopez-Cabrera M, Selgas R. Effects of rapamycin on the epithelial-to-mesenchymal transition of human peritoneal mesothelial cells. *Int J Artif Organs* 2005;28:164–169.
44. Lamouille S, Derynck R. Emergence of the phosphoinositide 3-kinase-Akt-mammalian target of rapamycin axis in transforming growth factor- β -induced epithelial-mesenchymal transition. *Cells Tissues Organs* 2011; 193:8–22.
45. Menendez JA, Cufí S, Oliveras-Ferraro C, Vellon L, Joven J, Vazquez-Martin A. Gerosuppressant Metformin: Less is more. *Aging (Albany NY)* 2011;4:348–362.
46. Cufí S, Vazquez-Martin A, Oliveras-Ferraro C, Martin-Castillo B, Joven J, Menendez JA. Metformin against TGF β -induced epithelial-to-mesenchymal transition (EMT): From cancer stem cells to aging-associated fibrosis. *Cell Cycle* 2010;9:4461–4468.
47. Oliveras-Ferraro C, Cufí S, Vazquez-Martin A, Torres-Garcia VZ, Del Barco S, Martin-Castillo B, Menendez JA. Micro(mi)RNA expression profile of breast cancer epithelial cells treated with the anti-diabetic drug metformin: Induction of the tumor suppressor miRNA let-7a and suppression of the TGF β -induced oncomiR miRNA-181a. *Cell Cycle* 2011;10:1144–1151.
48. Vazquez-Martin A, Oliveras-Ferraro C, Cufí S, Del Barco S, Martin-Castillo B, Menendez JA. Metformin regulates breast cancer stem cell ontogeny by transcriptional regulation of the epithelial-mesenchymal transition (EMT) status. *Cell Cycle* 2010;9:3807–3814.
49. Vazquez-Martin A, Oliveras-Ferraro C, Del Barco S, Martin-Castillo B, Menendez JA. The anti-diabetic drug metformin suppresses self-renewal and proliferation of trastuzumab-resistant tumor-initiating breast cancer stem cells. *Breast Cancer Res Treat* 2011;126:355–364.
50. Vazquez-Martin A, Oliveras-Ferraro C, Cufí S, Martin-Castillo B, Menendez JA. Metformin and energy metabolism in breast cancer: from insulin physiology to tumour-initiating stem cells. *Curr Mol Med* 2010;10:674–691.
51. Jensen SR, Franzky H, Wallander E. Chemotaxonomy of the Oleaceae: Iridoids as taxonomic markers. *Phytochemistry* 2002;60:213–231.
52. Bendini A, Cerretani L, Carrasco-Pancorbo A, Gómez-Caravaca AM, Segura-Carretero A, Fernández-Gutiérrez A, Lercker G. Phenolic molecules in virgin olive oils: A survey of their sensory properties, health effects, antioxidant activity and analytical methods. An overview of the last decade. *Molecules* 2007;12:1679–1719.
53. Lozano-Sánchez J, Segura-Carretero A, Menendez JA, Oliveras-Ferraro C, Cerretani L, Fernández-Gutiérrez A. Prediction of extra virgin olive oil varieties through their phenolic profile. Potential cytotoxic activity against human breast cancer cells. *J Agric Food Chem* 2010;58:9942–9955.
54. García-Villalba R, Carrasco-Pancorbo A, Oliveras-Ferraro C, Vázquez-Martín A, Menéndez JA, Segura-Carretero A, Fernández-Gutiérrez A. Characterization and quantification of phenolic compounds of extra-virgin olive oils with anticancer properties by a rapid and resolutive LC-ESI-TOF MS method. *J Pharm Biomed Anal* 2010;51:416–429.
55. Oliveras-Ferraro C, Vazquez-Martin A, Martin-Castillo B, Cufí S, Del Barco S, Lopez-Bonet E, Brunet J, Menendez JA. Dynamic emergence of the mesenchymal CD44(pos)CD24(neg/low) phenotype in HER2-gene amplified breast cancer cells with de novo resistance to trastuzumab (Herceptin). *Biochem Biophys Res Commun* 2010;397:27–33.
56. Oliveras-Ferraro C, Fernández-Arroyo S, Vazquez-Martin A, Lozano-Sánchez J, Cufí S, Joven J, Micol V, Fernández-Gutiérrez A, Segura-Carretero A, Menendez JA. Crude phenolic extracts from extra virgin olive oil circumvent de novo breast cancer resistance to HER1/HER2-targeting drugs by inducing GADD45-sensed cellular stress, G2/M arrest and hyperacetylation of Histone H3. *Int J Oncol* 2011;38:1533–1547.
57. Singleton YL, Rossi JA. Colorimetry of total phenolics with phosphomolybdic-phosphotungstic acid reagents. *Am J Enol Vitic* 1965;16:144–158.
58. Fu SP, Segura-Carretero A, Arráez-Román D, Menéndez JA, De La Torre A, Fernández-Gutiérrez A. Tentative Characterization of Novel Phenolic Compounds in Extra Virgin Olive Oils by Rapid-Resolution Liquid Chromatography Coupled with Mass Spectrometry. *J Agric Food Chem* 2009;57:11140–11147.
59. Sobrado VR, Moreno-Bueno G, Cubillo E, Holt LJ, Nieto MA, Portillo F, Cano A. The class I bHLH factors E2-2A and E2-2B regulate EMT. *J Cell Sci* 2009;122:1014–1024.
60. Jayachandran A, Königshoff M, Yu H, Rupniewska E, Hecker M, Klepetko W, Seeger W, Eickelberg O. SNAI transcription factors mediate epithelial-mesenchymal transition in lung fibrosis. *Thorax* 2009;64:1053–1061.
61. Freytag J, Wilkins-Port CE, Higgins CE, Higgins SP, Samarakoon R, Higgins PJ. PAI-1 mediates the TGF- β 1 + EGF-induced “scatter” response in transformed human keratinocytes. *J Invest Dermatol* 2010;130:2179–2190.
62. Senoo T, Hattori N, Tanimoto T, Furonaka M, Ishikawa N, Fujitaka K, Haruta Y, Murai H, Yokoyama A, Kohno N. Suppression of plasminogen activator inhibitor-1 by RNA interference attenuates pulmonary fibrosis. *Thorax* 2010;65: 334–340.
63. Chagraoui J, Lepage-Noll A, Anjo A, Uzan G, Charbord P. Fetal liver stroma consists of cells in epithelial-to-mesenchymal transition. *Blood* 2003;101:2973–2982.



64. Saika S, Shirai K, Yamanaka O, Miyazaki K, Okada Y, Kitano A, Flanders KC, Kon S, Uede T, Kao WW, Rittling SR, Denhardt DT, Ohnishi Y. Loss of osteopontin perturbs the epithelial-mesenchymal transition in an injured mouse lens epithelium. *Lab Invest* 2007;87:130–138.
65. Rödder S, Scherer A, Raulf F, Berthier CC, Hertig A, Couzi L, Durrbach A, Rondeau E, Marti HP. Renal allografts with IF/TA display distinct expression profiles of metzincins and related genes. *Am J Transplant* 2009;9:517–526.
66. Das S, Becker BN, Hoffmann FM, Mertz JE. Complete reversal of epithelial to mesenchymal transition requires inhibition of both ZEB expression and the Rho pathway. *BMC Cell Biol* 2009;10:94.
67. Belguise K, Guo S, Sonenshein GE. Activation of FOXO3a by the green tea polyphenol epigallocatechin-3-gallate induces estrogen receptor alpha expression reversing invasive phenotype of breast cancer cells. *Cancer Res* 2007;67:5763–5770.
68. Belguise K, Guo S, Yang S, Rogers AE, Seldin DC, Sherr DH, Sonenshein GE. Green tea polyphenols reverse cooperation between c-Rel and CK2 that induces the aryl hydrocarbon receptor, slug, and an invasive phenotype. *Cancer Res* 2007;67:11742–11750.
69. Xiao H, Ma X, Feng W, Fu Y, Lu Z, Xu M, Shen Q, Zhu Y, Zhang Y. Metformin attenuates cardiac fibrosis by inhibiting the TGFbeta1-Smad3 signalling pathway. *Cardiovasc Res* 2010;87:504–513.
70. Mishra R, Cool BL, Laderoute KR, Foretz M, Violette B, Simonson MS. AMP-activated protein kinase inhibits transforming growth factor-beta-induced Smad3-dependent transcription and myofibroblast transdifferentiation. *J Biol Chem* 2008;283:10461–10469.
71. Collins QF, Liu HY, Pi J, Liu Z, Quon MJ, Cao W. Epigallocatechin-3-gallate (EGCG), a green tea polyphenol, suppresses hepatic gluconeogenesis through 5'-AMP-activated protein kinase. *J Biol Chem* 2007;282:30143–30149.
72. Murase T, Misawa K, Haramizu S, Hase T. Catechin-induced activation of the LKB1/AMP-activated protein kinase pathway. *Biochem Pharmacol* 2009;78:78–84.
73. Huang CH, Tsai SJ, Wang YJ, Pan MH, Kao JY, Way TD. EGCG inhibits protein synthesis, lipogenesis, and cell cycle progression through activation of AMPK in p53 positive and negative human hepatoma cells. *Mol Nutr Food Res* 2009;53:1156–1165.
74. Nerstedt A, Johansson A, Andersson CX, Cansby E, Smith U, Mahlapuu M. AMP-activated protein kinase inhibits IL-6-stimulated inflammatory response in human liver cells by suppressing phosphorylation of signal transducer and activator of transcription 3 (STAT3). *Diabetologia* 2010;53:2406–2416.
75. Lo HW, Hsu SC, Xia W, Cao X, Shih JY, Wei Y, Abbruzzese JL, Hortobagyi GN, Hung MC. Epidermal growth factor receptor cooperates with signal transducer and activator of transcription 3 to induce epithelial-mesenchymal transition in cancer cells via up-regulation of TWIST gene expression. *Cancer Res* 2007;67:9066–9076.
76. Sullivan NJ, Sasser AK, Axel AE, Vesuna F, Raman V, Ramirez N, Oberyszyn TM, Hall BM. Interleukin-6 induces an epithelial-mesenchymal transition phenotype in human breast cancer cells. *Oncogene* 2009;28:2940–2947.
77. Shankar S, Nall D, Tang S-N, Meeker D, Passarini J, Sharma J, Srivastava RK. Resveratrol inhibits pancreatic cancer stem cell characteristics in human and *Kras^{G12D}* transgenic mice by inhibiting pluripotency maintaining factors and epithelial-mesenchymal transition. *PLoS One* 2011;6:e16530.
78. Tryndyak VP, Beland FA, Pogribny IP. E-cadherin transcriptional down-regulation by epigenetic and microRNA-200 family alterations is related to mesenchymal and drug-resistant phenotypes in human breast cancer cells. *Int J Cancer* 2010;126:2575–2583.
79. Li J, Qu X, Ricardo SD, Bertram JF, Nikolic-Paterson DJ. Resveratrol inhibits renal fibrosis in the obstructed kidney: Potential role in deacetylation of Smad3. *Am J Pathol* 2010;177:1065–1071.
80. Li C, Cai F, Yang Y, Zhao X, Wang C, Li J, Jia Y, Tang J, Liu Q. Tetrahydroxystilbene glucoside ameliorates diabetic nephropathy in rats: involvement of SIRT1 and TGF-beta1 pathway. *Eur J Pharmacol* 2010;649:382–389.
81. Tang SN, Singh C, Nall D, Meeker D, Shankar S, Srivastava RK. The dietary bioflavonoid quercetin synergizes with epigallocatechin gallate (EGCG) to inhibit prostate cancer stem cell characteristics, invasion, migration and epithelial-mesenchymal transition. *J Mol Signal* 2010;5:14.
82. Srivastava RK, Tang SN, Zhu W, Meeker D, Shankar S. Sulforaphane synergizes with quercetin to inhibit self-renewal capacity of pancreatic cancer stem cells. *Front Biosci (Elite Ed)* 2011;3:515–528.
83. Turner N, Li JY, Gosby A, To SW, Cheng Z, Miyoshi H, Taketo MM, Cooney GJ, Kraegen EW, James DE, Hu LH, Li J, Ye JM. Berberine and its more biologically available derivative, dihydroberberine, inhibit mitochondrial respiratory complex I: A mechanism for the action of berberine to activate AMP-activated protein kinase and improve insulin action. *Diabetes* 2008;57:1414–1418.
84. Gledhill JR, Montgomery MG, Leslie AG, Walker JE. Mechanism of inhibition of bovine F1-ATPase by resveratrol and related polyphenols. *Proc Natl Acad Sci USA* 2007;104:13632–13637.
85. Hwang JT, Kwon DY, Yoon SH. AMP-activated protein kinase: A potential target for the diseases prevention by natural occurring polyphenols. *New Biotechnol* 2009;26:17–22.
86. Lee KW, Lee HJ. The roles of polyphenols in cancer chemoprevention. *Biofactors* 2006;26:105–121.
87. Rahman I, Biswas SK, Kirkham PA. Regulation of inflammation and redox signaling by dietary polyphenols. *Biochem Pharmacol* 2006;72:1439–1452.
88. Page MM, Robb EL, Salway KD, Stuart JA. Mitochondrial redox metabolism: Aging, longevity and dietary effects. *Redox Ageing Dev* 2010;131:242–252.
89. Katsiki M, Chondrogianni N, Chinou I, Rivett AJ, Gonos ES. The olive constituent oleuropein exhibits proteasome stimulatory properties in vitro and confers life span extension of human embryonic fibroblasts. *Rejuvenation Res* 2007;10:157–172.
90. Paiva-Martins F, Fernandes J, Rocha S, Nascimento H, Vitorino R, Amado F, Borges F, Belo L, Santos-Silva A. Effects of olive oil polyphenols on erythrocyte oxidative damage. *Mol Nutr Food Res* 2009;53:609–616.
91. Stefanatos R, Sanz A. Mitochondrial complex I: A central regulator of the aging process. *Cell Cycle* 2011;10.
92. Fulco M, Cen Y, Zhao P, Hoffman EP, McBurney MW, Sauve AA, Sartorelli V. Glucose restriction inhibits skeletal myoblast differentiation by activating SIRT1 through AMPK-mediated regulation of Namp1. *Dev Cell* 2008;14:661–673.
93. Guarente L. Connecting the dots: Linking sirtuins and AMPK in metabolism and aging. *Dev Cell* 2011;20:e1.
94. Wang Y, Liang Y, Vanhoutte PM. SIRT1 and AMPK in regulating mammalian senescence: A critical review and a working model. *FEBS Lett* 2011;585:986–994.



95. Scheepens A, Tan K, Paxton JW. Improving the oral bioavailability of beneficial polyphenols through designed synergies. *Genes Nutr* 2010;5:75–87.
96. Vauzour D, Rodriguez-Mateos A, Corona G, Oruna-Concha MJ, Spencer JPE. Polyphenols and human health: Prevention of disease and mechanisms of action. *Nutrients* 2010;2:1106–1131.
97. Visioli F, de la Lastra CA, Andres-Lacueva X, Aviram M, Calhau C, Cassano A, D'Archivio M, Faria A, Favé G, Fogliano V, Llorach R, Vitaglione P, Zoratti M, Edeas M. Polyphenols and human health: A prospectus. *Crit Rev Food Sci Nutr* 2011;51:524–546.
98. Vissers MN, Zock PL, Roodenburg AJC, Leenen R, Katan, MB. Olive oil phenols are absorbed in humans. *J Nutr* 2002;132:409–417.
99. Zhang L, Zuo Z, Lin G. Intestinal and hepatic glucuronidation of flavonoids. *Mol Pharm* 2007;4:833–845.
100. Lambert JD, Sang SM, Yang CS. Biotransformation of green tea polyphenols and the biological activities of those metabolites. *Mol Pharmaceutics* 2007;4:819–825.
101. Landis-Piwowar KR, Dou QP. Polyphenols: Biological activities, molecular targets, and the effect of methylation. *Curr Mol Pharmacol* 2008;1:233–243.
102. Chang HC, Churchwell MI, Delclos KB, Newbold RR, Doerge DR. Mass spectrometric determination of Genistein tissue distribution in diet exposed Sprague-Dawley rats. *J Nutr* 2000;130:1963–1970.
103. Datla KP, Christidou M, Widmer WW, Rooprai HK, Dexter DT. Tissue distribution and neuroprotective effects of citrus flavonoid tangeretin in a rat model of Parkinson's disease. *Neuroreport* 2001;12:3871–3875.
104. Schramm D, Collins H, German B. Flavonoid transport by mammalian endothelial cells. *J Nutr Biochem* 1999;10:193–197.
105. Suganuma M, Okabe S, Oniyama M, Tada Y, Ito H, Fujiki H. Wide distribution of [3H](-)-epigallocatechin gallate, a cancer preventive tea polyphenol, in mouse tissue. *Carcinogenesis* 1998;19:1771–1776.
106. Gao S, Hu M. Bioavailability challenges associated with development of anti-cancer phenolics. *Mini Rev Med Chem* 2010;10:550–567.
107. Selma MV, Espin JC, Tomas-Barberan FA. Interaction between phenolics and gut microbiota: role in human health. *J Agric Food Chem* 2009;57:6485–6501.
108. Singh J, Dubey RK, Atal CK. Piperine-mediated inhibition of glucuronidation activity in isolated epithelial cells of the guinea-pig small intestine: evidence that piperine lowers the endogenous UDP-glucuronic acid content. *J Pharmacol Exp Ther* 1986;236:488–493.
109. Reen RK, Jamwal DS, Taneja SC, Koul JL, Dubey RK, Wiebel FJ, Singh J. Impairment of UDP-glucose dehydrogenase and glucuronidation activities in liver and small intestine of rat and guinea pig in vitro by piperine. *Biochem Pharmacol* 1993;46:229–238.
110. Shoba G, Joy D, Joseph T, Majeed M, Rajendran R, Srinivas PS. Influence of piperine on the pharmacokinetics of curcumin in animals and human volunteers. *Planta Med* 1998;64:353–356.
111. Lambert JD, Hong J, Kim DH, Mishin VM, Yang CS. Piperine enhances the bioavailability of the tea polyphenol (-)-epigallocatechin-3-gallate in mice. *J Nutr* 2004;134:1948–1952.
112. Johnson JJ, Nihal M, Siddiqui IA, Scarlett CO, Bailey HH, Mukhtar H, Ahmad N. Enhancing the bioavailability of resveratrol by combining it with piperine. *Mol Nutr Food Res* 2011;55:1169–1176.
113. Nair HB, Sung B, Yadav VR, Kannappan R, Chaturvedi MM, Aggarwal BB. Delivery of antiinflammatory nutraceuticals by nanoparticles for the prevention and treatment of cancer. *Biochem Pharmacol* 2010;80:1833–1843.
114. Goulas V, Exarchou V, Troganis AN, Psomiadou E, Fotsis T, Briasoulis E, Gerotheranassis IP. Phytochemicals in olive-leaf extracts and their antiproliferative activity against cancer and endothelial cells. *Mol Nutr Food Res* 2009;53:600–608.
115. Menendez JA, Vazquez-Martin A, Colomer R, Brunet J, Carrasco-Pancorbo A, Garcia-Villalba R, Fernandez-Gutierrez A, Segura-Carretero A. Olive oil's bitter principle reverses acquired autoresistance to trastuzumab (Herceptin) in HER2-overexpressing breast cancer cells. *BMC Cancer* 2007;7:80.
116. Menendez JA, Vazquez-Martin A, Oliveras-Ferreros C, Garcia-Villalba R, Carrasco-Pancorbo A, Fernandez-Gutierrez A, Segura-Carretero A. Analyzing effects of extra-virgin olive oil polyphenols on breast cancer-associated fatty acid synthase protein expression using reverse-phase protein microarrays. *Int J Mol Med* 2008;22:433–439.
117. Menendez JA, Vazquez-Martin A, Oliveras-Ferreros C, Garcia-Villalba R, Carrasco-Pancorbo A, Fernandez-Gutierrez A, Segura-Carretero A. Extra-virgin olive oil polyphenols inhibit HER2 (erbB-2)-induced malignant transformation in human breast epithelial cells: relationship between the chemical structures of extra-virgin olive oil secoiridoids and lignans and their inhibitory activities on the tyrosine kinase activity of HER2. *Int J Oncol* 2009;34:43–51.
118. Menendez JA, Vazquez-Martin A, Garcia-Villalba R, Carrasco-Pancorbo A, Oliveras-Ferreros C, Fernandez-Gutierrez A, Segura-Carretero A. Anti-HER2 (erbB-2) oncogene effects of phenolic compounds directly isolated from commercial Extra-Virgin Olive Oil (EVOO). *BMC Cancer* 2008;8:377.

Address correspondence to:

Javier A. Menendez, Ph.D.

Catalan Institute of Oncology, Girona (ICO-Girona)

Dr. Josep Trueta University Hospital

Avenida de França s/n

E-17007 Girona, Catalonia

Spain

E-mail: jmenendez@iconcologia.net; jmenendez@idibgi.org

Antonio Segura-Carretero, Ph.D.

Department of Analytical Chemistry

Faculty of Sciences, University of Granada

Avenida Fuentenueva s/n

E-18071 Granada, Andalusia

Spain

E-mail: ansegura@ugr.es

Received: May 4, 2011

Accepted: July 25, 2011









CAPÍTULO 6. Application of nanoLC-ESI-TOF-MS for the metabolomic analysis of phenolic compounds from extra-virgin olive oil in treated colon cancer cells.





Contents lists available at SciVerse ScienceDirect

Journal of Pharmaceutical and Biomedical Analysis

journal homepage: www.elsevier.com/locate/jpba

Application of nanoLC-ESI-TOF-MS for the metabolomic analysis of phenolic compounds from extra-virgin olive oil in treated colon-cancer cells

S. Fernández-Arroyo^{a,b,1}, A. Gómez-Martínez^{c,1}, L. Rocamora-Reverte^c, R. Quirantes-Piné^{a,b}, A. Segura-Carretero^{a,b,*}, A. Fernández-Gutiérrez^{a,b}, J.A. Ferragut^{c,**}^a Department of Analytical Chemistry, Faculty of Sciences, University of Granada, C/Fuentenueva S/N, 18071 Granada, Spain^b Functional Food Research and Development Center, Health Science Technological Park, Avenida del Conocimiento S/N, 18100 Armilla, Granada, Spain^c Instituto de Biología Molecular y Celular, Miguel Hernández University, Avenida de la Universidad S/N, 03202 Elche, Alicante, Spain

ARTICLE INFO

Article history:

Received 25 October 2011

Received in revised form 23 January 2012

Accepted 24 January 2012

Available online 1 February 2012

Keywords:

NanoLC-TOF-MS

Olive oil

Phenolic compounds

Colon adenocarcinoma

Metabolomic

ABSTRACT

Crude phenolic extracts (PE) have been obtained from naturally bearing Spanish extra-virgin olive oil (EVOO) showing different polyphenol families such as secoiridoids, phenolic alcohols, lignans, and flavones. EVOO-derived complex phenols (especially from the Arbequina variety olive) have been shown to suppress cell growth of SW480 and HT29 human colon adenocarcinoma cell lines. Inhibition of proliferation by EVOO-PE Arbequina variety extract was accompanied by apoptosis in both colon-cancer-cell lines and a limited G₂M cell-cycle arrest in the case of SW480 cells. The metabolized compounds from EVOO-PE in culture medium and cytoplasm of both cell lines were analyzed using nano-liquid chromatography (nanoLC) coupled with electrospray ionization-time-of-flight-mass spectrometry (ESI-TOF-MS). The results showed many phenolic compounds and their metabolites both in the culture medium as well as in the cytoplasm. The main compounds identified from EVOO-PE were hydroxylated luteolin and decarboxymethyl oleuropein aglycone.

© 2012 Elsevier B.V. All rights reserved.

1. Introduction

Several studies have reported that olive-oil consumption has potential protective effects against several pathologies, especially those related to cancer [1]. For years, the healthy properties of EVOO were attributed exclusively to its high monounsaturated fatty acid (MUFA) content, mostly in the form of oleic acid, and also the long-chain n-3 polyunsaturated fatty acids, such as conjugated linoleic acid and gamma-linolenic acid have shown tumor-inhibitory effects [2]. In addition to fatty acids, evidence has mounted concerning the bioactivity of minor components of EVOO, particularly phenolic compounds [3]. The main families of phenolic compounds in olive oil are: simple phenols, lignans, flavonoids, and secoiridoids [4]. These compounds are also present in by-products generated during olive-oil production, such as olive

leaves, although they appear mainly as glycosides [5]. A large body of evidence indicates that polyphenols can exert chemopreventive effects against different cancers, and several studies have explored the anticarcinogenic activity of olive-oil polyphenols, mainly in *in vitro* studies where individual compounds or olive-oil extracts were incubated in different types of human cancer-cell lines (prostate, leukemic, breast) [6]. These studies suggest that the olive-oil polyphenols analyzed are able to affect the overall process of carcinogenesis, because they have the abilities to inhibit the cell cycle, cell proliferation or oxidative stress, improve the efficacy of detoxification enzymes, induce apoptosis, and stimulate the immune system. Recently, Menendez et al. [7] have also studied the effect of olive-oil polyphenols, supplemented individually or in the oil matrix, in different human breast-cancer lines and their findings revealed that the presence of these polyphenols, especially those fractions rich in lignans and secoiridoids had a significantly stronger ability to decrease cell viability [8] and the expression status of HER2, one of the most commonly analyzed protooncogenes in human-cancer studies.

However, although there is evidence suggesting that olive-oil polyphenols show anticarcinogenic activity, the molecular mechanism of the uptake and metabolism of these compounds in the cancer cells has not yet been investigated, and only *in vitro* studies with cells of the gastrointestinal tract, CaCo-2 cells [9], and a human hepatoma cell line (HepG2) [10] have been undertaken.

Abbreviations: EVOO, extra-virgin olive oil; PE, phenolic extract; CRC, colorectal cancer; nanoLC, nano-liquid chromatography; MeOH, methanol; DOA, decarboxymethyl oleuropein aglycone; FCM, flow cytometry.

* Corresponding author at: Functional Food Research and Development Center, Health Science Technological Park, Avenida del Conocimiento S/N, E-18100 Granada, Spain. Tel.: +34 958 243296; fax: +34 958 249510.

** Corresponding author. Tel.: +34 966658431; fax: +34 966658758.

E-mail addresses: ansegura@ugr.es (A. Segura-Carretero), ja.ferragut@umh.es (J.A. Ferragut).

¹ These authors have equally contributed to this research.



Colorectal cancer (CRC) represents one of the most frequent malignancies worldwide with distant recurrence primarily affecting the liver as the predominant cause of CRC-related mortality. The 5-year survival rate of 90% in patients with tumor restricted to the colon decreases to 10% in the presence of distant metastasis [11]. Risk factors suggested in CRC etiology include genetic predisposition and dietary intake, such as high consumption of fat and low intake of fibers and flavonoids [12]. It is demonstrated that the phenolic compounds from EVOO prevent the carcinogenesis and invasion of colon-cancer cells and metastasis [13], including hydroxytyrosol and oleuropein aglycone [14].

Nano-liquid chromatography coupled to electrospray ionization-time-of-flight mass spectrometry (nanoLC-ESI-TOF MS) is a new powerful analytical tool, providing a wide number of important applications, especially in proteomics and also in fields such as pharmaceutical, environmental and enantiomeric analysis. The application of nanoLC in the field of food analysis is very limited, but we have recently demonstrated the potential of this technique in the determination and quantification of polyphenols from olive-oil samples [8]. The first attempts to use packed capillary columns with very small inside diameters, ranging from 20 to 70 μm , and flow rates on the order of 50–200 nL/min were reported by Novotny [15]. From a theoretical standpoint, it has been demonstrated that sensitivity can increase on decreasing the column inside diameter. This effect can be ascribed to both a reduction of analyte chromatographic dilution and greater efficiency [16]. A complementary approach to increase the sensitivity in nanoLC involves the coupling of separation system with mass spectrometry. Hyphenation is easy to achieve because of the relatively low flow rate involved in the separation process. Indeed, when the electrospray ionization (ESI) is used as the continuous-flow ionization technique, a lower flow rate raises the number ions in the gas phase and, consequently, augments sensitivity [17].

In this context, the present paper uses nanoLC-ESI-TOF-MS to elucidate for the first time the uptake, antiproliferative activity, and metabolism of the main families of olive-oil polyphenols in relation to human colon adenocarcinoma cells (SW480 and HT29) with an exogenous supplementation of olive-oil extracts.

2. Materials and methods

2.1. Chemicals

All chemicals were of analytical reagent grade. For the optimization of the extraction procedure, methanol and hexane were purchased from Panreac (Barcelona, Spain), hydrochloric acid from Scharlau (Barcelona, Spain), and ethyl acetate from Lab-Scan (Dublin, Ireland). Methanol from Lab-Scan (Dublin, Ireland) and acetic acid from Fluka (Buchs, Switzerland) were used for preparing mobile phases and also for the extraction procedures. Water was deionized by using a Milli-Q-system (Millipore, Bedford, MA, USA).

The EVOOs used corresponded to five different olive varieties from different geographic zones in Spain: two Hojiblanca variety olive oils produced in Málaga (EVOO 01) and Seville (EVOO 09), seven Picual variety oils produced in Málaga (EVOO 02), Jaén (EVOOs 04, 10 and 11), and Granada (EVOOs 05, 06 and 07); one Cornezuelo variety oil produced in Granada (EVOO 03); one Manzanilla variety oil produced in Seville (EVOO 08); and three Arbequina variety oils produced in Tarragona (EVOO 12) and Seville (EVOOs 13 and 14).

2.2. Extraction and characterization of phenolic compounds from extra-virgin olive oil

As indicated in the literature [18], after conditioning a Diol-cartridge with 10 mL of methanol and 10 mL of hexane, 60 g of EVOO

dissolved in 60 mL of hexane were passed through the cartridge. The non-polar fraction was eluted with 15 mL of hexane, and then 40 mL of methanol was passed to recover the phenolic compounds. The eluted solutions were dried in a vacuum system at 35 °C, and the residues were dissolved in 2 mL of methanol. For the supplementation to the cells, and to avoid the toxic effect of methanol, 1 mL of the methanol extract was evaporated and reconstituted in 125 μL of ethanol, since this solvent has a lower toxic effect on the cells.

These phenolic extracts were completely characterized using HPLC-ESI-TOF-MS by Lozano-Sánchez et al. [4].

2.3. Cell culture and cell-extract preparation

Colon adenocarcinoma HT29 and SW480 cells from IMIM (Institut Municipal d'Investigació Mèdica, Barcelona, Spain) and ATCC (American Type Culture Collection, LGC Promochem, UK), respectively, were grown in DMEM supplemented with heat-inactivated fetal bovine serum (5%), L-glutamine (2 mM), penicillin G (50 U/mL), and streptomycin (50 $\mu\text{g}/\text{mL}$), at 37 °C in a humidified atmosphere and 5% CO_2 . Cells were plated at a density of 10,000 cells/ cm^2 in 60 mm-diameter culture plates and permitted to adhere overnight at 37 °C. When cells reached 80% confluence, they were trypsinized (1 mL/25 cm^2), neutralized with culture medium at a 1:5 ratio (trypsin:medium) and pelleted for further analysis.

The cytosolic fraction of control (untreated HT-29 and SW480 cells) and HT29 or SW480 cells treated with olive-oil extracts, was obtained upon cell disruption with a Polytron homogenizer at 4 °C. First, cells were washed with phosphate-buffered saline (PBS) solution (Sigma-Aldrich Madrid, Spain) and sedimented. The pellet was resuspended with homogenization buffer Tris-HCl (10 mM, pH 7.4) containing EDTA (5 mM), NaCl (120 mM) and a protease inhibitor cocktail (Sigma-Aldrich Madrid, Spain), containing 4-(2-aminoethyl)benzenesulfonyl fluoride (AEBSF), pepstatin A, E-64, bestatin, leupeptin, and aprotinin. Upon centrifugation at 14,000 $\times g$ for 14 min at 4 °C, the pellet was discarded and supernatant was centrifuged for 1 h at 100,000 $\times g$ and 4 °C. The supernatant (cytosolic fraction) was stored at –80 °C until the metabolite-extraction procedure was performed. At this temperature, enzyme activity is stopped and samples can safely be stored without continuing metabolic activity.

2.4. Cell proliferation, apoptosis, and cell-cycle analysis

Cell proliferation was determined by the crystal-violet-staining assay. Cells were analyzed in 96-well plates at a density in the range of 4–6 $\times 10^6$ cells per well and treated with different rates of olive extracts (0.01% or 0.1%) in ethanol using six wells per treatment for 24 h. Then, cells were fixed and stained with a crystal-violet paraformaldehyde solution. Excess crystal-violet dye was removed by washing with deionized water, and culture plates were dried overnight. The crystal-violet dye was released from cells by brief incubation with HCl (0.1 M) and shaking. The optical density of each well was measured by a microplate reader at 620 nm (Anthos 2001 Labtec Instruments GmbH, Wals, Austria).

The cell cycle was analyzed essentially as described in [19]. Briefly, for cell-cycle distribution of DNA content, control and cells treated with the different olive-oil extracts were trypsinized, washed with PBS, and fixed with 75% cold ethanol at –20 °C for at least 1 h. Then, cells were incubated with Triton X-100 (0.5%) and RNase A (25 $\mu\text{g}/\text{mL}$) in PBS, stained with propidium iodide (25 $\times 10^{-3}$ $\mu\text{g}/\text{mL}$), incubated for 30 min in the dark and analyzed using an Epics XL flow cytometer equipped with a 0.75 W argon laser set at 488 nm (Beckman Coulter Co., Miami, FL, USA).

The apoptosis induced by treatment of the cells with 0.1% EVOO-PE14 for 24 h, was measured by flow cytometry by determining



the amount of apoptotic cells in the sub-G1 peak, as previously described [19].

Flow-cytometry data were analyzed upon gating the cells to eliminate dead cells and debris. A total of 10^5 cells were measured during each sample analysis.

2.5. Treatment of biological samples for the identification of metabolites

The treatment of biological samples was based on a previous study described in the literature [8]. The optimal extraction procedure was basically a liquid–liquid extraction with ethyl acetate including certain slight differences according to the type of sample. For the culture media, the best extraction procedure was as follows: 1 mL of the culture medium was mixed with 1 mL of ethyl acetate, extracted for 10 min using a vortex, centrifuged at $18,800 \times g$ at 4°C for 10 min and the supernatant was evaporated to dryness. The dried sample was reconstituted in $200 \mu\text{L}$ of water/acetic acid/MeOH (79.5/0.5/20, v/v/v).

For the cytoplasm samples the extraction procedure consisted of stirring $100 \mu\text{L}$ of cytoplasm with $100 \mu\text{L}$ of MeOH–HCl (0.5 M) $200 \mu\text{L}$ of ethyl acetate for 10 min using a vortex. The mixture was maintained in the freezer for 1 h at -20°C . After the samples reached room temperature, they were centrifuged at $18,800 \times g$ for 10 min at 4°C and the supernatant was evaporated to dryness. The dried sample was reconstituted in $100 \mu\text{L}$ of water/acetic acid/MeOH (79.5/0.5/20, v/v/v).

2.6. NanoLC-ESI-TOF-MS analysis

2.6.1. NanoLC

The chromatographic conditions were optimized following García-Villalba et al. [8]. A commercially available instrumentation EASY-nLC™ (Bruker Daltonik GmbH, Bremen, Germany) was used, composed of one module equipped with three pumps, three pressure sensors, four valves, two flow sensors, an autosampler, and a touchscreen.

A short capillary trapping column ($100 \mu\text{m}$ inside diameter, effective length 20 mm, $5 \mu\text{m}$ particle size) and a fused silica capillary column ($75 \mu\text{m}$ inside diameter, effective length 10 cm, $3 \mu\text{m}$ particle size), both packed with C18 stationary phase, were used for the chromatographic separation. The mobile phases were composed of water with acetic acid (0.25%) (phase A) and methanol (phase B) with the following gradient: 0 min, 5% B; 7 min, 35% B; 12 min, 45% B; 17 min, 50% B; 22 min, 60% B; 25 min, 95% B; 27 min, 5% B, and finally a conditioning cycle of 5 min with the same conditions for the next analysis. Before the following analysis was started, the pre-column and column were re-equilibrated with phase A at $6 \mu\text{L}/\text{min}$ for 2 min and $0.6 \mu\text{L}/\text{min}$ for 8 min, respectively. The flow rate used to elute the compounds in the analytical column was $300 \text{ nL}/\text{min}$ at 25°C and $5 \mu\text{L}$ of the sample was injected into the loop.

2.6.2. Mass spectrometry

The nanoLC system was coupled to a Bruker Daltonik microTOF mass spectrometer (Bruker Daltonik, Bremen, Germany) using electrospray ionization (ESI).

The nanoLC system was interfaced to the mass spectrometry using a commercial sheathless nano-spray interface with a tapered fused silica sprayer tip. The key parameters of the nano-ESI were adjusted for the flow rate used ($300 \text{ nL}/\text{min}$) to achieve stable spray across the entire gradient range: pressure 0.4 bar, dry gas flow $4 \text{ L}/\text{min}$ and a dry gas temperature of 150°C .

The mass spectrometer was run in the negative mode and was operated to acquire spectra in the range of 50–1000 m/z . The accurate mass data of the molecular ions, provided by the TOF analyzer,

were processed by DataAnalysis 4.0 software (Bruker Daltonik GmbH), which lists possible molecular formulas consistent with the accurate mass measurement and the true isotopic pattern. High mass accuracy requires mass calibration. For this, we used a mixture of well-known phenols present in the olive-oil extracts as an internal calibration, giving mass peaks throughout the desired range of 100–400 m/z , according to García-Villalba et al. [8].

3. Results and discussion

3.1. Screening of antiproliferative activity of EVOO-PE

Growth inhibition of colon-cancer HT29 and SW480 cells by treatments with each of the 14 olive-oil extracts at concentrations 0.01% and 0.1% for 24 h, was measured by the crystal-violet assay. Depending on the extract and on the concentration used, the effect on cell proliferation was very different (Tables 1A and 1B). Thus, while concentrations of 0.1% reduced cell growth by up to 20% with respect to control of untreated cells in both cell lines (Table 1B), inhibition of cell proliferation at 0.01% was much less drastic (Table 1A).

Also, the antiproliferative activity of the olive-oil extracts preferentially affected the SW480 cells, with significant differences in growth inhibition induced by some of the 14 olive-oil samples. All of

Table 1A

Cell proliferation of human colon cells upon incubation with 0.01% of 14 olive-oil crude extracts for 24 h.

	SW480	HT29
Control	100	100
EVOO-PE01	83.1 ± 2.6*	101.6 ± 6.4
EVOO-PE02	79.0 ± 2.9*	108.6 ± 3.8*
EVOO-PE03	75.1 ± 2.5*	101.5 ± 6.5
EVOO-PE04	82.5 ± 2.1*	96.9 ± 4.6
EVOO-PE05	85.7 ± 3.5*	93.7 ± 3.6
EVOO-PE06	79.0 ± 4.1*	94.4 ± 5.6
EVOO-PE07	89.5*	93.3 ± 2.2
EVOO-PE08	79.5 ± 4.0*	82.8 ± 4.3*
EVOO-PE09	77.0 ± 4.6*	84.5 ± 1.8*
EVOO-PE10	80.0 ± 6.4*	90.0 ± 3.8*
EVOO-PE11	86.1 ± 4.3*	93.1 ± 3.1
EVOO-PE12	80.0 ± 3.1*	95.3 ± 2.3
EVOO-PE13	79.2 ± 4.1*	96.9 ± 3.2
EVOO-PE14	76.9 ± 4.9*	87.9 ± 2.0*

Data are expressed as percentages of cell growth with respect to control of untreated cells ± SEM ($n = 3$).

* Significance value ($p < 0.01$) by a one-way ANOVA with respect to control.

Table 1B

Cell proliferation of human colon cells upon incubation with 0.1% of 14 olive-oil crude extracts for 24 h.

	SW480	HT29
Control	100	100
EVOO-PE01	37.4 ± 1.3*	51.1 ± 5.0*
EVOO-PE02	38.3 ± 1.1*	50.4 ± 6.8*
EVOO-PE03	36.8 ± 1.7*	45.8 ± 3.9*
EVOO-PE04	41.2 ± 2.1*	51.9 ± 6.6*
EVOO-PE05	21.7 ± 1.2*	34.9 ± 3.1*
EVOO-PE06	22.7 ± 0.8*	37.8 ± 3.9*
EVOO-PE07	26.8 ± 5.7*	39.6 ± 1.8*
EVOO-PE08	23.5 ± 1.5*	39.0 ± 2.6*
EVOO-PE09	23.1 ± 0.8*	24.2 ± 0.8*
EVOO-PE10	20.7 ± 1.6*	23.9 ± 0.8*
EVOO-PE11	22.6 ± 1.5*	24.8 ± 0.9*
EVOO-PE12	56.8 ± 2.8*	24.3 ± 2.0*
EVOO-PE13	40.6 ± 5.4*	21.9 ± 0.8*
EVOO-PE14	33.3 ± 4.2*	22.9 ± 1.5*

Data are expressed as percentages of cell growth with respect to control of untreated cells ± SEM ($n = 3$).

* Significance value ($p < 0.01$) by a one-way ANOVA with respect to control.

**Table 2**

Retention time, [M–H][–] measured, error (in ppm) between the theoretical calculated and measured masses, and the molecular formula of phenolic compounds from EVOO-PE14 and their metabolites found in culture medium and cytoplasm of HT29 and SW480 cell lines.

Compound	Retention time (min)	[M–H] [–]	Error (ppm)	Molecular formula	Culture medium		Cytoplasm	
					HT29	SW480	HT29	SW480
Phenolic compounds								
DOA	11.65	319.1165	4.1	C ₁₇ H ₂₀ O ₆				X
Vanillin	11.7	151.0401	0.3	C ₈ H ₈ O ₃	X	X		
Oleuropein aglycone	11.95	377.1247	1.7	C ₁₉ H ₂₂ O ₈				X
4-OH-benzoic acid	12.35	137.0244	0.1	C ₇ H ₆ O ₃	X	X		
Vanillic acid	12.6	167.0348	0.7	C ₈ H ₈ O ₄	X			
Hydroxytyrosol acetate	20.05	195.0661	0.6	C ₁₀ H ₁₂ O ₄	X			
10-H-oleuropein aglycone	20.1	393.1205	4.8	C ₁₉ H ₂₂ O ₉	X			
Syringaresinol	21	417.153	5.3	C ₂₂ H ₂₆ O ₈		X		
Acetoxy-pinoresinol	21.55	415.1378	4.5	C ₂₂ H ₂₄ O ₈	X	X	X	X
Pinoresinol	21.8	357.1339	1.3	C ₂₀ H ₂₂ O ₆		X		
Hydroxytyrosol	23.1	153.0555	0.7	C ₈ H ₁₀ O ₃	X	X		
Elenolic acid	25.8	241.0714	1.0	C ₁₁ H ₁₄ O ₆		X	X	
Luteolin	27.3	285.0399	1.9	C ₁₅ H ₁₀ O ₆	X	X		
Methyl-DOA	30.5	333.1152	3.0	C ₁₈ H ₂₂ O ₆	X		X	
Apigenin	31.1	269.0468	4.3	C ₁₅ H ₁₀ O ₅		X		
Metabolites								
Quercetin	38	301.0352	0.5	C ₁₅ H ₁₀ O ₇				X
Methyl-hydroxy-DOA	38.1	349.1278	5.0	C ₁₈ H ₂₂ O ₇			X	X
Methyl-luteolin	38.2	299.0574	4.3	C ₁₆ H ₁₂ O ₆				X

DOA, decarboxymethyl oleuropein aglycone.

these have been completely characterized by Lozano-Sánchez et al. [4]. While other EVOO-PEs present high antiproliferative activity, EVOO-PE14 displays a notable and quite different antiproliferative activity both in HT29 and in SW480 cells, and therefore it was selected for further analysis. This extract, belonging to the Arbequina variety from Seville (Spain), is characterized by a high content in lignans (especially in decarboxymethyl oleuropein aglycone, DOA). Furthermore, its traceability is well documented.

3.2. Metabolomic analysis using nanoLC-ESI-TOF-MS

The optimum nanoLC-ESI-TOF-MS method was applied to analyze EVOO-PE14 phenolic compounds derived from the treatment of HT29 and SW480 cells with this extract in either culture medium or in the cytosolic fraction of the cells.

The method proved the specificity for these compounds, since no interfering endogenous compounds were detected at the elution times of the polyphenols in the extracted ion chromatograms, when blank samples were analyzed. To identify the phenolic compounds in their free form and their possible metabolites formed after incubation, we used the information available in literature, the polarity of the compounds in the reverse phase, and the valuable information provided by the TOF analyzer. This provided a list of possible molecular formulas using the information on mass accuracy and the isotopic pattern of the compounds.

Table 2 shows the compounds from EVOO-PE14 and their metabolites found in the culture medium and the cytoplasm of HT29 and SW480 cell lines. Three metabolites deriving from EVOO-PE14 were found in the cytoplasm due to the metabolism of the cells, namely, methyl-hydroxy-DOA, methyl-luteolin, and quercetin (by hydroxylation of luteolin). Fig. 1 shows the extracted ion chromatograms (EIC) of some of the compounds found in both the culture medium as well as the cytoplasm. It should be highlighted that quercetin was the main compound found in cytoplasm, with much higher intensity than other compounds. Decarboxymethyl oleuropein aglycone (DOA) also presented high intensity, although lower than quercetin.

The complexity of crude olive-oil extracts makes hard to assign the above antiproliferative activity to individual components of the extracts. However, it is noteworthy that, according to Table 2

and Fig. 1, oleuropein (or its metabolic derivatives) and quercetin, were the two main phenolic compounds found in the cytoplasm of the EVOO-PE14-treated colon-cancer cells. Both compounds have demonstrated to possess antiproliferative activity in colon-cancer-cell lines [20], acting through diverse mechanisms including protein inhibition [21], apoptosis [22], or inhibition of enzyme activities [14,23]. In our case, we found that apoptosis (see below) accompanies the inhibition of proliferation upon treatment of the cells with the EVOO-PE14 olive-oil extract, regardless of the presence of other mechanisms that could also be present.

3.3. Cell-cycle analysis

Fig. 2 shows the distribution of DNA from control and EVOO-PE14-treated HT29 and SW480 cells determined by flow cytometry (FCM).

Tables 3A and 3B display the DNA content of the different phases of cell cycle corresponding to control and HT29 or SW480 cells treated with olive-oil-extract EVOO-PE14 according to Fig. 2. It can be seen that EVOO-PE14 induced apoptosis in HT29 and SW480 cells (10% and 14%, respectively, Table 3A), indicated by an arrow signaling the SubG1 phase in Fig. 2. However, the DNA-distribution profile was found to be quite different between the two cell lines when the relative DNA content of each phase was estimated assuming that 100% refers to the sum of the G1, S, and G₂M phases, i.e. without taking into account the contribution of the apoptotic cell population SubG1 (Table 3B). Thus, no significant changes were

Table 3A

Distribution of DNA from control and HT29 or SW480 cells treated with 0.1% of EVOO-PE14 for 24 h.

Phase	HT29		SW480	
	Control	EVOO-PE14	Control	EVOO-PE14
G1	40.7 ± 1.1	35.7 ± 6.3	64.5 ± 5	41.2 ± 4.9**
S	28.3 ± 7.4	25.1 ± 1.3	18.0 ± 1.5	15.3 ± 7.4
G ₂ M	28.5 ± 8.1	28.2 ± 11.7	15.3 ± 2.5	18.4 ± 2.5
SubG1	1.9 ± 0.3	10.3 ± 3.4*	1.3 ± 0.7	14.2 ± 8.9

Data are expressed as percentages of the cells ± SD estimated by FCM (n = 3).

* p < 0.05 between control and EVOO-PE14-treated cells (paired t-test).

** p < 0.01 between control and EVOO-PE14-treated cells (paired t-test).

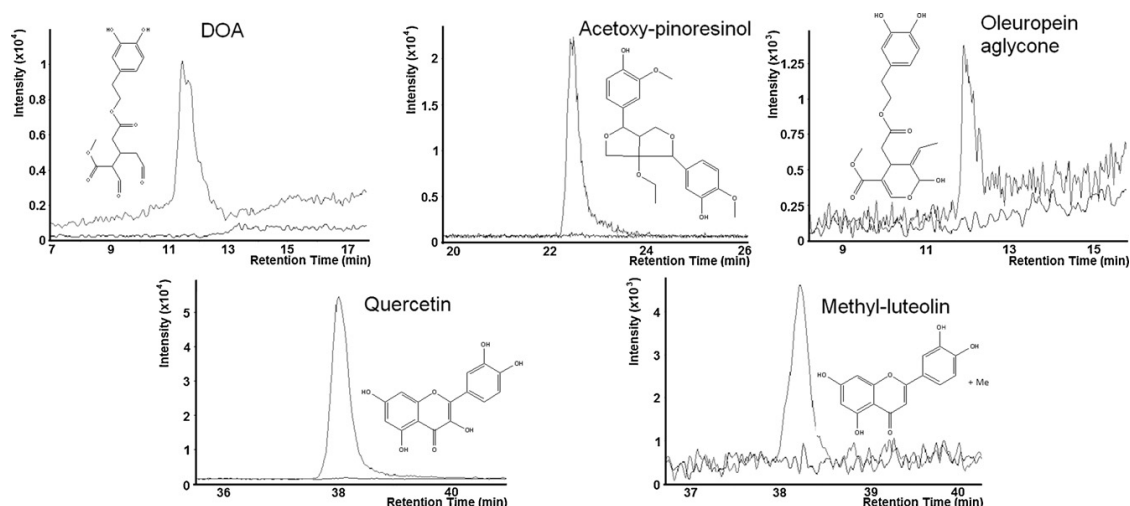


Fig. 1. Extracted ion chromatogram (EIC) of the main compounds and their metabolites found in culture medium and cytoplasm of HT29 and SW480 cell lines. For each identified compound, two signals of EIC corresponding to untreated and EVOO-PE14-treated cell lines are represented. DOA, decarboxymethyl oleuropein aglycone.

found in the cell cycle between control and HT29 EVOO-PE14-treated cells, despite a decrease in G1 concomitant with an increase in G₂M in SW480 EVOO-PE14-treated cells with respect to control SW480 cells. This observation indicates that EVOO-PE14: (a) induces a cytotoxic effect in HT29 and SW480 cells, promoting

apoptosis; and (b) also exerts a cytostatic effect in SW480 cells indicated by cell arrest in G₂M, probably as a step prior to apoptosis.

Several works have demonstrated that olive-oil polyphenols act as inhibitors of cell proliferation in human tumor-cell lines from lung [24], liver [25], leukemia [26], and colon [22], involving

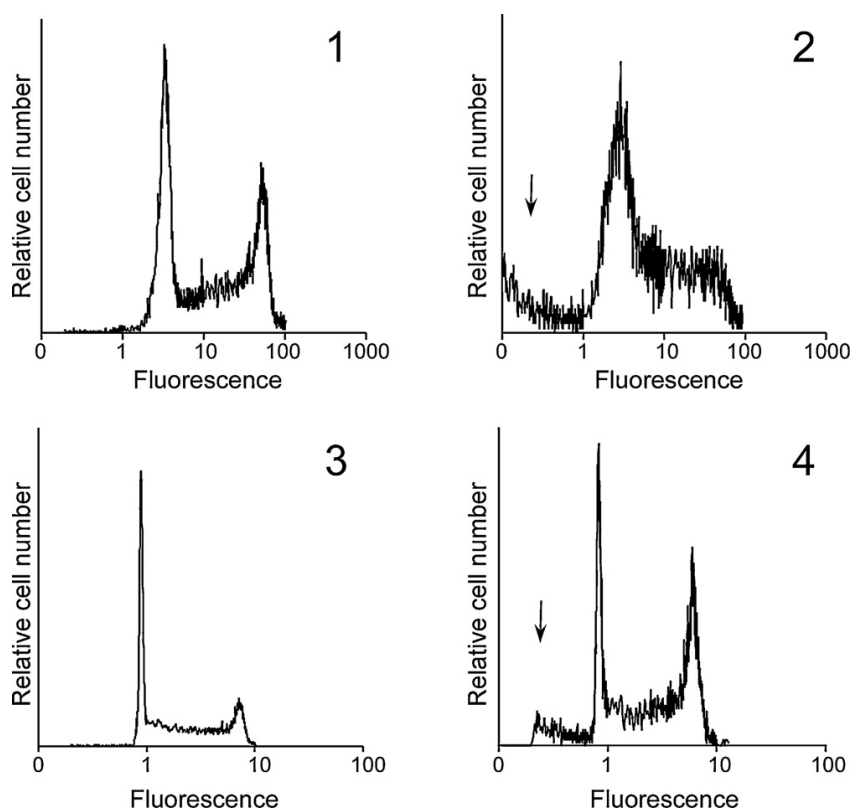


Fig. 2. Distribution of cellular DNA in control HT29 or SW480 cells (panels 1 and 3, respectively) and 0.1% EVOO-PE14-treated HT-29 (panel 2) or SW-480 (panel 4) cells for 24 h, determined by FCM. Arrows on panels 2 and 4 indicate the apoptotic cell population (sub-G1 phase).

**Table 3B**

Distribution of DNA from control and HT29 or SW480 cells treated with 0.1% of EVOOPE14 for 24 h after subtracting the content of the subG1 phase (apoptosis) included in Table 3A.

Phase	HT29		SW480	
	Control	EVOO-PE14	Control	EVOO-PE14
G1	41.5 ± 1.1	40.5 ± 5.6	65.3 ± 4.9	55 ± 4.2
S	27.6 ± 7.2	28.3 ± 1.1	18.2 ± 1.5	20.5 ± 6.3
G ₂ M	27.7 ± 7.9	32 ± 10.5	15.5 ± 2.5	24.5 ± 2.1**

Data are expressed as percentages of the cells ± SD estimated by FCM ($n=3$).

** $p < 0.01$ between control and EVOO-PE14-treated cells (paired t -test).

many different action mechanisms. Thus, oleuropein inhibits cell growth in SW620 human colon-cancer cells [14], while quercetin down-regulates Erb2/Erb3 signaling [21], activates AMPK signaling pathway [27], depresses cyclooxygenase-2 expression [23] in HT29 cells, and inhibits β -catenin/Tcf signaling in SW480 cells [28].

The relative high abundance of quercetin or oleuropein aglycone (and its derivatives) in the cytoplasm of the EVOO-PE14-treated cells (Table 2), points to these two components as apoptosis inducers in HT29 and SW480 cells. It seems reasonable to assume that the absence of quercetin, the flavonoid most commonly related to apoptosis, in the cytoplasm of HT29 EVOO-PE14-treated cells (Table 2), could be responsible for the lower degree of apoptosis found in these cells (10%) with respect to that observed in the SW480 cells (14%). Metabolic derivatives of quercetin and oleuropein aglycone, such as those listed in Table 2, might also be involved in the induction of apoptosis. In addition to the antiproliferative activity shown by individual phenolic compounds against colon-cancer-cell lines, synergic effects leading to apoptosis between the compounds listed in Table 2 cannot be ruled out.

Although the present work demonstrates the antiproliferative and pro-apoptotic activities of olive-oil extracts on colon-cancer cells, new experimental studies are needed to clarify the molecular and cellular mechanisms underlying the dietary benefits of olive-oil consumption with respects to human cancer.

4. Concluding remarks

New and powerful analytical tools able to characterize the cellular metabolites are needed to elucidate the action mechanism of phenolic compounds in cancer cells. In the present work, the cellular uptake and metabolism of olive-oil polyphenols in human colon adenocarcinoma cells are evaluated, taking advantage of the sensitivity of the nanoLC-ESI-TOF-MS. This analytical platform has demonstrated its potential in the analysis of small molecules in biological fluids. The analysis of culture medium and cytoplasm suggests that some compounds, mainly quercetin and oleuropein aglycone (and its derivatives), are the main compounds exerting an antiproliferative effect in SW480 and HT29 cell lines. These metabolites could affect some signaling pathways and cause apoptosis, promoting the entry into subG1 phase.

Conflict of interest

The authors have declared no conflict of interest.

Acknowledgements

The authors are grateful to the Spanish Ministry of Education and Science for the projects AGL2008-05108-C03-03 and AGL2011-29857-C03-02 and to Andalusian Regional Government Council of Innovation and Science for the projects P07-AGR-02619, P09-CTS-4564 and P10-FQM-6563.

References

- [1] C. Pelucchi, C. Bosetti, E. Negri, L. Lipworth, C. La Vecchia, Olive oil and cancer risk: an update of epidemiological findings through 2010, *Curr. Pharm. Des.* 17 (2011) 805–812.
- [2] E. Escrich, M. Solanas, R. Moral, I. Costa, L. Grau, Are the olive oil and other dietary lipids related to cancer? Experimental evidence, *Clin. Transl. Oncol.* 8 (2006) 868–883.
- [3] R.W. Owen, A. Giacosa, W.E. Hull, R. Haubner, B. Spiegelhalder, H. Bartsch, The antioxidant/anticancer potential of phenolic compounds isolated from olive oil, *Eur. J. Cancer.* 36 (2000) 1235–1247.
- [4] J. Lozano-Sanchez, A. Segura-Carretero, J.A. Menendez, C. Oliveras-Ferraras, L. Cerretani, A. Fernandez-Gutierrez, Prediction of extra virgin olive oil varieties through their phenolic profile. Potential cytotoxic activity against human breast cancer cells, *J. Agric. Food Chem.* 58 (2010) 9942–9955.
- [5] D. Arraez-Roman, S. Sawalha, A. Segura-Carretero, J. Menendez, A. Fernandez-Gutierrez, Identification of phenolic compounds in olive leaves using CE-ESI-TOF-MS, *Agro Food Ind. Hi-Tech.* 19 (2008) 18–22.
- [6] T.G. Sotiroudis, S.A. Kyrtopoulos, A. Xenakis, G.T. Sotiroudis, Chemopreventive potential of minor components of olive oil against cancer, *Ital. J. Food Sci.* 15 (2003) 169–185.
- [7] J.A. Menéndez, A. Vazquez-Martin, C. Oliveras-Ferraras, R. Garcia-Villalba, A. Carrasco-Pancorbo, A. Fernandez-Gutierrez, A. Segura-Carretero, Extra-virgin olive oil polyphenols inhibit HER2 (erbB-2)-induced malignant transformation in human breast epithelial cells: relationship between the chemical structures of extra-virgin olive oil secoiridoids and lignans and their inhibitory activities on the tyrosine kinase activity of HER2, *Int. J. Oncol.* 34 (2009) 43–51.
- [8] R. García-Villalba, A. Carrasco-Pancorbo, G. Zurek, M. Behrens, C. Baessmann, A. Segura-Carretero, A. Fernández-Gutiérrez, Nano and rapid resolution liquid chromatography–electrospray ionization-time of flight mass spectrometry to identify and quantify phenolic compounds in olive oil, *J. Sep. Sci.* 33 (2010) 2069–2078.
- [9] C. Manna, P. Galletti, G. Maisto, V. Cucciolla, S. D'Angelo, V. Zappia, Transport mechanism and metabolism of olive oil hydroxytyrosol in CaCo-2 cells, *FEBS Lett.* 470 (2000) 341–344.
- [10] L. Goya, R. Mateos, L. Bravo, Effect of the olive oil phenol hydroxytyrosol on human hepatoma HepG2 cells – protection against oxidative stress induced by tert-butylhydroperoxide, *Eur. J. Nutr.* 46 (2007) 70–78.
- [11] A. Jemal, T. Murray, E. Ward, A. Samuels, R.C. Tiwari, A. Ghafoor, E.J. Feuer, M.J. Thun, *Cancer statistics, 2005, CA-Cancer J. Clin.* 55 (2005) 10–30.
- [12] S.A. Bingham, N.E. Day, R. Luben, P. Ferrari, N. Slimani, T. Norat, F. Clavel-Chapelon, E. Kesse, A. Nieters, H. Boeing, A. Tjonneland, K. Overvad, C. Martinez, M. Dorronsoro, C.A. Gonzalez, T.J. Key, A. Trichopoulou, A. Naska, P. Vineis, R. Tumino, V. Krogh, H.B. Bueno-de-Mesquita, P.H.M. Peeters, G. Berglund, G. Hallmans, E. Lund, G. Skeie, R. Kaaks, E. Riboli, Dietary fibre in food and protection against colorectal cancer in the European Prospective Investigation into Cancer and Nutrition (EPIC): an observational study, *Lancet* 361 (2003) 1496–1501.
- [13] Y.Z.H. Hashim, I.R. Rowland, H. McGlynn, M. Servili, R. Selvaggini, A. Taticchi, S. Esposto, G. Montedoro, L. Kaisalo, K. Wahala, C.I.R. Gill, Inhibitory effects of olive oil phenolics on invasion in human colon adenocarcinoma cells in vitro, *Int. J. Cancer* 122 (2008) 495–500.
- [14] M. Notarnicola, S. Pisanti, V. Tutino, D. Bocale, M.T. Rotelli, A. Gentile, V. Memeo, M. Bifulco, E. Perri, M.G. Caruso, Effects of olive oil polyphenols on fatty acid synthase gene expression and activity in human colorectal cancer cells, *Genes Nutr.* 6 (2011) 63–69.
- [15] K.E. Karlsson, M. Novotny, Separation efficiency of slurry-packed liquid-chromatography microcolumns with very small inner diameters, *Anal. Chem.* 60 (1988) 1662–1665.
- [16] J.P.C. Vissers, Recent developments in microcolumn liquid chromatography, *J. Chromatogr. A* 856 (1999) 117–143.
- [17] C. Legido-Quigley, N.W. Smith, D. Mallet, Quantification of the sensitivity increase of a micro-high-performance liquid chromatography–electrospray ionization mass spectrometry system with decreasing column diameter, *J. Chromatogr. A* 976 (2002) 11–18.
- [18] A.M. Gómez Caravaca, A. Carrasco Pancorbo, B. Cañabate Díaz, A. Segura Carretero, A. Fernández Gutiérrez, Electrophoretic identification and quantitation of compounds in the polyphenolic fraction of extra-virgin olive oil, *Electrophoresis* 26 (2005) 3538–3551.
- [19] E. Carrasco-García, M. Saceda, S. Grasso, L. Rocamora-Reverte, M. Conde, Á. Gómez-Martínez, P. García-Morales, J.A. Ferragut, I. Martínez-Lacaci, Small tyrosine kinase inhibitors interrupt EGFR signaling by interacting with erbB3 and erbB4 in glioblastoma cell lines, *Exp. Cell Res.* 317 (2011) 1476–1489.
- [20] S. Kuo, Antiproliferative potency of structurally distinct dietary flavonoids on human colon cancer cells, *Cancer Lett.* 110 (1996) 41–48.
- [21] W.K. Kim, M.H. Bang, E.S. Kim, N.E. Kang, K.C. Jung, H.J. Cho, J.H.Y. Park, Quercetin decreases the expression of ErbB2 and ErbB3 proteins in HT-29 human colon cancer cells, *J. Nutr. Biochem.* 16 (2005) 155–162.
- [22] C.P.R. Xavier, C.F. Lima, A. Preto, R. Seruca, M. Fernandes-Ferreira, C. Pereira-Wilson, Luteolin, quercetin and ursolic acid are potent inhibitors of proliferation and inducers of apoptosis in both KRAS and BRAF mutated human colorectal cancer cells, *Cancer Lett.* 281 (2009) 162–170.



- [23] R. Narayansingh, R.A.R. Hurta, Cranberry extract and quercetin modulate the expression of cyclooxygenase-2 (COX-2) and I kappa B alpha in human colon cancer cells, *J. Sci. Food Agric.* 89 (2009) 542–547.
- [24] T. Nguyen, E. Tran, T. Nguyen, P. Do, T. Huynh, H. Huynh, The role of activated MEK-ERK pathway in quercetin-induced growth inhibition and apoptosis in A549 lung cancer cells, *Carcinogenesis* 25 (2004) 647–659.
- [25] A. Belen Granado-Serrano, M. Angeles Martin, L. Bravo, L. Goya, S. Ramos, Quercetin induces apoptosis via caspase activation, regulation of Bcl-2, and inhibition of PI-3-kinase/Akt and ERK pathways in a human hepatoma cell line (HepG2), *J. Nutr.* 136 (2006) 2715–2721.
- [26] J. Duraj, K. Zazrivcova, J. Bodo, M. Sulikova, J. Sedlak, Flavonoid quercetin, but not apigenin or luteolin, induced apoptosis in human myeloid leukemia cells and their resistant variants, *Neoplasma* 52 (2005) 273–279.
- [27] H. Kim, S. Kim, B. Kim, S. Lee, Y. Park, B. Park, S. Kim, J. Kim, C. Choi, J. Kim, S. Cho, J. Jung, K. Roh, K. Kang, J. Jung, Apoptotic effect of quercetin on HT-29 colon cancer cells via the AMPK signaling pathway, *J. Agric. Food Chem.* 58 (2010) 8643–8650.
- [28] C.H. Park, J.Y. Chang, E.R. Hahm, S. Park, H.K. Kim, C.H. Yang, Quercetin, a potent inhibitor against beta-catenin/Tcf signaling in SW480 colon cancer cells, *Biochem. Biophys. Res. Commun.* 328 (2005) 227–234.









BLOQUE III.

Hibiscus sabdariffa







CAPÍTULO 7. Quantification of the polyphenolic fraction and *in vitro* antioxidant and *in vivo* anti-hyperlipemic activities of *Hibiscus sabdariffa* aqueous extract.





Contents lists available at ScienceDirect

Food Research International

journal homepage: www.elsevier.com/locate/foodres

Quantification of the polyphenolic fraction and *in vitro* antioxidant and *in vivo* anti-hyperlipemic activities of *Hibiscus sabdariffa* aqueous extract

Salvador Fernández-Arroyo^{a,b}, Inmaculada C. Rodríguez-Medina^{a,b}, Raúl Beltrán-Debón^c, Federica Pasini^e, Jorge Joven^c, Vicente Micol^d, Antonio Segura-Carretero^{a,b,*}, Alberto Fernández-Gutiérrez^{a,b}

^a Department of Analytical Chemistry, University of Granada, Avda. Fuentenueva s/n, 18003 Granada, Spain

^b Functional Food Research and Development Center, Health Science Technological Park, Avenida del Conocimiento s/n, E-18100 Granada, Spain

^c Centre de Recerca Biomèdica, Hospital Universitari Sant Joan de Reus, IISPV-Institut d'Investigació Sanitària Pere Virgili, Universitat Rovira i Virgili, C/Sant Joan s/n, 43201 Reus (Tarragona), Spain

^d Molecular and Cellular Biology Institute, University Miguel Hernández, Avda. de la Universidad, s/n, 03202 Elche (Alicante), Spain

^e Dipartimento di Scienze degli Alimenti (DISA), Università degli Studi di Bologna, Piazza Goidanich 60, Cesena (FC) Italy

ARTICLE INFO

Article history:

Received 9 December 2010

Received in revised form 14 March 2011

Accepted 20 March 2011

Keywords:

Hibiscus sabdariffa
HPLC-DAD/ESI-TOF-MS
Polyphenols
Antioxidant capacity
Anti-hyperlipemic activity

ABSTRACT

In the present study the quantification of the polyphenolic fraction, anthocyanins and other polar compounds, the antioxidant capacity and the anti-hyperlipemic action of the aqueous extract of *Hibiscus sabdariffa* has been achieved. Seventeen compounds were successfully quantified either by HPLC-DAD or HPLC-ESI-TOF-MS. Six of them were directly quantified by their corresponding standards, whereas the rest were indirectly quantified as equivalents using standards of similar compounds. The antioxidant capacity have also been estimated by comparing different assays, i.e. Trolox equivalent antioxidant capacity (TEAC), ferric reducing antioxidant power (FRAP), oxygen radical absorbance capacity (ORAC), and measurement of thiobarbituric acid reacting substances (TBARS). *H. sabdariffa* showed high reducing capacity in FRAP assay and significant capability to scavenge peroxyl radicals in the ORAC assay. Nevertheless, the extract exhibited poor efficacy to inhibit peroxyl radicals in lipid systems. The plant extract also exhibited the capacity to decrease serum triglyceride concentration on hyperlipemic mouse model.

© 2011 Elsevier Ltd. All rights reserved.

1. Introduction

The *Hibiscus sabdariffa* L. (family: *Malvaceae*), usually named bissap, karkade or roselle is a tropical plant commonly used as local soft drink. It is highly appreciated all over the world for the particular sensation of freshness conveyed. Traditionally, it has been used effectively against hypertension, inflammation, and liver disorders (Wang et al., 2000). Previous studies showed that *H. sabdariffa* possesses anti-tumoral, anti-oxidant and anti-hyperlipemic activities (Chen et al., 2003; Hou, Tong, Terahara, Luo, & Fujii, 2005; Kao et al., 2009; Lin, Huang et al., 2007; Lin, Lin et al., 2007; Tseng et al., 1997, 2000). Recently, it was reported that the extract of *H. sabdariffa* inhibited the LDL oxidation and lowered serum triglycerides, cholesterol and LDL-cholesterol in animal models (Chen et al., 2003; Lin, Huang et al., 2007; Lin, Lin et al., 2007). Histological examination revealed that it could reduce foam cell formation and inhibit VSMC proliferation and migration, suggesting the anti-atherosclerotic effect of *H. sabdariffa*. In addition, studies on humans show the anti-

hypertensive and anti-inflammatory effects of *H. sabdariffa* consumption (Beltrán-Debón et al., 2010; Herrera-Arellano, Flores-Romero, Chavez-Soto, & Tortoriello, 2004). The brilliant red color and unique flavor make it a valuable food product. The anthocyanin pigments that create the color (Tsai & Ou, 1996) are responsible for the wide range of coloring in many foods. The *H. sabdariffa* petals are potentially a good source of antioxidant agents as anthocyanins (Segura-Carretero et al., 2008). Overall, there is now increasing evidence that antioxidants in the human diet are of major benefit for health and well-being. The antioxidant properties of *H. sabdariffa* and other hibiscus species have been widely studied (Büyükbalci & El, 2008; Oboh & Rocha, 2008; Vankar & Srivastava, 2008).

In this work we focused on quantifying the phenolic fraction, anthocyanins and other polar compounds in the aqueous extract of *H. sabdariffa*. This quantification was achieved using two detection systems, i.e. RP-HPLC coupled to DAD or RP-HPLC coupled to ESI-TOF-MS. Recently, the qualitative characterization of the compounds present in the aqueous extract of *H. sabdariffa* was carried out successfully (Rodríguez-Medina et al., 2009). These methods were also suitable for the quantification of these substances. To evaluate the antioxidant capacities of foods, numerous *in vitro* methods have been developed and reviewed. However, there has not been a consensus for the preferred method. ORAC (Oxygen Radical Absorbance Capacity),

* Corresponding author at: Functional Food Research and Development Center, Health Science Technological Park, Avenida del Conocimiento s/n, E-18100 Granada, Spain. Tel.: +34 958 243296; fax: +34 958 249510.

E-mail address: ansegura@ugr.es (A. Segura-Carretero).



TBARS (Thiobarbituric Acid Reactive Substances), TEAC (Trolox Equivalent Antioxidant Capacity) and FRAP (Ferric Reducing Antioxidant Power) assays are among the more popular methods that have been used (Wua et al., 2004). Advantages and disadvantages of these methods have been fully discussed in several reviews (Frankel & Meyer, 2000; Prior, Wu, & Schaich, 2005; Sánchez-Moreno, 2002; Strube, Haenen, Van Den Berg, & Bast, 1997). In this work we have studied the antioxidant capacity of *H. sabdariffa* aqueous extract using four different methods TEAC and FRAP (based on electron transference) vs. TBARS and ORAC (based on hydrogen atom transference) (Huang, Ou, & Prior, 2005). To further assess *H. sabdariffa* aqueous extract bioactivity, it was administered as sole drinking fluid to mice fed with a high fat-high cholesterol diet in order to assay its anti-hyperlipemic effects.

2. Materials and methods

2.1. Chemicals and reagents

All chemicals were of analytical HPLC reagent grade and used as received. Formic acid and acetonitrile used for preparing mobile phases were purchased from Fluka, Sigma-Aldrich (Steinheim, Germany) and Lab-Scan (Gliwice, Sowińskiego, Poland) respectively. Solvents were previously filtered using a Solvent Filtration Apparatus 58061 (Supelco, Bellefonte, PA, USA). The standards, for the calibration curves, chlorogenic acid, quercetin 3-rutinoside, quercetin 3-glucoside, kaempferol 3-O-rutinoside and kaempferol 3-(*p*-coumaroylglucoside), quercetin, 4-hydroxycoumarin and delphinidin-3-sambubioside were purchased either from Fluka, Extrasynthese (Genay Cedex, France) or Polyphenols (Polyphenols Laboratories AS, Hanaveien Sandnes, Norway). The stock solutions containing these analytes were prepared in methanol (Lab-Scan). The reagents to measure the antioxidant capacity, EYPC (egg yolk phosphatidylcholine), AAPH (2,2'-Azobis (2-methyl-propionamide) dihydrochloride), BHT (butylhydroxytoluene), TEP (1,1',3,3'-tetraethoxypropane), SDS (Sodium Dodecyl Sulfate), TBA (thiobarbituric acid), TPTZ (Tripyridyltriazine), ABTS (2,2'-azinobis (3-ethylbenzothiazoline-6-sulphonate), fluorescein, Trolox and ferric sulfate were purchased from Sigma-Aldrich. Sodium acetate, ferric chloride, sodium chloride, hydrochloric acid, sulphuric acid, acetic acid, chloroform, ethanol, TRIS (Tris(hydroxymethyl)aminomethane) were purchased from Panreac (Barcelona, Spain).

2.2. Sample preparation

The *H. sabdariffa* plant was originally from the village of Guerle in Senegal. It was kindly provided by Centre de Recerca Biomèdica, Hospital Universitari de Sant Joan (Reus, Tarragona, Spain). The dry calices from the plant were manually mill grounded and mixed with ultrapure water, up to a concentration of 25 g/l, stirred it in vortex until dissolved, filtered with units of single use Filters Millex (Millipore, Bedford, MA, USA) and directly injected into the HPLC system for the direct and indirect quantifications. On the other hand, the aqueous extract of *H. sabdariffa* for the different antioxidant capacity determinations was conveniently diluted in order to comply with the working range of each spectrophotometric method.

2.3. Instrumentation

HPLC analyses were performed with a RRLC 1200 series (Agilent Technologies, Palo Alto, CA), equipped with a binary pump with Zorbax Eclipse Plus C₁₈ 4.6 × 150 mm, 1.8 μm column. Prefilters were used as precolumn, RRLC in-line filters, 4.6 mm, 0.2 μm supplied by Agilent Technologies. The mobile phase flow rate was 0.5 ml min⁻¹. HPLC was equipped with DAD and coupled to a TOF mass spectrometer equipped with an orthogonal electrospray interface

ESI (model G1607A from Agilent Technologies, Palo Alto, CA, USA) operating in negative mode and positive mode of ionization. (MS-Instrument: microTOF, ESI-TOF mass spectrometer) (Bruker Daltonik GmbH, Bremen, Germany). Fluorescence (ORAC and TBARS) and absorbance (FRAP and TEAC) measures were carried out on a spectrofluorimeter Polarstar Omega (BMG Labtechnologies, GMBH; Offenburg, Germany) (Thermostated at 37 °C for the ORAC assay).

2.4. Chromatographic, UV and spectrophotometric conditions

The compounds of the aqueous extract of *H. sabdariffa* were separated by the C18 column at room temperature at a flow rate of 0.5 ml/min and the injection volume was 10 μl for both gradient elution programs. The use of the prefilters as guard column also provided some protection against decomposition and blocking of the working column. The linear gradient used for the analysis, separation and identification of the polyphenols, hydroxycitric acid and its lactone (gradient program 1) was as follow: Mobile phases: A: water/ACN (acetonitrile) 90:10 (1% HCOOH) and B: ACN. The linear gradient elution program was run as stated: 0 min, 5% (B); 20 min 20% (B); 25 min 40% (B); 30 min 5% (B); 35 min, isocratic of B 5%. Anthocyanins, due to their acid-base equilibrium, needed lower pH to be resolved, and a different chromatographic method (gradient program 2) was employed. Solvents that constituted the mobile phases were: A, water (10% HCOOH) and B, ACN. The applied elution conditions were: 0 min, 0% (B); 13 min 20% (B); 20 min 30% (B); 25 min 80% (B); 30 min 0% (B); 35 min, isocratic of B 0%. The DAD coupled to the HPLC system was set in a spectrum range starting at 190 nm and ending at 950 nm. The excitation and emission wavelengths were 485 and 520 nm respectively for the ORAC assay, whereas these sets were 500 and 530 nm for the TBARS determination. The absorbance wavelength for FRAP and TEAC assays were 593 and 734 nm respectively.

2.5. ESI-TOF-MS conditions

TOF-MS transfer parameters were optimized by direct infusion experiments with Tunning mix (Agilent Technologies). The trigger time was set to 53 s (50 s for setting transfer time and 3 s for pre-pulse storage time), corresponding to a mass range of 50–1000 *m/z*. The other optimum values of the ESI-MS parameters were capillary, 4500 V gas heater temperature, 200 °C; drying gas flow, 7 l/min; nebulizing gas pressure, 1.5 bar and the spectra rate was 1 Hz. At this stage the use of a splitter was required to the coupling with the MS detector as the flow which arrived to the ESI-micro-TOF detector had to be 0.25 ml/min in order to obtain reproducible results. The TOF mass spectrometer was equipped with an ESI interface operating in both, negative and positive, polarity modes. To tune the detector to optimal conditions calibration was performed with sodium formate clusters (5 mM sodium hydroxide in water/isopropanol 1/1 (v/v), with 0.2% (v/v) of formic and acetic acids) in quadratic + high precision calibration (HPC) regression mode. The calibration solution was injected at the beginning of the run and all the spectra were calibrated prior the polyphenol identification. The accurate mass data for the molecular ions were processed using the software DataAnalysis 4.0 (Bruker Daltonik), which provided a list of possible elemental formula by using the GenerateMolecularFormula™ editor. The GenerateFormula™ editor uses the sigmaFit™ algorithm, CHNO algorithm, which provides standard functionalities such as minimum/maximum elemental range, electron configuration and ring plus double bonds equivalents, as well as a sophisticated comparison of the theoretical with the measured isotope pattern (SigmaValue™) for increased confidence in the suggested molecular form (Bruker Daltonik, Technical Note 008; Rodríguez-Medina et al., 2009). The use of isotopic abundance patterns as a single further constraint removes >95% of false candidates. This orthogonal filter can condense



several thousand candidates down to only a small number of molecular formulas.

2.6. Antioxidant capacity assays

The Trolox equivalent antioxidant capacity (TEAC) assay, which measures the reduction of the ABTS radical cation by antioxidants, was based on method previously described by Miller, Rice-Evans, Davies, Gopinathan, and Milner (1993) and Re et al. (1999) and performed as in Laporta, Pérez-Fons, Mallavia, Caturla, and Micol (2007). The quantitative evaluation of the antioxidant capacity of the compounds against lipid peroxidation was determined through thiobarbituric acid reactive substances (TBARS) assay. Small unilamellar vesicles (SUVs) were prepared as previously described (Caturla, Vera-Samper, Villalaín, Reyes-Mateo, & Micol, 2003). Then, TBARS assay was performed as in Laporta et al. (2007). To assay the capacity of the extracts to scavenge peroxy radicals a validated ORAC method, which uses fluorescein (FL) as the fluorescent probe (ORAC_{FL}), was utilized (Ou, Hampsch-Woodill, & Prior, 2001) and performed as in Laporta et al. (2007). The final ORAC values were calculated by using a regression equation between the Trolox concentration and the net area of the FL decay curve (area under curve, AUC) as previously described (Ou et al., 2001). The ferric reducing antioxidant power (FRAP) was performed according to Al-Duais, Müller, Böhm, and Jetschke (2009). Ferrous sulfate solutions (0–300 µM) were used for calibration.

2.7. Hypolipemic effect of *H. sabdariffa*

Male LDLr^{-/-} mice (n=32) were purchased from the Jackson Laboratory (Bar Harbor, Me). In accordance with our institutional guidelines, animals were housed under standard conditions and given a commercial mouse diet (14% Protein Rodent Maintenance diet, Harlan, Barcelona, Spain). At 10-weeks of age, animals were distributed into two dietary experimental groups (n=16/group). One group was feed with the same maintenance diet (Chow diet, 3% fat and 0.03% cholesterol, w/w) and the other group was feed with a Western-type diet (High fat diet, 20% fat and 0.25% cholesterol, w/w). Each dietary group was divided into two groups (n=8). One of them consumed water during the study while the second group consumed only *H. sabdariffa* aqueous extract at final concentration of 10 g/l. Plant calyxes were grounded and heated until boil in tap water. Infusion was then cooled down to room temperature and filtered to discard insoluble fraction. Extract was prepared freshly every two days and liquid in both groups was administered *ad libitum*. Animals were

sacrificed at 24-weeks of age. The size of the experiment was planned according to previous data (Joven et al., 2007) and the animals were randomly assigned into experimental groups. Autoanalyser Synchron LXi 725 system (Beckman Coulter, IZASA, Barcelona, Spain) was used to determine cholesterol and triglyceride serum concentrations. SPSS/PC + 15.0 (SPSS, Chicago, IL) software was used and differences between groups were analyzed using U Mann–Whitney test with the level of significance set at p<0.05.

3. Results and discussion

3.1. HPLC-UV and HPLC-ESI-TOF-MS quantification

3.1.1. Sensitivity and repeatability

The sensitivity of the method was studied by defining the limits of detection (LODs) and limits of quantification (LOQs) for individual compounds in standard solutions for the UV spectra measured at the optimum wavelength. Four different wavelengths were considered at 325, 312, 350, 370 and 520 nm for the different compounds, except for the determination of the hydroxycitric acid and its lactone, the hibiscus acid in which the MS detection, based in the extract ion chromatogram, was used to measure the area peaks as the two above compounds did not present a measurable absorbance. Table 1 indicates the way the areas were obtained for the different analytes in terms of the detection system used in order to obtain the calibration curves, as well as molecular formula, *m/z* and UV–vis absorption bands of each compound from *H. sabdariffa* aqueous extract. Table 2 summarizes the analytical parameters for the different compounds present in the aqueous extract of *H. sabdariffa*. Seven standards were available and the rest of the compounds were expressed as equivalent of those, except for the hydroxycitric and hibiscus acids which were expressed as equivalents of caffeic acid (not present in the aqueous extract of *H. sabdariffa*, but used as standard for the quantification of these two compounds). Calibration curves were obtained for each standard with high linearity ($r^2 > 0.99$) by plotting the standard concentration as a function of the peak area obtained from HPLC–UV and HPLC–ESI–TOF–MS analyses. The limit of detection (LOD) and the limit of quantification (LOQ) were calculated according to IUPAC recommendation (Currie, 1995). Intraday and interday precisions were developed to evaluate the repeatability of HPLC–UV and HPLC–ESI–TOF–MS methods. A sample of the aqueous extract was injected (n=2) on the same day (intraday precision) for 3 consecutive days (interday precision, n=6). The intraday repeatability of peak area, expressed as the RSD, varied between the interval of 0.16% and 4.6% whereas the interday repeatability was between 0.87% and 6.12%.

Table 1
Molecular formula, [M–H]⁻, UV–vis absorption bands and used technique for the quantification of each compound in *H. sabdariffa* aqueous extract.

Compound	Molecular formula	[M–H] ⁻	UV–vis (nm)	Quantification technique
Hydroxycitric acid	C ₆ H ₈ O ₈	207.0140	–	MS-TOF (m/z 207)
Hibiscus acid	C ₆ H ₆ O ₇	189.0035	–	MS-TOF (m/z 189)
Chlorogenic acid (isomer I)	C ₁₆ H ₁₈ O ₉	353.0891	297, 324	DAD-UV (325 nm)
Chlorogenic acid	C ₁₆ H ₁₈ O ₉	353.0872	297, 324	DAD-UV (325 nm)
Chlorogenic acid (isomer II)	C ₁₆ H ₁₈ O ₉	353.0871	297, 324	DAD-UV (325 nm)
Myricetin-3-arabinogalactose	C ₂₆ H ₂₈ O ₁₇	611.1271	352	DAD-UV (350 nm)
Quercetin-3-sambubioside	C ₂₆ H ₂₈ O ₁₆	595.1309	345	DAD-UV (350 nm)
5-O-Caffeoylshikimic acid	C ₁₆ H ₁₆ O ₈	335.0768	296, 326	DAD-UV (325 nm)
Quercetin-3-rutinoside	C ₂₇ H ₃₀ O ₁₆	609.1462	255, 353	DAD-UV (350 nm)
Quercetin-3-glucoside	C ₂₁ H ₂₀ O ₁₂	463.0873	253, 356	DAD-UV (350 nm)
Kaempferol-3-O-rutinoside	C ₂₇ H ₃₀ O ₁₅	593.1512	265, 350	DAD-UV (350 nm)
N-Feruloyltyramine	C ₁₈ H ₂₀ NO ₄	312.1234	286, 316	DAD-UV (325 nm)
Kaempferol-3-(p-coumarylglucoside)	C ₃₀ H ₂₆ O ₁₃	593.1312	312	DAD-UV (312 nm)
Quercetin	C ₁₅ H ₁₀ O ₇	301.0339	253, 372	DAD-UV (370 nm)
7-Hydroxycoumarin	C ₉ H ₆ O ₃	161.0244	300	DAD-UV (300 nm)
Delphinidin-3-sambubioside	C ₂₆ H ₃₀ O ₁₆	595.1446	280, 520	DAD-UV (520 nm)
Cyanidin-3-sambubioside	C ₂₆ H ₃₀ O ₁₅	579.1493	280, 520	DAD-UV (520 nm)

**Table 2**

Calibration and standard deviation data, where RSD is the relative standard deviation, LOD is the limit of detection and LOQ is the limit of quantification. LOD and LOQ values were calculated for the available standards solely.

Analyte	RSD intraday	RSD interday	LOD (µg/ml)	LOQ (µg/ml)	Calibration range (µg/ml)	Calibration equations	r ²
Hydroxycitric acid	4.619	4.797	–	–	100–1000	Y = 1214164.4 X + 649809.3	0.9958
Hibiscus acid	3.607	3.626	–	–	100–1000	Y = 1214164.4 X + 649809.3	0.9958
Chlorogenic acid isomer I	1.575	2.266	–	–	5–100	y = 5268.2 X – 119.8	0.9951
Chlorogenic acid	0.707	2.011	0.235	0.782	5–100	y = 5268.2 X – 119.8	0.9951
Chlorogenic acid isomer II	1.977	1.629	–	–	5–100	y = 5268.2 X – 119.8	0.9951
Myricetin 3-arabinogalactose	1.714	4.384	–	–	0.5–10	Y = 3737.3 X – 5.0	0.9993
Quercetin 3-sambubioside	0.601	1.939	–	–	0.5–10	Y = 3737.3 X – 5.0	0.9993
5-O-Caffeoylshikimic acid	0.788	4.037	–	–	0.5–10	Y = 4313.0 X – 14.1	0.9958
Quercetin 3-rutinoside	1.197	0.876	0.116	0.386	5–100	Y = 3750.4 X + 26.0	0.9991
Quercetin 3-glucoside	1.93	1.501	0.102	0.341	0.5–10	Y = 4642.0 X – 6.0	0.9996
Kaempferol 3-O-rutinoside	3.084	2.477	0.088	0.293	0.5–10	Y = 4516.1 X – 4.6	0.9994
N-Feruloyltyramine	1.13	1.819	–	–	0.5–10	Y = 4313.0 X – 14.1	0.9958
Kaempferol 3-(p-coumarylglucoside)	1.837	1.698	0.086	0.288	0.5–10	Y = 6660.9 X – 19.4	0.9967
Quercetin	1.849	1.658	0.048	0.156	0.5–10	Y = 8831.1 X – 22.0	0.9988
7-Hydroxycoumarin	0.341	1.377	–	–	1–100	Y = 7451.0 X – 74.2	0.9961
Delphinidin 3-sambubioside	0.658	6.128	0.184	0.612	1–100	Y = 3418.9 X + 9.1	0.9983
Cyanidin 3-sambubioside	0.162	2.025	–	–	1–100	Y = 3418.9 X + 9.1	0.9983

3.1.2. Calibration curves

In order to quantify the amount of each compound in the aqueous extract of *H. sabdariffa*, seven calibration curves were prepared with the seven standards available, chlorogenic acid, quercetin 3-rutinoside (rutin), quercetin 3-glucoside, kaempferol 3-O-rutinoside, kaempferol 3-(p-coumarylglucoside), quercetin, 4-hydroxycoumarin and delphinidin 3-sambubioside. The other compounds, for which no commercially standards were available, were tentatively quantified on basis of the other compounds bearing similar structures. 7-Hydroxycoumarin was quantified with 4-hydroxycoumarin. A calibration curve of caffeic acid was also prepared for the quantification of hydroxycitric acid and its lactone, the hibiscus acid. The ranges are also stated in Table 2, including the RSD values obtained for two replicates of each calibration point. The calibration plots indicate good correlation between peak areas and the analyte concentrations. All calibration curves showed good linearity in the studied range of concentration. Regression coefficients were higher than 0.99 for all the compounds and for the considered ranges. All the features of the proposed method are summarized in Tables 1 and 2.

3.1.3. Quantification of compounds in the aqueous extract of *H. sabdariffa*

A previous method optimized in our laboratory was applied to the quantification of the seventeen compounds qualitatively characterized and present in the aqueous extract of *H. sabdariffa* (Rodríguez-Medina et al., 2009). The concentration of the extract was set at 25 g/l

Table 3

Quantification of polyphenolic fraction from *H. sabdariffa* aqueous extract, expressed in ppm (m/m).

Analyte	<i>Hibiscus sabdariffa</i>
Hydroxycitric acid	8288.03 ± 397.63
Hibiscus acid	31122.02 ± 1128.39
Chlorogenic acid isomer I	2755.15 ± 62.42
Chlorogenic acid	1923.72 ± 38.69
Chlorogenic acid isomer II	1041.19 ± 16.96
Myricetin 3-arabinogalactose	57.32 ± 2.51
Quercetin 3-sambubioside	304.02 ± 5.90
5-O-Caffeoylshikimic acid	171.47 ± 6.92
Quercetin 3-rutinoside	495.70 ± 4.34
Quercetin 3-glucoside	143.74 ± 2.16
Kaempferol 3-O-rutinoside	91.86 ± 2.28
N-Feruloyltyramine	98.97 ± 1.80
Kaempferol 3-(p-coumarylglucoside)	28.37 ± 0.48
Quercetin	121.24 ± 2.01
7-Hydroxycoumarin	1839.20 ± 25.34
Delphinidin 3-sambubioside	2701.21 ± 165.55
Cyanidin 3-sambubioside	1939.15 ± 39.27

in all the cases in order to fix in the considered working ranges. Two replicates of the extract in three consecutive days were carried out and the results, expressed in mg analyte/Kg of dry weighted extract (n = 6; value = X ± SD), are summarized in Table 3.

3.2. Antioxidant capacity

Four different methods were used to evaluate the antioxidant capacity of the aqueous extract of *H. sabdariffa* utilized in this study. TEAC and FRAP methods are based on electron transfer mechanisms (ET), i.e. reducing capacity. On the contrary, TBARS and ORAC methods are based on hydrogen atom transfer (HAT) reactions, which scavenge the generation of peroxy radicals through decomposition of azo compounds (Huang et al., 2005; Prior & Cao, 1999). Therefore, we tried to study deeply the performance of *H. sabdariffa* extract under these two different antioxidant mechanisms. *H. sabdariffa* aqueous extract was compared to another extract with proven antioxidant properties, i.e. olive leaf extract containing 25% oleuropein and also pomegranate extract (*Punica granatum* L.) which has a high content in anthocyanins (Alighourchi et al. 2008; Gil, Tomás-Barberán, Hess-Pierce, Holcroft, & Kader, 2000; Martin, Krueger, Rodríguez, Dreher, & Reed, 2008). Results are summarized in Table 4. As expected, *H. Sabdariffa* showed a different behavior in relation to olive leaf and pomegranate extracts depending on the antioxidant measurement considered.

TEAC value was higher for the olive leaf extract (0.92 vs. 0.16 mmol Trolox equivalent/g extract), indicating the lower reducing capacity of *H. sabdariffa* aqueous extract. However, the values obtained in the FRAP assay for *H. sabdariffa* aqueous extract doubled

Table 4

Results of antioxidant capacity assays.

ASSAY	<i>Hibiscus sabdariffa</i>	Olive leaf	Pomegranate
TEAC ^a	0.16 ± 0.005	0.92 ± 0.12 ^b	0.25 ± 0.02 ^c
FRAP ^d	2.31 ± 0.09	1.24 ± 0.02	1.68 ± 0.26 ^e
TBARS (IC ₅₀) ^f	163.66 ± 5.28	7.00 ± 1.20 ^b	32.40 ± 1.70 ^g
ORAC ^h	2307 ± 10	4950 ± 300 ⁱ	3210 ± 11 ^e

^a Expressed in mmol Trolox equivalent/g extract.

^b Data obtained from Funes et al. (2009).

^c Data obtained from Zhang, Wang, Lee, Henning, and Heber (2009).

^d Expressed in mmol FeSO₄ equivalent/g extract.

^e Data obtained from Madrigal-Carballo, Rodríguez, Krueger, Dreher, and Reed (2009).

^f Expressed in mg/l of extract able to inhibit 50% of lipid peroxidation.

^g Data obtained from Kulkarni, Aradhya, and Divakar (2004).

^h Expressed in µmol Trolox equivalent/g extract.

ⁱ Data obtained from Laporta et al. (2007).

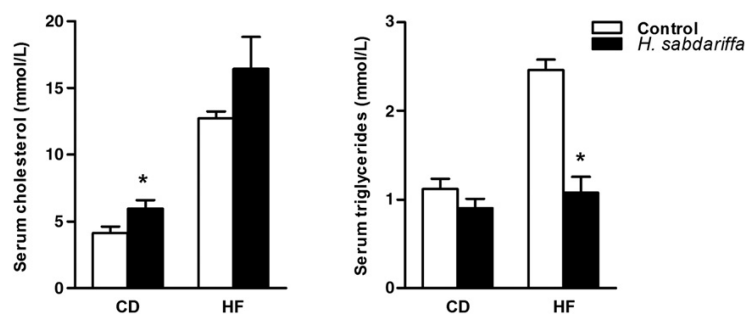


Fig. 1. Serum cholesterol and triglyceride concentrations were measured after treatment with *H. sabdariffa* extract. Cholesterol concentrations trend to increase in both dietary groups, but this difference was only significant in chow diet dietary group (CD). Serum triglyceride concentration was effectively reduced in both dietary groups, being significant in the high-fat diet (HF) fed animals. Differences are marked with * ($p < 0.05$).

those obtained for olive leaf extract, although this was also an ET-based assay too. The high FRAP value of the *H. sabdariffa* aqueous extract could be explained through the reported efficacy of chlorogenic acid and derivatives as reductants (De Leonardi, Pizzella, & Macciola, 2008; Wu, 2007), which are the main compounds in *H. sabdariffa* aqueous extract (Table 3).

Moreover, *H. sabdariffa* aqueous extract exhibited a significant ORAC value and a very low potency in the TBARS assay as revealed by its elevated IC₅₀ value (concentration of extract able to inhibit 50% of lipid peroxidation). Although both methods take place through HAT-based mechanisms, ORAC measures the capacity of antioxidants to scavenge peroxy radicals in a water environment, whereas TBARS assay determines the same capacity under a lipophilic environment, i.e. in the presence of a phospholipid membrane. Major antioxidant compounds in *H. sabdariffa* aqueous extract are chlorogenic acid derivatives and anthocyanins (delphinidin 3-sambubioside and cyanidin 3-sambubioside), which are highly hydrophilic antioxidants and hence these compounds may have worse interaction with lipid peroxy radicals that are the main radical species generated in the TBARS assay. It has been reported that delphinidin and cyanidin, which lack methoxy group in their B ring, are less antioxidant in lipid systems than malvidin or peonidin due to their higher polarity (Kähkönen & Heinonen, 2003). In addition, glycosylated flavonoids such as anthocyanins showed less antioxidant potency than their corresponding aglycones in lipid systems, since glycosylation decreases the access of the compound to the lipid phase what reinforces our hypothesis (Fukumoto & Mazza, 2000; Kähkönen & Heinonen, 2003).

The comparison of the *H. sabdariffa* aqueous extract vs. Pomegranate extract showed the similarity between the action mechanisms of the antioxidant capacity in TEAC and ORAC assays. However, the low value in FRAP assay could be due to the absence of chlorogenic acid in pomegranate extract. The low value for pomegranate extract in TBARS assay was due to the presence of ellagic acid and ellagitannins, which exhibit a high antioxidant capacity to prevent the lipid peroxidation (Yu, Chang, Wu, & Chian, 2005).

3.3. Effects of *H. sabdariffa* extract on serum lipid concentrations

H. sabdariffa hypolipemic effects were tested on low density lipoprotein receptor deficient mice (LDLr^{-/-}). Lipid metabolism has been largely studied on this animal model since these animals develop hyperlipemia when feed with hypercaloric diets.

Cholesterol and triglycerides concentration were measured in both dietary groups (chow diet, CD; high fat diet, HF) after 14 weeks of treatment. Serum cholesterol concentration increased in both dietary groups compared to the control, but this difference was only significant in those animals fed with chow diet (Fig. 1A). The strongest effect was observed on serum triglyceride concentration

when a high fat diet was fed. Serum triglycerides were reduced more than 50% in mice treated with *H. sabdariffa* infusion (Fig. 1B), compared to control. However, no change in serum triglycerides was observed in the chow diet group. Animals that consumed *H. sabdariffa* aqueous extract and were treated with high fat diet, showed a triglyceride concentration similar to that one observed in the chow diet group. Taken together, these results point to lipoprotein metabolism modulation by the *Hibiscus sabdariffa* extract. Triglyceride concentration reduction could be because a reduction in VLDL concentrations, the major triglyceride-containing lipoprotein. This effect could be observed in other polyphenol-rich plant extracts (Beltrán-Debón et al., 2010). On the other hand, the higher cholesterol concentration after *H. sabdariffa* treatment could be explained by an increase in LDL and HDL concentrations.

4. Concluding remarks

The proposed method exhibited excellent performance in the determination of the different families of phenolic compounds in *H. sabdariffa* plant material. The method used for the characterization of the aqueous extract of *H. sabdariffa* has been successfully validated and has proven to be suitable for quantification purposes. Using this method, seventeen main phenolic compounds in *H. sabdariffa* aqueous extract have been quantified. *H. sabdariffa* aqueous extract possesses a significant antioxidant capacity to reduce peroxy radicals by hydrogen atom transfer (ORAC). Moreover, *H. sabdariffa* exhibited a stronger capacity to donate electrons (FRAP) in the presence of metals than the strong antioxidant olive leaf extract (25% oleuropein). In addition, *H. sabdariffa* aqueous extract showed hypolipemic properties in a hyperlipemic mouse model through the reduction of 50% of serum triglyceride concentration under hypercaloric diet for several weeks.

Acknowledgments

This investigation has been supported by Grants P07-AGR-02619, P09-CTS-4564 AGL2007-60778 and AGL2008-05108-C03-03. RBD is a recipient of fellowship from the *Comissionat per a Universitats i Recerca del Departament d'Innovació, Universitats i Empresa de la Generalitat de Catalunya i del Fons Social Europeu*. The authors also thank Isabel Borrás, Jesús Lozano and Rosa Quirantes from the Analytical Chemistry department, University of Granada for their invaluable help.

References

- Alighourchi, H., Barzegar, M., & Abbasi, S. (2008). Anthocyanins characterization of 15 Iranian pomegranate (*Punica granatum* L.) varieties and their variation after cold storage and pasteurization. *European Food Research and Technology*, 227, 881–887.



- Al-Duais, M., Müller, L., Böhm, V., & Jatschke, G. (2009). Antioxidant capacity and total phenolics of *Cyphostemma digitatum* before and after processing: use of different assays. *European Food Research and Technology*, 228, 813–821.
- Beltrán-Debón, R., Alonso-Villaverde, C., Aragónes, G., Rodríguez-Medina, I., Rull, A., Micol, V., et al. (2010). The aqueous extract of *Hibiscus sabdariffa* calices modulates the production of monocyte chemoattractant protein-1 in humans. *Phytomedicine*, 17, 186–191.
- Bruker Daltonik. New technology for detection of true isotopic pattern in orthogonal TOF-mass spectrometry. Technical Note 008.
- Büyükbacı, A., & El, S. N. (2008). Determination of *in vitro* antidiabetic effects, antioxidant activities and phenol contents of some herbal teas. *Plant Foods for Human Nutrition*, 63, 27–33.
- Caturla, N., Vera-Samper, E., Villalán, J., Reyes-Mateo, C., & Micol, V. (2003). The relationship between the antioxidant and the antibacterial properties of galloylated catechins and the structure of phospholipid model membranes. *Free Radical Biology & Medicine*, 34, 648–662.
- Chen, C. C., Hsu, J. D., Wang, S. F., Chiang, H. C., Yang, M. Y., Kao, E. S., et al. (2003). *Hibiscus sabdariffa* extract inhibits the development of atherosclerosis in cholesterol-fed rabbits. *Journal of Agricultural and Food Chemistry*, 51, 5472–5477.
- Currie, L. A. (1995). Nomenclature in evaluation of analytical methods including detection and quantification capabilities. *Pure and Applied Chemistry*, 67, 1699–1723.
- De Leonardis, A., Pizzella, L., & Macciola, V. (2008). Evaluation of chlorogenic acid and its metabolites as potential antioxidants for fish oils. *European Journal of Lipid Science and Technology*, 110, 941–948.
- Frankel, E. N., & Meyer, A. S. (2000). The problems of using one-dimensional methods to evaluate multifunctional food and biological antioxidants. *Journal of the Science of Food and Agriculture*, 80, 1925–1941.
- Fukumoto, L. R., & Mazza, G. (2000). Assessing antioxidant and prooxidant activities of phenolic compounds. *Journal of Agricultural and Food Chemistry*, 48, 3597–3604.
- Funes, L., Fernández-Arroyo, S., Laporta, O., Pons, A., Roche, E., Segura-Carretero, A., et al. (2009). Correlation between plasma antioxidant capacity and verbascoide levels in rats alter oral administration of lemon verbena extract. *Food Chemistry*, 117, 589–598.
- Gil, M. I., Tomás-Barberán, F. A., Hess-Pierce, B. H., Holcroft, D. M., & Kader, A. A. (2000). Antioxidant activity of pomegranate juice and its relationship with phenolic composition and processing. *Journal of Agricultural and Food Chemistry*, 48, 4581–4589.
- Herrera-Arellano, A., Flores-Romero, S., Chavez-Soto, M. A., & Tortoriello, J. (2004). Effectiveness and tolerability of a standardized extract from *Hibiscus sabdariffa* in patients with mild to moderate hypertension: A controlled and randomized clinical trial. *Phytomedicine*, 11, 375–382.
- Hou, D. X., Tong, X., Terahara, N., Luo, D., & Fujii, M. (2005). Delphinidin 3-sambubioside, a *Hibiscus* anthocyanin, induces apoptosis in human leukemia cells through reactive oxygen species-mediated mitochondrial pathway. *Archives of Biochemistry and Biophysics*, 440, 101–109.
- Huang, D., Ou, B., & Prior, R. L. (2005). The Chemistry behind antioxidant capacity assays. *Journal of Agricultural and Food Chemistry*, 53, 1841–1856.
- Joven, J., Rull, A., Ferre, N., Escolá-Gil, J. C., Marsillach, J., Coll, B., et al. (2007). The results in rodent models of atherosclerosis are not interchangeable: The influence of diet and strain. *Atherosclerosis*, 195, e85–e92.
- Kähkönen, M. P., & Heinonen, M. (2003). Antioxidant activity of anthocyanins and their aglycons. *Journal of Agricultural and Food Chemistry*, 51, 628–633.
- Kao, E. S., Hsu, J. D., Wang, C. J., Yang, S. H., Cheng, S. Y., & Lee, H. J. (2009). Polyphenols extracted from *Hibiscus sabdariffa* L. inhibited lipopolysaccharide-induced inflammation by improving antioxidative conditions and regulating cyclooxygenase-2 expression. *Bioscience, Biotechnology, and Biochemistry*, 73, 385–390.
- Kulkarni, A. P., Aradhya, S. M., & Divakar, S. (2004). Isolation and identification of a radical scavenging antioxidant –punicalagin from pith and carpellary membrane of pomegranate fruit. *Food Chemistry*, 87, 551–557.
- Laporta, O., Pérez-Fons, L., Mallavia, R., Caturla, N., & Micol, V. (2007). Isolation, characterization and antioxidant capacity assessment of the bioactive compounds derived from *Hypoxis rooperi* corm extract (African potato). *Food Chemistry*, 101, 1425–1437.
- Lin, H. H., Huang, H. P., Huang, C. C., Chen, J. H., & Wang, C. J. (2007). *Hibiscus* polyphenol-rich extract induces apoptosis in human gastric carcinoma cells via p53 phosphorylation and p38 MAPK/FasL cascade pathway. *Molecular Carcinogenesis*, 43, 86–99.
- Lin, T. L., Lin, H. H., Chen, C. C., Lin, M. C., Chou, M. C., & Wang, C. J. (2007). *Hibiscus sabdariffa* extract reduces serum cholesterol in men and women. *Nutrition Research*, 27, 140–145.
- Madrigal-Carballo, S., Rodríguez, G., Krueger, C. G., Dreher, M., & Reed, J. D. (2009). Pomegranate (*Punica granatum*) supplements: Authenticity, antioxidant and polyphenol composition. *Journal of Functional Foods*, 1, 324–329.
- Martin, K. R., Krueger, C. G., Rodríguez, G., Dreher, M., & Reed, J. D. (2008). Development of a novel pomegranate standard and new method for the quantitative measurement of pomegranate polyphenols. *Journal of the Science of Food and Agriculture*, 89, 157–162.
- Miller, N. J., Rice-Evans, C., Davies, M. J., Gopinathan, V., & Milner, A. (1993). A novel method for measuring antioxidant capacity and its application to monitoring the antioxidant status in premature neonates. *Clinical Science*, 84, 407–412.
- Oboh, G., & Rocha, J. B. T. (2008). Antioxidant and neuroprotective properties of sour tea (*Hibiscus sabdariffa*, calyx) and green tea (*Camellia sinensis*) on some pro-oxidant-induced lipid peroxidation in brain *in vitro*. *Food Biophysics*, 3, 382–389.
- Ou, B., Hampsch-Woodill, M., & Prior, R. L. (2001). Development and validation of an improved oxygen radical absorbance capacity assay using fluorescein as the fluorescent probe. *Journal of Agricultural and Food Chemistry*, 49, 4619–4626.
- Prior, R. L., & Cao, G. (1999). *In vivo* total antioxidant capacity: Comparison of different analytical methods. *Free Radical Biology & Medicine*, 27, 1173–1181.
- Prior, R. L., Wu, X., & Schaich, K. (2005). Standardized methods for the determination of antioxidant capacity and phenolics in foods and dietary supplements. *Journal of Agricultural and Food Chemistry*, 53, 4290–4302.
- Re, R., Pellegrini, N., Proteggente, A., Pannala, A., Yang, M., & Rice-Evans, C. (1999). Antioxidant activity applying an improved ABTS radical cation decolorization assay. *Free Radical Biology & Medicine*, 26, 1231–1237.
- Rodríguez-Medina, I. C., Beltrán-Debón, R., Micol-Molina, V., Alonso-Villaverde, C., Joven, J., Menéndez, J., et al. (2009). Direct characterization of aqueous extract of *Hibiscus sabdariffa* using HPLC with diode array detection coupled to ESI and ion trap MS. *Journal of Separation Science*, 32, 3441–3448.
- Sánchez-Moreno, C. (2002). Review: Methods used to evaluate the free radical scavenging activity in foods and biological systems. *Food Science and Technology International*, 8, 121–139.
- Segura-Carretero, A., Puertas-Mejía, M. A., Cortacero-Ramírez, S., Beltrán, R., Alonso-Villaverde, C., Joven, J., et al. (2008). Selective extraction, separation, and identification of anthocyanins from *Hibiscus sabdariffa* L. using solid phase extraction-capillary electrophoresis mass spectrometry (time-of-flight/ion trap). *Electrophoresis*, 29, 2852–2861.
- Strube, M., Haenen, G. R. M. M., Van Den Berg, H., & Bast, A. (1997). Pitfalls in a method for assessment of total antioxidant capacity. *Free Radical Research*, 26, 515–521.
- Tsai, P. J., & Ou, A. S. M. (1996). Colour degradation of dried roselle during storage. *Journal of Food Science*, 23, 629–640.
- Tseng, T. H., Kao, E. S., Chu, C. Y., Chou, F. P., Lin, W. H., & Wang, C. J. (1997). Protective effects of dried flower extracts of *Hibiscus sabdariffa* L. against oxidative stress in rat primary hepatocytes. *Food and Chemical Toxicology*, 35, 1159–1164.
- Tseng, T. H., Kao, E. S., Chu, C. Y., Chou, F. P., Lin, W. L., & Wang, C. J. (2000). Induction of apoptosis by *Hibiscus* protocatechuic acid in human leukemia cells via reduction of retinoblastoma (RB) phosphorylation and Bcl-2 expression. *Biochemical Pharmacology*, 60, 307–315.
- Vankar, P. S., & Srivastava, J. (2008). Comparative study of total phenol, flavonoid contents and antioxidant activity in *Canna indica* and *Hibiscus rosa sinensis*: Prospective natural food dyes. *International Journal of Food Engineering*, 4 Article number 4.
- Wang, C. J., Wang, J. M., Lin, W. L., Chu, C. Y., Chou, F. P., & Tseng, T. H. (2000). Protective effect of *Hibiscus* anthocyanins against tert-butyl hydroperoxide-induced hepatic toxicity in rats. *Food and Chemical Toxicology*, 38, 411–416.
- Wu, L. (2007). Effect of chlorogenic acid on antioxidant activity of *Flos Ionicerae* extracts. *Journal of Zhejiang University. Science B*, 8, 673–679.
- Wua, X., Gua, L., Holden, J., Haytowitz, D. B., Gebhardt, S. E., Beecher, G., et al. (2004). Development of a database for total antioxidant capacity in foods: A preliminary study. *Journal of Food Composition and Analysis*, 17, 407–422.
- Yu, Y. M., Chang, W. C., Wu, C. H., & Chian, S. Y. (2005). Reduction of oxidative stress and apoptosis in hyperlipidemic rabbits by ellagic acid. *The Journal of Nutritional Biochemistry*, 16, 675–681.
- Zhang, Y., Wang, D., Lee, R., Henning, S. M., & Heber, D. (2009). Absence of pomegranate ellagitannins in the majority of commercial pomegranate extracts: Implications for standardization and quality control. *Journal of Agricultural and Food Chemistry*, 57, 7395–7400.







CAPÍTULO 8. Synergism of plant-derived polyphenols in adipogenesis: perspectives and implications.





Synergism of plant-derived polyphenols in adipogenesis: Perspectives and implications

María Herranz-López^{a,1}, Salvador Fernández-Arroyo^{b,1}, Almudena Pérez-Sánchez^a, Enrique Barrajon-Catalán^a, Raúl Beltrán-Debón^c, Javier Abel Menéndez^d, Carlos Alonso-Villaverde^e, Antonio Segura-Carretero^b, Jorge Joven^c, Vicente Micol^{a,*}

^a Instituto de Biología Molecular y Celular (IBMC), Universidad Miguel Hernández, Elche, Alicante, Spain

^b Department of Analytical Chemistry, Faculty of Sciences, University of Granada, Av/Fuentenueva, 18071 Granada, Spain

^c Centre de Recerca Biomèdica, Hospital Universitari de Sant Joan, IISPV, Universitat Rovira i Virgili, C/Sant Joan s/n, 43201 Reus, Spain

^d Catalan Institute of Oncology (ICO), Girona, Catalonia, Spain

^e Servei de Medicina Interna, Hospital Son Llàtzer, Palma, Illes Balears, Spain

ARTICLE INFO

Keywords:

Adipogenesis
Hibiscus sabdariffa
 Leptin
 MCP-1
 Polyphenols
 Synergism

ABSTRACT

Dietary polyphenols may exert their pharmacological effect via synergistic interactions with multiple targets. Putative effects of polyphenols in the management of obesity should be primarily evaluated in adipose tissue and consequently in well-documented cell model. We used *Hibiscus sabdariffa* (HS), a widely recognised medicinal plant, as a source of polyphenols with a number of salutary effects previously reported. We present here the full characterisation of bioactive components of HS aqueous extracts and document their effects in a model of adipogenesis from 3T3-L1 cells and in hypertrophic and insulin-resistant adipocytes. Aqueous extracts were up to 100 times more efficient in inhibiting triglyceride accumulation when devoid of fibre and polysaccharides. Significant differences were also observed in reactive oxygen species generation and adipokine secretion. We also found that, when polyphenols were fractionated and isolated, the benefits of the whole extract were greater than the sum of its parts, which indicated a previously unnoticed synergism. In conclusion, polyphenols have interactive and complementary effects, which suggest a possible application in the management of complex diseases and efforts to isolate individual components might be irrelevant for clinical medicine and/or human nutrition.

© 2012 Elsevier GmbH. All rights reserved.

Introduction

Obesity-associated metabolic, oxidative and inflammatory disturbances are a growing epidemic and are associated with at least six of the top ten causes of death (McGeer and McGeer 2004). Adipocytes store excess energy, but when overloaded they become resistant to insulin, which compromises their ability to accumulate

lipids and facilitates alterations in structure and metabolism in remote tissues, such as the pancreas, liver and muscle (Yu and Zhu 2004; Jernas et al. 2006; Rull et al. 2010). Excessive oxidation in adipose cells is common and triggers cellular stress (Furukawa et al. 2004; Yeop Han et al. 2010). The resulting sequence of events remains poorly understood in humans but tends to self-perpetuate if untreated. Initially, there is a complex process of cellular adaptation, monitored by tissue-resident macrophages. When failure and malfunction become extreme, a chronic inflammatory response is unleashed (Rull et al. 2010).

If assumptions are accurate, it is conceivable that antioxidant and/or anti-inflammatory therapies that act on adipose tissue may have potential benefits in the amelioration of obesity-related diseases. However, current available drugs have not been assayed yet. The only validated therapeutic measure consists of preventing hypertrophy in adipocytes via caloric restriction or increased caloric expenditure, but changes in lifestyle are difficult to achieve. Plant-derived polyphenols may provide a similar effect without restricting caloric intake (Lamming et al. 2004; Howitz and Sinclair 2008). Polyphenols are antioxidant and anti-inflammatory

Abbreviations: HS, *Hibiscus sabdariffa*; AHS, aqueous extract of *H. sabdariffa*; PEHS, phenolic extract of *H. sabdariffa*; FBS, foetal bovine serum; TNF- α , tumour necrosis factor- α ; IGF1, insulin-like growth factor-1; IL-6, interleukin-6; VEGF, vascular endothelial growth factor; IL-1 α , interleukin-1 α ; IL-1 β , interleukin-1 β ; MCP-1, monocyte chemoattractant protein-1; IBMX, 3-isobutyl-1-methylxanthine.

* Corresponding author at: Instituto de Biología Molecular y Celular, Universidad Miguel Hernández, Avda. de la Universidad s/n, 03202 Elche, Alicante, Spain. Tel.: +34 96 6658430; fax: +34 96 6658758.

E-mail address: vmicol@umh.es (V. Micol).

¹ These authors have equally contributed to this research and are listed in random order.



molecules that interact in humans with molecular targets involved in stress response pathways, and increased ingestion of dietary polyphenols could be helpful. However, plant-derived polyphenols are secondary metabolites that are synthesised in response to a major stress event; consequently, the expected amount of polyphenols in our commonly consumed food is very low. We reasoned that tropical plant-derived products could be a potential source of polyphenol concentrate and could be used to design dietary supplements. Recent data indicate that aqueous extracts of *Hibiscus sabdariffa* (HS) might ameliorate metabolic disturbances (Carvajal-Zarrabal et al. 2005; Alarcon-Aguilar et al. 2007; Kim et al. 2007), but human trials have been generally unsatisfactory, due to an incomplete characterisation of the essential bioactive components (Beltrán-Debón et al. 2009; Mozaffari-Khosravi et al. 2009; Kuriyan et al. 2010). In this study, we address this issue, document the effects of polyphenols on mouse adipocytes and provide data that support multi-target action in the same signalling cascades or response networks.

Materials and methods

Materials

3T3-L1 cells were purchased from the American Type Culture Collection (Manassas, VA, USA). Dexamethasone, 3-isobutyl-1-methylxanthine, insulin, crystal violet, Ascentis C18 preparative reverse phase column, formic acid, acetonitrile and ethanol were obtained from Sigma–Aldrich (Madrid, Spain). Dulbecco's modified Eagle's medium, calf serum, foetal bovine serum, and an antibiotic mixture (penicillin–streptomycin) were purchased from PAA Laboratories (Linz, Austria). Sodium pyruvate and trypsin–EDTA were obtained from Invitrogen (Carlsbad, CA). Polyvinylidene fluoride (PVD) filters, 0.22 µm, were obtained from Millipore (Bedford, MA). AdipoRed™ Assay Reagent was obtained from Lonza (Walkersville, MD USA). The resin used for the preparative chromatography was Amberlite™ FPX66 (Rohm and Haas, Philadelphia, USA). The standards for the calibration curves, chlorogenic acid, quercetin-3-rutinoside, quercetin-3-glucoside, kaempferol-3-O-rutinoside, kaempferol 3-(*p*-coumaroylglucoside), quercetin, 4-hydroxycoumarin and delphinidin-3-sambubioside were purchased either from Fluka, Extrasynthese (Genay, France) or Polyphenols Laboratories (Hanaveien, Norway).

Methods of extraction and fractionation of polyphenols

Primary aqueous extract (AHS) was obtained from sun-dried calyces from plants harvested by investigators in Senegal with an approximate plant-to-extract ratio of 5:1 as previously described (Beltrán-Debón et al. 2009). The purified extract (PEHS) was prepared by removing fibre and polysaccharides by precipitation in 85% ethanol (v/v). Extracts were reconstituted in water at 170 mg/ml and loaded onto a 1.5 cm × 25 cm chromatography column containing Amberlite™ FPX66. The retained phenolic fraction was finally eluted with 95% ethanol and 0.01% trifluoroacetic acid, rotary evaporated and freeze-dried. Total phenolic content in AHS and PEHS was measured with the Folin–Ciocalteu method (Huang et al. 2005). To further characterise the bioactive components, PEHS was dissolved in distilled water to a concentration of 230 mg/ml, filtered through a 0.45 µm PVD filter and fractionated using a WellChrom preparative HPLC system (Merck–Knauer, Berlin, Germany). We used an Ascentis C18 preparative reverse phase column (10 µm, 25 cm × 21.2 mm), and elution was performed using acetonitrile as a mobile phase in a multistep linear gradient at room temperature with a flow rate of 19 ml/min. The preparative version of EuroChrom® software, version 3.01, was

used for data acquisition and analysis. We obtained 35 fractions representing distinct combinations of components, which were identified and quantified. We then lyophilised the resulting fractions for assays described below.

Characterisation and quantification of polyphenols

Analysis was performed in a Rapid Resolution Liquid Chromatography 1200 (Agilent Technologies, Palo Alto, CA) using a Zorbax Eclipse Plus C₁₈, 4.6 mm × 150 mm, 1.8 µm column at room temperature with a flow rate of 0.5 ml/min and an injection volume of 10 µl (Rodríguez-Medina et al. 2009). The chromatographic system was coupled to a time-of-flight (TOF) mass spectrometer (MS) (Bruker Daltonic Bremen, Germany) that was equipped with an orthogonal electrospray interface (ESI; model G1607A from Agilent Technologies, Palo Alto, CA, USA) that operated in negative and positive modes of ionisation. Compound identification was made by comparing the retention times and mass spectra obtained by TOF-MS with those of authentic standards or interpreted according to previously obtained mass spectra. Quantification of the major compounds in AHS, PEHS and the isolated fractions was carried out using commercially available standards when available or previously reported structurally similar compounds (Fernandez-Arroyo et al., 2011).

In vitro experimental models

The 3T3-L1 preadipocytes were propagated and differentiated according to described procedures (Green and Kehinde 1975) (see also supporting information). Differential effects on adipogenesis were assayed by adding extracts and fractions in pre-designed concentrations to the media at the beginning of the induction period; these conditions were maintained until cells were harvested. The absence of cytotoxicity was ascertained by the crystal violet method. In all experiments, more than 90% of the cells were mature adipocytes after 8–10 days of incubation. For other experiments, we used hypertrophied, insulin-resistant adipocytes obtained by increasing the time of incubation (22 days) in 25 mM glucose (Yeop Han et al. 2010). In these cases, extracts and fractions were added at day 18 and allowed to incubate for 4 days before harvesting. We assessed triglyceride accumulation with AdipoRed™; extracts and fractions were added either at day 8 (mature adipocytes) or at day 18 (hypertrophied adipocytes) after induction and were incubated for 2 or 4 additional days, respectively. Fat droplets were analysed with a Nikon Eclipse TE 2000U fluorescence microscope controlled by NIS-Elements software.

Measurement of intracellular reactive oxygen species (ROS) and secreted adipokines

Measurements were performed on hypertrophied adipocytes in 25 mM glucose to assess the effect of proposed extracts. These extracts were added to adipocytes at day 18 after inducing differentiation, and incubation proceeded for four additional days under the same conditions. ROS generation was assessed with 2',7'-dichlorodihydrofluorescein diacetate as described (Yeop Han et al. 2010), and fluorescence was measured in a multiwell plate reader (POLARstar Omega microplate) with excitation at 485 nm and emission at 520 nm. In separate experiments, several cytokines (leptin, tumour necrosis factor- α (TNF- α), insulin-like growth factor-1 (IGF-1), interleukin-6 (IL-6), vascular endothelial growth factor (VEGF), interleukin-1 alpha (IL-1 α), interleukin-1 beta (IL-1 β) and monocyte chemoattractant protein-1 (MCP-1)) were measured by ELISA (Signosis, Inc., Sunnyvale, CA, USA) in resulting supernatants following the manufacturer's instructions.

Statistical analyses

Values were represented as means \pm standard deviation. Differences between two or more groups were compared using non-parametric tests and were considered statistically significant when $p < 0.05$. The means of quantitative variables were analysed using one-way ANOVA, the Student *t*-test for unpaired samples and Tukey test for multiple comparisons. All statistical analyses were performed with the Statistical Package for Social Science version 17.0 (SPSS, Chicago, IL, USA).

Results

Relative composition of candidate bioactive components

There were no major qualitative differences in polyphenol content between AHS and PEHS; therefore, the precipitation procedures used to remove other soluble material did not result in selective losses in benefit (Fig. 1A and B and Table 1). However, such manipulations resulted in immediately apparent quantitative differences and subsequent changes in relative contribution (Table 2). The phenolic content of AHS, as expressed in gallic acid equivalents, was significantly ($p < 0.001$) lower (2.26 ± 0.11 g/100 g) than that of PEHS (28.42 ± 0.33 g/100 g). Relative differences were observed in organic acids and all families of phenolic compounds: organic acid derivatives (hydroxycitric and hibiscus acids), anthocyanins (delphinidin-3-sambubioside and cyanidin-3-sambubioside), phenolic acid derivatives (chlorogenic acid and 5-*O*-caffeoylshikimic acid), and several flavonol derivatives (quercetin, myricetin and kaempferol glycosides) (Table 2). PEHS was fractionated into 35 different fractions, and only fractions 6, 9 and 14 (Fig. 1C–E

and Table 2) significantly inhibited adipogenesis at concentrations ranging from 10 to 40 μ g/ml. For clarity, negative results for the remaining fractions are not shown. During the fractionation procedure and the subsequent concentration, significant peaks were additionally detected and identified in PEHS (hibiscus acid dimethyl ester, coumaroylquinic acid, leucoside (kaempferol-3-*O*-sambubioside)) and several unidentified compounds. At least six new identified peaks (numbers 32–37) appeared only in isolated fractions. The composition of these fractions differed notably. The major component of fraction 6 was delphinidin-3-sambubioside, fraction 9 contained cyanidin-3-sambubioside, chlorogenic acid and tetra-*O*-methyljeediflavanone as major components, and fraction 14 was especially rich in glycosylated flavonols, such as quercetin-3-sambubioside and myricetin-3-glucoside (Table 2).

Phenolic compounds inhibited adipogenic differentiation of 3T3-L1 cells: fibre and/or polysaccharides were either inactive or interfered in the model

We found that AHS significantly inhibited lipid accumulation and adipogenic differentiation of pre-adipocytes but only at concentrations ≥ 500 μ g/ml, which are not likely to be achieved *in vivo*. However, the relative activity of PEHS was much higher and evident even at concentrations < 10 μ g/ml. Both extracts showed a significant reduction in the number of differentiated cells when compared with the control, as well as a dose-dependent response in the reduction in the accumulation of triglycerides (Fig. 2A–E). Cells differentiated in the presence of adipogenic agents plus 1000 μ g/ml AHS or 40 μ g/ml PEHS extracts accumulated 44.4% and 19.3% of triglyceride, respectively, as compared to levels normally observed

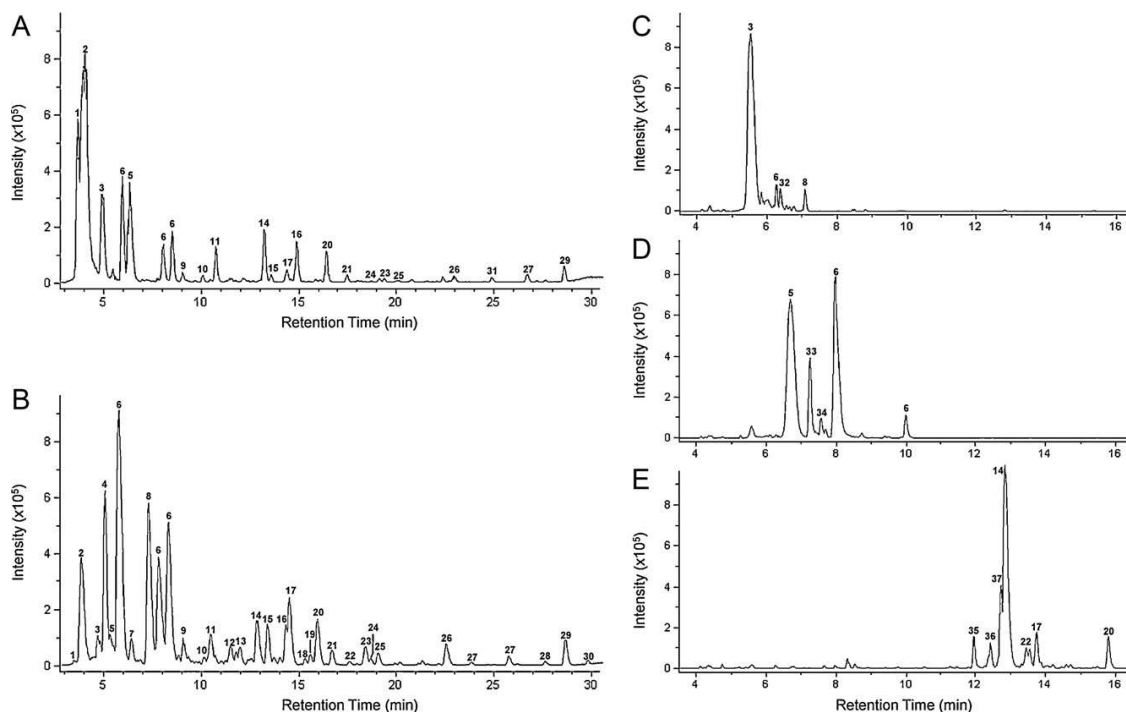


Fig. 1. Representative base peak chromatograms obtained by HPLC–ESI–TOF–MS of *Hibiscus sabdariffa* AHS (A) and PEHS (B) extracts at 50 mg/ml and 5 mg/ml, respectively. Qualitative differences between AHS and PEHS were deemed negligible, but quantitative differences were evident, especially with respect to the content of phenolic acids, anthocyanins and flavonols. Fractionation of PEHS, obtained through semipreparative liquid chromatography, showed that only a few fractions (C–E) were active in adipocytes.

**Table 1**

Relevant analytical data for components isolated in AHS and PEHS (see also Fig. 1). Note that peaks 31–37 were only identified after a further process of purification.

Peak number	Compound	Retention time (min)	Molecular formula	[M–H] ⁻	UV–Vis (nm)
1	Hydroxycitric acid	4.35	C ₆ H ₈ O ₈	207.0140	–
2	Hibiscus acid	4.72	C ₆ H ₆ O ₇	189.0035	–
3	Delphinidin-3-sambubioside	5.50	C ₂₆ H ₃₀ O ₁₆	595.1446	280, 520
4	Unknown	5.86	C ₈ H ₁₂ O ₈	235.0461	278, 334
5	Cyanidin-3-sambubioside	6.11	C ₂₆ H ₃₀ O ₁₅	579.1493	280, 520
6	Chlorogenic acid	6.52/8.41/8.92	C ₁₆ H ₁₈ O ₉	353.0891	297, 324
7	Unknown	7.13	–	230.0127	272, 298
8	Hibiscus acid dimethyl ester	7.91	C ₈ H ₁₀ O ₇	217.0354	292
9	Methyl digallate	9.62	C ₁₅ H ₁₂ O ₉	335.0409	278
10	2-O-Trans-caffeoyl-hydroxycitric acid	10.60	C ₁₅ H ₁₄ O ₁₁	369.0463	285, 330
11	Myricetin-3-arabinogalactoside	10.91	C ₂₆ H ₂₈ O ₁₇	611.1254	260, 354
12	Coumaroylquinic acid	11.86	C ₁₆ H ₁₈ O ₈	337.0929	310
13	Unknown	12.34	C ₁₁ H ₁₁ NO ₅	236.0564	272
14	Quercetin-3-sambubioside	13.11	C ₂₆ H ₂₈ O ₁₆	595.1309	345
15	Unknown	13.63	C ₁₆ H ₂₀ O ₁₀	371.0984	278
16	Quercetin-3-rutinoside	14.50	C ₂₇ H ₃₀ O ₁₆	609.1462	255, 353
17	5-O-Caffeoylshikimic acid	14.69	C ₁₆ H ₁₆ O ₈	335.0768	296, 326
18	Leucoside (kaempferol-3-O-sambubioside)	15.44	C ₂₆ H ₂₈ O ₁₅	579.1355	278, 505
19	Unknown	15.69	C ₁₇ H ₂₂ O ₁₀	385.1140	270
20	Quercetin-3-glucoside	16.04	C ₂₁ H ₂₀ O ₁₂	463.0873	253, 356
21	Kaempferol-3-O-rutinoside	16.71	C ₂₇ H ₃₀ O ₁₅	593.1512	265, 350
22	Unknown	17.58	C ₁₈ H ₂₂ O ₉	381.1191	278
23	Unknown	18.33	C ₂₁ H ₃₀ O ₁₁	457.1715	–
24	Methyl-epigallocatechin	18.60	C ₁₆ H ₁₆ O ₇	319.0823	268, 336
25	Unknown	18.93	–	503.1759	278
26	Myricetin	22.19	C ₁₅ H ₁₀ O ₈	317.0298	372
27	N-Feruloyltyramine	23.40/25.19	C ₁₈ H ₂₀ NO ₄	312.1234	286, 316
28	Unknown	26.94	–	307.0726	288, 353, 414
29	Quercetin	28.67	C ₁₅ H ₁₀ O ₇	301.0339	253, 372
30	Unknown	29.89	C ₁₈ H ₃₄ O ₅	329.2333	–
31	Prodelfinidin B3	24.82	C ₃₀ H ₂₆ O ₁₄	609.1250	312
32	Tetra-O-methyljeediflavanone	4.30	C ₃₄ H ₃₀ O ₁₁	613.1715	341
33	Unknown	6.11	C ₂₆ H ₃₀ O ₁₆	597.1461	338
34	Caffeoylglucose	6.46	C ₁₅ H ₁₈ O ₉	341.0878	314
35	Unknown	11.37	C ₂₆ H ₄₄ O ₁₆	611.2557	277
36	Unknown	11.93	C ₂₇ H ₃₂ O ₁₇	627.1567	278
37	Myricetin-3-glucoside	12.25	C ₂₁ H ₂₀ O ₁₃	479.0831	355

in control cells. The extract concentration that led to 50% of inhibition of triglyceride accumulation (IC₅₀) was 799 ± 225 µg/ml for AHS and 9.1 ± 2.8 µg/ml for PEHS, respectively. This result revealed that PEHS was approximately 90–100 times more effective in reducing triglyceride accumulation. This difference was around 10 times higher than that expected for actual polyphenol concentrations, which indicated that the absence of polysaccharides and other soluble material improved the inhibition of triglyceride cellular uptake in this model.

Anti-adipogenic activity of polyphenols was no longer conserved in most isolated fractions

Only 3 of 35 polyphenolic fractions (numbers 6, 9 and 14; Fig. 1C–E) significantly inhibited adipogenesis. The efficacy of these fractions was dose-dependent; fraction 14 was the most active throughout the dosing range (Fig. 2F). None of these fractions at 40 µg/ml achieved the effectiveness that was obtained with the total mixture of polyphenols (PEHS). Changes in activity with combinations of these fractions at different concentrations were negligible. None of the binary combinations (20 or 30 µg/ml of each fraction) achieved higher activities than the individual fractions. Moreover, the strong inhibitory action of fraction 14 was maintained when using pairs 6/14 and 9/14. Finally, the combination of three of the fractions (20 µg/ml of each) also failed to improve the anti-adipogenic activity, as compared with both isolated fractions and combinations. Taking all results into account, the presence of all polyphenols was necessary in order to achieve maximum efficacy, and the relative proportion was potentially a relevant factor.

Phenolic compounds were active in mature as well as hypertrophied and insulin-resistant adipocytes

When extracts were assayed in mature adipocytes, the addition of AHS did not significantly affect triglyceride content, even at 1000 µg/ml, but 40 µg/ml of PEHS decreased triglyceride content by 20–30% when assayed at 40 µg/ml (Supporting Information; Fig. 2). These novel findings prompted the exploration of the effects of PEHS in a cell model of adipocyte hypertrophy in the context of insulin resistance, similar to that observed in the adipose tissue of obese patients (Yu and Zhu 2004; Jernas et al. 2006; Takahashi et al. 2008; Yeop Han et al. 2010). Surprisingly, we found significant effects with AHS and that both AHS and PEHS were more efficient at reducing triglyceride accumulation in insulin-resistant adipocytes than in mature adipocytes (1000 µg/ml AHS: 19% mean values reduction; 40 µg/ml PEHS: 38% mean values reduction) (Fig. 3). It appeared that the PEHS-mediated reduction in triglyceride accumulation was significantly higher during the adipogenesis process than in mature or hypertrophic adipocytes but we found a differential response with both extracts. The generation of endogenous ROS was not affected by AHS (Fig. 4A and B), but the effect of PEHS was significant and dose-dependent, achieving a 30% reduction, which indicated that the removed material might have deleterious effects on either the diffusibility or the intrinsic antioxidant activity of phenolic compounds. These deleterious effects were not observed with their putative anti-inflammatory properties. We observed that both extracts at the tested concentrations significantly decreased the amount of secreted adipokines with respect to controls (Fig. 4C). This result indicated that the effect of fibre and/or saccharides could be specific. For most of the adipokines assayed,



Table 2
Quantitative data in ppm (m/m) for major components found in extracts and fractions with significant biological activity.

Peak number	Compound	Quantification technique	AHS	PEHS	Fraction 6	Fraction 9	Fraction 14
1	Hydroxyacetic acid	MS-TOF (m/z 207)	8288.0 ± 397.6	-	-	-	-
2	Hibiscus acid	MS-TOF (m/z 189)	311.22.0 ± 1128.4	-	-	-	-
3	Delphinidin-3-sambubioside	DAD-UV (520nm)	2701.2 ± 165.6	128.134.2 ± 9486.9	-	-	-
5	Cyanidin-3-sambubioside	DAD-UV (520nm)	1939.2 ± 39.3	207.315.5 ± 1807.6	415,227.9 ± 18,558.3	-	-
6	Chlorogenic acid	DAD-UV (325 nm)	5720.0 ± 39.4	87,143.1 ± 393.1	-	193,354.1 ± 3119.0	-
8	Hibiscus acid dimethyl ester	MS-TOF (m/z 217)	-	106,469.9 ± 1182.0	5381.5 ± 173.9	137,219.1 ± 1425.8	-
9	Methyl digallate	DAD-UV (270nm)	-	2802.3 ± 46.6	5300.5 ± 325.9	-	-
11	Myricetin-3-arabinogalactose	DAD-UV (350nm)	57.3 ± 2.5	4755.5 ± 53.8	-	-	-
12	Coumaroylquinic acid	DAD-UV (310nm)	-	772.9 ± 10.4	-	-	-
14	Quercetin-3-sambubioside	DAD-UV (350nm)	304.0 ± 5.9	7673.8 ± 34.6	-	-	113,130.2 ± 2356.4
16	Quercetin-3-rutinoside	DAD-UV (325 nm)	495.7 ± 4.3	4953.2 ± 47.9	-	-	-
17	5-O-Caffeoylshikimic acid	DAD-UV (350 nm)	171.5 ± 6.9	3526.7 ± 49.2	-	-	7312.7 ± 168.9
18	Leucoside	DAD-UV (350nm)	-	1123.0 ± 25.4	-	-	-
20	Quercetin-3-glucoside	DAD-UV (350nm)	143.7 ± 2.2	3071.6 ± 15.9	-	-	12,789.1 ± 268.6
21	Kaempferol-3-O-rutinoside	DAD-UV (350nm)	91.9 ± 2.3	2185.5 ± 15.5	-	-	-
24	Methyl-epigallocatechin	DAD-UV (270nm)	-	310.9 ± 5.5	-	-	-
26	Myricetin	DAD-UV (370nm)	-	4765.9 ± 49.1	-	-	-
27	N-Feruloyltyramine	DAD-UV (325 nm)	99.0 ± 1.8	867.9 ± 8.6	-	-	-
29	Quercetin	DAD-UV (370nm)	121.2 ± 2.0	5795.2 ± 61.7	-	-	-
31	Prodphinidin B3	DAD-UV (310nm)	1839.2 ± 25.3	327.0 ± 2.9	-	-	-
32	Tetra-O-methyljeediflavanone	DAD-UV (350nm)	-	-	13,515.7 ± 125.8	-	-
34	Caffeoylglucose	MS-TOF (m/z 341)	-	-	-	2902.1 ± 67.5	-
37	Myricetin-3-glucoside	DAD-UV (350 nm)	-	-	-	-	29,383.6 ± 1245.1

both extracts showed the same quantitative efficacy. A differential response, higher for PEHS than for AHS, was only observed with the secretion of leptin and MCP-1.

Discussion

The efficacy of phytotherapy is currently under intense debate (Wagner 2011). To firmly establish beneficial effects that may yield valuable nutritional advice or dietary supplements, human studies demand (Mozaffari-Khosravi et al. 2009; Kuriyan et al. 2010) full chemical characterisation of the source of polyphenols and the effect of further manipulation in the relative composition. Our novel findings suggested that the previous removal of fibre and polysaccharides, which represent up to 60% of the total weight of soluble extracts (Müller and Franz 1992), might significantly increase the activity of a polyphenolic mixture. Adipogenesis was substantially inhibited by a standardised *Hibiscus sabdariffa* extract, and the effect of the full extract was higher than the sum of its parts, which provided further evidence that a combination of bioactive components was superior to isolated constituents. In essence, the assayed extracts are a complex mixture of anthocyanins, organic acids, phenolic acids and flavonols (Rodríguez-Medina et al. 2009). Nevertheless, our results revealed that some compounds can have a higher contribution to the observed effects, which suggested the importance of relative composition and that different formulations might yield different outcomes. For instance, the putative hypolipidemic effects of polyphenolic mixtures have been mainly associated with the presence of organic acids (Carvajal-Zarrabal et al. 2005). In contrast, the described effects of PEHS in adipogenesis were obtained in a scenario in which the proportion of phenolic compounds was higher than that of organic acids. From data obtained from isolated fractions, it could be concluded that glycosylated flavonols were the most active compounds amongst individual components, but this finding seemed irrelevant when compared to the action of the full mixture. Although other isolated phenolic compounds (apigenin, epigallocatechin gallate, resveratrol and quercetin) have also shown to inhibit adipogenesis in 3T3-L1 adipocytes in similar concentrations (10–50 µg/ml, Lin et al. 2005; Bandyopadhyay et al. 2006; Yang et al. 2008), cytotoxicity was readily observed. This point is extremely important because plant-derived polyphenols are a complex mixture that interacts with numerous endogenous molecular targets in humans but are surprisingly safe even at high doses (Corson and Crews 2007; Goel et al. 2008; Efferth and Koch 2011).

Another novel finding was that PEHS also actively diminished triglyceride accumulation in mature and even insulin-resistant hypertrophied adipocytes, which suggested an induction in the lipolysis rate (Yu and Zhu 2004; Takahashi et al. 2008). This effect could be important in the management of metabolic disturbances because the uninhibited release of fatty acids from hypertrophied adipocytes might lead to systemic lipotoxicity and insulin resistance (Unger 1995). It was also established that excess triglyceride accumulation in adipocytes generated an excess of ROS that triggered inflammation (Yeop Han et al. 2010). Although the differential abilities observed between AHS and PEHS deserve further consideration, PEHS clearly possesses antioxidative and anti-inflammatory actions in mature and hypertrophied adipocytes. These properties might also have therapeutic implications because these are important processes in 3T3-L1 adipocytes that are directly related to the accumulation of fat and with potential regulation via JNK/NF-κB pathways as described (Furukawa et al. 2004; Takahashi et al. 2008; Yeop Han et al. 2010). Once again we highlight the importance of a particular formulation of phenolic compounds because PEHS was particularly active in inhibiting the secretion of leptin and MCP-1, which are important adipokines

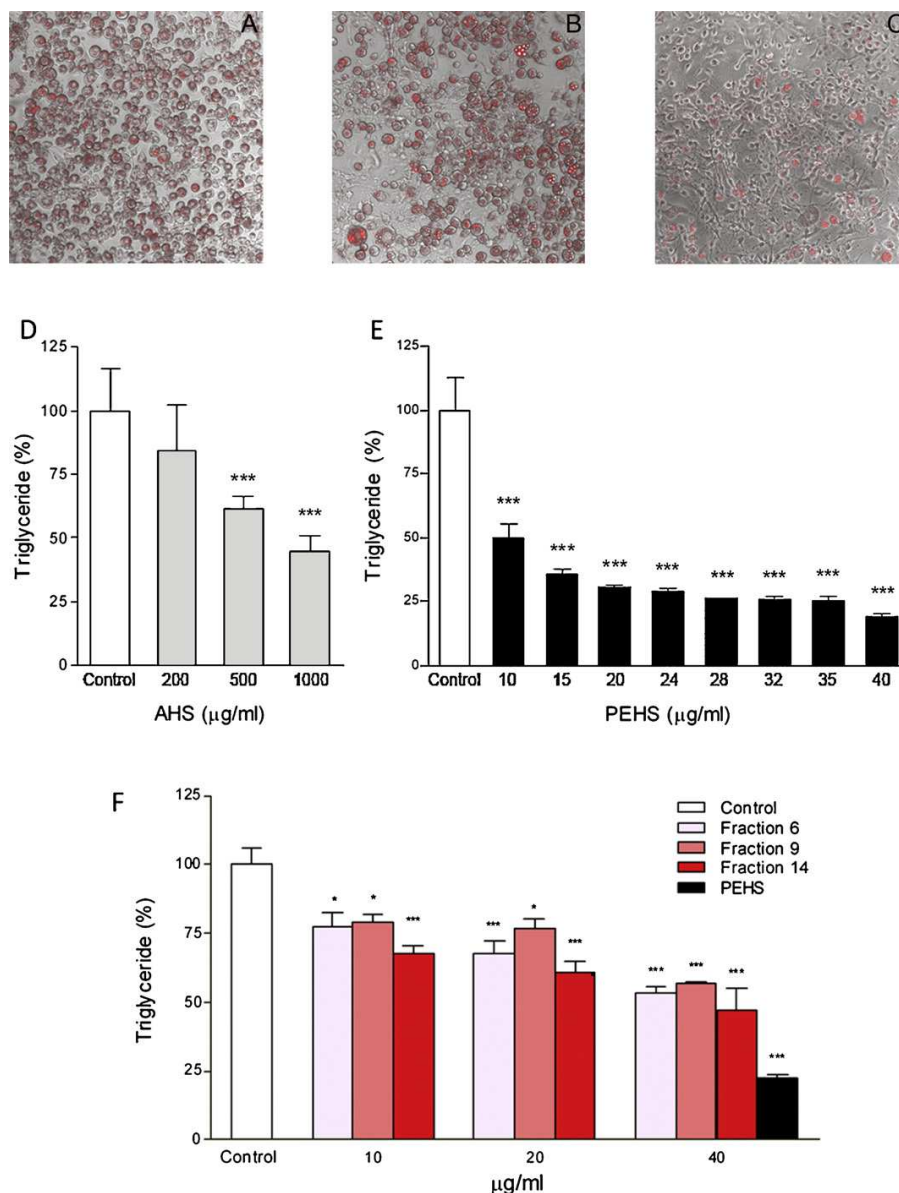


Fig. 2. Polyphenols from *Hibiscus sabdariffa* significantly inhibited the accumulation of triglycerides in 3T3-L1 preadipocytes and programmed adipogenesis. Representative microphotographs of cells stained with AdipoRed™ (treatment groups: control, 1000 $\mu\text{g/ml}$ AHS or 40 $\mu\text{g/ml}$ PEHS; A–C), demonstrate that the number of mature adipocytes was substantially decreased in cells treated with extracts. The quantitative effects of different doses on the final content of triglyceride are also shown (D–E). The effect of selected fractions in the accumulation of triglycerides in 3T3-L1 preadipocytes is shown in (F). Cell viability was unaffected even at higher concentrations. * $p < 0.05$ and *** $p < 0.001$ versus control.

that regulate the migration of non-resident macrophages to the adipose tissue and overall systemic metabolism (Furukawa et al. 2004). This anti-inflammatory effect has also been observed with resveratrol or alpha lipoic acid (Szkudelska et al. 2009; Prieto-Hontoria et al. 2011).

The apparently additive, synergistic or even antagonistic action of each polyphenol and the intrinsic complications of understanding adipocyte metabolism without knowledge of genetic and proteomic kinetics impede efforts to describe the possible biological reactions and metabolic networks involved. Polyphenol reaction and diffusion rates also confound these efforts. Moreover,

the process of transformation and regeneration in these particular cells, and the effects that we described strongly suggested the presence of repeat-pattern mechanisms (Gierer and Meinhardt 1972), which is a self-organising, self-repairing, reaction–diffusion system (Turing 1990).

We speculate that this relationship can be applied to every combination of polyphenols with medicinal effects, but at least two major points should be highlighted. Leptin production correlates positively with insulin resistance, fat mass and adipocyte volume in response to metabolic stress (Frederich et al. 1995). The observed benefit with PEHS was comparatively higher than that observed

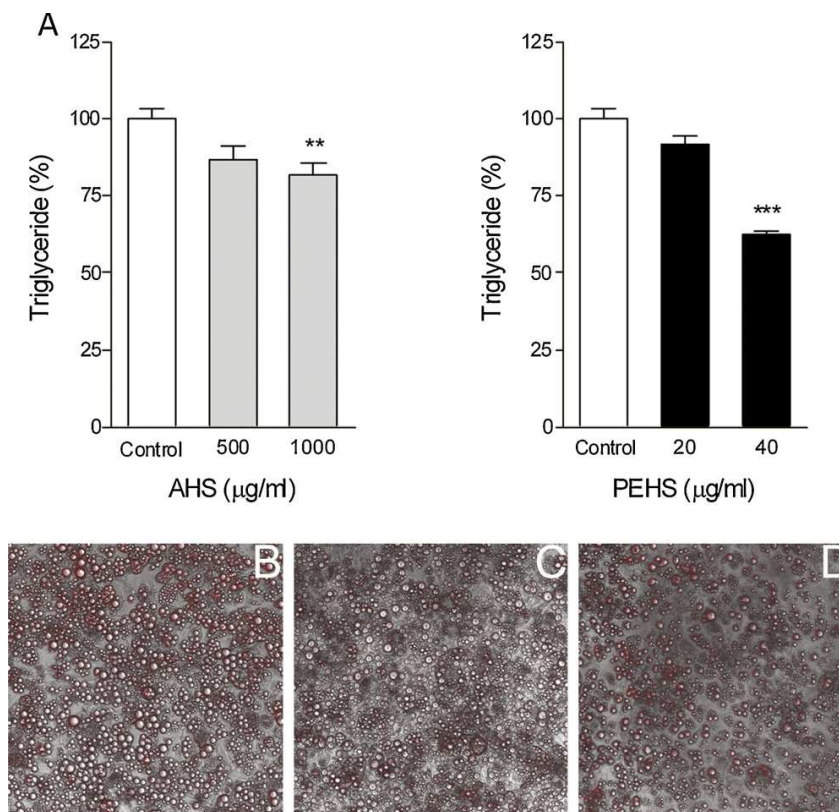


Fig. 3. Polyphenols from *Hibiscus sabdariffa* significantly decreased the accumulation of triglycerides in 3T3-L1 hypertrophied/insulin-resistant adipocytes (A). Effects are shown for AHS (500–1000 µg/ml) (left panel) and PEHS (20–40 µg/ml) (right panel). (B)–(D) are representative microphotographs of cells stained with AdipoRed™; treatment groups: control, 1000 µg/ml AHS or 40 µg/ml PEHS, respectively. The number of fat droplets per cell was decreased in the experiments with PEHS. Cell viability was unaffected even at higher concentrations. ** $p < 0.01$ and *** $p < 0.001$ versus control.

with triglyceride accumulation, which suggested that leptin gene expression was a possible pharmacologic target, although this is effect obviously modulated by actions on a variety of other targets (Frederich et al. 1995; Rupnick et al. 2002; Tilg and Moschen 2006; Samuni et al. 2010). Results with MCP-1 excretion were expected. We have previously reported in humans that these polyphenolic extracts significantly reduce the concentration of circulating MCP-1, which is relevant because MCP-1 has been proposed as a biomarker and therapeutic target in the management of obesity and its related complications (Beltrán-Debón et al. 2009).

We should express caution, however, when interpreting *in vitro* data to actual actions of polyphenols in the body, especially if no data have been collected regarding the action of physiological metabolites of tested polyphenols on the same cell systems. First, the intestinal flora is likely to metabolise some of these compounds. Once the glucoside cleaved, the released aglycone is subjected to the action of specific enzymes in the wall of the small intestine leading to glucuronide, sulphated, and methylated metabolites, which may reach their target tissues and organs. Obviously, our *in vitro* assays do not take into account the *in vivo* bioavailability issue and can lead to false positive interpretations. To date, there is no data about human or animal studies on metabolites deriving from HS polyphenols. Although some bioavailability studies on phenolic acids, anthocyanins and flavonols are available, these are contained in very different food matrices what may radically modify the interaction amongst these compounds in the gastrointestinal tract and therefore their absorption. Whilst human

absorption and bioavailability studies have revealed that phenolic acids and anthocyanins can be retrieved in plasma and urine in their intact form after food consumption (Paredes-Lopez et al. 2010; Williamson et al. 2011), flavonols and flavanols seem to be found in various forms, free or conjugated with glucuronide, sulphate or methyl groups (Day et al. 2001; Williamson et al. 2011).

Because in studies with green tea polyphenols, the metabolites mostly had reduced biological activity, it might be tempting to suggest that conversion of HS polyphenols into less-active metabolites would compromise the cellular effects denoted in the present study. In some systems, however, polyphenols-derived metabolites were found to have the equivalent or even greater activity than the parental polyphenols (Lambert et al. 2007). In the present study, PEHS contains up to thirty identifiable phenolic compounds by HPLC–MS. Accepting that absorption of many of these compounds is negligible; still several of them will be conjugated and will interact with multiple metabolic targets. Thus, to study the effects of all possible metabolites becomes an enormous and fascinating target, which will be undoubtedly matter for future research.

In conclusion, we propose that this particular formulation of polyphenols should be assayed in clinical trials because of its observed regulation of adipogenesis, its regulation of oxidative stress signalling pathways in mature and/or hypertrophied adipocytes and its subsequent ability to alter the expression of adipokines. In regards to the preparation of phytopharmaceuticals or dietary supplements, we propose that the separation of soluble material other than polyphenols prior to use will increase

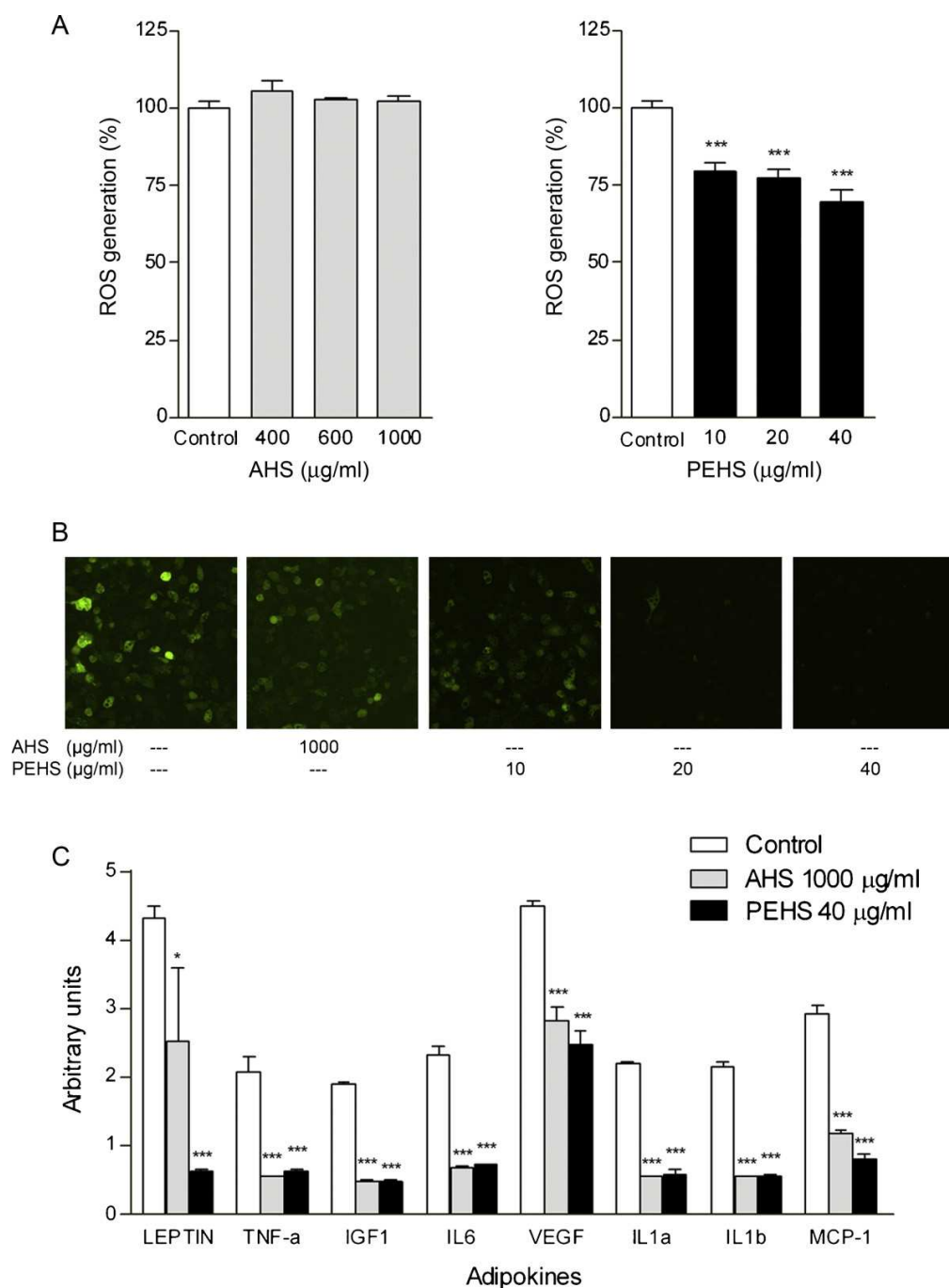


Fig. 4. The phenolic fraction from *Hibiscus sabdariffa* inhibited ROS generation and modulated the concentration of secreted adipokines in hypertrophied 3T3-L1 adipocytes (A). Cells were incubated with different doses of AHS (400–1000 µg/ml) (left panel) or PEHS (10–40 µg/ml) (right panel) and ROS generation was measured by H₂DCFDA labelling. Whereas PEHS affected ROS generation in a dose-dependent manner, AHS did not. Representative fluorescence microphotographs of cells stained with H₂DCFDA are shown in (B). Although the secretion of assayed adipokines was efficiently decreased with both extracts, a differential response was obtained with leptin and MCP-1 (C). **p* < 0.05 and ****p* < 0.001 versus control.

the possibility of safely obtaining synergistic effects. Although bioavailability and safety issues require further studies, we have demonstrated the potential pharmacological and therapeutic superiority of a combination of polyphenols with respect to their

individual components. The existence of synergistic efficacy of binary combinations of compounds has been evaluated and verified by Berenbaum's isobole method (Berenbaum 1989; Wagner 2011). Unfortunately, this method cannot be applied in our case at



this stage due to the complexity of the polyphenol mixture. It is possible that the benefits of polyphenols are the result of mere additive effects or simple combinatory actions, but the data suggest a synergistic effect at least in the sense of that described by Mark Twain: “a bonus achieved when things work together harmoniously”.

Conflict of interest statement

The authors declare that there are no conflicts of interest.

Acknowledgements

We thank MONTELOEDER, SL for providing raw plant material and for advice on the extraction and purification procedures. RBD and MHL were the recipients of fellowships from the Comissionat per a Universitat i Recerca del Departament d'Innovació, Universitat i Empresa de la Generalitat de Catalunya and Programa Vali-d from Generalitat Valenciana, respectively. We thank Andalusian Regional Government Council of Innovation and Science for granted Excellence Project

Appendix A. Supplementary data

Supplementary data associated with this article can be found, in the online version, at doi:10.1016/j.phymed.2011.12.001.

References

- Alarcon-Aguilar, F.J., Zamilpa, A., Perez-García, M.D., Almanza-Perez, J.C., Romero-Núñez, E., Campos-Sepulveda, E.A., Vazquez-Carrillo, L.L., Roman-Ramos, R., 2007. Effect of *Hibiscus sabdariffa* on obesity in MSG mice. *J. Ethnopharmacol.* 114, 66–71.
- Bandyopadhyay, S., Lion, J.M., Mentaverri, R., Ricupero, D.A., Kamel, S., Romero, J.R., Chattopadhyay, N., 2006. Attenuation of osteoclastogenesis and osteoclast function by apigenin. *Biochem. Pharmacol.* 72, 184–197.
- Beltrán-Debón, R., Alonso-Villaverde, C., Aragonés, G., Rodríguez-Medina, I., Rull, A., Micol, V., Segura-Carretero, A., Fernández-Gutiérrez, A., Camps, J., Joven, J., 2009. The aqueous extract of *Hibiscus sabdariffa* calices modulates the production of monocyte chemoattractant protein-1 in humans. *Phytomedicine* 17, 186–191.
- Berenbaum, M.C., 1989. What is synergy? *Pharmacol. Rev.* 41, 93–141.
- Carvajal-Zarrabal, O., Waliszewski, S.M., Barradas-Dermitz, D.M., Orta-Flores, Z., Hayward-Jones, P.M., Nolasco-Hipolito, C., Angulo-Guerrero, O., Sanchez-Ricano, R., Infanzon, R.M., Trujillo, P.R., 2005. The consumption of *Hibiscus sabdariffa* dried calyx ethanolic extract reduced lipid profile in rats. *Plant Foods Hum. Nutr.* 60, 153–159.
- Corson, T.W., Crews, C.M., 2007. Molecular understanding and modern application of traditional medicines: triumphs and trials. *Cell* 130, 769–774.
- Day, A.J., Mellon, F., Barron, D., Sarrazin, G., Morgan, M.R., Williamson, G., 2001. Human metabolism of dietary flavonoids: identification of plasma metabolites of quercetin. *Free Radic. Res.* 35, 941–952.
- Efferth, T., Koch, E., 2011. Complex interactions between phytochemicals. The multi-target therapeutic concept of phytotherapy. *Curr. Drug Targets* 12, 122–132.
- Fernandez-Arroyo, S., Rodriguez-Medina, I.C., Beltrán-Debón, R., Pasini, F., Joven, J., Micol, V., Segura-Carretero, A., Fernandez-Gutiérrez, A., 2011. Quantification of the polyphenolic fraction and in vitro antioxidant and in vivo anti-hyperlipemic activities of *Hibiscus sabdariffa* aqueous extract. *Food Res. Int.* 44, 1490–1495.
- Frederich, R.C., Hamann, A., Anderson, S., Lollmann, B., Lowell, B.B., Flier, J.S., 1995. Leptin levels reflect body lipid content in mice: evidence for diet-induced resistance to leptin action. *Nat. Med.* 1, 1311–1314.
- Furukawa, S., Fujita, T., Shimabukuro, M., Iwaki, M., Yamada, Y., Nakajima, Y., Nakayama, O., Makishima, M., Matsuda, M., Shimomura, I., 2004. Increased oxidative stress in obesity and its impact on metabolic syndrome. *J. Clin. Invest.* 114, 1752–1761.
- Gierer, A., Meinhardt, H., 1972. A theory of biological pattern formation. *Kybernetik* 12, 30–39.
- Goel, A., Jhurani, S., Aggarwal, B.B., 2008. Multi-targeted therapy by curcumin: how spicy is it? *Mol. Nutr. Food Res.* 52, 1010–1030.
- Green, H., Kehinde, O., 1975. An established preadipose cell line and its differentiation in culture. II. Factors affecting the adipose conversion. *Cell* 5, 19–27.
- Howitz, K.T., Sinclair, D.A., 2008. Xenohormesis: sensing the chemical cues of other species. *Cell* 133, 387–391.
- Huang, D., Boxin, O.U., Prior, R.L., 2005. The chemistry behind antioxidant capacity assays. *J. Agric. Food Chem.* 53, 1841–1856.
- Jernas, M., Palming, J., Sjöholm, K., Jennische, E., Svensson, P.-A., Gabriellsson, B.G., Levin, M., Sjögren, A., Rudemo, M., Lystig, T.C., Carlsson, B., Carlsson, L.M.S., Lonn, M., 2006. Separation of human adipocytes by size: hypertrophic fat cells display distinct gene expression. *FASEB J.* 20, 1540–1542.
- Kim, J.K., So, H., Youn, M.J., Kim, H.J., Kim, Y., Park, C., Kim, S.J., Ha, Y.A., Chai, K.Y., Kim, S.M., Kim, K.Y., Park, R., 2007. *Hibiscus sabdariffa* L. water extract inhibits the adipocyte differentiation through the PI3-K and MAPK pathway. *J. Ethnopharmacol.* 114, 260–267.
- Kuriyan, R., Kumar, D.R., R., Kurpad, A.V., 2010. An evaluation of the hypolipidemic effect of an extract of *Hibiscus sabdariffa* leaves in hyperlipidemic Indians: a double blind, placebo controlled trial. *BMC Complement. Altern. Med.* 10, 27.
- Lambert, J.D., Sang, S., Yang, C.S., 2007. Biotransformation of green tea polyphenols and the biological activities of those metabolites. *Mol. Pharm.* 4, 819–825.
- Lamming, D.W., Wood, J.G., Sinclair, D.A., 2004. Small molecules that regulate lifespan: evidence for xenohormesis. *Mol. Microbiol.* 53, 1003–1009.
- Lin, J., Della-Fera, M.A., Baile, C.A., 2005. Green tea polyphenol epigallocatechin gallate inhibits adipogenesis and induces apoptosis in 3T3-L1 adipocytes. *Obes. Res.* 13, 982–990.
- McGeer, P.L., McGeer, E.G., 2004. Inflammation and the degenerative diseases of aging. *Ann. N.Y. Acad. Sci.* 1035, 104–116.
- Mozaffari-Khosravi, H., Jalali-Khanabadi, B.A., Afkhami-Ardekani, M., Fatehi, F., 2009. Effects of sour tea (*Hibiscus sabdariffa*) on lipid profile and lipoproteins in patients with type II diabetes. *J. Altern. Complement. Med.* 15, 899–903.
- Müller, B.M., Franz, G., 1992. Chemical structure and biological activity of polysaccharides from *Hibiscus sabdariffa*. *Planta Med.* 58, 60–67.
- Paredes-Lopez, O., Cervantes-Ceja, M.L., Vigna-Perez, M., Hernandez-Perez, T., 2010. Berries: improving human health and healthy aging, and promoting quality life – a review. *Plant Foods Hum. Nutr.* 65, 299–308.
- Prieto-Hontoria, P.L., Perez-Matute, P., Fernandez-Galilea, M., Martinez, J.A., Moreno-Aliaga, M.J., 2011. Lipic acid inhibits leptin secretion and Sp1 activity in adipocytes. *Mol. Nutr. Food Res.* 55, 1–11.
- Rodríguez-Medina, I.C., Beltrán-Debón, R., Micol, V., Alonso-Villaverde, C., Joven, J., Menéndez, J.A., Segura-Carretero, A., Fernández-Gutiérrez, A., 2009. Direct characterization of aqueous extract of *Hibiscus sabdariffa* using HPLC with diode array detection coupled to ESI and ion trap MS. *J. Sep. Sci.* 32, 3441–3448.
- Rull, A., Camps, J., Alonso-Villaverde, C., Joven, J., 2010. Insulin resistance, inflammation, and obesity: role of monocyte chemoattractant protein-1 (or CCL2) in the regulation of metabolism. *Mediators Inflamm.* 2010, 326580.
- Rupnick, M.A., Panigrahy, D., Zhang, C.Y., Dallabrida, S.M., Lowell, B.B., Langer, R., Folkman, M.J., 2002. Adipose tissue mass can be regulated through the vasculature. *Proc. Natl. Acad. Sci. U.S.A.* 99, 10730–10735.
- Samuni, Y., Cook, J.A., Choudhuri, R., Degraff, W., Sowers, A.L., Krishna, M.C., Mitchell, J.B., 2010. Inhibition of adipogenesis by Tempol in 3T3-L1 cells. *Free Radic. Biol. Med.* 49, 667–673.
- Szkudelska, K., Nogowski, L., Szkudelski, T., 2009. The inhibitory effect of resveratrol on leptin secretion from rat adipocytes. *Eur. J. Clin. Invest.* 39, 899–905.
- Takahashi, K., Yamaguchi, S., Shimoyama, T., Seki, H., Miyokawa, K., Katsuta, H., Tanaka, T., Yoshimoto, K., Ohno, H., Nagamatsu, S., Ishida, H., 2008. JNK- and I[math>\kappaB]-dependent pathways regulate MCP-1 but not adiponectin release from artificially hypertrophied 3T3-L1 adipocytes preloaded with palmitate in vitro. *Am. J. Physiol. Endocrinol. Metab.* 294, E898–E909.
- Tilg, H., Moschen, A.R., 2006. Adipocytokines: mediators linking adipose tissue, inflammation and immunity. *Nat. Rev. Immunol.* 6, 772–783.
- Turing, A.M., 1990. The chemical basis of morphogenesis. 1953. *Bull. Math. Biol.* 52, 153–197 (discussion 119–152).
- Unger, R.H., 1995. Lipotoxicity in the pathogenesis of obesity-dependent NIDDM. Genetic and clinical implications. *Diabetes* 44, 863–870.
- Wagner, H., 2011. Synergy research: approaching a new generation of phytopharmaceuticals. *Fitoterapia* 82, 34–37.
- Williamson, G., Dionisi, F., Renouf, M., 2011. Flavonols from green tea and phenolic acids from coffee: critical quantitative evaluation of the pharmacokinetic data in humans after consumption of single doses of beverages. *Mol. Nutr. Food Res.* 55, 864–873.
- Yang, J.Y., Della-Fera, M.A., Rayalam, S., Ambati, S., Hartzell, D.L., Park, H.J., Baile, C.A., 2008. Enhanced inhibition of adipogenesis and induction of apoptosis in 3T3-L1 adipocytes with combinations of resveratrol and quercetin. *Life Sci.* 82, 1032–1039.
- Yeop Han, C., Kargi, A.Y., Omer, M., Chan, C.K., Wabitsch, M., O'Brien, K.D., Wight, T.N., Chait, A., 2010. Differential effect of saturated and unsaturated free fatty acids on the generation of monocyte adhesion and chemotactic factors by adipocytes: dissociation of adipocyte hypertrophy from inflammation. *Diabetes* 59, 386–396.
- Yu, Y.H., Zhu, H., 2004. Chronological changes in metabolism and functions of cultured adipocytes: a hypothesis for cell aging in mature adipocytes. *Am. J. Physiol. Endocrinol. Metab.* 286, E402–E410.









CAPÍTULO 9. HPLC-ESI-TOF-MS
bioavailability study in rats after oral
ingestion of *Hibiscus sabdariffa*
polyphenol-enriched extract.





HPLC-ESI-TOF-MS bioavailability study in rats after oral ingestion of *Hibiscus sabdariffa* polyphenol-enriched extract

Salvador Fernández-Arroyo^{a,†}, María Herranz-López^{b,†}, Raúl Beltrán-Debón^c, Isabel Borrás Linares^a, Enrique Barraión-Catalán^b, Jorge Joven^c, Alberto Fernández-Gutiérrez^a, Antonio Segura-Carretero^{a,*} and Vicente Micol^b

^aDepartment of Analytical Chemistry, Faculty of Sciences, University of Granada, Av/ Fuentenueva, 18071, Granada, Spain.

^bInstitute of Molecular and Cell Biology (IMCB). Miguel Hernández University. Elche, Alicante. Spain.

^cCentre de Recerca Biomèdica, Hospital Universitari de Sant Joan, IISPV, Universitat Rovira i Virgili, C/ Sant Joan s/n, 43201, Reus, Spain.

†These authors have equally contributed to this research and are listed in random order.

*Corresponding author. Address: Department of Analytical Chemistry, Faculty of Sciences, University of Granada, Av/ Fuentenueva, 18071, Granada, Spain. Tel.: +34-958243296. E-mail address: ansegura@ugr.es (A. Segura Carretero)

**Abstract**

In this bioavailability study, 17 polyphenols and metabolites have been detected and quantified in rat plasma by high-performance liquid chromatography coupled to time-of-flight mass spectrometry (HPLC-ESI-TOF-MS) after the oral ingestion of *Hibiscus sabdariffa* polyphenolic-enriched extract. Eleven of these compounds were metabolites. Whereas phenolic acids were found in plasma without any modification in their structures, most flavonols were found as quercetin or kaempferol glucuronide conjugates. An average of 5 μM equivalents of plasma circulating flavonols was found at their highest determined concentration. Flavonol glucuronide conjugates, which show longer half-life elimination values, are proposed to contribute to the observed lipid peroxidation inhibitory activity in cellular membranes. By contrast, phenolic acids appear to exert their antioxidant activity through ferric ion reduction and superoxide scavenging at shorter times. No anthocyanins were detected in the plasma samples. We propose that flavonol-conjugated forms (quercetin and kaempferol) may be the compounds responsible for the observed antioxidant effects and thus contribute to the healthy effects of *Hibiscus sabdariffa* polyphenolic extract.

Keywords: HPLC-ESI-TOF-MS / bioavailability / *Hibiscus sabdariffa* / phenolic extract / antioxidant capacity / quercetin glucuronide



1. Introduction

The demonstration of the beneficial effects of dietary polyphenols on health is becoming an important issue. Although most cellular studies have proven their biological effects at the *in vitro* level, the correlation between the *in vivo* observed effects and the presence of the responsible metabolites is still a great challenge. The estimated total dietary intake of polyphenols is about 1g/day, distributed among about one-third of phenolic acids and two-thirds of flavonoids. Nevertheless, bioavailability of phenolic compounds in humans is very low due to poor intestinal absorption and because gut microbiota, which reflect a complex interplay of diet and genetics, heavily metabolize the phytonutrients. After acute consumption of up to 100 mg of a single compound, the maximum concentration in plasma rarely exceeds 1 μ M [1, 2].

Hibiscus sabdariffa (HS) L. (family: *Malvaceae*), called bissap, karkade or roselle, is a tropical plant commonly used as local soft drink. The calyces are rich in polysaccharides [3] and phenolic compounds. Our group has contributed substantially to the characterization and quantification of the composition of this plant, which contains organic acids, phenolic acids, anthocyanins, and flavonols as main compounds [4, 5].

The aqueous extracts of HS have been commonly used in folk medicine to treat hypertension, fever, inflammation, liver disorders, and obesity. Previous studies have shown that HS possesses anti-tumor and antioxidant properties [6-8]. In humans, HS significantly decreases MCP-1 plasma concentration, suggesting that HS may be a valuable traditional herbal medicine for treating chronic inflammatory diseases [9]. Recent data also indicate that aqueous extracts of *H. Sabdariffa* might ameliorate metabolic disturbances [10-12][10, 11]. The antioxidant and antihyperlipemic properties of HS aqueous extract have been previously reported by our group using a mouse model [5]. Moreover, the strong antioxidative and hypolipidemic properties of a HS polyphenolic extract have been recently reported in a cell model for adipogenesis and insulin resistance [13]. In any case, the compounds or metabolites responsible for such activities have not yet been identified.



In this study, the major metabolites present in the plasma of rats after acute ingestion of a polyphenol-enriched *Hibiscus sabdariffa* extract (PEHS) were identified and quantified by high-performance liquid chromatography with diode-array detection coupled to electrospray time-of-flight mass spectrometry (HPLC-DAD-ESI-TOF-MS). This analytical technique is a powerful tool for the metabolomic analysis of phenolic metabolites [14]. The antioxidant status of the plasma samples was also measured through several complementary antioxidant techniques: the ferric reducing ability of plasma (FRAP) method, the thiobarbituric acid reactive substances (TBARS) assay, and the superoxide dismutase activity assay (SOD).

2. Material and Methods

2.1. Chemicals

All chemicals were of analytical HPLC reagent grade and used as received. Formic acid and acetonitrile used for preparing mobile phases were purchased from Fluka, Sigma-Aldrich (Steinheim, Germany) and Lab-Scan (Gliwice, Sowinskiego, Poland), respectively. Solvents were previously filtered using a Solvent Filtration Apparatus 58061 (Supelco, Bellefonte, PA, USA). The standards for the calibration curves, citric acid, chlorogenic acid, methylgallate, N-feruloyltyramine, quercetin 3-glucoside, quercetin, isorhamnetin and kaempferol were purchased either from Fluka, Sigma-Aldrich (Steinheim, Germany), Extrasynthese (Genay Cedex, France) or Polyphenols (Polyphenols Laboratories AS, Hanaveien Sandnes, Norway). The stock solutions containing these analytes were prepared in deionized water except flavonols, which were prepared in methanol (Lab-Scan). Trichloroacetic acid (TCA), thiobarbituric acid (TBA), 1,1,3,3-tetraethoxypropane (TEP), 2,4,6-tripyridyl-S-triazine (TPTZ), ferric chloride (FeCl_3); ferric sulfate (FeSO_4), xanthine, xanthine oxidase, and cytochrome C were purchased from Sigma–Aldrich Corp. (St. Louis, MO, USA).

2.2. Extraction Method of *Hibiscus sabdariffa* phenolic compounds (PEHS)



First, an aqueous extract was obtained from sun-dried calyces of plants harvested by researchers in Senegal with an approximate plant-to-extract ratio of 5:1 as previously described [9]. The purified extract (PEHS) was prepared removing fiber and polysaccharides in a precipitation step using 85% ethanol (v/v). Then, the extract was reconstituted in water at 170 mg/ml and loaded onto a 1.5 cm x 25 cm chromatography column containing Amberlite™ FPX66 (Rohm and Haas, Philadelphia, PA, USA). The phenolic fraction retained was finally eluted with 95% ethanol and 0.01% trifluoroacetic acid, rotary evaporated and freeze-dried.

2.3. Animals

Sixteen male Wistar rats (240-280 g) were housed in standard cages at room temperature with free access to food and water for two weeks. Throughout the experiments, the animals were processed according to the suggested ethical guidelines for the care of laboratory animals [15]. After being food deprived 18 h before testing, the rats were orally treated with PEHS (1200 mg/kg) via gastric gavage. For the administration, the extract was resuspended in saline buffer (1 mL). The control group (four rats) received only buffer. The animals were anesthetized using isoflurane and the blood samples were withdrawn via cardiac puncture into heparinized tubes at 0 (control group), 20, 60, and 120 min post dosing (four animals per time). All blood samples were centrifuged at 1000 g for 15 min at 4°C, and then plasma was stored at -80°C.

2.4. Bioavailability study in plasma by HPLC-ESI-TOF-MS

Plasma (200 µL) was mixed with 1000 µL of 0.2 M HCl in methanol. After 2 h at -20 °C, the mixture was centrifuged at 18,800 g for 5 min at 4°C, and the supernatant was evaporated to dryness. The dried sample was reconstituted in 100 µL of mobile phase (1% formic acid in water-acetonitrile 90:10). The chromatographic, UV and ESI-TOF-MS conditions were performed as previously reported [5]. The rest of the compounds were quantified using the respective pure standard compound. C_{max} and t_{max} were determined by experimental observation. The half-life ($t_{1/2}$) was calculated as $\ln 2 / k_{el}$, where k_{el} (elimination rate constant) was established from the slope of the elimination phase in the concentration vs. time plot. For identification, quercetin, kaempferol, and chlorogenic acid were compared with their



corresponding standards using TOF-MS. N-feruloyltyramine, methylgallate, hibiscus acid, hibiscus acid hydroxyethyl ester, and hydroxycitric acid were compared with the retention time of these compounds in PEHS and the accuracy mass and molecular formula provided by the TOF-MS. Glucuronidated flavonols were identified by comparing their mass spectra obtained by TOF-MS with those interpreted according to previously reported data. The compounds were quantified using citric acid for organic acids, quercetin for quercetin derivatives and kaempferol for kaempferol derivatives. The rest of compounds were quantified using their respective standards.

2.5. Analysis of plasma MDA

50 μL of plasma were mixed with 50 μL of 0.05% BHT in ethanol and 50 μL of TCA 20% in HCl 0.6 M. These samples were incubated 15 min on ice and centrifuged at 5000 g for 15 min at 4°C. Then 100 μL of TBA 0.6% in water were added to 100 μL of supernatant. Subsequently, the mixture was incubated at 97°C for 1 h, allowed to cool and extracted with 300 μL of n-butanol through vigorous shaking, and then samples were centrifuged at 10,000 g for 3 min. The TBA-MDA chromogen was determined by using HPLC coupled to fluorescence detection as reported [16], using 515 and 553 nm as excitation and emission wavelengths, respectively. A calibration curve of MDA (0-3.2 nmol), obtained by acidic hydrolysis of 1,1,3,3-tetraethoxypropane (TEP), was used. This was done by preparing a solution of 10 mM TEP in 1% H_2SO_4 and allowing the mixture to stand at room temperature for 24 h before use. The results were expressed as nmol MDA / ml of rat plasma.

2.6. Ferric-reducing ability of plasma (FRAP)

For an assessment of the plasma antioxidant capacity, the ferric-reducing ability of plasma (FRAP) was measured as previously described [17]. Briefly, 40 μL of diluted plasma samples (1:2) were mixed on a 96-well plate with 250 μL of freshly prepared FRAP reagent. Samples were incubated for 10 min at 37°C and then absorbance at 593 nm was recorded during 4 min on a microplate reader (SPECTROstar Omega, BMG LabTech GmbH, Offenburg, Germany). FRAP values were calculated using $\text{FeSO}_4 \cdot 7\text{H}_2\text{O}$ as standard and were expressed as μM FeSO_4 .



2.7. Superoxide dismutase (SOD) activity in plasma

SOD activity was measured through an adaptation of a previously reported method [18]. The xanthine/xanthine oxidase system was used to generate the superoxide anion. This anion reduced cytochrome C, which was monitored at 550 nm. The SOD-like activity of the tested sample removed the superoxide anion and inhibited the cytochrome C reduction. The activity was determined with a SPECTROstar Omega microplate reader at 37°C.

2.8. Statistical analysis

Statistical analysis was performed using the Microcal Origin 8.5 software (OriginLab). Values were represented as means \pm standard deviation. Differences between two or more groups were compared using non-parametric tests and were considered statistically significant when $p < 0.05$. The means of quantitative variables were analyzed using a one-way ANOVA, Student's t-test for unpaired samples, and Tukey's test for multiple comparisons.

3. Results and discussion

3.1. Bioavailability analysis after oral ingestion of HS polyphenols

The detailed composition of the *Hibiscus sabdariffa* polyphenolic extract (PEHS) used for the study has been reported previously (Supplementary information, Table 1) [13]. The rats were orally administered to determine the presence of phenolic compounds and their metabolites in rat plasma.

A total of 17 compounds were detected in plasma samples using HPLC-ESI-TOF-MS (Fig. 1). Table 1 lists the retention times of these compounds, the accuracy mass and molecular formula provided by the TOF-MS. Six compounds were already present in the original extract: chlorogenic acid, N-feruloyltyramine, quercetin, methylgallate, hibiscus acid, and hibiscus acid hydroxyethyl ester (Supplementary information, Table 1). Eleven compounds were metabolites: hydroxycitric acid, four quercetin diglucuronide isomers, two quercetin glucuronide isomers, a



methyl quercetin derivative (isorhamnetin or tamarixetin), kaempferol and two kaempferol glucuronide isomers (Fig. 1). Nevertheless, hydroxycitric acid is naturally present in *Hibiscus sabdariffa* raw material, but PEHS was devoid of this compound since this extract was obtained after reverse chromatographic separation in non-polar solvent. Therefore, we assume that the hydroxycitric acid found in the rat plasma derived most probably from metabolized hibiscus acid, or hibiscus acid ester derivatives.

After oral administration, deglycosylation of flavonoids is likely to occur either pre- or post-absorption in rats [19, 20] but also in other mammals. Therefore, all quercetin glucuronide conjugates determined in this study (phase II metabolites) must derive from the pool of quercetin aglycone to which different quercetin glycosylated and non-glycosylated forms present in PEHS contribute (quercetin-3-sambubioside, quercetin-3-rutinoside, quercetin-3-glucoside, and quercetin; Supplementary information, Table 1). Similarly, kaempferol glucuronides found in rat plasma must derive from kaempferol derivatives present in the extract.

The pharmacokinetic parameters and the quantification of each compound appear in Table 2. The organic acids hibiscus acid, hibiscus acid hydroxyethyl ester, and the metabolite hydroxycitric acid reached high concentrations in plasma at $t_{\max} \geq 120$ min (>100 μM for hibiscus acid), contributing to micromole amounts of organic acids in plasma. Phenolic acid derivatives found in rat plasma were chlorogenic acid, methyl digallate, and N-feruloyltyramine. Chlorogenic acid reached 3.8 μM at 60 min and methyl digallate and N-feruloyltyramine registered concentration values below 1 μM , at 60 and 20 min, respectively. These compounds also exhibited low elimination half-life values most probably indicating a lack of tissue accumulation.

Considering a total dose of 1200 mg/Kg (360 mg of extract administered to each rat), all quercetin derivatives in PEHS (quercetin-3-sambubioside, quercetin-3-rutinoside, quercetin-glucoside, and quercetin; Supplementary information, Table 1) accounted for 16.8 μmol , whereas kaempferol derivatives in PEHS totaled 2.0 μmol equivalents. Most quercetin conjugated forms were within the low micromolar range in rat plasma. The highest concentrations were found for quercetin glucuronide (isomer 1) and quercetin, i.e. 2.17 μM and



1.57 μM , respectively. The rest of quercetin conjugated forms, including a methyl-quercetin derivative (isorhamnetin or tamarixetin), were found at concentrations lower than 1 μM . The methylated forms of quercetin have been found as phase II metabolites after quercetin administration in previous studies [21]. All kaempferol derivatives were also found in concentrations lower than 1 μM . The total concentration of flavonol conjugated forms (quercetin + kaempferol) in plasma obtained from the concentrations determined at t_{max} yielded about 4.3 μM at 20-60 min and 5.5 μM at 120 min. These values agree with those reported for the oral administration of other quercetin-enriched extracts in rats [20, 22].

Among all the quercetin derivatives, quercetin-3-glucoside reportedly has better absorption than does quercetin aglycone or other glycosides bearing a rhamnose moiety [23]. Hence, this compound in PEHS must be the one that contributes most to the different glucuronidated forms of quercetin in rat plasma. However, we cannot rule out that some of the quercetin conjugates found in plasma could also derive from glycosylated kaempferol derivatives present in PEHS through oxidative conversion and conjugation, as reported elsewhere [24]. It is also remarkable that quercetin conjugates have longer elimination half-life values than those of phenolic acids, especially quercetin diglucuronide (isomer 4), indicating that these compounds may accumulate in the tissues and could be responsible for long-term effects.

Consequently, the total flavonol concentration found in rat plasma after a dose of 1200 mg/kg of hibiscus polyphenols was about 5 μM within the 60-120 min period following ingestion. Since the elimination rate of quercetin metabolites has been reported to be very low [21], higher plasma quercetin concentration could be easily maintained in rats with a subchronic administration of hibiscus polyphenolic extract, a possibility that may deserve further research.

3.2. Antioxidant activity of plasma

Despite of the abovementioned low bioavailability of most polyphenols, some studies have reported the enhancement of plasma antioxidant status after oral administration of polyphenol-enriched extracts in animal models. In the present study, the *ex vivo* antioxidant activity of plasma samples from rats previously fed with a polyphenol-enriched *H. sabdariffa* extract was determined. Several free-radical scavenging measurements were performed in the same



samples in which the bioavailability study was conducted: determination of the level of plasma malondialdehyde (MDA) by HPLC, the ferric-reducing ability of plasma (FRAP value), and the superoxide dismutase (SOD) activity.

3.2.1. Radical-scavenging capacity by measurement of the inhibition of malondialdehyde (MDA) generation

MDA, a thiobarbituric reactive substance (TBARS), is considered a reactive species that derives from oxidation of polyunsaturated lipids causing toxic stress and advanced lipoxidation end products. This compound is generally accepted as a biomarker of oxidative stress [25]. Upon PEHS ingestion, the amount of plasma MDA was decreasing with the time of sample extraction showing a minimum value at the latest time tested, i.e. 120 min (Figure 2A). Organic acids such as hydroxycitric acid are less likely to inhibit lipid oxidation. Phenolic acids reached their maximum concentration at 20-60 min, implying that at 120 min these compounds would be in the elimination phase. Therefore, this result indicates that antioxidant compounds promoting a maximum antioxidant activity against lipid peroxidation would be those having the highest concentration at the longest times of the study (60-120 min), such as some quercetin glucuronide or kaempferol glucuronide conjugates (Table 2). This may also indicate that the potential molecular site of these compounds is located at phospholipid cell membranes or plasma lipoproteins, to protect them from ROS peroxidative attack, as postulated previously [26].

3.2.2. Ferric Reducing Ability of Plasma (FRAP)

The FRAP method measures the capacity of antioxidant compounds to reduce the ferric ions by an electron transfer (ET) mechanism. The results show that the maximum ferric reducing activity was achieved fairly fast, i.e. in plasma samples taken at 20 min after oral ingestion (Figure 2B). At 60 and 120 min, FRAP values were decreasing, but significant differences still appeared compared with control samples ($p < 0.05$). The fast response of this free-radical scavenging activity in plasma may be related to phenolic compounds that promote a fast absorption process in the small intestine. This correlates with the presence of phenolic acids



such as chlorogenic acid, methylgallate or even N-feruloyltyramine, which reach their maximum concentration at 20-60 min. In agreement with this statement, chlorogenic, ferulic, and caffeic acid derivatives have shown fast absorption process when administered in complex food matrixes [16, 27].

3.2.3. Superoxide Dismutase (SOD) Activity

The capability of rat plasma samples to scavenge superoxide radicals was determined by using the xanthine/xanthine oxidase system coupled to superoxide dismutase (SOD) (Figure 2C). The results showed that maximum capacity to inhibit the formation of the superoxide anion radicals in plasma, i.e. SOD-like activity, was also reached at 20 min after oral ingestion of PEHS. Significant differences in SOD activity were also observed at 60 min compared to control ($p < 0.05$). This result agrees with the result found in the FRAP determination, which may indicate that both activities are due to the same plasma compounds. It has been reported that chlorogenic acid was the main contributor among other phenolic compounds to SOD-like activity in apple vinegar [28].

The biological activity of quercetin-related metabolites has recently attracted much interest. Quercetin methylated conjugates have provided oxidative-stress resistance, thermotolerance, and life-span properties in *C. elegans* [29]. Quercetin metabolites, especially quercetin 3-O-*beta*-D-glucuronide, retain significant antioxidant activity compared to quercetin aglycone and accumulate in aortic tissue [30]. Quercetin-3-glucuronide has shown antioxidant capacity against copper-ion-induced oxidation of human plasma LDL [31] and inhibits myeloperoxidase activity in activated neutrophils [32, 33]. Quercetin glucuronides also inhibit glucotoxicity and apoptosis in human umbilical-vein endothelial cells [34]. Macrophages were found to be targets of quercetin glucuronides, by suppressing factors which contribute to foam-cell formation [35]. Moreover, quercetin glucuronides do not show pro-oxidant properties as quercetin does [36]. All this evidence strengthens the contention that quercetin metabolites may have a protective role in chronic inflammatory conditions such as cardiovascular disease.



Many different bioavailability studies on phenolic acids, anthocyanins, and flavonols contained in different food matrixes are available in the literature. Nevertheless, studies focusing on the particular combination of polyphenols in *Hibiscus sabdariffa* may be necessary because their interaction and absorption in the gastrointestinal tract may have particular determinants. The identification of the flavonol metabolites after the ingestion of *Hibiscus* polyphenols in humans requires further research in order to identify the compounds responsible for the healthful effects. It has been reported that the metabolite profile of human plasma after the intake of onions is similar to that with intragastric administration in rats [37]. Thus, the results in the present work may offer a plausible approach.

The maximum concentration of plasma-circulating flavonols determined in this study after a single oral administration of hibiscus polyphenols was about 5 μM within the 60-120 min period following ingestion. It was reported that even higher concentrations might be easily maintained in plasma with a regular supply of flavonols in the diet [21]. Considering all these facts, and taking into account that flavonols metabolites in the different tissues were not determined in this study, we can regard the use of flavonol metabolites in cell models within the high micromolar range as being a physiological situation. Recently, we have demonstrated the potential pharmacological and therapeutic superiority of the combination of polyphenols from HS with respect to their individual components in cell models [13]. Nevertheless, it remains to be ascertained whether or not the flavonol glucuronides found in the present study retain the biological activity of their parental polyphenols in similar cell models.

4. Conclusions

In conclusion, a total of 17 compounds were detected by HPLC-ESI-TOF-MS in the plasma of rats after the oral ingestion of *H. sabdariffa* polyphenolic-enriched extract. Six of these were already in the extract while 11 were metabolites. Phenolic acids remained intact in plasma but most flavonols were found as quercetin or kaempferol glucuronide conjugates. The highest concentration of plasma-circulating flavonols was about 5 μM within the 60- to 120-min period



following ingestion. Flavonol glucuronide conjugates are proposed to account for the inhibition of lipid peroxidation in cellular membranes at longer times. By contrast, phenolic acids are postulated to exert their reduction and superoxide-scavenging capacities at shorter time intervals and are ruled out as candidates for long-term health benefits, since they do not accumulate. No anthocyanins were detected in the plasma samples. Therefore, we suggest that flavonol-conjugated forms (quercetin and kaempferol) may be the compounds responsible for the observed antioxidant effects and thus contribute to the healthy effects of *Hibiscus sabdariffa*. Hence, the study of the molecular and cellular targets of these metabolites in different cell models deserves further attention in future studies.

5. Acknowledgements

We thank MONTELOEDER, SL for providing raw plant material and for advice on the extraction and purification procedures. The authors are grateful to the Spanish Ministry of Science and Innovation for the projects AGL2008-05108-C03-03/ALI and AGL2011-29857-C03-02, Andalusian Regional Government Council of Innovation and Science for the excellence projects P09-CTS-4564, P10-FQM-6563 and P11-CTS-7625 and to GREIB.PT.2011.18 projects. SFA would like to thank Andalusian Regional Government Council of Innovation and Science for the fellowship P07-AGR-02619. RBD and MHL were the recipients of fellowships from the Comissionat per a Universitats I Recerca del Departament d'Innovació, Universitats I Empresa de la Generalitat de Catalunya and Programa Vali+d from Generalitat Valenciana, respectively. IBL acknowledges financial support from the Spanish Ministry of Education and Science (FPI grant, BES-2009-028128).

The authors declare that there are no conflicts of interest.

6. References



- [1] Manach C, Williamson G, Morand C et al (2005) Bioavailability and bioefficacy of polyphenols in humans. I. Review of 97 bioavailability studies RID C-9684-2010. *Am J Clin Nutr* 81:2
- [2] Scalbert A, Williamson G (2000) Dietary intake and bioavailability of polyphenols RID C-9684-2010. *J Nutr* 130:2073S
- [3] MULLER B, FRANZ G (1992) Chemical-Structure and Biological-Activity of Polysaccharides from Hibiscus-Sabdariffa. *Planta Med* 58:60
- [4] Rodriguez-Medina IC, Beltran-Debon R, Micol Molina V et al (2009) Direct characterization of aqueous extract of Hibiscus sabdariffa using HPLC with diode array detection coupled to ESI and ion trap MS. *Journal of Separation Science* 32:3441
- [5] Fernández-Arroyo S, Rodríguez-Medina IC, Beltrán-Debón R et al (2011) Quantification of the polyphenolic fraction and in vitro antioxidant and in vivo anti-hyperlipemic activities of Hibiscus sabdariffa aqueous extract. *Food Res Int* 44:1490
- [6] Chang YC, Huang HP, Hsu JD et al (2005) Hibiscus anthocyanins rich extract-induced apoptotic cell death in human promyelocytic leukemia cells. *Toxicol Appl Pharmacol* 205:201
- [7] Farombi EA, Fakoya A (2005) Free radical scavenging and antigenotoxic activities of natural phenolic compounds in dried flowers of Hibiscus sabdariffa L. *Molecular Nutrition & Food Research* 49:1120
- [8] Ochani PC, D'Mello P (2009) Antioxidant and antihyperlipidemic activity of Hibiscus sabdariffa Linn. leaves and calyces extracts in rats. *Indian J Exp Biol* 47:276
- [9] Beltran-Debon R, Alonso-Villaverde C, Aragonés G et al (2010) The aqueous extract of Hibiscus sabdariffa calices modulates the production of monocyte chemoattractant protein-1 in humans. *Phytomedicine* 17:186
- [10] Carvajal-Zarrabal O, Waliszewski SM, Barradas-Dermitz DMA et al (2005) The consumption of Hibiscus sabdariffa dried calyx ethanolic extract reduced lipid profile in rats. *Plant Foods for Human Nutrition* 60:153
- [11] Alarcon-Aguilar FJ, Zamilpa A, Perez-Garcia MD et al (2007) Effect of Hibiscus sabdariffa on obesity in MSG mice. *J Ethnopharmacol* 114:66
- [12] Kim J, So H, Youn M et al (2007) Hibiscus sabdariffa L. water extract inhibits the adipocyte differentiation through the PI3-K and MAPK pathway. *J Ethnopharmacol* 114:260
- [13] Herranz-López M, Fernández-Arroyo S, Pérez-Sánchez A et al Synergism of plant-derived polyphenols in adipogenesis: perspectives and implications. *Phytomedicine*
- [14] Neumann S, Bocker S (2010) Computational mass spectrometry for metabolomics: identification of metabolites and small molecules. *Anal Bioanal Chem* 398:2779
- [15] Morton D, Jennings M, Buckwell A et al (2001) Refining procedures for the administration of substances. *Lab Anim* 35:1
- [16] Funes L, Fernandez-Arroyo S, Laporta O et al (2009) Correlation between plasma antioxidant capacity and verbascoside levels in rats after oral administration of lemon verbena extract. *Food Chem* 117:589



- [17] Benzie I, Strain J (1996) The ferric reducing ability of plasma (FRAP) as a measure of "antioxidant power": The FRAP assay. *Anal Biochem* 239:70
- [18] MCCORD J, FRIDOVIC.I (1969) Superoxide Dismutase an Enzymic Function for Erythrocyte (Hemocytin). *J Biol Chem* 244:6049
- [19] van der Woude H, Boersma MG, Vervoort J et al (2004) Identification of 14 quercetin phase II mono- and mixed conjugates and their formation by rat and human phase II in vitro model systems. *Chem Res Toxicol* 17:1520
- [20] Zhao G, Zou L, Wang Z et al (2011) Pharmacokinetic Profile of Total Quercetin after Single Oral Dose of Tartary Buckwheat Extracts in Rats. *J Agric Food Chem* 59:4435
- [21] Manach C, Morand C, Demigne C et al (1997) Bioavailability of rutin and quercetin in rats. *FEBS Lett* 409:12
- [22] Carbonaro M, Grant G (2005) Absorption of quercetin and rutin in rat small intestine. *Ann Nutr Metab* 49:178
- [23] Morand C, Manach C, Crespy V et al (2000) Respective bioavailability of quercetin aglycone and its glycosides in a rat model. *Biofactors* 12:169
- [24] Barve A, Chen C, Hebbar V et al (2009) Metabolism, oral bioavailability and pharmacokinetics of chemopreventive kaempferol in rats. *Biopharm Drug Dispos* 30:356
- [25] Del Rio D, Stewart AJ, Pellegrini N (2005) A review of recent studies on malondialdehyde as toxic molecule and biological marker of oxidative stress. *Nutr Metab Cardiovasc Dis* 15:316
- [26] Shirai M, Moon JH, Tsushida T et al (2001) Inhibitory effect of a quercetin metabolite, quercetin 3-O-beta-D-glucuronide, on lipid peroxidation in liposomal membranes. *J Agric Food Chem* 49:5602
- [27] Stalmach A, Mullen W, Barron D et al (2009) Metabolite Profiling of Hydroxycinnamate Derivatives in Plasma and Urine after the Ingestion of Coffee by Humans: Identification of Biomarkers of Coffee Consumption RID B-3250-2009 RID C-9684-2010. *Drug Metab Disposition* 37:1749
- [28] Nakamura K, Ogasawara Y, Endou K et al (2010) Phenolic Compounds Responsible for the Superoxide Dismutase-like Activity in High-Brix Apple Vinegar. *J Agric Food Chem* 58:10124
- [29] Surco-Laos F, Cabello J, Gomez-Orte E et al (2011) Effects of O-methylated metabolites of quercetin on oxidative stress, thermotolerance, lifespan and bioavailability on *Caenorhabditis elegans*. *Food Funct* 2:445
- [30] Duenas M, Gonzalez-Manzano S, Gonzalez-Paramas A et al (2010) Antioxidant evaluation of O-methylated metabolites of catechin, epicatechin and quercetin. *J Pharm Biomed Anal* 51:443
- [31] Moon JH, Tsushida T, Nakahara K et al (2001) Identification of quercetin 3-O-beta-D-glucuronide as an antioxidative metabolite in rat plasma after oral administration of quercetin. *Free Radic Biol Med* 30:1274
- [32] Loke WM, Proudfoot JM, McKinley AJ et al (2008) Quercetin and its in vivo metabolites inhibit neutrophil-mediated low-density lipoprotein oxidation. *J Agric Food Chem* 56:3609



[33] Shiba Y, Kinoshita T, Chuman H et al (2008) Flavonoids as substrates and inhibitors of myeloperoxidase: molecular actions of aglycone and metabolites. *Chem Res Toxicol* 21:1600

[34] Chao CL, Hou YC, Chao PD et al (2009) The antioxidant effects of quercetin metabolites on the prevention of high glucose-induced apoptosis of human umbilical vein endothelial cells. *Br J Nutr* 101:1165

[35] Kawai Y, Nishikawa T, Shiba Y et al (2008) Macrophage as a target of quercetin glucuronides in human atherosclerotic arteries: implication in the anti-atherosclerotic mechanism of dietary flavonoids. *J Biol Chem* 283:9424

[36] Lodi F, Jimenez R, Menendez C et al (2008) Glucuronidated metabolites of the flavonoid quercetin do not auto-oxidise, do not generate free radicals and do not decrease nitric oxide bioavailability. *Planta Med* 74:741

[37] Kawai Y, Saito S, Nishikawa T et al (2009) Different profiles of quercetin metabolites in rat plasma: comparison of two administration methods. *Biosci Biotechnol Biochem* 73:517



Table 1. Relevant analytical data for the compounds identified in the samples of rat plasma after the ingestion of a polyphenolic-enriched *H. sabdariffa* extract (PEHS) (see also Figure 1).

Peak num	Compound	Retention time (min)	Molecular Formula	[M-H] ⁻
1	Hydroxycitric acid	2.65	C ₆ H ₈ O ₈	207.0140
2	Hibiscus acid	3.10	C ₆ H ₆ O ₇	189.0035
3	Hibiscus acid hydroxyethyl ester	3.88	C ₈ H ₁₂ O ₈	235.0461
4	Chlorogenic acid	5.53	C ₁₆ H ₁₈ O ₉	353.0891
5	Methyl digallate	7.42	C ₁₅ H ₁₂ O ₉	335.0409
6	Quercetin diglucuronide (isomer 1)	10.15	C ₂₇ H ₂₆ O ₁₉	653.0996
7	Quercetin diglucuronide (isomer 2)	11.75	C ₂₇ H ₂₆ O ₁₉	653.0996
8	Quercetin diglucuronide (isomer 3)	13.05	C ₂₇ H ₂₆ O ₁₉	653.0996
9	Quercetin diglucuronide (isomer 4)	14.38	C ₂₇ H ₂₆ O ₁₉	653.0996
10	Quercetin glucuronide (isomer 1)	15.57	C ₂₁ H ₁₈ O ₁₃	477.0674
11	Quercetin glucuronide (isomer 2)	16.20	C ₂₁ H ₁₈ O ₁₃	477.0674
12	Kaempferol glucuronide (isomer 1)	19.45	C ₂₁ H ₁₈ O ₁₂	461.0726
13	Kaempferol glucuronide (isomer 2)	20.25	C ₂₁ H ₁₈ O ₁₂	461.0726
14	N-Feruloyltyramine	25.60	C ₁₈ H ₂₀ NO ₄	312.1234
15	Quercetin	27.58	C ₁₅ H ₁₀ O ₇	301.0339
16	Kaempferol	29.92	C ₁₅ H ₁₀ O ₆	285.0405
17	Methyl-Quercetin	30.06	C ₁₆ H ₁₂ O ₇	315.0510



Table 2. Total administered and circulating plasma moles, and pharmacokinetic parameters of rat plasma phenolic compounds and their metabolites after oral administration of PEHS. Metabolites are indicated in italics.

Compound	Administered dose (μmol) ^a	Plasma max. amount (nmol) ^b	C _{max} (μM)	t _{max} (min)	t _{1/2} (min)
Hibiscus acid	244.1	1,749.6 \pm 71.2	112.50 \pm 4.57 ^c	$\geq 120^c$	--- ^d
Hibiscus acid hydroxyethylester	125.3	94.8 \pm 12.1	6.07 \pm 0.77 ^c	$\geq 120^c$	--- ^d
<i>Hydroxycitric acid</i>	---	196.5 \pm 24.1	12.59 \pm 1.55 ^c	$\geq 120^c$	--- ^d
Hibiscus acid derivatives	499.8	2,041.0			
Chlorogenic acid	108.2	58.8 \pm 5.4	3.77 \pm 0.35	60	77.0
Methyldigallate	3.0	5.0 \pm 0.8	0.32 \pm 0.05	60	38.3
N-feruloyltyramine	1.0	8.3 \pm 2.5	0.54 \pm 0.16	20	46.8
Quercetin	6.9	24.4 \pm 2.7	1.57 \pm 0.18	60	81.5
<i>Quercetin diglucuronide (isomer 1)</i>	---	11.1 \pm 2.1	0.71 \pm 0.13 ^c	$\geq 120^c$	--- ^d
<i>Quercetin diglucuronide (isomer 2)</i>	---	3.6 \pm 0.4	0.23 \pm 0.02 ^c	$\geq 120^c$	--- ^d
<i>Quercetin diglucuronide (isomer 3)</i>	---	14.4 \pm 0.3	0.92 \pm 0.02	60	70.7
<i>Quercetin diglucuronide (isomer 4)</i>	---	11.4 \pm 1.9	0.73 \pm 0.12	60	433.2
<i>Quercetin glucuronide (isomer 1)</i>	---	33.9 \pm 1.9	2.17 \pm 0.12 ^c	$\geq 120^c$	--- ^d
<i>Quercetin glucuronide (isomer 2)</i>	---	12.4 \pm 0.5	0.79 \pm 0.03	20	80.6
<i>Methyl-Quercetin</i>	---	13.7 \pm 1.2	0.88 \pm 0.08 ^c	$\geq 120^c$	--- ^d
Quercetin derivatives	16.8				
<i>Kaempferol</i>	---	12.7 \pm 1.3	0.81 \pm 0.08 ^c	$\geq 120^c$	--- ^d
<i>Kaempferol glucuronide (isomer 1)</i>	---	4.2 \pm 0.2	0.27 \pm 0.01	60	43.3
<i>Kaempferol glucuronide (isomer 2)</i>	---	11.4 \pm 1.5	0.73 \pm 0.09 ^c	$\geq 120^c$	--- ^d
Kaempferol derivatives	2.0				

^a Quantification of total administered polyphenol amount was made on the basis of the concentration (w/w) of each compound in PEHS extract (supplementary information) and total administered extract.

^b Total moles at t_{max} considering an average plasma volume of 60 ml/Kg (6% of body weight).

^c t_{max} was not calculated because C_{max} was not achieved. Data indicate the time and concentration at maximum time assayed.

^d t_{1/2} was not calculated since descent curve was not achieved.



Figure Captions

Fig. 1. Representative base peak chromatograms obtained by HPLC-ESI-TOF-MS of rat plasma samples at 0 (control), and 20, 60 and 120 min following the oral ingestion of *Hibiscus* polyphenols. ESI-TOF-MS spectra of the main compounds found in plasma samples: hydroxycitric acid (1), hibiscus acid (2), hibiscus acid hydroxyethyl ester (3), chlorogenic acid (4), methylgallate (5), quercetin diglucuronide isomers (6-9), quercetin glucuronide isomers (10, 11), kaempferol glucuronide isomers (12, 13), N-feruloyltyramine (14), quercetin (15), kaempferol (16) and methyl-quercetin (17).

Fig. 2. (A) Variation of MDA concentration determined by HPLC-fluorescence in rat plasma samples at 20, 60 and 120 min after the oral ingestion of *Hibiscus* polyphenols. Each bar represents the mean \pm SD (n=6). **(B)** Ferric-reducing capacity of plasma (FRAP) in rats at 20, 60 and 120 min after being orally treated with *Hibiscus* polyphenols. Each bar represents the mean \pm SD (n=8). **(C)** Superoxide dismutase activity in plasma of rats at the same time intervals than those abovementioned after the oral ingestion of *Hibiscus* polyphenols. Each bar represents the mean \pm SD (n=8); *($p < 0.05$) indicates statistically significant differences compared to control.

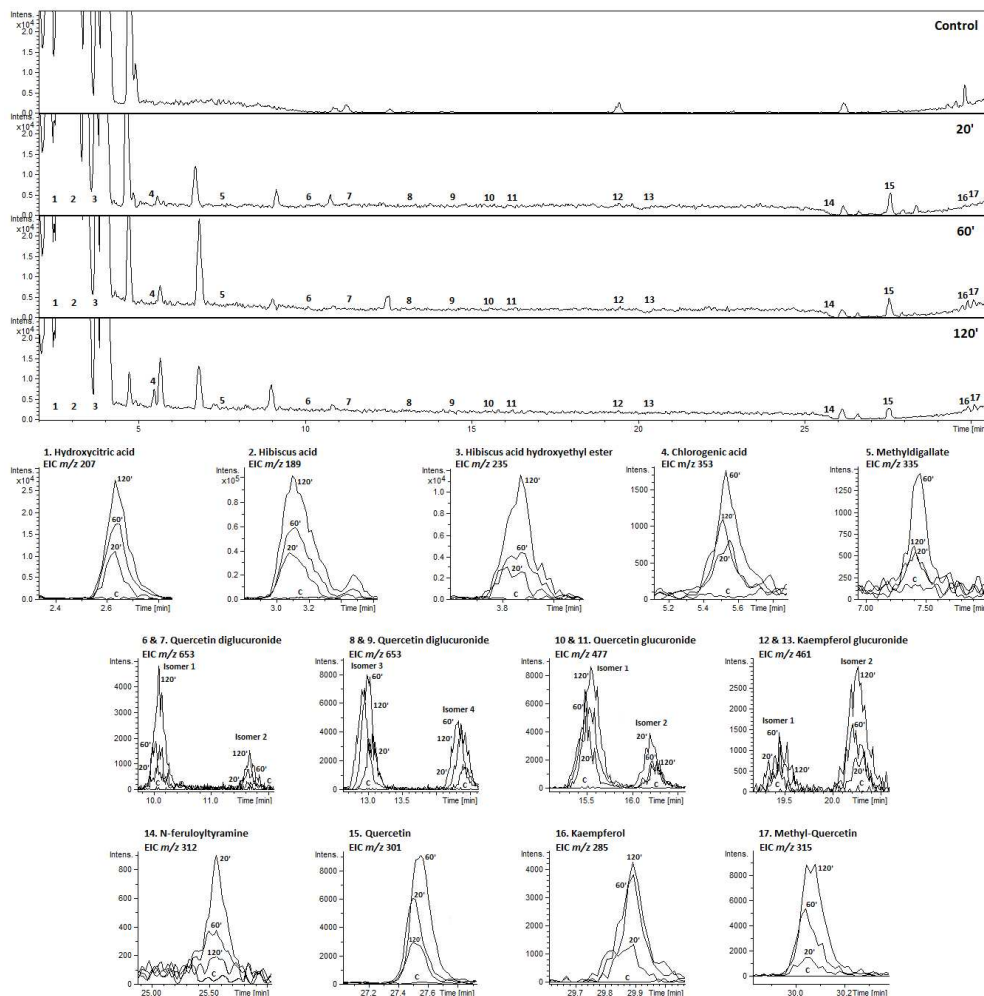


Fig. 1. Representative base peak chromatograms obtained by HPLC-ESI-TOF-MS of rat plasma samples at 0 (control), and 20, 60 and 120 min following the oral ingestion of Hibiscus polyphenols.

ESI-TOF-MS spectra of the main compounds found in plasma samples: hydroxycitric acid (1), hibiscus acid (2), hibiscus acid hydroxyethyl ester (3), chlorogenic acid (4), methylgallate (5), quercetin diglucuronide isomers (6-9), quercetin glucuronide isomers (10, 11), kaempferol glucuronide isomers (12, 13), N-feruloyltyramine (14), quercetin (15), kaempferol (16) and methyl-quercetin (17).

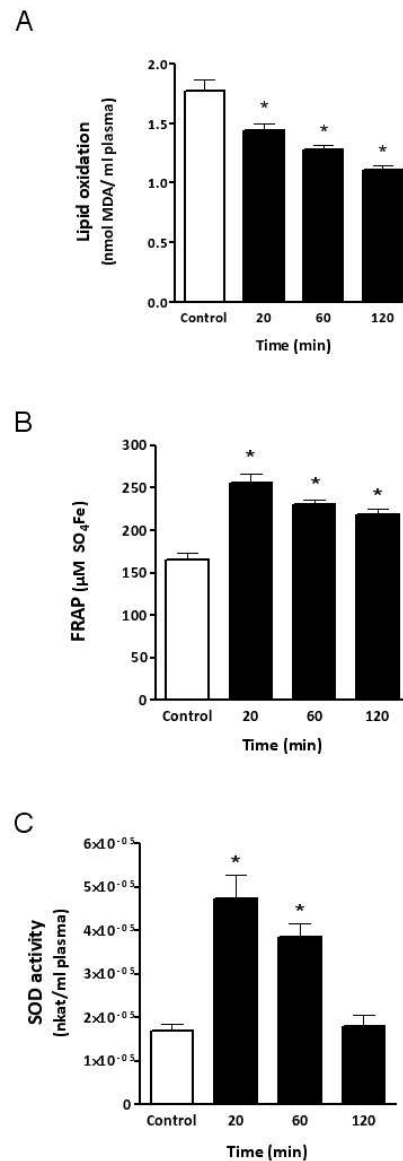


Fig. 2. (A) Variation of MDA concentration determined by HPLC-fluorescence in rat plasma samples at 20, 60 and 120 min after the oral ingestion of Hibiscus polyphenols. Each bar represents the mean \pm SD (n=6). (B) Ferric-reducing capacity of plasma (FRAP) in rats at 20, 60 and 120 min after being orally treated with Hibiscus polyphenols. Each bar represents the mean \pm SD (n=8). (C) Superoxide dismutase activity in plasma of rats at the same time intervals than those abovementioned after the oral ingestion of Hibiscus polyphenols. Each bar represents the mean \pm SD (n=8); *(p<0.05) indicates statistically significant differences compared to control. 141x375mm (72 x 72 DPI)



Table S1. Quantitative data in ppm (w/w) for major components found in the polyphenol-enriched *H. sabdariffa* extract used in the study (PEHS) determined by high-performance liquid chromatography with diode array detection coupled to electrospray time-of-flight mass spectrometry (HPLC-DAD-ESI-TOF-MS).

Compound	Quantification Technique	Concentration (ppm)
Hibiscus acid	MS-TOF (m/z 189)	128134.2 ± 9486.9
Delphinidin-3-sambubioside	DAD-UV (520 nm)	207315.5 ± 1807.6
Hibiscus acid hydroxyethyl ester	MS-TOF (m/z 235)	82132.4 ± 1416.4
Cyanidin-3-sambubioside	DAD-UV (520 nm)	87143.1 ± 393.1
Chlorogenic acid	DAD-UV (325 nm)	106469.9 ± 1182.0
Hibiscus acid dimethyl ester	MS-TOF (m/z 217)	79045.1 ± 1154.2
Methyl digallate	DAD-UV (270 nm)	2802.3 ± 46.6
Myricetin-3-arabinogalactose	DAD-UV (350 nm)	4755.5 ± 53.8
Coumaroylquinic acid	DAD-UV (310 nm)	772.9 ± 10.4
Quercetin-3-sambubioside	DAD-UV (350 nm)	7673.8 ± 34.6
Quercetin-3-rutinoside	DAD-UV (350 nm)	4953.2 ± 47.9
5-O-Caffeoylshikimic acid	DAD-UV (325 nm)	3526.7 ± 49.2
Leucoside	DAD-UV (350 nm)	1123.0 ± 25.4
Quercetin-3-glucoside	DAD-UV (350 nm)	3071.6 ± 15.9
Kaempferol-3-O-rutinoside	DAD-UV (350 nm)	2185.5 ± 15.5
Methyl epigallocatechin	DAD-UV (270 nm)	310.9 ± 5.5
Myricetin	DAD-UV (370 nm)	4765.9 ± 49.1
N-Feruloyltyramine	DAD-UV (325 nm)	867.9 ± 8.6
Quercetin	DAD-UV (370 nm)	5795.2 ± 61.7
Prodelfinidin B3	DAD-UV (310 nm)	327.0 ± 2.9







CAPÍTULO 10. *Hibiscus sabdariffa*

rescues achondroplastic RCJ-
FGFR3^{G380R} chondrocytes from
achondroplasia.





***Hibiscus sabdariffa* rescues achondroplastic RCJ-FGFR3^{G380R} chondrocytes from achondroplasia**

Salvador Fernández-Arroyo^{1,2}, Fernando Huete-Toral³, María Jesús Pérez de Lara³,
María Herranz-López⁴, Vicente Micol⁴, Antonio Segura-Carretero^{1,2}, Laurence Legeai-
Mallet⁵, Jesús Pintor^{3*}

¹ Analytical Chemistry Department, Faculty of Sciences, University of Granada, Av/ Fuentenueva, 18071, Granada, Spain.

² Functional Food Research and Development Center, Health Science Technological Park, Avenida del Conocimiento s/n, E-18100 Armilla (Granada), Spain

³ Biochemistry Department, E.U. Óptica, Universidad Complutense de Madrid, C/Arcos de Jalón 118, 28037 Madrid, Spain

⁴ Institute of Molecular and Cell Biology (IMCB). Miguel Hernández University. 03202 Elche, Alicante. Spain.

⁵ Institut National de la Santé et de la Recherche Médicale (INSERM). Hôpital Necker-Enfants Malades. 149 rue de Sèvres 75743 Paris cedex 15. France.

* Corresponding author:

Jesús Pintor

Adress: Biochemistry Department, E.U. Óptica, Universidad Complutense de Madrid, C/Arcos de Jalón 118, 28037 Madrid, Spain.

E-mail: jpintor@vet.ucm.es

Running title: *Hibiscus sabdariffa* rescues achondroplastic cells



Grants, sponsors and funding sources

The authors are grateful to the Areces Foundation (Acondroplasia 2010) project support, Fundación MAGAR, Spanish Ministry of Education and Science for the project AGL2011-29857-C03-02, to Andalusian Regional Government Council of Innovation and Science for the excellence projects P09-CTS-4564, P10-FQM-6563 and P11-CTS-7625 and to GREIB.PT.2011.18 projects and we also thank MONTELOEDER, S.L. for providing us with the plant extracts.

Keywords: Achondroplasia; *Hibiscus sabdariffa*; chloride efflux; extracellular matrix; cell viability; P-ERK1/2

Abstract

Achondroplasia is the most common form of dwarfism. This skeletal dysplasia is due to a mutation in the gene that encodes for the FGFR3 receptor, the recurrent mutation G380R responding of 97 % of all dwarfism cases. Conventional strategies for the treatment of achondroplasia are surgical-intervention. However, in recent years, new pharmacological strategies are being studied in achondroplastic cell lines. The aim of this work was to evaluate the effect of the natural source of polyphenols in the treatment of achondroplasia. *Hibiscus sabdariffa* is effective on FGF9-induced chloride flux changes, restore extracellular matrix, avoid rapid cell death and modify ERK1/2 phosphorylation.



1. Introduction

Chondrocytes are important cells of the cartilage and are involved in the endochondral bone growth process in mammals. Several molecules, hormones, cytokines and growth factors drive the progress of epiphyseal growth plate chondrocytes during endochondral ossification [1,2].

Achondroplasia, also known as dwarfism, is one of the most representative types of congenital skeletal dysplasias. This pathology is due to a mutation in the gene that encodes for the FGFR3 receptor, being the change of Gly380 to Arg (G380R) the most common mutation.

Several mechanisms have been reported to explain how mutant FGFR3 enhances these signals. One of the mechanisms described suggests that the mutation stabilizes the dimeric state of the receptor, thus, permitting its prolonged signaling [3]. On the other hand, a slow down-regulation of the mutant receptor [4], and a defective lysosomal targeting of mutant FGFR3 has also been observed [5]. Concerning the signal transduction pathways downstream of FGFR3, the ERK1/2 (MAPK) pathway is mainly involved in chondrocyte differentiation process [6] and reduces the synthesis of the components of the extracellular matrix [7]. The main processes altered in achondroplasia are the defective ability of activated FGFR3 to mobilize calcium [8], the defect of chondrocyte proliferation [9,10] and the turnover of the extracellular matrix homeostasis [10,11]. The fibroblast growth factor 9 (FGF9) is the preferred ligand for FGFR3 and stimulate all of these changes in achondroplastic chondrocytes.

Typical radiological features include shortening of the tubular bones and macrocephaly, due to disruption of endochondral ossification, and a delay in bone age was observed shortly after birth [12].



Conventional strategies for the treatment of achondroplasia are surgical-intervention. However, in recent years, new pharmacological strategies are being studied in achondroplastic cell lines, for example the treatment with the dinucleotide diadenosine tetraphosphate (Ap₄A). This dinucleotide is effective on FGF9-induced chloride flux changes [13], restoring extracellular matrix, avoiding premature cell death [14] and reestablish Ca²⁺ transients, all these processes mediated by P2Y receptor activation [15].

The aim of this work is to evaluate the effect of the natural source of polyphenols as possible treatment for achondroplasia. In this sense, the complete aqueous extract from *Hibiscus sabdariffa* (roselle) and its purified phenolic extract, *Lippia citriodora* (lemon verbena) extract (27% verbascoside, w/w), *Hypoxis rooperi* (african potato) extract, grape fruit extract (45% naringin, w/w), olive leaf extract (40% oleuropein, w/w), *Citrus aurantium* (bitter orange) extract (25% naringin, 25% neohesperidin, w/w) and *Aspalathus linearis* (roiboos) extract were tested in FGF9-stimulated mouse achondroplastic cell line (ACH).

2. Material and Methods

2.1. Reagents and antibodies

Tetracycline, α -MEM, heat-inactivated fetal bovine serum and antibiotics (penicillin, streptomycin and hygromycin) were purchased from Invitrogen (Carlsbad, CA, USA). FGF9, Tris, NaCl, NP-40, sodium desoxycholate, SDS, phenylmethylsulphonyl fluoride (PMSF), sodium fluoride (NaF), sodium orthovanadate (Na₃VO₄), Tween-20, BSA, aprotinin, pepstatin and leupeptin were obtained from Sigma (St. Louis, MO, USA).



Antibodies against phospho-ERK1/2, ERK1/2 and horse radish peroxidase-conjugated goat anti-mouse IgG were purchased from Santa Cruz Biotechnology (Santa Cruz, CA, USA).

2.2. Plant extracts

Eight plant extracts were tested in this study. Rooibos tea, grape fruit extract, *Citrus aurantium* (bitter orange), *Lippia citriodora* standardized with 27 % verbascoside (PLX 27%), *Hypoxis rooperi* (*H. rooperi*), and *Hibiscus sabdariffa* extract (HS) at final concentration of 100 µg/mL in water. Olive leaf extract standardized with 40 % oleuropein at final concentration of 100 µg/mL in DMSO. A purified and concentrated phenolic fraction of HS (PEHS), obtained as previously reported [22], was tested at final concentration of 10 µg/mL in water. The botanical ingredients were provided by MONTELOEDER, S.L. (Elche, Alicante, Spain).

2.3. Cell line and cell culture

Non-transformed mouse chondrocytes (RCJ3.1C5.18) were transfected with full-length human mutant (ACH) FGFR3, FGFR3^{G380R}, as described elsewhere [4]. Expression of FGFR3 was regulated by a tetracycline suppression system (Tet-off system), the receptor is expressed in the absence of tetracycline in the culture medium. Standard culture medium was α-MEM supplemented with 15% heat-inactivated fetal bovine serum (FBS) and antibiotics (600 µg/mL geneticin, 100 U/mL penicillin/streptomycin, 2 µg/mL tetracycline, 50 µg/mL hygromycin). Cells were incubated at 37 °C with 5% CO₂.



2.4. MQAE measurements

Intracellular chloride concentration was measured using MQAE as a fluorescent indicator [16]. MQAE has a high sensitivity to chloride, which interacts with and quenches the dye in its excited state. Changes in MQAE fluorescence should, therefore, inversely reflect changes in intracellular chloride concentration. Thus, a decrease in intracellular MQAE fluorescence indicates an increase in intracellular chloride concentration [17]. The MQAE experiment was performed according to Huete-Toral *et al.* (2011) protocol designed for achondroplastic cells [13]. ACH cells were grown to confluence in 96-well plates and loaded overnight with 0.8 mM MQAE at 37 °C. Before the experiment started, the medium was removed, and each well was washed three times with chloride-containing buffer. The composition of the chloride-containing buffer was: 2.4 mM K₂HPO₄, 0.6 mM KH₂PO₄, 1 mM CaSO₄, 1 mM MgSO₄, 10 mM HEPES, 10 mM D-glucose and 130 mM NaCl. The cells were incubated with chloride-containing buffer (to induce chloride channel activation) for 10 min at 37 °C. The buffer was then removed and replaced by 100 µl of chloride-free buffer containing the different extracts with and without FGF9 as stimulant at the desired concentration (10 or 100 µg/mL for extracts and 25 ng/mL for FGF9). The composition of this buffer was identical to that with chloride except that the NaCl was replaced with equimolar NaNO₃. The plates were then read on a Fluoroskan Ascent F1 (Thermo Systems) at 360 nm excitation wavelength and emission at wavelength 460 nm. Data are expressed in relative fluorescence units (RFU), as fluorescence variation (F_t-F₀), where F_t is the fluorescence at final time recorded in the experiment and F₀ is the initial fluorescence.



2.5. Extracellular matrix studies

Cartilage matrix deposition in chondrocytes was quantified by Alcian blue staining. Cells were seeded at a density of 2×10^5 cells/well in six-well dishes. After reaching the confluence, the differentiation was induced by adding 10 mM β -glycerophosphate and 50 $\mu\text{g}/\text{mL}$ ascorbic acid to the medium. Under these conditions, the presence of cartilage matrix (proteoglycan synthesis) can be detected at 3, 7 and at 10 days of culture, as previously described [18]. FGF9 (25 ng/mL) alone, or FGF9 together extracts (10-100 $\mu\text{g}/\text{mL}$) were also added with the fresh growth medium. Differentiating cultures were fed supplemented media every 2 days. At different time points cells were washed with PBS and stained with Alcian blue (1% in 3% acetic acid) for 30 min, washed three times for 2 min in 3% acetic acid and rinsed with distilled water. After cells were solubilized in 1% SDS and heat 1 h at 90 °C, the absorbance at 605 nm was measured for triplicate samples.

2.6. Cell viability

Cell viability was determined by trypan blue staining. Viable (unstained) cells were counted using a hemocytometer. Experiments were performed in triplicate.

2.7. Western blot analysis

In order to analyze phosphorylation status of ERK1/2 protein expression, 2×10^4 cell/cm² were plated onto tissue culture dishes. Two days later, culture medium was replaced by fresh one without tetracycline and cells were incubated during 20 h. After this, the cells were exposed for 1 h and at the indicated concentrations with the different extracts (10-100 $\mu\text{g}/\text{mL}$) either with or without FGF9 (25 ng/mL). After stimulation, cells were lysed in buffer (50 mM Tris-HCl pH 8.0, 150 mM NaCl, 1% NP-40, 0.5% sodium



deoxycholate, 0.1% SDS, 1mM PMSF, 1 mM NaF, 2mM Na₃VO₄, 10µg/mL aprotinin, 5 µg/mL pepstatin and 10µg/mL leupeptin). Lysates were clarified at 13,000 x g for 20 min at 4 °C. Protein concentration was determined by the Bio-Rad protein assay (Bio-Rad laboratories, Hercules, CA, USA).

Protein extracts from each sample (45 µg) were subjected to 10% SDS-polyacrilamide gels and were transferred to nitrocellulose membranes (Amersham-Pharmacia-Biotech, Buckinghamshire, UK). Thereafter, membranes were blocked and incubated overnight in the primary antibody appropriately diluted in TBS (1:1000 for p-ERK1/2 and 1:100 for FGFR3) containing 5% skimmed milk and 0.1% Tween-20. After washing, blots were incubated with horse radish peroxidase-conjugated goat anti-mouse IgG secondary antibody (1:2000). Development was performed using ECL system (Amersham-Pharmacia-Biotech, Buckinghamshire, UK).

To verify equal loading, membranes were stripped in 62.5 mM Tris-HCl pH 6.8, 2% SDS and 100 mM β-mercaptoethanol and re-blotted with proper antibodies diluted in TBS (1:1000 for ERK1/2 and GAPDH).

Films were scanned and a densitometric analysis was performed using Kodak GL 200 Imaging System and Kodak Molecular Imaging Software (Kodak, Rochester, NY, USA). All the data shown are representative of three independent experiments.

2.8. Statistical analysis

All data are presented as the mean ± SD. Significant differences were determined by two-tailed Student's t test. The plotting curves was carried out with Prism5 (GraphPad Software, Inc).



3. Results

3.1. Identifying new compounds to rescue chondrocytes from achondroplasia

We have recently designed a method to test compounds that may have anti-achondroplastic properties. The method is based on the chloride fluxes these cells have and how anti-achondroplastic compounds can reverse the effect of FGF9 [13].

Using the mentioned approach, we have analyzed the ability of 8 plant extracts to prevent the effect of FGF9 on achondroplastic chondrocytes. FGF9 activates FGFR3 receptor causing all the endochondral ossification defects, starting at the molecular level but reflecting them into the typical phenotype of achondroplasia (dwarfism).

In this sense, among the assayed compounds only two depicted interesting properties ameliorating the effect of FGF9. As it is shown in figure 1A, the extract of *Hibiscus sabdariffa*, abbreviated as HS (100 µg/mL), was able to reverse the effect of FGF9 (25 ng/mL) produced in achondroplastic chondrocytes regarding Cl⁻ concentrations (figure 1A). The phenolic fraction of *Hibiscus sabdariffa*, abbreviated as PEHS (10 µg/mL) did produce a similar effect but no so evident as the one produced by HS. Relating the changes to the effect produced by FGF9 on chloride concentrations, *Hibiscus sabdariffa* reversed the effect produced by FGF9 returning to control values (58.83% reduction of the effect produced by FGF9), while PEHS produced a similar effect returning FGF9 values but to a lesser extent (6.28% reduction of FGF9 total effect) (figure 1B). All the other tested extracts produced variable behaviors which can be seen in detail in figure 1B.

3.2. HS and PEHS modify FGF9 ERK1/2 phosphorylation

One of the intracellular pathways which are triggered by FGF9 after receptor activation is ERK1/2 cascade (p42 and p44 phosphorylation). Achondroplastic cells challenged



with FGF9 elicited a significant ERK1/2 phosphorylation when compared to untreated cells (control).

The application of HS alone (100 $\mu\text{g}/\text{mL}$) produced an increase in the phosphorylation level of p42 and p44 compared to the control (figure 2A). On the other hand, PEHS (10 $\mu\text{g}/\text{mL}$) alone did not significantly modify the level of phosphorylation of ERK1/2 compared to control, and even reduced phosphorylation (figure 2). No apparent changes were observed when HS was assayed in the presence of FGF9 when compared to HS alone. Nevertheless, when PEHS was tested in the presence of FGF9 (25 ng/mL), phosphorylation of ERK1/2 was clearly and statistically reduced comparing to FGF9 alone (n=6, figure 2B).

3.3. HS and PEHS rescue achondroplastic chondrocytes restoring extracellular matrix

One of the main problems of achondroplastic chondrocytes is the lack of extracellular matrix production [10]. This effect relies directly on the over-activation of the FGFR3 after FGF stimulation [7].

When HS and PEHS were tested in their ability to modify intracellular matrix deposition, both PEHS showed a better ability to rescue chondrocytes from its conditions in terms of extracellular matrix production even in the presence of FGF9. (n=6, figure 3). Interestingly, HS was unable to reverse the effect of FGF9 while this extract, when applied alone; it did improve extracellular matrix production when compared to control (figure 3). On the other hand, PEHS did significantly produce more extracellular matrix which was only measurable ten days after the treatment (figure 3).



3.4. Cellular survival after treatment with HS and PEHS

One of the features of achondroplastic chondrocytes, among those already commented, is the rapid maturation of these cells which implies a rapid cell death [19]. In this sense, the application of FGF9 (25 ng/mL) drops cell survival dramatically the remaining cells being roughly one third of the initial ones in 24 hours (figure 4). When this experiment was performed in the presence of HS (100 µg/mL) this extract protected significantly the achondroplastic chondrocytes from death as it can be observed in figure 4. In this sense HS was able to keep 78 ± 2.5 % of cells alive (n=6) when comparing with the FGF9 achondroplastic treated cells.

The application of PEHS (10 µg/mL) in the presence of FGF9 also resulted in the survival of the cells being 88.3 ± 3.2 % alive (n=6, figure 4). The application of both HS and PEHS alone did not significantly modify the rate of cell survival as it can be seen in figure 4.

4. Discussion

There is a lack of compounds which can be used for the treatment of an orphan skeletal disease such as achondroplasia. Basic research points towards the existence of potential compounds that might be used for the treatment of this disease. These include nucleotides, derivatives of pyridoxal phosphate, C-natriuretic peptide, inhibitors of tyrosine kinase activity or more recently siRNAs [7,14,20-22]. Since the previous results are not yet conclusive, it is matter of interest to look not only for new compounds but also for new sources for such compounds. In this sense, we introduce here a different approach in which we tested the ability of plant extracts to rescue achondroplastic chondrocytes phenotype from its condition.



The combination of extracts from plants together with a fluorimetric technique described by Huete-Toral and co-workers (2011) [13], have permitted a rapid screening of a series of compounds selecting those which were potentially anti-achondroplastic, since they counteracts FGF9 actions in this cellular model. Among the tested extracts two depicted interesting behavior in chloride studies, the extract of *Hibiscus sabdariffa* (HS) and a phenolic fraction of the same plant (PEHS). These two were then taken for a subsequent study. The phenolic profile of HS and PEHS has been completely characterized and quantified previously [23]. Biochemical analysis on their ability to modify FGF9 phosphorylation of ERK1/2, confirmed that only PEHS was able to reduced ERK1/2 phosphorylation. This does not mean that HS was useless. It is necessary to bear in mind that part from the ERK1/2 pathway, FGFR3 which is mutated in achondroplasia, involves the recruitment of other pathways among which STAT-1 has been already demonstrated [24-26]. It can be the case that HS, by an unknown mechanism, can modulate STAT-1 pathway not altering ERK1/2 cascade. This means that more experiments are necessary to investigate this possibility.

Among the experiments performed with HS and PEHS, the ones related with the extracellular matrix deposition are of interest. Extracellular matrix is poor in achondroplastic condition therefore any compound restoring conditions in which that extracellular matrix is enriched is an indication of a change in the chondrocyte physiology. Between the two tested extracts only PEHS was able to reverse FGF9 effect and to permit a more abundant extracellular matrix. Nevertheless, PEHS was unable to return extracellular matrix to the values of control chondrocytes. This implies that either higher concentrations of the phenolic extract are necessary or a longer exposure time.



Cell viability is always affected in achondroplastic chondrocytes which enters in apoptosis quicker than normal chondrocytes [19,27]. In our experiments both, HS and PEHS did permit achondroplastic chondrocytes to survive longer than those which were untreated with the mentioned extracts. In this case both were able to help cells to survive for a longer period of time. Interestingly HS was able to produce that effect. This result may be related to STAT-1 pathway which is involved in cells survival [26]. If we combine the lack of reduction carried out by HS on ERK1/2, with the no effect of HS on extracellular matrix together with the effect of cell survival, altogether may suggest that this extract contains a component capable to alter STAT-1 pathway. On the other hand, as it has been reported [23], PEHS differs substantially from HS in a variety of compounds and their concentration, and that may produce longer chondrocyte survival and selectively more ERK1/2 inhibition with the concomitant extracellular matrix recovery. A recent study has shown that HS is especially enriched in organic acids whereas PEHS contains higher amounts of anthocyanins and flavonols, which correlates with the stronger hypolipidemic effects of PEHS [22]. Therefore, this class of compounds might be also related to cellular protection and restoration of cellular matrix observed in chondrocytes. Any how, further investigations are required in order to identify the responsible compounds and their molecular mechanism.

5. Concluding remarks

Due to the conventional strategies for the treatment of achondroplasia are surgical-type, new pharmacological strategies are being studied in achondroplastic cell lines in recent years. Furthermore, we have evaluated the effect of the natural sources of polyphenols as possible treatment for achondroplasia. Among of them, only *Hibiscus sabdariffa* extract and its enriched phenolicone have achieved to rescue of achondroplastic cell line



from achondroplasia due to chloride efflux induction and cell death prevention. *H. sabdariffa* phenolic-enriched extract (PEHS), also restore the extracellular matrix and inhibits ERK1/2 phosphorylation.

6. References

- [1] Kobayashi T, Kronenberg H. Minireview: Transcriptional regulation in development of bone. *Endocrinology*. 2005;146:1012-1017.
- [2] Provot S, Schipani E. Molecular mechanisms of endochondral bone development. *Biochem Biophys Res Commun*. 2005;328:658-665.
- [3] Webster M, Donoghue D. Constitutive activation of fibroblast growth factor receptor 3 by the transmembrane domain point mutation found in achondroplasia. *EMBO J*. 1996;15:520-527.
- [4] Monsonogo-Ornan E, Adar R, Feferman T, Segev O, Yayon A. The transmembrane mutation G380R in fibroblast growth factor receptor 3 uncouples ligand-mediated receptor activation from down-regulation. *Mol Cell Biol*. 2000;20:516-522.
- [5] Cho J, Guo C, Torello M, Lunstrum G, Iwata T, Deng C, Horton W. Defective lysosomal targeting of activated fibroblast growth factor receptor 3 in achondroplasia. *Proc Natl Acad Sci U S A*. 2004;101:609-614.
- [6] Raucci A, Laplantine E, Mansukhani A, Basilico C. Activation of the ERK1/2 and p38 mitogen-activated protein kinase pathways mediates fibroblast growth factor-induced growth arrest of chondrocytes. *J Biol Chem*. 2004;279:1747-1756.
- [7] Yasoda A, Komatsu Y, Chusho H, Miyazawa T, Ozasa A, Miura M, Kurihara T, Rogi T, Tanaka S, Suda M, Tamura N, Ogawa Y, Nakao K. Overexpression of CNP in



chondrocytes rescues achondroplasia through a MAPK-dependent pathway. *Nat Med.* 2004;10:80-86.

[8] Nguyen HB, Estacion M, Gargus JJ. Mutations causing achondroplasia and thanatophoric dysplasia alter bFGF-induced calcium signals in human diploid fibroblasts. *Hum Mol Genet.* 1997;6:681-688.

[9] Segev O, Chumakov I, Nevo Z, Givol D, Madar-Shapiro L, Sheinin Y, Weinreb M, Yaron A. Restrained chondrocyte proliferation and maturation with abnormal growth plate vascularization and ossification in human FGFR-3(G380R) transgenic mice. *Hum Mol Genet.* 2000;9:249-258.

[10] Krejci P, Masri B, Fontaine V, Mekikian P, Weis M, Prats H, Wilcox W. Interaction of fibroblast growth factor and C-natriuretic peptide signaling in regulation of chondrocyte proliferation and extracellular matrix homeostasis. *J Cell Sci.* 2005;118:5089-5100.

[11] Urban JPG, Hall AC, Gehl KA. Regulation of matrix synthesis rates by the ionic and osmotic environment of articular chondrocytes. *J Cell Physiol.* 1993;154:262-270.

[12] Pannier S, Mugniery E, Jonquoy A, Benoist-Lasselín C, Odent T, Jais J, Munnich A, Legeai-Mallet L. Delayed bone age due to a dual effect of FGFR3 mutation in Achondroplasia. *Bone.* 2010;47:905-915.

[13] Huete F, Guzman-Aranguez A, Ortín J, Hoyle CHV, Pintor J. Effects of diadenosine tetraphosphate on FGF9-induced chloride flux changes in achondroplastic chondrocytes. *Purinergic Signalling.* 2011;7:243-249.



- [14] Guzman-Aranguez A, Irazu M, Yayon A, Pintor J. Effect of diadenosine polyphosphates in achondroplastic chondrocytes: Inhibitory effect of Ap(4)A on FGF9 induced MAPK cascade. *Biochem Pharmacol.* 2007;74:448-456.
- [15] Guzman-Aranguez A, Irazu M, Yayon A, Pintor J. P2Y receptors activated by diadenosine polyphosphates reestablish Ca²⁺ transients in achondroplastic chondrocytes. *Bone.* 2008;42:516-523.
- [16] Koncz C, Daugirdas JT. Use of MQAE for measurement of intracellular [Cl⁻] in cultured aortic smooth muscle cells. *American Journal of Physiology - Heart and Circulatory Physiology.* 1994;267:H2114-H2123.
- [17] Marandi N, Konnerth A, Garaschuk O. Two-photon chloride imaging in neurons of brain slices. *Pflugers Archiv European Journal of Physiology.* 2002;445:357-365.
- [18] Lunstrum G, Keene D, Weksler N, Cho Y, Cornwall M, Horton W. Chondrocyte differentiation in a rat mesenchymal cell line. *Journal of Histochemistry & Cytochemistry.* 1999;47:1-6.
- [19] L'Hote C, Knowles M. Cell responses to FGFR3 signalling: growth, differentiation and apoptosis. *Exp Cell Res.* 2005;304:417-431.
- [20] Guzman-Aranguez A, Crooke A, Yayon A, Pintor J. Effect of PPADS on achondroplastic chondrocytes: Inhibition of FGF receptor type 3 over-activity. *Eur J Pharmacol.* 2008;584:72-77.
- [21] Shukla V, Coumoul X, Wang RH, Kim HS, Deng CX. RNA interference and inhibition of MEK-ERK signaling prevent abnormal skeletal phenotypes in a mouse model of craniosynostosis. *Nat Genet.* 2007;39:1145-1150.



- [22] Jonquoy A, Mugniery E, Benoist-Lasselín C, Kaci N, Le Corre L, Barbault F, Girard AL, Le Merrer Y, Busca P, Schibler L, Munnich A, Legeai-Mallet L. A novel tyrosine kinase inhibitor restores chondrocyte differentiation and promotes bone growth in a gain-of-function *Fgfr3* mouse model. *Hum Mol Genet.* 2012;21:841-851.
- [23] Herranz-López M, Fernández-Arroyo S, Pérez-Sánchez A, Barraón-Catalán E, Beltrán-Debón R, Menéndez JA, Alonso-Villaverde C, Segura-Carretero A, Joven J, Micol V. Synergism of plant-derived polyphenols in adipogenesis: Perspectives and implications. *Phytomedicine.* 2011;(in press) DOI: 10.1016/j.phymed.2011.12.001.
- [24] Sahni M, Ambrosetti D-, Mansukhani A, Gertner R, Levy D, Basilico C. FGF signaling inhibits chondrocyte proliferation and regulates bone development through the STAT-1 pathway. *Genes and Development.* 1999;13:1361-1366.
- [25] Sahni M, Raz R, Coffin J, Levy D, Basilico C. STAT1 mediates the increased apoptosis and reduced chondrocyte proliferation in mice overexpressing FGF2. *Development.* 2001;128:2119-2129.
- [26] Harada D, Yamanaka Y, Ueda K, Nishimura R, Morishima T, Seino Y, Tanaka H. Sustained phosphorylation of mutated FGFR3 is a crucial feature of genetic dwarfism and induces apoptosis in the ATDC5 chondrogenic cell line via PLC gamma-activated STAT1. *Bone.* 2007;41:273-281.
- [27] Krejci P, Bryja V, Pachernik J, Hampl A, Pogue R, Mekikian P, Wilcox WR. FGF2 inhibits proliferation and alters the cartilage-like phenotype of RCS cells. *Exp Cell Res.* 2004;297:152-164.



Figure legends

Figure 1. A) Effect of *Hibiscus sabdariffa* (HS) on chloride flux in RCJ-FGFR3-G380R-tet cells with or without FGF9 vs. Control. HS reversed the inhibitory effect of FGF9 in chloride efflux. **B)** Bar graphs showing the changes in chloride efflux of each plant extract referred to % of FGF9 inhibitory chloride efflux activity. Only HS and EHS show significant reduction FGF9 inhibitory activity (two-way anova)*** $P < 0.001$ (n=6).

Figure 2. Analysis of extracts action on ERK1/2 phosphorylation. Cells were incubated during 20 h in fresh medium without tetracycline. After this, the cells were incubated for 1 h with the different extracts, with or without FGF9. Cell lysates were successively immunoblotted with antiphospho-ERK 1/2 and anti-ERK2 antibody to verify loading. Histograms represent the levels of phosphorylated ERK 1/2 intensity obtained in the western blot analysis. ERK1/2 has been used as control charge. Only PEHS significantly reduced FGF9 phosphorylation levels (n=6; *** $P < 0.001$).

Figure 3. Extracellular matrix deposition at days 3, 7 and 10 of untreated cells (control), FGF9-activated receptor and treated cells with HS and PEHS with or without FGF9. At the indicated times, extracellular matrix was quantified by Alcian blue staining of cell layers, following solubilization, dye uptake was quantified at 605 nm for triplicate samples (n=6).

Figure 4. Viable chondrocytes precursors were determined by trypan blue method. Bar graphs compare untreated cells (control), FGF9-activated receptor and treated cells with HS and PEHS with or without FGF9. Both, HS and PEHS, reversed de effect of FGF9; increasing cell survival (n=6; ** $P < 0.05$ vs. FGF9).



Figure 1.

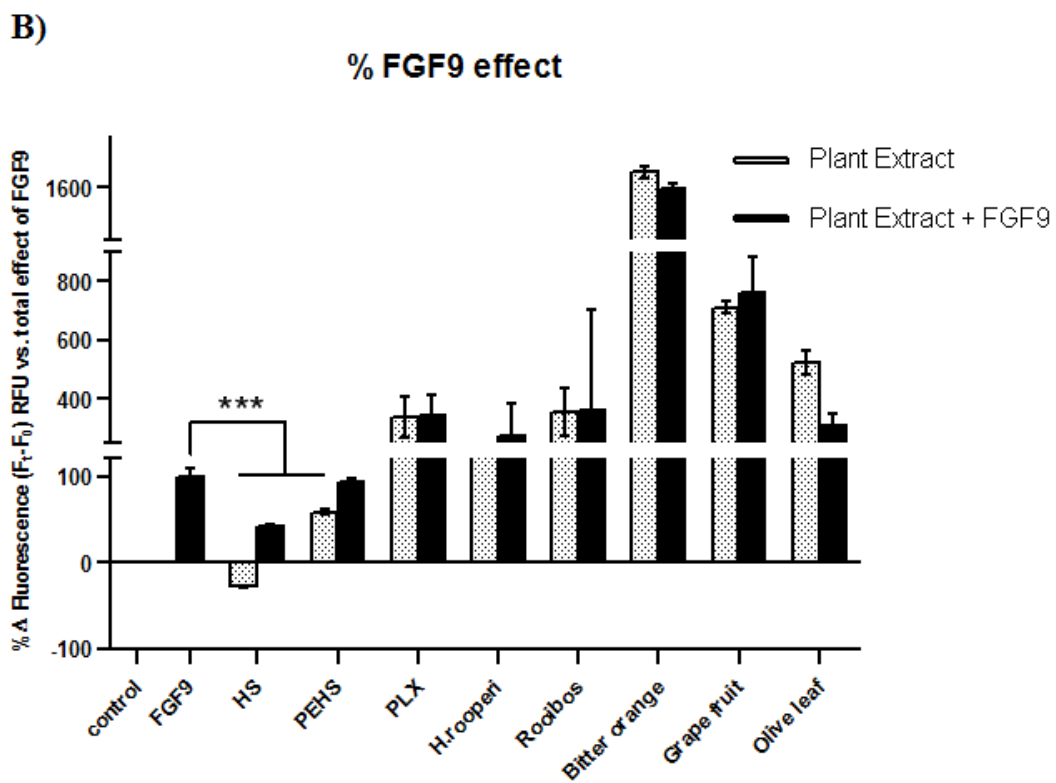
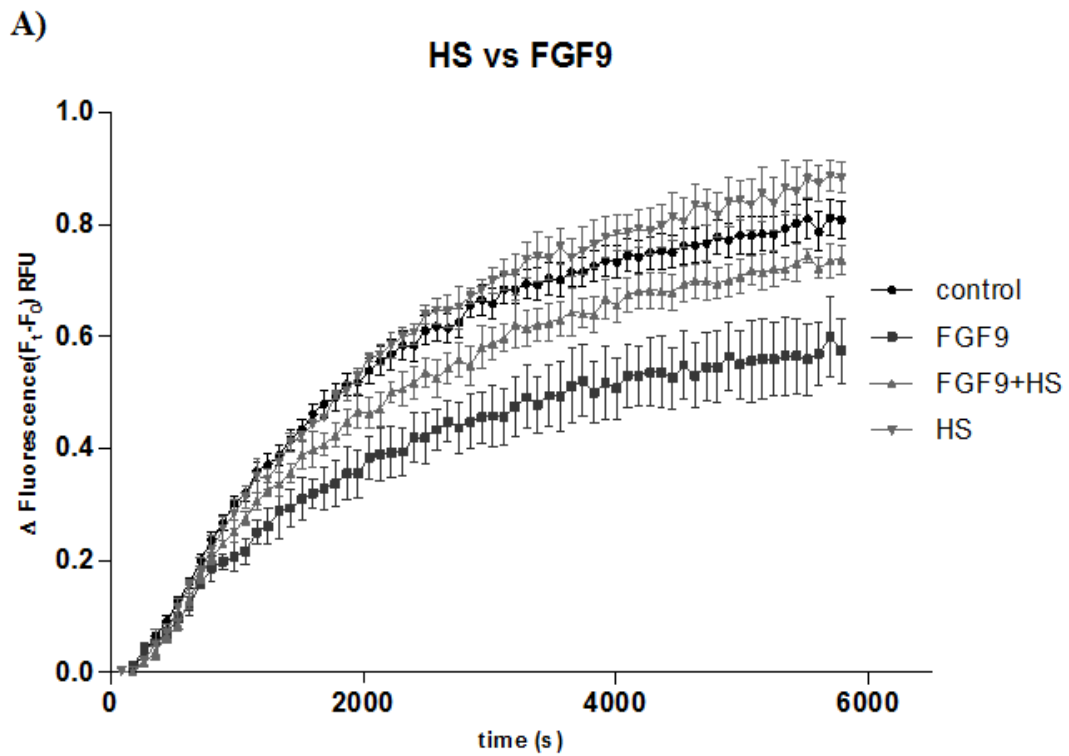




Figure 2.

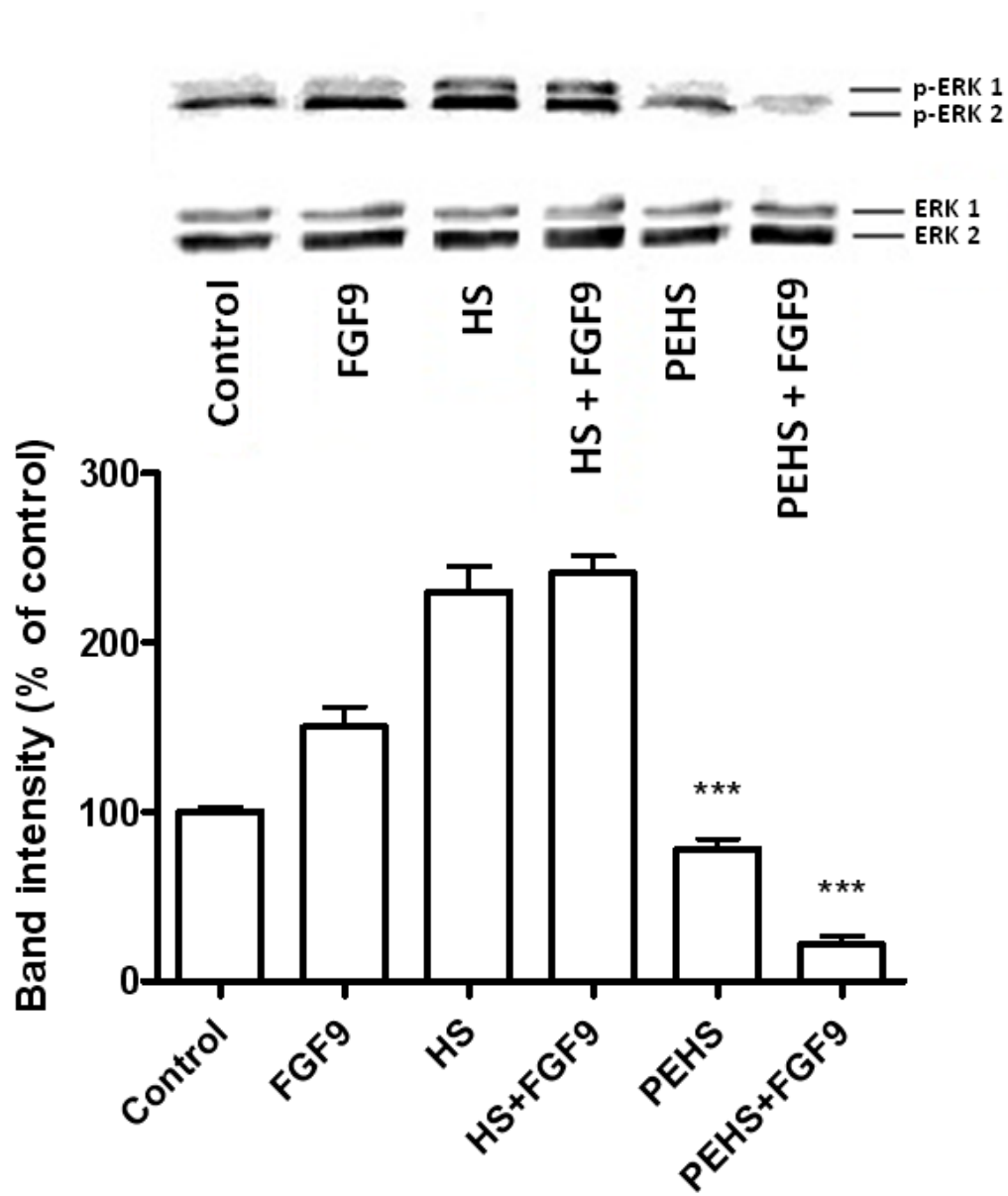
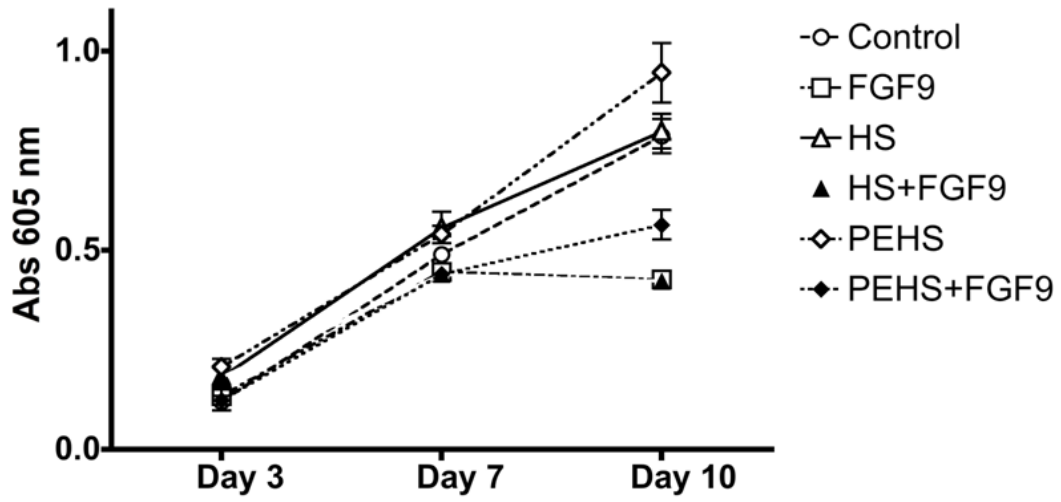
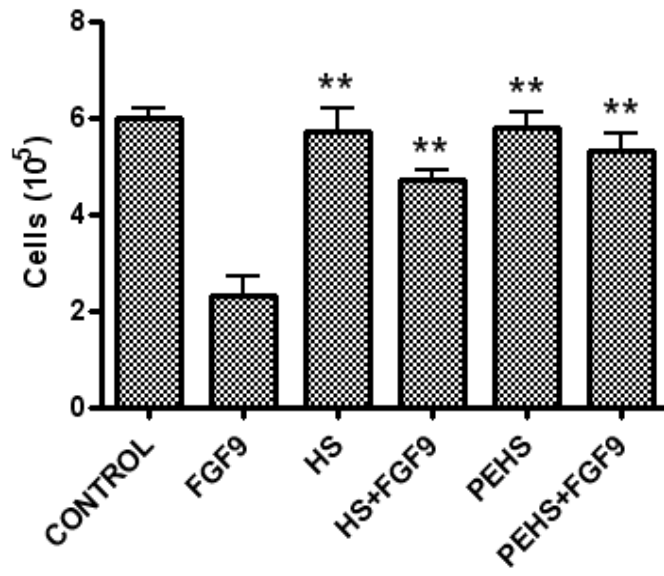




Figure 3.



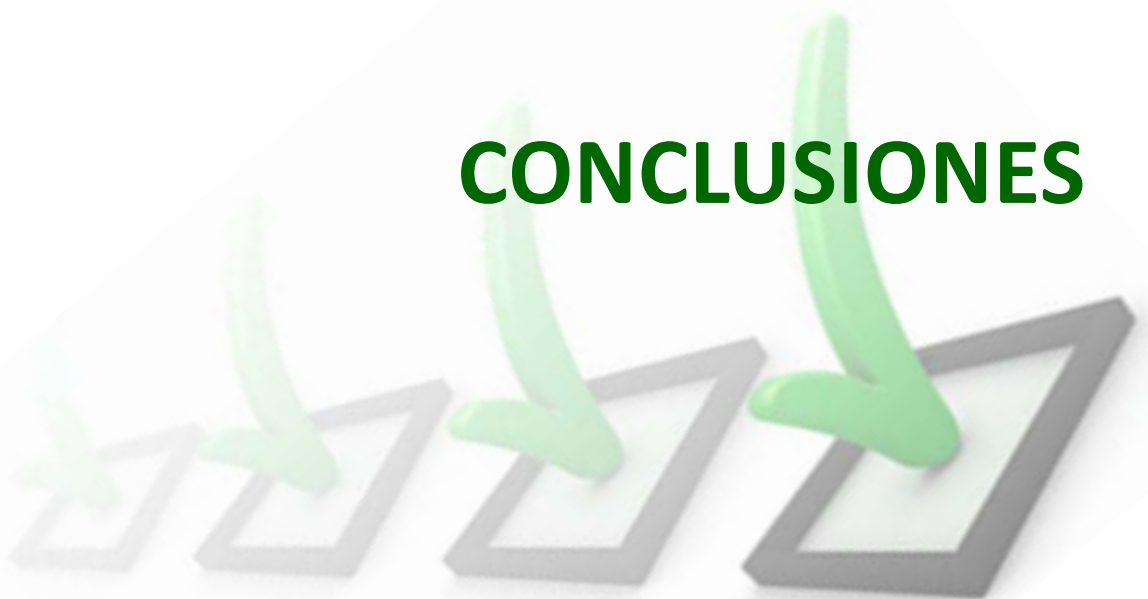
**Figure 4.**







CONCLUSIONES







El perfil polifenólico de *Cistus ladanifer* se ha caracterizado por primera vez utilizando HPLC acoplado a espectrometría de masas de tiempo de vuelo y trampa de iones, habiendo identificado mediante la masa exacta, distribución isotópica y patrón de fragmentación de cada compuesto 7 ácidos fenólicos, 13 flavonoides, 6 derivados del ácido elágico, 5 derivados del hexahidroxidifenoilo, 5 compuestos no pertenecientes a ninguna de las familias de compuestos fenólicos y 21 compuestos desconocidos.

El perfil polifenólico es similar para especies del género *Cistus* englobadas dentro del mismo subgénero, y difiere significativamente entre los tres subgéneros existentes. El subgénero *Cistus* es el que se diferencia más en el perfil fenólico, diferenciándose de los otros dos en la carencia de elagitaninos, mientras que los subgéneros *Leucocistus* y *Halimioides* tienen más relación entre sí, corroborando los estudios taxonómicos filogenéticos y evolutivos existentes.

Cistus populifolius presenta un mayor contenido de polifenoles totales, de flavonoides y de taninos que *Cistus ladanifer*. Además, *C. populifolius* tiene una mayor capacidad antioxidante mediante transferencia de electrones. Sin embargo, *Cistus ladanifer* posee un mayor poder antioxidante para donar átomos de hidrógeno en un medio hidrofílico. Por otro lado se observa una elevada capacidad antibacteriana de estos extractos debido, seguramente, a la elevada concentración en elagitaninos, siendo *Cistus ladanifer* especialmente potente contra *Staphylococcus aureus* y *Cistus populifolius* contra *Escherichia coli*.

Los ensayos citotóxicos preliminares con *Cistus ladanifer* y *Cistus populifolius* en diferentes líneas celulares cancerígenas han puesto de manifiesto un importante efecto en la línea celular M220 de adenocarcinoma pancreático



primario humano y en las líneas celulares MCF7/HER2 y JIMT-1 de cáncer de mama. Aunque los mecanismos de acción todavía no se conocen, los extractos de *Cistus* estudiados parecen afectar las vías de señalización relacionadas con HER2 en la línea MCF7/HER2 y las vías de modulación de la proliferación celular en JIMT-1.

Se ha evaluado la bioactividad de 14 aceites de oliva virgen extra pertenecientes a 5 variedades de aceituna distintas (2 de la variedad Hojiblanca, 7 de la Picual, 1 de la Cornezuelo, 1 de la Manzanilla y 3 de la Arbequina) que difieren en su perfil polifenólico. Los datos de cuantificación ponen de manifiesto un menor contenido en secoiridoides y mayor en lignanos en aceites de la variedad Arbequina, siendo todos los demás aceites mucho más enriquecidos en secoiridoides que en lignanos (sobre todo los aceites de la variedad Picual).

Los aceites ricos en secoiridoides y bajo contenido en lignanos (especialmente los de la variedad Picual) inhiben la proliferación celular en líneas JIMT-1 de cáncer de mama resistentes al tratamiento anti-HER2 mediante activación de los genes de estrés celular y daño del ADN de la familia GADD45 que producen una parada del ciclo celular en fase G2/M, hiperacetilación de la histona H3 indicando un desempaquetamiento de la cromatina que permite la expresión de genes represores de tumores y activación de Stat3, NF- κ B, y especialmente de MEK1 y MAK/p38.

Los aceites de la variedad Picual ricos en secoiridoides previenen la transición epitelial-mesenquimal (EMT) fibrogénica y oncogénica promovida por TGF- β 1 evitando la pérdida de proteínas de adhesión (E-caderina) y la síntesis de proteínas asociadas a la migración (vimentina y fibronectina) mediante inhibición de la acumulación de SNAI2 (Slug) y SMAD3/4 en el núcleo.



Los aceites con alto contenido en lignanos y pobres en secoiridoides (variedad Arbequina) son capaces de inhibir la proliferación de las líneas celulares HT29 y SW480 de adenocarcinoma de colon en un 78.1 % un 66.7 % respectivamente induciendo la entrada de las células en fase SubG1 y promoviendo la apoptosis, siendo más significativo en SW480. Se ha realizado un análisis metabolómico mediante nLC-ESI-TOF-MS de los compuestos provenientes del aceite de oliva virgen extra y sus metabolitos tanto en el medio de cultivo como en el citoplasma celular. Se han encontrado 9 compuestos originales del aceite de oliva en los medios de cultivo y 3 en los citoplasmas celulares, siendo estos diferentes para cada línea celular en ambos casos. Sólo en el citoplasma se han observado metabolitos de los polifenoles, 1 en la línea celular HT29 (metil-hidroxi-DOA) y 3 en SW480 (metil-hidroxi-DOA, metil-luteolina y quercetina). La quercetina y la oleuropeína aglicona son los compuestos más abundantes en el citoplasma celular. La presencia de quercetina únicamente en SW480 podría ser la causa de un mayor grado de apoptosis en esta línea celular que en HT29.

Se ha validado un método analítico mediante HPLC-DAD-ESI-TOF-MS estableciendo los límites de detección y cuantificación, la reproducibilidad y la repetibilidad para cuantificar los compuestos fenólicos de un extracto acuoso de *Hibiscus sabdariffa*. Se han calculado las concentraciones de 17 compuestos (donde se incluyen 7 flavonoles, 4 ácidos cinámicos, 1 cumarina, 2 antocianinas y 3 compuestos no fenólicos). Destacan las elevadas concentraciones de los ácidos hidroxycítrico, hibísico y clorogénico en el extracto acuoso.

Se ha obtenido un extracto polifenólico enriquecido de *Hibiscus sabdariffa* (PEHS) al que se le han eliminado los polisacáridos y la fibra. Mediante caracterización analítica con HPLC-DAD-ESI-TOF-MS se han descrito 5 nuevos compuestos que no se observaban en el extracto acuoso de *H. sabdariffa* (1 ácido benzoico, 1 ácido cinámico, 2 flavonoles y 1 flavan-3-ol). La cuantificación



de este extracto pone de manifiesto su alto contenido en ácido hibísico, antocianinas (delfinidina-3-sambubiósido y cianidina-3-sambubiósido) y ácido clorogénico, destacando también el alto contenido en flavonoles glicosilados. Mediante el fraccionamiento de PEHS se obtuvieron 35 fracciones. De todas ellas se seleccionaron las fracciones 6, 9 y 14 por presentar la mayor bioactividad. Mediante HPLC-DAD-ESI-TOF-MS se caracterizaron 2 nuevos compuestos en la fracción 6 (un derivado del ácido hibísico y una flavanona), 1 en la 9 (un glucósido del ácido cafeico) y 1 en la 14 (un glucósido de miricetina). La fracción 6 es especialmente rica en la antocianina delfinidina-3-sambubiósido. La fracción 9 en cianidina-3-sambubiósido y ácido clorogénico y la fracción 14 en quercetina-3-sambubiósido.

La capacidad antioxidante del extracto de *Hibiscus sabdariffa* es muy diferente según el ensayo utilizado. El ensayo TEAC indica una pobre capacidad reductora del extracto, aunque el alto valor de FRAP puede deberse a la presencia de ácido clorogénico, el cual está demostrado que posee una gran capacidad para reducir iones metálicos. El elevado valor de ORAC y de TBARS dan a entender que el extracto de *H. sabdariffa* es un potente antioxidante en un medio hidrofílico y pobre en un medio lipofílico, debido a la presencia de ácido clorogénico y antocianinas con elevada hidrofiliidad, impidiendo su interacción con lípidos.

El extracto acuoso de *Hibiscus sabdariffa* disminuye la concentración sérica de triglicéridos sin mostrar diferencias significativas en los niveles de colesterol en ratones obesos LDLr^{-/-} alimentados con una dieta rica en grasas durante 14 semanas. La disminución en los niveles de triglicéridos puede deberse a una disminución en las lipoproteínas VLDL.



Tanto el extracto acuoso de *H. sabdariffa*, como el extracto polifenólico purificado (PEHS) y las fracciones obtenidas de éste último se ensayaron en células preadipocíticas 3T3-L1, observándose una disminución de la acumulación de triglicéridos dentro de los adipocitos en todos los casos. Sin embargo, la bioactividad del extracto PEHS ($IC_{50} = 9,1 \mu\text{g/mL}$) es muy superior a la observada en el extracto acuoso de *H. sabdariffa* ($IC_{50} = 799 \mu\text{g/mL}$) y a la de las fracciones ensayadas o combinaciones de éstas. Los mismos resultados se observan en adipocitos maduros por diferenciación de las células 3T3-L1 y en adipocitos hipertrofiados resistentes a insulina. Esta elevada bioactividad del extracto PEHS se debe al aumento en la concentración de los compuestos del extracto original y a la eliminación de los polisacáridos y fibras que podrían interferir en la acción de los polifenoles. Además, se pone de manifiesto el efecto sinérgico de los polifenoles del extracto ya que con las fracciones aisladas no se obtuvieron los resultados esperados. Por último, en adipocitos hipertrofiados, sólo PEHS fue capaz de inhibir la generación de especies reactivas del oxígeno con una relación dosis/respuesta, mientras que todas las adipoquinas estudiadas disminuyeron de igual forma con el extracto acuoso de *H. sabdariffa* ($1000 \mu\text{g/mL}$) y con PEHS ($40 \mu\text{g/mL}$), excepto la leptina y la MCP-1 cuya disminución fue más acusada en el caso de PEHS, demostrando así el efecto antioxidante y antiinflamatorio de *H. sabdariffa*.

Se ha analizado la biodisponibilidad de los compuestos del extracto polifenólico purificado de *Hibiscus sabdariffa* (PEHS) mediante HPLC-DAD-ESI-TOF-MS y el estatus oxidativo en plasma de rata después de una ingesta forzada de este extracto. Se han identificado 6 compuestos originales del extracto (ácido hibísico, ácido hibísico hidroxietiléster, ácido clorogénico, metildigalato, N-feruloiltiramina y quercetina) y 11 metabolitos (ácido hidroxicítrico, metilquercetina, 2 isómeros de la quercetina glucurónido, 4 isómeros de la quercetina diglucurónido, kaempferol y dos isómeros del kaempferol



glucurónido). Los derivados del ácido hibísico son los más abundantes en plasma con 2041 nmoles totales a un tiempo máximo superior a los 120 minutos. La disminución de la generación de MDA a los 120 minutos puede atribuirse a los ácidos orgánicos, aunque pueden tener un efecto sinérgico algunos isómeros de la quercetina glucurónido y kaempferol glucurónido. La elevada actividad de la enzima superóxido dismutasa y la alta capacidad del plasma reduciendo iones férricos a los 20 minutos pueden correlacionarse especialmente con el ácido clorogénico, aunque también con el metildigalato o incluso con la N-feruloiltiramina.

El extracto acuoso de *Hibiscus sabdariffa* es capaz de rescatar a la línea celular acondroplásica murina RCJ con una mutación $FGFR3^{G380R}$ de la acondroplasia mediante un aumento del eflujo de Cl^- y un aumento de la proliferación celular (incluso con el efector FGF9 presente en ambos casos) y un aumento en la generación de matriz extracelular únicamente cuando no existe FGF9 en el medio. El extracto polifenólico purificado de *Hibiscus sabdariffa* (PEHS) tiene el mismo efecto disminuyendo la acumulación de Cl^- en el citoplasma sólo cuando FGF9 no está presente y aumentando la generación de matriz extracelular y la proliferación celular incluso con FGF9 presente en el medio. Además, PEHS es capaz de inhibir la fosforilación de ERK1/2 por debajo de los niveles basales tanto en ausencia como en presencia de FGF9 (21.8 % y 78.4 % respectivamente).







CONCLUSIONS







On a caractérisé le profil polyphénolique de *Cistus ladanifer* par première fois en utilisant HPLC couplé à spectrométrie de masses de temps de vol et piège d'ions, en identifiant, moyennant la masse exacte, la distribution isotopique et le patron de fragmentation de chaque composée, 7 acides phénoliques, 13 flavonoïdes, 6 dérivés de l'acide ellagique, 5 dérivés du hexahydroxydiphénol, 5 composés qui n'appartiennent à aucune famille de composés phénoliques et 21 composés non identifiés.

Le profil polyphénolique est similaire pour les espèces du genre *Cistus* englobées dans le même sous-genre, et différent d'une manière significative entre les trois sous-genres existants. Le sous-genre *Cistus* est celui qui diffère le plus des autres deux, dont manque l'ellagitannin. Par contre, il y a une relation entre les sous-genres *Leucocistus* et *Halimioides*, en corroborant les études taxonomiques phylogénétiques et évolutives existantes.

Cistus populifolius présente une teneur plus élevée en polyphénols totaux, flavonoïdes et tanins que *Cistus ladanifer*. En outre, *C. populifolius* a une plus grande capacité antioxydante par transfert d'électrons. Cependant, *Cistus ladanifer* a plus de pouvoir antioxydant en donnant des atomes d'hydrogène sur un milieu hydrophile. D'autre part, ces extraits montrent une forte capacité antibactérienne, due, sûrement, à l'haute concentration d'ellagitannins qu'ils contiennent, étant *Cistus ladanifer* particulièrement puissante contre *Staphylococcus aureus* et *Cistus populifolius* contre *Escherichia coli*.

Les essais cytotoxiques préliminaires avec *Cistus ladanifer* et *Cistus populifolius* dans différentes lignées cellulaires cancéreuses ont montré un effet significatif sur la lignée cellulaire M220 d'adénocarcinome primaire pancréatique humain et dans les lignées MCF7/HER2 et JIMT-1 du cancer du sein. Bien que les mécanismes d'action ne sont pas encore connus, les extraits de *Cistus* étudiés



semblent affecter les voies de signalisation connexes à HER2 dans la lignée MCF7/HER2 et les voies de modulation de la prolifération cellulaire dans JIMT-1.

La bioactivité de 14 huiles d'olive extra vierge appartenant à 5 variétés d'olives différentes (2 de la variété Hojiblanca, 7 de la Picual, 1 de la Cornezuelo, 1 de la variété Manzanilla et 3 de l'Arbequina) qui diffèrent dans le profil polyphénolique a été évaluée. Les données de quantification révèlent une teneur inférieure des sécoiridoïdes et majeur de lignanes dans les huiles d'olive de la variété Arbequina, tandis que toutes les autres huiles sont enrichies en sécoiridoïdes et un bas teneur en lignanes (notamment les huiles de la variété Picual).

Les huiles riches en sécoiridoïdes et un faible teneur en lignanes (surtout la variété Picual) inhibent la prolifération des cellules dans la lignée JIMT-1 du cancer de sein résistant au traitement anti-HER2, grâce à l'activation des gènes de la famille GADD45 de stress cellulaire et dégât à l'ADN, un arrêt du cycle cellulaire en phase G2/M, hiperacetilación de l'histone H3 indiquant un déroulement de la chromatine en permettant l'expression de gènes répresseurs de tumeurs et l'activation de gènes comme Stat3, NF- κ B et surtout de MEK1 et MAK/p38.

Les huiles riches en sécoiridoïdes de la variété Picual préviennent la transition épithélium-mésenchymateuse (EMT) fibrogénique et oncogénique promue par TGF- β 1, évitant la perte de protéines d'adhésion (E-cadhérine) et la synthèse de protéines associées à la migration (vimentine et la fibronectine) via l'inhibition de l'accumulation de SNAI2 (Slug) et SMAD3/4 dans le noyau cellulaire.

Huiles à teneur élevée en lignanes et pauvres en sécoiridoïdes (variété Arbequina) sont capables d'inhiber la prolifération des lignées cellulaires HT29



et SW480 d'adénocarcinome du côlon dans une 78,1 % 66,7 % respectivement en induisant l'entrée dans la phase SubG1 de cellules et la promotion de l'apoptose, étant plus important en SW480. On a effectué un analyse métabolomique par nLC-ESI-TOF-MS des composés de l'huile d'olive vierge extra et de leurs métabolites dans le milieu de culture et dans le cytoplasme cellulaire. On a trouvé 9 composés originaux de l'huile d'olive dans les milieux de culture et 3 dans le cytoplasme de la cellule, ceux-ci étant différents pour chaque lignée cellulaire dans les deux cas. Uniquement dans le cytoplasme on a observé les métabolites des polyphénols, 1 dans la lignée HT29 (méthyl-hydroxy-DOA) et 3 dans SW480 (méthyl-hydroxy-DOA, méthyl-lutéoline et quercétine). La quercétine et l'oleuropéine aglycone sont les composés plus abondants dans le cytoplasme cellulaire. La présence de quercétine dans SW480 pourrait être la cause d'un degré plus élevé de l'apoptose dans cette lignée de cellules que à HT29.

Une méthode analytique par HPLC-DAD-ESI-TOF-MS a été validée par l'établissement des limites de détection et de quantification, de la reproductibilité et de la répétabilité, pour quantifier les composés phénoliques d'un extrait aqueux d'*Hibiscus sabdariffa*. On a calculé les concentrations de 17 composés (qui comprend 7 flavanols, 4 acides cinnamiques, 1 coumarine, 2 anthocyanes et 3 composés non phénoliques). On remarque les hautes concentrations d'acides hydroxycitrique, hibiscique et chlorogénique dans l'extrait aqueux d'*H. sabdariffa*.

On a purifié un extrait polyphénolique enrichi d'*Hibiscus sabdariffa* (PEHS) dont on a enlevé les polysaccharides et les fibres. Grâce à la caractérisation analytique par HPLC-DAD-ESI-TOF-MS on a décrit 5 nouveaux composés qui n'ont pas été observés à l'extrait aqueux d'*H. sabdariffa* (1 acide benzoïque, 1 acide cinnamique, 2 flavonols et 1 flavan-3-ol). La quantification de cet extrait



montre sa haute teneur en acide hibiscique et anthocyanes (delphinidine-3-sambubioside et cyanidine-3-sambubioside) et acide chlorogénique, soulignant également son élevé contenu en flavanols glycosés. 35 fractions ont été obtenues par fractionnement du PEHS. On a sélectionné les fractions 6, 9 et 14 qui présentent une majeure bioactivité. On a caractérisé par HPLC-DAD-ESI-TOF-MS 2 nouveaux composés dans la fraction 6 (un dérivé de l'acide hibiscique et une flavanone), 1 composé dans la fraction 9 (un glucoside de l'acide caféique) et 1 dans la 14 (un glycoside de myricétine). La fraction 6 est particulièrement riche en anthocyanes delphinidine-3-sambubioside. La fraction 9 en acide chlorogénique et cyanidine-3-sambubioside et la fraction 14 en quercétine-3-sambubioside.

La capacité antioxydante de l'extrait d'*Hibiscus sabdariffa* est très différente selon l'essai utilisé. La méthode TEAC suggère une mauvaise capacité de l'extrait comme réducteur, bien que la valeur élevée du FRAP peut être due à la présence de l'acide chlorogénique, dont est démontré sa grande capacité de réduire les ions métalliques. La valeur élevée du ORAC et TBARS donne à comprendre que l'extrait d'*H. sabdariffa* est un puissant antioxydant dans un milieu hydrophile et pauvre dans un milieu lipophile, du à la présence de l'acide chlorogénique et anthocyanes avec une haute hydrophilité, empêchant son interaction avec les lipides.

L'extrait aqueux d'*Hibiscus sabdariffa* diminue les triglycérides sériques sans montrer des différences significatives de cholestérol au niveau des souris obèses LDLr^{-/-} nourris avec une alimentation riche en graisses durant 14 semaines. La diminution des niveaux de triglycérides peut être due à une diminution des lipoprotéines VLDL.



L'extrait aqueux d'*Hibiscus sabdariffa*, l'extrait polyphénolique enrichi purifié (PEHS) et les fractions obtenues à partir de cette dernière ont été testés dans des cellules préadipocytiques 3T3-L1, notant une diminution de l'accumulation de triglycérides dans les adipocytes dans tous les cas. Cependant, la bioactivité de l'extrait PEHS ($IC_{50} = 9.1 \mu\text{g/mL}$) est beaucoup plus élevée que celle observée dans l'extrait aqueux ($IC_{50} = 799 \mu\text{g/mL}$) ou dans les fractions et ses combinaisons. Les mêmes résultats peuvent être vus dans les adipocytes matures par différenciation des cellules 3T3-L1 et dans adipocytes hypertrophiques résistant à l'insuline. Cette bioactivité élevée de l'extrait de PEHS est due à l'augmentation de la concentration des composés de l'extrait original et l'élimination des polysaccharides et des fibres qui pourraient interférer avec l'action des polyphénols. En outre, se révèle la synergie des polyphénols de l'extrait car avec les fractions isolés on n'a pas obtenu les résultats attendus. Finalement, dans les adipocytes hypertrophiques, PEHS est capable d'inhiber la production d'espèces réactives de l'oxygène avec une relation dose/réponse, tandis que l'ensemble d'adipokines étudiées ont diminuée d'une manière similaire avec l'extrait aqueux d'*H. sabdariffa* (1000 $\mu\text{g/mL}$) et PEHS (40 $\mu\text{g/mL}$), sauf la leptine et le MCP-1, dont le déclin a été plus marqué dans le cas de PEHS, démontrant l'effet antioxydant et anti-inflammatoire d'*Hibiscus sabdariffa*.

On a étudié la biodisponibilité des composés polyphénoliques de l'extrait purifié enrichi d'*Hibiscus sabdariffa* (PEHS) par HPLC-DAD-ESI-TOF-MS et le statut oxydatif du plasma chez le rat après une ingestion forcée de cet extrait. 6 composés originaux de l'extrait ont été identifiés (acide hibiscique, acide hibiscique hydroxyéthylester, acide chlorogénique, méthylgalate, N-feruloyltyramine et quercétine) et 11 métabolites de ces polyphénols (acide hydroxycitrique, méthylquercétin, 2 isomères de quercétine glucuronide, 4 isomères de quercétine diglucuronide, kaempférol et 2 isomères de kaempférol



glucuronide). Les métabolites dérivés de l'acide hibiscique sont les plus abondants dans le plasma avec 2041 nmol totaux dans un temps maximum de plus de 120 minutes. La diminution de la production de MDA à 120 minutes peut être attribuée à des acides organiques, mais peut avoir un effet synergique entre les isomères de la quercétine glucuronide et le kaempférol glucuronide. La forte activité de l'enzyme superoxyde dismutase (SOD) et l'haute capacité du plasma en réduisant les ions ferriques au 20 minutes peuvent être corrélées, en particulier, avec l'acide chlorogénique, mais aussi avec le méthylgalate ou même avec la N-feruloyltyramine.

L'extrait aqueux d'*Hibiscus sabdariffa* est capable d'arracher la lignée cellulaire murine achondroplasique RCJ exprimant une mutation FGFR3^{G380R} en augmentant l'efflux de Cl⁻ et la prolifération cellulaire (même avec l'effecteur FGF9 présente dans les deux cas) et une augmentation de la production de matrice extracellulaire uniquement lorsqu'il y a FGF9 dans le milieu. L'extrait polyphénolique d'*H. sabdariffa* purifié (PEHS) a le même effet en diminuant l'accumulation de Cl⁻ dans le cytoplasme seulement si FGF9 n'est pas présente, et en augmentant la production de matrice extracellulaire et la prolifération cellulaire même lorsque FGF9 est présente. En outre, PEHS est capable d'inhiber la phosphorylation de ERK1/2 ci-dessous des niveaux de base à la fois en absence et en présence de FGF9 (21,8% et 78,4% respectivement).







ABREVIATURAS







AAPH: 2,2'-Azobis-(2-aminopropano)-dihidrocloruro

ABTS: 2,2'-azinobis 3-etilbenzotiazolin-6-sulfonato

ADN: ácido desoxiribonucleico

AKT1 (PKB): serin-treonin proteína kinasa 1 (proteína kinasa B)

APC: gen de la Poliposis adenomatosa

APCI: ionización química a presión atmosférica

ARN: ácido ribonucleico

AUC: área bajo la curva

CBG: β -glucosidasa citosólica

CCR: cáncer colorectal

Cdk: ciclinas dependientes de kinasas

COL2A1: colágeno tipo II alpha 1

COMT: catecol-O-metiltransferasas

DAD: detector de batería de diodos

DTDST: transportador de sulfatos en la displasia diastrófica

EGCG: epigallocatequina galato

EI: impacto electrónico

EMT: transición epitelial-mesenquimal

ErbB2 (HER2): oncogen B de la eritroblastosis aviar 2 (Receptor para el factor de crecimiento epidérmico humano 2)

ERO: especies reactivas del oxígeno

ESI: ionización por electrospray

FAS: sintasa de ácidos grasos

FBS: suero fetal bovino

FGF: factor de crecimiento de fibroblastos

FGFR1-4: receptor 1-4 del factor de crecimiento de fibroblastos

FRAP: poder antioxidante reduciendo iones férricos

GADD: familia de proteínas implicadas en la parada del crecimiento y el daño del ADN



H2AX: histona 2AX

HAT: acetiltransferasa de histonas / transferencia de átomos de hidrógeno

HDAC: desacetilasa de histonas

HPLC: cromatografía líquida de alta resolución

IGF-1: factor de crecimiento insulínico 1

IL: interleuquinas

INT: cloruro de 2-(p-iodofenil)-3-(p-nitrofenil)5-feniltetrazolio

IR: infrarojo

IT: trampa de iones

K-ras: oncogén homólogo del virus del sarcoma murino de Kirsten

LDL: lipoproteínas de baja densidad

LDLr: receptor de las lipoproteínas de baja densidad

LPH: lactasa floridzin hidrolasa

MAPK1/2 (ERK1/2): proteínas kinasas activadas por mitógeno 1 y 2 (kinasas reguladoras de la señal extracelular 1 y 2)

MCP1: proteína quimioatrayente de monocitos 1

MDA: malondialdehido

MEK1/2 (MAP2K1/2): kinasa de la MAPK1/2 (proteína kinasa kinasa activada por mitógenos 1 y 2)

MIC: concentración inhibitoria mínima

MLH1: homólogo 1 de Mut L

MS: espectrometría de masas

MSH2: homólogo 2 de Mut S

MTT: bromuro de 3-(4,5-dimetiltiazol-2-il)-2,5-difeniltetrazolio

m/z: relación masa/carga

NASH: esteatosis hepática no alcohólica

NF-κB: factor nuclear kappa beta

nLC: nanocromatografía líquida

OMS: organización mundial de la salud



- ORAC: capacidad para absorber radicales de oxígeno
- PEA3: potenciador del activador del poliomavirus 3
- PPAR- γ : receptor γ de la proliferación del peroxisoma
- PPO: polifenol oxidasa
- RAF: acelerador rápido del fibrosarcoma (serin-treonin kinasa)
- RAS: proteína del sarcoma de rata (proteína GTPasa)
- RE: receptor de estrógenos
- RMN: resonancia magnética nuclear
- SET: transferencia de un electrón
- SOD: superóxido dismutasa
- Stat1/3: transductor de señal y activador de la transcripción 1 y 3
- SULT (P-PST): fenol sulfotransferasas
- TBA: ácido tiobarbitúrico
- TBARS: sustancias reactivas al ácido tiobarbitúrico
- TEAC: capacidad antioxidante en equivalentes de Trolox
- TGF- β : factor de transformación del crecimiento β
- TLC: cromatografía en capa fina
- TNF- α : factor de necrosis tumoral α
- TOF: tiempo de vuelo
- TPTZ: 2,4,6-tripiridil-s-triazina
- UGT: UDP glucuronil transferasa
- UV-Vis: ultravioleta-visible
- VEGF: factor de crecimiento vascular endotelial





BIBLIOGRAFÍA





1. Chaves, N.; Escudero, J. Allelopathic effect of *Cistus ladanifer* on seed germination. *Funct. Ecol.* **1997**, *11*, 432-440.
2. Chaves, N.; Sosa, T.; Alias, J.; Escudero, J. Identification and effects of interaction phytotoxic compounds from exudate of *cistus ladanifer* leaves. *J. Chem. Ecol.* **2001**, *27*, 611-621.
3. Chaves, N.; Sosa, T.; Escudero, J. Plant growth inhibiting flavonoids in exudate of *cistus ladanifer* and in associated soils. *J. Chem. Ecol.* **2001**, *27*, 623-631.
4. Deforce, K. The historical use of ladanum. Palynological evidence from 15th and 16th century cesspits in northern Belgium. *Vegetation History and Archaeobotany* **2006**, *15*, 145-148.
5. Sosa, T.; Chaves, N.; Alias, J.; Escudero, J.; Henao, F.; Gutierrez-Merino, C. Inhibition of mouth skeletal muscle relaxation by flavonoids of *Cistus ladanifer* L.: A plant defense mechanism against herbivores. *J. Chem. Ecol.* **2004**, *30*, 1087-1101.
6. Greche, H.; Mrabet, N.; Zrira, S.; Ismaili-Alaoui, M.; Benjilali, B.; Boukir, A. The Volatiles of the Leaf Oil of *Cistus ladanifer* L. var. *albiflorus* and Labdanum Extracts of Moroccan Origin and their Antimicrobial Activities. *J. Essent. Oil Res.* **2009**, *21*, 166-173.
7. Sanchez De Rojas, V.R.; Ortega, T.; Villar, A. Inhibitory effects of *Cistus populiofolius* on contractile responses in the isolated rat duodenum. *J. Ethnopharmacol.* **1995**, *46*, 59-62.
8. Somoza, B.; deRojas, V.R.S.; Ortega, T.; Villar, A.M. Vasodilator effects of the extract of the leaves of *Cistus populifolius* on rat thoracic aorta. *Phytotherapy Research* **1996**, *10*, 304-308.



9. de Andres, A.I.; Gomez-Serranillos, M.P.; Iglesias, I.; Villar, A.M. Effects of extract of *Cistus populifolius* L. on the central nervous system. *Phytotherapy Research* **1999**, *13*, 575-579.
10. Qa'dan, F.; Petereit, F.; Mansour, K.; Nahrstedt, A. Antioxidant oligomeric proanthocyanidins from *Cistus salvifolius*. *Planta Med.* **2006**, *72*, 1072-1073.
11. Gurbuz, P.; Kuruuzum, U.A.; Guvenalp, Z.; Kazaz, C.; Demirezer, L.O. Free Radical Scavenging Activities of Flavonoids from *Cistus salviifolius* L. *Planta Med.* **2011**, *77*, 1385-1385.
12. Kuehn, C.; Arapogianni, N.E.; Halabalaki, M.; Hempel, J.; Hunger, N.; Wober, J.; Skaltsounis, A.L.; Vollmer, G. Constituents from *Cistus salvifolius* (Cistaceae) Activate Peroxisome Proliferator-Activated Receptor-gamma but Not -delta and Stimulate Glucose Uptake by Adipocytes. *Planta Med.* **2011**, *77*, 346-353.
13. Kreimeyer, J.; Petereit, F.; Nahrstedt, A. Separations of flavan-3-ols and dimeric proanthocyanidins by capillary electrophoresis. *Planta Med.* **1998**, *64*, 63-67.
14. Saracini, E.; Tattini, M.; Traversi, M.L.; Vincieri, F.F.; Pinelli, P. Simultaneous LC-DAD and LC-MS determination of ellagitannins, flavonoid glycosides, and acyl-glycosyl flavonoids in *Cistus salvifolius* L. leaves. *Chromatographia* **2005**, *62*, 245-249.
15. Guinea, M.; Elbl, G.; Wagner, H. Screening of *Cistus-Clusii* Extract for Cyclooxygenase and Angiotensin-Converting Enzyme Inhibitory Activity. *Planta Med.* **1990**, *56*, 664.
16. Stübing, G.; Peris, J.B. *Plantas Medicinales de la Comunidad Valenciana*. Generalitat Valenciana. Conselleria de Medi Ambient: Valencia, 1998;



17. Kupeli, E.; Yesilada, E. Flavonoids with anti-inflammatory and antinociceptive activity from *Cistus laurifolius* L. leaves through bioassay-guided procedures. *J. Ethnopharmacol.* **2007**, *112*, 524-530.
18. Sadhu, S.K.; Okuyama, E.; Fujimoto, H.; Ishibashi, M.; Yesilada, E. Prostaglandin inhibitory and antioxidant components of *Cistus laurifolius*, a Turkish medicinal plant. *J. Ethnopharmacol.* **2006**, *108*, 371-378.
19. Vitali, F.; Pennisi, G.; Attaguile, G.; Savoca, F.; Tita, B. Antiproliferative and cytotoxic activity of extracts from *Cistus incanus* L. and *Cistus monspeliensis* L. on human prostate cell lines. *Natural Product Research* **2011**, *25*, 188-202.
20. Pomponio, R.; Gotti, R.; Santagati, N.A.; Cavrini, V. Analysis of catechins in extracts of *Cistus* species by microemulsion electrokinetic chromatography. *Journal of Chromatography a* **2003**, *990*, 215-223.
21. Goncalves, S.; Xavier, C.; Costa, P.; Albericio, F.; Romano, A. Extracts from *Cistus albidus* are effective antioxidants and inhibitors of cell proliferation in vitro. *Planta Med.* **2009**, *75*, 973-973.
22. Qa'dan, F.; Petereit, F.; Nahrstedt, A. Prodelphinidin trimers and characterization of a proanthocyanidin oligomer from *Cistus albidus*. *Pharmazie* **2003**, *58*, 416-419.
23. Bouamama, H.; Villard, J.; Benharref, A.; Jana, M. Antibacterial and antifungal activities of *Cistus incanus* and *C. monspeliensis* leaf extracts. *Therapie* **1999**, *54*, 731-733.
24. Lendeckel, U.; Arndt, M.; Wolke, C.; Reinhold, D.; Kahne, T.; Ansorge, S. Inhibition of human leukocyte function, alanyl aminopeptidase (APN, CD13) and dipeptidylpeptidase IV (DP IV, CD26) enzymatic activities by aqueous extracts of *Cistus incanus* L. ssp *incanus*. *J. Ethnopharmacol.* **2002**, *79*, 221-227.



25. Petereit, F.; Nahrstedt, A.; Innerlich, B. Antiinflammatory Activity of the Traditionally used Herb of *Cistus-Incanus*. *Planta Med.* **1989**, *55*, 650.
26. Attaguile, G.; Caruso, A.; Pennisi, G.; Savoca, F. Gastroprotective Effect of Aqueous Extract of *Cistus-Incanus* L in Rats. *Pharmacological Research* **1995**, *31*, 29-32.
27. Droebner, K.; Ehrhardt, C.; Ludwig, S.; Planz, O. CYSTUS052, a New Compound Against Seasonal and Pandemic Influenza Virus. *Antiviral Res.* **2010**, *86*, A33-A33.
28. Chinou, I.; Demetzos, C.; Harvala, C.; Roussakis, C.; Verbist, J.F. Cytotoxic and Antibacterial Labdane-Type Diterpenes from the Aerial Parts of *Cistus-Incanus* Subsp *Creticus*. *Planta Med.* **1994**, *60*, 34-36.
29. Santagati, N.A.; Salerno, L.; Attaguile, G.; Savoca, F.; Ronsisvalle, G. Simultaneous determination of catechins, rutin, and gallic acid in *Cistus* species extracts by HPLC with diode array detection. *J. Chromatogr. Sci.* **2008**, *46*, 150-156.
30. Servili, M.; Selvaggini, R.; Esposto, S.; Taticchi, A.; Montedoro, G.; Morozzi, G. Health and sensory properties of virgin olive oil hydrophilic phenols: agronomic and technological aspects of production that affect their occurrence in the oil. *Journal of Chromatography A* **2004**, *1054*, 113-127.
31. Baccouri, O.; Guerfel, M.; Baccouri, B.; Cerretani, L.; Bendini, A.; Lercker, G.; Zarrouk, M.; Ben Miled, D.D. Chemical composition and oxidative stability of Tunisian monovarietal virgin olive oils with regard to fruit ripening. *Food Chem.* **2008**, *109*, 743-754.
32. Esti, M.; Contini, M.; Moneta, E.; Sinesio, F. Phenolics compounds and temporal perception of bitterness and pungency in extra-virgin olive oils: Changes occurring throughout storage. *Food Chem.* **2009**, *113*, 1095-1100.



33. Suárez, M.; Macià, A.; Romero, M.; Motilva, M. Improved liquid chromatography tandem mass spectrometry method for the determination of phenolic compounds in virgin olive oil. *Journal of Chromatography A* **2008**, *1214*, 90-99.
34. Lozano-Sanchez, J.; Segura-Carretero, A.; Menendez, J.A.; Oliveras-Ferraros, C.; Cerretani, L.; Fernandez-Gutierrez, A. Prediction of Extra Virgin Olive Oil Varieties through Their Phenolic Profile. Potential Cytotoxic Activity against Human Breast Cancer Cells. *J. Agric. Food Chem.* **2010**, *58*, 9942-9955.
35. Dolores Mesa, M.; Aguilera, C.M.; Ramirez-Tortosa, C.L.; Gil, A.; Carmen Ramirez-Tortosa, M. *Effect of Olive Oil on Cardiovascular Risk Factor, LDL Oxidation and Atherosclerosis Development*. 2006; pp. 222.
36. Wolfrey, B.; Wilson, T.A.; Nicolosi, R.J. Feeding of olive oil reduces LDL oxidation and aortic cholesterol compared to sunflower oil in hamsters. *Faseb Journal* **2001**, *15*, A273-A273.
37. Gorinstein, S.; Leontowicz, H.; Lojek, A.; Leontowicz, M.; Ciz, M.; Krzeminski, R.; Gralak, M.; Czerwinski, J.; Jastrzebski, Z.; Trakhtenberg, S.; Grigelmo-Miguel, N.; Soliva-Fortuny, R.; Martin-Belloso, O. Olive oils improve lipid metabolism and increase antioxidant potential in rats fed diets containing cholesterol. *J. Agric. Food Chem.* **2002**, *50*, 6102-6108.
38. Chan, Y.; Dernonty, I.; Pelled, D.; Jones, P.J.H. Olive oil containing olive oil fatty acid esters of plant sterols and dietary diacylglycerol reduces low-density lipoprotein cholesterol and decreases the tendency for peroxidation in hypercholesterolaemic subjects. *Br. J. Nutr.* **2007**, *98*, 563-570.
39. Rosenblat, M.; Volkova, N.; Coleman, R.; Almagor, Y.; Aviram, M. Antiatherogenicity of extra virgin olive oil and its enrichment with green tea



polyphenols in the atherosclerotic apolipoprotein-E-deficient mice: enhanced macrophage cholesterol efflux. *J. Nutr. Biochem.* **2008**, *19*, 514-523.

40. Loizzo, M.R.; Di Lecce, G.; Menichini, F.; Boselli, E.; Menichini, F.; Frega, N.G. In Vitro Evaluation of Phenolics from Italian Extra Virgin Olive Oil for Diabetes Type II, Obesity and Hypertension Management. *Annals of Nutrition and Metabolism* **2009**, *55*, 595-595.

41. Panagiotakos, D.B.; Pitsavos, C.; Arvaniti, F.; Stefanadis, C. Adherence to the Mediterranean food pattern predicts the prevalence of hypertension, hypercholesterolemia, diabetes and obesity, among healthy adults; the accuracy of the MedDietScore. *Prev. Med.* **2007**, *44*, 335-340.

42. Di Fronzo, V.; Gente, R.; Pacioni, D.; Riccio, E.; Ferrara, L.A. Olive oil and health effects - on blood pressure, diabetes, arteriosclerosis, cancer and inflammatory diseases. *Agro Food Industry Hi-Tech* **2007**, *18*, 4-5.

43. Pasinetti, G.M.; Eberstein, J.A. Metabolic syndrome and the role of dietary lifestyles in Alzheimer's disease. *J. Neurochem.* **2008**, *106*, 1503-1514.

44. Owen, R.W.; Giacosa, A.; Hull, W.E.; Haubner, R.; Spiegelhalder, B.; Bartsch, H. The antioxidant/anticancer potential of phenolic compounds isolated from olive oil. *Eur. J. Cancer* **2000**, *36*, 1235-1247.

45. Menendez, J.A.; Vazquez-Martin, A.; Oliveras-Ferraros, C.; Garcia-Villalba, R.; Carrasco-Pancorbo, A.; Fernandez-Gutierrez, A.; Segura-Carreter, A. Extra-virgin olive oil polyphenols inhibit HER2 (erbB-2)-induced malignant transformation in human breast epithelial cells: Relationship between the chemical structures of extra-virgin olive oil secoiridoids and lignans and their inhibitory activities on the tyrosine kinase activity of HER2. *Int. J. Oncol.* **2009**, *34*, 43-51.

46. Sirianni, R.; Chimento, A.; De Luca, A.; Casaburi, I.; Rizza, P.; Onofrio, A.; Iacopetta, D.; Puoci, F.; Ando, S.; Maggiolini, M.; Pezzi, V. Oleuropein and



hydroxytyrosol inhibit MCF-7 breast cancer cell proliferation interfering with ERK1/2 activation. *Molecular Nutrition & Food Research* **2010**, *54*, 833-840.

47. Notarnicola, M.; Pisanti, S.; Tutino, V.; Bocale, D.; Rotelli, M.T.; Gentile, A.; Memeo, V.; Bifulco, M.; Perri, E.; Caruso, M.G. Effects of olive oil polyphenols on fatty acid synthase gene expression and activity in human colorectal cancer cells. *Genes and Nutrition* **2011**, *6*, 63-69.

48. Bulotta, S.; Corradino, R.; Celano, M.; D'Agostino, M.; Maiuolo, J.; Oliverio, M.; Procopio, A.; Iannone, M.; Rotiroti, D.; Russo, D. Antiproliferative and antioxidant effects on breast cancer cells of oleuropein and its semisynthetic peracetylated derivatives. *Food Chem.* **2011**, *127*, 1609-1614.

49. Birgit, D. Medicinal Plants of the World, Volume I, Chemical Constituents, Traditional and Modern Uses: Ivan A. Ross, Humana Press, Totowa, NJ, USA, ISSN 1-58829-281-9, 2003, 492 pp., US\$ 99.50. *Plant Science* **2004**, *166*, 255.

50. Ajay, M.; Chai, H.J.; Mustafa, A.M.; Gilani, A.H.; Mustafa, M.R. Mechanisms of the anti-hypertensive effect of Hibiscus sadariffa L. calyces. *J. Ethnopharmacol.* **2007**, *109*, 388-393.

51. Mozaffari-Khosravi, H.; Jalali-Khanabadi, B.; Afkhami-Ardekani, M.; Fatehi, F.; Noori-Shadkam, M. The effects of sour tea (Hibiscus sabdariffa) on hypertension in patients with type II diabetes. *J. Hum. Hypertens.* **2009**, *23*, 48-54.

52. McKay, D.L.; Chen, C.O.; Saltzman, E.; Blumberg, J.B. Hibiscus Sabdariffa L. Tea (Tisane) Lowers Blood Pressure in Prehypertensive and Mildly Hypertensive Adults. *J. Nutr.* **2010**, *140*, 298-303.

53. Liu, J.Y.; Chen, C.C.; Wang, W.H.; Hsu, J.D.; Yang, M.Y.; Wang, C.J. The protective effects of Hibiscus sabdariffa extract on CCl4-induced liver fibrosis in rats. *Food and Chemical Toxicology* **2006**, *44*, 336-343.



54. Yang, M.; Peng, C.; Chan, K.; Yang, Y.; Huang, C.; Wang, C. The Hypolipidemic Effect of Hibiscus sabdariffa Polyphenols via Inhibiting Lipogenesis and Promoting Hepatic Lipid Clearance. *J. Agric. Food Chem.* **2010**, *58*, 850-859.
55. Yin, G.; Cao, L.; Xu, P.; Jeney, G.; Nakao, M. Hepatoprotective and antioxidant effects of Hibiscus sabdariffa extract against carbon tetrachloride-induced hepatocyte damage in *Cyprinus carpio*. *In Vitro Cellular & Developmental Biology-Animal* **2011**, *47*, 10-15.
56. Farombi, E.A.; Fakoya, A. Free radical scavenging and antigenotoxic activities of natural phenolic compounds in dried flowers of Hibiscus sabdariffa L. *Molecular Nutrition & Food Research* **2005**, *49*, 1120-1128.
57. Christian, K.R.; Nair, M.G.; Jackson, J.C. Antioxidant and cyclooxygenase inhibitory activity of sorrel (Hibiscus sabdariffa). *Journal of Food Composition and Analysis* **2006**, *19*, 778-783.
58. Oboh, G.; Rocha, J.B.T. Antioxidant and Neuroprotective Properties of Sour Tea (Hibiscus sabdariffa, calyx) and Green Tea (Camellia sinensis) on some Pro-oxidant-induced Lipid Peroxidation in Brain in vitro. *Food Biophysics* **2008**, *3*, 382-389.
59. Mohd-Esa, N.; Hern, F.S.; Ismail, A.; Yee, C.L. Antioxidant activity in different parts of roselle (Hibiscus sabdariffa L.) extracts and potential exploitation of the seeds. *Food Chem.* **2010**, *122*, 1055-1060.
60. Ajiboye, T.O.; Salawu, N.A.; Yakubu, M.T.; Oladiji, A.T.; Akanji, M.A.; Okogun, J.I. Antioxidant and drug detoxification potentials of Hibiscus sabdariffa anthocyanin extract. *Drug Chem. Toxicol.* **2011**, *34*, 109-115.
61. Olaleye, M.T. Cytotoxicity and antibacterial activity of Methanolic extract of Hibiscus sabdariffa. *Journal of Medicinal Plants Research* **2007**, *1*, 9-13.



62. Kang, P.; Seok, J.; Kim, Y.; Eun, J.; Oh, S. Antimicrobial and antioxidative effects of roselle (*Hibiscus sabdariffa* L.) flower extract and its fractions on skin microorganisms and oxidation. *Food Science and Biotechnology* **2007**, *16*, 409-414.
63. Mounnissamy, V.M.; Gopal, V.; Gunasegaran, R.; Saraswathy, A. Antiinflammatory activity of gossypetin isolated from *Hibiscus sabdariffa*. *Indian Journal of Heterocyclic Chemistry* **2002**, *12*, 85-86.
64. Fakeye, T. Toxicity and immunomodulatory activity of fractions of *Hibiscus sabdariffa* Linn (family Malvaceae) in animal models. *African Journal of Traditional Complementary and Alternative Medicines* **2008**, *5*, 394-398.
65. Kao, E.; Hsu, J.; Wang, C.; Yang, S.; Cheng, S.; Lee, H. Polyphenols Extracted from *Hibiscus sabdariffa* L. Inhibited Lipopolysaccharide-Induced Inflammation by Improving Antioxidative Conditions and Regulating Cyclooxygenase-2 Expression. *Bioscience Biotechnology and Biochemistry* **2009**, *73*, 385-390.
66. Beltran-Debon, R.; Alonso-Villaverde, C.; Aragonés, G.; Rodríguez-Medina, I.; Rull, A.; Micol, V.; Segura-Carretero, A.; Fernández-Gutierrez, A.; Camps, J.; Joven, J. The aqueous extract of *Hibiscus sabdariffa* calices modulates the production of monocyte chemoattractant protein-1 in humans. *Phytomedicine* **2010**, *17*, 186-191.
67. Amos, S.; Binda, L.; Chindo, B.A.; Tseja, A.; Odutola, A.A.; Wambebe, C.; Gamaniel, K. Neuropharmacological effects of *Hibiscus sabdariffa* aqueous extract. *Pharm. Biol.* **2003**, *41*, 325-329.
68. Olvera-García, V.; Castano-Tostado, E.; Rezendiz-López, R.I.; Reynoso-Camacho, R.; de Mejía, E.G.; Elizondo, G.; Loarca-Pina, G. *Hibiscus sabdariffa* L. extracts inhibit the mutagenicity in microsuspension assay and the proliferation of HeLa cells. *J. Food Sci.* **2008**, *73*, T75-T81.



69. Lin, H.; Chen, J.; Wang, C. Chemopreventive Properties and Molecular Mechanisms of the Bioactive Compounds in Hibiscus Sabdariffa Linne. *Curr. Med. Chem.* **2011**, *18*, 1245-1254.
70. Hou, D.X.; Tong, X.; Terahara, N.; Luo, D.; Fujii, M. Delphinidin 3-sambubioside, a Hibiscus anthocyanin, induces apoptosis in human leukemia cells through reactive oxygen species-mediated mitochondrial pathway. *Arch. Biochem. Biophys.* **2005**, *440*, 101-109.
71. Lin, H.H.; Huang, H.P.; Huang, C.C.; Chen, J.H.; Wang, C.J. Hibiscus polyphenol-rich extract induces apoptosis in human gastric carcinoma cells via p53 phosphorylation and p38 MAPK/FasL cascade pathway. *Mol. Carcinog.* **2005**, *43*, 86-99.
72. Lin, H.; Chen, J.; Kuo, W.; Wang, C. Chemopreventive properties of Hibiscus sabdariffa L. on human gastric carcinoma cells through apoptosis induction and JNK/p38 MAPK signaling activation. *Chem. Biol. Interact.* **2007**, *165*, 59-75.
73. Chang, Y.; Huang, K.; Huang, A.; Ho, Y.; Wang, C. Hibiscus anthocyanins-rich extract inhibited LDL oxidation and oxLDL-mediated macrophages apoptosis. *Food and Chemical Toxicology* **2006**, *44*, 1015-1023.
74. Alarcon-Aguilar, F.J.; Zamilpa, A.; Perez-Garcia, M.D.; Almanza-Perez, J.C.; Romero-Nunez, E.; Campos-Sepulveda, E.A.; Vazquez-Carrillo, L.I.; Roman-Ramos, R. Effect of Hibiscus sabdariffia on obesity in MSG mice. *J. Ethnopharmacol.* **2007**, *114*, 66-71.
75. Carvajal-Zarrabal, O.; Hayward-Jones, P.M.; Orta-Flores, Z.; Nolasco-Hipolito, C.; Barradas-Dermitz, D.M.; Aguilar-Uscanga, M.G.; Pedroza-Hernandez, M.F. Effect of Hibiscus sabdariffa L. Dried Calyx Ethanol Extract on Fat Absorption-Excretion, and Body Weight Implication in Rats. *Journal of Biomedicine and Biotechnology* **2009**, 394592.



76. Kao, E.; Tseng, T.; Lee, H.; Chan, K.; Wang, C. Anthocyanin extracted from *Hibiscus attenuate* oxidized LDL-mediated foam cell formation involving regulation of CD36 gene. *Chem. Biol. Interact.* **2009**, *179*, 212-218.
77. Kuriyan, R.; Kumar, D.R.; Rajendran, R.; Kurpad, A.V. An evaluation of the hypolipidemic effect of an extract of *Hibiscus Sabdariffa* leaves in hyperlipidemic Indians: a double blind, placebo controlled trial. *Bmc Complementary and Alternative Medicine* **2010**, *10*, 27.
78. Olatunji, L.A.; Adebayo, J.O.; Adesokan, A.A.; Olatunji, V.A.; Soladoye, A.O. Chronic administration of aqueous extract of *Hibiscus sabdariffa* enhances Na⁺-K⁺-ATPase and Ca²⁺-Mg²⁺-ATPase activities of rat heart. *Pharm. Biol.* **2006**, *44*, 213-216.
79. Gurrola-Diaz, C.M.; Garcia-Lopez, P.M.; Sanchez-Enriquez, S.; Troyo-Sanroman, R.; Andrade-Gonzalez, I.; Gomez-Leyva, J.F. Effects of *Hibiscus sabdariffa* extract powder and preventive treatment (diet) on the lipid profiles of patients with metabolic syndrome (MeSy). *Phytomedicine* **2010**, *17*, 500-505.
80. Esselen, W.B.; Sammy, G.M. Roselle: a natural red colorant for foods? *Food Product and Development* **1975**, *7*, 80-82.
81. Segura-Carretero, A.; Puertas-Mejia, M.A.; Cortacero-Ramirez, S.; Beltran, R.; Alonso-Villaverde, C.; Joven, J.; Dinelli, G.; Fernandez-Gutierrez, A. Selective extraction, separation, and identification of anthocyanins from *Hibiscus sabdariffa* L. using solid phase extraction capillary electrophoresis mass spectrometry (time-of-flight ion trap). *Electrophoresis* **2008**, *29*, 2852-2861.
82. Cisse, M.; Dornier, M.; Sakho, M.; Ndiaye, A.; Reynes, M.; Sock, O. The bissap (*Hibiscus sabdariffa* L.): composition and principal uses. *Fruits* **2009**, *64*, 179-193.



83. Rodriguez-Medina, I.C.; Beltran-Debon, R.; Micol Molina, V.; Alonso-Villaverde, C.; Joven, J.; Menendez, J.A.; Segura-Carretero, A.; Fernandez-Gutierrez, A. Direct characterization of aqueous extract of Hibiscus sabdariffa using HPLC with diode array detection coupled to ESI and ion trap MS. *Journal of Separation Science* **2009**, *32*, 3441-3448.
84. Yamada, T.; Hida, H.; Yamada, Y. Chemistry, physiological properties, and microbial production of hydroxycitric acid. *Appl. Microbiol. Biotechnol.* **2007**, *75*, 977-982.
85. Fabricant, D.S.; Farnsworth, N.R. The value of plants used in traditional medicine for drug discovery. *Environ. Health Perspect.* **2001**, *109*, 69-75.
86. Robards, K.; Prenzler, P.D.; Tucker, G.; Swatsitang, P.; Glover, W. Phenolic compounds and their role in oxidative processes in fruits. *Food Chem.* **1999**, *66*, 401-436.
87. Puupponen-Pimia, R.; Nohynek, L.; Meier, C.; Kahkonen, M.; Heinonen, M.; Hopia, A.; Oksman-Caldentey, K.M. Antimicrobial properties of phenolic compounds from berries. *J. Appl. Microbiol.* **2001**, *90*, 494-507.
88. Mastuda, H.; Morikawa, T.; Ueda, K.; Managi, H.; Yoshikawa, M. Structural requirements of flavonoids for inhibition of antigen-Induced degranulation, TNF- α and IL-4 production from RBL-2H3 cells. *Bioorg. Med. Chem.* **2002**, *10*, 3123-3128.
89. Norata, G.D.; Marchesi, P.; Passamonti, S.; Pirillo, A.; Violi, F.; Catapano, A.L. Anti-inflammatory and anti-atherogenic effects of catechin, caffeic acid and trans-resveratrol in apolipoprotein E deficient mice. *Atherosclerosis* **2007**, *191*, 265-271.



90. Kostyuk, V.A.; Potapovich, A.I.; Suhan, T.O.; de Luca, C.; Korkina, L.G. Antioxidant and signal modulation properties of plant polyphenols in controlling vascular inflammation. *Eur. J. Pharmacol.* **2011**, *658*, 248-256.
91. Singh, R.; Akhtar, N.; Haqqi, T.M. Green tea polyphenol epigallocatechi3-gallate: Inflammation and arthritis. *Life Sci.* **2010**, *86*, 907-918.
92. Maria, D. Polyphenols as antimicrobial agents. *Curr. Opin. Biotechnol.* **2011**,
93. Fernandez-Panchon, M.S.; Villano, D.; Troncoso, A.M.; Garcia-Parrilla, M.C. Antioxidant activity of phenolic compounds: from in vitro results to in vivo evidence. *Crit. Rev. Food Sci. Nutr.* **2008**, *48*, 649-671.
94. Nadochiy, S.M.; Redman, E.K. Mediterranean diet and cardioprotection: The role of nitrite, polyunsaturated fatty acids, and polyphenols. *Nutrition* **2011**, *27*, 733-744.
95. Taguri, T.; Tanaka, T.; Kouno, I. Antimicrobial activity of 10 different plant polyphenols against bacteria causing food-borne disease. *Biological and Pharmaceutical Bulletin* **2004**, *27*, 1965-1969.
96. International Agency for research on cancer GLOBOCAN 2008 (IARC). **2011**, *2011*,
97. Willingham, A.T.; Deveraux, Q.L.; Hampton, G.M.; Aza-Blanc, P. RNAi and HTS: exploring cancer by systematic loss-of-function. *Oncogene* **2004**, *23*, 8392-8400.
98. Hartwell, L.H.; Kastan, M.B. Cell-Cycle Control and Cancer. *Science* **1994**, *266*, 1821-1828.
99. Marston, A.L.; Amon, A. Meiosis: Cell-cycle controls shuffle and deal. *Nature Reviews Molecular Cell Biology* **2004**, *5*, 983-997.



100. Porter, L.A.; Donoghue, D.J. Cyclin B1 and CDK1: nuclear localization and upstream regulators. *Prog. Cell Cycle Res.* **2003**, *5*, 335-347.
101. Smith, M.L.; Chen, I.T.; Zhan, Q.M.; Bae, I.S.; Chen, C.Y.; Gilmer, T.M.; Kastan, M.B.; Oconnor, P.M.; Fornace, A.J. Interaction of the P53-Regulated Protein Gadd45 with Proliferating Cell Nuclear Antigen. *Science* **1994**, *266*, 1376-1380.
102. Levine, A.J.; Finlay, C.A.; Hinds, P.W. P53 is a tumor suppressor gene. *Cell* **2004**, *S116*, S67-S69.
103. Rothkamm, K.; Kruger, I.; Thompson, L.; Lobrich, M. Pathways of DNA double-strand break repair during the mammalian cell cycle. *Mol. Cell. Biol.* **2003**, *23*, 5706-5715.
104. Bartkova, J.; Horejsi, Z.; Koed, K.; Kramer, A.; Tort, F.; Zieger, K.; Guldborg, P.; Sehested, M.; Nesland, J.; Lukas, C.; Orntoft, T.; Lukas, J.; Bartek, J. DNA damage response as a candidate anti-cancer barrier in early human tumorigenesis. *Nature* **2005**, *434*, 864-870.
105. Kuo, M.; Allis, C. Roles of histone acetyltransferases and deacetylases in gene regulation. *Bioessays* **1998**, *20*, 615-626.
106. Mai, A.; Massa, S.; Rotili, D.; Cerbara, I.; Valente, S.; Pezzi, R.; Simeoni, S.; Ragno, R. Histone deacetylation in epigenetics: An attractive target for anticancer therapy. *Med. Res. Rev.* **2005**, *25*, 261-309.
107. Nicholson, K.; Anderson, N. The protein kinase B/Akt signalling pathway in human malignancy. *Cell. Signal.* **2002**, *14*, 381-395.
108. ZHONG, Z.; WEN, Z.; DARNELL, J. Stat3 - a Stat Family Member Activated by Tyrosine Phosphorylation in Response to Epidermal Growth-Factor and Interleukin-6. *Science* **1994**, *264*, 95-98.



109. MacDonald, T.; Brown, K.; LaFleur, B.; Peterson, K.; Lawlor, C.; Chen, Y.; Packer, R.; Cogen, P.; Stephan, D. Expression profiling of medulloblastoma: PDGFRA and the RAS/MAPK pathway as therapeutic targets for metastatic disease. *Nat. Genet.* **2001**, *29*, 143-152.
110. Ryan, K.; Ernst, M.; Rice, N.; Vousden, K. Role of NF-kappa B in p53-mediated programmed cell death. *Nature* **2000**, *404*, 892-897.
111. Jiang, Y.; Li, Z.; Schwarz, E.; Lin, A.; Guan, K.; Ulevitch, R.; Han, J. Structure-function studies of p38 mitogen-activated protein kinase - Loop 12 influences substrate specificity and autophosphorylation, but not upstream kinase selection. *J. Biol. Chem.* **1997**, *272*, 11096-11102.
112. Clarke, R.; Dickson, R.B.; Brunner, N. The Process of Malignant Progression in Human Breast-Cancer. *Annals of Oncology* **1990**, *1*, 401-407.
113. Ruizcabello, J.; Berghmans, K.; Kaplan, O.; Lippman, M.E.; Clarke, R.; Cohen, J.S. Hormone Dependence of Breast-Cancer Cells and the Effects of Tamoxifen and Estrogen - P-31 Nmr-Studies. *Breast Cancer Res. Treat.* **1995**, *33*, 209-217.
114. White, R.; Parker, M.G. Molecular mechanisms of steroid hormone action. *Endocr. Relat. Cancer* **1998**, *5*, 1-14.
115. Shao Zhiming, J.M.; Yu Liming; Han Qixia; Shen Zhenzhou Estrogen receptor-negative breast cancer cells transfected with estrogen receptor exhibit decreased tumour progression and sensitivity to growth inhibition by estrogen. *Chinese Medical Sciences Journal* **1997**, *12*, 11-14.
116. Collingwood, T.N.; Urnov, F.D.; Wolffe, A.P. Nuclear receptors: coactivators, corepressors and chromatin remodeling in the control of transcription. *J. Mol. Endocrinol.* **1999**, *23*, 255-275.



117. Kavanagh, K.T.; Hafer, L.J.; Kim, D.W.; Mann, K.K.; Sherr, D.H.; Rogers, A.E.; Sonenshein, G.E. Green tea extracts decrease carcinogen-induced mammary tumor burden in rats and rate of breast cancer cell proliferation in culture. *J. Cell. Biochem.* **2001**, *82*, 387-398.
118. Deguchi, H.; Fujii, T.; Nakagawa, S.; Koga, T.; Shirouzu, K. Analysis of cell growth inhibitory effects of catechin through MAPK in human breast cancer cell line T47D. *Int. J. Oncol.* **2002**, *21*, 1301-1305.
119. Roper, K.I.; Whitley, B.R.; Ma, A.; Church, F.C. Effect of polyphenols on breast cancer cell proliferation, adhesion, and migration. *Faseb Journal* **2002**, *16*, A143-A143.
120. Kushima, Y.; Iida, K.; Nagaoka, Y.; Kawaratani, Y.; Shirahama, T.; Sakaguchi, M.; Baba, K.; Hara, Y.; Uesato, S. Inhibitory Effect of (-)-Epigallocatechin and (-)-Epigallocatechin Gallate against Heregulin beta 1-Induced Migration/Invasion of the MCF-7 Breast Carcinoma Cell Line. *Biol. Pharm. Bull.* **2009**, *32*, 899-904.
121. Liao, S.S.; Umekita, Y.; Guo, J.T.; Kokontis, J.M.; Hiipakka, R.A. Growth-Inhibition and Regression of Human Prostate and Breast-Tumors in Athymic Mice by Tea Epigallocatechin Gallate. *Cancer Lett.* **1995**, *96*, 239-243.
122. Nakachi, K.; Suemasu, K.; Suga, K.; Takeo, T.; Imai, K.; Higashi, Y. Influence of drinking green tea on breast cancer malignancy among Japanese patients. *Jap. J. Cancer Res.* **1998**, *89*, 254-261.
123. Iwasaki, M.; Inoue, M.; Sasazuki, S.; Miura, T.; Sawada, N.; Yamaji, T.; Shimazu, T.; Willett, W.C.; Tsugane, S. Plasma tea polyphenol levels and subsequent risk of breast cancer among Japanese women: a nested case-control study. *Breast Cancer Res. Treat.* **2010**, *124*, 827-834.
124. Sartippour, M.R.; Pietras, R.; Marquez-Garban, D.C.; Chen, H.; Heber, D.; Henning, S.M.; Sartippour, G.; Zhang, L.; Lu, M.; Weinberg, O.; Rao, J.Y.; Brooks,



M.N. The combination of green tea and tamoxifen is effective against breast cancer. *Carcinogenesis* **2006**, *27*, 2424-2433.

125. Schlachterman, A.; Valle, F.; Wall, K.M.; Azios, N.G.; Castillo, L.; Morell, L.; Washington, A.V.; Cubano, L.A.; Dharmawardhane, S.F. Combined Resveratrol, Quercetin, and Catechin Treatment Reduces Breast Tumor Growth in a Nude Mouse Model. *Translational Oncology* **2008**, *1*, 19-27.

126. Li, Y.; Yuan, Y.; Meeran, S.M.; Tollefsbol, T.O. Synergistic epigenetic reactivation of estrogen receptor-alpha (ER alpha) by combined green tea polyphenol and histone deacetylase inhibitor in ER alpha-negative breast cancer cells. *Molecular Cancer* **2010**, *9*, 274.

127. Damianaki, A.; Bakogeorgou, E.; Kampa, M.; Notas, G.; Hatzoglou, A.; Panagiotou, S.; Gemetzi, C.; Kouroumalis, E.; Martin, P.M.; Castanas, E. Potent inhibitory action of red wine polyphenols on human breast cancer cells. *J. Cell. Biochem.* **2000**, *78*, 429-441.

128. Hakimuddin, F.; Paliyath, G.; Meckling, K. Treatment of MCF-7 breast cancer cells with a red grape wine polyphenol fraction results in disruption of calcium homeostasis and cell cycle arrest causing selective cytotoxicity. *J. Agric. Food Chem.* **2006**, *54*, 7912-7923.

129. Kim, N.D.; Mehta, R.; Yu, W.P.; Neeman, I.; Livney, T.; Amichay, A.; Poirier, D.; Nicholls, P.; Kirby, A.; Jiang, W.G.; Mansel, R.; Ramachandran, C.; Rabi, T.; Kaplan, B.; Lansky, E. Chemopreventive and adjuvant therapeutic potential of pomegranate (*Punica granatum*) for human breast cancer. *Breast Cancer Res. Treat.* **2002**, *71*, 203-217.

130. Mehta, R.; Lansky, E.P. Breast cancer chemopreventive properties of pomegranate (*Punica granatum*) fruit extracts in a mouse mammary organ culture. *European Journal of Cancer Prevention* **2004**, *13*, 345-348.



131. Levi, F.; Pasche, C.; Lucchini, F.; Ghidoni, R.; Ferraroni, M.; La Vecchia, C. Resveratrol and breast cancer risk. *European Journal of Cancer Prevention* **2005**, *14*, 139-142.
132. Wang, Y.; Lee, K.W.; Chan, F.L.; Chen, S.A.; Leung, L.K. The red wine polyphenol resveratrol displays bilevel inhibition on aromatase in breast cancer cells. *Toxicological Sciences* **2006**, *92*, 71-77.
133. Filomeni, G.; Graziani, I.; Rotilio, G.; Ciriolo, M.R. trans-Resveratrol induces apoptosis in human breast cancer cells MCF-7 by the activation of MAP kinases pathways. *Genes and Nutrition* **2007**, *2*, 295-305.
134. Murias, M.; Miksits, M.; Aust, S.; Spatzenegger, M.; Thalhammer, T.; Szekeres, T.; Jaeger, W. Metabolism of resveratrol in breast cancer cell lines: Impact of sulfotransferase 1A1 expression on cell growth inhibition. *Cancer Lett.* **2008**, *261*, 172-182.
135. Hsieh, T.; Wong, C.; Bennett, D.J.; Wu, J.M. Regulation of p53 and cell proliferation by resveratrol and its derivatives in breast cancer cells: an in silico and biochemical approach targeting integrin alpha v beta 3. *International Journal of Cancer* **2011**, *129*, 2732-2743.
136. Whitsett, T.G., Jr.; Lamortiniere, C.A. Genistein and resveratrol: mammary cancer chemoprevention and mechanisms of action in the rat. *Expert Review of Anticancer Therapy* **2006**, *6*, 1699-1706.
137. Nifli, A.P.; Kampa, M.; Alexaki, V.I.; Notas, G.; Castanas, E. Polyphenol interaction with the T47D human breast cancer cell line. *J. Dairy Res.* **2005**, *72*, 44-50.
138. Strati, A.; Papoutsis, Z.; Lianidou, E.; Moutsatsou, P. Effect of ellagic acid on the expression of human telomerase reverse transcriptase (hTERT) alpha plus



beta plus transcript in estrogen receptor-positive MCF-7 breast cancer cells. *Clin. Biochem.* **2009**, *42*, 1358-1362.

139. Bachmeier, B.E.; Nerlich, A.G.; Iancu, C.M.; Cilli, M.; Schleicher, E.; Vene, R.; Dell'Eva, R.; Jochum, M.; Albini, A.; Pfeffer, U. The chemopreventive polyphenol Curcumin prevents hematogenous breast cancer metastases in immunodeficient mice. *Cellular Physiology and Biochemistry* **2007**, *19*, 137-152.

140. Carroll, C.E.; Eilersieck, M.R.; Hyder, S.M. Curcumin inhibits MPA-induced secretion of VEGF from T47-D human breast cancer cells. *Menopause-the Journal of the North American Menopause Society* **2008**, *15*, 570-574.

141. Faria, A.; Pestana, D.; Teixeira, D.; de Freitas, V.; Mateus, N.; Calhau, C. Blueberry Anthocyanins and Pyruvic Acid Adducts: Anticancer Properties in Breast Cancer Cell Lines. *Phytotherapy Research* **2010**, *24*, 1862-1869.

142. Ullah, M.F.; Ahmad, A.; Zubair, H.; Khan, H.Y.; Wang, Z.; Sarkar, F.H.; Hadi, S.M. Soy isoflavone genistein induces cell death in breast cancer cells through mobilization of endogenous copper ions and generation of reactive oxygen species. *Molecular Nutrition & Food Research* **2011**, *55*, 553-559.

143. Limer, J.L.; Speirs, V. Phyto-oestrogens and breast cancer chemoprevention. *Breast Cancer Research* **2004**, *6*, 119-127.

144. van Zanden, J.J.; Geraets, L.; Wortelboer, H.M.; van Bladeren, P.J.; Rietjens, I.M.C.M.; Cnubben, N.H.P. Structural requirements for the flavonoid-mediated modulation of glutathione S-transferase P1-1 and GS-X pump activity in MCF7 breast cancer cells. *Biochem. Pharmacol.* **2004**, *67*, 1607-1617.

145. Lin, Y.; Hou, Y.C.; Lin, C.; Hsu, Y.; Sheu, J.J.C.; Lai, C.; Chen, B.; Chao, P.L.; Wan, L.; Tsai, F. Puerariae radix isoflavones and their metabolites inhibit growth and induce apoptosis in breast cancer cells. *Biochem. Biophys. Res. Commun.* **2009**, *378*, 683-688.



146. Noratto, G.; Porter, W.; Byrne, D.; Cisneros-Zevallos, L. Identifying Peach and Plum Polyphenols with Chemopreventive Potential against Estrogen-Independent Breast Cancer Cells. *J. Agric. Food Chem.* **2009**, *57*, 5219-5226.
147. Pick, A.; Mueller, H.; Mayer, R.; Haenisch, B.; Pajeva, I.K.; Weigt, M.; Boenisch, H.; Mueller, C.E.; Wiese, M. Structure-activity relationships of flavonoids as inhibitors of breast cancer resistance protein (BCRP). *Bioorg. Med. Chem.* **2011**, *19*, 2090-2102.
148. Solanas, M.; Hurtado, A.; Costa, I.; Moral, R.; Menendez, J.A.; Colomer, R.; Escrich, E. Effects of a high olive oil diet on the clinical behavior and histopathological features of rat DMBA-induced mammary tumors compared with a high corn oil diet. *Int. J. Oncol.* **2002**, *21*, 745-753.
149. Menendez, J.A.; Vellon, L.; Colomer, R.; Lupu, R. Oleic acid, the main monounsaturated fatty acid of olive oil, suppresses Her-2/neu (erb B-2) expression and synergistically enhances the growth inhibitory effects of trastuzumab (Herceptin (TM)) in breast cancer cells with Her-2/neu oncogene amplification. *Annals of Oncology* **2005**, *16*, 359-371.
150. Menendez, J.A.; Papadimitropoulou, A.; Vellon, L.; Lupu, R. A genomic explanation connecting "Mediterranean diet", olive oil and cancer: Oleic acid, the main monounsaturated fatty acid of olive oil, induces formation of inhibitory "PEA3 transcription factor-PEA3 DNA binding site" complexes at the Her-2/neu (erbB-2) oncogene promoter in breast, ovarian and stomach cancer cells. *Eur. J. Cancer* **2006**, *42*, 2425-2432.
151. Menendez, J.A.; Vazquez-Martin, A.; Colomer, R.; Brunet, J.; Carrasco-Pancorbo, A.; Garcia-Villalba, R.; Fernandez-Gutierrez, A.; Segura-Carretero, A. Olive oil's bitter principle reverses acquired autoresistance to trastuzumab (Herceptin (TM)) in HER2-overexpressing breast cancer cells. *BMC Cancer* **2007**, *7*, 80-80.



152. Menendez, J.A.; Vazquez-Martin, A.; Garcia-Villalba, R.; Carrasco-Pancorbo, A.; Oliveras-Ferraros, C.; Fernandez-Gutierrez, A.; Segura-Carretero, A. Anti-HER2 (erbB-2) oncogene effects of phenolic compounds directly isolated from commercial Extra-Virgin Olive Oil (EVOO). *BMC Cancer* **2008**, *8*, 377-377.
153. Menendez, J.A.; Vazquez-Martin, A.; Oliveras-Ferraros, C.; Garcia-Villalba, R.; Carrasco-Pancorbo, A.; Fernandez-Gutierrez, A.; Segura-Carretero, A. Analyzing effects of extra-virgin olive oil polyphenols on breast cancer-associated fatty acid synthase protein expression using reverse-phase protein microarrays. *Int. J. Mol. Med.* **2008**, *22*, 433-439.
154. Han, J.; Talorete, T.P.N.; Yamada, P.; Isoda, H. Anti-proliferative and apoptotic effects of oleuropein and hydroxytyrosol on human breast cancer MCF-7 cells. *Cytotechnology* **2009**, *59*, 45-53.
155. Jemal, A.; Murray, T.; Ward, E.; Samuels, A.; Tiwari, R.C.; Ghafoor, A.; Feuer, E.J.; Thun, M.J. Cancer statistics, 2005. *CA-Cancer J. Clin.* **2005**, *55*, 10-30.
156. Bingham, S.A.; Day, N.E.; Luben, R.; Ferrari, P.; Slimani, N.; Norat, T.; Clavel-Chapelon, F.; Kesse, E.; Nieters, A.; Boeing, H.; Tjonneland, A.; Overvad, K.; Martinez, C.; Dorronsoro, M.; Gonzalez, C.A.; Key, T.J.; Trichopoulou, A.; Naska, A.; Vineis, P.; Tumino, R.; Krogh, V.; Bueno-de-Mesquita, H.B.; Peeters, P.H.M.; Berglund, G.; Hallmans, G.; Lund, E.; Skeie, G.; Kaaks, R.; Riboli, E. Dietary fibre in food and protection against colorectal cancer in the European Prospective Investigation into Cancer and Nutrition (EPIC): an observational study. *Lancet* **2003**, *361*, 1496-1501.
157. Christensen, K.Y.; Naidu, A.; Marie-Elise, P.; Pintos, J.; Siemiatycki, J.; Koushik, A. The Risk of Lung Cancer Related to Dietary Intake of Flavonoids. *Am. J. Epidemiol.* **2010**, *171*, S4-S4.



158. Konishi, M.; KikuchiYanoshita, R.; Tanaka, K.; Muraoka, M.; Onda, A.; Okumura, Y.; Kishi, N.; Iwama, T.; Mori, T.; Koike, M.; Ushio, K.; Chiba, M.; Nomizu, S.; Konishi, F.; Utsunomiya, J.; Miyaki, M. Molecular nature of colon tumors in hereditary nonpolyposis colon cancer, familial polyposis, and sporadic colon cancer. *Gastroenterology* **1996**, *111*, 307-317.
159. Aaltonen, L.A.; Peltomaki, P.; Leach, F.S.; Sistonen, P.; Pylkkanen, L.; Mecklin, J.P.; Jarvinen, H.; Powell, S.M.; Jen, J.; Hamilton, S.R.; Petersen, G.M.; Kinzler, K.W.; Vogelstein, B.; Delachapelle, A. Clues to the Pathogenesis of Familial Colorectal-Cancer. *Science* **1993**, *260*, 812-816.
160. Kinzler, K.W.; Vogelstein, B. Lessons from hereditary colorectal cancer. *Cell* **1996**, *87*, 159-170.
161. Aaltonen, L.A.; Salovaara, R.; Kristo, P.; Canzian, F.; Hemminki, A.; Peltomaki, P.; Chadwick, R.B.; Kaariainen, H.; Eskelinen, M.; Jarvinen, H.; Mecklin, J.P.; de la Chapelle, A.; Percesepe, A.; Ahtola, H.; Harkonen, N.; Julkunen, R.; Kangas, E.; Ojala, S.; Tulikoura, J.; Valkamo, E. Incidence of hereditary nonpolyposis colorectal cancer and the feasibility of molecular screening for the disease. *N. Engl. J. Med.* **1998**, *338*, 1481-1487.
162. Pretlow, T.P.; Brasitus, T.A.; Fulton, N.C.; Cheyer, C.; Kaplan, E.L. K-Ras Mutations in Putative Preneoplastic Lesions in Human Colon. *J. Natl. Cancer Inst.* **1993**, *85*, 2004-2007.
163. Ekelund, S.; Papadogiannakis, N.; Olivecrona, H.; Lindfors, U. Tissue sampling for mutation analysis in colorectal cancer: K-ras is homogeneously distributed throughout the tumor tissue. *Oncol. Rep.* **2011**, *25*, 253-258.
164. Hollstein, M.; Sidransky, D.; Vogelstein, B.; Harris, C.C. P53 Mutations in Human Cancers. *Science* **1991**, *253*, 49-53.



165. Shaw, P.; Bovey, R.; Tardy, S.; Sahli, R.; Sordat, B.; Costa, J. Induction of Apoptosis by Wild-Type P53 in a Human Colon Tumor-Derived Cell-Line. *Proc. Natl. Acad. Sci. U. S. A.* **1992**, *89*, 4495-4499.
166. Hosokawa, N.; Hosokawa, Y.; Sakai, T.; Yoshida, M.; Marui, N.; Nishino, H.; Kawai, K.; Aoike, A. Inhibitory Effect of Quercetin on the Synthesis of a Possibly Cell-Cycle-Related 17-Kda Protein, in Human Colon Cancer-Cells. *International Journal of Cancer* **1990**, *45*, 1119-1124.
167. Tanaka, T.; Yoshimi, N.; Sugie, S.; Mori, H. Protective Effects Against Liver, Colon, and Tongue Carcinogenesis by Plant Phenols. *ACS Symp. Ser.* **1992**, *507*, 326-337.
168. Tamura, H.; Matsui, M. Inhibitory effects of green tea and grape juice on the phenol sulfotransferase activity of mouse intestines and human colon carcinoma cell line, Caco-2. *Biol. Pharm. Bull.* **2000**, *23*, 695-699.
169. Pahlke, G.; Ngiewih, Y.; Kern, M.; Jakobs, S.; Marko, D.; Eisenbrand, G. Impact of quercetin and EGCG on key elements of the Wnt pathway in human colon carcinoma cells. *J. Agric. Food Chem.* **2006**, *54*, 7075-7082.
170. Singh, B.N.; Shankar, S.; Srivastava, R.K. Green tea catechin, epigallocatechin-3-gallate (EGCG): Mechanisms, perspectives and clinical applications. *Biochem. Pharmacol.* **2011**, *82*, 1807-1821.
171. Tanaka, T.; Miyamoto, S.; Suzuki, R.; Yasui, Y. Chemoprevention of colon carcinogenesis by dietary non-nutritive compounds. *Current Topics in Nutraceutical Research* **2006**, *4*, 127-151.
172. Kulisic-Bilusic, T.; Schnaebeler, K.; Schmoeller, I.; Dragovic-Uzelac, V.; Krisko, A.; Dejanovic, B.; Milos, M.; Pifat, G. Antioxidant activity versus cytotoxic and nuclear factor kappa B regulatory activities on HT-29 cells by natural fruit juices. *European Food Research and Technology* **2009**, *228*, 417-424.



173. Shan, B.; Wang, M.; Li, R. Quercetin Inhibit Human SW480 Colon Cancer Growth in Association with Inhibition of Cyclin D1 and Survivin Expression through Wnt/-Catenin Signaling Pathway. *Cancer Invest.* **2009**, *27*, 604-612.
174. Xavier, C.P.R.; Lima, C.F.; Preto, A.; Seruca, R.; Fernandes-Ferreira, M.; Pereira-Wilson, C. Luteolin, quercetin and ursolic acid are potent inhibitors of proliferation and inducers of apoptosis in both KRAS and BRAF mutated human colorectal cancer cells. *Cancer Lett.* **2009**, *281*, 162-170.
175. Kim, H.; Kim, S.; Kim, B.; Lee, S.; Park, Y.; Park, B.; Kim, S.; Kim, J.; Choi, C.; Kim, J.; Cho, S.; Jung, J.; Roh, K.; Kang, K.; Jung, J. Apoptotic Effect of Quercetin on HT-29 Colon Cancer Cells via the AMPK Signaling Pathway. *J. Agric. Food Chem.* **2010**, *58*, 8643-8650.
176. Fabiani, R.; De Bartolomeo, A.; Rosignoli, P.; Servili, M.; Montedoro, G.F.; Morozzi, G. Cancer chemoprevention by hydroxytyrosol isolated from virgin olive oil through G(1) cell cycle arrest and apoptosis. *European Journal of Cancer Prevention* **2002**, *11*, 351-358.
177. [Anon] Anti-metastatic effects of olive oil phenolics in colon cancer cell line. *Cellular Oncology* **2005**, *27*, 139-140.
178. Hashim, Y.Z.H.-.; Rowland, I.R.; McGlynn, H.; Servili, M.; Selvaggini, R.; Taticchi, A.; Esposito, S.; Montedoro, G.; Kaisalo, L.; Wahala, K.; Gill, C.I.R. Inhibitory effects of olive oil phenolics on invasion in human colon adenocarcinoma cells in vitro. *International Journal of Cancer* **2008**, *122*, 495-500.
179. Gill, C.I.R.; Boyd, A.; McDermott, E.; McCann, M.; Servili, M.; Selvaggini, R.; Taticchi, A.; Esposito, S.; Montedoro, G.; McGlynn, H.; Rowland, I. Potential anti-cancer effects of virgin olive oil phenols on colorectal carcinogenesis models in vitro. *International Journal of Cancer* **2005**, *117*, 1-7.



180. Emilia Juan, M.; Wenzel, U.; Ruiz-Gutierrez, V.; Daniel, H.; Planas, J.M. Olive fruit extracts inhibit proliferation and induce apoptosis in HT-29 human colon cancer cells. *J. Nutr.* **2006**, *136*, 2553-2557.
181. Hashim, Y.Z.H.Y.; Gill, C.I.R.; McGlynn, H.; Rowland, I.R. Components of olive oil and chemoprevention of colorectal cancer. *Nutr. Rev.* **2005**, *63*, 374-386.
182. Sanchez-Fidalgo, S.; Villegas, I.; Cardeno, A.; Talero, E.; Sanchez-Hidalgo, M.; Motilva, V.; Alarcon de la Lastra, C. Extra-virgin olive oil-enriched diet modulates DSS-colitis-associated colon carcinogenesis in mice. *Clinical Nutrition* **2010**, *29*, 663-673.
183. Corona, G.; Deiana, M.; Incani, A.; Vauzour, D.; Dessi, M.A.; Spencer, J.P.E. Hydroxytyrosol inhibits the proliferation of human colon adenocarcinoma cells through inhibition of ERK1/2 and cyclin D1. *Molecular Nutrition & Food Research* **2009**, *53*, 897-903.
184. Fini, L.; Hotchkiss, E.; Fogliano, V.; Romano, M.; Devol, E.B.; Qin, H.B.; Boland, r.; Ricciardiello, L. Chemopreventive properties of pinoresinol-enriched olives involve a selective activation of the p53 cascade in colon cancer cells. *Gastroenterology* **2007**, *132*, A434-A434.
185. Fini, L.; Hotchkiss, E.; Fogliano, V.; Graziani, G.; Romano, M.; De Vol, E.B.; Qin, H.; Selgrad, M.; Boland, C.R.; Ricciardiello, L. Chemopreventive properties of pinoresinol-rich olive oil involve a selective activation of the ATM-p53 cascade in colon cancer cell lines. *Carcinogenesis* **2008**, *29*, 139-146.
186. Thiery, J.P.; Acloque, H.; Huang, R.Y.J.; Nieto, M.A. Epithelial-Mesenchymal Transitions in Development and Disease. *Cell* **2009**, *139*, 871-890.



187. Lee, J.; Dedhar, S.; Kalluri, R.; Thompson, E. The epithelial-mesenchymal transition: new insights in signaling, development, and disease. *J. Cell Biol.* **2006**, *172*, 973-981.
188. Wu, Y.; Zhou, B.P. New insights of epithelial-mesenchymal transition in cancer metastasis. *Acta Biochimica Et Biophysica Sinica* **2008**, *40*, 643-650.
189. Zeisberg, M.; Yang, C.; Martino, M.; Duncan, M.B.; Rieder, F.; Tanjore, H.; Kalluri, R. Fibroblasts derive from hepatocytes in liver fibrosis via epithelial to mesenchymal transition. *J. Biol. Chem.* **2007**, *282*, 23337-23347.
190. Yeh, Y.; Wei, W.; Wang, Y.; Lin, S.; Sung, J.; Tang, M. Transforming Growth Factor-beta 1 Induces Smad3-Dependent beta(1) Integrin Gene Expression in Epithelial-to-Mesenchymal Transition during Chronic Tubulointerstitial Fibrosis. *Am. J. Pathol.* **2010**, *177*, 1743-1754.
191. Belguise, K.; Guo, S.; Sonenshein, G.E. Activation of FOXO3a by the green tea polyphenol epigallocatechin-3-gallate induces estrogen receptor alpha expression reversing invasive phenotype of breast cancer cells. *Cancer Res.* **2007**, *67*, 5763-5770.
192. Belguise, K.; Guo, S.; Yang, S.; Rogers, A.E.; Seldin, D.C.; Sherr, D.H.; Sonenshein, G.E. Green tea polyphenols reverse cooperation between c-Rel and CK2 that induces the Aryl hydrocarbon receptor, Slug, and an invasive phenotype. *Cancer Res.* **2007**, *67*, 11742-11750.
193. Chen, P.; Chu, S.; Kuo, W.; Chou, M.; Lin, J.; Hsieh, Y. Epigallocatechin-3 Gallate Inhibits Invasion, Epithelial-Mesenchymal Transition, and Tumor Growth in Oral Cancer Cells. *J. Agric. Food Chem.* **2011**, *59*, 3836-3844.
194. Organización Mundial de la Salud (OMS) Obesidad y sobrepeso. Nota informativa N° 311. **2011**,



195. Avram, M.M.; Avram, A.S.; James, W.D. Subcutaneous fat in normal and diseased states - 3. Adipogenesis: From stem cell to fat cell. *J. Am. Acad. Dermatol.* **2007**, *56*, 472-492.
196. Hausman, G.; Richardson, R. Adipose tissue angiogenesis. *J. Anim. Sci.* **2004**, *82*, 925-934.
197. Bray, G. Medical consequences of obesity. *Journal of Clinical Endocrinology & Metabolism* **2004**, *89*, 2583-2589.
198. Bahceci, M.; Gokalp, D.; Bahceci, S.; Tuzcu, A.; Atmaca, S.; Arikan, S. The correlation between adiposity and adiponectin tumor necrosis factor alpha, interleukin-6 and high sensitivity C-reactive protein levels. Is adipocyte size associated with inflammation in adults? *J. Endocrinol. Invest.* **2007**, *30*, 210-214.
199. Monteiro, R.; Assuncao, M.; Andrade, J.P.; Neves, D.; Calhau, C.; Azevedo, I. Chronic Green Tea Consumption Decreases Body Mass, Induces Aromatase Expression, and Changes Proliferation and Apoptosis e Rat Adipose Tissue. *J. Nutr.* **2008**, *138*, 2156-2163.
200. Chen, N.; Bezzina, R.; Hinch, E.; Lewandowski, P.A.; Cameron-Smith, D.; Mathai, M.L.; Jois, M.; Sinclair, A.J.; Begg, D.P.; Wark, J.D.; Weisinger, H.S.; Weisinger, R.S. Green tea, black tea, and epigallocatechin modify body composition, improve glucose tolerance, and differentially alter metabolic gene expression in rats fed a high-fat diet. *Nutr. Res.* **2009**, *29*, 784-793.
201. Chen, Y.; Cheung, C.; Reuhl, K.R.; Liu, A.B.; Lee, M.; Lu, Y.; Yang, C.S. Effects of Green Tea Polyphenol (-)-Epigallocatechin-3-gallate on Newly Developed High-Fat/Western-Style Diet-Induced Obesity and Metabolic Syndrome in Mice. *J. Agric. Food Chem.* **2011**, *59*, 11862-11871.



202. Chan, C.Y.; Wei, L.; Castro-Munozledo, F.; Koo, W.L. (-)-Epigallocatechin-3-gallate blocks 3T3-L1 adipose conversion by inhibition of cell proliferation and suppression of adipose phenotype expression. *Life Sci.* **2011**, *89*, 779-785.
203. Park, H.J.; Lee, J.; Chung, M.; Park, Y.; Bower, A.M.; Koo, S.I.; Giardina, C.; Bruno, R.S. Green Tea Extract Suppresses NF kappa B Activation and Inflammatory Responses in Diet-Induced Obese Rats with Nonalcoholic Steatohepatitis. *J. Nutr.* **2012**, *142*, 57-63.
204. Terra, X.; Montagut, G.; Bustos, M.; Llopiz, N.; Ardevol, A.; Blade, C.; Fernandez-Larrea, J.; Pujadas, G.; Salvado, J.; Arola, L.; Blay, M. Grape-seed procyanidins prevent low-grade inflammation by modulating cytokine expression in rats fed a high-fat diet. *J. Nutr. Biochem.* **2009**, *20*, 210-218.
205. Chuang, C.; McIntosh, M.K. Potential Mechanisms by Which Polyphenol-Rich Grapes Prevent Obesity-Mediated Inflammation and Metabolic Diseases. *Annual Review of Nutrition, Vol 31* **2011**, *31*, 155-176.
206. Charradi, K.; Sebai, H.; Elkahoui, S.; Ben Hassine, F.; Limam, F.; Aouani, E. Grape Seed Extract Alleviates High-Fat Diet-Induced Obesity and Heart Dysfunction by Preventing Cardiac Siderosis. *Cardiovascular Toxicology* **2011**, *11*, 28-37.
207. Ahn, J.; Lee, H.; Kim, S.; Ha, T. Curcumin-induced suppression of adipogenic differentiation is accompanied by activation of Wnt/beta-catenin signaling. *American Journal of Physiology-Cell Physiology* **2010**, *298*, C1510-C1516.
208. Ejaz, A.; Wu, D.; Kwan, P.; Meydani, M. Curcumin Inhibits Adipogenesis in 3T3-L1 Adipocytes and Angiogenesis and Obesity in C57/BL Mice. *J. Nutr.* **2009**, *139*, 919-925.
209. Chuang, C.C.; Martinez, K.; Xie, G.; Kennedy, A.; Bumrungpert, A.; Overman, A.; Jia, W.; McIntosh, M.K. Quercetin is equally or more effective than



resveratrol in attenuating tumor necrosis factor-alpha-mediated inflammation and insulin resistance in primary human adipocytes. *Am. J. Clin. Nutr.* **2010**, *92*, 1511-1521.

210. Provot, S.; Schipani, E. Molecular mechanisms of endochondral bone development. *Biochem. Biophys. Res. Commun.* **2005**, *328*, 658-665.

211. He, L.; Shobnam, N.; Wimley, W.C.; Hristova, K. FGFR3 Heterodimerization in Achondroplasia, the Most Common Form of Human Dwarfism. *J. Biol. Chem.* **2011**, *286*, 13272-13281.

212. Shiang, R.; Thompson, L.M.; Zhu, Y.-.; Church, D.M.; Fielder, T.J.; Bocian, M.; Winokur, S.T.; Wasmuth, J.J. Mutations in the transmembrane domain of FGFR3 cause the most common genetic form of dwarfism, achondroplasia. *Cell* **1994**, *78*, 335-342.

213. Raucci, A.; Laplantine, E.; Mansukhani, A.; Basilico, C. Activation of the ERK1/2 and p38 mitogen-activated protein kinase pathways mediates fibroblast growth factor-induced growth arrest of chondrocytes. *J. Biol. Chem.* **2004**, *279*, 1747-1756.

214. Krejci, P.; Masri, B.; Fontaine, V.; Mekikian, P.; Weis, M.; Prats, H.; Wilcox, W. Interaction of fibroblast growth factor and C-natriuretic peptide signaling in regulation of chondrocyte proliferation and extracellular matrix homeostasis. *J. Cell. Sci.* **2005**, *118*, 5089-5100.

215. Huete, F.; Guzman-Aranguez, A.; Ortin, J.; Hoyle, C.H.V.; Pintor, J. Effects of diadenosine tetraphosphate on FGF9-induced chloride flux changes in achondroplastic chondrocytes. *Purinergic Signalling* **2011**, *7*, 243-249.

216. Eswarakumar, V.P.; Lax, I.; Schlessinger, J. Cellular signaling by fibroblast growth factor receptors. *Cytokine Growth Factor Rev.* **2005**, *16*, 139-149.



217. Koel, M.; Borissova, M.; Vaher, M.; Kaljurand, M. Developments in the application of Green Chemistry principles to food analysis Capillary electrophoresis for the analysis of ingredients in food products. *Agro Food Industry Hi-Tech* **2011**, *22*, 27-29.
218. Castro-Puyana, M.; Garcia-Canas, V.; Simo, C.; Cifuentes, A. Recent advances in the application of capillary electromigration methods for food analysis and Foodomics. *Electrophoresis* **2012**, *33*, 147-167.
219. Soleas, G.J.; Goldberg, D.M. Analysis of antioxidant wine polyphenols by gas chromatography mass spectrometry. *Oxidants and Antioxidants, Pt a* **1999**, *299*, 137-151.
220. Gomez-Caravaca, A.M.; Gomez-Romero, M.; Arraez-Roman, D.; Segura-Carretero, A.; Fernandez-Gutierrez, A. Advances in the analysis of phenolic compounds in products derived from bees. *J. Pharm. Biomed. Anal.* **2006**, *41*, 1220-1234.
221. Bruckner, K.J.; Charalam.G; Hardwick, W.A.; Linnebac.AI Separation, Identification, and Quantitative-Determination of Certain Beer Flavor Compounds by High-Pressure Liquid Chromatography. *Abstracts of Papers of the American Chemical Society* **1973**, 49-&.
222. Karlsson, K.E.; Novotny, M. Separation Efficiency of Slurry-Packed Liquid-Chromatography Microcolumns with very Small Inner Diameters. *Anal. Chem.* **1988**, *60*, 1662-1665.
223. Hsieh, S.C.; Jorgenson, J.W. Preparation and evaluation of slurry-packed liquid chromatography microcolumns with inner diameters from 12 to 33 μ m. *Anal. Chem.* **1996**, *68*, 1212-1217.



224. Fanali, S.; Camera, E.; Chankvetadze, B.; D'Orazio, G.; Quaglia, M.G. Separation of tocopherols by nano-liquid chromatography. *J. Pharm. Biomed. Anal.* **2004**, *35*, 331-337.
225. Hernandez-Borges, J.; Aturki, Z.; Rocco, A.; Fanali, S. Recent applications in nanoliquid chromatography. *Journal of Separation Science* **2007**, *30*, 1589-1610.
226. Hernandez-Borges, J.; D'Orazio, G.; Aturki, Z.; Fanali, S. Nano-liquid chromatography analysis of dansylated biogenic amines in wines. *Journal of Chromatography a* **2007**, *1147*, 192-199.
227. Garcia-Villalba, R.; Carrasco-Pancorbo, A.; Zurek, G.; Behrens, M.; Baessmann, C.; Segura-Carretero, A.; Fernandez-Gutierrez, A. Nano and rapid resolution liquid chromatography-electrospray ionization-time of flight mass spectrometry to identify and quantify phenolic compounds in olive oil. *Journal of Separation Science* **2010**, *33*, 2069-2078.
228. Pellizza, Ed; Chuang, C.M.; Kuc, J.; Williams, E.B. Gas Chromatography and Mass Spectroscopy of Plant Phenolics and Related Compounds. *J. Chromatogr.* **1969**, *40*, 285-&.
229. Powell-Braxton, L.; Veniant, M.; Latvala, R.D.; Hirano, K.I.; Won, W.B.; Ross, J.; Dybdal, N.; Zlot, C.H.; Young, S.G.; Davidson, N.O. A mouse model of human familial hypercholesterolemia: Markedly elevated low density lipoprotein cholesterol levels and severe atherosclerosis on a low-fat chow diet. *Nat. Med.* **1998**, *4*, 934-938.
230. Karadag, A.; Ozcelik, B.; Saner, S. Review of Methods to Determine Antioxidant Capacities. *Food Analytical Methods* **2009**, *2*, 41-60.
231. Sheweita, S. Drug-metabolizing enzymes: Mechanisms and functions. *Curr. Drug Metab.* **2000**, *1*, 107-132.



232. Barnes, S.; Prasain, J.; D'Alessandro, T.; Arabshahi, A.; Botting, N.; Lila, M.A.; Jackson, G.; Janle, E.M.; Weaver, C.M. The metabolism and analysis of isoflavones and other dietary polyphenols in foods and biological systems. *Food & Function* **2011**, *2*, 235-244.
233. Williamson, G.; Day, A.; Plumb, G.; Couteau, D. Human metabolic pathways of dietary flavonoids and cinnamates. *Biochem. Soc. Trans.* **2000**, *28*, 16-22.
234. Scalbert, A.; Williamson, G. Dietary intake and bioavailability of polyphenols. *J. Nutr.* **2000**, *130*, 2073S-2085S.
235. Nielsen, S.; Breinholt, V.; Justesen, U.; Cornett, C.; Dragsted, L. In vitro biotransformation of flavonoids by rat liver microsomes. *Xenobiotica* **1998**, *28*, 389-401.
236. Wormhoudt, L.; Commandeur, J.; Vermeulen, N. Genetic polymorphisms of human N-acetyltransferase, cytochrome P450, glutathione-S-Transferase, and epoxide hydrolase enzymes: Relevance to xenobiotic metabolism and toxicity. *Crit. Rev. Toxicol.* **1999**, *29*, 59-124.
237. Doménech-Berrozpe, J., Martínez-Lanao, J., & Plá Delfina, J. M. (2001). *Biofarmacia y Farmacocinética volumen I: Farmacocinética*. Madrid: Síntesis.
238. Domínguez-Gil Hurlé, A. La circulación del medicamento en el organismo. Farmacocinética. In Anonymous ;2001; Vol.Ed. Farmaindustria, serie Científica pp. 25-44.
239. Bravo, L. Polyphenols: Chemistry, dietary sources, metabolism, and nutritional significance. *Nutr. Rev.* **1998**, *56*, 317-333.

